

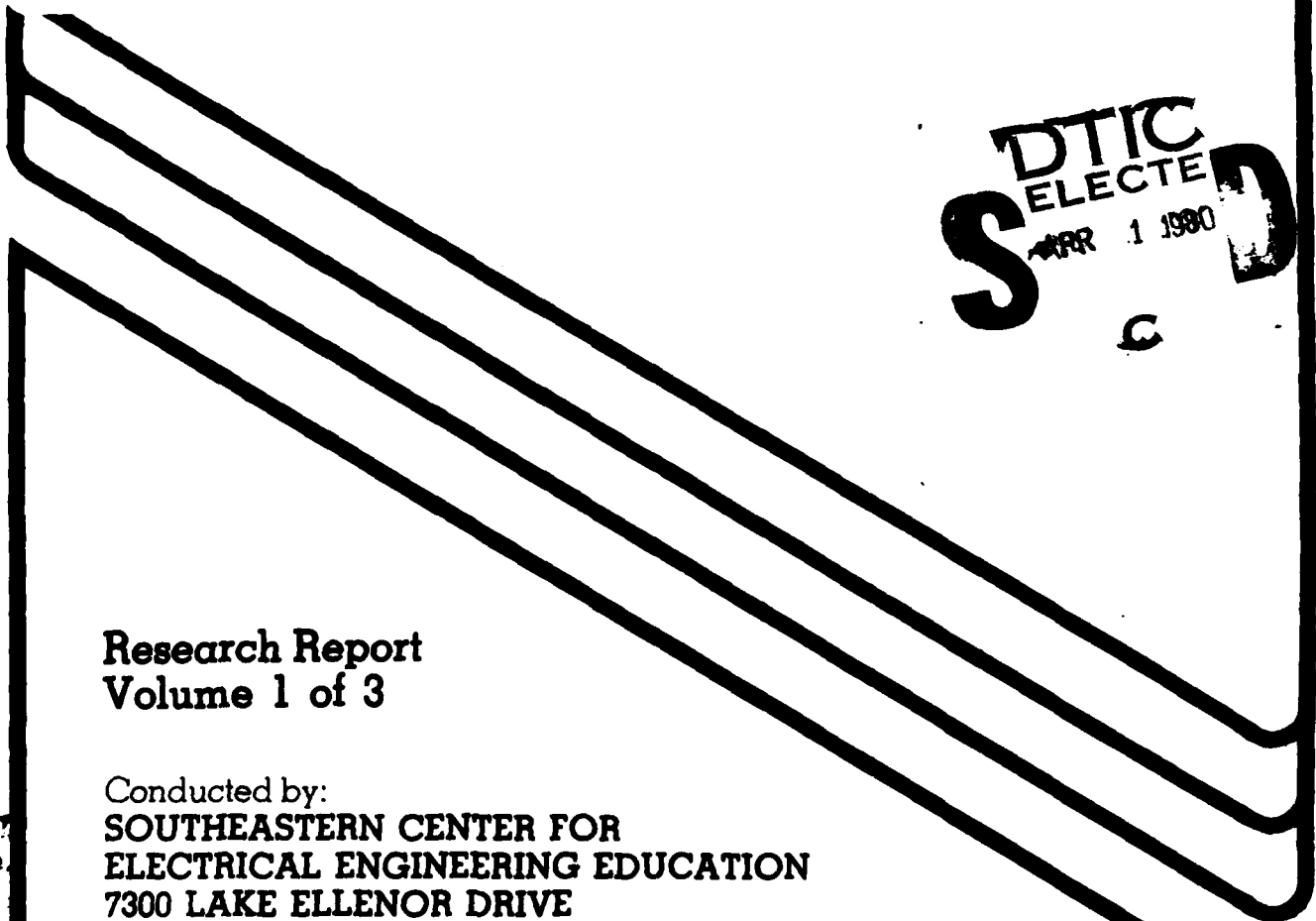
9

AL A 082402

~~LEVEL II~~

1979 USAF

# SUMMER FACULTY RESEARCH PROGRAM



DTIC  
ELECTE  
APR 1 1980  
S  
C

Research Report  
Volume 1 of 3

Conducted by:  
SOUTHEASTERN CENTER FOR  
ELECTRICAL ENGINEERING EDUCATION  
7300 LAKE ELLENOR DRIVE  
ORLANDO, FLORIDA  
DECEMBER, 1979

Approved for public release;  
distribution unlimited.

80 3 20 050

UNCLASSIFIED

SECURITY CLASSIFICATION OF THIS PAGE (When Data Entered)

REPORT DOCUMENTATION PAGE		READ INSTRUCTIONS BEFORE COMPLETING FORM
1. REPORT NUMBER <b>AFOSR-TR- 80 - 02 47</b> ✓	2. GOVT ACCESSION NO.	3. RECIPIENT'S CATALOG NUMBER
4. TITLE (and Subtitle) 1979 USAF Summer Faculty Research Program Volume 1 of 3		5. TYPE OF REPORT & PERIOD COVERED Final
7. AUTHOR(s) Richard N. Miller		6. PERFORMING ORG. REPORT NUMBER
9. PERFORMING ORGANIZATION NAME AND ADDRESS ✓ Southeastern Center for Electrical Engineering Education 7300 Lake Ellenor Drive Orlando, Florida 32809		8. CONTRACT OR GRANT NUMBER(s) ✓ F49620-79-C-0038
11. CONTROLLING OFFICE NAME AND ADDRESS Air Force Office of Scientific Research/XOP Bldg. 410 Bolling Air Force Base, DC 20332		10. PROGRAM ELEMENT, PROJECT, TASK AREA & WORK UNIT NUMBERS 61102F 2305/D5
14. MONITORING AGENCY NAME & ADDRESS (if different from Controlling Office)		12. REPORT DATE December 1979
		13. NUMBER OF PAGES 690
		15. SECURITY CLASS. (of this report) UNCLASSIFIED
		15a. DECLASSIFICATION/DOWNGRADING SCHEDULE
16. DISTRIBUTION STATEMENT (of this Report) Approved for public release; distribution unlimited.		
17. DISTRIBUTION STATEMENT (of the abstract entered in Block 20, if different from Report)		
18. SUPPLEMENTARY NOTES		
19. KEY WORDS (Continue on reverse side if necessary and identify by block number)  Summer Faculty Research Program		
20. ABSTRACT (Continue on reverse side if necessary and identify by block number) This Volume 1 of 3 volumes presents the final research reports of the 1979 Summer Faculty Research Program participants. The program designed to stimulate scientific and engineering interaction between university faculty members and technical personnel at the Air Force laboratories, centers, and divisions has four specific objectives: (1) To develop the basis for continuing research of interest to the Air Force at the faculty member's institution. (2) To further the research objectives of the Air Force. →		

DD FORM 1473

1 JAN 73

EDITION OF 1 NOV 65 IS OBSOLETE

UNCLASSIFIED

UNCLASSIFIED

SECURITY CLASSIFICATION OF THIS PAGE(When Data Entered)

- (3) To stimulate continuing relations among faculty members and their peers in the Air Force.
- (4) To enhance the research interests and capabilities of scientific and engineering educators. ←

UNCLASSIFIED

9

6 ~~SECRET~~ USAF/SCEEE SUMMER FACULTY RESEARCH PROGRAM Volume I.

Conducted by (1979).

The Southeastern Center

for

Electrical Engineering Education, Inc. under

USAF Contract Number F49620-79-C-0038 (15)

DTIC ELECTED APR 1 1980 S D C

PARTICIPANTS' RESEARCH REPORTS

Volume I of III

Submitted to (9) Final rpt.

Air Force Office of Scientific Research

Bolling Air Force Base Washington, D.C.

(16) 2395 (17) 25

by

(10) Richard N. Miller SFRP Director Southeastern Center for Electrical Engineering Education

(18) AFOSP (19)

TR-EP-025

(11) Sep 1979 Dec

(12) 7LQ

AIR FORCE OFFICE OF SCIENTIFIC RESEARCH (AFOSR) NOTICE This report is approved for distribution under AFOSR-12 (7b). A. D. [Name] Technical Information Officer

Approved for public release; distribution unlimited.

## P R E F A C E

The United States Air Force Summer Faculty Research Program (USAF-SFRP) is a program designed to introduce university/college faculty members to Air Force research. This is accomplished by the faculty members being selected on a competitive basis for a ten-week assignment during the summer intercession to perform research in Air Force laboratories/centers. Each assignment is in a subject area and at an Air Force facility mutually agreed upon by the faculty member and the Air Force. The assigned faculty member is compensated for his time and reimbursed for his travel. The USAF-SFRP is sponsored by the Air Force Office of Scientific Research/Air Force Systems Command, United States Air Force, and is conducted by the Southeastern Center for Electrical Engineering Education, Inc.

The specific objectives of the 1979 USAF-SFRP are:

- (1) To develop the basis for continuing research of interest to the Air Force at the faculty member's institution.
- (2) To further the research objectives of the Air Force.
- (3) To stimulate continuing relations among faculty members and their professional peers in the Air Force.
- (4) To enhance the research interests and capabilities of scientific and engineering educators.

In the 1979 USAF-SFRP seventy appointments were made to faculty members from across the US. These professors were assigned to twenty-three USAF laboratories/centers ranging in location from California to Massachusetts. This three-volume document is a compilation of the final reports written by the assigned faculty members about their summer research efforts.

1979 USAF/SCEEE SUMMER FACULTY RESEARCH PROGRAM

LIST OF PARTICIPANTS

NAME/ADDRESS

DEGREE, SPECIALTY, & LABORATORY  
ASSIGNMENT

Dr. Yelagalawadi V. Acharya  
Professor, Mechanical Engineering Dept.  
West Virginia Tech  
Montgomery, WV 25136  
(304) 442-3289 [REDACTED]

Degree: D. Sc., Aeronautics, 1954  
Specialty: Fluid Mechanics, Aero-  
dynamics  
Assigned: AFFDL (Wright-Patterson)  
[REDACTED]

Dr. Adel A. Aly  
Associate Professor  
Dept. of Industrial Engineering  
University of Oklahoma  
202 W. Boyd, Suite 124  
Norman, OK 73019  
(405) 325-3721 [REDACTED]

Degree: PhD., Industrial Eng., 1975  
Specialty: Applied OR, Math Prog.,  
Facility design and location theory  
and routing and distribution systems  
Assigned: AFRADC (Griffiss)  
[REDACTED]

Dr. Clarence A. Bell  
Associate Professor  
Dept. of Mechanical Engineering  
Texas Tech University  
Lubbock, TX 79409  
(806) 742-3563 [REDACTED]

Degree: PhD., Mechanical Eng., 1971  
Specialty: Vibrations, Dynamics,  
Applied Mathematics  
Assigned: AFWL (Kirtland)  
[REDACTED]

Dr. Warren W. Bowden  
Professor of Chemical Engineering  
Rose-Hulman Institute of Technology  
5500 Wabash Avenue  
Terre Haute, IN 47803  
(812) 877-1511 [REDACTED]

Degree: PhD., Chemical Eng., 1965  
Specialty: Physical properties, Phase  
equilibrium, Computer utilization  
Assigned: AFAEDC (Arnold)  
[REDACTED]

Mr. Barry D. Bullard  
Instructor  
Dept. of Engineering Technology  
University of Central Florida  
P.O. Box 25000  
Orlando, FL 32816  
(305) 275-2710/2268 [REDACTED]

Degree: MS, Electrical Eng., 1977  
Specialty: Electronic Communications-  
Antennas and Microwave  
Assigned: SAMTEC (Patrick)  
[REDACTED]

Dr. James A Cadzow  
Professor, Dept. of Electrical Engineering  
Virginia Polytechnic Institute  
Blacksburg, VA 24061  
(703) 961-5694 [REDACTED]

Degree: PhD., Electrical Eng., 1964  
Specialty: Communications, Controls  
& Digital Signal Processing  
Assigned: AFRADC (Griffiss)  
[REDACTED]

Dr. Malcolm D. Calhoun  
Assistant Professor  
Dept. of Electrical Engineering  
Mississippi State University  
Drawer EE  
Mississippi State, MS 39762  
(601) 325-3912/3073 [REDACTED]

Degree: PhD., Electrical Eng., 1976  
Specialty: Electronics, Communications  
Assigned: AFAL (Wright-Patterson)  
[REDACTED]

1979 PARTICIPANTS

Page Two

NAME/ADDRESS

DEGREE, SPECIALTY, & LABORATORY  
ASSIGNMENT

Dr. William R. Carper  
Professor, Dept. of Chemistry  
Wichita State University  
Wichita, KS 67208  
(316) 689-3120 [REDACTED]

Degree: PhD., Physical Chemistry, 1963  
Specialty: Kinetics, Molecular Spectroscopy  
Assigned: AFFJSRL (USAF Academy)  
[REDACTED]

Dr. Chi Hau Chen  
Professor and Chairman  
Electrical Engineering Dept.  
Southeastern Massachusetts University  
N. Dartmouth, MA 02747  
(617) 999-8475 [REDACTED]

Degree: PhD., Electrical Eng., 1965  
Specialty: Signal Processing, Pattern Recognition and Communications  
Assigned: AFGL (Hanscom)  
[REDACTED]

Dr. Donald C. Chiang  
Professor  
Division of Civil and Mechanical Engineering  
Rose-Hulman Institute of Technology  
5500 Wabash Avenue  
Terre Haute, IN 47803  
(812) 877-1511, EXT. 323 [REDACTED]

Degree: PhD., Fluid Mechanics, 1965  
Specialty: Fluid Mechanics, Thermodynamics, Heat Transfer, Analog Computer  
Assigned: AFFDL (Wright-Patterson)  
[REDACTED]

Dr. Aaron S. Collins  
Assistant Professor  
Electrical Engineering Dept.  
Tennessee Technological University  
Box 5004-TTU  
Cookeville, TN 39501  
(615) 528-3352 [REDACTED]

Degree: PhD., Electrical Eng., 1973  
Specialty: Classical and Modern Control Theory, Computers, Simulation, Numerical Methods  
Assigned: AFAL (Wright-Patterson)  
[REDACTED]

Dr. William A. Davis  
Assistant Professor  
Electrical Engineering Dept.  
Virginia Polytechnic Institute  
and State University  
Blacksburg, VA 24061  
(703) 961-6307 [REDACTED]

Degree: PhD., Electrical Eng., 1974  
Specialty: Electromagnetics  
Assigned: AFWL (Kirtland)  
[REDACTED]

Dr. Alan S. Edelstein  
Associate Professor, Dept. of Physics  
University of Illinois at Chicago Circle  
P.O. Box 4348  
Chicago, IL 60680  
(312) 996-5348/3400 [REDACTED]

Degree: PhD., Physics, 1963  
Specialty: Solid State Physics, Magnetism, Superconductivity  
Assigned: AFML (Wright-Patterson)  
[REDACTED]

Mr. Willard R. Fey  
Associate Professor  
Dept. of Industrial and Systems Engineering  
Georgia Institute of Technology  
Atlanta, GA 30332  
(404) 894-2359 [REDACTED]

Degree: MS, Electrical Eng., 1961  
Specialty: System Dynamics  
Assigned: AFESC (Tyndall)  
[REDACTED]

1979 PARTICIPANTS

Page Three

NAME/ADDRESS

Dr. John T. Foley  
Assistant Professor of Physics Dept.  
Mississippi State University  
Mississippi State, MS 39762  
(601) 325-2806 [REDACTED]

Dr. Garabet J. Gabriel  
Associate Professor  
Dept. of Electrical Engineering  
Notre Dame University  
Notre Dame, IN 46556  
(219) 283-7531 [REDACTED]

Dr. James A. Gessaman  
Associate Professor of Biology Dept.  
Utah State University  
UMC 53  
Logan, UT 84332  
(801) 752-4100, EXT. 7876 [REDACTED]

Dr. Paul K. Grogger  
Assistant Professor  
Dept. of Geography and Environmental Studies  
University of Colorado  
Colorado Springs, CO 80907  
(303) 598-3737, EXT. 273/217 [REDACTED]

Dr. William D. Gunther  
Professor of Economics  
University of Alabama  
P.O. Box 650  
University, AL 35486  
(205) 348-7842 [REDACTED]

Dr. John Hadjilogiou  
Associate Professor  
Electrical Engineering Dept.  
Florida Institute of Technology  
P.O. Box 1150  
Melbourne, FL 32901  
(305) 723-3701, EXT. 217 [REDACTED]

Dr. Keith M. Hagenbuch  
Assistant Professor of Physics  
Behrend College of  
Pennsylvania State University  
Station Road  
Erie, PA 16563  
(814) 898-1511 [REDACTED]

DEGREE, SPECIALTY, & LABORATORY  
ASSIGNMENT

Degree: PhD., Physics, 1977  
Specialty: Optics  
Assigned: AFWL (Kirtland)

Degree: PhD., Electrical Eng., 1964  
Specialty: Electromagnetics  
Assigned: AFAPL (Wright-Patterson)

Degree: PhD., Zoology, 1968  
Specialty: Thermoregulation, Ecological  
Energetics  
Assigned: USAFSAM (Brooks)

Degree: PhD., Geology  
Specialty: Utilization of conservation  
and solar energy, Investigation of  
land use planning by remote sensing  
Assigned: AFESC (Tyndall)

Degree: PhD., Economics, 1969  
Specialty: Regional Economics  
Assigned: AFESC (Tyndall)

Degree: PhD., Electrical Eng., 1970  
Specialty: Digital Systems  
Assigned: AFHRL/FTE (Williams)

Degree: PhD., Physics, 1967  
Specialty: Electricity and Magnetism  
Assigned: AFFDL (Wright-Patterson)

Accession For  
NTIS  
DOC TAB  
Unannounced  
Justification  
BY  
Dis. Information  
Availability  
1st  
A

1979 PARTICIPANTS

Page Four

NAME/ADDRESS

Dr. Donald F. Hanson  
Assistant Professor  
Electrical Engineering Dept.  
University of Mississippi  
University, MS 38677  
(601) 232-7231 [REDACTED]

Dr. Charles Hays  
Associate Professor  
Dept. of Manufacturing Technology  
University of Houston  
Houston, TX 77004  
(713) 749-4652 [REDACTED]

Dr. Michael J. Henschman  
Associate Professor of Chemistry Dept.  
Brandeis University  
Waltham, MA 02154  
(617) 647-2821 [REDACTED]

Dr. Manuel A. Huerta  
Associate Professor of Physics Dept.  
University of Miami  
Coral Gables, FL 33124  
(305) 284-2323 [REDACTED]

Dr. Frank M. Ingels  
Professor  
Electrical Engineering Dept.  
Mississippi State University  
Drawer EE  
Mississippi State, MS 39762  
(601) 325-3912/6067 [REDACTED]

Dr. Prasad K. Kadaba  
Professor  
Electrical Engineering Dept.  
University of Kentucky  
Lexington, KY 40506  
(606) 258-2966/257-1856 [REDACTED]

Dr. Madhoo Kanal  
Professor  
Dept. of Physics  
Clark University  
Worcester, MA 01610  
(617) 793-7366 [REDACTED]

DEGREE, SPECIALTY, & LABORATORY  
ASSIGNMENT

Degree: PhD., Electrical Eng., 1976  
Specialty: Numerical Solution of  
Electromagnetics Problems  
Assigned: AFWL (Kirtland)  
[REDACTED]

Degree: PhD., Metallurgical Eng., 1973  
Specialty: Metallurgy, Metallography,  
Alloying, Materials requirements  
Assigned: AFML (Wright-Patterson)  
[REDACTED]

Degree: PhD., Chemistry, 1961  
Specialty: Physical Chemistry,  
Reaction Kinetics  
Assigned: AFGL (Hanscom)  
[REDACTED]

Degree: PhD., Physics, 1970  
Specialty: Plasma Physics, MHD, Fluid  
Mechanics, Electromagnetic Wave  
Propagation and Doppler Radar, Acoustics,  
Tomography  
Assigned: AFATL (Eglin)  
[REDACTED]

Degree: PhD., Electrical Eng., 1967  
Specialty: Communications, Error  
Correcting Codes, Signal Tracking  
Electronics  
Assigned: AFATL (Eglin)  
[REDACTED]

Degree: PhD., Physics, 1950  
Specialty: Microwave Absorption &  
Dielectric Relaxation of various  
materials, Microwave Measurements,  
Magnetic Resonance, Application of  
new techniques to evaluate toxic  
effluents.  
Assigned: AFML (Wright-Patterson)  
[REDACTED]

Degree: PhD., Physics, 1969  
Specialty: Transport Theory  
Assigned: AFGL (Hanscom)  
[REDACTED]

1979 PARTICIPANTS

Page Five

NAME/ADDRESS

Dr. William D. Kane, Jr.  
Assistant Professor  
Dept. of Management and Marketing  
Western Carolina University  
Cullowhee, NC 28723  
(704) 227-7401, EXT. 26 [REDACTED]

Dr. Allen E. Kelly  
Associate Professor of Civil Engineering  
Oklahoma State University  
Stillwater, OK 74074  
(405) 624-5206 [REDACTED]

Dr. Robert V. Kenyon  
Post Doctoral Fellow  
Dept. of Optometry  
University of California  
Berkeley, CA 94705  
(415) 642-7196 [REDACTED]

Dr. Keith Koenig  
Assistant Professor  
Dept. of Aerospace Engineering  
Mississippi State University  
Drawer A  
Mississippi State, MS 39762  
(601) 325-3623 [REDACTED]

Dr. John R. Lakey  
Assistant Professor  
Psychology Dept.  
University of Evansville  
Evansville, IN 47702  
(812) 479-2531 [REDACTED]

Dr. Gordon K. Lee  
Assistant Professor  
Dept. of Electrical Engineering  
Colorado State University  
Ft. Collins, CO 80523  
(303) 491-5767 [REDACTED]

Dr. Jack C. Lee  
Associate Professor  
Mathematics Dept.  
Wright State University  
Dayton, OH 45435  
(513) 873-2433 [REDACTED]

DEGREE, SPECIALTY, & LABORATORY  
ASSIGNMENT

Degree: PhD., Organizational Behavior,  
1977  
Specialty: Behavioral Science as it  
applies to Management of Organizations  
Assigned: AFHRL/ASR (Wright-Patterson)  
[REDACTED]

Degree: PhD., Civil Eng., 1970  
Specialty: Structural Eng. &  
Mechanics  
Assigned: AFATL (Eglin)  
[REDACTED]

Degree: PhD., Physiological Optics, 1971  
Specialty: Visual Science, Eye  
Movement Control Systems, Information  
Processing for Motor Control  
Assigned: AFHRL/FTE (Williams)  
[REDACTED]

Degree: PhD., Aeronautics, 1978  
Specialty: Bluff Body Separated Flows,  
Laser Doppler Velocimetry  
Assigned: AFFJSRL (USAF Academy)  
[REDACTED]

Degree: PhD., Physiological Psychology,  
1973  
Specialty: Sensory Processors  
Assigned: USAFSAM (Brooks)  
[REDACTED]

Degree: PhD., Electrical Eng., 1978  
Specialty: Multivariable Control  
Systems  
Assigned: AFATL (Eglin)  
[REDACTED]

Degree: PhD., Statistics, 1972  
Specialty: Multivariate Analysis and  
Application of Statistics to different  
Disciplines  
Assigned: AFAMRL (Wright-Patterson)  
[REDACTED]

1979 PARTICIPANTS

Page Six

NAME/ADDRESS

DEGREE, SPECIALTY, & LABORATORY  
ASSIGNMENT

Dr. Robert D. Lyng  
Assistant Professor  
Dept. of Biological Sciences  
Indiana University - Purdue University  
2101 Coliseum Blvd. E.  
Ft. Wayne, IN 46805  
(219) 482-5798/5271 [REDACTED]

Degree: PhD., Zoology, 1969  
Specialty: Development Biology  
Assigned: AFANRL (Wright-Patterson)  
[REDACTED]

Dr. Arlyn J. Melcher  
Professor of Administrative Sciences  
Kent State University  
Kent, OH 44242  
(216) 672-2750 [REDACTED]

Degree: PhD., Industrial Relations,  
1964

Specialty: Organizational Analysis  
Assigned: AFBRC (Wright-Patterson)  
[REDACTED]

Dr. Bonita H. Melcher  
Assistant Professor of Management  
University of Akron  
Akron, OH 44325  
(216) 375-7037 [REDACTED]

Degree: DBA, Organization Theory &  
Administration, 1975  
Specialty: Organization Design  
Assigned: AFBRC (Wright-Patterson)  
[REDACTED]

Dr. Andrew U. Meyer  
Professor of Electrical Engineering  
New Jersey Institute of Technology  
323 High Street  
Newark, NY 07102  
(201) 645-5468/5472 [REDACTED]

Degree: PhD., Electrical Eng., 1961  
Specialty: Automatic Control Systems,  
Application of System Analysis to  
Biomedical Engineering  
Assigned: AFANRL (Wright-Patterson)  
[REDACTED]

Dr. Jerrel R. Mitchell  
Associate Professor of Electrical Engineering  
Mississippi State University  
P.O. Drawer EE  
Mississippi State, MS 39762  
(601) 325-3912/6064 [REDACTED]

Degree: PhD., Electrical Eng., 1972  
Specialty: Control Systems  
Assigned: AFWL (Kirtland)  
[REDACTED]

Dr. William T. Morris  
Professor  
Dept. of Industrial and Systems Engineering  
Ohio State University  
1971 Neil Avenue  
Columbus, OH 43210  
(614) 422-2178 [REDACTED]

Degree: PhD., Industrial Eng., 1956  
Specialty: Industrial Engineering,  
Engineering Economics, Productivity  
Improvement  
Assigned: AFBRC (Wright-Patterson)  
[REDACTED]

Dr. Stephen E. Mudrick  
Assistant Professor  
Dept. of Atmospheric Science  
University of Missouri-Columbia  
701 Hitt Street  
Columbia, MO 65211  
(314) 882-6591 [REDACTED]

Degree: PhD., Meteorology, 1973  
Specialty: Dynamic Meteorology,  
Numerical Modeling of Atmosphere  
Assigned: AFGL (Hanscom)  
[REDACTED]

1979 PARTICIPANTS

Page Seven

NAME/ADDRESS

Dr. William C. Mundy  
Associate Professor of Physics  
Pacific Union College  
Angwin, CA 94508  
(707) 965-7269 [REDACTED]

Dr. Maurice C. Neveu  
Associate Professor  
Dept. of Chemistry  
State University of New York  
Fredonia, NY 14063  
(716) 673-3285 [REDACTED]

Dr. Charles E. Nuckolls  
Associate Professor  
Mechanical Engineering and Aerospace Science  
University of Central Florida  
P.O. Box 25000  
Orlando, FL 32816  
(305) 275-2242 [REDACTED]

Dr. Nicholas G. Odrey  
Assistant Professor  
Industrial Engineering Dept.  
University of Rhode Island  
103 Gilbreth Hall  
Kingston, RI 02881  
(401) 792-2455 [REDACTED]

Dr. William J. Ohley  
Assistant Professor  
Dept. of Electrical Engineering  
University of Rhode Island  
Kingston, RI 02881  
(401) 792-2505 [REDACTED]

Dr. John V. Oldfield  
Professor  
Dept. of Electrical and Computer Engineering  
113 Link Hall  
Syracuse, NY 13210  
(315) 423-4443 [REDACTED]

Dr. John M. Owens  
Associate Professor  
Electrical Engineering Dept.  
University of Texas  
Arlington, TX 76019  
(817) 273-2671 [REDACTED]

DEGREE, SPECIALTY, & LABORATORY  
ASSIGNMENT

Degree: Ph.D., Physics, 1972  
Specialty: Raman Spectroscopy &  
Mie Scattering  
Assigned: AFRPL (Edwards)  
[REDACTED]

Degree: Ph.D., Physical-Organic  
Chemistry, 1959  
Specialty: Physical-Organic Chemistry,  
Kinetics, Catalysis, Reaction Mechanisms  
Enzyme Chemistry  
Assigned: AFATL (Eglin)  
[REDACTED]

Degree: Ph.D., Mechanical Eng., 1970  
Specialty: Engineering Mechanics  
Assigned: AFAEDC (Arnold)  
[REDACTED]

Degree: Ph.D., Industrial Eng., 1978  
Specialty: Manufacturing Engineering  
Assigned: AFML (Wright-Patterson)  
[REDACTED]

Degree: Ph.D., Electrical Eng., 1976  
Specialty: Biomedical Engineering  
Assigned: AFHRL/ASR (Wright-Patterson)  
[REDACTED]

Degree: Ph.D., Electrical Eng., 1958  
Specialty: Computer-aided Electronic  
Design, Graphical Display  
Assigned: AFRADC (Griffiss)  
[REDACTED]

Degree: Ph.D., Electrical Eng., 1968  
Specialty: Electrical Engineering  
Assigned: AFRADC/ET (Hanscom)  
[REDACTED]

1979 PARTICIPANTS

Page Eight

NAME/ADDRESS

DEGREE, SPECIALTY, & LABORATORY  
ASSIGNMENT

Dr. Michael J. Pappas  
Associate Professor of Mechanical Engineering  
New Jersey Institute of Technology  
323 High Street  
Newark, NJ 07102  
(201) 645-5367 [REDACTED]

Degree: PhD., Mechanical Eng., 1970  
Specialty: Structural Optimization  
Assigned: AFFDL (Wright-Patterson)  
[REDACTED]

Dr. Steven E. Poltrock  
Assistant Professor  
Dept. of Psychology  
University of Denver  
2030 S. York  
Denver, CO 80210  
(303) 753-2478 [REDACTED]

Degree: PhD., Psychology, 1976  
Specialty: Cognitive Psychology  
Assigned: AFHRL/TTY (Lowry)  
[REDACTED]

Dr. Douglas Preis  
Assistant Professor of Electrical Engineering  
Tufts University  
Medford, MA 02115  
(617) 628-5000, EXT. 287 [REDACTED]

Degree: PhD., Electrical Eng., 1969  
Specialty: Electromagnetics, Signal  
Processing, Acoustics  
Assigned: ESD (Hanscom)  
[REDACTED]

Dr. Rangaiya A. Rao  
Associate Professor  
Dept. of Electrical Engineering  
San Jose State University  
S. 7th Street  
San Jose, CA 95192  
(408) 277-2459 [REDACTED]

Degree: PhD., Electrical Eng., 1966  
Specialty: Semiconductor device  
Physics and Technology, Solar  
Cells, Semiconductor Crystal Growth,  
III-V Compound Semiconductors,  
Photodetectors, Microwave Devices,  
Characterization of Semiconductors  
Assigned: AFAL (Wright-Patterson)  
[REDACTED]

Dr. Stephen M. Rappaport  
Assistant Professor  
Dept. of Biomedical and Environmental  
Health Sciences  
University of California  
Berkeley, CA 94720

Degree: PhD., Environmental Science  
and Eng., 1974  
Specialty: Industrial Hygiene  
Assigned: USAFSAM (Brooks)  
[REDACTED]

Dr. Jane A. Rysberg  
Assistant Professor of Psychology  
Ohio State University  
1680 University Drive  
Mansfield, OH 44906  
(419) 755-4277 [REDACTED]

Degree: PhD., Educational Psychology,  
1977  
Specialty: Educational Psychology,  
Cognitive Development  
Assigned: AFHRL/PE (Brooks)  
[REDACTED]

Dr. Michael C. Smith  
Assistant Professor  
Dept. of Industrial Engineering  
Oregon State University  
Corvallis, OR 97331  
(503) 754-2365 [REDACTED]

Degree: PhD., Industrial Eng., 1977  
Specialty: Operations Analysis,  
Analysis of Capital Investment, Health  
Systems Design  
Assigned: AFLC (Wright-Patterson)  
[REDACTED]

1979 PARTICIPANTS  
Page Nine

NAME/ADDRESS

DEGREE, SPECIALTY, & LABORATORY  
ASSIGNMENT

Dr. Walther D. Stanaland  
Assistant Professor  
Dept. of Systems Science  
University of Western Florida  
Pensacola, FL 32504  
(904) 476-9500, EXT. 495 [REDACTED]

Degree: PhD., Electrical Eng., 1979  
Specialty: Electrical Properties of  
Dielectric Materials  
Assigned: AFATL (Eglin)  
[REDACTED]

Dr. Edwin F. Strother  
Associate Professor  
Dept. of Physics/Space Science  
Florida Institute of Technology  
Melbourne, FL 32901  
(305) 723-3701, EXT. 326/240 [REDACTED]

Degree: PhD., Physics, 1971  
Specialty: Experimental Physics  
Assigned: AFGL (Hanscom)  
[REDACTED]

Dr. Edgar C. Tacker  
Professor  
Dept. of Electrical Engineering  
University of Houston  
Houston, TX 77004  
(713) 749-4416 [REDACTED]

Degree: PhD., Electrical Eng., 1964  
Specialty: Systems (Decision  
Processes, Estimation, Control, and  
Modeling)  
Assigned: AFFJSRL (USAF Academy)  
[REDACTED]

Dr. Richard H. Tipping  
Associate Professor  
Physics Dept.  
University of Nebraska  
Omaha, NB 68182  
(402) 554-2510 [REDACTED]

Degree: PhD., Physics, 1969  
Specialty: Molecular Spectroscopy  
Assigned: AFGL (Hanscom)  
[REDACTED]

Dr. Pramod K. Varshney  
Assistant Professor  
Electrical and Computer Engineering  
Syracuse University  
Link Hall  
Syracuse, NY 13210  
(315) 423-4432 [REDACTED]

Degree: PhD., Electrical Eng., 1976  
Specialty: Communications and  
Computers  
Assigned: AFRADC (Griffiss)  
[REDACTED]

Dr. Ghasi R. Verma  
Associate Professor  
Dept. of Mathematics  
University of Rhode Island  
Kingston, RI 02881  
(401) 792-2889 [REDACTED]

Degree: PhD., Mathematics, 1957  
Specialty: Mathematics  
Assigned: AFFDL (Wright-Patterson)  
[REDACTED]

Dr. Ta-hsien Wei  
Assistant Professor  
Electrical Engineering Dept.  
North Carolina A & T State University  
Greensboro, NC 27411  
(919) 379-7760 [REDACTED]

Degree: PhD., Physics, 1964  
Specialty: Systems Engineering  
Assigned: AFAPL (Wright-Patterson)  
[REDACTED]

1979 PARTICIPANTS

Page Ten

NAME/ADDRESS

Dr. Herschel Weil  
Professor  
Electrical and Computer Engineering  
University of Michigan  
4517 East Engineering  
Ann Arbor, MI 48109  
(313)764-4329

Dr. Bronel R. Whelchel  
Associate Professor of Electronic  
Data Processing  
Tennessee State University  
Nashville, TN 37203  
(615) 320-3i54

Dr. Charles R. Willis  
Professor of Physics  
Boston University  
111 Cummington Street  
Boston, MA 02215  
(617) 353-2600

Dr. Dennis E. Wilson  
Assistant Professor  
Dept. of Engineering  
University of South Carolina  
Columbia, SC 29208  
(803) 777-7118/4185

Dr. Gerald A. Woelfl  
Assistant Professor  
Dept. of Civil Engineering  
Marquette University  
1515 W. Wisconsin Avenue  
Milwaukee, WI 53233  
(414) 224-7384

Dr. John C. Wolfe  
Assistant Professor  
Dept. of Electrical Engineering  
University of Houston  
4800 Calhoun  
Houston, TX 77004  
(713) 749-2506

Dr. Richard G. Yalman  
Professor of Chemistry  
Antiock University  
Yellow Springs Campus  
Yellow Springs, OH 45387  
(513) 767-7331

DEGREE, SPECIALTY, & LABORATORY  
ASSIGNMENT

Degree: PhD., Applied Math, 1948  
Specialty: Electromagnetic Theory  
and Applications  
Assigned: AFAPL (Wright-Patterson)

Degree: PhD., Education & Business  
Administration  
Specialty: Systems Analysis and  
Design, Electronic Data Processing  
Assigned: AFHRL/PE (Brooks)

Degree: PhD., Physics, 1957  
Specialty: Theoretical Physics,  
Quantum Optics, Statistical  
Mechanics  
Assigned: AFRADC/ET (Hanscom)

Degree: PhD., Mechanical Eng., 1976  
Specialty: Viscous Flow, Analytical  
and Approximate Methods  
Assigned: AFAEDC (Arnold)

Degree: PhD., Civil Eng., 1971  
Specialty: Highway and Construction  
Materials  
Assigned: AFESC (Tyndall)

Degree: PhD., Physics, 1974  
Specialty: Electrical Engineering  
Materials  
Assigned: AFAL (Wright-Patterson)

Degree: PhD., Organic Chemistry, 1949  
Specialty: Coordination Chemistry,  
Organic Chemistry  
Assigned: AFAL (Wright-Patterson)

PARTICIPANT LABORATORY ASSIGNMENT

1979 USAF/SCEEE SUMMER FACULTY RESEARCH PROGRAM

AFAEDC AIR FORCE ARNOLD ENGINEERING DEVELOPMENT CENTER  
(Arnold Air Force Station)  
1. Dr. Warren Bowden - Rose-Hulman Institute of Technology  
2. Dr. Charles Nuckolls - University of Central Florida  
3. Dr. Dennis Wilson - University of South Carolina

AFHRL/PE AIR FORCE HUMAN RESOURCES LABORATORY  
(Brooks Air Force Base)  
1. Dr. Jane Rysberg - Ohio State University  
2. Dr. Bronel Whelchel - Tennessee State University

USAFSAM UNITED STATES AIR FORCE SCHOOL OF AEROSPACE MEDICINE  
(Brooks Air Force Base)  
1. Dr. James Gessaman - Utah State University  
2. Dr. John Lakey - University of Evansville  
3. Dr. Stephen Rappaport - University of California

AFRPL AIR FORCE ROCKET PROPULSION LABORATORY  
(Edwards Air Force Base)  
1. Dr. Bill Mundy - Pacific Union College

AFATL AIR FORCE ARMAMENT DEVELOPMENT AND TEST CENTER  
(Eglin Air Force Base)  
1. Dr. Manuel Huerta - University of Miami  
2. Dr. Frank Ingels - Mississippi State University  
3. Dr. Allen Kelly - Oklahoma State University  
4. Dr. Gordon Lee - Colorado State University  
5. Dr. Maurice Neveu - State University College of Fredonia/NY  
6. Dr. Walter Stanaland - University of Western Florida

AFRADC AIR FORCE ROME AIR DEVELOPMENT CENTER  
(Griffiss Air Force Base)  
1. Dr. Adel Aly - University of Oklahoma  
2. Dr. James Cadzow - Virginia Polytechnic Institute/State Univ.  
3. Dr. John Oldfield - Syracuse University  
4. Dr. Pramod Varshney - Syracuse University

AFGL AIR FORCE GEOPHYSICS LABORATORY  
(Hanscom Air Force Base)  
1. Dr. Chi Hau Chen - Southeastern Massachusetts University  
2. Dr. Michael Henschman - Brandeis University  
3. Dr. Madhoo Kanal - Clark University  
4. Dr. Steven Mudrick - University of Missouri/Columbia  
5. Dr. Edwin Strother - Florida Institute of Technology  
6. Dr. Richard Tipping - University of Nebraska/Omaha

AFRADC/ET AIR FORCE ROME AIR DEVELOPMENT CENTER  
(Hanscom Air Force Base)  
1. Dr. John Owens - University of Texas  
2. Dr. Charles Willis - Boston University

**PARTICIPANT LABORATORY ASSIGNMENT (Continued)**

**ESD**                   **ELECTRONICS SYSTEMS DIVISION**  
(Hanscom Air Force Base)  
1. Dr. Douglas Preis - Tufts University

**AFWL**                   **AIR FORCE WEAPONS LABORATORY**  
(Kirtland Air Force Base)  
1. Dr. Clarence Bell - Texas Tech University  
2. Dr. William Davis - Virginia Polytechnic Institute/State Univ.  
3. Dr. John Foley - Mississippi State University  
4. Dr. Donald Hanson - University of Mississippi  
5. Dr. Jerrel Mitchell - Mississippi State University

**AFHRL/TTY**           **AIR FORCE HUMAN RESOURCES LABORATORY**  
(Lowry Air Force Base)  
1. Dr. Steven Poltrock - University of Denver

**SAMTEC/TOEI**       **SPACE AND MISSILE TEST CENTER**  
(Patrick Air Force Base)  
1. Mr. Barry Bullard - University of Central Florida

**AFESC**               **AIR FORCE ENGINEERING TECHNOLOGY OFFICE**  
(Tyndall Air Force Base)  
1. Mr. Willard Fey - Georgia Institute of Technology  
2. Dr. Paul Grogger - University of Colorado/Colorado Springs  
3. Dr. William Gunther - University of Alabama  
4. Dr. Gerald Woelfl - Marquette University

**AFFJSRL**           **AIR FORCE FRANK J. SEILER RESEARCH LABORATORY**  
(United States Air Force Academy)  
1. Dr. William Carper - Wichita State University  
2. Dr. Keith Koenig - Mississippi State University  
3. Dr. Edgar Tacker - University of Houston

**AFHRL/FTE**       **AIR FORCE HUMAN RESOURCES LABORATORY**  
(Williams Air Force Base)  
1. Dr. John Hadjiligiou - Florida Institute of Technology  
2. Dr. Robert Kenyon - University of California

**AFAL**               **AIR FORCE AVIONICS LABORATORY**  
(Wright-Patterson Air Force Base)  
1. Dr. Malcolm Calhoun - Mississippi State University  
2. Dr. Aaron Collins - Tennessee State University  
3. Dr. Rangaiya Rao - San Jose State University  
4. Dr. John Wolfe - University of Houston  
5. Dr. Richard Yalman - Antioch University

**AFAMRL**           **AIR FORCE AEROSPACE MEDICAL RESEARCH LABORATORY**  
(Wright-Patterson Air Force Base)  
1. Dr. Jack Lee - Wright State University  
2. Dr. Robert Lyng - Indiana Univ. - Purdue Univ./Ft. Wayne  
3. Dr. Andrew Meyer - New Jersey Institute of Technology

PARTICIPANT LABORATORY ASSIGNMENT (Continued)

AFAPL AIR FORCE AEROPROPULSION LABORATORY  
(Wright-Patterson Air Force Base)  
1. Dr. Garabet Gabriel - Notre Dame University  
2. Dr. Ta-hsien Wei - North Carolina A&T State University  
3. Dr. Herschel Weil - University of Michigan

AFBRMC AIR FORCE BUSINESS RESEARCH MANAGEMENT CENTER  
(Wright-Patterson Air Force Base)  
1. Dr. Arlyn Melcher - Kent State University  
2. Dr. Bonita Melcher - University of Akron  
3. Dr. William Morris - Ohio State University

AFFDL AIR FORCE FLIGHT DYNAMICS LABORATORY  
(Wright-Patterson Air Force Base)  
1. Dr. Yelagalawadi Acharya - West Virginia Tech  
2. Dr. Donald Chiang - Rose-Hulman Institute of Technology  
3. Dr. Keith Hagenbuch - Pennsylvania State Univ./Behrend College  
4. Dr. Michael Pappas - New Jersey Institute of Technology  
5. Dr. Ghasi Verma - University of Rhode Island

AFHRL/ASR AIR FORCE HUMAN RESOURCES LABORATORY  
(Wright-Patterson Air Force Base)  
1. Dr. William Kane, Jr. - University of Western Carolina  
2. Dr. William Ohley - University of Rhode Island

AFLC AIR FORCE LOGISTICS COMMAND  
(Wright-Patterson Air Force Base)  
1. Dr. Michael Smith - Oregon State University

AFML AIR FORCE MATERIALS LABORATORY  
(Wright-Patterson Air Force Base)  
1. Dr. Alan Edelstein - University of Illinois/Chicago Circle  
2. Dr. Charles Hays - University of Houston  
3. Dr. Prasad Kadaba - University of Kentucky  
4. Dr. Nicholas Odrey - University of Rhode Island

RESEARCH REPORTS

1979 USAF-SCEEE SUMMER FACULTY RESEARCH PROGRAM

VOLUME I  
Report No.

Title

Research Associates

<u>Report No.</u>	<u>Title</u>	<u>Research Associates</u>
1	Thermodynamic and Aerodynamic Analysis of of High Speed Ejectors	Dr. Yelagalawadi Acharya
2	Optimum Design of Built-in-Test Diagnostic System	Dr. Adel A. Aly
3	Effects of Nuclear Blast Double Shock on Airborne Aircraft	Dr. Clarence A. Bell
4	Icing Testing with Models-Similitude Considerations	Dr. Warren W. Bowden
5	Shipboard Antenna Placement Optimization- (SAPO)	Mr. Barry D. Bullard
6	ARMA Spectral Estimation: An Efficient Closed Form Procedure	Dr. James A. Cadzow
7	A Study of Two Avionics Multiplex Simulation Models: SNS and MUXSIM	Dr. Malcolm D. Calhoun
8	Laser Candidate and Energetic Material Studies	Dr. William R. Carper
9	A Non-Linear Maximum Entropy Method for Spectral Estimation	Dr. Chi-Hau Chen
10	Computer Codes Applicable to the Determi- nation of Ejection Seat/Man Aerodynamic Parameters	Dr. Donald C. Chiang
11	Petri Net-Related Models for Avionics Systems	Dr. Aaron S. Collins
12	Bounding Signal Levels at Wire Terminations Behind Apertures	Dr. William A. Davis
13	Photoconductivity of Extrinsic Silicon	Dr. Alan S. Edelstein
14	System Analysis of the Environmental Tech- nical Information System (ETIS)	Mr. Willard Fey
15	The Uniqueness of Phase Retrieval From Intensity Measurements	Dr. John T. Foley
16	High Speed Electromagnetic Transients on Superconducting Coils	Dr. Garabet J. Gabriel

RESEARCH REPORTS (Continued)

<u>Report No.</u>	<u>Title</u>	<u>Research Associates</u>
17	Part I: Effects of Dehydration and Heat on Acceleration Response in Man Part II: Relationships Between Total Body Sweating Rate and Localized Sweating Rate	Dr. James A. Gessaman
18	The Utilization of Geothermal Resources at United States Air Force Bases	Dr. Paul K. Grogger
19	A Critical Evaluation of the USAF Methodology for Assessing the Socioeconomic Impact of Proposed Base Realignment	Dr. William D. Gunther
20	Analysis of the Advanced Simulator for Pilot Training (ASPT): Computer System Architecture	Dr. John Hadjilgiou
21	Optimized Holography of Microscopic Particles	Dr. Keith M. Hagenbuch
<u>VOLUME II</u>		
22	Electromagnetic Diffraction by a Narrow Slit in an Impedance Sheet--E--Polarization	Dr. Donald F. Hanson
23	Part I: Technology Assessment on the Critical and Strategic Status of Tantalum Metal Part II: Technology Assessment Concerning the Current Status of Alloy and Coating Development Programs for Refractory Metal Systems Containing Cb, Mo, Ta, and W	Dr. Charles Hays
24	Gas Phase Reactions of Some Hydrated Ions	Dr. Michael J. Henchman
25	Detonation Physics of Nonideal Explosives with Analytical Results for Detonation Failure Diameter	Dr. Manuel A. Huerta
26	Cepstrum Analysis Techniques for Possible Applications to Seismic/Acoustic Ranging	Dr. Franklin M. Ingels
27	A NMR Study of Absorbed Water in the Anodized Oxide Layer and Paper Spacer of Electrolytic Capacitors	Dr. Prasad K. Kadaba
28	On Remote Sensing of the Atmospheric Temperature: An Analysis of the Discrepancy Between the Measured and Calculated Values of the Radiance	Dr. Madhoo Kanai
29	A Heuristic Model of Air Force Maintenance Performance	Dr. William Kane, Jr.

RESEARCH REPORTS (Continued)

<u>Report No.</u>	<u>Title</u>	<u>Research Associates</u>
30	An Evaluation of a Method for Assessing Aircraft Structural Damage from Multiple Fragment Impact	Dr. Allen E. Kelly
31	Groundwork for Oculomotor Research in Simulators	Dr. Robert V. Kenyon
32	Redesign of a Laser Doppler Velocimeter System for Unsteady, Separated Flow Studies	Dr. Keith Koenig
33	Electromyographic Correlates of Flight-Crew Performance	Dr. John R. Lakey
34	Investigation of Time-to-Go Algorithms for Air-to-Air Missiles	Dr. Gordon K. F. Lee
35	Some Statistical Analysis Issues for System Simulation Research	Dr. Jack C. Lee
36	Effects of Hydrazine on Pregnant ICR Mice	Dr. Robert D. Lyng
37	Organizational Analysis of an Acquisition Organization	Dr. Arlyn J. Melcher
38	Organizational Analysis of An Acquisition Organization	Dr. Bonita S. Melcher
39	Dynamics of Two-Dimensional Eye-Head Tracking	Dr. Andrew U. Meyer
40	Optimization of the Feed Forward Technique for Beam Control in the APT	Dr. Jerrel R. Mitchell
41	Predicting the Impacts of USAF Personnel Cuts	Dr. William T. Morris
42	Attempts to Simulate "Realistic" Atmospheric Motion with a Simple Numerical Model	Dr. Stephen Mudrick
<u>VOLUME III</u>		
43	Plume Properties Measurement Research in a Solid Rocket Motor Exhaust	Dr. Bill Mundy
44	A Search for New Fuel Components in Non-Ideal Explosives Mixtures	Dr. Maurice C. Neveu
45	Vibration Diagnostics for Turbofan Engines	Dr. Charles E. Nuckolls
46	Goal Programming: Functional Decomposition and Consideration Within an Integrated Computer-Aided Manufacturing Decision Support System (IDSS)	Dr. Nicholas G. Odrey

RESEARCH REPORTS (Continued)

<u>Report No.</u>	<u>Title</u>	<u>Research Associates</u>
47	A Computer Model of Saccadic Suppression	Dr. William J. Ohley
48	Special-Purpose Processors for the Image-Processing Requirements of Automatic Feature Extraction Systems	Dr. John V. Oldfield
49	Magnetostatic Wave Decay and Filter Devices	Dr. John M. Owens
50	Improved Methods for Large Scale Structural Synthesis	Dr. Michael Pappas
51	Educational Implications of Cognitive Research on Imagery	Dr. Steven E. Poltrock
52	Adaptive Signal Processing for Array Antennas	Dr. Douglas Preis
53	Deep Levels in $\text{Al}_x\text{Ga}_{1-x}\text{As}$	Dr. Rangaiya A. Rao
54	Development of Air-Sampling and Analytical Method for Diisocyanates	Dr. Stephen M. Rappaport
55	Civilian Appraisal System	Dr. Jane A. Rysberg
56	A Study of Opportunistic Maintenance Policies for the F100PW100 Aircraft Engine	Dr. Michael C. Smith
57	Error Analysis for a Radio-Frequency Systems Simulation Facility	Dr. Walter D. Stanaland
58	A High Altitude Tethered Aerostat System Study	Dr. Edwin F. Strother
59	Pattern Recognition/Image Processing in Optical Tracking	Dr. Edgar C. Tacker
60	Atmospheric Absorption of Radiation by $\text{H}_2\text{O}$ and $\text{CO}_2$	Dr. Richard H. Tipping
61	Study and Evaluation of SIIDS and ADPT Systems	Dr. Pramod K. Varshney
62	Stability Analysis of the Lower Branch Solutions of the Falkner-Skan Equations	Dr. Ghasi R. Verma
63	Inductance Matrix of a Permanent Magnet Alternator	Dr. Ta-hsien Wei
64	Analysis for Coherent Anti-Stokes Raman Spectroscopy (CARS)	Dr. Herschel Weil

RESEARCH REPORTS (Continued)

<u>Report No.</u>	<u>Title</u>	<u>Research Associates</u>
65	An Investigation of One and Three Parameter Item Response Models with Implications for Computerized Adaptive Testing	Dr. Bronel R. Whelchel
66	Modulated Spontaneous Raman Effect for Laser All-Optical Frequency Standards	Dr. Charles R. Willis
67	Unsteady Laminar Boundary Layers Due to Transverse Cylinder & Free Stream Oscillations	Dr. Dennis E. Wilson
68	Response of Airfield Pavement to Large Magnitude Dynamic Loads	Dr. Gerald A. Woelfl
69	Analysis of the Role of High Brightness Electron Guns in Lithography	Dr. John C. Wolfe
70	Impurities in Communications Grade GaAs	Dr. Richard G. Yalman

UNITED STATES AIR FORCE

SUMMER FACULTY RESEARCH PROGRAM

PARTICIPANTS' RESEARCH REPORTS

**1979 USAF - SCEE Summer Faculty Research Program**

**Sponsored by the**

**Air Force Office of Scientific Research**

**Conducted by the**

**Southeastern Center for Electrical Engineering Education**

**FINAL REPORT**

---

**HIGH SPEED EJECTORS**

**Prepared By:** Y.V.G. Acharya

**Academic Rank:** Professor

**Department and University:** Mechanical Engineering  
West Virginia Institute of Technology

**Research Location:** Aerodynamics Branch  
Air Force Flight Dynamics Laboratory  
WPAFB, Dayton, OH

**USAF Research Colleague:** K. S. Nagaraja

**Date:** August 20, 1979

**Contract No.:** F49620-79-C-0038

ABSTRACT

Thermodynamic and Aerodynamic Analysis

of

High Speed Ejectors

by

Y.V.G. Acharya

Ejectors have been used for quite a long time for pumping fluids. While the approximate performance of ejectors is well known due to a variety of tests from which engineering designs have evolved, there is yet quite a lot of unknown areas in the analytical design of ejectors. An early attempt by the author<sup>(1)</sup> gave some insight into the incompressible ejector. The bibliography of work done during the intervening period is quite long<sup>(2)</sup>

Recently the problem has been further investigated<sup>(4-6)</sup> and the present study is a reevaluation of the efficiency and the thrust augmentation of high speed ejectors. A brief introduction is given; after which the problem for one dimensional flow including turbulence and friction is stated and the general equations derived.

These equations are solved by lumping together the effect of the turbulence and friction by a friction factor. These solutions can be considered as only a first approximation.

Actually one has to take into account the effects of compressibility on the turbulence factors as well as the effect of structure of the flow for supersonic jets and its interaction with the boundary layer. These are left for a later investigation.

### ACKNOWLEDGMENTS

The author would like to thank the Air Force Systems Command, the Air Force Office of Scientific Research, the Wright Patterson Air Force Base and the Southeastern Center for Electrical Engineering Education for the opportunity to do meaningful research work during the summer of 1979. Thanks are due to Dr. R.N. Miller for the careful planning of the program.

Thanks are due to Dr. T.M. Weeks, Technical Manager of the External Aerodynamics Branch at the Air Force Flight Dynamics Laboratory for the help he gave in providing a good environment for work. Special thanks are due to Captain J. DeJongh for helping me in developing the computer program and getting the computed results, and to Ms. Doris Appel for typing the report. Finally thanks are due to Dr. K.S. Nagaraja for sponsoring my visit and providing the large amount of recent references in the area of this investigation.

## I. INTRODUCTION

Ejectors have been the subject of investigations over the past 75 years and thousands of reports have been written<sup>(2)</sup>. Ejectors have been used for pumping applications, increase of lift over airfoils and augmentation of thrust.

Recently much attention has been focussed on the increase of lift by the use of ejectors for VTOL/STOL aircraft. The author recently analyzed the effect of ejectors under transonic conditions for helicopter rotors, which are called Controlled Circulation Rotors (CCR), with some success<sup>(3)</sup>.

Over the past 15 to 20 years fundamental analytical and experimental studies were done on ejectors at the Aerospace Research Laboratories of the Wright Patterson Air Force Base<sup>(4)</sup>. But it remains a fact that the actual performance of the ejector is less than that expected. So it is proposed to investigate the ejector flows both experimentally and analytically more systematically and thoroughly.

As part of this effort the recent work of Nagaraja et al<sup>(5)</sup>, Alperin<sup>(6)</sup> and Porter<sup>(2)</sup> are examples. An experimental program has been initiated at the WPAFB and the mixing problem is being contracted out to some well known investigators in the universities.

The present investigation is a part of this overall effort.

## II. OBJECTIVES

The primary objective is the formulation of the ejector flow equations for (A.1) one dimensional,

(A.2) two dimensional,

and (A.3) axi-symmetric flows;

including the effects of

(B.1) compressibility

(B.2) turbulence

(B.3) friction

and (B.4) shockwave and boundary layer interaction;

for (C.1) Low speed

(C.2) Subsonic

(C.3) Transonic

and (C.4) Supersonic ranges,  
with (D.1) constant area  
or (D.2) constant pressure  
mixing of primary and secondary flows occurring  
either (E.1) subsonically  
or (E.2) supersonically

In addition the analytical model should include the geometric features of the secondary channel or tube - and that of the diffuser.

This is a formidable problem. Once the analytical formulation is done, the objective is to develop a comprehensive computer program for all the variables (A, B, C, D, E) as inputs.

But since we had only ten weeks for this effort, it was decided to narrow the objective to consider only the performance of an ejector with one dimensional flow (A.1), which is compressible (B.1) either subsonic or supersonic: (C.2) or (C.4). The primary and secondary streams mix at constant pressure (D.2) and either subsonically or supersonically: (E.1 or (E.2).

The influence of compressibility on turbulence is neglected in this effort. Later investigations can be done taking it into account, as has been done previously by the author<sup>(7)</sup>. But at present the effect of turbulence and friction is taken into account by means of a pseudo coefficient of friction.

### III. EJECTOR MODEL

Fig. 1 gives the basic configuration. The stagnation conditions for the primary stream are  $P_{op}$ ,  $T_{op}$ , and for the secondary stream the stagnation condition are  $P_{oo}$ ,  $T_{oo}$ . Section (1) is the plane at which the primary and secondary streams are unmixed. It is assumed that the pressure is constant in this plane. The efficiency of the primary nozzle and the secondary inlet are taken as unity. There is no difficulty in introducing those efficiencies for a practical case.

Section (2) is the plane where complete mixing has taken place. Again we take the flow characteristics are constant over this plane. Actually we have to consider the mixing process, in which case the velocity profile is known <sup>(1)</sup>. But we have not introduced this variation in this investigation.

Section (3) is the plane at the diffuser exit, where the pressure is constant, namely,  $P_\infty$ .

#### IV. FUNDAMENTAL EQUATIONS

We shall assume that the flow through the ejector is steady state steady flow, then from thermodynamics, if  $h$  is the enthalpy at any point and  $h_0$  is the stagnation enthalpy:

$$h_0 = h + \frac{u^2}{2} \quad (1)$$

where  $u$  is the local velocity. If we assume that the fluid is a perfect gas we further have

$$c_p T_0 = c_p T + \frac{u^2}{2} \quad (2)$$

with the velocity of sound defined as

$$c = \left(\frac{\partial p}{\partial \rho}\right)_s = \gamma R T$$

$$(2) \text{ becomes } T_0 = T \left(1 + \frac{\gamma-1}{2} M^2\right) \quad (3)$$

In the mixing region, we shall assume that there will be turbulence such that

$$\begin{aligned} u &= \bar{u} + u' \\ p &= \bar{p} + p' \end{aligned} \quad (4)$$

#### V. PRIMARY JET

$T_{or}$  = stagnation temperature at the reservoir (e.g. gas generator)

$T_{op}$  = stagnation temperature at the nozzle exit.

$u_{p\infty}$  = velocity at the nozzle exit where the back pressure is  $p_\infty$

$u_{p1}$  = velocity at nozzle exit when the back pressure is  $p_1$ .

Using equation (2)

$$u_{p0} = \sqrt{[2C_p(T_{op} - T_{\infty})]} \quad (5)$$

$$u'_{p0} = \sqrt{[2C_p(T_{or} - T_{\infty})]} \quad (6)$$

$$\eta_N = u_{p0} / u'_{p0} \quad (7)$$

We need not consider (6) unless  $\eta_N$  is desired.

Now we can use the flow in the nozzle as isentropic and consider only  $T_{op}$  in which case, we have

$$\frac{P_{op}}{P_{\infty}} = \left(\frac{T_{op}}{T_{\infty}}\right)^{\frac{\gamma}{\gamma-1}} \quad (8)$$

if we define  $(\gamma-1)/\gamma = n$

$$\frac{T_{op}}{T_{\infty}} = \left(\frac{P_{op}}{P_{\infty}}\right)^n \quad (9)$$

An isentropic nozzle with the stagnation temperature  $T_{or}$ , will have the relation

$$T_{or}/T_{\infty} = (P_{or}/P_{\infty})^n$$

If we consider the nozzle to be isenergetic i.e.  $T_{op} = T_{or}$ , we have from (7)

$$\eta_N = \sqrt{\left[ \frac{1 - \left(\frac{P_{\infty}}{P_{op}}\right)^n}{1 - \left(\frac{P_{\infty}}{P_{or}}\right)^n} \right]}$$

or 
$$P_{\infty}/P_{op} = \left\{ 1 - \eta_N^2 \left[ 1 - \left(\frac{P_{\infty}}{P_{or}}\right)^n \right] \right\}^{\frac{1}{n}} \quad (10)$$

## VI. GAS GENERATOR

Either the gas generator or the compressor increases the pressure of the incoming gas. Its temperature is increased by the burner in the latter case, whereas in the former case, it is increased due to the gas generation process.

Now we consider that  $u_{\infty}$  is the velocity of the air entering the compressor at  $T_{\infty}$  such that

$$\begin{aligned} h_{0\infty} &= h_{\infty} + \frac{u_{\infty}^2}{2} \\ h_{0r} &= h_{0\infty} + q \end{aligned} \quad (11)$$

where  $q$  is the effective amount of heat added during the process. Now using (2) we have

$$\frac{T_{02}}{T_{01}} = 1 + \frac{\gamma-1}{2} K_0^2 \quad (12)$$

### VII. REFERENCE THRUST

The thrust of the nozzle, when the back pressure is atmospheric is due to the primary jet only. If  $\dot{m}_p$  is the primary mass flow, then

$$T_{Ref.} = \dot{m}_p (u_{p0} - u_{\infty}) \quad (13)$$

where the mass flow

$$\dot{m}_p = A_p \rho_{p0} u_{p0}$$

where  $A_p$  = cross section at nozzle exit.

### VIII. SECONDARY STREAM

There is a loss of pressure in the inlet such that

$$P_{0i} - P_{01} = \Delta p_i = \frac{1}{2} \rho_i u_i^2 C_{di} \quad (14)$$

where  $C_{di}$  is the drag or the loss coefficient and  $P_{01}$  is the stagnation pressure at section (1) and  $P_{0i}$  is that at the inlet;

leading to

$$\frac{P_{0i}}{P_{01}} = 1 - \frac{C_{di}}{\gamma} \left( \frac{\rho_i}{\rho_{01}} \right) \left[ \left( \frac{P_{0i}}{P_{01}} \right)^{\frac{\gamma}{\gamma-1}} - 1 \right]. \quad (15)$$

If  $C_{di} = 0$ ,  $P_{0i} = P_{01}$ .

Again by disregarding the inlet loss, we have from (3)

$$\begin{aligned} T_{0i} &= T_i \left( 1 + \frac{\gamma-1}{2} K_i^2 \right) \\ P_{0i} &= P_i \left( 1 + \frac{\gamma-1}{2} K_i^2 \right)^{\frac{\gamma}{\gamma-1}} \end{aligned} \quad (16)$$

### IX. ENTRAINMENT

The amount of secondary flow induced by the primary flow is the entrainment ( $r$ )

$$r = \dot{m}_c / \dot{m}_p = (A_i u_i \rho_i) / (A_p u_{p0} \rho_{p0}) \quad (17)$$

where

$$u_{p0} = \sqrt{2 c_d (T_{0p} - T_{p0})} \quad (18)$$

If the mixing channel has a constant area of  $A_2$ , from section (1) to (2).

$$A_2 = A_1 + A_p$$

and defining  $\alpha = A_2/A_p$ ;  $\lambda_1 = u_1/u_{b1}$

we have

$$\lambda = \frac{\rho_1}{\rho_{b1}} (\alpha - 1) \lambda_1 \quad (19)$$

#### X. ENTROPY AT SECTION 1

The change in entropy for any perfect gas flow is:

$$\Delta s = c_v \ln \frac{p_2/p_1}{(\rho_2/\rho_1)^\gamma} \quad (20)$$

The change of entropy for the primary stream is:

$$s_{p1} - s_{p0} = c_v \ln \left[ (p_{b1}/p_{b0}) / (\rho_{b1}/\rho_{b0})^\gamma \right] \quad (21)$$

The change of entropy for the secondary stream is:

$$s_1 - s_0 = c_v \ln \left[ (p_1/p_0) / (\rho_1/\rho_0)^\gamma \right] \quad (22)$$

#### XI. FLOW CHARACTERISTICS AT SECTION 2

At this section mixing has already taken place and if we use the similarity of profiles we can write an equation for the velocity profile from the considerations of mixing<sup>(1)</sup>. We will return to that in a later investigation. At present, we will assume that

$$\begin{aligned} \rho_2(y) &= \bar{\rho}_2 + \rho_2'(y) \\ u_2(y) &= \bar{u}_2 + u_2'(y) \end{aligned} \quad (23)$$

Hence, except for turbulence, we will consider that the mean quantities are constant in the section.

Since the flow is isenergetic, we have

$$T_{0p} \dot{m}_p + T_{0c} \dot{m}_c = \bar{T}_{02} (\dot{m}_p + \dot{m}_c)$$

or

$$\bar{T}_{02} = (T_{0p} + \lambda T_{0c}) / (1 + \lambda) \quad (24)$$

Considering the momentum integral equation between section (1) and (2), we have:

$$\dot{m}_p u_{b1} + \dot{m}_c u_1 + p_{b1} A_p + p_1 A_1 = p_2 A_2 + \int_{A_2} \rho u^2 dA + F \quad (25)$$

where F is the frictional component.

Noting that  $p_{b_1} = p_1$ ,  $A_0 = A_1 + A_F$

$$\frac{(p_0 - p_1) A_0}{\dot{m}_p u_{p_1}} = 1 + \lambda \lambda_1 - \frac{\int \rho_0 u_0^2 dA}{\dot{m}_p u_{p_1}} - \frac{F}{\dot{m}_p u_{p_1}} \quad (26)$$

now

$$\int \rho_0 u_0^2 dA = \int (\bar{\rho}_0 + \rho'_0) (\bar{u}_0 + u'_0)^2 dA = \bar{\rho}_0 \bar{u}_0^2 A_0 \left( 1 + 2 \frac{\bar{\rho}'_0 \bar{u}'_0}{\bar{\rho}_0 \bar{u}_0} + \frac{\bar{u}'_0^2}{\bar{u}_0^2} \right)$$

$$\dot{m}_p + \dot{m}_c = \int \rho_0 (\bar{\rho}_0 + \rho'_0) (\bar{u}_0 + u'_0) dA = \bar{\rho}_0 \bar{u}_0 A_0 \left( 1 + \frac{\bar{\rho}'_0 \bar{u}'_0}{\bar{\rho}_0 \bar{u}_0} \right)$$

$$\therefore \bar{\rho}_0 \bar{u}_0 A_0 = \dot{m}_p (1 + \lambda) \left( 1 - \frac{\bar{\rho}'_0 \bar{u}'_0}{\bar{\rho}_0 \bar{u}_0} \right)$$

hence equation (26) becomes:

$$\frac{(p_0 - p_1) A_0}{\dot{m}_p u_{p_1}} = 1 + \lambda \lambda_1 - \dot{m}_p (1 + \lambda) \left( 1 - \frac{\bar{\rho}'_0 \bar{u}'_0}{\bar{\rho}_0 \bar{u}_0} \right) \cdot \frac{u_2}{\dot{m}_p u_{p_1}} \left( 1 + 2 \frac{\bar{\rho}'_0 \bar{u}'_0}{\bar{\rho}_0 \bar{u}_0} + \frac{\bar{u}'_0^2}{\bar{u}_0^2} \right) - \frac{F}{\dot{m}_p u_{p_1}}$$

that is

$$\frac{(p_0 - p_1) A_0}{\rho_{b_1} u_{p_1}^2} = 1 + \lambda \lambda_1 - (1 + \lambda) \beta_2 \left( 1 + \frac{\bar{\rho}'_0 \bar{u}'_0}{\bar{\rho}_0 \bar{u}_0} + \frac{\bar{u}'_0^2}{\bar{u}_0^2} + \frac{1}{2} C_F \right) \quad (27)^*$$

where

$$C_F = F / \left( \frac{1}{2} \bar{\rho}_0 \bar{u}_0^2 A_0 \right)$$

Now let us consider the energy equation for the section (2):

$$\dot{m}_c \bar{T}_{0_2} = \dot{m}_c T_2 + \frac{\dot{m}_c u_2^2}{2} = \frac{\dot{m}_c}{\gamma - 1} \frac{p_2}{\rho_2} + \frac{\dot{m}_c u_2^2}{2} \quad (28)$$

integrating and noting:  $\dot{m}_p + \dot{m}_c = \rho_0 u_0 A_0$

$$\frac{\dot{m}_c}{\gamma - 1} \rho_0 \bar{u}_0 A_0 + \frac{1}{2} \int \rho_0 (\bar{\rho}_0 + \rho'_0) (\bar{u}_0 + u'_0)^2 dA = \dot{m}_c \bar{T}_{0_2} (\dot{m}_p + \dot{m}_c) \quad (29)$$

the h and performing integration

$$\frac{1}{2} \int \rho_0 (\bar{\rho}_0 + \rho'_0) (\bar{u}_0 + u'_0)^2 dA = \frac{1}{2} \bar{\rho}_0 \bar{u}_0^2 A_0 \left( 1 + 3 \frac{\bar{u}'_0^2}{\bar{u}_0^2} + 3 \frac{\bar{\rho}'_0 \bar{u}'_0}{\bar{\rho}_0 \bar{u}_0} \right)$$

$$\dot{m}_p + \dot{m}_c = \bar{\rho}_0 \bar{u}_0 A_0 \left( 1 + \frac{\bar{\rho}'_0 \bar{u}'_0}{\bar{\rho}_0 \bar{u}_0} \right)$$

\* Equation (27) when compared with equation (13) of Nagaraja et al (5) gives the skewness factor

$$\beta_2 = 1 + \frac{\bar{\rho}'_0 \bar{u}'_0}{\bar{\rho}_0 \bar{u}_0} + \frac{\bar{u}'_0^2}{\bar{u}_0^2}$$

$$\text{and } \chi = \frac{1}{2} C_F$$

In their computation they have assumed  $\beta_2 \approx 1$  and  $0.02 \leq \chi \leq 0.06$

Following the same heuristic reasoning, we compute for empirical values of a pseudo coefficient of friction (CF)

Defining  $J = \frac{2c_p \bar{T}_{02}}{u_{b1}^2}$  after some algebra

$$\frac{b_2 \alpha}{\rho_{b1} u_{b1}^2} = \frac{\eta J}{2} \frac{(1+\lambda)}{\lambda_2} \left[ 1 - \frac{\lambda_2^2}{\gamma} \left( 1 + 3 \frac{\bar{u}_2^2}{u_2^2} + 2 \frac{\bar{u}_2' u_2'}{\bar{u}_2 u_2} \right) \right] \quad (30)$$

So finally we get another value for

$$\frac{(p_2 - p_1) \alpha}{\rho_{b1} u_{b1}^2} = \frac{\eta J}{2} \frac{(1+\lambda)}{\lambda_2} \left[ 1 - \frac{\lambda_2^2}{\gamma} \left( 1 + 3 \frac{\bar{u}_2^2}{u_2^2} + 2 \frac{\bar{u}_2' u_2'}{\bar{u}_2 u_2} \right) \right] - \frac{\eta \alpha}{2(\gamma_{02}/\gamma_{01} - 1)} \quad (31)$$

We can now equate the values of  $(p_2 - p_1)$  as given by equations (27) and (31), and get an equation for  $\lambda_2$ , which we write as

$$K \lambda_2^2 - L \lambda_2 + M = 0 \quad (32)$$

where

$$K = \frac{\gamma+1}{2\gamma} + \frac{3-\gamma}{2\gamma} \cdot \frac{\bar{u}_2^2}{u_2^2} + \frac{1}{\gamma} \frac{\bar{u}_2' u_2'}{\bar{u}_2 u_2} + \frac{1}{2} CF$$

$$L = \left[ 1 + \lambda \lambda_1 + \frac{\eta \alpha}{2(\gamma_{02}/\gamma_{01} - 1)} \right] / (1+\lambda) \quad (32a)$$

$$M = \eta J / 2$$

where

$$\lambda_2 = [L \pm \sqrt{L^2 - 4KN}] / (2K) \quad (32b)$$

We will see in the computation that the negative sign gives  $M_2 < 1$ , and the positive sign gives  $M_2 > 1$ . Hence there are two solutions to the given problem, where the mixing is subsonic and another where the mixing is supersonic. This can also be proved analytically.

Computed values of  $M_2$  are shown for a particular case in Fig. 2.3. In the computations we have taken  $K = (2-\gamma)/2 + CF$ , with  $0.02 \leq CF \leq 0.08$ .

## XII. ENTROPY AT SECTION 2

Considering equations (21) and (22) the total change of entropy between section (2) and (1) is

$$S_2 - S_1 = m_1 c_p \ln \frac{h_2/h_1}{(\bar{p}_2/\rho_{b1})^\gamma} + m_2 c_p \ln \frac{h_2/h_1}{(\bar{p}_2/\rho_{b1})^\gamma} \quad (33)$$

if we disregard turbulence. Even if we consider  $S_1 = S_{01}$ , for a natural process, according to the second law of thermodynamics, the change of entropy should be greater than or equal to zero.

We can write

$$S_2 - S_1 = (1+\lambda) \frac{w_p c_p}{\rho_1} \ln \frac{b_2/b_1}{(\bar{\rho}_2/\rho_1)^{\gamma}} + w_p c_p \ln \left( \frac{\rho_1}{\rho_2} \right)^{\gamma} \geq 0 \quad (34)$$

We have assumed constant pressure mixing,  $b_{b_1} = b_1$ . Therefore, in our computation,  $\rho_{p1}$  for the case  $\lambda_{p1} - \lambda_0 = \lambda_1 - \lambda_0 = 0$ , we have  $\rho_{p1} = \rho_1$ . The test that the flow is real is then:

$$b_2/b_1 \geq (\bar{\rho}_2/\rho_1)^{\gamma}$$

### XIII. CHARACTERISTICS AT SECTION (3)

Equation (30) can be written as

$$\frac{p_2}{p_0} = \frac{\bar{T}_{02}}{\bar{T}_0} \cdot \frac{\bar{p}_2}{\rho_0} \left[ 1 + \frac{\bar{\rho}_2 \bar{u}_2^2}{\bar{p}_2 \bar{u}_2} \right] \left[ 1 - \frac{\lambda_2^2}{\gamma} \left( 1 + \frac{\bar{u}_2^2}{\bar{u}_2^2} + 2 \frac{\bar{p}_2 \bar{u}_2^2}{\bar{p}_2 \bar{u}_2} \right) \right] \quad (35)$$

Since the flow is isenergetic and mixed, we have

$$\bar{T}_{02} = \bar{T}_{03}$$

Also at the exit of diffuser

$$b_3 = b_0$$

(36)

Hence writing an analogous equation to (35), we have, using (36):

$$\frac{p_3}{p_0} = 1 = \frac{\bar{T}_{02}}{\bar{T}_0} \cdot \frac{\bar{p}_3}{\rho_0} \left( 1 + \frac{\bar{\rho}_3 \bar{u}_3^2}{\bar{p}_3 \bar{u}_3} \right) \left[ 1 - \frac{\lambda_3^2}{\gamma} \left( 1 + \frac{\bar{u}_3^2}{\bar{u}_3^2} + 2 \frac{\bar{p}_3 \bar{u}_3^2}{\bar{p}_3 \bar{u}_3} \right) \right] \quad (37)$$

In addition, we have the entropy equation:

$$\frac{b_3}{b_0} = \left\{ \frac{\bar{p}_3 \left[ 1 + \frac{1}{2} \left( \frac{\bar{\rho}_3^2}{\bar{p}_3^2} + 2 \frac{\bar{\rho}_3 \bar{u}_3^2}{\bar{p}_3 \bar{u}_3} \right) \right]}{\bar{p}_3 \left[ 1 + \frac{1}{2} \left( \frac{\bar{\rho}_2^2}{\bar{p}_2^2} + 2 \frac{\bar{\rho}_2 \bar{u}_2^2}{\bar{p}_2 \bar{u}_2} \right) \right]} \right\} \exp \left[ \frac{\lambda \gamma}{1+\lambda} \frac{S_2 - S_3}{w_p R} \right] \quad (38)$$

One more equation is the continuity equation

$$\bar{\rho}_2 \bar{u}_2 A_2 \left( 1 + \frac{\bar{\rho}_2 \bar{u}_2^2}{\bar{p}_2 \bar{u}_2} \right) = \bar{\rho}_3 \bar{u}_3 A_3 \left( 1 + \frac{\bar{\rho}_3 \bar{u}_3^2}{\bar{p}_3 \bar{u}_3} \right) \quad (39)$$

For the special case, where we disregard turbulence or when we make an empirical approximation to the correlations, we can compute the values of  $\bar{\rho}_3$ ,  $\lambda_3$ ,  $\bar{T}_3$  and  $M_3$ , provided we take  $S_2 - S_3 = 0$ . We can then determine  $\delta = A_3/A_2$ , as the diffuser area ratio.

#### XIV. THRUST AUGMENTATION

The actual thrust of the ejector is:

$$T_{ej} = (\dot{m}_p + \dot{m}_e) u_j - \dot{m}_p u_\infty - \dot{m}_e u_c \quad (40)$$

The reference thrust is that due to the primary jet only:

$$T_{ref} = \dot{m}_p (u_{p0} - u_\infty) \quad (41)$$

Hence the increase in thrust due to the ejector is:

$$\Phi = T_{ej} / T_{ref}$$

dividing through by  $u_{p1}$

$$\Phi = \frac{(1+\lambda) \lambda_3 - \lambda_\infty - \lambda \lambda_c}{(u_{p0}/u_{p1}) - \lambda_\infty} \quad (42)$$

The above ratio does not give an idea of the actual thrust developed, hence we have derived a coefficient of thrust

$$C_T = T_{ej} / (2 C_p \rho_0 T_\infty A_p) \quad (43)$$

Using  $C_T$  one can determine the variation of the actual thrust for a given area of the primary nozzle and the ambient conditions.

#### XV. EFFICIENCY

The efficiency of an ejector can be stated in different ways, depending on the circumstance.

##### (a) Propulsive Efficiency

Considering the ejector as a propulsive device, we can compare the work output to the mechanical energy input. Thus:

$$\begin{aligned} \eta_{p.e.j} &= \frac{\text{Work done by Thrust}}{\text{Available Mechanical Energy}} \\ &= \frac{T_{ej} \cdot u_\infty}{\frac{1}{2} \dot{m}_p (u_{p0}^2 - u_\infty^2)} \\ &= \frac{2 \Phi \lambda_\infty}{(u_{p0}/u_{p1}) + \lambda_\infty} \end{aligned}$$

$$\eta_{p,ef} = \frac{2\phi \dot{m}_p (u_{p\infty} - u_\infty) u_\infty}{\dot{m}_p (u_{p\infty}^2 - u_\infty^2)}$$

Hence

$$\eta_{p,ef} = (2\phi \lambda_\infty) / [(u_{p\infty}/u_{p1}) + \lambda_\infty] \quad (44)$$

This will be zero for static conditions when  $u_\infty = 0$ . Hence it is necessary in that case to define an efficiency which is meaningful.

(b) Energy Efficiency

If we compare the energy gained by the flow in the ejector to the thermal energy available in the primary flow this will always give us a finite value for the ratio. This ratio can be called energy efficiency. It can also be called the thermal efficiency (not to be confused with the thermodynamic cycle efficiency).

$$\begin{aligned} \eta_{t,ef} &= \frac{\frac{1}{2} (\dot{m}_p + \dot{m}_e) (u_3^2 - u_\infty^2)}{\dot{m}_p (h_{0p} - h_{0\infty})} \\ &= \frac{(1+\lambda) (\lambda_3^2 - \lambda_\infty^2)}{\frac{2c_p \bar{T}_{0\infty}}{u_{p1}^2} (\frac{T_{0p}}{T_{0\infty}} - \frac{T_{0e}}{T_{0\infty}})} \\ \eta_{t,ef} &= \frac{(1+\lambda)}{J} \frac{(\lambda_3^2 - \lambda_\infty^2)}{(T_{0p} - T_{0\infty}) / \bar{T}_{0\infty}} \end{aligned} \quad (45)$$

(c) Overall Efficiency

If we consider the ejector as producing thrust for the aircraft (or any other vehicle), then we can combine the concepts of (a) and (b) and define the ratio of the work output to the enthalpy energy input as an overall efficiency.

$$\begin{aligned} \eta_{o,ef} &= \frac{\text{Work Output}}{\text{Enthalpy input}} = \frac{\phi \dot{m}_p (u_{p\infty} - u_\infty) u_\infty}{\dot{m}_p c_p (T_{0e} - T_{0\infty})} \\ &= \frac{2\phi [(u_{p\infty}/u_{p1}) - \lambda_\infty] \lambda_\infty}{J (T_{0e} - T_{0\infty}) / \bar{T}_{0\infty}} \end{aligned} \quad (46)$$

We note that the overall efficiency defined in this manner vanishes for the static ejector just like the propulsive efficiency.

that is  $\eta_{o,ei} = \eta_{p,ei} (u_{p\infty}^2 - u_{\infty}^2) / (u_{p\infty}'^2 - u_{\infty}^2)$

where  $u_{p\infty}'/u_{p\infty} = \eta_n$ , the velocity coefficient for the nozzle. If we take  $\eta_n = 1$ , there is no difference between the propulsive and overall efficiencies.

#### XVI. NUMERICAL COMPUTATION

Computer programs have been developed to compute all the flow characteristics of the ejector. The input for the program consists of the following:

- ALO =  $\frac{A_2}{A_{\infty}}$  an assigned value (e.g. 20)
- PR =  $\frac{P_{op} - P_{\infty}}{P_{\infty}}$  a variable
- MO =  $M_{\infty}$  Flight Mach number. Variable
- MI =  $M_1$  Mach number at Section 1. Variable
- TA =  $T_i$  Temperature of secondary flow at inlet. Constant
- TO =  $T_{\infty}$  Ambient temperature of fluid. Constant
- G =  $\gamma = C_p/C_v$  for the fluid. Constant
- CF = an empirical value for the coefficient of friction and turbulence (see eq. 32a)

The output of the program consists of a tabulation of  $PR_1 = p_1/p_{\infty}$ ;  $TR_1 = T_1/T_{\infty}$ ;  $AR = A_2/A_p$ ;  $PR_2 = p_2/p_{\infty}$ ;  $MP_1 = M_{p_1}$ , Mach number of flow at nozzle exit;  $TR_2 = T_2/T_{\infty}$ ;  $TR_3 = T_3/T_{\infty}$ ;  $M_2 = M_2$ , Mach number of flow at section 2, entrance to diffuser;  $DEL = A_3/A_2$ , ratio of exit to entrance areas of diffuser;  $M_3 = M_3$ , Mach number of flow at the exit of diffuser,  $PHI = \phi$ , Thrust augmentation factor,  $LI = \lambda_1 = u_1/u_{p_1}$ ;  $R = \lambda$  Entrainment; CT = pseudo thrust coefficient defined by e.g. 43;

All these characteristics are tabulated for values of  $M_1$  varying from 0.1 to 2.0 for subsonic mixing (Root I) and supersonic mixing (Root II).

The input for each case: ALO, PR, MO, TA, TO, G, and CF are listed.

At present the input data used are:

ALO = 20, 10

PR = 0.1, 0.2, 0.4, 0.6, 0.8, 1, 2, 5, 10.

MO = 0, 0.1, 0.2, 0.3, 0.4, 0.5, 0.6, 0.7, 0.8.

TA = 520

TO = 520

G = 1.4

and CF = 0, .02, .03, .04, .05, .06, .07, .08, .09

But they can be easily changed to cover a wider range of values or a particular value as desired.

Basically this program has been written to enable calculations involving  $\eta_n = 0$  and  $C_{di} = 0$ . i.e. friction-less flow in the nozzle and the secondary inlet. This enables us to assume constant entropy in this section.

We have also assumed that the entropy is a constant in the diffuser section of the ejector.

Hence only approximate results are available. The appended figures show the various characteristics.

## XVII. CONCLUSION

The scope of this study is restricted, as explained before. Even then, we can derive some general conclusions:

- (1) Mixing can be either subsonic or supersonic (Fig. 2.3)
- (2) For a static ejector ( $M_\infty=0$ ) (Figs. 2-6, 9)
  - (a) Thrust augmentation decreases with increase in pressure ratio;
  - (b) Thrust coefficients increase with increase in pressure ratio;
  - (c) Maximum values of  $\Phi$  occur at  $M_1 = 1.0$  for subsonic mixing;
  - (d) Maximum values of  $C_T$  occur at  $M_1 < 1$ , for supersonic mixing;
  - (e) Diffuser area ratios decrease with increase in pressure ratio;
  - (f) Maximum values of thrust augmentation;
    - (i) decrease with increase in pressure ratio;
    - (ii) increase with increase in mixing tube area.

- (g) Maximum values of thrust coefficients
    - (i) increase with increase in pressure ratio;
    - (ii) increase with increase in mixing tube area.
  - (h) Both maximum values of  $\Phi$  and  $C_T$  are higher for supersonic mixing than for subsonic mixing.
- (3) For a moving ejector: When the flight Mach number ( $M_\infty$ ) increases (Figs. 7, 8):
- (a) Mixing tube ratios decrease with increase in pressure ratio;
  - (b) Diffuser area ratios decrease with increase in pressure ratio;
  - (c) Thrust augmentation decreases with increase in pressure ratio. Supersonic mixing is better than subsonic mixing;
  - (d) Thrust coefficients increase with pressure ratio but decrease with increase in  $M_\infty$ ;
  - (e) The propulsive and thermal efficiencies increase with  $M_\infty$  but decrease with increase in pressure ratios.
- (4) In general (Fig. 6) the maximum values of  $C_T$
- (a) decrease with increase in friction and turbulence;
  - (b) increase with increase in pressure ratios;
  - (c) increase with increase in secondary to primary velocity ratios.
- (5) A general conclusion that can be drawn, for mixing tube ratios ( $\alpha_\infty$ ) larger than 10, is that maximum thrust augmentation factors of 1.6 to 2.5 could be practical for a well designed ejector. The performance is enhanced with lower flight Mach numbers and supersonic mixing in the ejector (Fig. 9).

#### XVIII. RECOMMENDATIONS

The results of this study are based on a thermodynamic analysis of the one-dimensional compressible flow through an ejector.

The flows in the inlet section, the nozzle and the diffuser have been taken as isentropic. Turbulence and friction have been taken into account by means of a pseudo friction factor. Hence, this investigation includes the considerations of References (4) to (6).

While showing the trend of the behavior of the flow characteristics, the results have yet to be compared with experimental results to obtain values of  $CF$ , which can be used.

The empiricism of the above results can be improved by further investigations. Which should include:

- (1) the nozzle efficiency;
- (2) the inlet loss;
- (3) the non-uniformity of flow in the mixing region - we could assume similarity of flow profiles in this region as has been done by the author in Ref. 1;
- (4) turbulence and density correlations;
- (5) the effect of compressibility on the apparent coefficient of viscosity as explained in Ref. 7;
- (6) the structure of the flow in sonic and supersonic primary jets;
- and (7) the boundary layer and its interaction with the flow, particularly when the primary and/or secondary streams are sonic or supersonic.

The above list does not contain all the parameters but the most important ones to consider in order to get meaningful results.

It is suggested that both experimental and analytical investigations be pursued to include all the effects listed above. It is hard to say, a priori, the exact influence of these parameters on the flow characteristics. But it may be substantial as shown by Figs. 3, 4, and 6. Only a systematic study will show which parameters are important.

A more detailed analysis of the mixing process and the effects of compressibility on it can be done by the author based on References (1) and (7), if he has the support for such an investigation. This would clearly be a first step. In the meanwhile, experimental studies to evaluate (4), (6), and (7) have to be undertaken.

The analytical studies also show that, with the increase in back pressure, secondary flows ensue. We did not have time to pursue this aspect of the problem. An investigation concerning this effect is necessary to determine optimum pressure ratios for efficient ejector performance.

This study does not include the geometry of the ejector, except for the area ratios. The length and shape of the inlet, nozzle, mixing

channel and diffuser depends essentially on the desired performance and a more detailed study of the losses due to friction. An approximate analysis has been done by the author, to obtain the length of the mixing channel, but this study has not been included in this report, as the study is not yet complete. It can be included in further investigation by the author.

#### REFERENCES

- (1) (a) Acharya, Y.V.G. The Design of a Cylindrical Injector  
Applied Scientific Research, Section A, Volume 5, 1954.
- (b) Acharya, Y.V.G. Momentum Transfer and Heat Diffusion in the Mixing of Coaxial Turbulent Jets Surrounded by a Pipe. Thesis (Dr.) Technische Hoogeschool. Delft, Netherlands, 1954.
- (2) Porter, J.L. A Summary/Overview of Ejector Theory and Performance  
ATC Report No. B-91100/8CR-125 Vought Corp Advanced Technology Center, Dallas, Texas, 1978.
- (3) Acharya, Y.V.G. Calculation of Lift and Pressure Distribution on Circulation Control Rotor Sections in the Transonic Range. NASA-Ames Research Center, 1977 (Report included in the NASA-ASEE-Stanford, 1977 Summary Faculty Fellowship Reports).
- (4) Nagaraja, K.S. Recent Developments in Ejector Technology in the Air Force: an Overview. AFFDL/WPAFB, Ohio, 1978.
- (5) Nagaraja, K.S., Hammond, D.L., and Graetch, J.E. One Dimensional Ejector Flows. AIAA/SAE 9th Propulsion Conference, Los Vegas, Nevada, 1973. AIAA Paper
- (6) Alperin, M, and Wu, J.J., High Speed Ejectors. Flight Dynamics Research Corporation, Van Nuys, CA, Report No. FDRC 3160-12-78, 1978.
- (7) Acharya, Y.V.G. The Mixing of Supersonic Under Expanded Nozzle Flow With a Subsonic Free Stream 30th DFD meeting of the American Physical Society, 1977.

## APPENDIX

### LIST OF FIGURES

1. Schematic Layout of Ejector
2. Flow characteristics vs  $M_1$ , with CF as parameter for  $PR=10$ ,  $\alpha_\infty = 20$ ,  $M_\infty = 0$ .
3. Thrust augmentation vs  $\lambda_1$ , for  $\alpha_\infty = 20$ ;  $M_\infty = 0$  and  $M_2 < 1$ .
4. Thrust factors vs PR, for  $\alpha_\infty = 20$ ,  $M_\infty = 0$  and  $M_2 < 1$  with CF as parameter.
5. Flow characteristics vs  $M_1$  for  $\alpha_\infty = 20$ ;  $M_\infty = 0$  and  $CF = 0$ , with PR as parameter.
6. Maximum thrust coefficient for  $\alpha_\infty = 20$ ;  $M_\infty = 0$ , with PR as parameter.
7. Flow characteristics vs  $M_\infty$  for  $M_1 = 0.8$  and  $CF = 0$  with PR as parameter.
8. Flow characteristics with subsonic nozzle and subsonic mixing, with  $M_1$  and  $M_\infty$  as parameters.
9. Maximum thrust augmentation and thrust coefficient vs PR, for  $M_\infty = 0$ ;  $CF = 0$ .
10. Flow characteristics for subsonic nozzle vs  $M_{p1}$ , for  $\alpha_\infty = 20$ ;  $M_\infty = 0$ ;  $CF = 0$ .





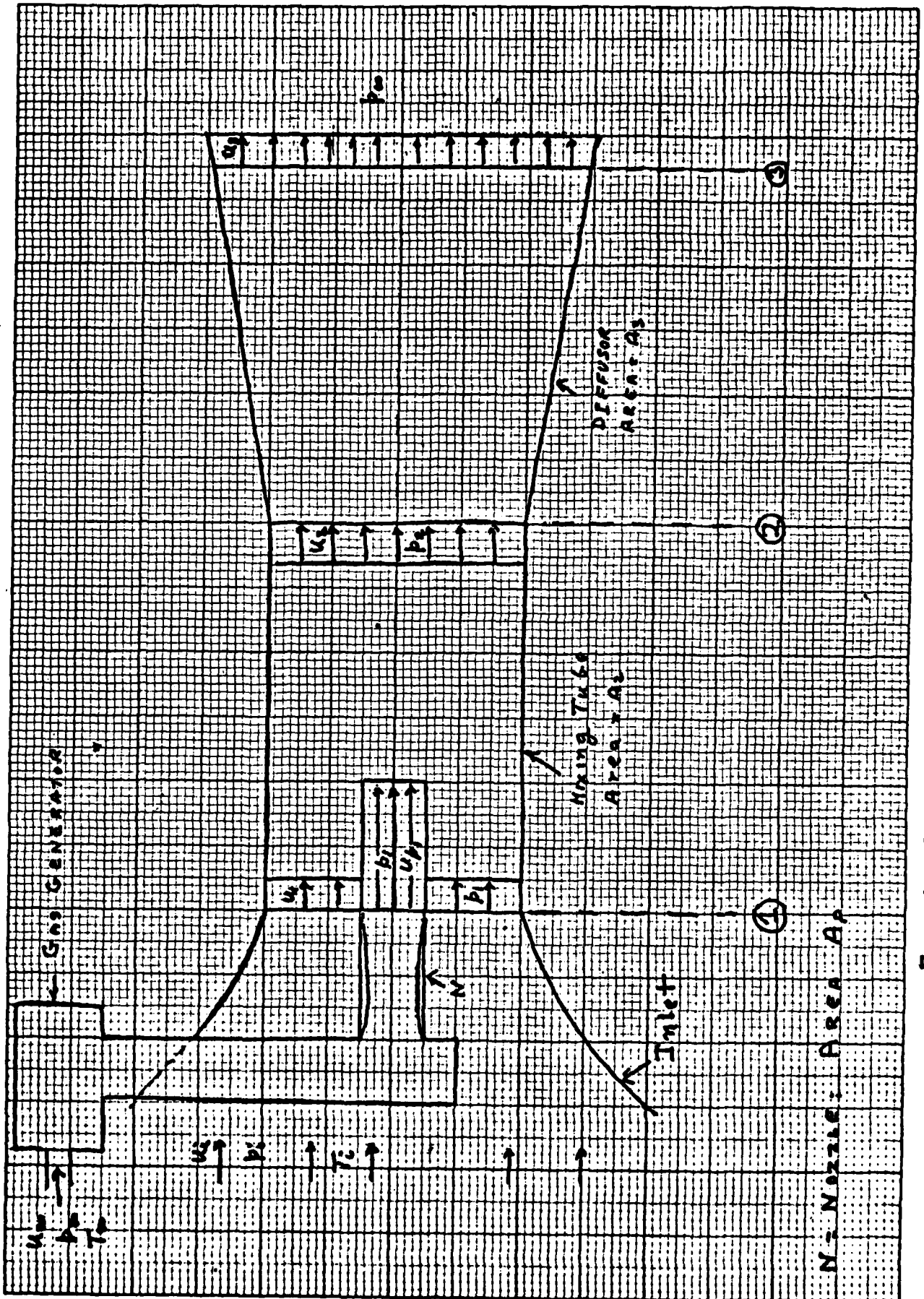
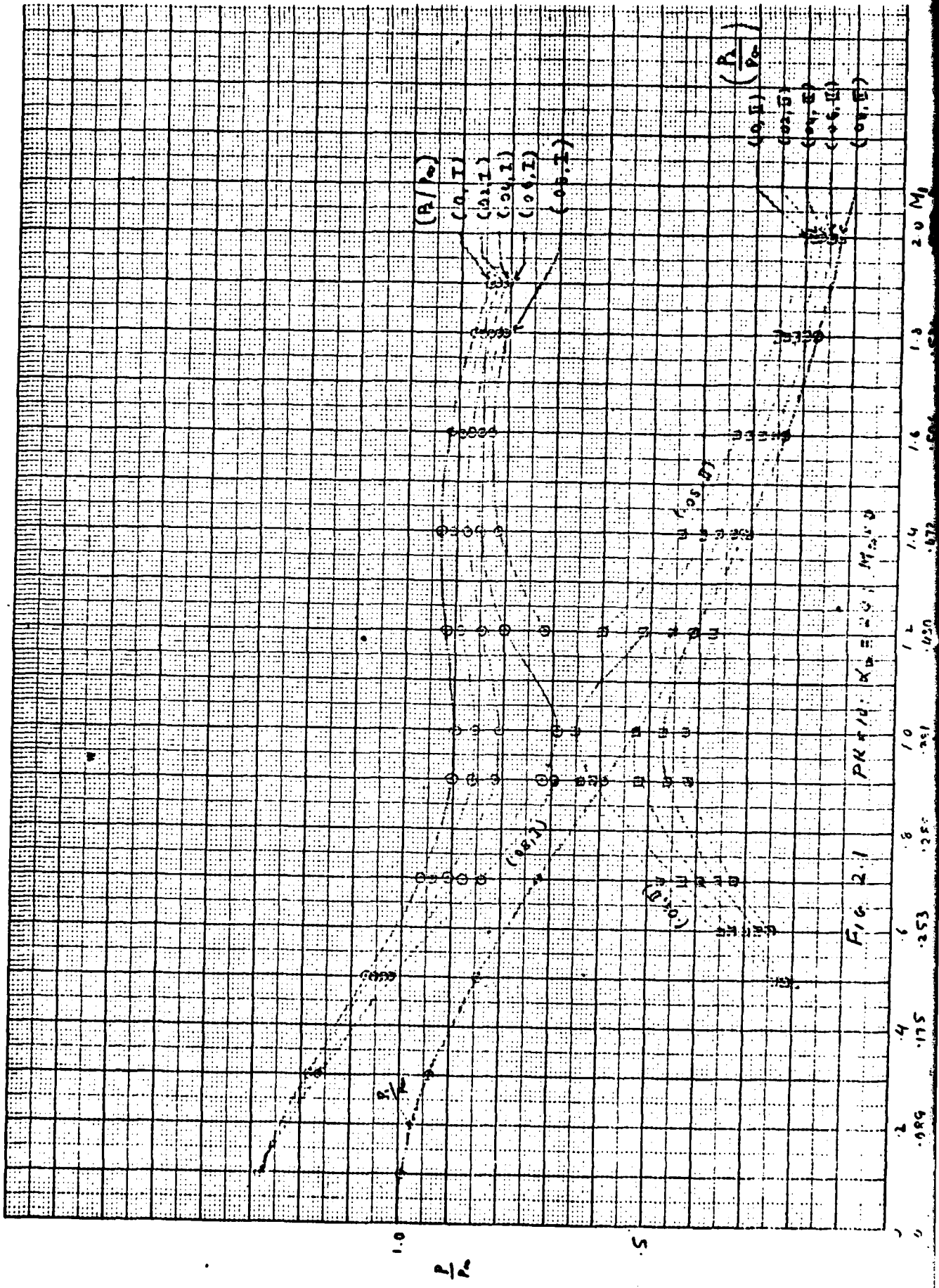


FIG. 1 SCHEMATIC OF EJECTOR





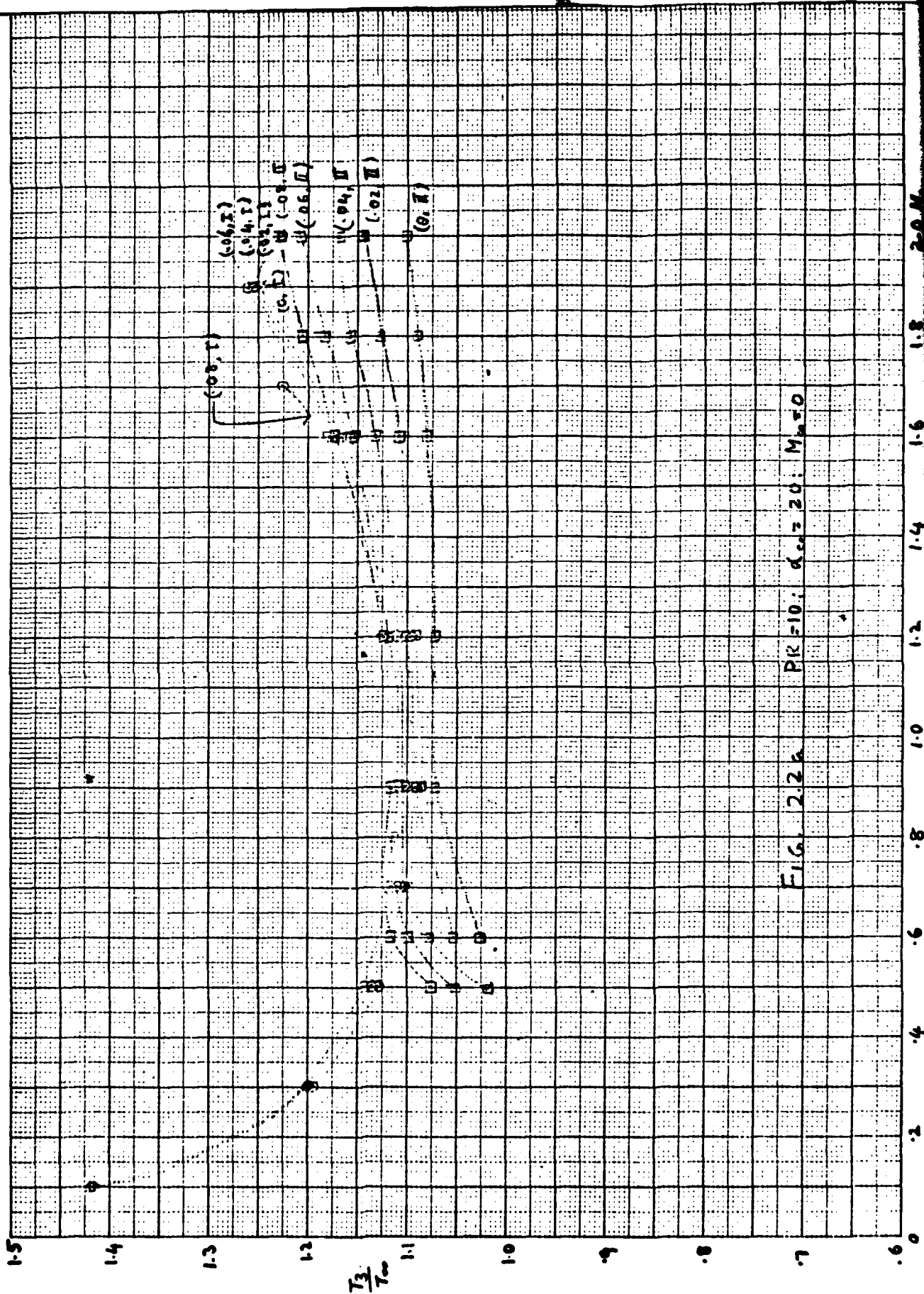


FIG. 2.2a PR=10;  $\alpha_{cc}=20$ ;  $M_{\infty}=0$

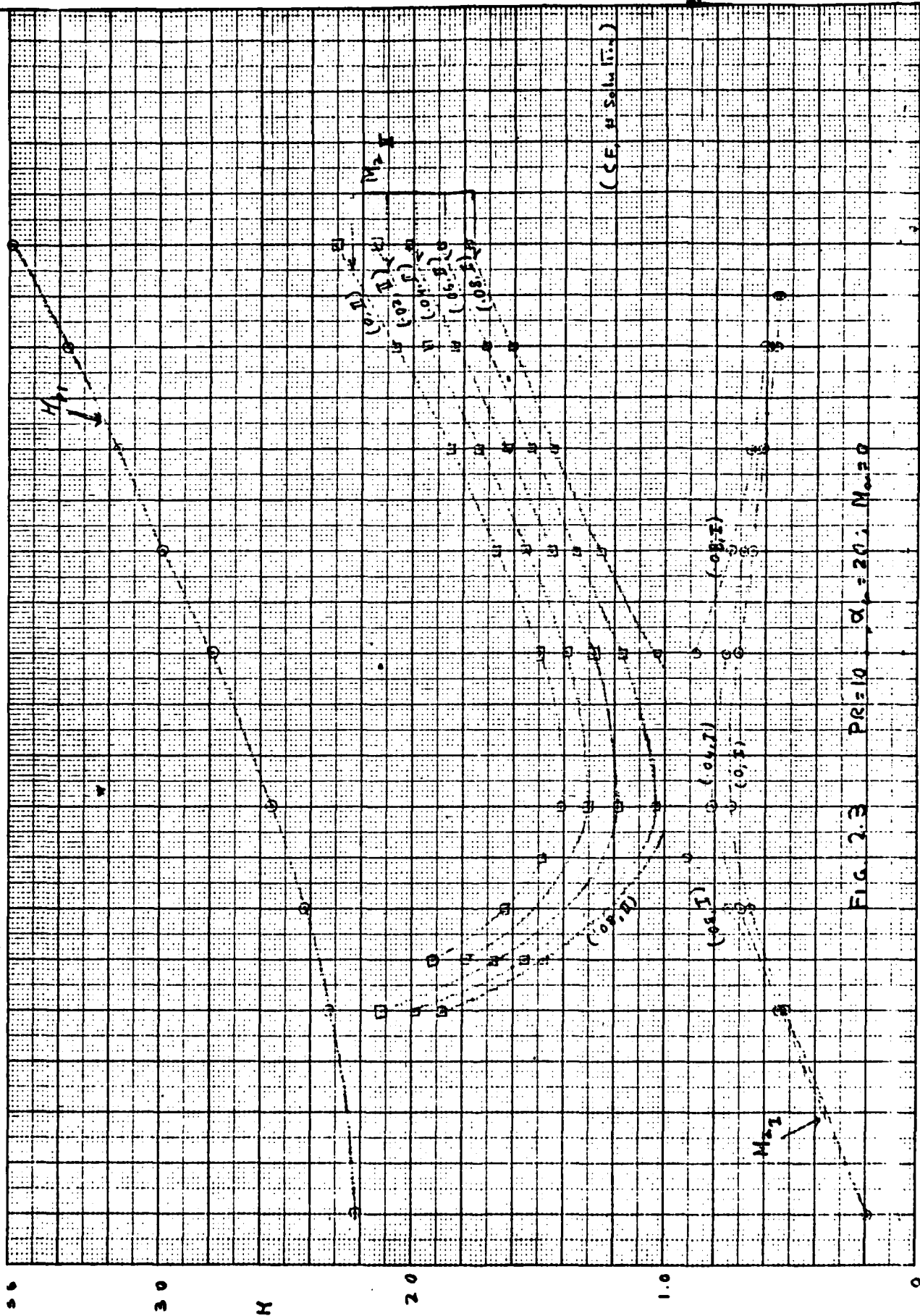


FIG. 2.3  $PR=10$ ,  $\alpha=20$ ,  $M_0=20$

$\lambda \rightarrow$   
558  $\lambda \rightarrow$

1.1 1.3 1.5 1.6 1.7 1.8

0.43 0.47 0.50 0.53 0.56 0.59

0.8 1.0 1.2 1.4 1.6 1.8

0.25 0.31 0.38 0.43 0.48 0.53

0.85 1.0 1.1 1.2 1.3 1.4

0.85 1.0 1.1 1.2 1.3 1.4

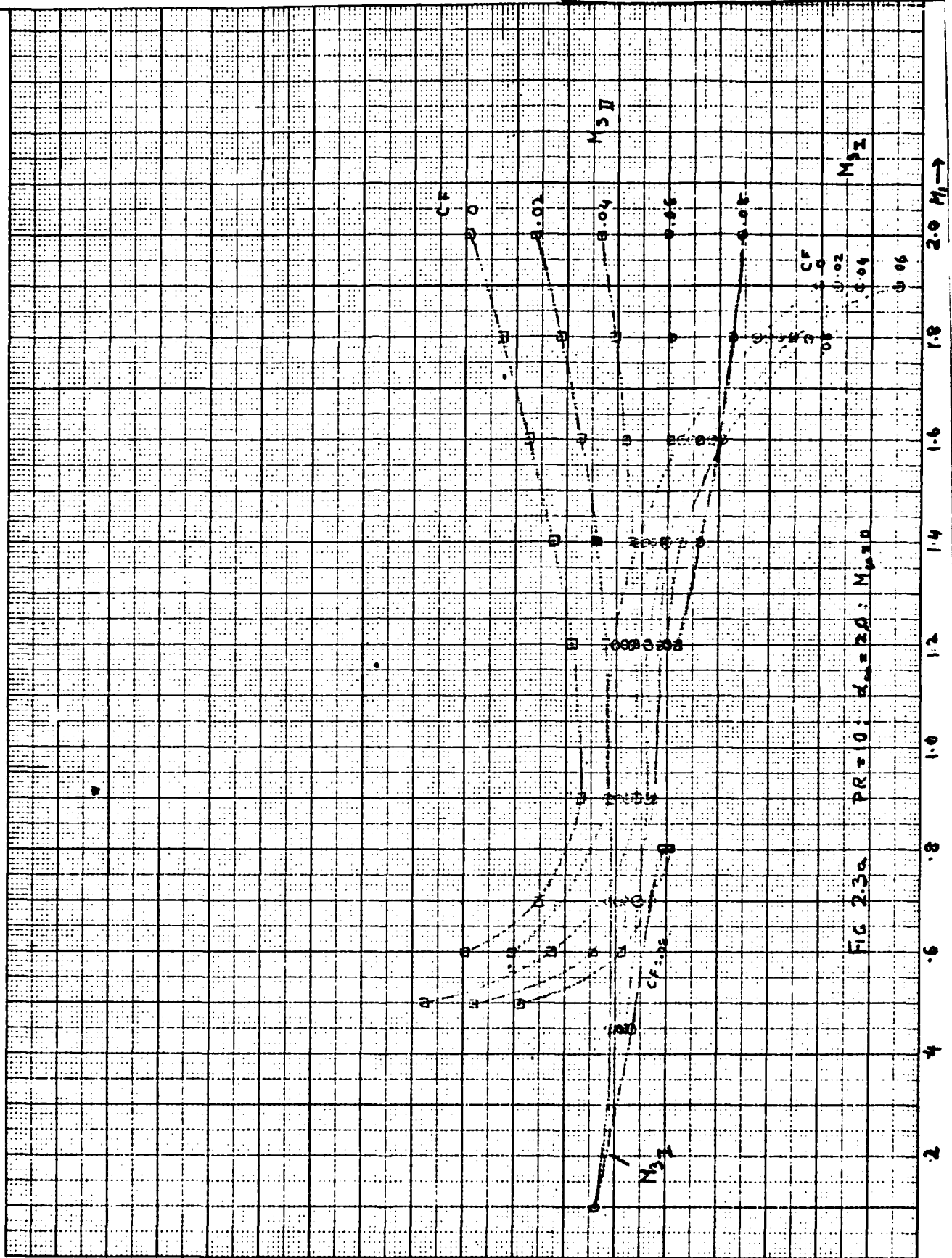


FIG 2.3a PR=10;  $M_1=20$ ;  $M_{10}=10$

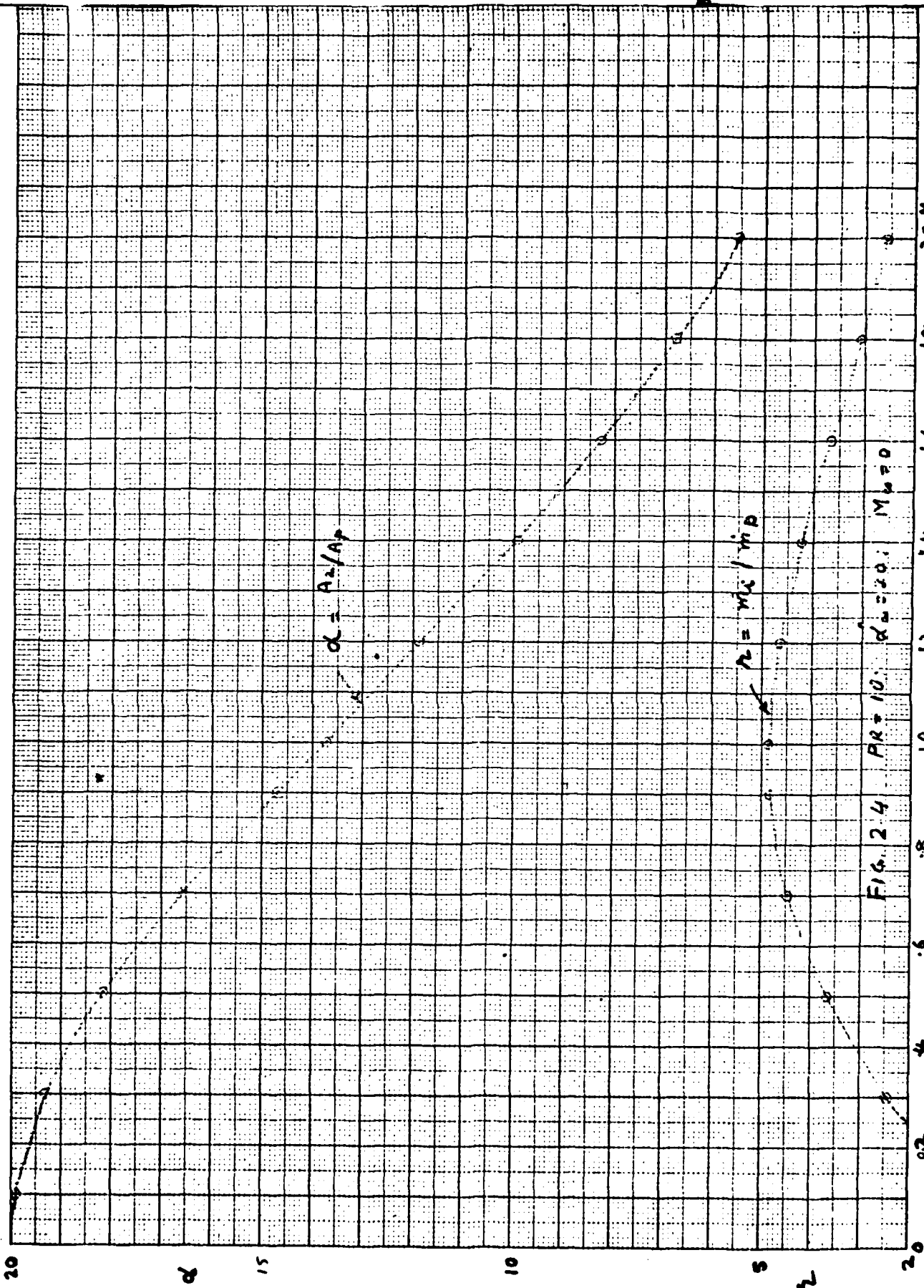


FIG. 24 PR = 10;  $\alpha_0 = 20$ ;  $M_0 = 0$

0	0.2	0.4	0.6	0.8	1.0	1.2	1.4	1.6	1.8	2.0
0	.089	.175	.253	.312	.351	.430	.472	.506	.534	.558

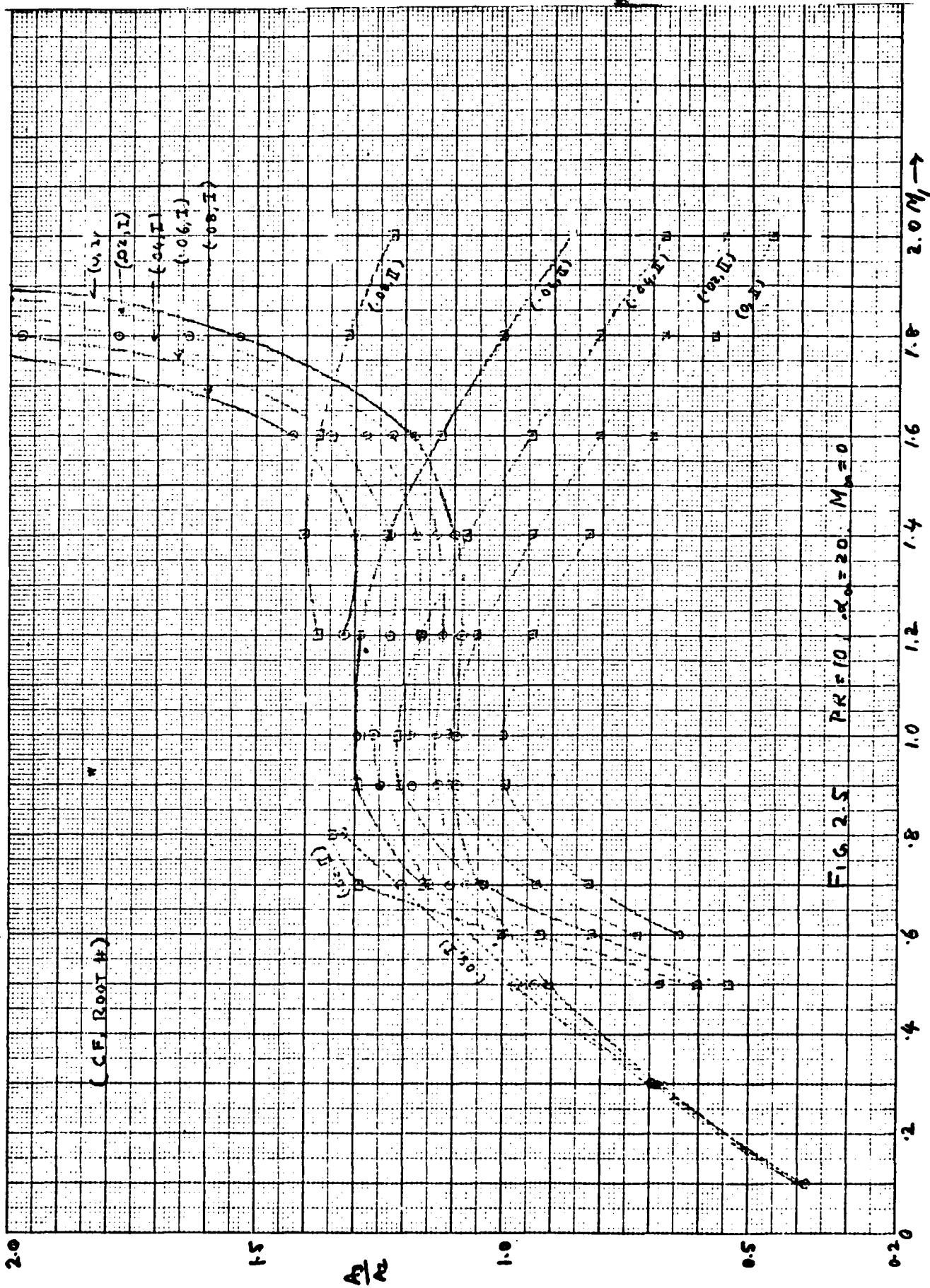


FIG. 2.5 PR=10,  $\alpha_0=20$ ,  $M_0=0$

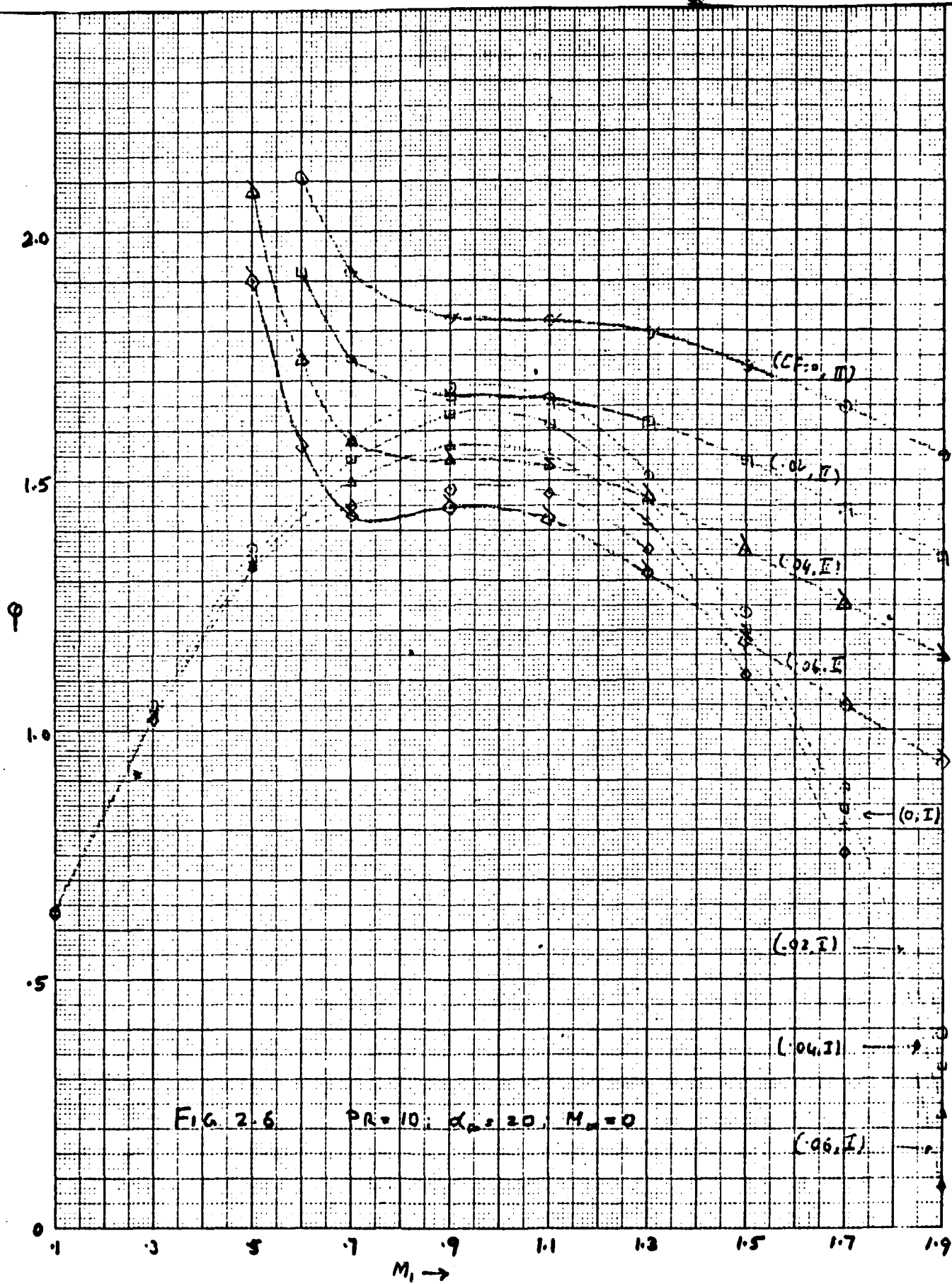


FIG. 2.6 PR = 10;  $\alpha_p = 20$ ;  $M_\infty = 0$

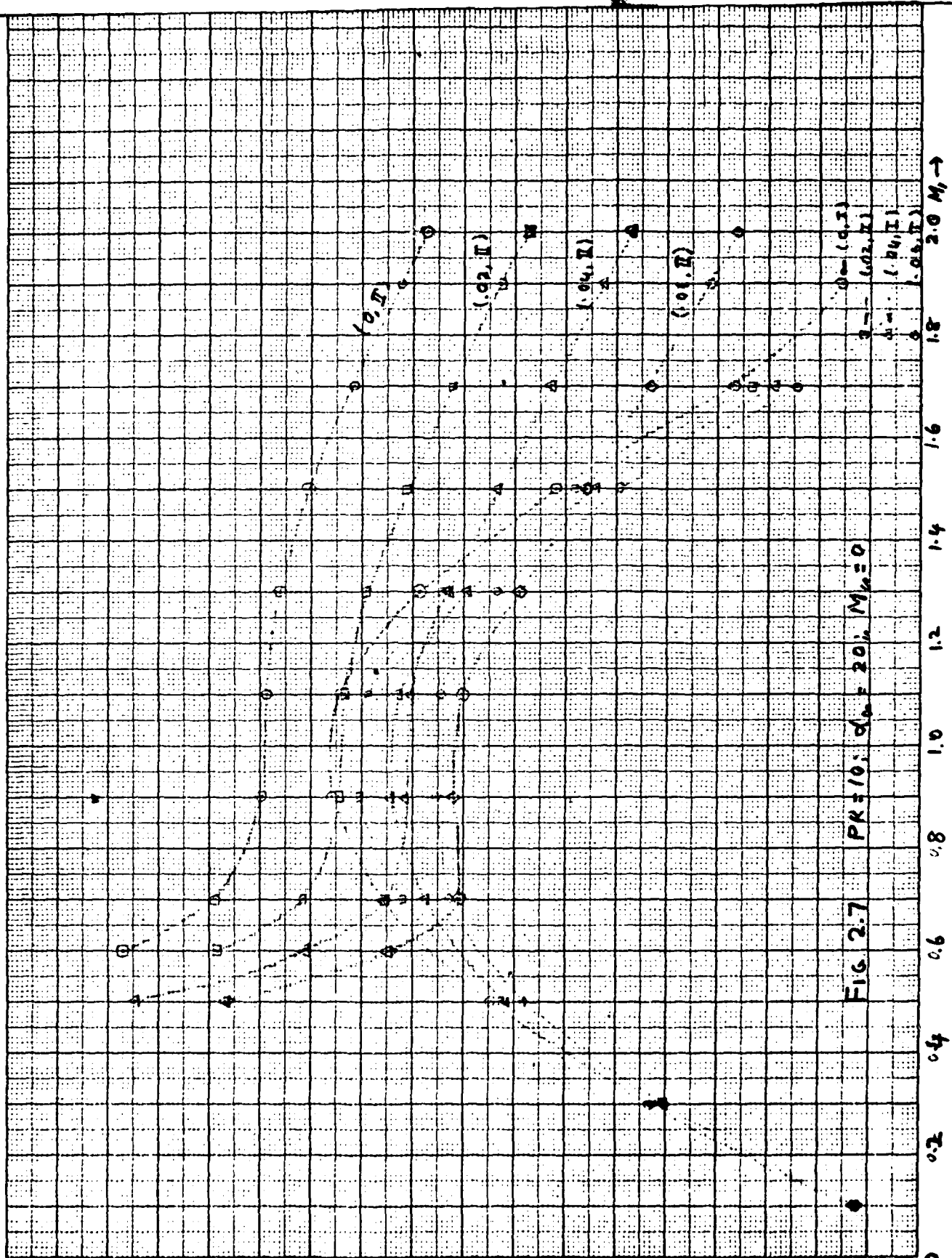
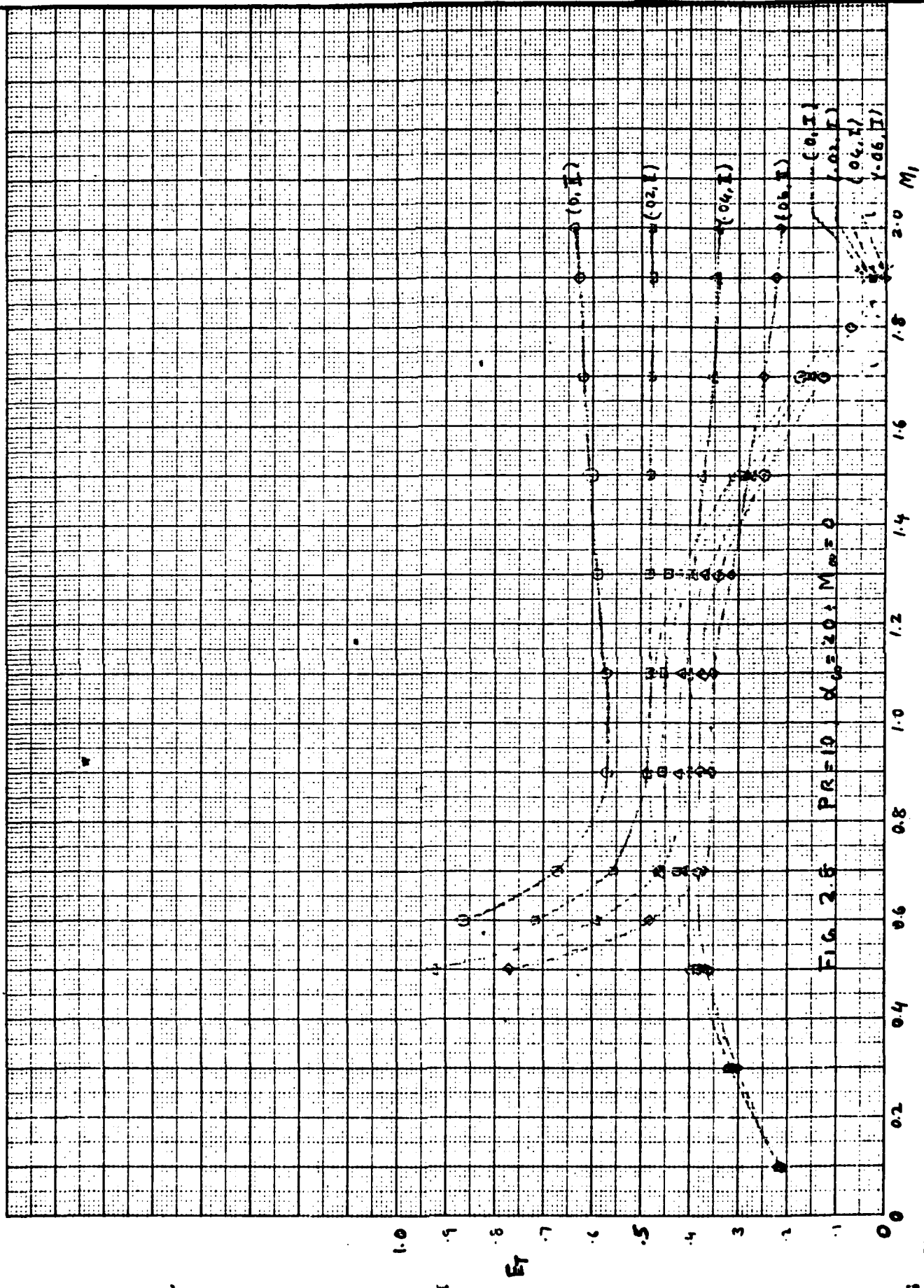


FIG. 2.7  $PK=10; \alpha_0=20; M_0=0$



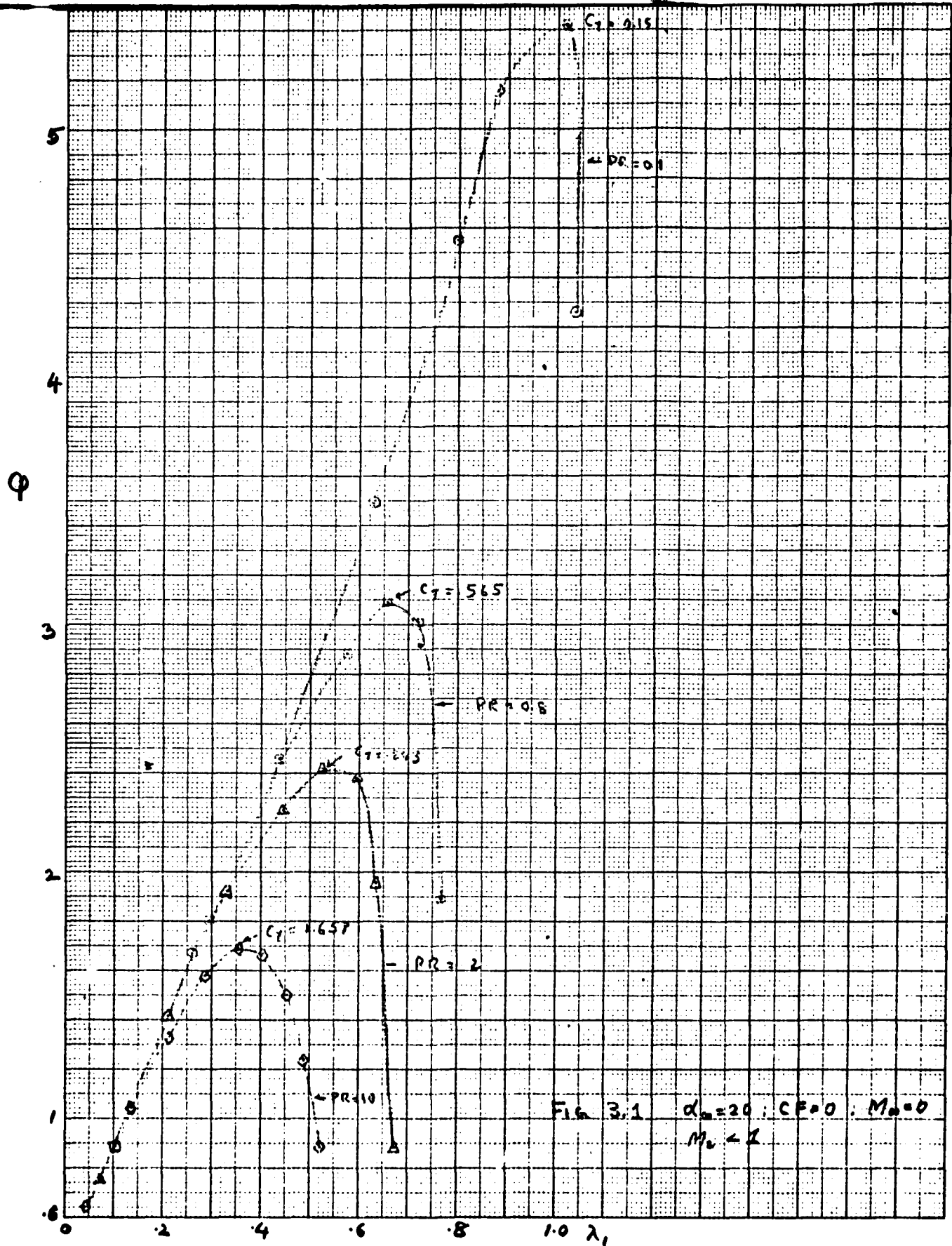


Fig 3.1  $\alpha_0 = 20$ ;  $CF = 0$ ;  $M_0 = 0$   
 $M_0 < 1$

PA	C <sub>1</sub>
1	.057
2	.200
4	.358
10	.424
20	.680
50	1.452
100	1.548

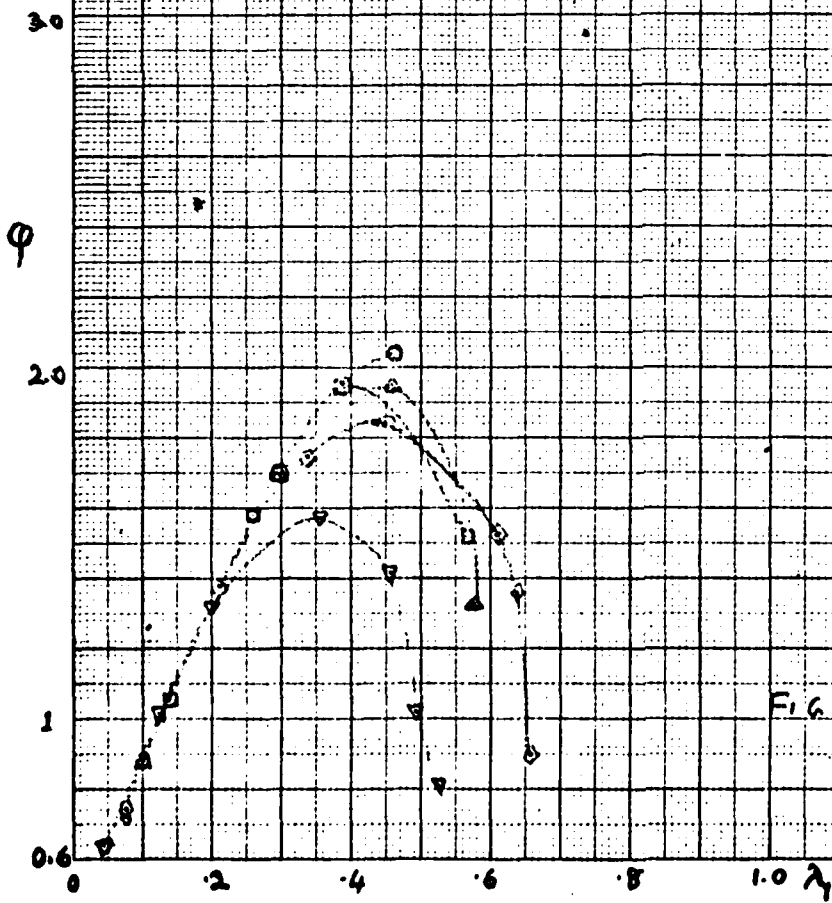


FIG. 3.2  $\alpha_0 = 20; M_0 = 0; CF = 0.00$   
 $M_0 < 1$

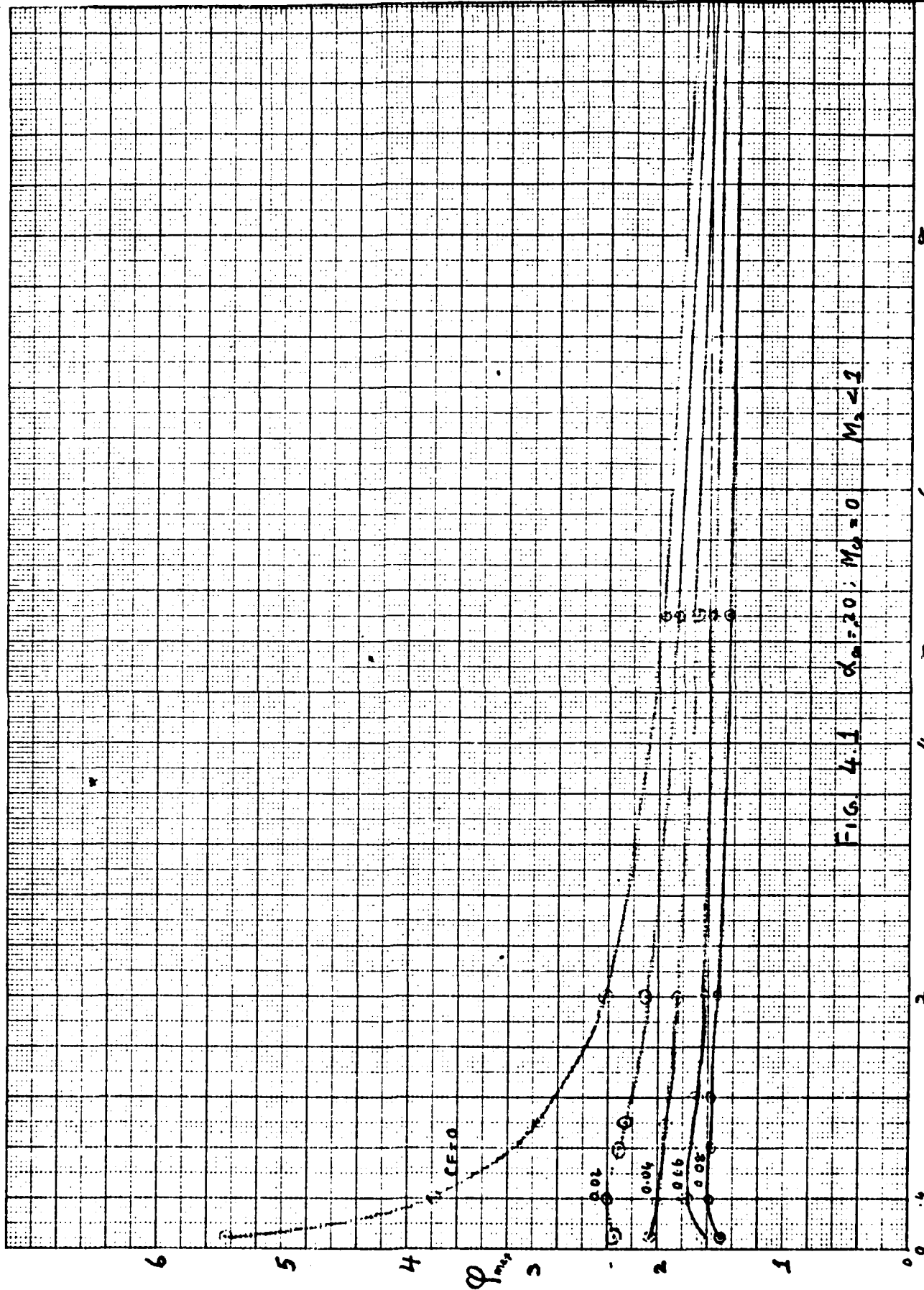


FIG. 4.1  $\alpha_m = 20$ ;  $M_0 = 0$   $M_2 = 1$

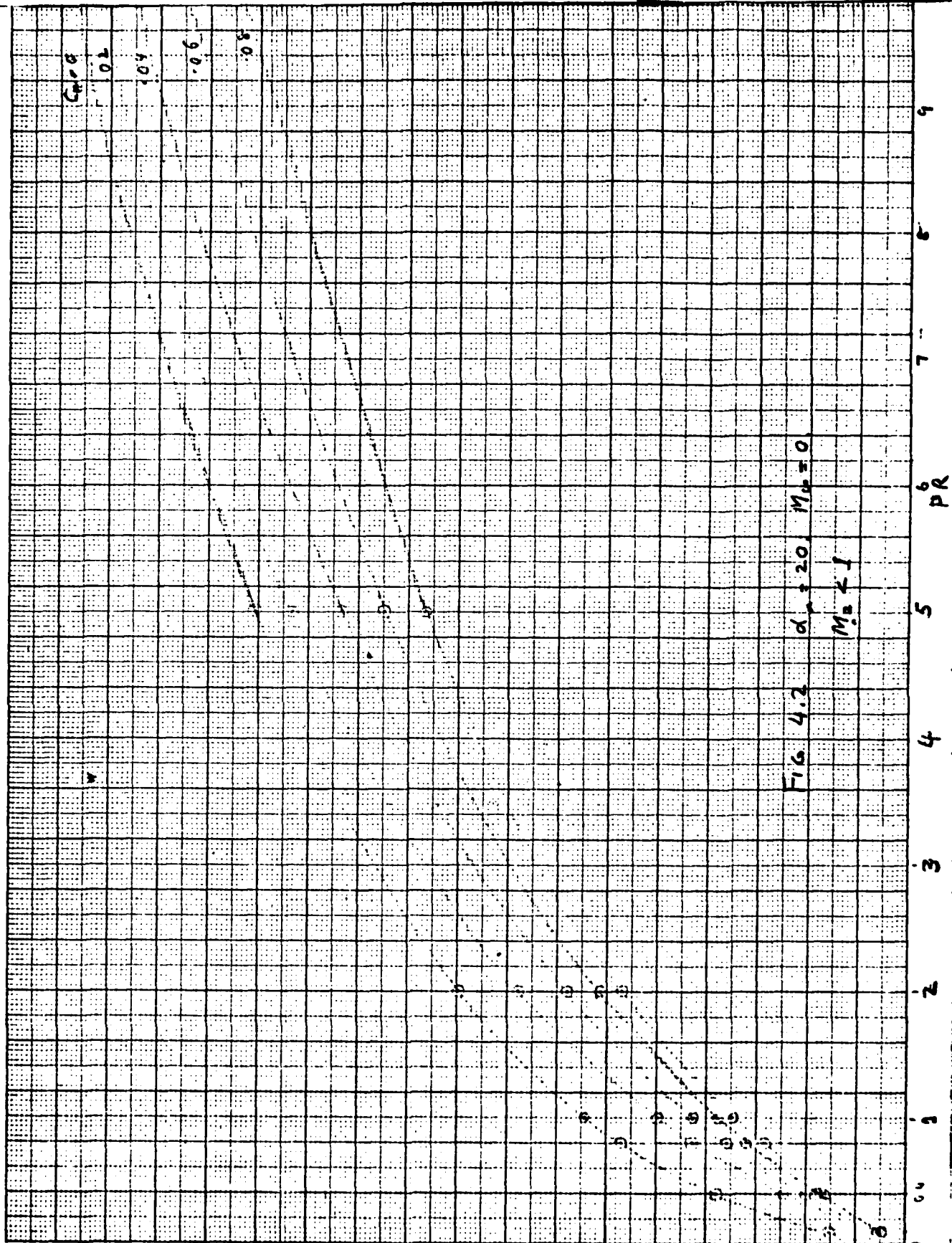


FIG. 4.2  $\alpha_1 = 2.0$   $M_0 = 0$   $M_1 = 1$

1.5

1.0

.5

0.0

CT  
Mod.

0

1

2

3

4

5

6

7

8

9

PR



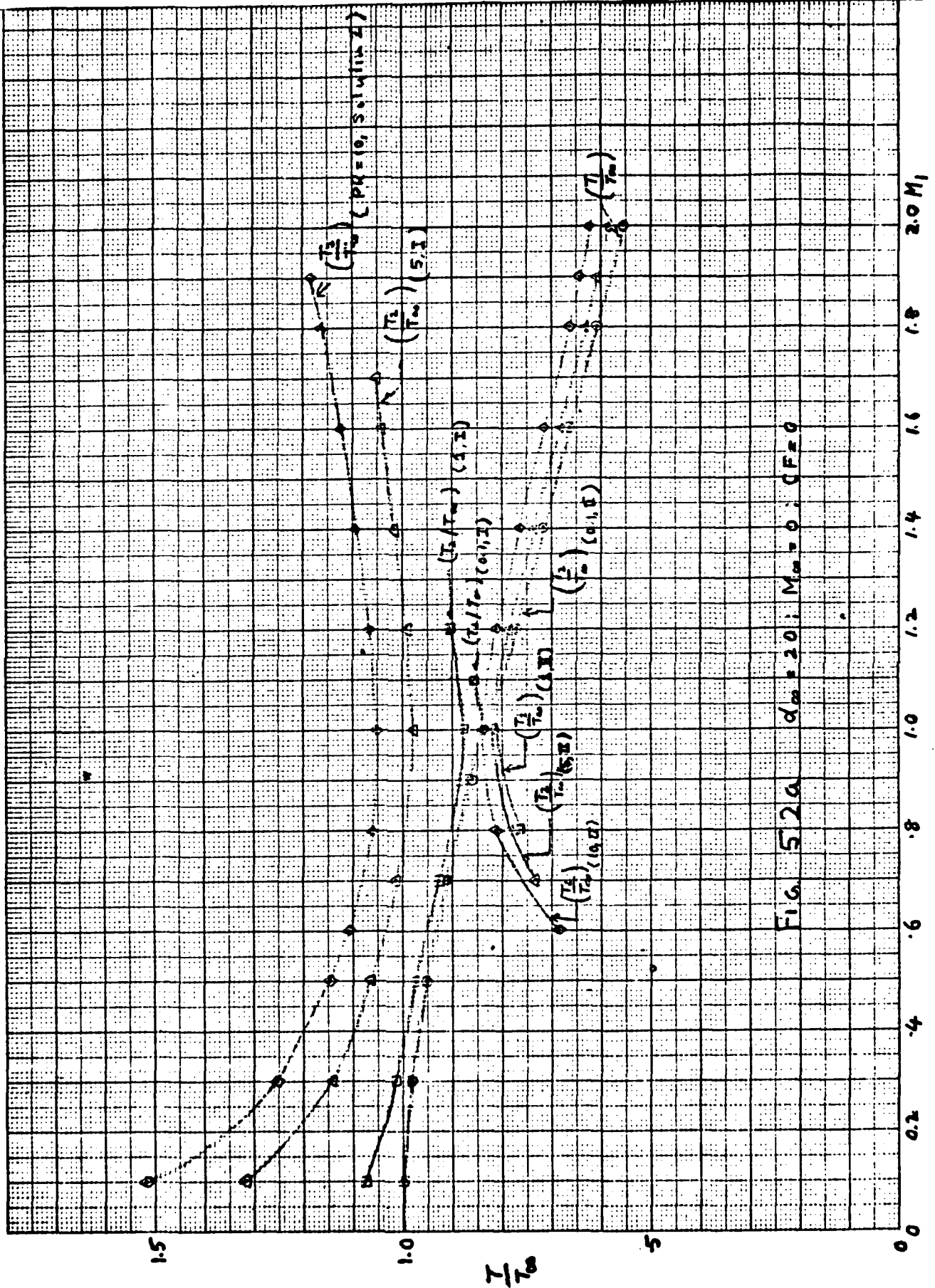


Fig. 52a  $d_0 = 20$ ;  $M_0 = 0$ ;  $(F = 0)$

0.0 0.2 0.4 0.6 0.8 1.0 1.2 1.4 1.6 1.8 2.0 M1

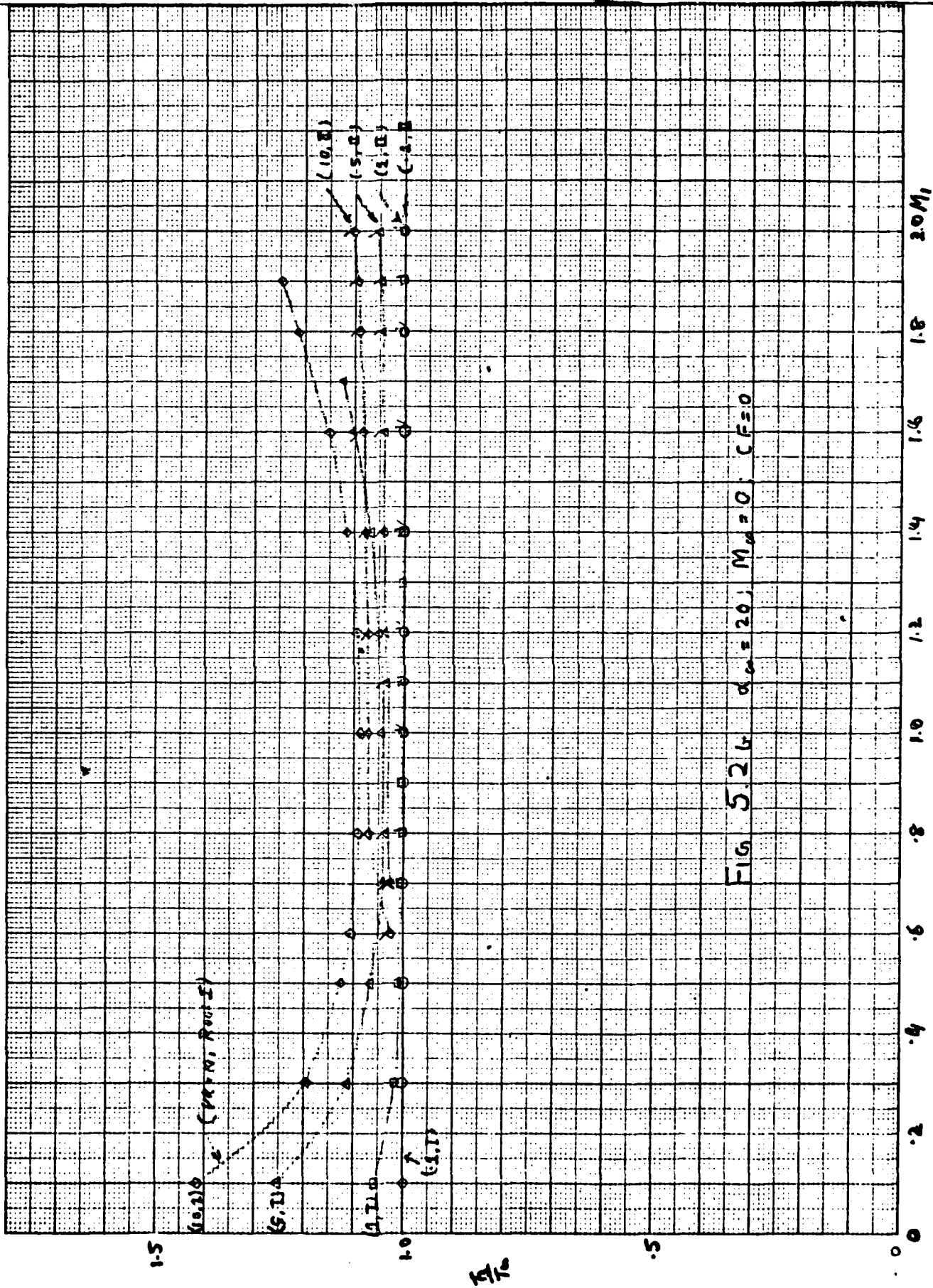


FIG 5.26  $\alpha_0 = 20$ ,  $M_0 = 0$ ,  $CF = 0$

2.0M

1.8

1.6

1.4

1.2

1.0

0.8

0.6

0.4

0.2

0

$\frac{M}{K_0}$

1.5

.5

0

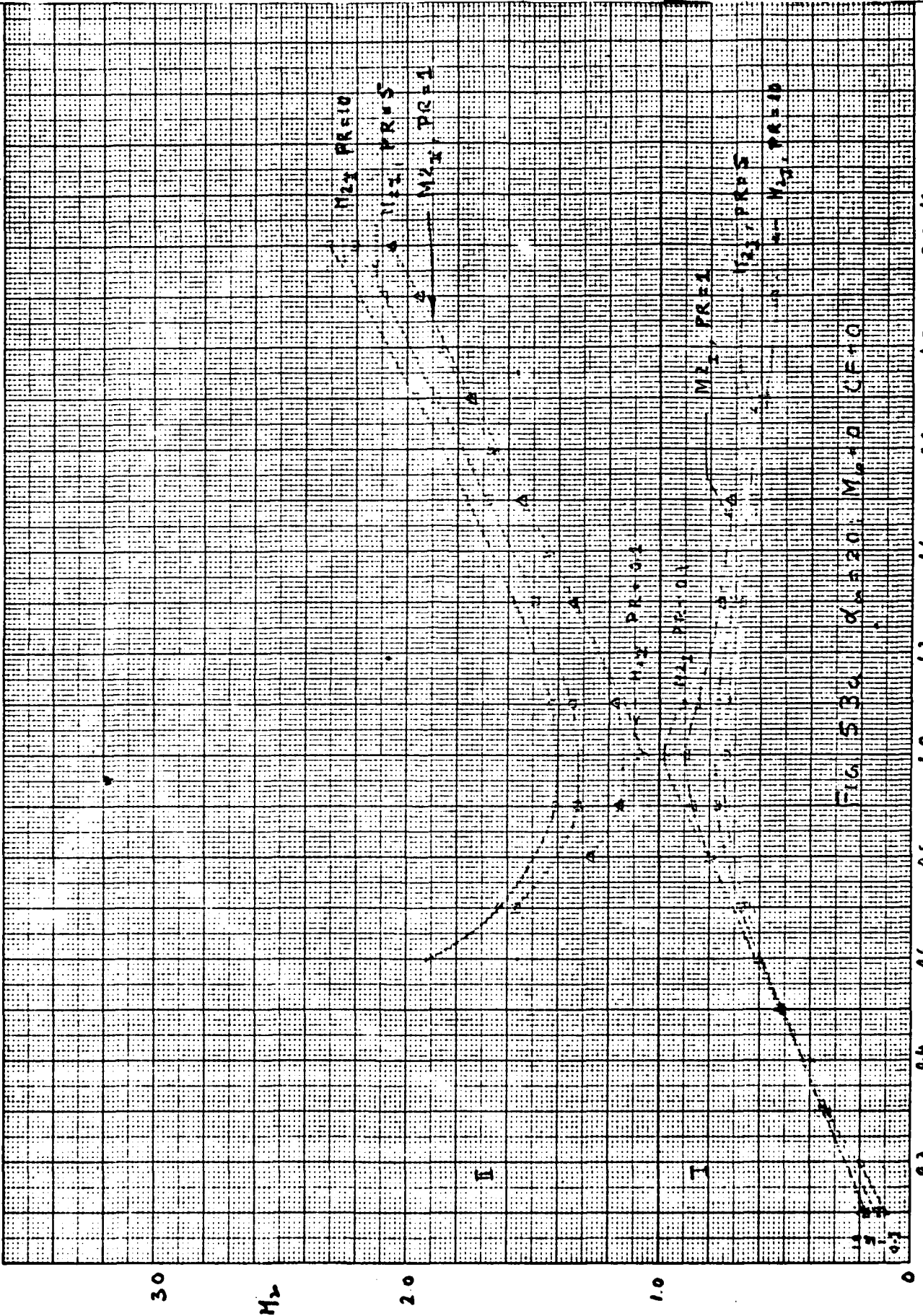


FIG. 5.34.  $d_0 = 20$ ;  $M_0 = 10$ ;  $CF = 10$

0.2 0.4 0.6 0.8 1.0 1.2 1.4 1.6 1.8 2.0 M1

$\mu = 0$  PR = 10 ;  $d_0 = 20$

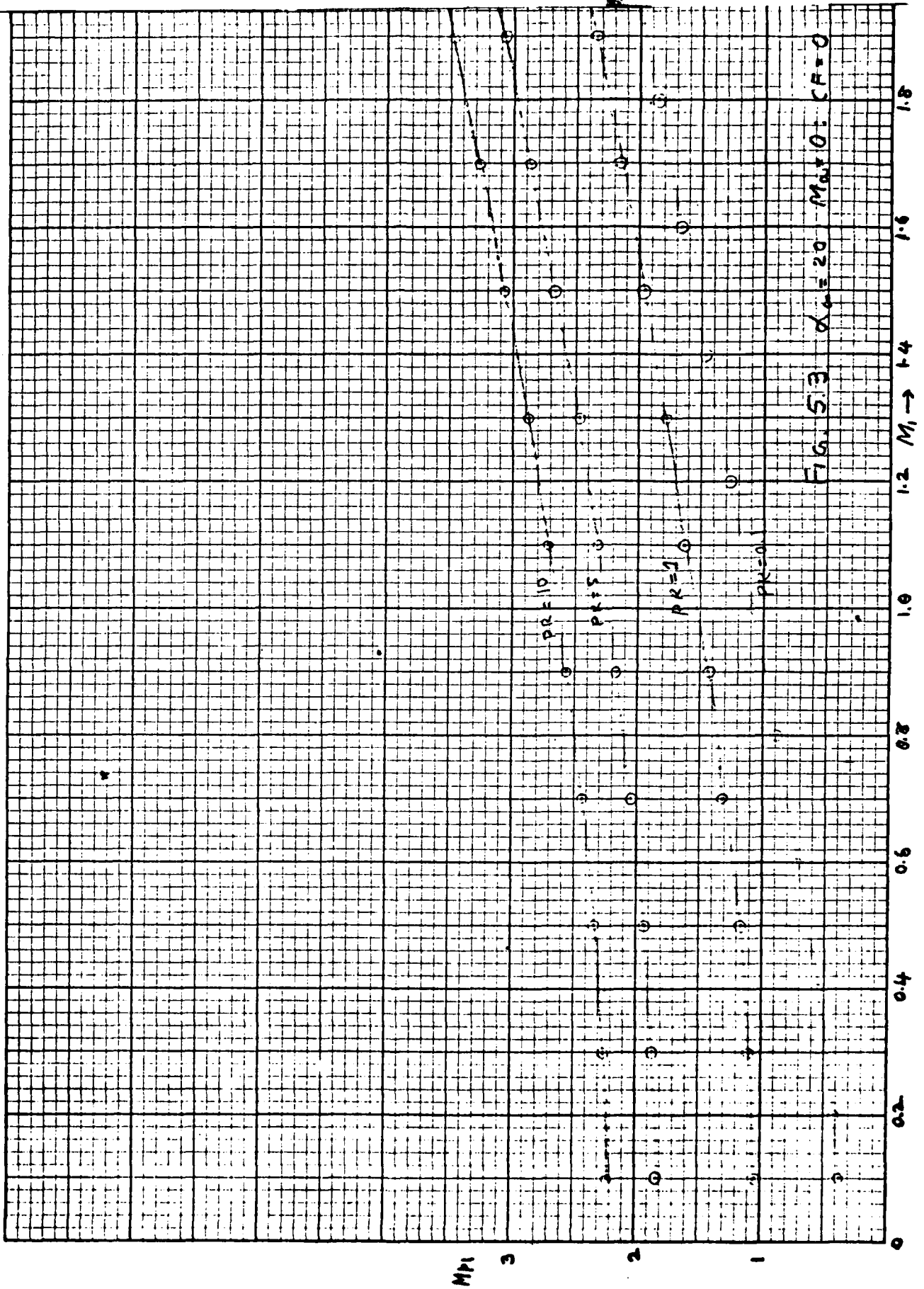


FIG. 5.3  $\alpha_0 = 20$   $M_{01} = 0$   $CF = 0$

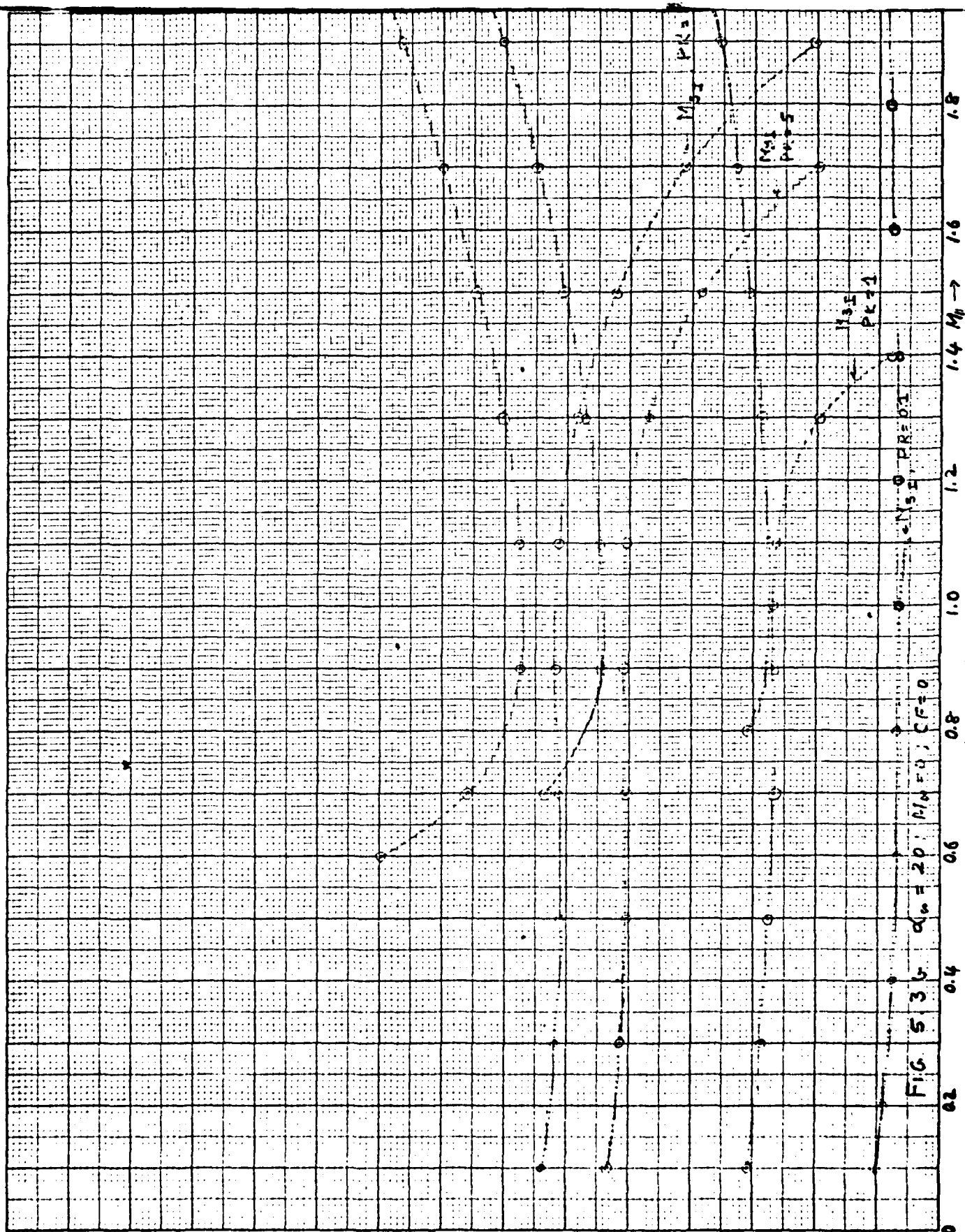


FIG 5 36  $\alpha_n = 20$ ,  $M_0 = 0$ ,  $CF = 0$

Fig. 5.4

$d_m = 20; k_0 = 0 \quad CF = 0$

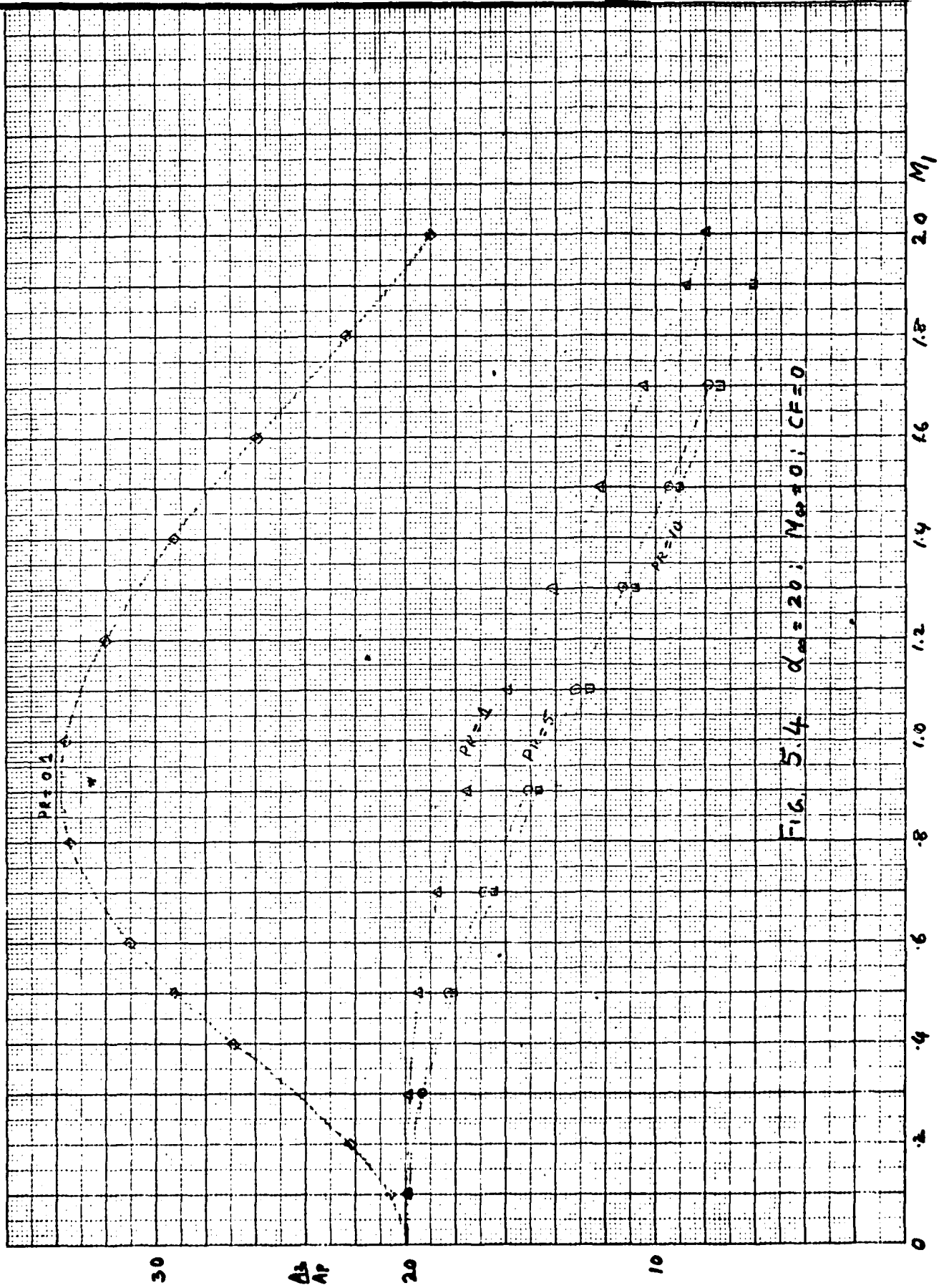
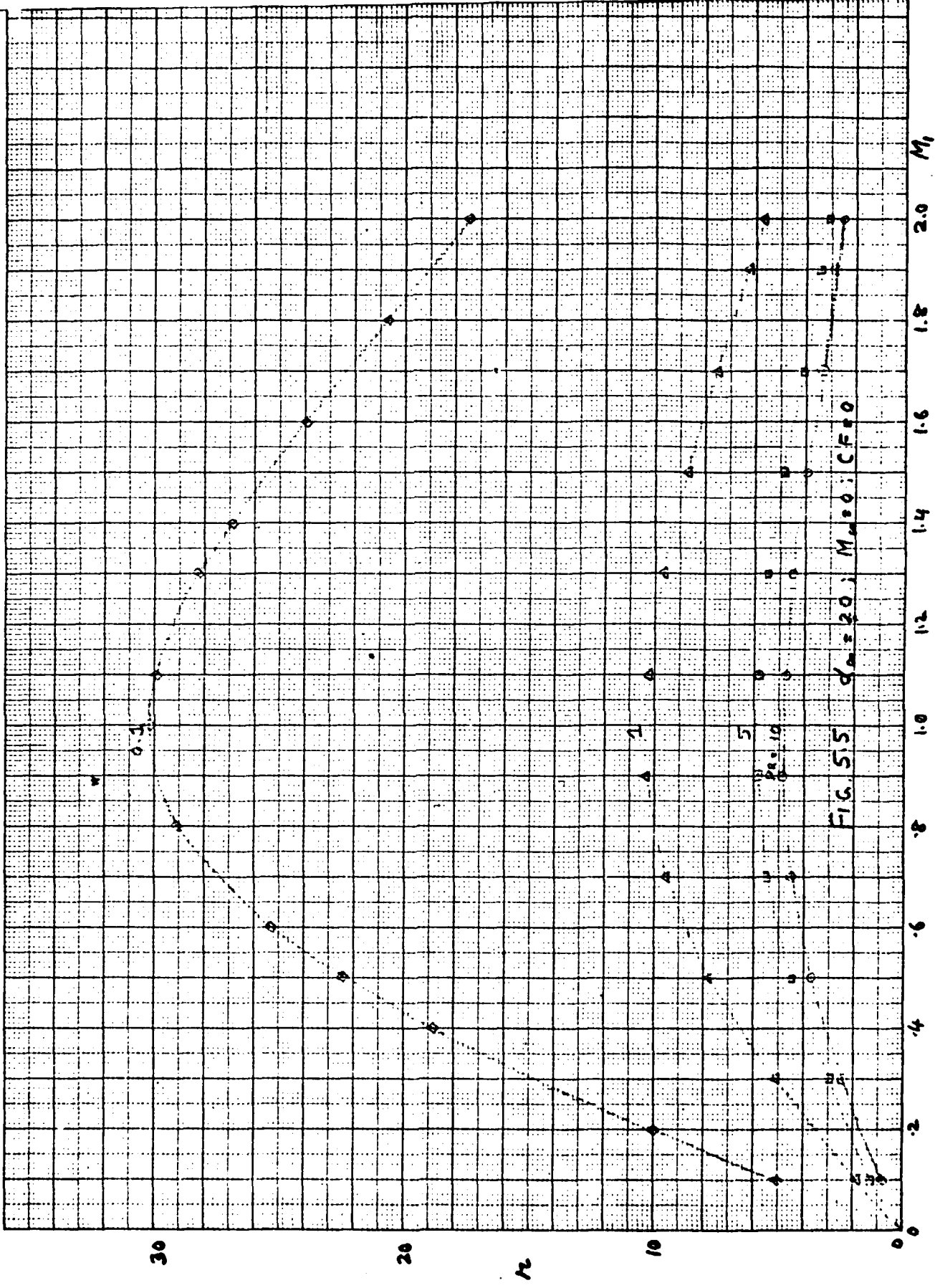


FIG. 5.4  $d_m = 20; M_0 = 10; CF = 0$



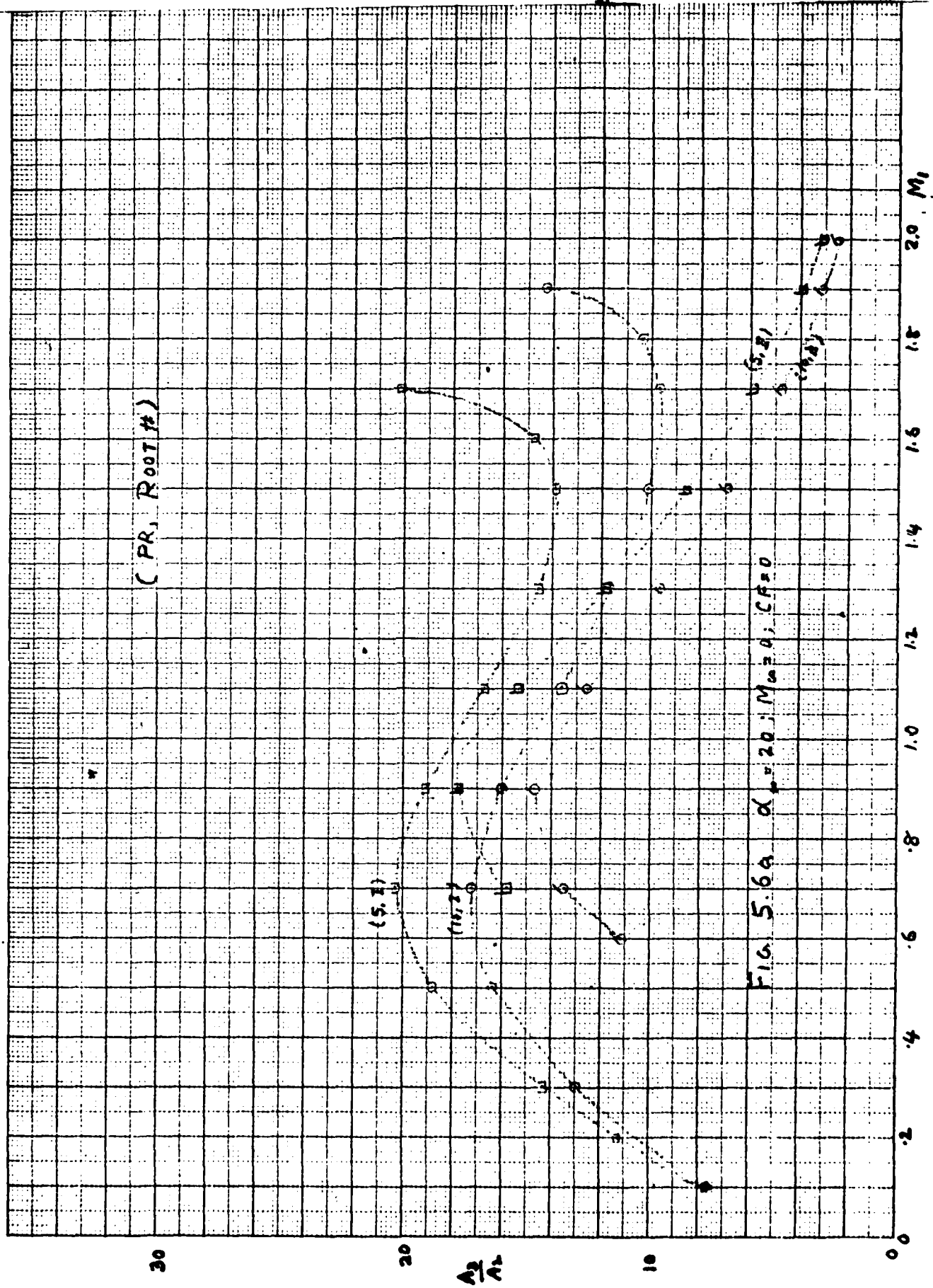


FIG. 5.6a  $\alpha = 20; M_0 = 2.0; CF = 0$

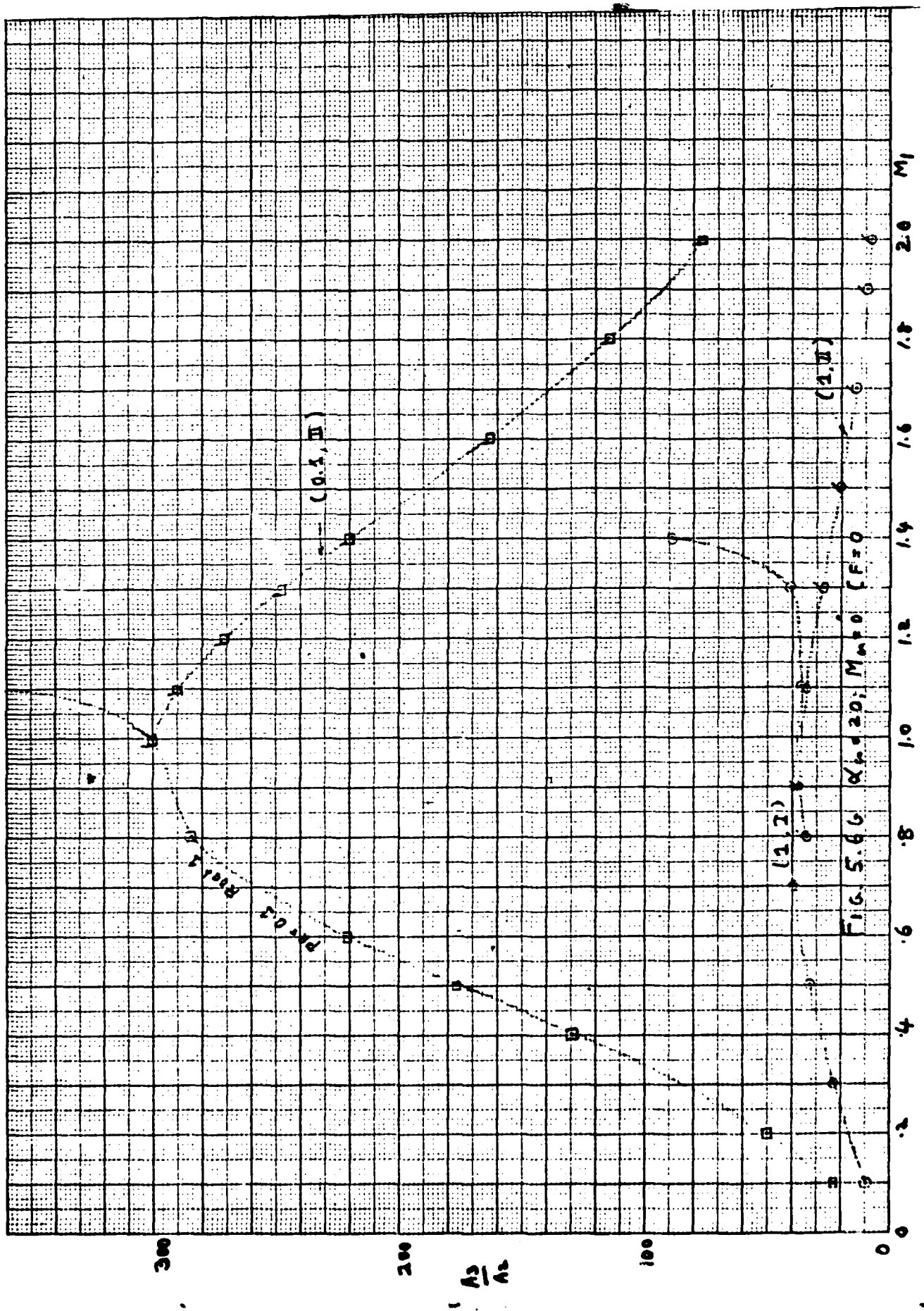


FIG. 5.66  $\alpha_n = 20; M_n = 0 (F=0)$

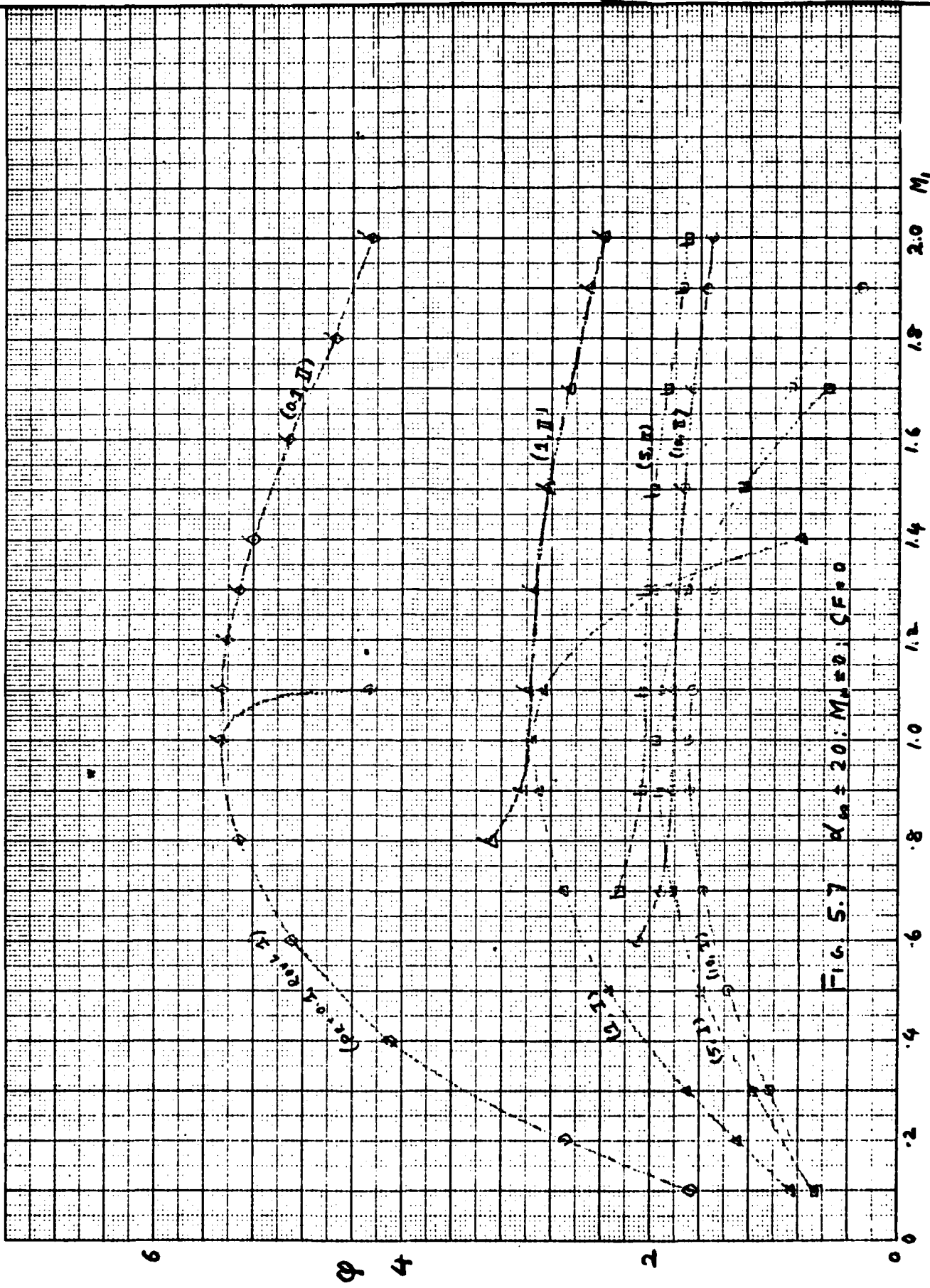
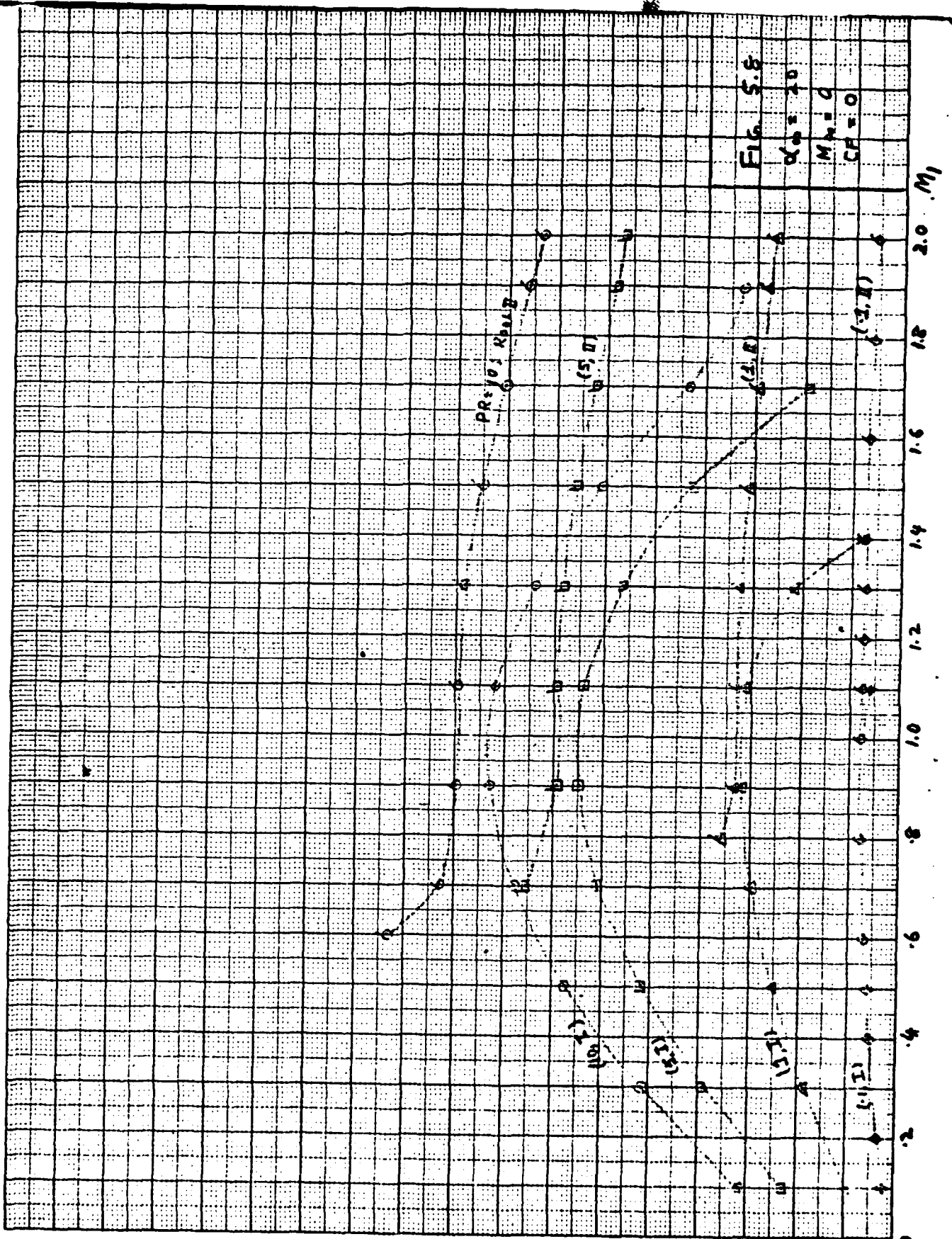


FIG. 5.7  $R_{0.2} = 20; M_{0.2} = 0; CF = 0$



-2

CT

1

0

0 .2 .4 .6 .8 1.0 1.2 1.4 1.6 1.8 2.0  $M_1$

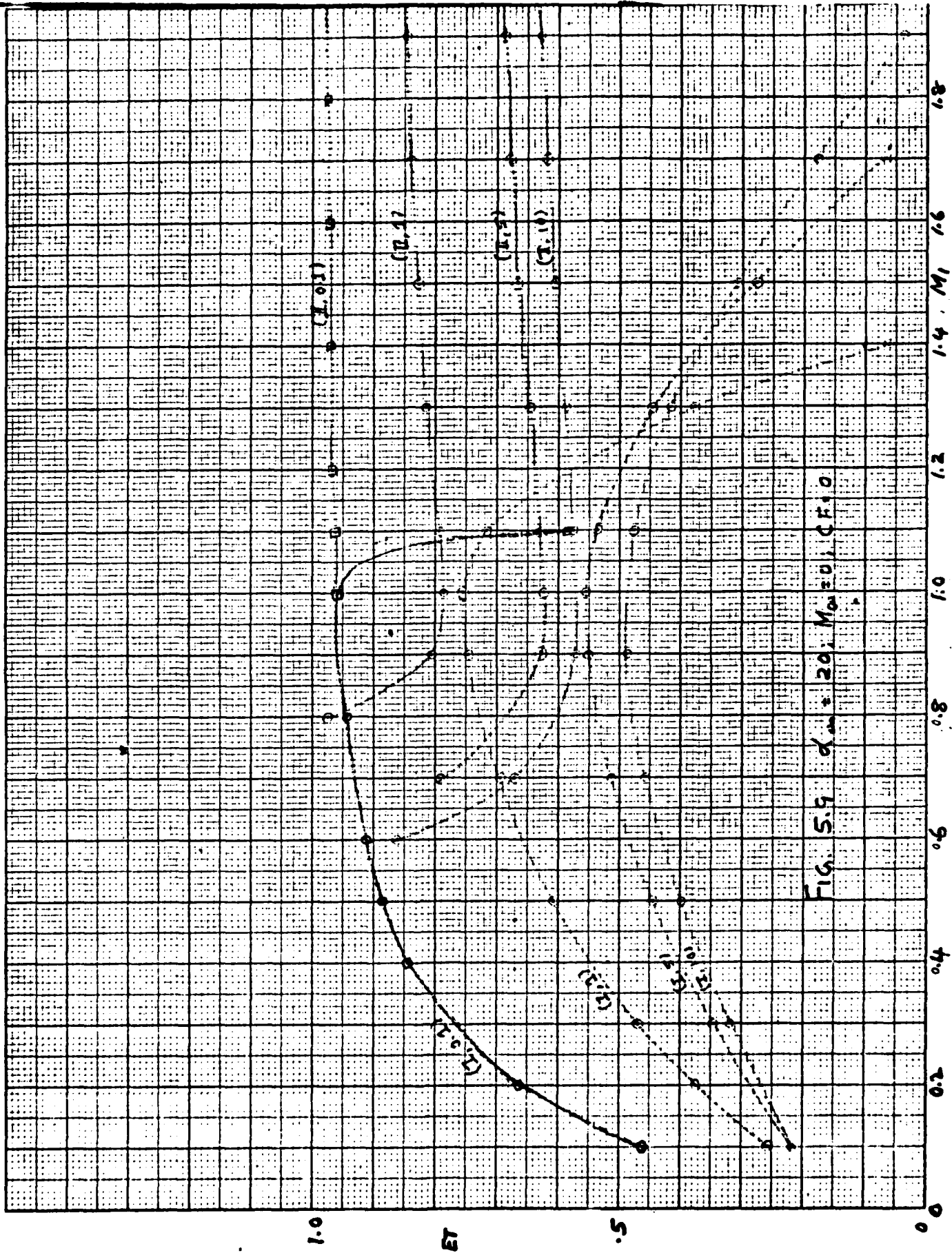


FIG. 5.9  $\alpha_{max} = 20$ ,  $M_{0.0} = 0$ ,  $CF = 0$

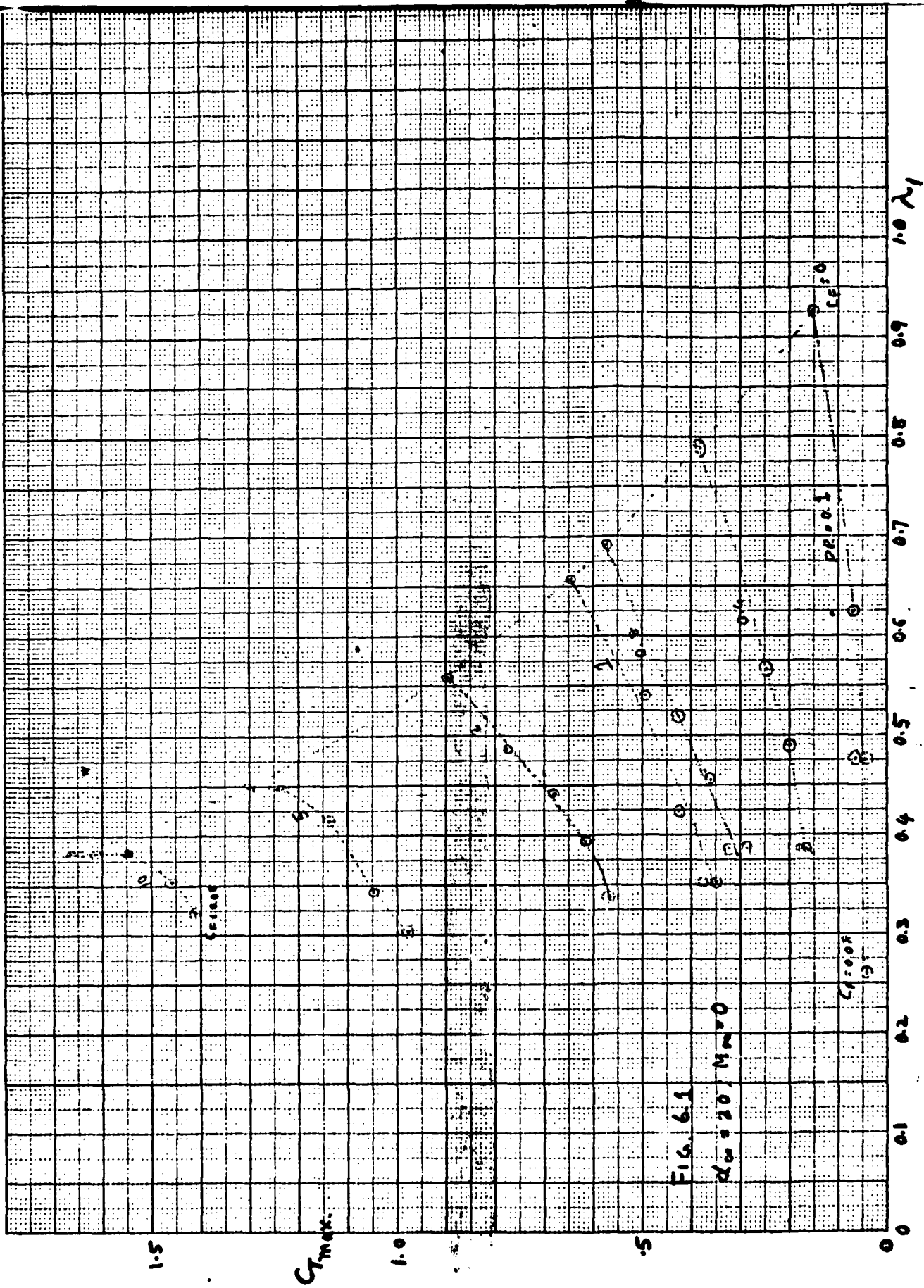


FIG. 6.1

$\alpha_0 = 20, M = 0$

$C_{Tmax}$

$\lambda$

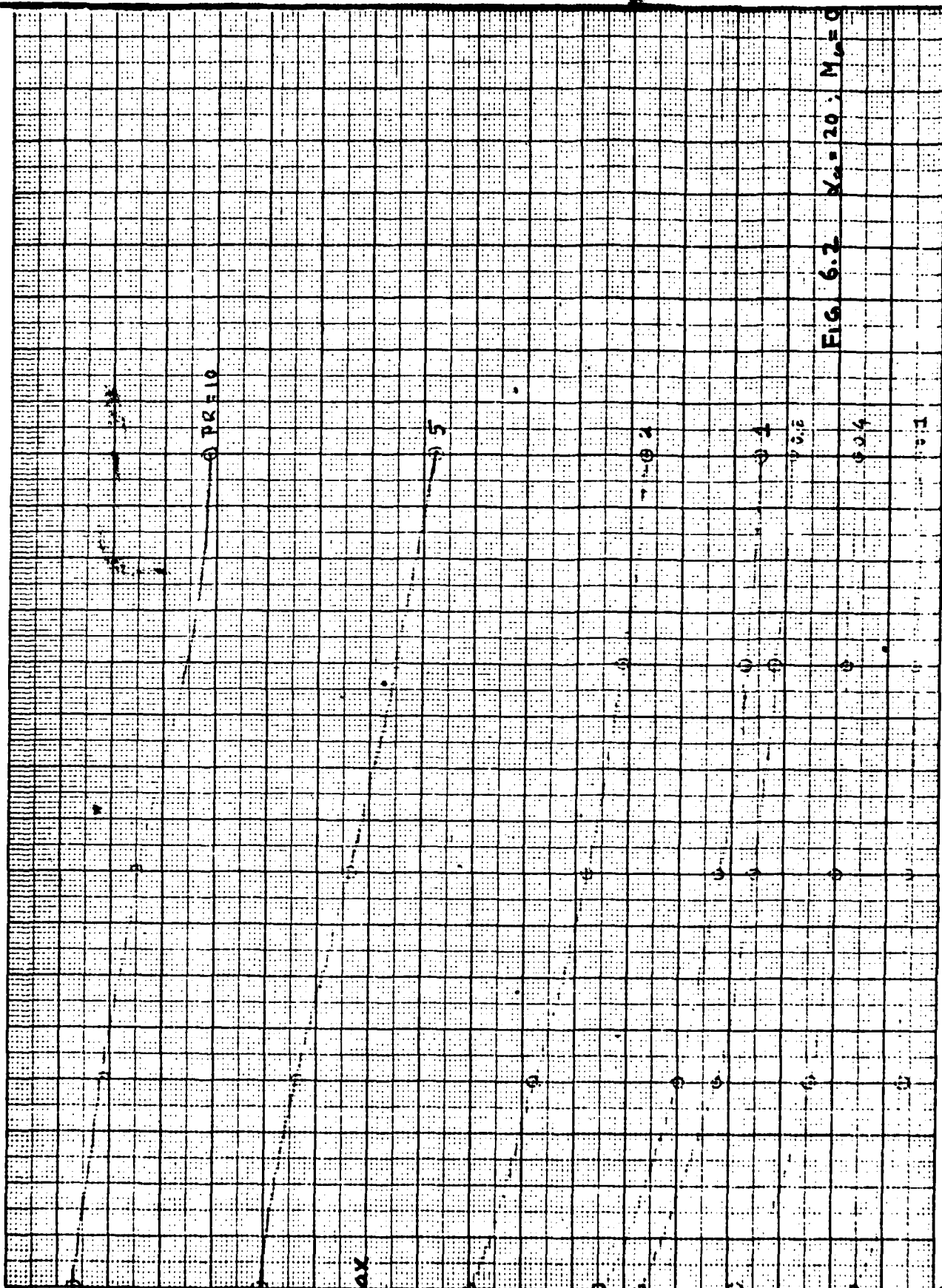


FIG. 6.2  $X_{0.2} = 2.0$ ;  $M_{0.2} = 0$

1.5

$CT_{max}$

1.0

THIS PAGE IS BEST QUALITY PRACTICABLE FROM COPY FURNISHED TO DDG

0.5

0.0

0.16

0.08

0.04

0.0

0.1

0.2

0.4

0.6

0.24

0.10

0.5

0.2

0.4

0.6

0.24

0.10

0.5

0.2

0.4

0.6

0.24

0.10

0.5

0.2

0.4

0.6

0.24

0.10

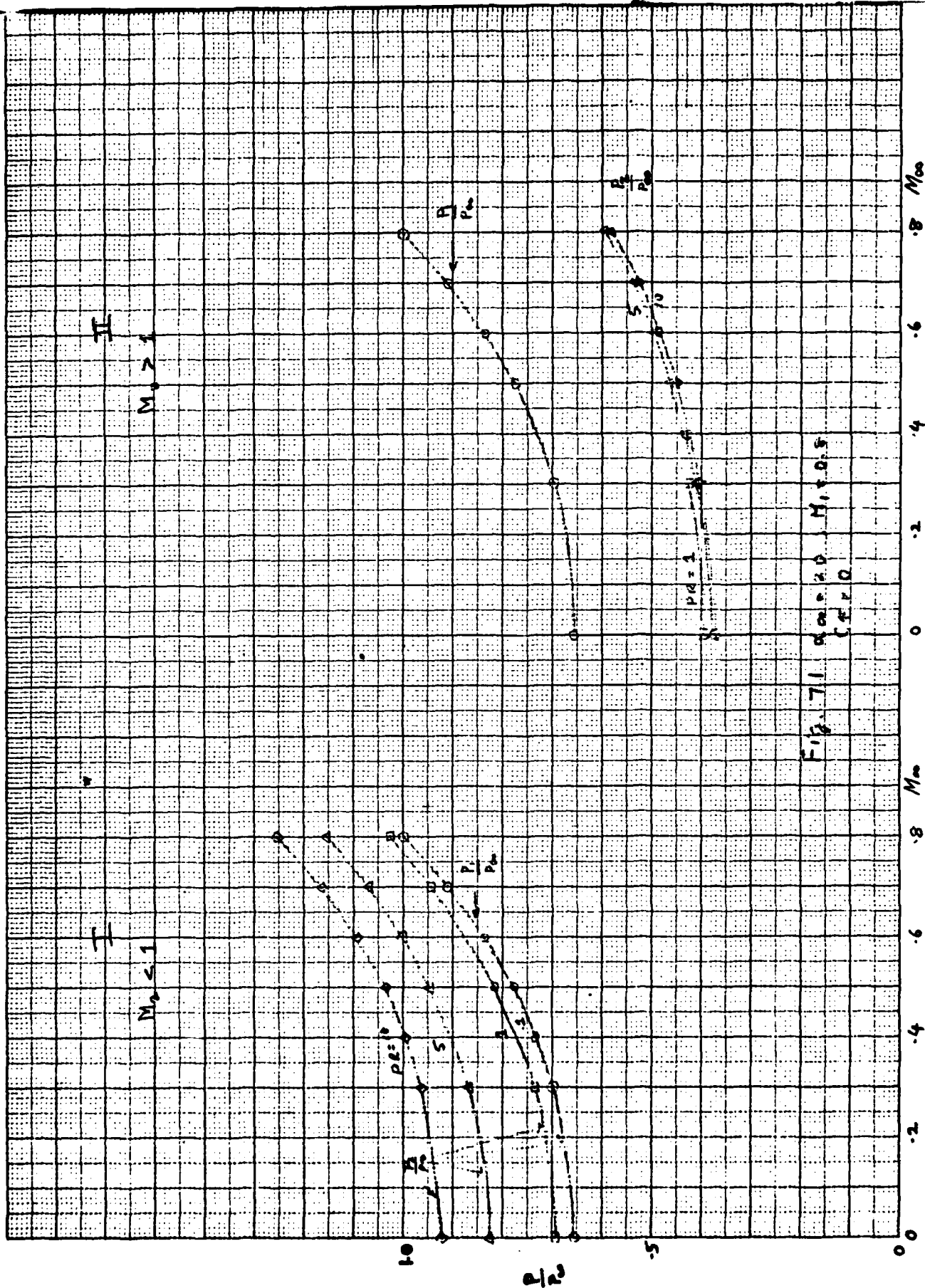


Fig. 71 of course 2.0 M<sub>0</sub> 0.5  
CF 10

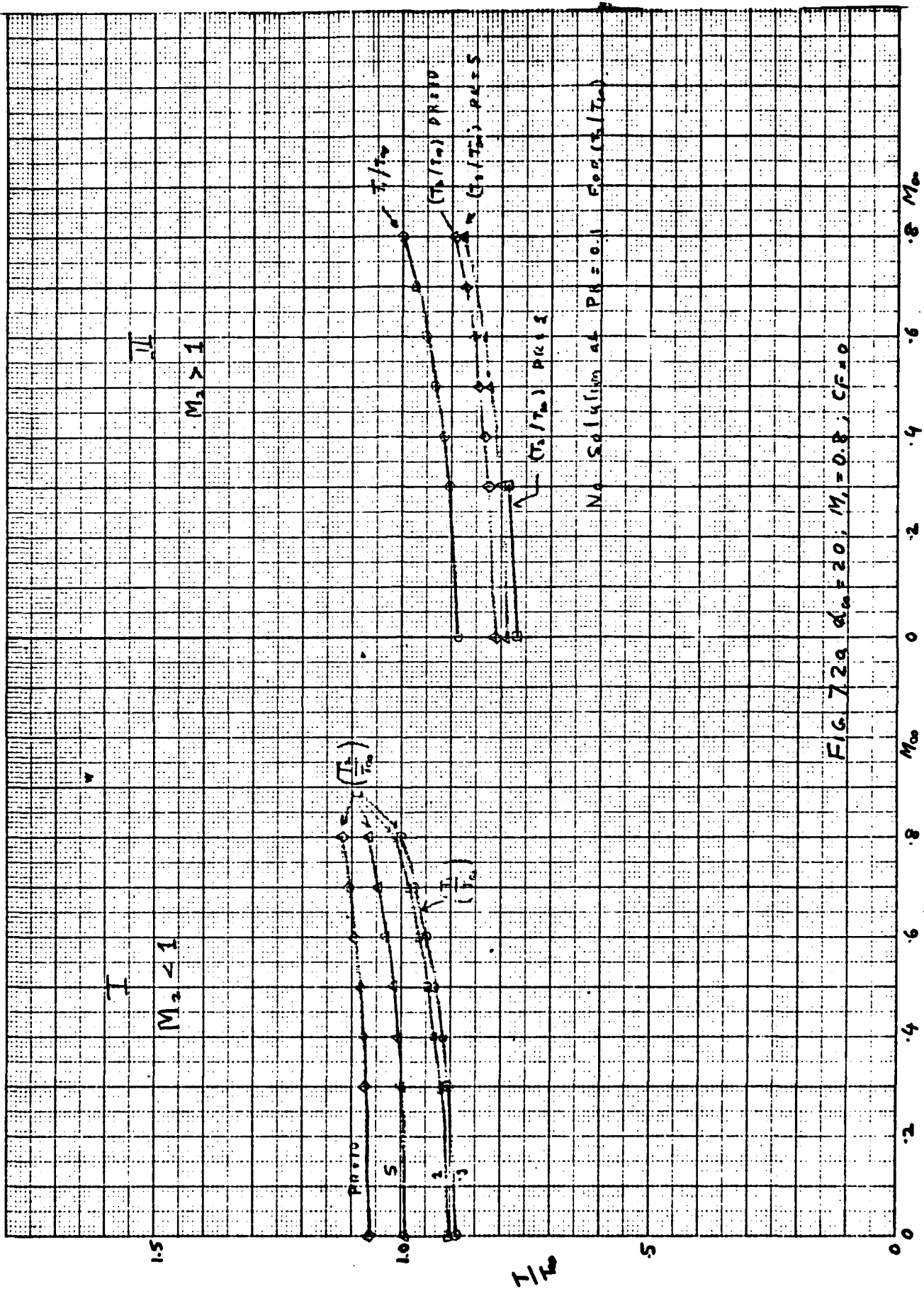


FIG. 729  $\alpha_0 = 20^\circ$ ,  $M_1 = 0.8$ ,  $CF = 0$

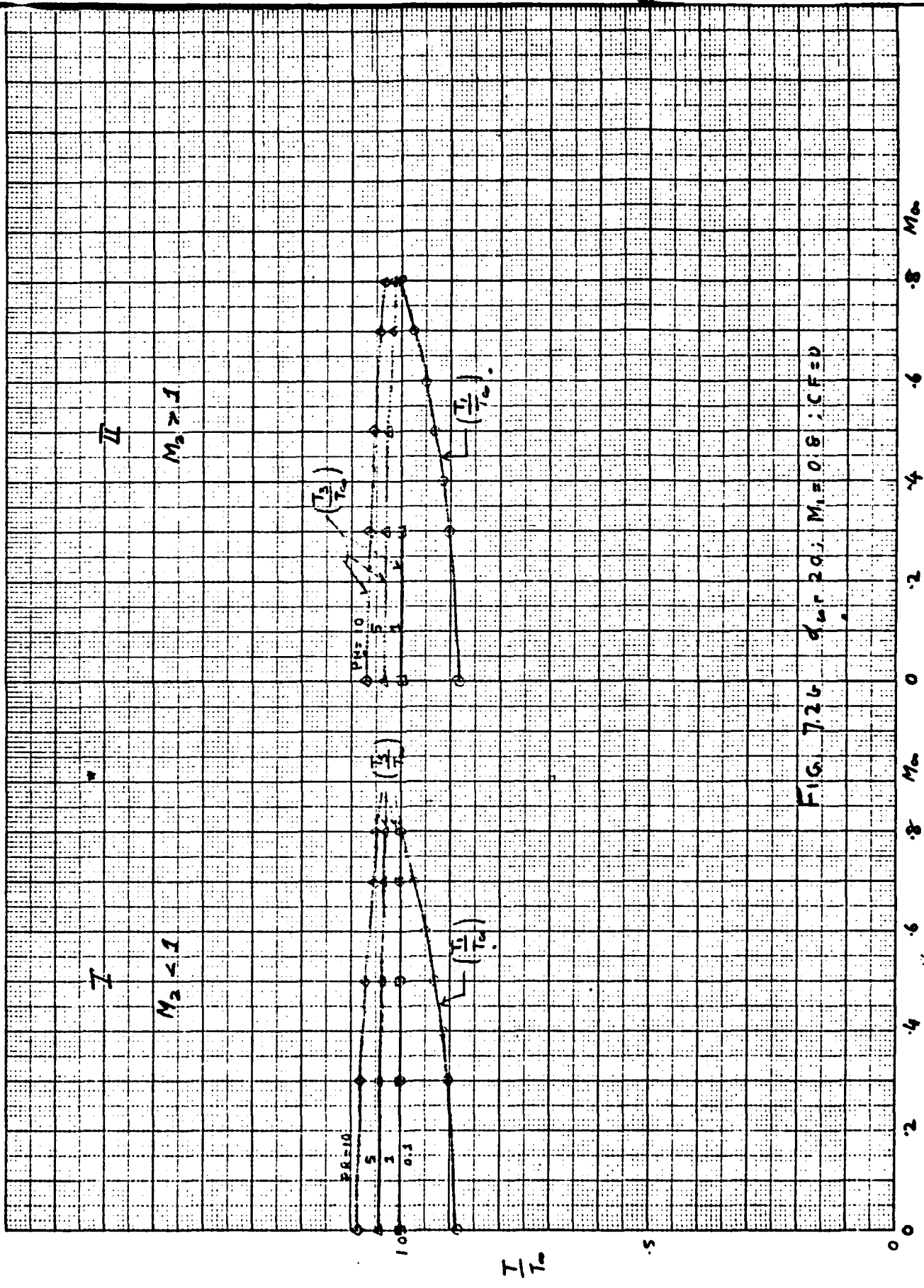


FIG. 7.26  $d_{10} = 20$ ;  $M_1 = 0.8$ ;  $CF = 0$

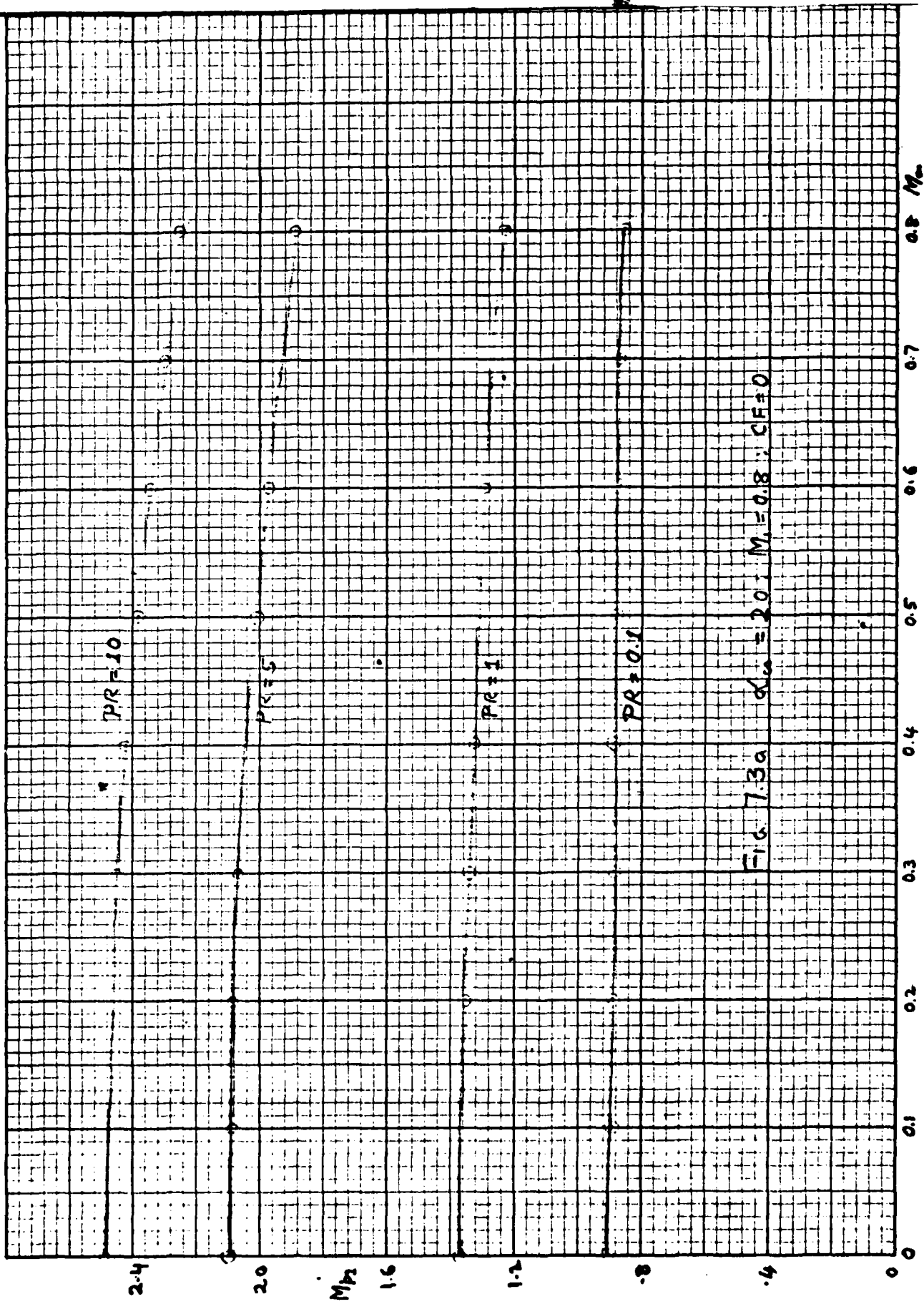
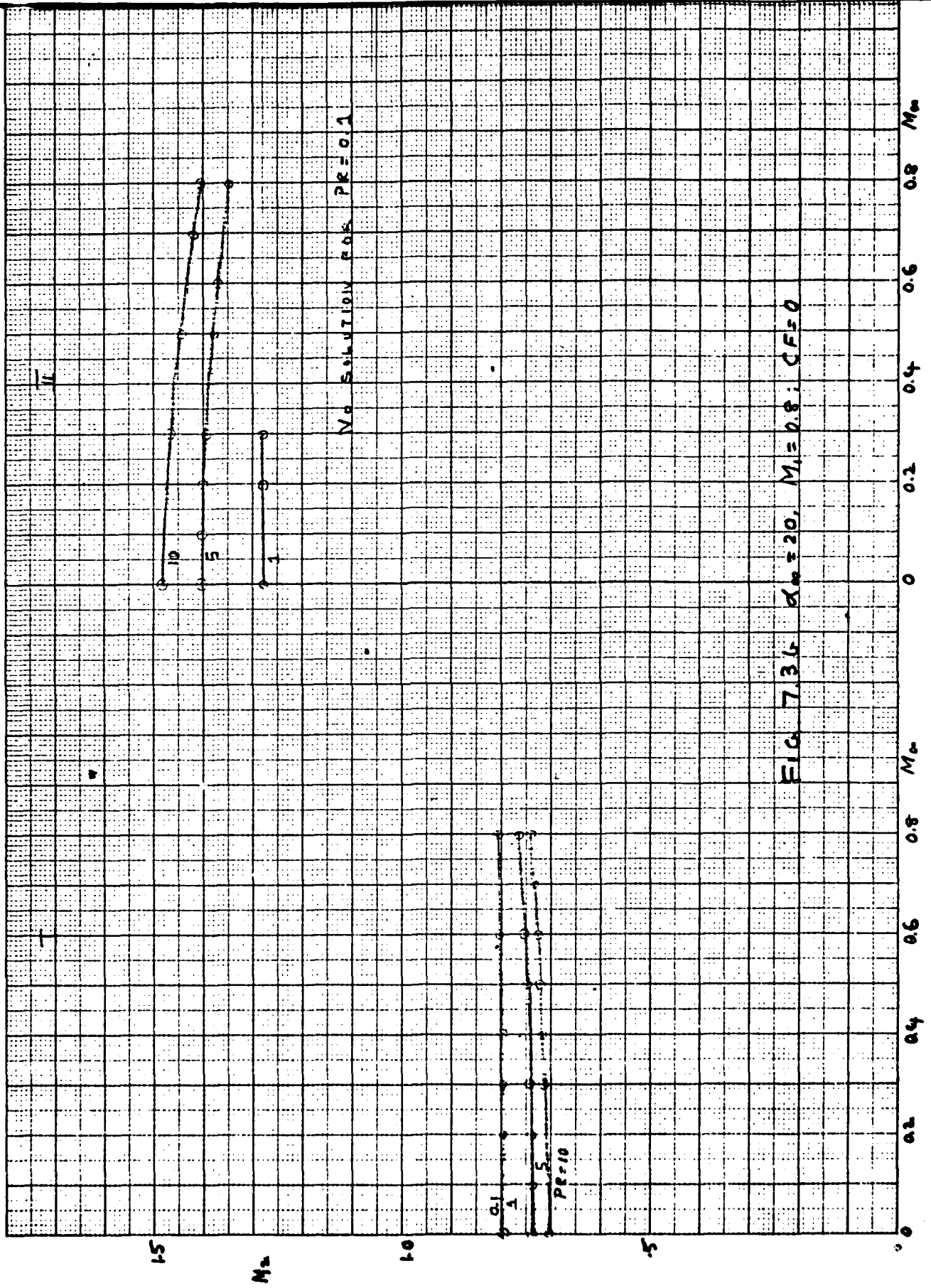


Fig. 7.3a  $\alpha_{60} = 20$ ;  $M_1 = 0.8$ ;  $CF = 0$



NO SOLUTION FOR  $PR=0.1$

FIG. 7.36.  $\alpha_n = 20$ ,  $M_1 = 0.8$ ,  $CF = 0$

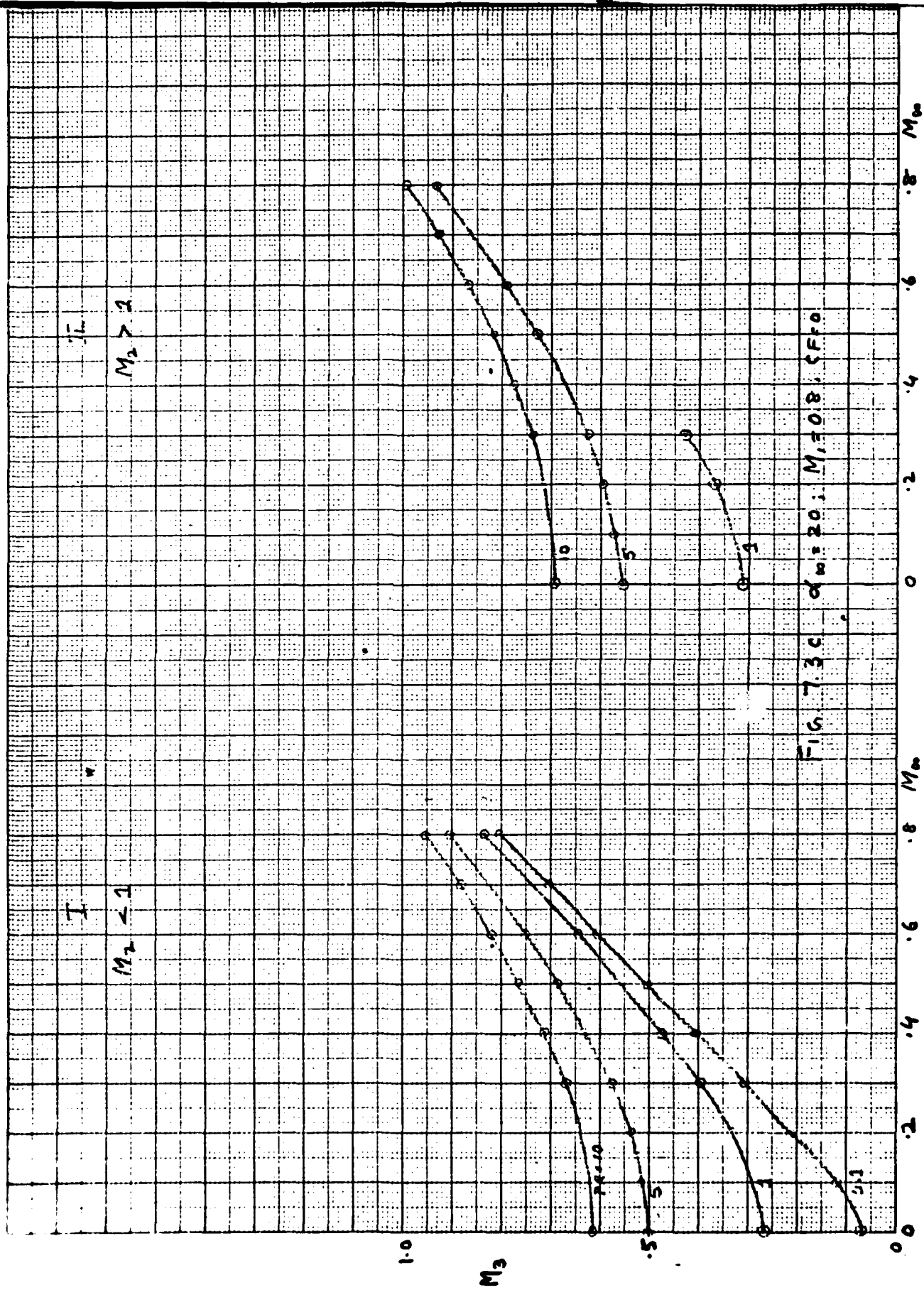


FIG. 7.3c.  $\alpha_w = 20$ ;  $M_1 = 0.8$ ;  $\zeta = 0$

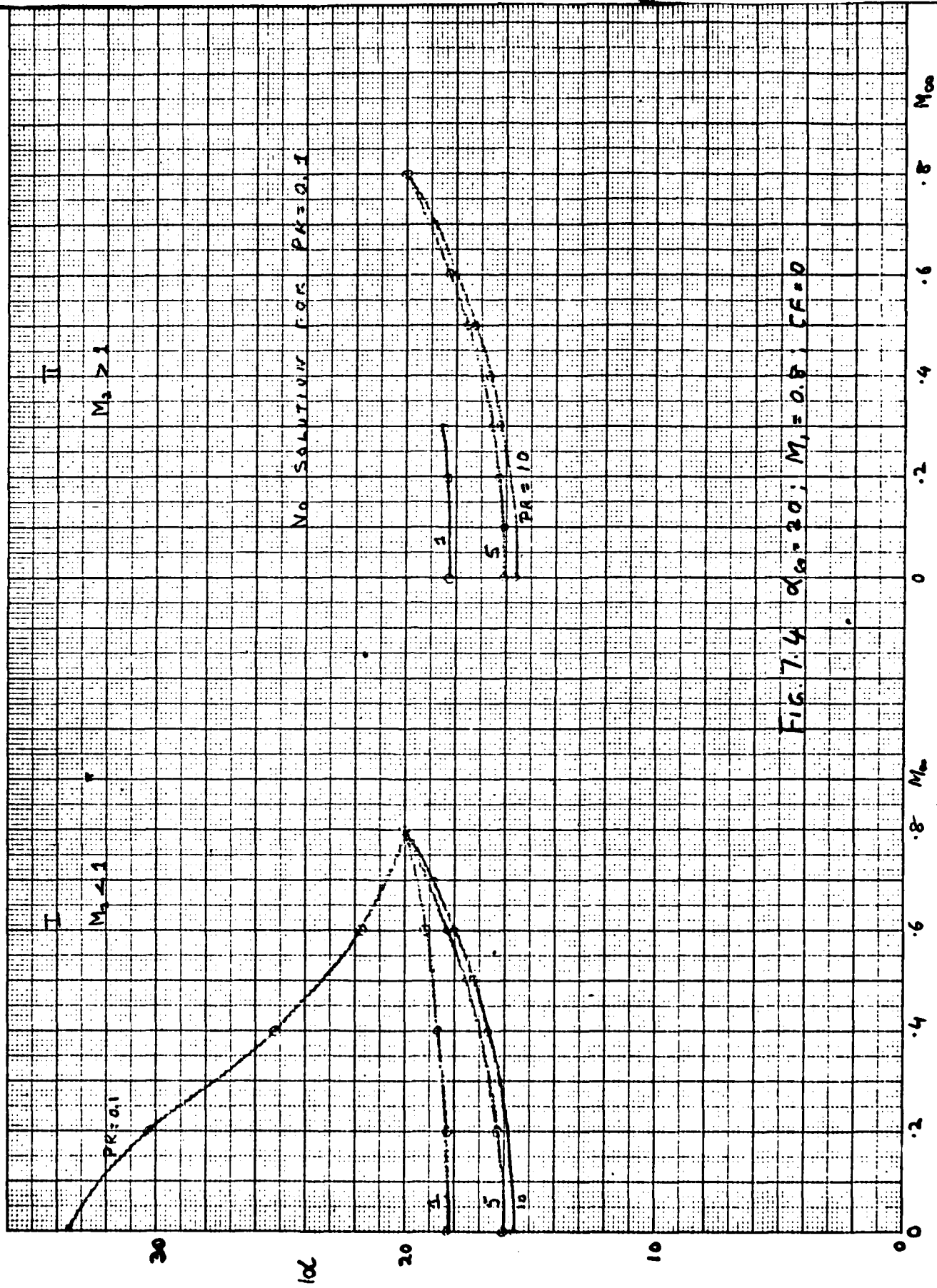


FIG. 7.4  $\alpha_{00} = 20$ ;  $M_1 = 0.8$ ;  $CF = 0$

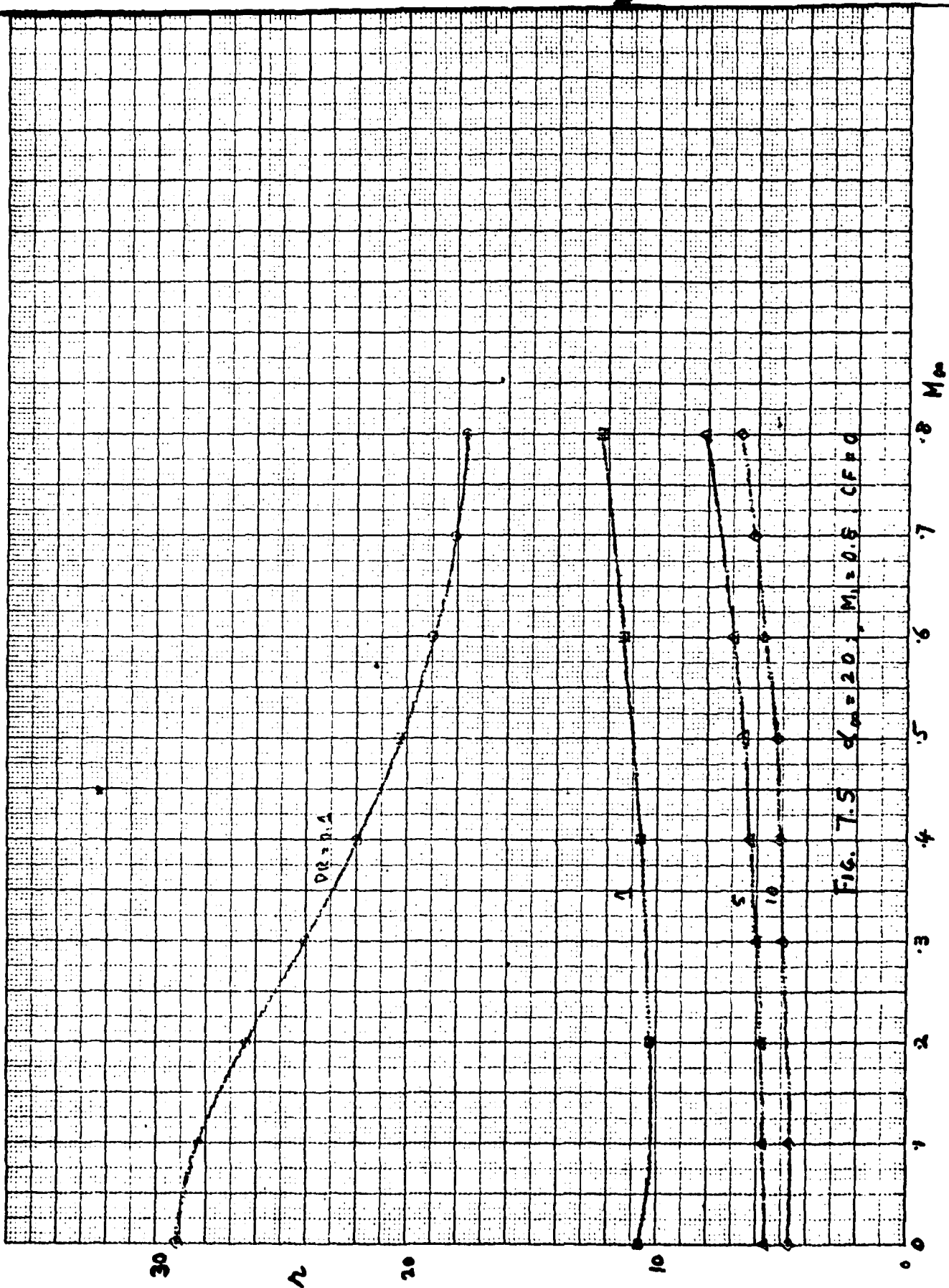
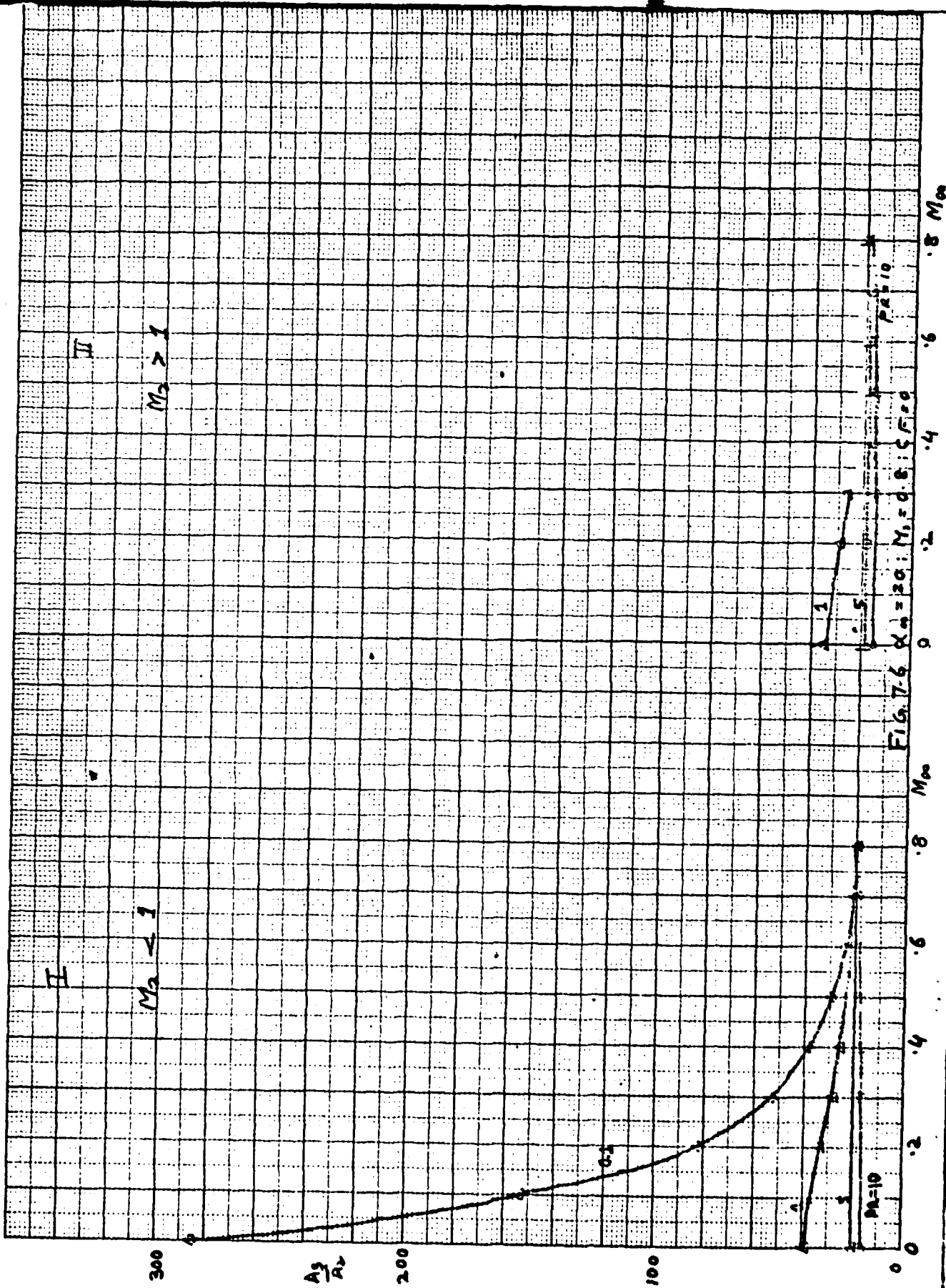


FIG. 7-5  $\alpha_m = 20$ ,  $M_1 = 0.8$  CFB



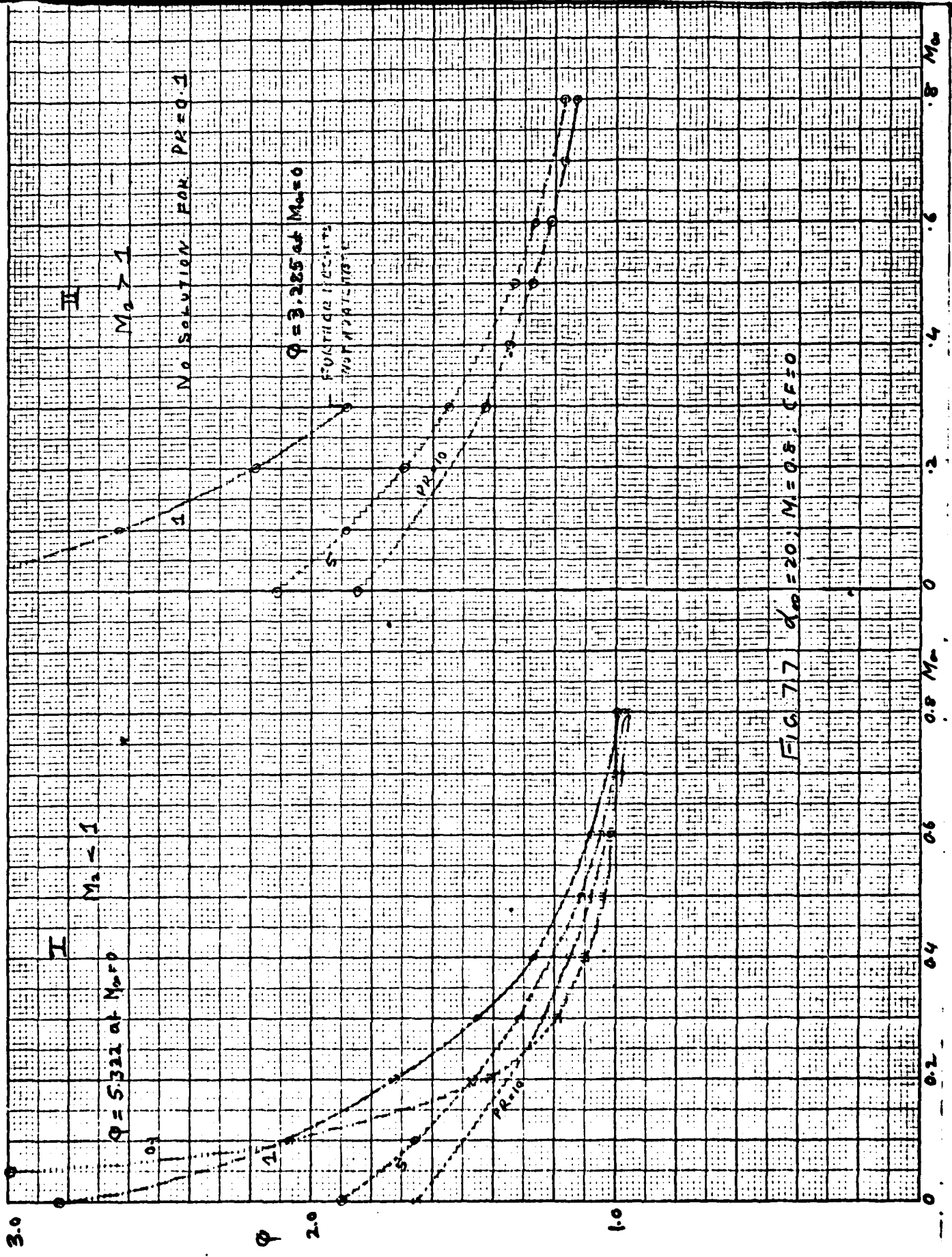
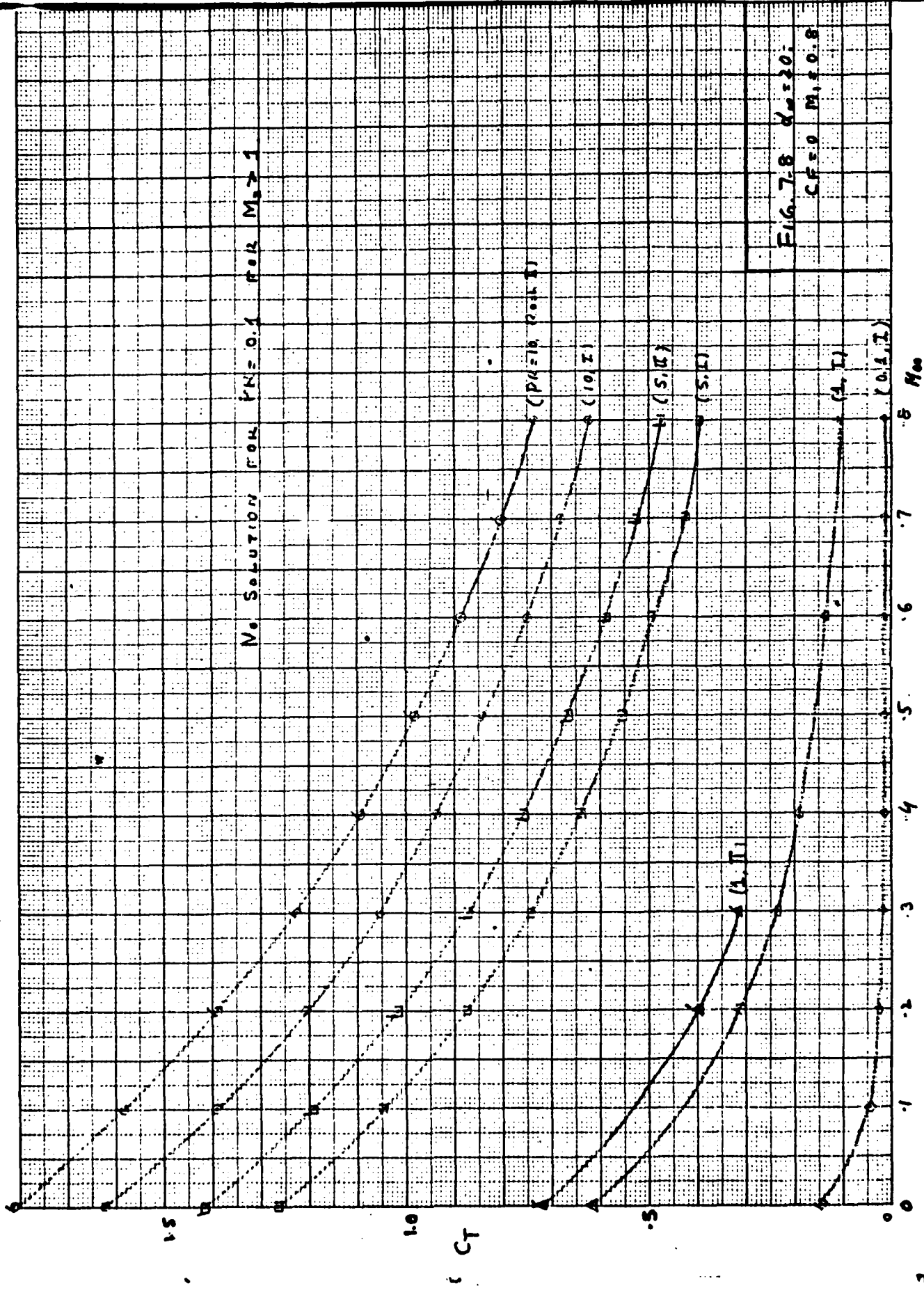
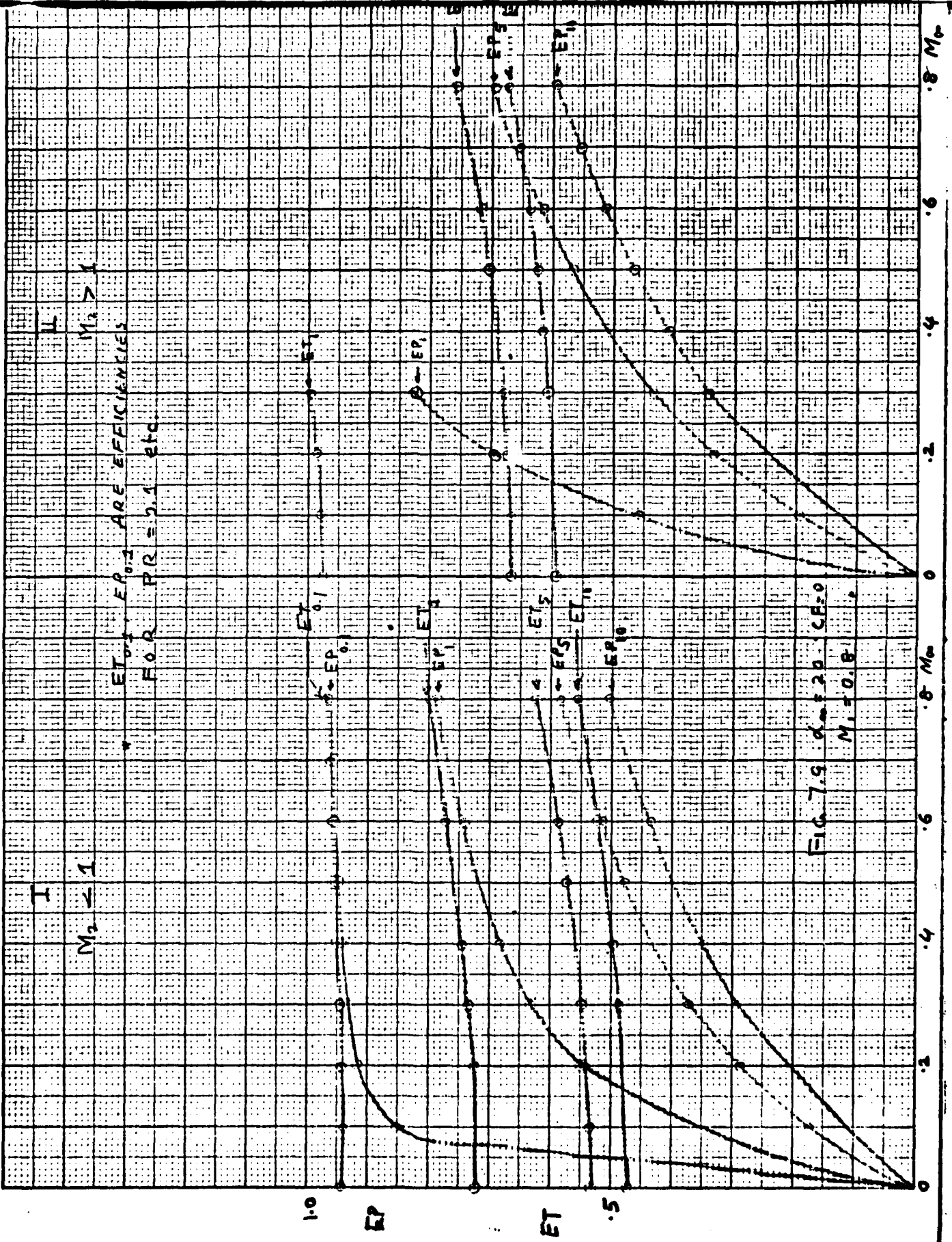


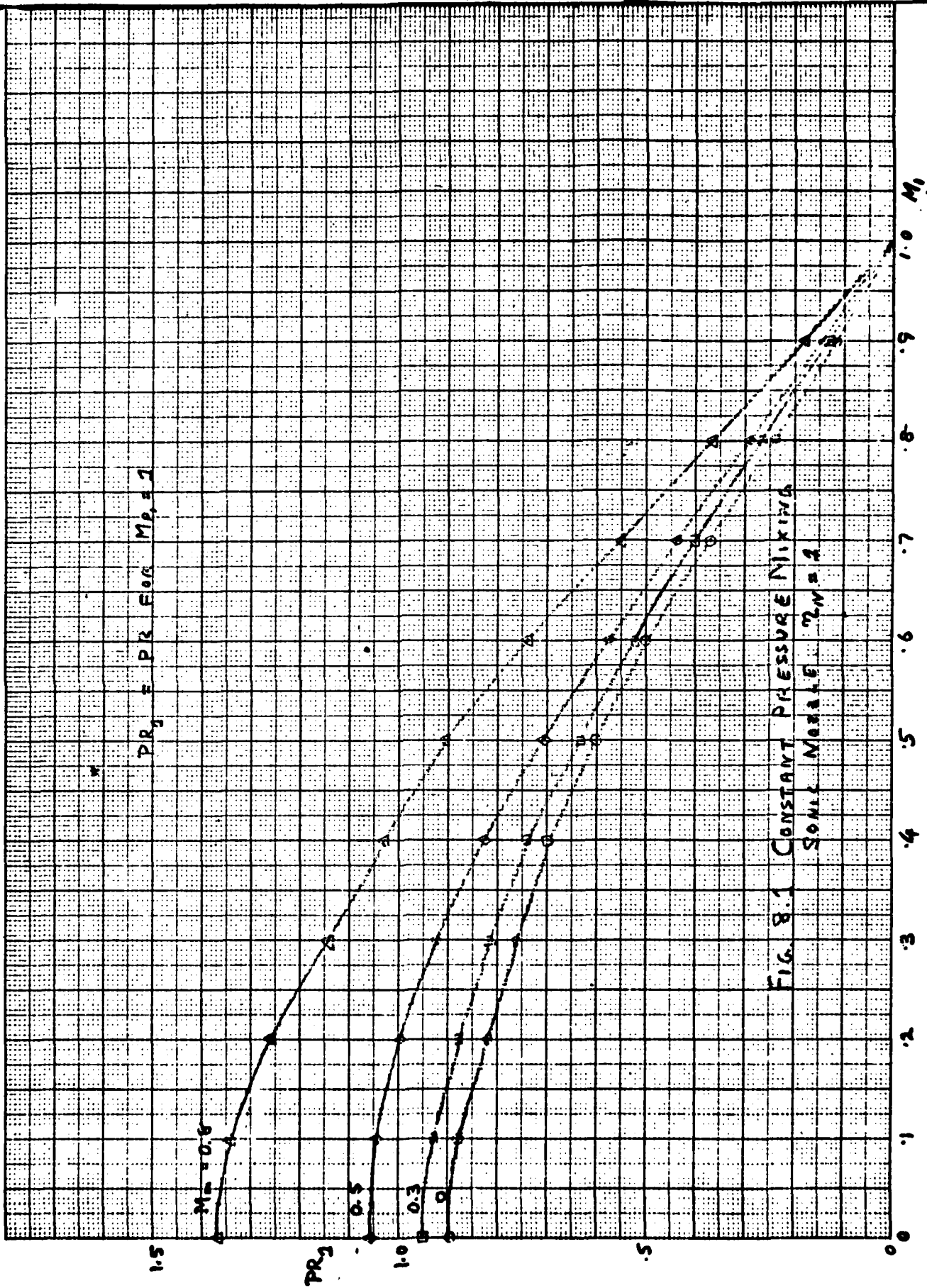
FIG. 77  $d_m = 20; M = 0.8; C_F = 0$



No. SOLUTION FOR  $\gamma_N = 0.1$  FOR  $M_N > 1$

FIG. 7-8  $\alpha_w = 20$   
 $CF = 0$   $M_1 = 0.8$





$PR_2$  F PR FOR  $M_n = 1$

FIG. 8.1 CONSTANT PRESSURE MIXING  
SOME MOLE  $M_n = 1$

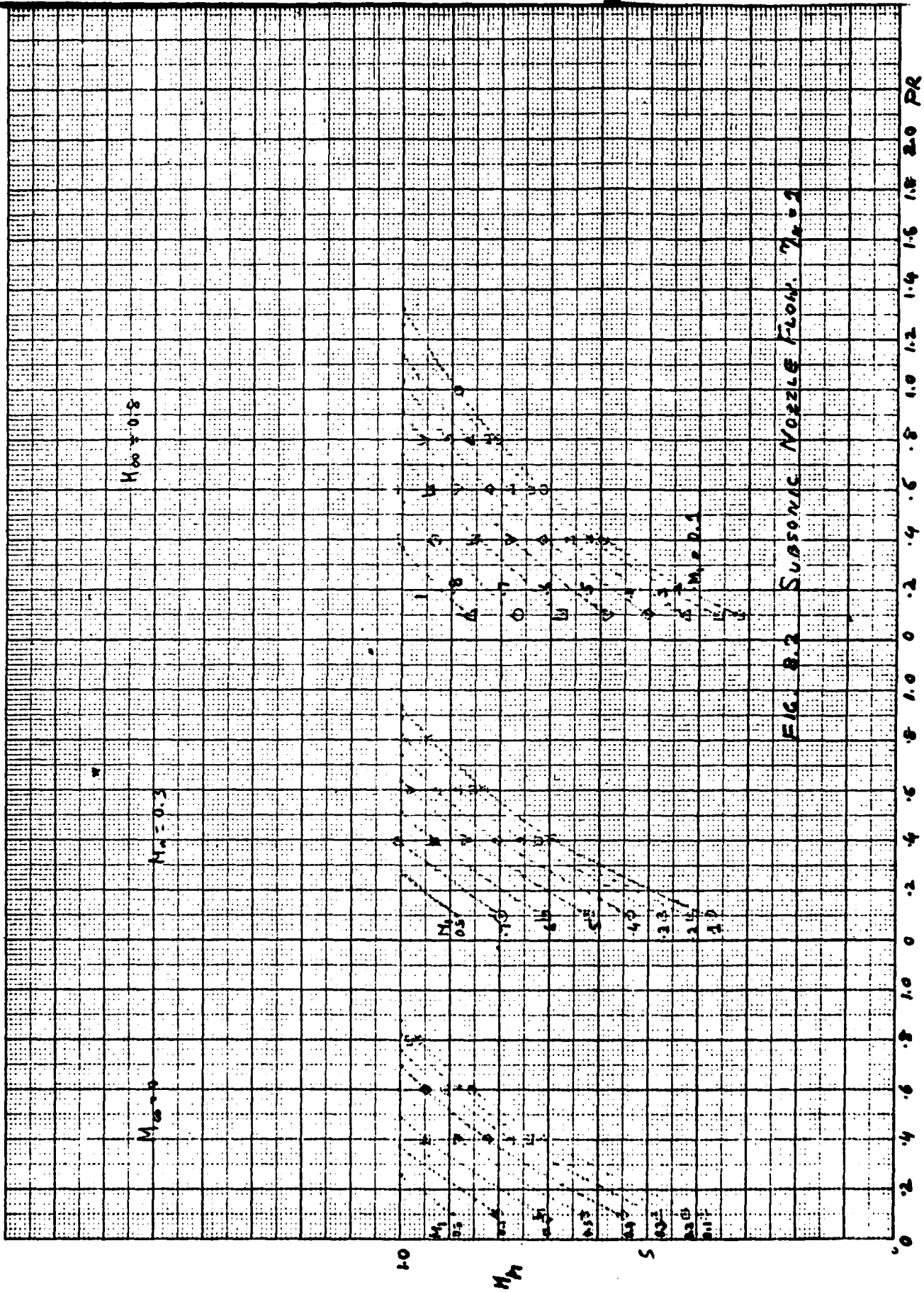


FIG. 8.2 SUBSONIC NOZZLE FLOW.  $\gamma = 1.4$

0 0.2 0.4 0.6 0.8 1.0 1.2 1.4 1.6 1.8 2.0 PR

# SUBSONIC MIXING

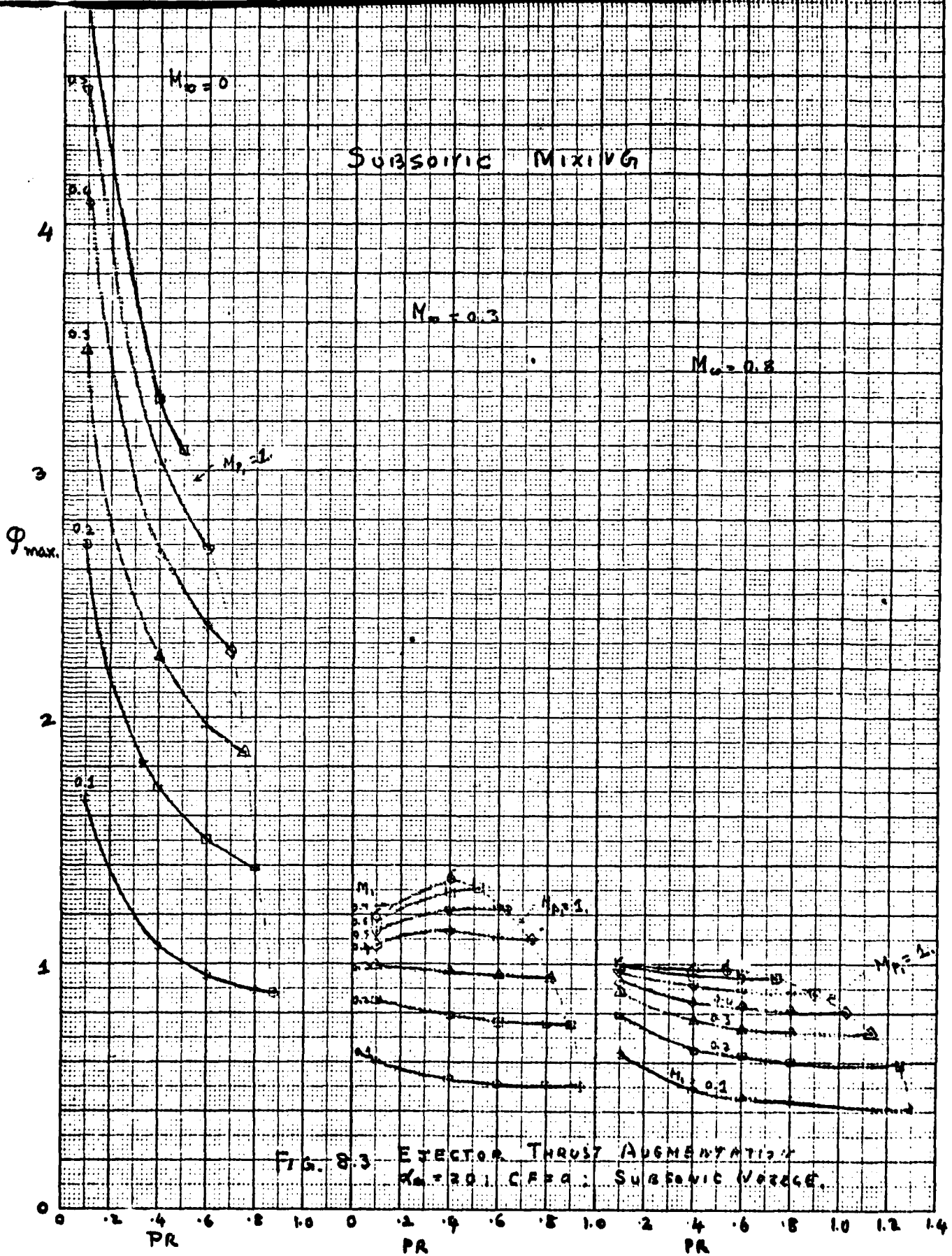
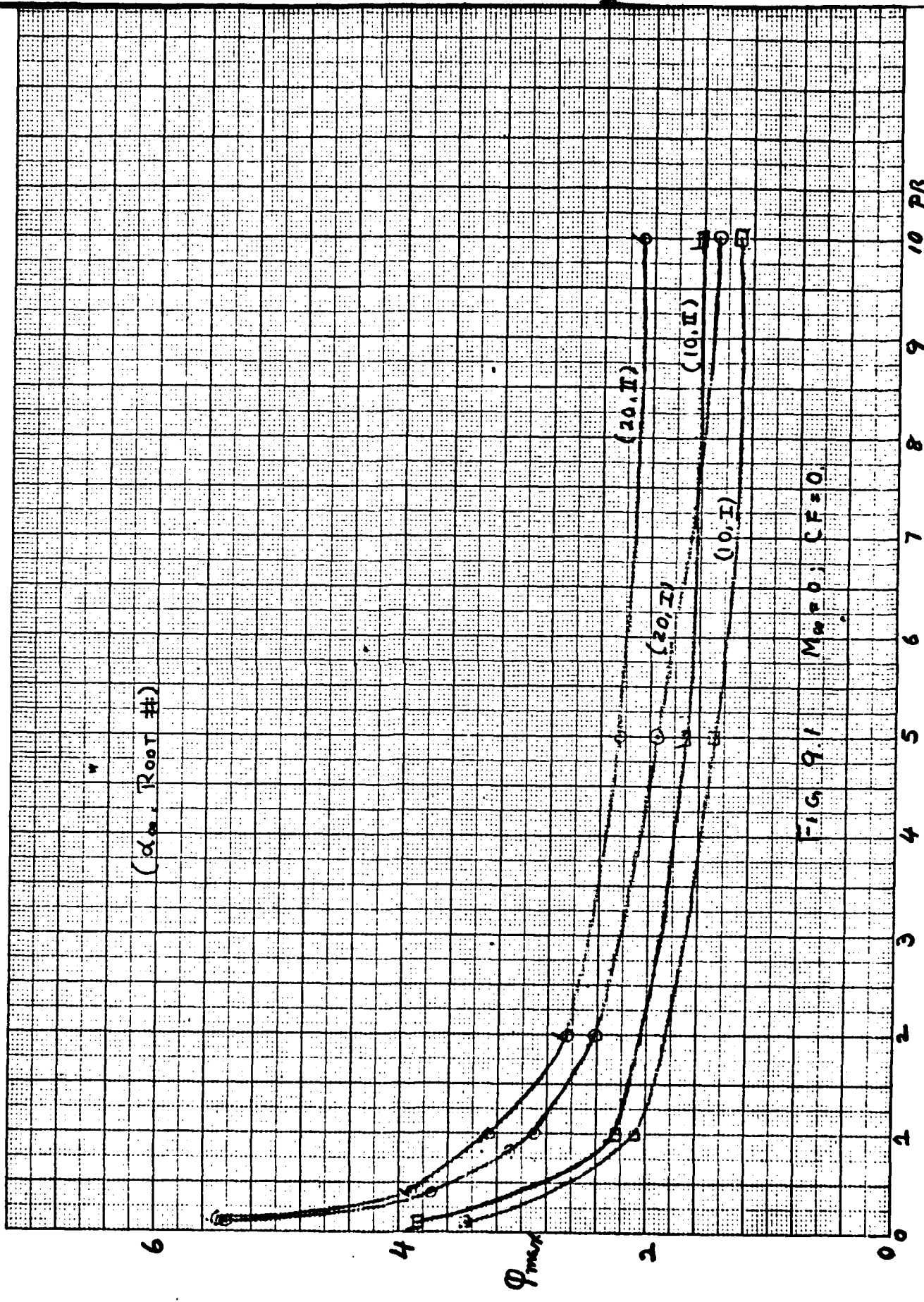


FIG. 8.3 EJECTOR THRUST AUGMENTATION  
 $\gamma = 1.4$ ,  $C_F = 0$ : SUBSONIC MIXING.



( $\alpha_m$ , Root #)

FIG. 9 /  $M_\infty = 0$ ;  $CF = 0$

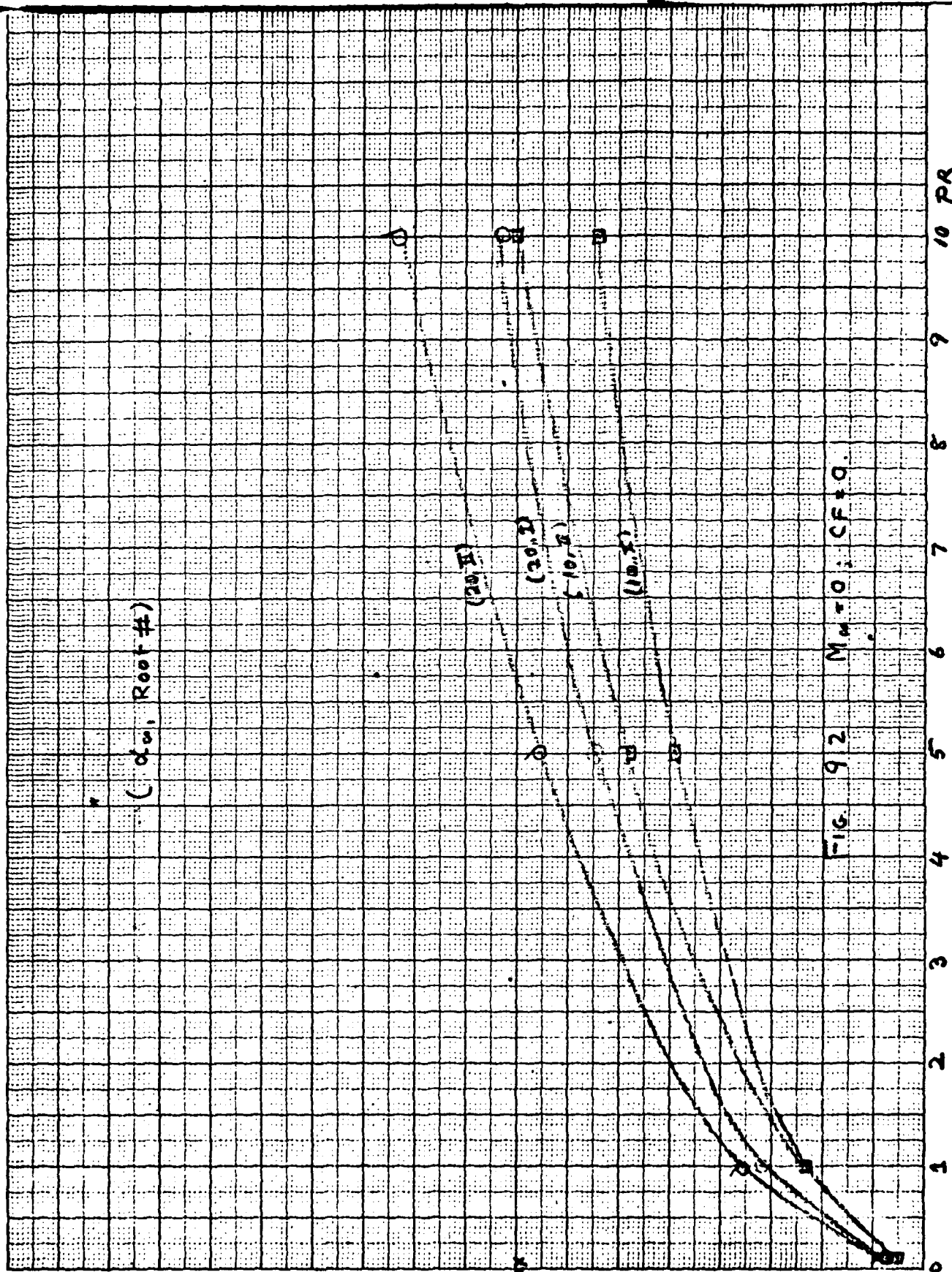


FIG. 92  $M_w = 0$ ;  $CF = 0$ .

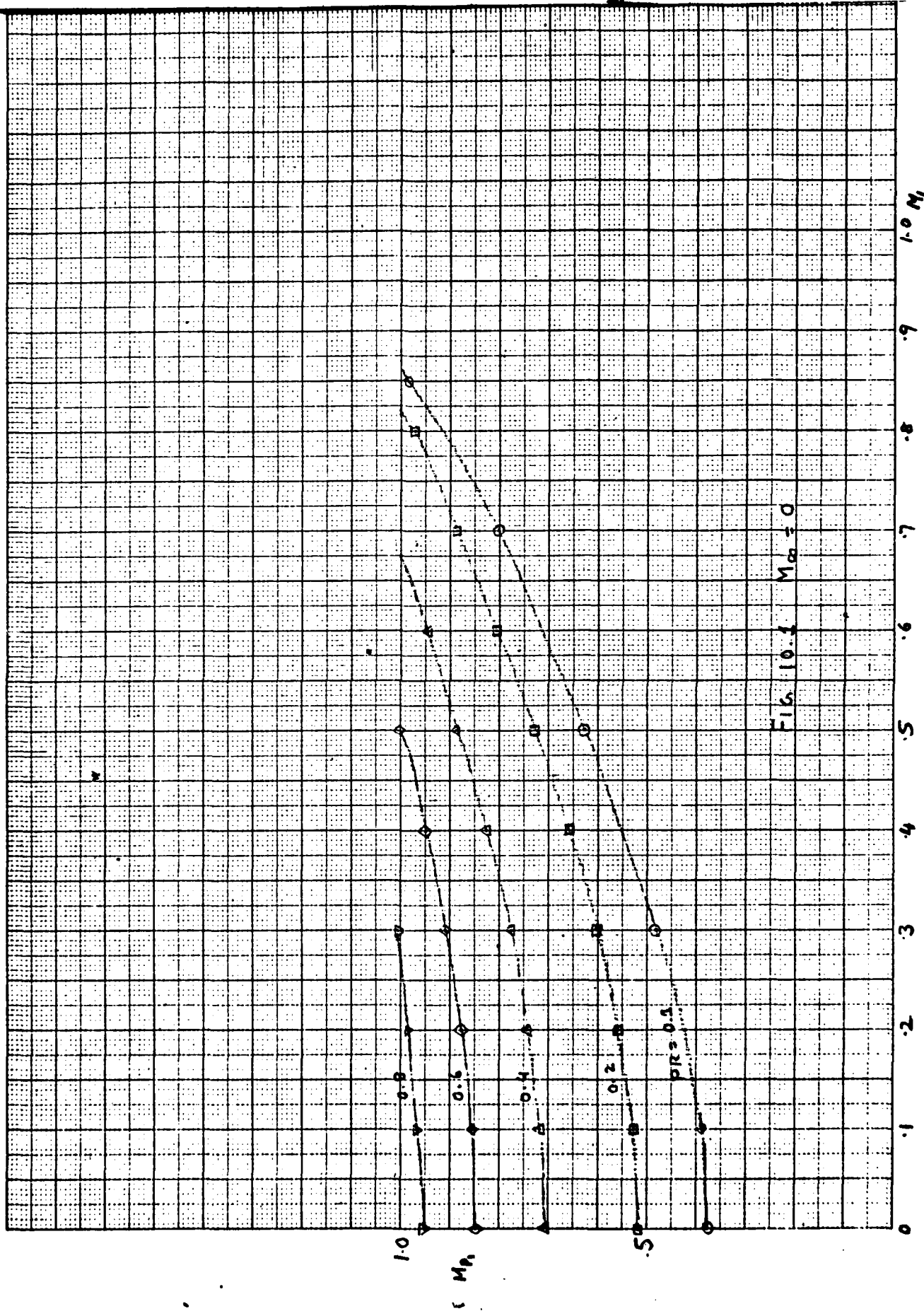


Fig. 10.1  $M_{00} = 0$

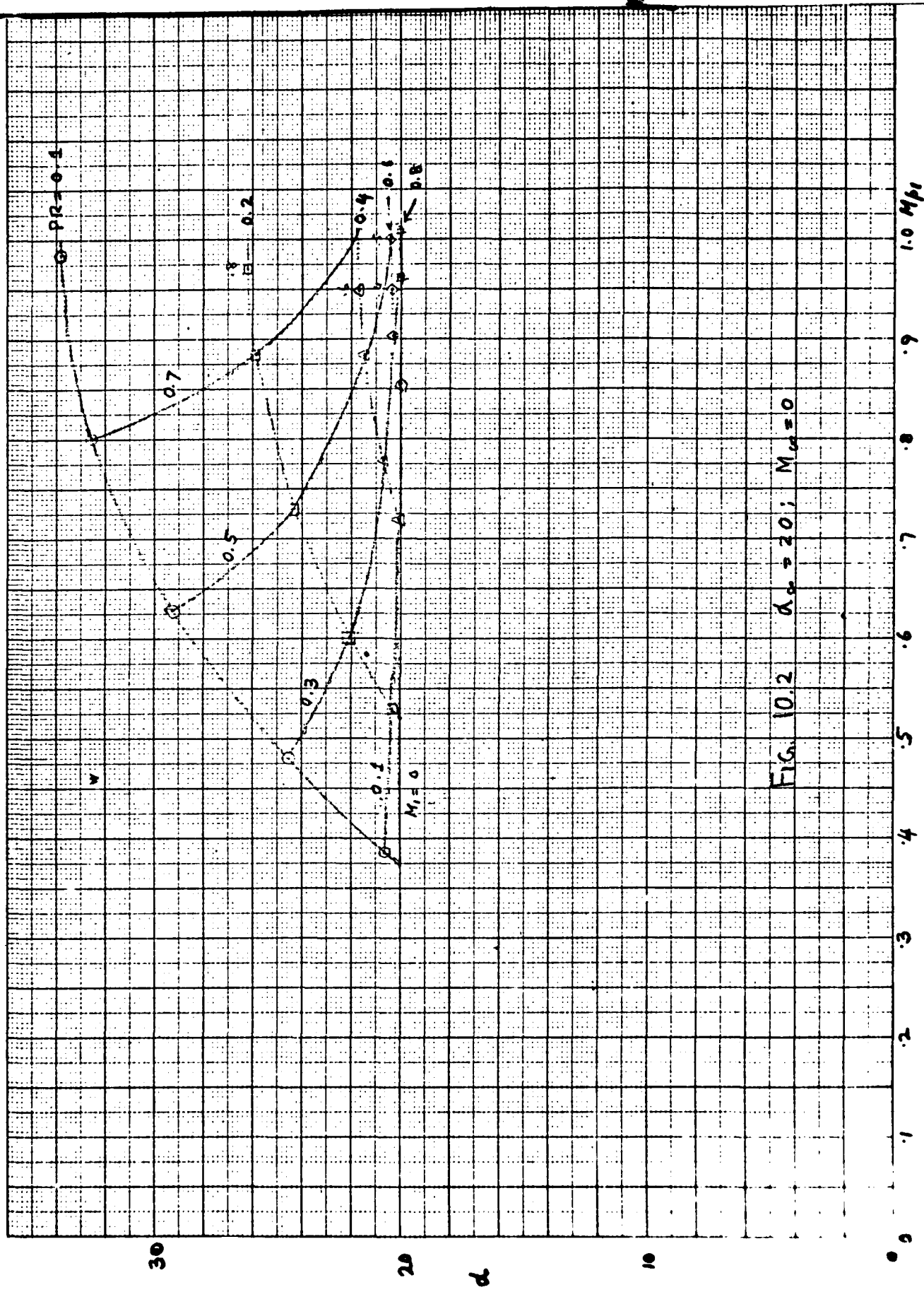


FIG. 10.2  $\alpha_0 = 20$ ;  $M_0 = 0$

1.0 Mpi

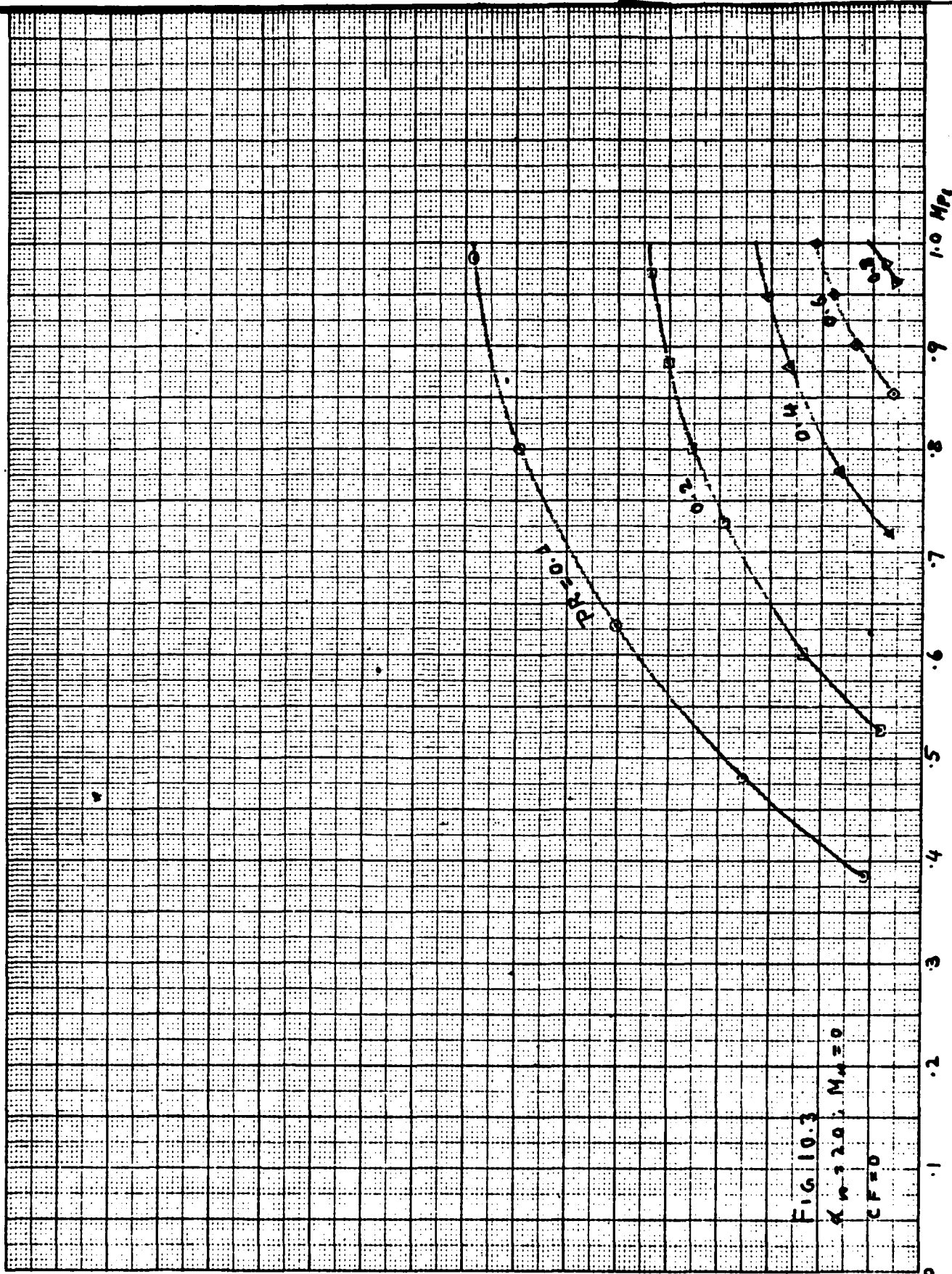


FIG 10.3

$\alpha = 20^\circ, M_1 = 0$

$CF = 0$

10

$A_3/A_2$

5

0.0

1.0 MFL

.9

.8

.7

.6

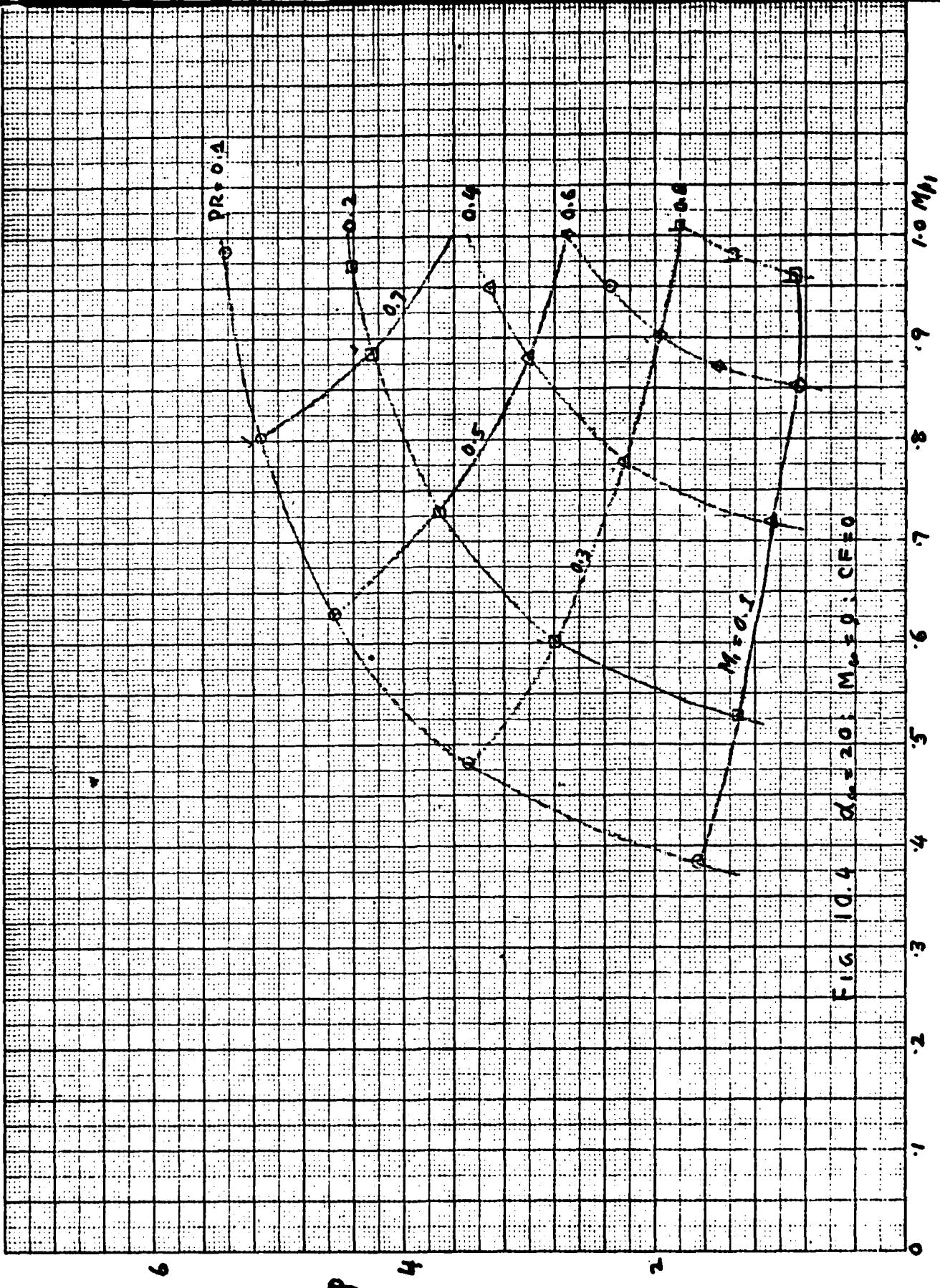
.5

.4

.3

.2

.1



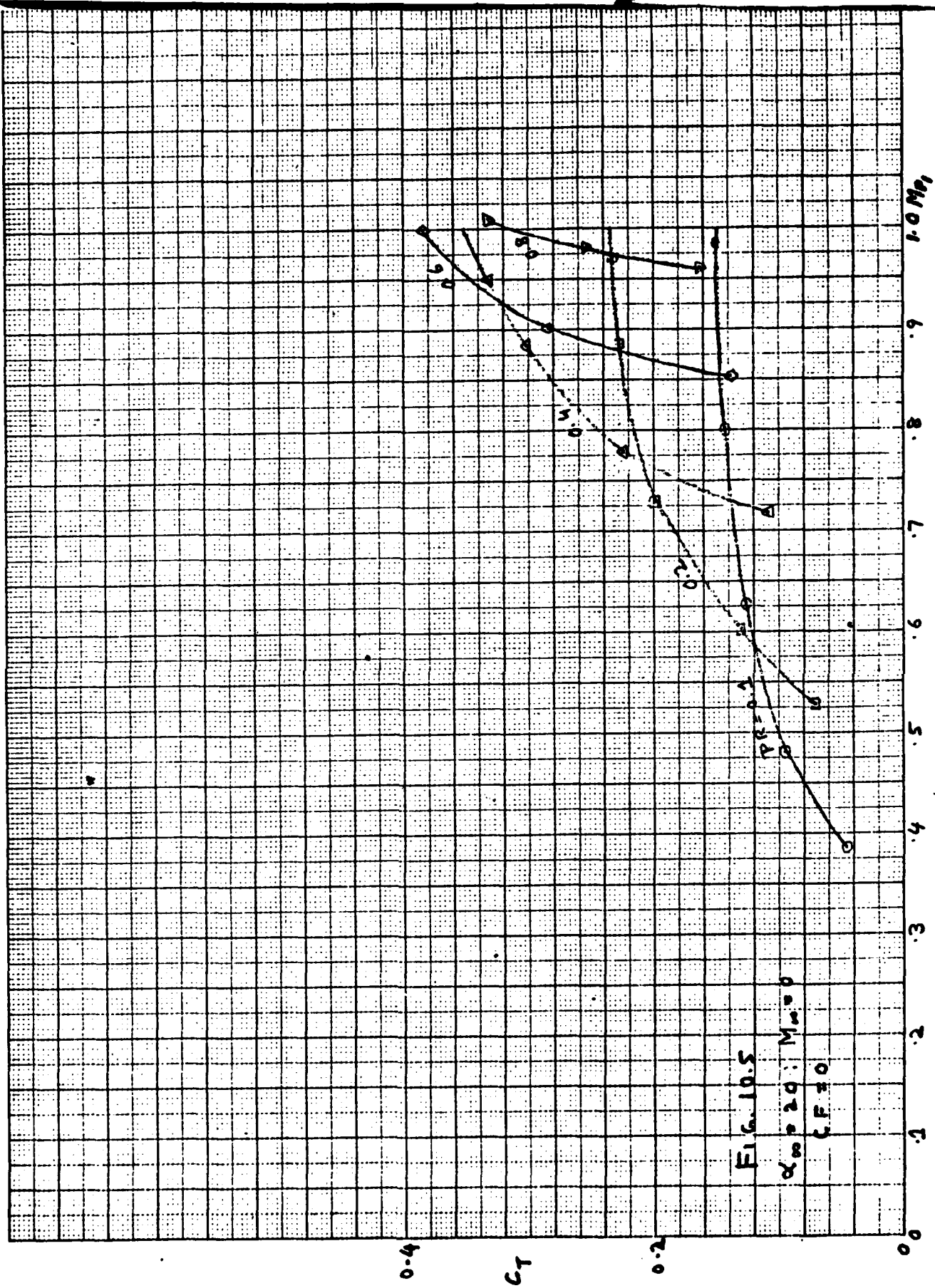


FIG. 10.5

$M_{\infty} = 2.0$ ;  $M_{\infty} = 0$

$CF = 1.0$

**1979 USAF - SCEEE SUMMER FACULTY RESEARCH PROGRAM**

**Sponsored by the**

**AIR FORCE OFFICE OF SCIENTIFIC RESEARCH**

**Conducted by the**

**SOUTHEASTERN CENTER FOR ELECTRICAL ENGINEERING EDUCATION**

**FINAL REPORT**

**OPTIMUM DESIGN OF BUILT-IN-TEST DIAGNOSTIC SYSTEM**

<b>Prepared By:</b>	<b>Adel A. Aly</b>
<b>Academic Rank:</b>	<b>Associate Professor</b>
<b>Department and University:</b>	<b>School of Industrial Engineering - University of Oklahoma</b>
<b>Research Location:</b>	<b>Rome Air Development Center-Reliability and Compatibility Division-Reliability Branch-Reliability and Maintainability Engineering Techniques Section.</b>
<b>USAF Research Colleague:</b>	<b>Jerome Klion</b>
<b>Contract No:</b>	<b>F49620-79-C-0038</b>

# OPTIMUM DESIGN OF BUILT-IN-TEST DIAGNOSTIC SYSTEM

By

ADEL A. ALY

## ABSTRACT

In this report, the problem of cost effective design of diagnostic and fault isolation procedures for BIT systems is investigated. The cost of BIT varies from a group of LRU's to another; also the probability of failure for LRU's within the module are different. The problem is to find the optimum sequence of tests (BIT) to be executed to isolate a failed unit such that the expected cost is minimized.

An optimum procedure based on Branch-and-Bound concept are developed. Several dominance and reductions rules are introduced. A small example is solved to demonstrate the efficiency of the developed algorithm.

### ACKNOWLEDGMENTS

The author wishes to express his appreciation to the U.S. Air Force Systems Command, Air Force Office of Scientific Research for providing the Summer Faculty Research Fellowship which made this research possible. The author is also grateful to RADC-RB division Chief, Col. David Luke and RADC-RBRT section Chief Mr. Anthony Coppola for their sincere hospitality. A special word of appreciation is given to Mr. Jerome Klion, USAF Research Colleague, for providing this research topic, his time, guidance, and encouragement during the course of this research. Appreciation is also extended to Dr. Richard N. Miller, SCEEE Director and his staff for their fine administration of SFRP.

## I. INTRODUCTION

The problem of fault isolation techniques has not advanced noticeably during the last two decades. The basic process existed was the manual signal tracing. This process relies heavily on the technical expertise of the maintenance technician. Even with highly skilled personnel this process is slow and difficult since it requires a large array of test equipment such as signal generators, oscilloscopes and voltmeters as well as extensive technical manuals. As a consequence many faults are not correctly diagnosed, also the extensive use of trial and error substitution as a means of identifying the faulty part.

Due to the above reasons, too much time is devoted to the fault isolation process which leads to reducing the systems availability. With the advance of the integrated circuit, the imminent LSI era, and a better packaging techniques the modular concept was introduced to a primary system. Therefore, the problem of diagnosis is shifted from locating the faulty discrete component to the identification of the line replaceable unit (LRU) in which the faulty component is resident. LRU may include smaller modules within it to facilitate - off - line replacement or it can itself be the lowest level of replacement.

The introduction of the digital computers and micro processors as part of the system provide an automatic testing procedure. Basically, the design of built - in - test (BIT) diagnostic subsystems along with the selection of test points where the test equipment are attached will provide an efficient, less expensive, and more reliable fault isolation procedure.

In this report, the optimal design for an on-aircraft (or a ground electronic equipment) fault diagnosis and isolation system is investigated. This work is applicable to the Air Force and other DOD branches in designing BIT equipment.

Throughout the report, it is assumed that the probability of simultaneous failure of two or more LRS's is so small as to be negligible. A self-diagnosability is recognized when the BIT will automatically execute a primary sequence of diagnostic test to identify, unambiguously, malfunctioning subsystems up to a given group of LRU's. As faults are localized, malfunctioning group of LRU's can be replaced (by switching on stand by spares) and a secondary isolation may be performed semi-automatically or manually to isolate the single failed LRU.

## II. OBJECTIVES

The objectives of this research effort are:

1. Searching the literature for relevant researchs dealing with optimization techniques applied to fault isolation process.
2. To explore and modify existing algorithms so as to demonstrate their computational capabilities.
3. To develop an optimization procedure which is capable of handling the dimensions of real world problems.

## III. PROBLEM DEFINITION

The problem solved in this research is the design of minimum expected cost BIT diagnostic procedures for detecting and isolating single faults in a primary system. The primary system is assumed to be a collection of elements (modules). It is assumed that each element has an estimated priori probability of failure. Tests are defined simply in terms of which elements each of them check. An arbitrary cost, reflecting the time, expense, or

difficulty involved in executing the test is assigned to each test.

#### IV. PREVIOUS WORK

A review of the technical literature yields a surprisingly small number of references to the general problem of efficient or optimum diagnostic procedures. One of the earliest models proposed for relating faults to diagnostic tests is that of Brule', et. al. [1]. In this model, the system is represented as an interconnected collection of functional elements with access to the terminals of the available elements. Tests are performed on collections of elements; hence the test-fault relationship is a test-element relationship and a fault is considered to be the failure of an element in performing its function. A related work by Johnson [8] discusses the generation of efficient sequential tests procedures by use of information theoretic methods to evaluate the amount of information provided by a test. Chang [3] develops a different criterion for evaluating the goodness of the available tests. He introduces the distinguishability criterion for a set of  $n$  singly occurring faults and  $m$  tests are considered for inclusion in a fixed test schedule. The model is  $r$  data matrix  $D$  having entry  $d_{ij}=1$  if test  $T_j$  fails for fault  $f_i$ , and  $d_{ij} = 0$  if test  $T_j$  passes for fault  $f_i$ . Distinguishability among the rows of the table is considered and the model is applied to the selection of a fixed set of diagnostic tests. Butterworth [2], Firstman and Gluss [5], and Gluss [6] develop search procedures to determine a sequence which minimizes the expected cost of secondary isolation to locate a failed element within a group of LRU's identified by the BIT primary diagnostic. Cohn and Ott [4] present an optimal algorithm to minimize the expected cost test tree. The test tree specifies an adaptive

testing procedure that detects a failure and isolates the faulty component. They utilize a recursive formula for their optimal search. Even though they recognize the similarity to the machine-setup problem and the applicability of dynamic programming technique to solve the problem, their adaptive procedures is exactly a dynamic programming procedure. Sheskin [13] develops a probabilistic dynamic programming procedure to determine the sequence of diagnostic tests to isolate the group of modules which contains the faulty unit.

From the above survey, only references [4] and [13] solve the sequencing problem optimally by utilizing dynamic programming. Unfortunately, no computational experiences are presented. If dynamic programming is used, and the number of elements in the equipment increases the computational and storage burden increase exponentially.

In this research effort, a Branch-and-Bound algorithm is presented to capitalize on some dominance and branching rules which may have a great impact in reducing the computational and storage requirements.

#### V. NETWORK REPRESENTATION

Following the notation of Brule', et al [1]. Assume that the primary system consists of  $n$  elements of different groups of LRU's identified as the smallest replaceable modules in the system. Therefore, the number of different tests which can exist is  $(2 - 1)^{n-1}$ . A test is defined by a sequence of  $n$  binary digits, one for each element in the system. Digit  $i$  is equal to 0 if the test checks element  $i$  and is equal to 1 if the test does not check element  $k$ , e.g.,  $T_{14}$  (01101) checks the first and the fourth elements. For each test  $T_k$  there corresponds a fixed cost  $C_k$ .  $S(t)$  denotes the state

of the equipment prior to performing test  $T_k$  at the  $t^{\text{th}}$  level in the testing procedure. A state is represented by an  $n$ -bit number containing only the bits 0 and 1. A 0 is assigned in position  $i$  of a state if an element is known to be good. A 1 is assigned in position  $i$  if the element is not yet tested.  $S(o)$  has 1's in all positions and  $S(n)$  has 0's in all positions.  $S_k(t+1)$  is the state of the equipment if test  $T_k$  passes. This state is computed by the AND operation of  $S$  and  $T_k$ .  $\bar{S}_k(t+1)$  is defined as the state of the equipment if test  $T_k$  fails. It is computed by AND operation  $S T'_k$  ( $T'_k$  is the complement NOT).

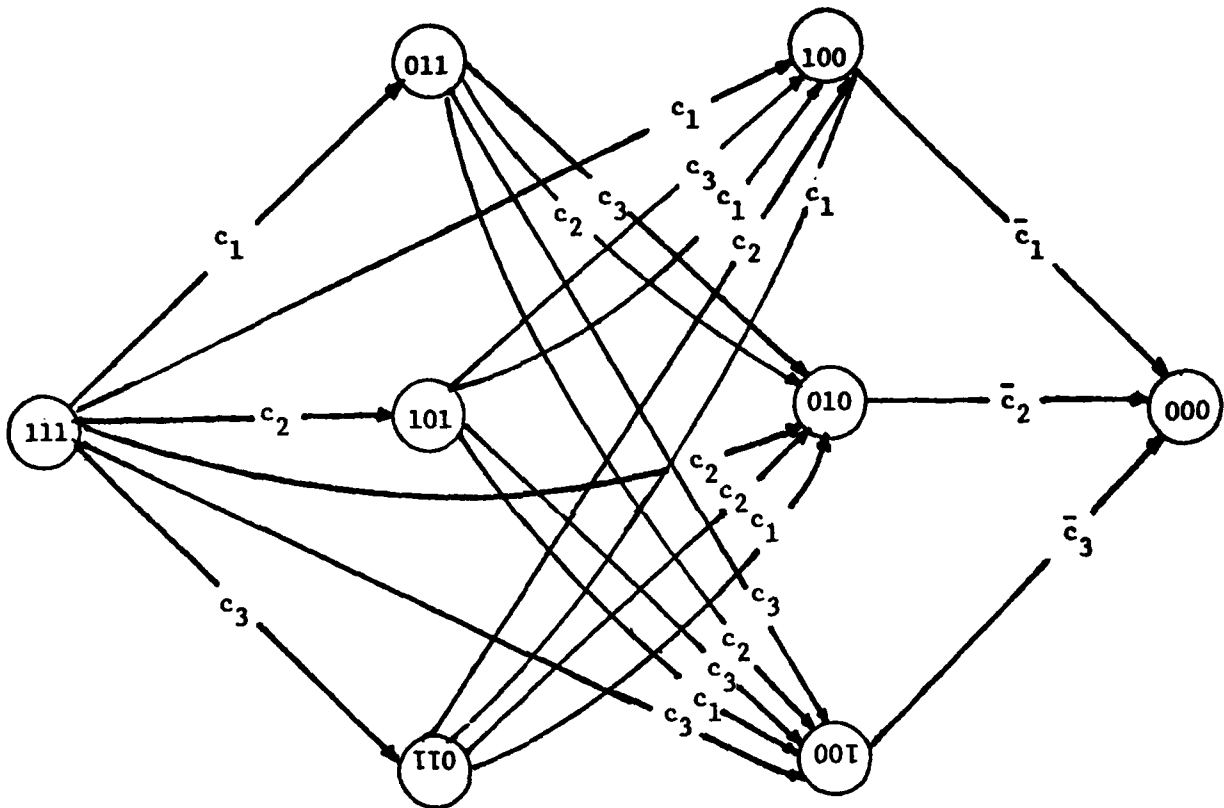
When dynamic programming is utilized to solve the optimum diagnostic problem, the procedure can be described by a decision tree structure with nodes labeled by states and arcs labeled by tests and their costs. For all possible tests, the decision tree could be constructed as a directed network from initial state node  $S(o)$  to final node  $S(n)$ . For a 3-element example the directed network is shown in Figure 1 and the problem is to find the path with minimum expected cost through a directed network. The network depicted in Figure 1 has a small number of nodes and a very large number of arcs.

In the directed network, a node  $S(t)$  may be reached from node  $S(o)$  by any of several paths (partial sequence). In the algorithm to be presented below, it is convenient to assign a node for each state in conjunction with a particular path to it from  $S(o)$ . Thus, any node will have only one entering arc, i.e., a unique predecessor.

The modified network for the 3-element example is shown in Figure 2. Note that some states appear more than once, where in Figure 1 they do not. The modified network has more nodes and less arcs compared to the directed network. The major drawback to the directed network approach is that every undominated node is extended.

$c_1$  is the cost of  $T_{100}$ ;  
 $c_2$  is the cost of  $T_{010}$ ;  
 $c_3$  is the cost of  $T_{001}$ ;

$\bar{c}_1$  is the cost of secondary isolation for  $LRU_1$   
 $\bar{c}_2$  is the cost of secondary isolation for  $LRU_2$   
 $\bar{c}_3$  is the cost of secondary isolation for  $LRU_3$



number of nodes = 8  
 number of arcs = 21

Figure 1. Network Flow Representation

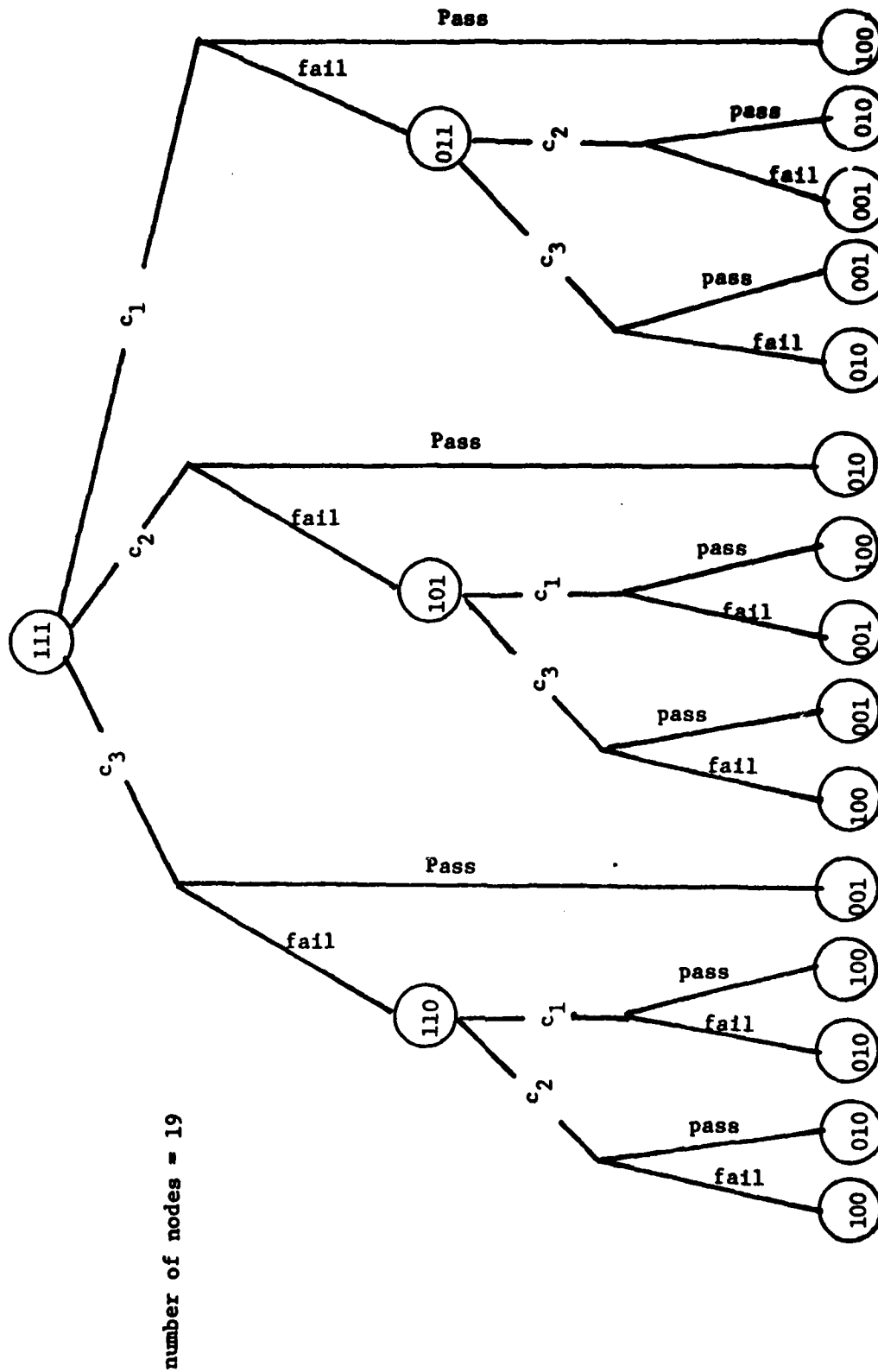


Figure 2. A Modified Network with All Paths

$c_1$  is the cost of  $T_{100}$ ;

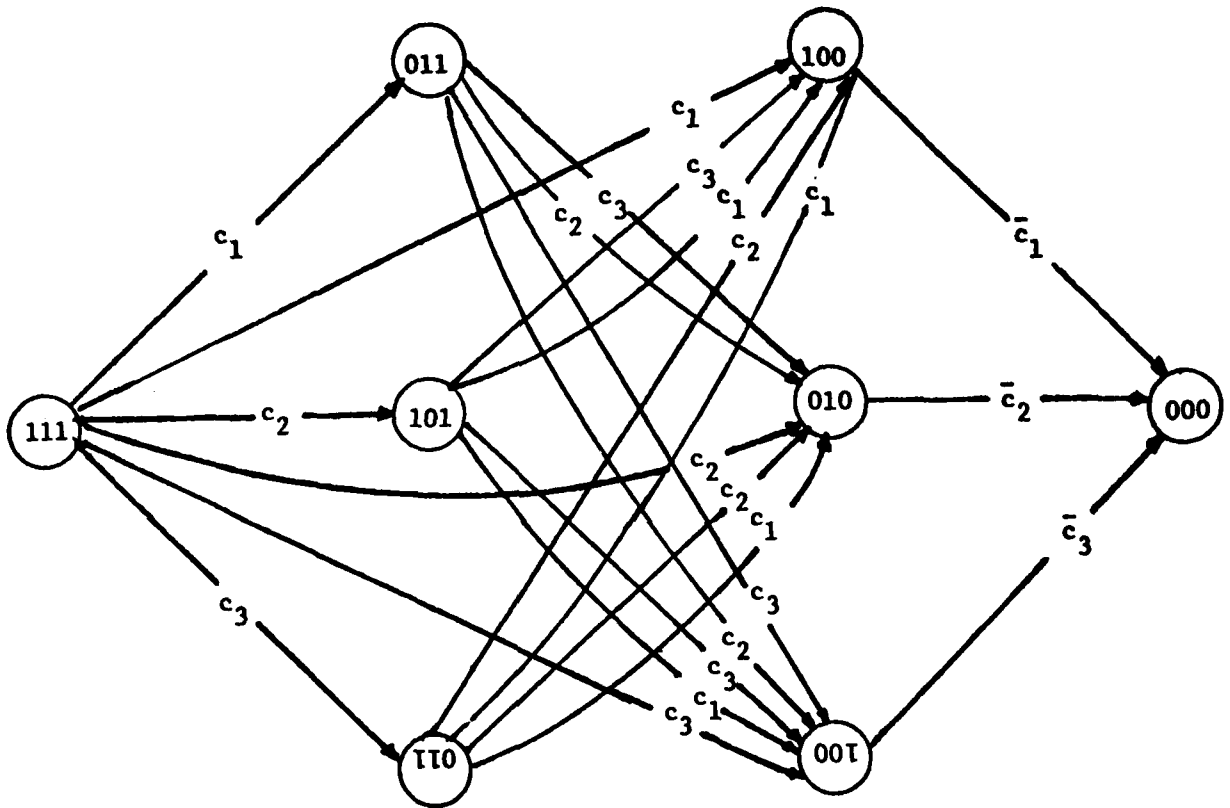
$c_2$  is the cost of  $T_{010}$ ;

$c_3$  is the cost of  $T_{001}$ ;

$\bar{c}_1$  is the cost of secondary isolation for  $LRU_1$

$\bar{c}_2$  is the cost of secondary isolation for  $LRU_2$

$\bar{c}_3$  is the cost of secondary isolation for  $LRU_3$



number of nodes = 8

number of arcs = 21

Figure 1. Network Flow Representation

In the sequel, a Branch-and-Bound algorithm is considered in an effort to arrive at an optimal solution, generating fewer nodes, and thereby reducing the computation and storage burdens.

#### VI. BRANCH - AND - BOUND APPROACH

Basically, Branch-and-Bound is a network emanating from an initial node  $\Omega$  which represents the space of all solutions. Branching corresponds to partitioning of the total space into smaller mutually exclusive and exhaustive subsets. Intermediate nodes generated from  $\Omega$  corresponds to these subsets. Figure 3 illustrates the branching procedure. A lower bound on the expected cost of solutions within the subset is associated with each node. The partitioning continues until a final node is found whose bound (actual expected cost) is less than the lower bound for all unbranched nodes.

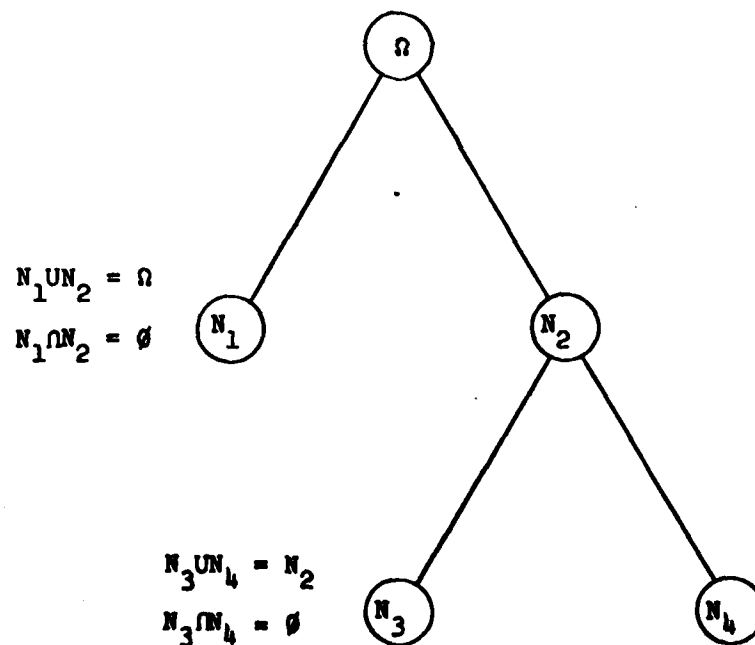


Figure 3. Partitioning the Solution Space

Frequently the basic scheme is augmented by application of necessary conditions to terminate branching with comparison with the expected cost of a known solution. There are many strategies for determining the next node to branch from, including the node with the minimum lower bound and the most recently generated node with the minimum lower bound. For further details on Branch-and-Bound, see Lawler and Wood [11] and Mitten [10].

Note that in the Branch-and-Bound Network an unbranched node is the node whose partial sequence has not been extended; a fathomed node is the one from which no further branching is considered (due to bounding, or dominance rule).

After a node or subset  $S$  has been partitioned, a lower bound is computed for each partition or succeeding node  $j$ . This bound is a lower bound on the objective function value that would be produced by any partial sequence containing the sequence that has been made at this node  $j$ . The lower bound will be a sum of two values. If the sum is greater than the current upper bound on the optimal objective function value, then further consideration of the node  $j$  will be unprofitable. The partial sequence it represents would never be part of the optimal scheme, thus the node is fathomed or no longer considered as a candidate for partitioning.

If, on the other hand, the lower bound on node  $j$  is less than the current upper bound on the optimal objective function value, its partial sequence is still a promising candidate as the optimal allocation scheme. The node is then partitioned and its successor nodes are placed under the same scrutiny for fathoming.

When the  $n - 1$  level is reached a complete sequence has been developed. Objective function values may be computed for each node at the  $n - 1$  level.

The node with the minimal objective function value that is still less than the current upper bound on the optimum represents the new best sequence, and its objective function value becomes the new upper bound on optimal. Otherwise, these nodes are fathomed and nothing is changed. If all nodes have either been fathomed or partitioned, then the current upper bound is taken as the optimal objective function value.

In this research a Branch-and-Bound algorithm which uses a depth approach of "backtracking" strategy is developed. In particular newly generated nodes are ranked and listed left to right such that the right-most node has the minimum lower bound. Subsequent branching emanates from the right-most (highest numbered) node of the set first generated.

The depth approach involves partitioning a node at level  $i$ . For its successor nodes at level  $i + 1$ , the lower bounds are computed and fathomed if possible. The unfathomed node with the minimal lower bound among these successors is chosen as the next node for partitioning. The other unfathomed nodes remain active. This procedure continues through the  $n - 1$  level. The predecessor node at the  $n - 3$  level is considered. If it has active nodes among its successors at the  $n - 2$  level, then another attempt can be made to fathom these active nodes with the new upper bound. If active nodes still remain, the active successor with the minimal lower bound is chosen for partitioning. If no active nodes remain among the successors, the predecessor node at the  $n - 4$  level is considered, and the process repeats.

As can be seen from the above discussion, the number of active nodes at any time is not too large unless the horizon is very long. A final node and thus upper bound is generally obtained quickly, and it is easy to

locate the next node to branch from.

#### VII. THE BRANCHING RULE

The branching rule is the criterion used to choose the next test in the sequence for an unfathomed node at a certain level. Johnson [8] shows that a highly efficient sequence of tests can be assured by choosing the tests on the basis of a figure of merit derived from information theory. The application of a test serves to remove some of the ambiguity  $j$  that is, it reduces the uncertainty as to the identity of the fault. At any level the "best" next test may be the one which results in the highest average information gain with minimum cost. Therefore, the figure of merit to be used is the ratio of ambiguity removed by a test to the cost of performing the test. That is

$$F_k = \frac{-P \log_2 P - (1-P) \log_2 (1-P)}{C_k} \quad (1)$$

where  $P$  is the a priori probability that the test will pass and  $C_k$  is the cost of performing the test.

In the proposed branch-and-Bound scheme instead of branching over all possible tests, choose the test with the highest  $F_k$  among all possible tests.

#### VIII. DOMINANCE RULE

Let  $N_t$  represent a node corresponding to state  $S(t)$  and a particular partial sequence. Let  $Q(N_t)$  be an optimal partial sequence from node  $S(o)$  to  $N_t$  and  $\bar{Q}(N_t)$  be the associated partial sequence. Hence,  $Q(N_t) \circ \bar{Q}(N_t)$  (where "o" indicates concatenation) represents a feasible testing sequence extending from  $S(o)$  to  $S(N)$  and passing through  $N_t$ . Define  $f(N_t)$  to be the expected cost associated with the partial sequence  $\bar{Q}(N_t)$ ;  $\phi(N_t)$  to be

the expected cost from node  $S(o)$  to node  $S(t)$ . Then the cost associated with  $Q(N_t) \circ \bar{Q}(N_t)$  is  $\phi(N_t) + f(N_t)$ .

Consider any two feasible schedules  $Q(N_t) \circ \bar{Q}(N_t)$  and  $Q(N_{t'}) \circ \bar{Q}(N_{t'})$ , let  $C(N_t)$  and  $C(N_{t'})$  be the associated expected total cost. If  $C(N_t) \leq C(N_{t'})$  node  $N_t$  "dominates"  $N_{t'}$ .

Theorem 1:

Consider two nodes  $N_t$  and  $N_{t'}$  such that  $t \leq t'$ , that is to say,  $S(t) \leq S(t')$ , (where  $\leq$  in terms of degrees of ambiguity). If  $f(N_t) \leq f(N_{t'})$ , then  $N_t$  dominates  $N_{t'}$ .

The proof follows from the fact that at a higher level in the tree if the expected cost incurred thusfar is relatively small then the expected cost of completion will be less.

Theorem 1 implies that if node  $N_{t'}$  is generated, and  $f(N_{t'})$  is computed and compared with  $f(N_t)$  for any previously generated node  $N_t$  such that  $S(t') \geq S(t)$ , and  $f(N_t)$  is found to be equal or smaller than  $f(N_{t'})$ , then branching from  $N_{t'}$  may be terminated.

IX. TESTS REDUCTION TECHNIQUE

As mentioned above the total number of significant tests equals  $(2^{n-1} - 1)$  where  $n$  is the number of elements in the system. In all previous work, no attempt to reduce the set of feasible tests at node  $S(o)$  has been tried.

In this section a reduction technique is utilized to minimize the number of tests. This problem is analogous to the method for the selection of prime implicants in digital system [12] or the covering problem in integer linear programming [14].

Arrange all tests in an  $(n \times 2^{n-1} - 1)$  array where the columns indicate the designated test and a row identify the possible faulty element. Let  $r_i$  denotes row  $i$ ,  $T_j$  denotes column  $j$  of the testing matrix  $||a_{ij}||$ .

Reduction 1: If  $r_i = e_k$  (the  $k^{\text{th}}$  unit vector) for some  $i, k$ , then  $T_k$  is the only test to identify a faulty element  $i$ , delete row  $i$ . Also, every row  $t$ , such that  $a_{tk} = 1$  may be deleted.

Reduction 2: If  $r_t \geq r_p$  (in a vector sense) for some  $t$  and  $p$ , then  $r_t$  may be deleted.

Reduction 3: If for some set of columns  $R$  and some column  $k$ ,

$$\sum_{j \in R} T_j \geq T_k \text{ and } \sum_{j \in R} C_j \leq C_k; \text{ column } k \text{ may be deleted.}$$

The last reduction's rule should be done iteratively. Define the order of tests as follows, the one which tests only one element has an order of one, the one which tests two elements has an order of two, and so on. Start the set  $R$  with tests of order one to try to eliminate tests of higher order. Increase the order of tests included in the set  $R$  to check others with at least the same order. To check the possibility of eliminating tests of order one, make sure that the tests included in  $R$  are capable among themselves to isolate the same element as the test of order one. These procedures are illustrated using the 4-element example problem in [13].

Table 1. Test of Primary System

$C_k$	3	5	4	1	6	2	7
$T_k$	$T_1$	$T_2$	$T_3$	$T_4$	$T_5$	$T_6$	$T_7$
$P_1 = .45$	1	1	1	1	0	0	0
$P_2 = .30$	1	0	0	0	1	0	0
$P_3 = .20$	0	1	0	0	0	1	0
$P_4 = .05$	0	0	1	0	0	0	1

Probabilities  
of Failure

1.  $R = \{4,6\}$ ; delete  $T_2$
2.  $R = \{3,4\}$ ; delete  $T_7$
3.  $R = \{1,4\}$ ; delete  $T_5$

This will reduce the number of the feasible sets to only 4 (knowing that the required number of tests is three) which reduces the dimensionality of the problem almost 43%.

In general, the test used at any node must cause the correct partition of the ambiguity subset; the effect of the test on elements outside the ambiguity subset is irrelevant. A test is sufficient at a node if it has 0's for elements in one class of the partition, 1's for elements in the complementary class, and either value for elements outside the ambiguity subset.

#### X. BOUNDING APPROACH

Nodes are numbered in the order in which they are generated, starting with  $\Omega$  as the initial node  $S(0)$ . Let  $|S(o)|$  denote the cardinality of the set  $S(o)$ , e.g.,  $|S(o)| - |S(1)| = 1$ . Let  $M_1$  be the set of nodes generated from the nodes in  $M_{i-1}$ . Denote by  $N_{j_p}$  the unique immediate predecessor of  $N_j$ . It should be noted that in applying Theorem 1 to a node  $N_j \in M_1$ ,  $N_j$  need only to be compared with other nodes  $N_k$ ,  $N_k \in M_1$ , i.e., it is not possible to have  $N_j \in M_j$ ,  $N_k \in M_j$ ,  $j < 1$ , such that  $S(N_j) \geq S(N_k)$ .

Let  $L(N_j)$  denote the lower bound on the objective function for all solutions associated with  $N_j$ , and define it as follows,

$$L(N_j) = \phi(N_j) + \lambda \quad (2)$$

where  $\lambda$  is a lower bound on the cost of partial sequence from  $N_j$  to a feasible final node, i.e.,  $\lambda \leq f(N_j)$ . Let  $E_j$  be the set of distinct feasible

tests such that none of them has been scheduled before reaching node  $N_j$ . Since each test will partition the set  $S(N_j)$  into two sets,  $N_j + 1, N_j + 1$ , depending on the outcome of the test (pass - fail) then,  $N'_{j+1}$  is the node representing the complement of  $S(N_j)$ ,  $S'(N_j)$ . Thus a lower bound for any node  $N_j$  such that  $|S(N_j)| \geq 2$  may be obtained as follows:

1. At Level 0: Notice that  $\phi(\Omega) = 0$  and there are  $n-1$  tests to be performed, therefore equation 2 is written as,

$$L(N_0) = \phi(\Omega) + \sum_{k=0}^{n-2} \min_{k \in E_0} (T_k) \sum_{i \in N_0} p_i \quad (3)$$

2. At Level j: If  $N_j$  has the property that  $|S(N_{j_p})| - 1 > |S(N_j)|$ , then

$$L(N_j) = \phi(N_j) + \sum_{k=j}^{n-2} \min_{k \in E_j} (T_k) \sum_{i \in N_j} p_i \quad (4)$$

otherwise,

$$L(N_j) = \phi(N_j) + \sum_{k=j}^{n-2} \min_{k \in E_j} (T_k) \sum_{i \in N_j} p_i + \sum_{i \notin N_j} p_i \quad (5)$$

3. At Level n-1: If the number of paths to reach node  $N_{n-1}$  equals  $n-1$ , then

$$L(N_{n-1}) = \phi(N_{n-1}) = U(N_{n-1}) \quad (6)$$

where  $U(N_{n-1})$  is the upper bound on the optimal solution, hence, an optimal solution is obtained.

Notice that after each branching process the two newly generated nodes will have the same lower bound. In the case when one of the two nodes has  $|S(N_j)| = 1$ , i.e., one element has been isolated explicitly, fathome this node and continue branching from its complement  $S'(N_j)$ .

## XI. A BRANCH-AND-BOUND ALGORITHM:

Define  $\phi^*(S)$  as the minimum value of  $\phi(N_j)$ . The set of previously generated states is designated by  $\pi$ , and the vector of the expected cost  $\phi$ . Whenever a new node  $N_j$  is generated,  $S(N_j)$  may be compared with the list, and if there is an  $S \in \pi$  such that  $S \leq S(N_j)$ , Theorem 1 may be applied. If  $N_j$  is dominated, back track. If there is the case that  $S = S(N_j)$  but  $\phi^*(S) > \phi(N_j)$ ,  $\phi^*(S)$  is set to be equal to  $\phi(N_j)$ .

An algorithm based on the above discussion is now presented as follows:

1. Initiate node  $\Omega$  by setting  $S(\Omega) = (1,1,\dots,1)$ ,  $\phi(\Omega) = 0$ , and both  $\pi$ ,  $\phi = \emptyset$ .
2. Generate up to  $m$  new nodes  $N_j$ , where  $m = |E_0|$ , compute the information-gain figure of merit,  $F_k$ , using (1). Compute  $\phi(N_j)$  and  $S(N_j)$  for each node and add to  $\pi$  and  $\phi$ . If no new nodes can be generated, there is no feasible solution. Stop. Otherwise, proceed to step 3.
3. Compute lower bound for each new node using (3,4,5,6). Label the nodes  $N_j$  with  $(L(N_j), \phi(N_j), N_{j_p})$ .
4. Branch from the unbranched node with the minimum lower bound, and branch with the test,  $T_k^* \in N_j$  where  $T_k^*$  has the  $\max_k \{F_k\}$ . For both newly generated nodes  $N_j, N'_j$  compute  $S(N_j), \phi(N_j)$  and add to  $\pi$  and  $\phi$ . If any node isolates a single element, fathom this node. Compute lower bound for the nodes and label  $N_j$  with  $(L(N_j), \phi(N_j), N_{j_p})$ .
5. Repeat step 4 until a final node with  $n-1$  tests is reached. Set  $U^* = L(N_{n-1})$ .

6. Trace back up the branch at any level where  $|N_{j_p}| - 1 \geq |N_j|$ , removing all previously branched nodes encountered and all unfathomed nodes  $N_k$  such that  $L(N_k) \geq U^*$ . If no such node is found, search for a node  $N_j$  up the tree such that  $L(N_j) < U^*$ . If no such node is found, the solution associated with  $U^*$  is optimal. Stop. Otherwise, proceed to step 7.
7. Branch from  $N_j$  using (1). For each newly generated node  $N_k$  compute the lower bound and compare it with  $U^*$ . If  $U^* \leq L(N_k)$ , remove  $N_k$ . For each remaining newly generated node  $N_k$  compute  $S(N_k)$  and  $\phi(N_k)$ . Apply Theorem 1 if possible. If an  $S$  is found such that  $N_k$  is dominated, fathome  $N_k$ . If no nodes remain afterwards, return to step 6. Otherwise, proceed to step 8.
8. Label each node  $N_j$  with  $(L(N_j), \phi(N_j), N_{j_p})$ .
9. Choose the node with the minimum lower bound and return to step 7, repeat steps 7 and 8 until a new final node  $N_k$  is reached. Compare  $U^*$  with  $L(N_k)$ . If  $L(N_k) \geq U^*$ , go to step 6. If  $L(N_k) < U^*$ , set  $U^* = L(N_k)$  and go to step 6.

## XII. NUMERICAL EXAMPLE

To illustrate the use of the algorithm presented above, the example in [13] is solved where the data are as in Table 1. The corresponding network is shown in Figure 4. The notation used is as follows,

The encircled number at the left of each node is the node number. The numbers inside the boxes represent the state. The number at the top, right of each box is the predecessor node number, the number at the top left indicates the isolated element, the number at the bottom right is  $\phi(\cdot)$ , and the one at the bottom left is  $L(N_j)$ . If  $L(N_j)$  is underlined, then the node has been fathomed. The solution proceeds as follows:

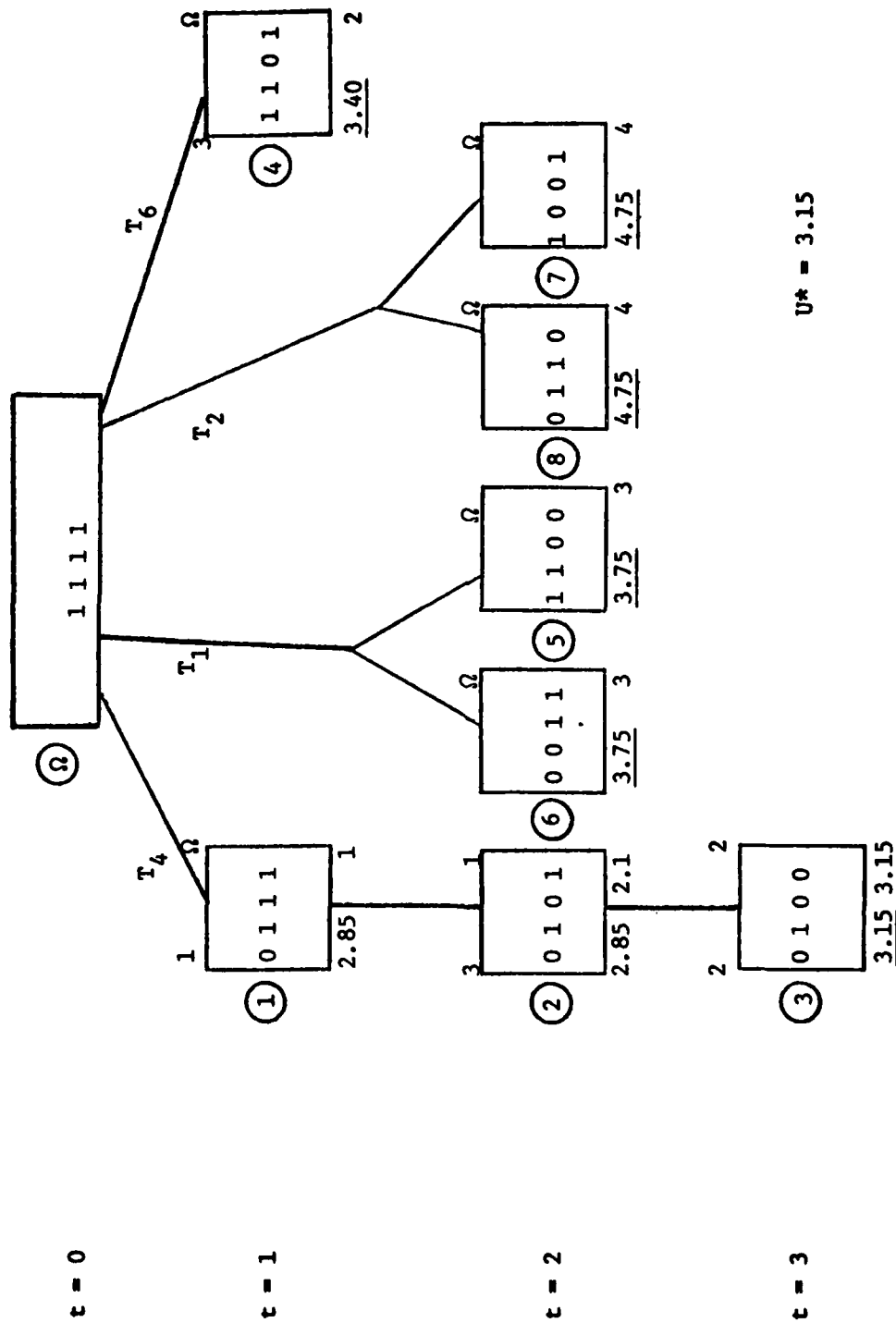


Figure 4. Branch-and-Bound network for a four-element example.

1. At node  $\Omega$ , using the reduced test matrix obtained in section 9, calculate  $F_k$  for  $k = 1, 2, 4, 6$ .  $F_\Omega = (.27, .25, .99, 36)$ , thus the maximum  $F_k$  corresponds to  $T_4$ . Branch with  $T_4$  to generate node  $N_1$ .
2.  $L(N_1) = 1 + 2x.25 + 3x.25 = 2.25$ . At  $N_1$ ,  $F_1 = (.33, .12, .47)$ . Therefore, branch with  $T_6$  to generate node  $N_2$ .
3.  $L(N_2) = 1 + 2x.25 + 3x.25 = 2.25$ . At  $N_2$ ,  $F_2 = (.197, .148)$ . Branch with  $T_1$  to generate node  $N_3$ . Since  $t = n-1$  and  $|S(n-1)| = 1$ . Stop.  $\phi(N_2) = L(N_2) = U^* = 3.15$  and Fathome node  $N_2$ .
4. Backtrack to node  $\Omega$  and the next test with maximum  $F_k$  is  $T_6$ . Generate node  $N_4$ .  $L(N_4) = 3.40 > U^*$ . Fathome the node and backtrack.
5. The next test with maximum  $F_k$  is  $T_1$ . Generate nodes  $N_5$  and  $N_6$ .  $L(N_5) = L(N_6) = 3.75 > U^*$ . Fathome both nodes and backtrack.
6. The only test left is  $T_2$ . Generate nodes  $N_7$  and  $N_8$ .  $L(N_7) = L(N_8) = 4.75 > U^*$ . Fathome both nodes and backtrack.
7. Since all nodes in the network are fathomed. Stop. The optimum expected cost,  $\phi^*(N_2)$ , equals 3.15 and the optimum sequence is  $\{T_4, T_6, T_1\}$ .

### XIII. CONCLUSIONS AND RECOMMENDATIONS

From the example problem, the maximum number of nodes generated equals 8. Where Figure 2 indicates that for a 3-element problem 19 nodes are required. In Johnson, et al [7] they approximate the number of testing trees if complete enumeration is used. For a 4-element problem the total number of testing trees equals 15. Thus, total number of nodes is  $2(n-1) \times 15 = 90$ . When  $n = 10$  (which is very reasonable in practical problems), there exists about  $3.44 \times 10^7$  trees, i.e.,  $6.19 \times 10^8$  nodes!

Comparing the above Branch-and-Bound algorithm with the dynamic programming approach for the same example. It is easily seen that the number of calculations and the storage requirements have been reduced dramatically.

We believe that a Branch-and-Bound approach is the best methodology in solving the design problem of diagnostic and fault isolation procedures. This approach will yield the optimum expected cost as the other procedures but, with a very high efficiency.

Since the algorithm was tested on a reasonably small problem,  $n = 4$ , a future research is recommended to determine its efficiency in solving practical problem of larger size, e.g.,  $n = 50$  which appears frequently in BIT diagnostic procedures. Mechanization of the algorithm will help the Air Force in evaluating their optimum procedures for BIT on site for a real life cycle cost data.

Also in the future, the Branch-and-Bound procedure should be modified to accommodate both the partitioning and secondary isolation problems as defined in MIL-STD-1591 [9].

## REFERENCES

1. Brule', J.D., R.A. Johnson, and E.J. Kletsy, "Diagnosis of Equipment Failures", IRE Transactions on Reliability and Quality Control, Vol. RQC-9, Pages 23-34, 1960.
2. Butterworth, R., "Some Reliability Fault-Testing Models", Operations Research, Vol. 20, Pages 335-343, 1972.
3. Chang, H.Y., "An Algorithm for Selecting an Optimum Set of Diagnostic Tests", IEEE Transactions on Electronic Computer, Vol. EC-14, Pages 706-711, 1965.
4. Cohn, M. and G. Ott, "Design of Adaptive Procedures for Fault Detection and Isolation", IEEE Transactions on Reliability, Vol. R-20, Pages 7-10, 1971.
5. Firstman, S. and B. Gluss, "Optimum Search Routines for Automatic Fault Location", Operations Research, Vol. 8, Pages 512-523, 1960.
6. Gluss, B., "An Optimum Policy for Detecting a Fault in a Complex System", Operations Research, Vol. 7, Pages 468-477, 1959.
7. Johnson, R.A., E.J. Kletsy, and J.D. Brule', "Diagnosis of Equipment Failures", RADC-TR-59-47, 1959.
8. Johnson, R.A., "An Information Theory Approach to Diagnosis", Proceedings of 6th Symposium on Reliability and Quality Control, Pages 102-109, 1960.
9. Military Standard on Aircraft, Fault-Diagnosis, Sub-Systems, Analysis/Synthesis of MIL-STD-1591, 1977.
10. Mitten, L.G., "Branch and Bound Methods", Operations Research, Vol. 18, Pages 24-34, 1970.
11. Lawler, E. and D. Wood, "Branch and Bound Methods: A Survey", Operations Research, Vol. 14, Pages 699-719, 1966.
12. Lee, S.C., Digital Circuits and Logic Design, Prentice-Hall, Inc., Englewood Cliffs, N.J., 1976.
13. Sheskin, T.J., "Sequencing of Diagnostic Tests for Fault Isolation by Dynamic Programming", IEEE Transaction on Reliability, Vol. R-27, Pages 353-358, 1978.
14. Taha, H.A., Integer Programming, Academic Press, Inc., New York, New York, 1975.

1979 USAF-SCEEE SUMMER FACULTY RESEARCH PROGRAM

Sponsored by

THE AIR FORCE OFFICE OF SCIENTIFIC RESEARCH

Conducted by the

SOUTHEASTERN CENTER FOR ELECTRICAL ENGINEERING EDUCATION

PARTICIPANT'S FINAL REPORT

EFFECTS OF NUCLEAR BLAST

DOUBLE SHOCK ON AIRBORNE AIRCRAFT

Prepared by:	Clarence A. Bell, Ph.D.
Academic Rank:	Associate Professor
Department and University:	Department of Mechanical Engineering Texas Tech University
Assignment:	Kirtland Air Force Base, New Mexico Air Force Weapons Laboratory
USAF Research Colleague:	Alfred L. Sharp
Date:	August 10, 1979
Contract No:	F49620-79-C-0038

EFFECTS OF NUCLEAR BLAST

DOUBLE SHOCK ON AIRBORNE AIRCRAFT

by

Clarence A. Bell

ABSTRACT

The response of aircraft to nuclear blasts is of considerable importance. Blast input from bombs detonated above ground consists of a primary blast and a reflected blast. This report describes studies of response of aircraft to two blast inputs, the first from the primary blast and the second from the reflected blast, which occur within a short time interval. Preliminary analyses indicate that response may be more severe when determined from a two-blast analysis.

#### ACKNOWLEDGEMENTS

The author would like to thank the Air Force Systems Command, Air Force Office of Scientific Research, and the Southeastern Center for Electrical Engineering Education for the opportunity to participate in the research program described in this report.

The author gratefully expresses his appreciation to the Air Force Weapons Laboratory for the cooperation and support he received throughout the ten-week period of this activity. In particular, thanks are extended to Dr. Authur Gunther, Chief Scientist, Major Terry Schmidt, and Mr. Gerald Campbell. The author especially wishes to express appreciation to Mr. Al Sharp for his spirit of support, encouragement and help in the project.

## PREFACE

This report describes research conducted by the author at the Air Force Weapons Laboratory (AFWL) at Kirtland Air Force Base (KAFB) in Albuquerque, New Mexico under sponsorship of the Southeastern Center for Electrical Engineering Education (SCEEE) during a ten-week period in the time span from April 29, 1979 to July 14, 1979.

## Introduction

It is well established that an important factor in the maintenance of world peace is the balance of power between the United States and potential adversaries. That is, it is believed that the capability of the United States Armed Forces to withstand a nuclear attack by an adversary and still be able to deliver a nuclear retaliatory attack of catastrophic magnitude is a major deterrent to such an initial attack. For this reason, the study of the vulnerability of aircraft to nuclear explosion is of significance. In the event of an attack, part of which is directed toward an Air Force base, it is anticipated that some degree of warning would be available and that an attempt would be made to launch a counterattack. Thus, it is assumed that some retaliatory aircraft would have been launched and would be sufficiently far from the explosion to be unaffected by it, some would still be on the ground and would be destroyed, and others would be airborne but would experience a considerable amount of blast input.

The survivability of aircraft in this last group would depend on many factors, such as proximity of the aircraft to the blast, the direction of the flight relative to the explosion location, the altitude of the aircraft and of the explosion and the maneuver status of the aircraft at blast intercept. Therefore, several strategies are available for the crews of these aircraft to pursue. Optimal escape strategy depends on a critical knowledge of aircraft response to various blast conditions. This is particularly true when the effects of the reflected shock wave (reflected from the ground) are taken into account.

The subject of this report is the survivability of airborne aircraft which have encountered a considerable amount of blast input from nuclear explosions.

#### Description of the Blast Environment

The blast environment has been studied extensively [1] and only a brief summary is provided in this report.

Atmospheric response to nuclear explosion can be characterized by near-field and far-field effects. Near-field effects can extend to several hundred or perhaps, to a few thousand feet and are associated with intense temperatures, pressures and radiation levels. Aircraft in the near-field have no probability of survival and, therefore, are not the subject of the study described in this report.

When a nuclear explosion occurs in the atmosphere above ground level it results in a step-function atmospheric pressure change (and the associated wind velocity gust which follows it) which moves away from the explosion as a shock wave front. In the near-field this wave front can move out at a rate of several thousand feet per second. As the wave progresses outward, it moves through an atmosphere which is more normal in its conditions and soon moves at a speed approaching the local sonic velocity.

When the shock wave encounters the ground, a reflected wave is formed, as shown in Figure 1. The reflected wave appears to emanate from a point the same distance below ground level as the nuclear explosion is above ground level. Both shock waves, the primary wave and the reflected wave, move outward and can encounter an aircraft in flight. Thus, the aircraft can experience two shocks if it is operating in the appropriate regime.

Since sonic velocity depends on the temperature of the medium (air) through which it moves, the primary and reflected waves do not generally move at the same velocity. Since atmospheric temperature decreases with altitude, the reflected wave (which is closer to the ground) moves at higher velocity and can overtake the primary wave. This situation is illustrated in Figure 2. The figure shows an iso-overpressure contour (a contour of constant incremental pressure) in the far field. The upper portion of the contour, labeled the primary region (sometimes called the region of free air shock) shows the iso-overpressure contour due to the primary wave front. An aircraft in this region would experience this overpressure pulse and, some time later, a weaker pulse from the reflected wave. In the bottom portion of the contour, labeled the mach shock region, is the region where the reflected front has caught up with the primary front and the resulting shock is the sum of the two shocks. In the middle portion, labeled the transition region, the primary shock is followed by the reflected shock, but the reflected shock is of greater magnitude than the primary shock. The intersection of these last two regions is called the triple point. Typical pressure time-histories in these three regions are shown as inserts in the figure. The iso-overpressure contour of Figure 2 is based on the maximum value of the overpressure, as shown in the inserts. That is, in the free-air shock region, the contour is based on the pressure value at the first peak; in the transition region it is based on the value at the second peak; and in the mach shock region it is based on the value of the single coalesced peak.

## Research Topic

The topic selected for research [2] concerns the dynamic response of aircraft to nuclear blast environment (overpressure and gust). The general methods for dynamic response calculations are well known and have been used for the past 20 years to predict stand-off ranges for nuclear tests in the atmosphere and for predictions of survivability in war games. These predictions were generally threshold-of-damage predictions and were labeled "suresafe." In recent years the emphasis has been placed on mission completion. That is, acceptance of the fact that some damage would occur and determination of the response corresponding to a standoff range which would just permit completion of the assigned mission. (The mission may consist of takeoff, climb, cruise, refuel penetration, etc). Associated with this emphasis is a new set of dynamic response problems, an important one of which involves consideration of response to double shock.

This research project emphasized a study of aircraft response in the transition region relatively close to the triple point. In a typical study case in this regime, the aircraft would be impacted by the primary wave front and started into its characteristic vibratory motion. Then, a short time later, the reflected wave front would impact the aircraft and result in additional input into the aircraft's vibration. It is felt that the damage resulting from the second input should depend critically on the vibratory displacement state of the aircraft at the time that the second input arrives.

To illustrate the point, consider a simplified example. Suppose the aircraft has experienced the primary wave input and has been set into vibration by it. If the wings are in the maximum upward position of their sinusoidal vibratory motion just as the reflected wave front arrives and causes an upward

aerodynamic force to be exerted on wings, considerable damage could occur. Conversely, if the secondary upward force arrives at another time, say just as the wings are moving through their equilibrium position with maximum downward velocity, it could actually alleviate structural loads. Thus the degree of damage depends upon modal frequencies and time of arrival of the second shock.

For this reason, consideration is turning toward use of the transition region to position aircraft and to evaluate the range at which mission completion damage occurs. Since this is a function of the response of the system when excited by the multiple shocks it may or may not be important to position the aircraft where the second peak is equal to some estimated value of hardness. The first peak may be the important response. The need exists, therefore, to study the response of a typical multi-degree of freedom system with multiple encounters to determine the important and controlling parameters. The payoff for this analysis would be a recommendation to the Strategic Air Command (SAC) to either fly low and fast to obtain a large range or climb above the triple point path. If the transition region is not as severe as postulated then an increased capability exists which should be incorporated in the SAC planning.

The specific research activity consisted of the development of a mathematical model of an aircraft typical of ones employed by SAC, such as the B-52H and KC-135, and the analysis of the response of this model to mathematically simulated blast input both with and without ground reflection effects. Two simultaneous approaches were employed: one approach was to generate a relatively simple model of an aircraft (with similarity to the B-52H), assuming a set of inertial and stiffness properties, determining the appropriate mode shapes and frequencies, using unsteady subsonic aerodynamics for the forcing functions, and calculating the resulting aircraft structural loads at a

few typical places. Based on this approach, the analyses would be conducted both with and without ground reflection effects. The other approach was to modify existing large-scale Air Force codes so as to reduce them in size and complexity and apply them to a study of the two shock problem. The model employed in this approach bore a similarity to the KC-135.

#### 1. Generation of a Simple Model

It was considered desirable to develop a simple model of an aircraft for the purposes of this research because a simple model would be relatively easy to change to accommodate varying refinements and because it would be relatively inexpensive in terms of digital computer costs to analyze many blast and flight conditions.

The model formulation followed standard methods (3) and was started by basing mass and stiffness on data obtained from the Boeing Company (4) for the B-52H. The Boeing data was obtained in a form suitable to be used to perform a large multi-degree-of-freedom analysis and had over 100 degrees of freedom. From this data the author reformed a model which consisted of 24 degrees of freedom. An attempt was made to use the mass and stiffness data of the 24 degree-of-freedom system with the first 24 modes of the Boeing vibration analysis to generate generalized mass and stiffness data. It was anticipated that there would be problems associated with this simple technique and these problems did, indeed, occur. The resulting generalized mass matrix (which should have been diagonal) had large off-diagonal terms and proved to be unusable.

Effort was directed toward obtaining the eigenvalues (frequencies) and eigenvectors (mode shapes) of the 24 degree-of-freedom system by adapting an

existing code, MASSMOD (5). This adaptation is partially successful but not complete as of this writing.

## 2. Modification of Existing Codes

Large complex codes for the dynamic analysis of aircraft exist (6, 7). One of these codes, a subsonic version of VIBRA4 was modified to reduce the size of the code and was employed, together with mass and stiffness data roughly simulating the KC-135, to analyze the dynamic response of the model to blast input both with and without ground reflection effects.

The modifications to VIBRA4 consisted of elimination of numerous calculations of stress levels on the aircraft, reduction of the number of degrees-of-freedom to a maximum of ten, elimination of the outputting of a considerable amount of miscellaneous data such as modal shapes, generalized masses, and structural loads, and display of time histories of input gust velocity and selected responses. These modifications resulted in a relatively inexpensive tool for analysis of double shock input.

A few analysis runs were made to examine the effects of neglecting double shock input. These runs are incomplete and preliminary but they seem to indicate that the double shock effect will produce higher loads than would be experienced by single shock at the same overpressures or gust velocities.

### Recommendations for Further Research

The research has resulted in the development of a tool for relatively inexpensive analysis of the double shock effect. This tool results from a modification of existing large-scale codes. It is effective but rather crude and could be refined to be a more useful and less expensive tool. It is recommended that activity continue to refine and simplify the code to produce a more useful and inexpensive analysis tool.

The analysis of the double shock phenomenon using the techniques developed is very preliminary. It is recommended that analyses continue, along with refinement in the methods, to investigate the significance of double shock effects.

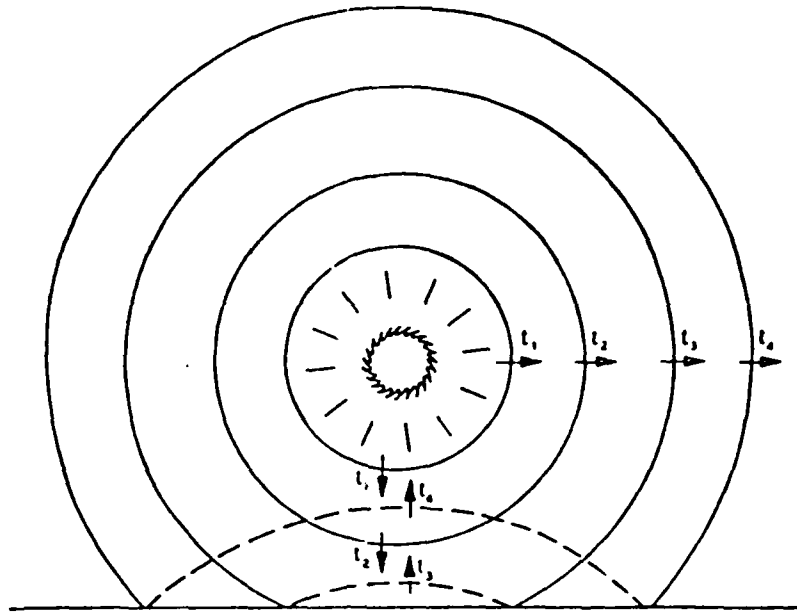


Figure 1. Reflection of Air Burst at Earth's Surface

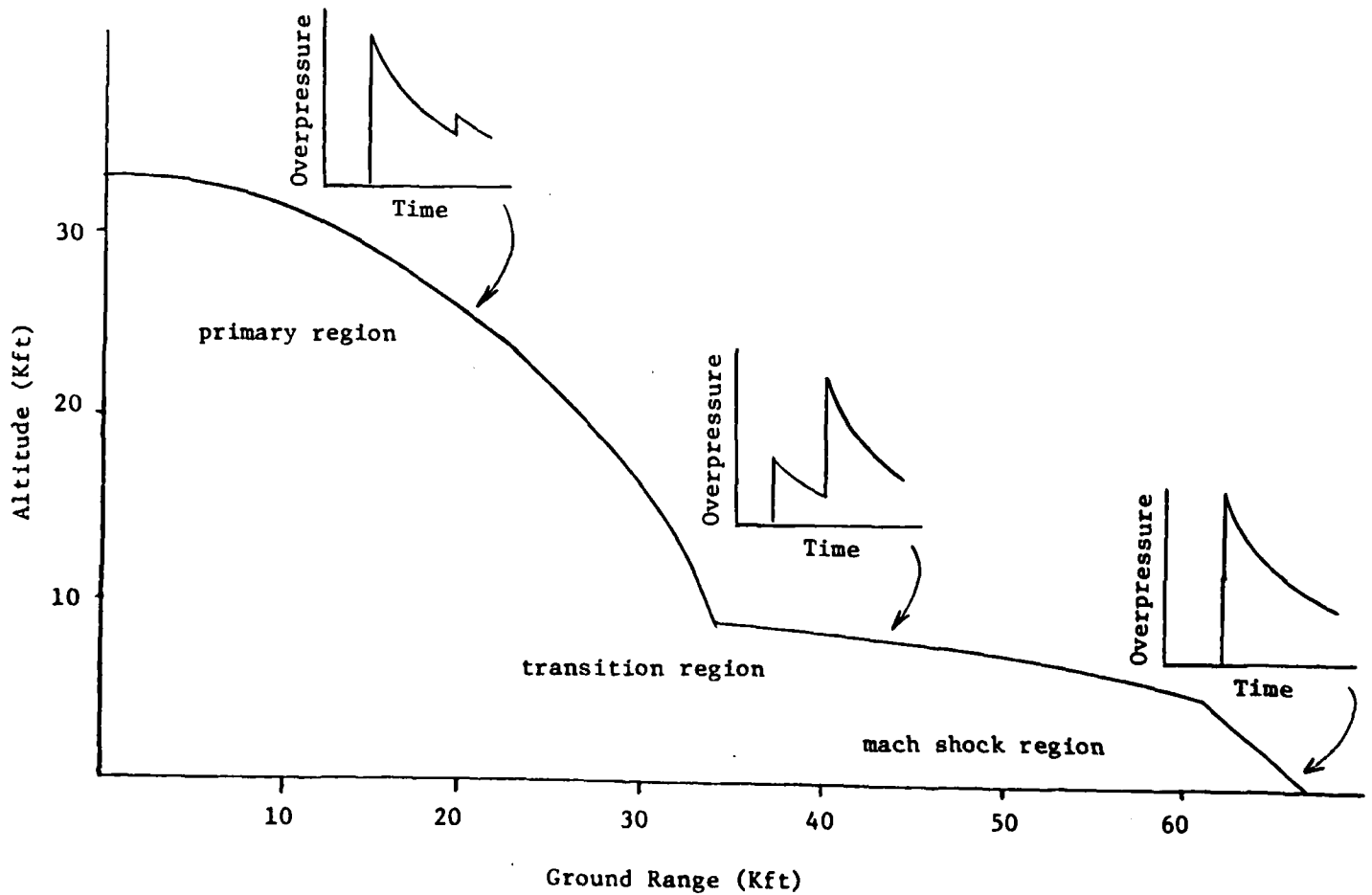


Figure 2. Iso-overpressure Contour

## References

1. Handbook for Analysis of Nuclear Weapon Effects, DNA 2048H-1, March 1976.
2. Sharp, A. L., Memo for the Record, DYV AFWL, KAFB, 15 May 1979.
3. Scanlan, R. H. and R. Rosenbaum, "Introduction to the Study of Aircraft Vibration and Flutter," Macmillan, 1951.
4. Shoup, G. S., Analytical Models for the B-52H, KC-135A, and 747-200 Aircraft, Vol. I, AFWL-TR-72-197, 1973.
5. Dalton, T. A., N. P. Hobbs, and J. M. Coco, MASM0D A Preprocessor Program for Preparing Dynamic Models for VIBRA-4, DNA 3050F, 1973.
6. Hobbs, N. P., G. Zartarian and J. P. Walsh, A Digital Computer Program for Calculating Blast Response of Aircraft to Nuclear Explosions, Vol. I, AFWL-TR-70-140, 1971.
7. McGrew, J. A., et al, Nuclear Blast Response Computer Program, Vol. I, AFWL-76-210, 1977.

1979 USAF - SCEEE SUMMER FACULTY RESEARCH PROGRAM

Sponsored by the

AIR FORCE OFFICE OF SCIENTIFIC RESEARCH

Conducted by the

SOUTHEASTERN CENTER FOR ELECTRICAL ENGINEERING EDUCATION

FINAL REPORT

ICING TESTING WITH MODELS - SIMILITUDE CONSIDERATIONS

Prepared by: Warren W. Bowden  
Academic Rank: Professor  
Department and University: Chemical Engineering, Rose-Hulman Institute of Technology  
Research Location: Arnold Engineering Development Center, Arnold AFS, TN 37389; Engine Test Facility, Technology Applications Branch, Fluid Mechanics Section  
USAF Research Colleague: Dr. Jay D. Hunt  
Date: August 21, 1979  
Contract No.: F49620-79-C-0038

## ICING TESTING WITH MODELS - SIMILITUDE CONSIDERATIONS

by

Warren W. Bowden

### ABSTRACT

Research on icing, anti-icing, and/or de-icing of aircraft surfaces would be less expensive and more flexible if it could be done using small-scale models. The reliable scale-up of test results from models depends, in theory, whether or not similitude can be maintained between the full scale equipment and its model.

The author (a) surveyed the literature on the application of similitude and the use of models in icing-, anti-icing- and de-icing- testing; (b) collected together the most valuable work on this subject; and (c) reviewed it critically with the aim of developing practical procedures for scaling up test results from models.

The conclusions resulting from this review are as follows:

(1) Most of those who have studied the use of models, scale-up and similitude in icing/anti-icing/de-icing of aircraft surfaces conclude that it is possible to scale up results from models.

(2) However, some authors express doubts whether valid scale-up is possible.

(3) Experimental data confirming (or disproving) valid scale-up are limited, mostly qualitative and not at all convincing one way or the other.

The author made recommendations as follows:

(1) Initiate a research program to establish whether or not icing, anti-icing and/or de-icing on models can be scaled up.

(2) Set up test equipment so as to maximize flexibility in the choice of individual test objectives.

(3) Develop computer programs to aid in the establishment of test conditions for models and the scale-up (or scale-down) of design data.

Contacts with NASA-Lewis makes it appear that a cooperative venture in this area between NASA-Lewis and Arnold Center is possible.

#### ACKNOWLEDGEMENT

The author thanks the Air Force Systems Command, Air Force Office of Scientific Research and the Southeastern Center for Electrical Engineering Education for giving him the opportunity to spend a rewarding and interesting summer at the Arnold Engineering Development Center. Special thanks go to Mr. Marshall Kingery at Arnold for numerous helpful suggestions.

Dr. Jay Hunt, ETF/TAB, provided sound direction and helpful discussions on this research project. Mr. Roy Schulz, ETF/TAB, cheerfully answered my questions concerning his work on supercooled water droplets and anti-icing heating.

## I. INTRODUCTION:

If one could carry out icing testing using reduced-scale models, one would accrue the advantages of economy, flexibility and an expanded range of available test conditions.

When models are used in icing testing or any sort of testing it must be shown that the results obtained on the model can be expected to scale up to the full scale equipment. It has been shown by rigorous argument and by experiment (1,2) that if similitude is maintained between the two scales, the results will scale up closely. Similitude in this context means that the model- and full scale-equipment are similar geometrically and are exposed to similar aerodynamic and heat transfer regimes.

This report summarizes the results from a survey of the literature on the application of similitude to icing testing. The rate of accretion of ice on a surface depends on the impingement flux,  $W''$ , surface conditions, and heat transfer. The impingement flux depends primarily on geometric and aerodynamic factors. The heat transfer effects depend upon geometric and aerodynamic considerations but also upon temperature and humidity driving forces. Hence, the two principal dependent variables are coupled. In this report impingement flux,  $W''$ , will be dealt with first, heat transfer next, and finally the interaction of the two.

Appendices A-I to A-IV contain summaries of several papers on the application of similitude to icing research.

Appendix B-I is a discussion of certain results in the seminal paper by Willbanks and Schulz (15) on the simulation of icing conditions in test cells.

Appendix B-II gives the derivations of steady and unsteady energy balances using the steady and unsteady First Law expressions. These derivations emphasize the implications of underlying assumptions of steady state conditions. Some of the widely-quoted equations (from (17), for example) are subject to considerable doubt if applied to a section undergoing freezing conditions.

## II. OBJECTIVES:

The objectives of this research were as follows:

- (1) To survey the literature on the use of models and similitude in icing-/anti-icing testing.
- (2) To collect together the most valuable work on this subject for convenient reference.
- (3) To review critically the application of similitude in icing-/anti-icing research and thus develop practical computational procedures for the use of models in this work.

## III. SURVEY OF LITERATURE:

The author made use of an on-line Information Retrieval Service (Lockheed DIALOG) and reports which Dr. Jay Hunt supplied in searching for previous work on the application of similitude to icing research. Some 15 papers/reports/sections of design manuals were found which contained pertinent material. These references are listed below under "References".

## IV. SUMMARY OF WORK ON APPLICATION OF SIMILITUDE TO ICING-/ANTI-ICING RESEARCH:

The work of four authors on this subject has been summarized in Appendices A-I through A-IV.

## V. CRITICAL REVIEW/COMPUTATIONAL PROCEDURES:

Reading the summaries in Appendices A-I through A-IV leads one to the following observations:

- (1) There are a variety of approaches to the application of similitude to icing research with varying degrees of rigor.
- (2) Similitude conditions with respect to drop trajectory/collection efficiency has been much more carefully worked out than that for heat transfer.
- (3) There is not a unanimity of opinion whether or not it is possible to maintain complete similitude between model and full scale equipment.
- (4) Experimental data confirming (or disproving) the applicability of similitude principles are not abundant and not convincing one way or the other.

As stated in the Introduction, computational procedures for maintenance of similitude of impingement flux, heat transfer, and the combination of these two are developed in separate sections below.

(A) Maintenance of Similitude with Respect to Impingement Flux,  $W''$ :

Impingement flux,  $W''$ , is the mass of water striking an appropriate unit area per unit time. As shown in reference (3),  $W''$  can be calculated from

$$W'' = (LWC)_o \left( \frac{HZ}{A_{wet}} \right) V_o E_M \quad (1)$$

wherein

$(LWC)_o$  = liquid water content of upstream air,  $M/L^3$

$\left( \frac{HZ}{A_{wet}} \right)$  = an appropriate geometric factor which allows for local water distribution (See (4) ), dimensionless

$V_o$  = uniform approach velocity upstream of object,  $L/\theta$

$E_M$  = overall impingement efficiency, dimensionless

The factor  $\left( \frac{HZ}{A_{wet}} \right)$  must be geometrically similar in the model and the full scale equipment in order to maintain similitude.  $(LWC)_o$  and  $V_o$  can be varied independently. The interaction of these variables and  $E_M$  required to maintain equal  $W''$  in the model and full scale equipment will be discussed after a detailed discussion of  $E_M$  in a subsection below.

Overall Collection Efficiency,  $E_M$ . As discussed in detail in reference (5),  $E_M$  is a complicated function of the impingement parameter,  $K_o$ , defined by Equation (2):

$$K_o = K \left( \frac{\lambda}{\lambda_s} \right) \quad (2)$$

wherein  $K = \text{inertia parameter} = \frac{2}{9} \left( \frac{d}{2} \right)^2 \frac{\rho_w V_o}{L_c M_o}$

and  $d$  = drop diameter,  $L$

$\rho_w$  = water density,  $M/L^3$

$V_o$  = uniform upstream velocity,  $L/\theta$

$M_o$  = viscosity of air,  $m/(L\theta)$

$L_c$  = characteristic length of object (See (6) for examples),  $L$

$\frac{\lambda}{\lambda_s}$  = (true droplet "range")/(Stokes' Law "range"), dimensionless

Obviously, in order to keep  $E_M$  the same for a full-scale object (subscript  $f$ ) and its reduced-scale model (subscript  $m$ ), one must maintain conditions such that  $K_{om} = K_{of}$ .

If the scale factor relating the sizes is  $R$ , then  $L_{cm} = RL_{cf}$  and from Equation (2)

$$\bar{d}_m^2 v_{om} \left( \frac{\lambda}{\lambda_s} \right)_m = R \bar{d}_f^2 v_{of} \left( \frac{\lambda}{\lambda_s} \right)_f$$

or

$$\bar{d}_m = \bar{d}_f \left( \frac{v_{of}}{v_{om}} R \right)^{1/2} \left[ \frac{\left( \frac{\lambda}{\lambda_s} \right)_f}{\left( \frac{\lambda}{\lambda_s} \right)_m} \right]^{1/2} \quad (3)$$

In obtaining (3) it has been assumed that  $\rho_w$  and  $M_o$  are constant. As shown by Pfeifer and Maier (7),  $\lambda/\lambda_s$  is a nearly linear function of the drop Reynolds number,  $N_{Re,d} = \bar{d} v_o \rho_w / M_o$ . The ratio  $\left[ \left( \frac{\lambda}{\lambda_s} \right)_f / \left( \frac{\lambda}{\lambda_s} \right)_m \right]$  is essentially related by the ratio  $(\bar{d} v_o)_m / (\bar{d} v_o)_f$ . Hence, one could write Equation (3) in the form

$$\bar{d}_m = \bar{d}_f \left( \frac{v_{of}}{v_{om}} R \right)^{1/2} \cdot f \left( \bar{d}_f, \frac{v_{of}}{v_{om}} \right) \quad (4)$$

Equation (4) can be written as

$$\bar{d}_m - \bar{d}_f \left( \frac{v_{of}}{v_{om}} R \right)^{1/2} \cdot f \left( \bar{d}_f, \frac{v_{of}}{v_{om}} \right) = 0 \quad (5)$$

and, for a given  $R$ ,  $v_{of}/v_{om}$  ratio and  $\bar{d}_f$ , solved for the  $\bar{d}_m$  required for the model to maintain dynamic similitude and thus the same  $E_M$ . The ratio  $v_{of}/v_{om}$  might need to differ from unity in order to maintain similitude with respect to heat transfer.

To demonstrate how this procedure would work and to check if a feasible mean drop diameter is obtained, consider the example given in (8):

$\bar{d}_f = 20 \mu m$ ,  $N_{Re,d_f} = 135$ ,  $v_o = 314$  ft/sec,  $\rho_w = 62.4$  lb/ft<sup>3</sup>,  $M_o = 1.1 \times 10^{-5}$  lb<sub>m</sub>/ft-sec. From Figure 3-6 in (8)  $\lambda/\lambda_s = 0.32$

Assume that for some reason:  $V_{of}/V_{om} = 1.8$   $R = 1/10$   
 Now, in Equation (3) or (5):

$$\bar{d}_m - 20 \left(1.8 \times \frac{1}{10}\right)^{1/2} \frac{(0.32)^{1/2}}{(\lambda/\lambda_s)_m^{1/2}} = 0$$

$$\text{or } \bar{d}_m - \frac{4.8}{(\lambda/\lambda_s)_m^{1/2}} = 0 \quad (A)$$

In the example referred to above:

$$\frac{\rho_w}{M_o} = \frac{135}{20 \times 314} = 0.02149, \quad V_{om} = \frac{314}{1.8} = 174.4 \quad \text{and}$$

$$N_{Re d_m} = d_m \times 174.4 \times 0.02149 = d_m \times 3.748$$

Now solve (A) by trial:

Trial	$\bar{d}_m$ Ass.	$N_{Re d_m}$	$(\lambda/\lambda_s)_m$	$\bar{d}_m$ Calc.	$\bar{d}_{Ass.} - \bar{d}_{Calc.}$
1	30	11.2	0.31	8.62	21.4
2	10	37.5	0.5	6.78	3.22
3	5	18.7	0.61	6.14	- 1.14
4	6	22.5	0.58	6.3	- 0.3
5	7	26.2	0.57	6.35	0.65

$$\text{So } \bar{d}_m = 6.3 + \frac{0.3}{0.95} = 6.6$$

$\bar{d}_m = 6.6 \mu\text{m}$

This means that if the full scale test were run as in the example given, and if it were necessary to have  $R = 1/10$ ,  $V_{of}/V_{om} = 1.8$ , then the test using a model would need to be run with an average drop size around  $7 \mu\text{m}$  in order to have the same  $E_M$ .

It should be pointed out that an examination of the  $E_M - K_o$  curves given by Pfeifer and Maier (9) shows that for values of  $K_o > \sim 10$   $E_M$  changes very little with  $K_o$ . Consequently, providing the impingement parameter,  $K_o$ , is maintained above 10, scaleup of results should be reliable even though similitude has not been maintained.

Impingement Flux,  $W''$ . From Equation (1), if the ratio  $(W''_m/W''_f)$  is to be unity,

$$(LWC)_{om} \left( \frac{HZ}{A_{wet}} \right)_m V_{om} E_{Mm} = (LWC)_{of} \left( \frac{HZ}{A_{wet}} \right)_f V_{of} E_{Mf} \quad (6)$$

The ratio  $(HZ/A_{wet})_m / (HZ/A_{wet})_f$  will, by virtue of geometric similitude, equal unity. If it has been possible to maintain  $E_{Mm}$  equal to  $E_{Mf}$ , then we have

$$(LWC)_{om} V_{om} = (LWC)_{of} V_{of} \quad (7)$$

If, for some reason, it is necessary to have a fixed ratio  $V_{of}/V_{om}$ , then the liquid water content for the model should be related to that of the full scale apparatus by

$$(LWC)_{om} = (LWC)_{of} \frac{V_{of}}{V_{om}} \quad (8)$$

Equation (8) gives the  $(LWC)_o$  needed to assure the same  $W''$  in model and full scale test object.

Ice Thickness,  $T_I$ . Ice thickness,  $T_I$ , is calculated from

$$T_I = \frac{W''}{\rho_{ice}} \gamma \quad (9)$$

In this expression  $\rho_{ice}$  is fixed and  $\gamma$ , the time of the experiment, can be varied independently of other factors. The impingement flux,  $W''$ , can be scaled up as described above.

Other References. Reference numbers 10-14 give alternate approaches to the maintenance of similitude during model testing. Summaries of the material on similitude in several of the papers/reports are given in Appendices A-I through A-IV.

(B) Similitude With Respect to Heat Transfer:

Case 1. No Freezing on Surface,  $T_s \geq 0^\circ C$ . For a case where there is no freezing on the surface, we can use the equation in the paper by Willbanks and Schulz (15)

$$Q = \frac{q_s''}{\bar{h}(T_s - T_r)} = 1 + \frac{\frac{h_{fg} \bar{M}_v}{C_p \bar{M}_a} \left[ \frac{P_r}{S_c} \right]^{0.67} \frac{(P_{vs} - P_{ve})}{P_e}}{T_s - T_r} + b \frac{T_s - T_c - T_e \frac{\gamma - 1}{2} \frac{C_p}{C_c} M_e^2}{T_s - T_r} \quad (10)$$

(See notation below.)

In Equation (10)  $Q$  is a dimensionless heat transfer parameter. In words, it is the ratio of the total anti-icing heat input flux,  $q_s''$ , (heat flow rate per unit area) to the convection heat transfer flux,  $(\bar{h}(T_s - T_r))$ . The factor  $b$  is the ratio of the sensible heat capacity ( $W_{C_c}$ ) to the convective heat transfer coefficient  $\bar{h}$ . At slow air speeds and if the droplet temperatures equal the air temperature,  $b$  would be the ratio of sensible heat to convective heat.

If one rewrites Equation (10) in the form

$$q_s'' = \bar{h}(T_s - T_r) + \frac{\bar{h} \bar{M}_v}{C_p \bar{M}_a} \left[ \frac{P_r}{S_c} \right]^{0.67} \frac{(P_{vs} - P_{ve})}{P_e} h_{fg} + b \bar{h} \left[ T_s - T_c - T_e \cdot \frac{\gamma - 1}{2} \cdot \frac{C_p}{C_c} \cdot M_e^2 \right] \quad (11)$$

one can immediately associate the first term with convective heat transfer, the second with evaporative heat effect and the third with the net sensible heat effect.

Consider now each of these phenomena in turn. In order to maintain similitude with respect to convective heat transfer, one must have equal transfer coefficients,  $\bar{h}$ , in the model and in the full scale. The heat transfer coefficient,  $\bar{h}$ , is a function primarily of the Reynolds number and Prandtl number. For example, from reference (3) the following equations are recommended:

(A) Leading edge of an airfoil

$$N_{NU,D} = \frac{h_o D}{K} = 1.14 (N_{Re,D})^{0.5} (N_{Pr})^{0.4} \left(1 - \left(\frac{\theta}{90}\right)^3\right) \quad (12)$$

wherein

$D = 2X$  (airfoil leading edge radius)

$\theta$  = angle from stagnation point ( $0^\circ - 80^\circ$ )

$$N_{Re,D} = \frac{\rho_o v_o D}{M_o}$$

$N_{Pr}$  = Prandtl number of air

$\rho_o, v_o, M_o$  = density, velocity, viscosity, respectively of the air

(B) Stagnation point on a nose cone or spinner,

wherein

$$N_{NU,D} = \frac{hD}{K} = 1.32 (N_{Re,D})^{0.5} (N_{Pr})^{0.4} \quad (13)$$

$$N_{Re,D} = \frac{\rho_o v_o D}{M_o}$$

(C) Side panel regions and surfaces of nose cones and spinners aft of the stagnation point (flat plate correlations):

$$N_{NU,S} = \frac{hS}{K} = 0.322 (N_{Re,S})^{0.5} (N_{Pr})^{0.33} \quad (\text{Laminar flow}) \quad (14)$$

$$N_{NU,S} = \frac{hS}{K} = 0.0296 (N_{Re,S})^{0.8} (N_{Pr})^{0.33} \quad (\text{Turbulent flow}) \quad (15)$$

wherein

$$N_{Re,S} = \frac{\rho_e v_e S}{M_e}$$

$S$  = characteristic dimension

(D) Internal anti-icing bleed air passages

$$N_{NU,De} = \frac{hDe}{K} = 0.023 (N_{Re,De})^{0.8} (N_{Pr})^{0.4} \quad (16)$$

wherein

$$N_{Re, De} = \frac{V De}{M} = 10000$$

$$De = \frac{4 \times (\text{cross-sectional flow area})}{\text{inside wetted perimeter}}$$

Hence, to maintain similitude with respect to convective heat transfer, one must keep  $N_{NU} = \frac{hL}{K}$  constant, where L is some characteristic

length. Now, L by necessity, must be different in model and full-scale equipment. Changing L changes the numerical value of  $N_{NU}$  and  $N_{Re}$ . In fact, h is proportional to  $L^{-0.2}$  or  $L^{-0.5}$  from the above equations. To carry through an analysis let subscript m refer to the model and f refer to the full scale and assume that Equation (15) applies:

$$\frac{h_m S_m}{K_m} = 0.0296 \left( \frac{\rho_m V_m S_m}{M_m} \right)^{0.8} \left( \frac{C_p M}{K} \right)_m^{0.33} \quad (17)$$

$$\frac{h_f S_f}{K_f} = 0.0296 \left( \frac{\rho_f V_f S_f}{M_f} \right)^{0.8} \left( \frac{C_p M}{K} \right)_f^{0.33} \quad (18)$$

S = a characteristic length

Divide Equation (17) by (18) with  $h_m = h_f$  to obtain

$$\frac{S_m}{S_f} = \frac{K_f}{K_m} \left[ \frac{\rho_m V_m}{M_m} \right]^{0.8} \left[ \frac{S_m}{S_f} \right]^{0.8} \left[ \frac{\left( \frac{C_p M}{K} \right)_m}{\left( \frac{C_p M}{K} \right)_f} \right]^{0.33}$$

or

$$\left( \frac{S_m}{S_f} \right)^{0.2} = \frac{K_f}{K_m} \left[ \frac{\rho_m V_m}{M_m} \right]^{0.8} \left[ \frac{\left( \frac{C_p M}{K} \right)_m}{\left( \frac{C_p M}{K} \right)_f} \right]^{0.33}$$

$$\text{or } \frac{S_m}{S_f} = \left(\frac{K_f}{K_m}\right)^5 \times \left[\frac{e_m v_m}{M_m}\right]^4 \times \left[\frac{\left(\frac{C M}{P K}\right)_m}{\left(\frac{C M}{P K}\right)_f}\right]^{1.65}$$

If one assumes that the ratios of physical properties do not change very much, then

$$\frac{S_m}{S_f} = \left(\frac{v_m}{v_f}\right)^4$$

$$\text{or } v_m = v_f \left(\frac{S_m}{S_f}\right)^{0.25}$$

If  $S_m/S_f = 1/10$ , then  $v_m = 0.562 v_f$ .

Looking now at the second term in Equation (11), the evaporative term: the rate of evaporation is proportional to the driving force,  $(P_{sat} - P_{ve}) / P_e$ , and the mass transfer coefficient,  $(\bar{h} \bar{M}_v / (\bar{M}_a C_p) \left(\frac{P_r}{S_c}\right)^{0.67})$ . The evaporative energy transfer rate is hence the product of (mass transfer rate) (Latent heat). Assuming a constant driving force this term depends on the same factors as convective heat transfer.

The third term in Equation (11) essentially concerns the sensible heat, the heat required to increase the temperature of the incoming water from  $T_c$  to the surface film temperature  $T_s$ . The coefficient  $(b\bar{h})$  equals  $W_c C_c$ , the total heat capacity of the incoming fluid. Thus,  $(b\bar{h})$  is a function of  $W'$  and the liquid water heat capacity  $C_c$ . The latter quantity is constant for all practical purposes.

#### Notation for Section V-B

- $b$  = sensible heating parameter =  $W_c C_c / \bar{h}$
- $c_p$  = air heat capacity
- $c_c$  = liquid water heat capacity
- $D$  = diffusion coefficient of water
- $\bar{h}$  = convective heat transfer coefficient

$h_{fg}$  = latent heat of evaporation  
 $K$  = thermal conductivity  
 $\bar{M}_v$  = molecular weight of water = 18.016  
 $\bar{M}_a$  = molecular weight of air = 28.996  
 $M_e$  = Mach number at outer edge of boundary layer = a function of  $M_\infty$ ,  $T_\infty$ ,  $T_e$  (see reference (20), pp. 162-169)  
 $M_\infty$  = Mach number of free air stream  
 $P_e$  = total pressure at outer edge of boundary layer  
 $P_r$  = Prandtl number of air =  $C_p M / K$   
 $P_{vs}$  = saturation vapor pressure of water  
 $P_{ve}$  = partial pressure of water in free stream  
 $q''_s$  = anti-icing heat transfer flux  
 $Q$  = dimensionless ratio defined by Equation (10)  
 $r$  = recovery factor =  $(P_r)^{1/3}$  (turbulent boundary layer)  
 $S_c$  = Schmidt number =  $M / \rho D$   
 $T_r$  = recovery temperature =  $T_e (1 + r \frac{\gamma - 1}{2} M_e^2)$   
 $T_s$  = film surface temperature  
 $T_e$  = temperature at outer edge of boundary layer = a function of  $M_\infty$  and  $M_e$  (see above-mentioned reference)  
 $T_{c\bullet}$  = temperature of approaching water droplets  
 $\gamma$  = heat capacity ratio =  $C_p / C_v$   
 $M$  = viscosity  
 $\rho$  = density

(C) Interaction of Impingement Flux and Heat Flux

It is clear from the discussion above that to maintain the sensible heat term constant it is necessary to keep  $W''$  constant. To keep  $W''$  constant one needs to keep the product  $(LWC)_o \left( \frac{HZ}{A_{wet}} \right) V_o E_M$  constant. The factor  $\left( \frac{HZ}{A_{wet}} \right)$  is fixed by geometry. If the maintenance of dynamic similitude with respect to convection heat transfer requires a change in  $V_o$ , this may trigger a change in  $E_M$ . Furthermore, a change in  $V_o$  will necessitate a change in  $(LWC)_o$ . Providing the ratio  $(V_{om}/V_{of})$  is such a value that it can be compensated for by changing  $(LWC)_o$ , equal values of  $W''$  can be maintained.

The above discussion leads one to the conclusion that it is important to know whether one or another of the three terms in Equation (11) predominates in any given situation. For example, if in a particular instance, the convection heat transfer rate were 90% of the total anti-icing heat transfer, then it would not be too important to maintain complete similitude with respect to the evaporative heat transfer or the sensible heat flow. On the other hand, if in a particular case the three are approximately equal, then it would be important to maintain dynamic similitude with respect to all three modes of heat transfer. For example, in the case discussed in Appendix B-I, when  $M_e = 0.4$ ,  $b = 0.251$ , the percent of anti-icing heat being used for sensible heat is 1.6%. Hence, for this case, one need not be very concerned about dynamic similitude with respect to the sensible heat effect.

On the other hand, when  $M_e = 0.4$ ,  $b = 2$ , the sensible heat effect predominates and similitude with respect to this effect would be especially important. In this particular case the latent heat and convective heat are about equal and of such a percentage that they also would have to be considered.

## RECOMMENDATIONS

In view of

- (a) the need for sound calculation procedures and reliable data for design of anti-icing and/or de-icing protection of aircraft surfaces,
- (b) the rather conspicuous advantages derived from the use of models in the determination of these data, and
- (c) the uncertainties which currently call into question the applicability of similitude and the validity of scale-up of anti-icing and de-icing results from models,

the writer makes the three recommendations below;

- (I.) Initiate a research program to establish whether or not results from models in icing-/anti-icing/de-icing tests can be validly scaled up.

The first of such tests should be on a body for which the collection efficiency is well known, a cylinder, for example. The primary objective of such tests would be to determine if heat transfer and the interaction of heat transfer with collection efficiency can be scaled up. The format of this investigation would be:

- (a) run tests on a full scale object under a given set of conditions,
- (b) run tests on a model under conditions calculated to be scaled down according to the laws of similitude, and
- (c) make a comparison of the results from the two above conditions by statistical criteria to determine whether or not the scale-down was indeed valid. A few such tests on each of a few shapes would confirm (or disprove) the validity of tests with models and the applicability of similitude principles.

A few comments on the nature of the above investigation are in order:

The key decision whether the tests should focus on anti-icing or de-icing, or "no protection" conditions is a difficult one. If one chooses the "no protection" option, he should consider that there is available now a corpus of qualitative data, that new data on this phenomena are likely to be qualitative or semiquantitative at best, that the impingement efficiency will be changing with time because the shape and size of the ice deposit changes with time, and that heat transfer effects are secondary. The choice between anti-icing and de-icing protection depends on many factors: the surface under consideration, the practical means of applying heat to the surface (resistive electrical heating,

double skin heat exchanger, heat pipe), the problems caused by "runoff" and/or shedding. If shedding can be tolerated, then intermittent electrical heating (de-icing) needs to be carefully considered. If runoff is no problem, then anti-icing protection probably should have top priority. Finally, experimental data comparing icing, anti-icing and de-icing occurring at altitude with that occurring at sea level should be obtained. All these comments lead to recommendation (II).

(II.) Set up test equipment so as to maximize flexibility in the choice of individual test objectives.

In other words, the shapes under study should be so equipped that the heat input can be intermittent or steady, the heat fluxes, the surface temperature and other important variables can be accurately measured. Plans for measurements to be taken, recorded, and to some extent analyzed, by microprocessors in real time deserve top consideration.

(III.) Develop computer programs to aid in the establishment of test conditions for models and the scale-up (or down) of design data.

In this situation the collection efficiency and heat transfer must be scaled down (or up) simultaneously according to the principles of similitude. As can be seen in other sections of this report, the required calculations are not simple. The time savings and flexibility afforded by appropriate computer programs cannot be overemphasized. Such programs would be quickly adapted for the microprocessor used to massage the data while it is being collected.

These programs should:

(a) be well-structured, i.e., easily understood, easily modified by programmers reasonably skilled in the art, free of unanticipated action and untoward output;

(b) be well documented; that is, provided with descriptions of calculation procedures, flow diagrams, subprogram descriptions, variable descriptions and specifications, and illustrative input/output;

(c) have checks of input data for reasonableness to avoid misuse and waste of execution time;

(d) have provisions to prevent ungraceful failure;

(e) have adequate error/warning messages to the user in situations where failure may occur; and

(f) be portable.

Communication with personnel at NASA-Lewis makes it seem likely that a cooperative Arnold/NASA-Lewis research program could be arranged.

## REFERENCES

1. Bridgman, P. W., Dimensional Analysis, 2nd Edition, Yale (1931), Wiley (1951).
2. Langham<sup>AN</sup>, H. L., Dimensional Analysis and Theory of Models, Wiley (1951).
3. Pfeifer, G. D., and G. P. Maier, Engineering Summary of Powerplant Icing, AD1A-045-087 (1977).
4. Ibid, pp. 3-10 to 3-13, and 3-28 to 3-30.
5. Ibid, pp. 3-8, 3-9 and 3-32 to 3-39.
6. Ibid, p. 3-9.
7. Ibid, p. 3-31.
8. Ibid, pp. 3-13, 3-14.
9. Ibid, pp. 3-35, 3-39.
10. Brun, E. A., AGARDOGRAPH 16, Section 2.2.2 (1957).
11. Armand, Claude, F. Charpin, and G. Leclere, AGARD-AR-127, pp. A6-1 to A6-23 (1978).
12. Flower, J. W., "The Determination of Ice Deposition on Slender Wings: An Experimental Technique and Simplified Theory," ICAS Proceedings 1974, pp. 397-408 (1974).
13. Bowden, D. T., A. E. Gensemer, and C. A. Speen, Engineering Summary of Airframe Icing Technical Data, FAA Technical Report ADS-4 (1964).
14. Lewis, J. P. and R. S. Ruggeri, "Experimental Droplet Impingement on Four Bodies of Revolution," NACA-TN-4092 (1957).
15. Willbanks, C. E., and R. J. Schulz, "Analytical Study of Icing Simulation for Turbine Engines in Altitude Test Cells," Journal of Aircraft, 12, 960-967 (1975).
16. Hardy, J. K., "Protection of Aircraft Against Ice," Royal Aircraft Establishment, Report No. S.M.E. 3380, July, 1946.
17. Messenger, B. L., "Equilibrium Temperature of an Unheated Icing Surface as a Function of Air Speed," J.A.S., 29-42 (1953).
18. Tribus, M., Intermittent Heating for Protection in Aircraft Icing, Ph.D. Thesis, U.C.L.A., August, 1949.
19. Neel, C. W. B., N. R. Bergium, D. Juckoff, and B. A. Schlaff, "The Calculation of the Heat Required for Wing Thermal Ice Prevention in Specified Icing Conditions," NACA-TN-1472, December, 1947.

20. Sogin, H. H., A Design Manual for Thermal Anti-Icing Systems,  
WADC TR 54-313.

Appendix A-I

Summary of Study by Armand, et al., on Similitude

Armand, Charpin, Fasso and Leclere (1) found that the model scale,  $K$ , is related to the other parameters by the expression

$$K = \frac{a_K^{2-x} V_K^{1-x}}{P_{aK}^x T_{aK}^{\frac{3-5x}{2}} (T_{a_m} + 117)/(T_{a_f} + 117)^{x-1}} \quad (\text{A-I, 1})$$

where  $x$  is chosen so that

$$\frac{C_D \cdot Re}{24} = K (Re)^x \quad (\text{A-I, 2})$$

represents the best fit of the drag coefficient with  $Re$ . For values of  $Re$  between 6 and 120 they found that the best  $x$  was around 0.39. In most cases  $T_{a_m}/T_{a_f}$  is close to 1, and a practical formula is:

$$K = \frac{a_K^{1.61} V_K^{0.61}}{P_{aK}^{0.39}} \quad (\text{A-I, 3})$$

The liquid water content ratio,  $LWC_K$ , and icing time ratio,  $\tau_K$ , are given by

$$LWC_K = \frac{P_{aK}^{0.8}}{K^{0.2} V_K^{0.2} T_{aK}^{1.6}} \quad (\text{A-I, 4})$$

and

$$\tau_K = \frac{K^{1.2} T_{aK}^{1.6}}{V_K^{0.8} P_{aK}^{0.8}} \quad (\text{A-I, 5})$$

Equations (A-I, 3) and (A-I, 4) are valid only if the relative heat factor,  $b$ , and icing fraction,  $n$ , (2) are equal in both scales. The equation derived in (2) relating these parameters is as follows:

$$\frac{1.06 \times 10^6}{P_a} = t_a (1 + b) + 1730 \frac{\bar{P}_a}{P_a} + 79.7nb + (3.65 + b) \frac{V_{\infty K}^2}{8370} \quad (\text{A-I, 6})$$

In the above equations, (A-I, 1) through (A-I, 6), the symbols have the following meaning:

$K$  = model scale

$P_{aK} = P_{am}/P_{af}$  = atmospheric pressure ratio

$V_{\infty K}$  = upstream velocity ratio

$T_{aK}$  = upstream air temperature ratio

$C_D$  = drag coefficient

$Re$  = Reynolds number

$a_K$  = drop diameter ratio

$\bar{P}_a$  = water partial pressure in free stream

$n$  = icing fraction

$b$  = relative heat factor =  $\frac{C_p W''}{h}$

$C_p$  = heat capacity of liquid water

$W''$  = water impingement rate

$h$  = convection heat transfer coefficient

The flight of an aircraft under any given conditions is characterized by the following:

$V_{\infty f}$  = velocity

$\alpha_f$  = angle of attack

$H_f$  = altitude corresponding to a pressure  $p_{af}$  and temperature  $t_{af}$

The icing cloud is characterized by its:

$(LWC)_f$  = liquid water content

$a_f$  = droplet median volume diameter

$\bar{p}_f$  = water partial pressure

The ice deposit on a wing or whatever depends on the above parameters and duration of the icing condition,  $\tau_t$ .

For aerodynamic similitude

$$\alpha_m = \alpha_f$$

(A-I, 7)

For similitude with respect to heat transfer, values of the parameters  $P_a$ ,  $t_a$ ,  $\bar{P}$  and  $V$  fix the rate at which heat transfer takes place. Hence, the relation between  $n$  and  $b$ , from Equation (A-I, 7) becomes

$$n = \frac{A_f + B_f b}{b} \quad (\text{A-I, 8})$$

For similitude to prevail with respect to heat transfer, the four variables just listed should lead to the same value of  $n$  for both scales, so

$$\frac{A_f + B_f b}{b} = \frac{A_m + B_m b}{b} \quad (\text{A-I, 9})$$

or  $A_m = A_f$  and  $B_m = B_f$  (A-I, 10)

wherein  $A$  and  $B$  are groups of variables in Equation (A-I, 6) when it is solved for  $n$ .

Similitude of droplet trajectory is ensured if the mean drop diameter ratio is chosen such that

$$a_K^{1.61} = \frac{K P_a K^{0.39}}{V_K^{0.61}} \quad (\text{A-I, 11})$$

Similitude of ice deposits depends on  $LWC$  and  $\gamma$ .

Similitude for rotary wing aircraft is also discussed briefly.

#### References:

- (1) Armand, Claude, F. Charpin, G. Fasso and G. Leclere. "Techniques and Facilities Used at the Onera Modane Centre for Icing Tests," Aircraft Icing, AGARD Advisory Report #127 (November, 1978).
- (2) Messenger, B. L., "Equilibrium Temperature of an Unheated Icing Surface as a Function of Air Speed," J. of A. S., 20, pp. 29-42 (1953).

## Appendix A-II

Abstract of "Theoretical and Experimental Study of the Influence of Various Parameters on the Icing of a Profile," by Jacques Bongrand.\*

### Theory:

One can cause the following parameters to vary:

1. The static pressure (represents altitude)
2. The static temperature of the external flow
3. The relative velocity at infinity
4. The concentration of water upstream
5. The average diameter of the water drops.

### Outline of Icing:

A general description of the phenomena.

### Trajectories of Drops

The magnitude of the force on the drop is calculated from an equation of the form:

$$R = \rho d^2 u^2 f\left(\frac{\rho V_d}{M}\right) \quad (\text{A-II, 1})$$

For a value of  $u$  of the order of 10 to 100 m/sec and  $d$  in the vicinity of 20 microns, one can take

$$f\left(\frac{\rho ud}{M}\right) \sim \left(\frac{\rho ud}{M}\right)^{-1/2} \quad (\text{A-II, 2})$$

To maintain similitude of capture one should maintain the expression

$$\rho^{1/2} d^{-3/2} v^{-1/2} \quad \text{constant.}$$

If this condition is realized, the fraction of water captured by the profile varies according to the product  $CV$ , where

$C$  = water content

$V$  = upstream velocity at infinity

### Heat Transfer

The various terms can be evaluated as follows:

1. Kinetic energy of the drops is  $V^2/2$  per unit mass or  $10^3 \text{ J/K}_g$  at 100 m/s and  $45 \times 10^3 \text{ J/K}_g$  at 300 m/s compared with the heat of fusion of  $\approx 330 \times 10^3 \text{ J/K}_g$ .

\* See end of this Appendix for reference.

## 2. Convection heat transfer

The magnitude of the heat flux "emitted" by the wall,  $F$ , is of the order

$$F_1 \sim v (\theta_p - \theta_e) \left( \frac{e v l}{M} \right)^{-0.2} \sim - (e v)^{0.8} \theta_e \quad (\text{A-II, 3})$$

Heat lost by vaporization of drops in the boundary layer. The quantity of water vaporized per unit volume of boundary layer is proportional to

$$P_s \left( \frac{\theta + \theta_r}{2} \right) - P_s(\theta)$$

whence the searched-for flux,  $F_2$  is:

$$F_2 \sim v \delta_1 \left[ P_s \left( \frac{\theta + \theta_r}{2} \right) - P_s(\theta) \right]$$

$$\sim -v^{0.8} e^{-0.2} P_s'(\theta) \theta$$

$$\text{where } \delta_1 \sim \left( \frac{e v l}{M} \right)^{-0.2} \quad (\text{A-II, 4})$$

is the displacement thickness of the boundary layer.

These results allow one to make explicit the "Equation of Thermal Equilibrium":

$$c' \theta + n L_1 = \frac{F_1 + F_2}{K CV} - \frac{v^2}{2} \quad (\text{A-II, 5})$$

wherein

$c'$  = heat capacity of water

$Q = K CV$  = fraction of water captured

The conversion into heat of the Kinetic energy of the drops does not intervene in a practical way for  $VL \ll 100 \text{m/sec}$ . One can also neglect the term  $c' \theta$ , in effect, numerically

$$\frac{c'}{L_1} \theta = \frac{\theta}{80} \quad (\text{A-II, 6})$$

$L_1$  = Latent heat of fusion

This relation is very small for temperature near  $0^\circ\text{C}$ .

Finally, the calculation of  $n$ , the fraction frozen, only intervenes through the ratios  $F_1/CV$  and  $F_2/CV$ , respectively, proportional to

$$c^{-1} \rho^{0.8} v^{-0.2} \theta_e \quad \text{and} \quad c^{-1} \rho^{-0.2} v^{-0.2} \theta$$

Similitude Laws

Identical trajectories:  $e^{1/2} d^{-3/2} v^{1/2}$

Fraction of water capture: CV

Heat exchange per unit mass of water captured:

$$c^{-1} \rho^{0.8} v^{-0.2} \theta_e \quad \text{and} \quad c^{-1} \rho^{-0.2} v^{-0.2} \theta$$

Modelling the effect of altitude: experimental data.

TABLE 1 - SELECTED EXPERIMENTAL DATA POINTS FROM REF. 1

Data Item

pt.	5	6	4	4'	a	d
$\phi$ veine	830	830	830	550	550	550
Mach veine	0,11	0,35	0,35	0,35	0,215	0,28
Altitude, m	0	5000	5000	5000	1500	1500
t, °C	-10	-10	-20	-20	-25,6	-20
LWC	2,2	2,2	0,3	0,3	0,424	0,38
$\bar{d}_d$	20	20	20	20	21,4	20
Debit Manche	24,9	14,6	14,9	14,1	15,3	17,6
Freq. Rot., Hz	50	51	50	0	0	0
Duree de l'essai/min.	7	7	28	20	16	20
Mass Captée	50/60	100	180	250	140	105

References:

- (1) Bongrand, J., "Etude Theorique et Experimental de L'Influence de Divers Parameters Sur Givrage D'un Profil," Icing Testing for Aircraft Engines, 10-1 to 10-13, AGARD Conference Proceedings Number 236, (August, 1978).

Notation:

R = Force acting on drop

$\rho$  = density of air

$u$  = velocity of drop relative to air

$M$  = viscosity of air

$V$  = velocity of air

$d$  = diameter of drop

$\theta_p$  = effective temperature of surface

$\theta$  = static temperature of air upstream from the obstacle

$\theta_e$  = equilibrium temperature of surface

$L_1$  = heat of fusion of  $H_2O$

### Appendix A-III

#### Summary of E. A. Brun's treatment of Similitude for Icing Testing (1)

The two conditions of similitude governing drop impingement are that the following groups should be the same in flight- and in model- tests:

$$Re = \frac{V D \rho_a}{M_a} \quad (\text{A-III, 1})$$

$$= 18 \frac{\rho_a^C}{\rho_d^D} \quad (\text{A-III, 2})$$

If similitude is to be maintained when the scale is changed by a factor  $n$ , quantities must be changed as follows:

$$C_m = n C_f, D_m = n D_f, V_m = V_f/n \quad (\text{A-III, 3})$$

$$\rho_{am} = \rho_{af}, M_{am} = M_{af}$$

The size of the model can be reduced only if the average diameter of the droplet is reduced and the air velocity is increased. In most cases it is not possible to increase the velocity to any extent and small scale experimentation cannot achieve similitude with its full scale counterpart.

Furthermore, if the test concerns the effectiveness of thermal de-icing or anti-icing systems, it is also necessary to conform to similitude with respect to heat transfer and mass transfer.

The additional conditions for similitude when heat transfer is involved are that the following dimensionless groups should be equal in the model- and full scale- object tests:

$$X = \frac{L v}{TC_p}, \frac{W}{\rho_a} ; P_e = \frac{V C}{a} = \frac{V C}{\gamma}, \frac{v}{a} = R_e P_r \quad (\text{A-III, 4})$$

(see end of this Appendix for notation)

It is possible, with ingenuity, to minimize the deficiencies of a small tunnel. One method of doing this is to distort the model so that the front part is full scale but the rear part is foreshortened enough to permit the model to go into the test section. The drop impingement and heat transfer

phenomena on the forward part of the model are little affected by the changes downstream and measurements approximate what they would be on a full scale model."

Notation:

$V_a$  = air velocity

$D$  = drop diameter

$\rho_a$  = density of air

$M_a$  = viscosity of air

$\rho_d$  = density of water

$L_v$  = latent heat of vaporization

$T$  = temperature of system

$C_p$  = heat capacity of air

$W$  = liquid water content

$C$  = heat capacity of water

$a$  = thermal diffusivity of air

$\gamma = M_a / \rho_a$

$R_a$  = Reynolds number air stream

$P_r$  = Prandtl number of air

Reference:

- (1) Brun, E. A., "Icing Wind Tunnel Tests," Icing Problems and Recommended Solutions, pp. 179-181, AGARDOGRAPH 16 (November, 1957).

Appendix A-IV

Abstract of "The Determination of Ice Deposition on Slender Wings; An Experimental Technique and Simplified Theory," by J. W. Flower (1).

The author used a water tunnel with small glass beads representing supercooled water droplets.

If conditions were such that the drag characteristics of the droplets could be represented by a constant drag coefficient, the conditions for similarity could be written

$$\left(\frac{d_m}{d_f}\right) \left(\frac{l_f}{l_m}\right) \left(\frac{\rho_f}{\rho_m}\right) \left(\frac{\rho_w - \rho_m}{\rho_w - \rho_f}\right) = 1 \quad (\text{A-IV, 1})$$

wherein

d = drop diameter

l - characteristic length

$\rho$  = free stream density

$\rho_w$  = density of water

Write Equation (A-IV, 1) in the form

$$\frac{d_m}{d_f} \frac{l_f}{l_m} \frac{\sigma_m - 1}{\sigma_f - 1} = 1 \quad (\text{A-IV, 2})$$

wherein

$$\sigma = \rho_w / \rho$$

The assumption of constant drag coefficient is not at all realistic for small droplet, small Reynolds number conditions. A more reasonable assumption would be that Stokes Law holds which implies that  $C_D$ , the drag coefficient, varies inversely with the Reynolds number. The condition for similarity with this assumption is:

$$\left(\frac{v_m}{v_f}\right) \left(\frac{d_m}{d_f}\right)^2 \left(\frac{l_f}{l_m}\right) \left(\frac{\nu_f}{\nu_m}\right) \left(\frac{\sigma_m - 1}{\sigma_f - 1}\right) = 1 \quad (\text{A-IV, 3})$$

wherein

v = free stream velocity

$\nu$  = Kinematic viscosity

Appendix A-IV

Abstract of "The Determination of Ice Deposition on Slender Wings: An Experimental Technique and Simplified Theory," by J. W. Flower (1).

The author used a water tunnel with small glass beads representing supercooled water droplets.

If conditions were such that the drag characteristics of the droplets could be represented by a constant drag coefficient, the conditions for similarity could be written

$$\left(\frac{d_m}{d_f}\right) \left(\frac{l_f}{l_m}\right) \left(\frac{\rho_f}{\rho_m}\right) \left(\frac{\rho_w - \rho_m}{\rho_w - \rho_f}\right) = 1 \quad (\text{A-IV, 1})$$

wherein

$d$  = drop diameter

$l$  = characteristic length

$\rho$  = free stream density

$\rho_w$  = density of water

Write Equation (A-IV, 1) in the form

$$\frac{d_m}{d_f} \frac{l_f}{l_m} \frac{\sigma_m - 1}{\sigma_f - 1} = 1 \quad (\text{A-IV, 2})$$

wherein

$$\sigma = \rho_w / \rho$$

The assumption of constant drag coefficient is not at all realistic for small droplet, small Reynolds number conditions. A more reasonable assumption would be that Stokes Law holds which implies that  $C_D$ , the drag coefficient, varies inversely with the Reynolds number. The condition for similarity with this assumption is:

$$\left(\frac{V_m}{V_f}\right) \left(\frac{d_m}{d_f}\right)^2 \left(\frac{l_f}{l_m}\right) \left(\frac{\nu_f}{\nu_m}\right) \left(\frac{\sigma_m - 1}{\sigma_f - 1}\right) = 1 \quad (\text{A-IV, 3})$$

wherein

$V$  = free stream velocity

$\nu$  = Kinematic viscosity

Intermediate Reynolds numbers may be taken into account by assuming

$$C_D = \frac{K}{Re^n} \quad (\text{A-IV, 4})$$

wherein

K = a constant

$n \leq 1.0$

The condition for similarity now is

$$\left(\frac{v_m}{v_f}\right)^n \left(\frac{d_m}{d_f}\right)^{1+n} \left(\frac{l_f}{l_m}\right) \left(\frac{\gamma_f}{\gamma_m}\right) \left(\frac{\sigma_m - 1}{\sigma_f - 1}\right) = 1 \quad (\text{A-IV, 5})$$

The water tunnel permits the use of solid spheres instead of water droplets. It could provide a large change in stream density. It would permit the use of more uniform particles whose diameters were more accurately determined.

There are several disadvantages:

- (a) impossibility of arranging for particles to stick to surface,
- (b) difficulty of having to track the particles.

Tests indicate that icing levels on the upper surfaces are unlikely to be serious. However, the results are not conclusive for various reasons:

- (a) Complete similarity was not possible because of limitations of "tunnel velocity"
- (b) unsteadyness of flow leading to uncertainty in impact position

Reference:

- (1) Flower, J. W., "The Determination of Ice Deposition on Slender Wings: An Experimental Technique and Simplified Theory," ICAS Proceedings, 1974, pp. 397-408, (1974).

Appendix B-I

Review of "Analytical Study of Icing Simulation for Turbine Engines  
in Altitude Cells" by C. E. Willbanks and R. J. Schulz (15)

Re: Figure 3, p. 963.

$$Q = \frac{q_s''}{\bar{h} (T_s - T_r)} = \frac{\text{anti-icing heat rate}}{\text{convection heat rate}}$$

wherein

$$q_s'' = \text{anti-icing heat rate} = (\text{convection heat rate}) + (\text{latent heat rate}) + (\text{sensible heat rate})$$

$$\bar{h} (T_s - T_r) = \text{convection heat rate}$$

$$\frac{1}{Q} = \frac{\text{convection heat rate}}{(\text{convection heat rate}) + (\text{sensible heat rate}) + (\text{latent heat rate})}$$

so,  $\frac{1}{Q}$  = fraction of anti-icing heat rate which goes out by convection

$$1 - \frac{1}{Q} = \text{fraction of anti-icing heat which goes to (sensible heat) + (latent heat)}$$

$$\text{now, } b = \frac{W_c C_c}{\bar{h}}$$

wherein

$$W_c = \text{flux of water striking surface, m/} \phi \text{ L}^2$$

$$C_c = \text{heat capacity of liquid water} = 1$$

$$\bar{h} = \text{convection heat transfer coefficient}$$

so, at constant  $\bar{h}$  and constant  $T_s - T_{\infty}$ ,  $b$  is simply a measure of rate of heat required to raise  $W_c$  mass/(unit area unit time) from  $T_{\infty}$  to  $T_s$ . An increase in  $b$  under these conditions simply means an increase of  $W_c$ .

On Figure 3 increasing  $b$  at constant  $M_{\infty}$  (and therefore constant  $\bar{h}$ ) implies simply an increase in  $W_c$ .

Looking at Figure 3, when  $M_{\infty} = 0.4$  and  $b = 0.0261$ ,  $1/Q = 0.5$  and when  $M_{\infty} = 0.4$ ,  $b = 2$ ,  $1/Q = 0.22$ . This means that when  $b = 0.0261$ , 50% of the anti-icing heat goes out by convection and 50% goes to heat the incoming water from  $456^{\circ}\text{R}$  to  $492^{\circ}\text{R}$  and to vaporize that amount at  $492^{\circ}\text{R}$  (according to statement at bottom of p. 962, top of p. 963).

Now, take as a basis 1 lb. of water coming in at 456°R. To heat this to 492°R takes 36 Btu; to vaporize it at 492°R takes 1075.5 Btu, a total of 1111.5 Btu. If this is 50% of the total, then the total is 2223 Btu and the heat loss by convection is 1111.5 Btu.

If b is set equal to 2, this implies a water rate of  $1 \times 2/0.0261 = 76.63$  lb. To heat this amount of water from 456°R to 492°R requires  $76.63 \times 36 = 2759$  Btu. Since  $T_g$  and  $T_r$  are the same as in the previous case, the convection is still 1111.5 Btu. Since  $1/Q = 0.22$ , the total heat equals  $1111.5/0.22 = 5052.3$  Btu. Hence, the evaporative heat transfer is  $5052.3 - 2759 - 1111.5 = 1181.8$  Btu. This corresponds to  $1181.8/1075.7 = 1.099$  lb. of water being vaporized whereas one would expect 1 lb. to be vaporized. This discrepancy can be eliminated by assuming that the minimum value of b is 0.0251 instead of 0.0261.

The heat flow rates by each mode and the percentage of each are given in the following table (valid for  $M_e = 0.4$ ):

Heat Flow Mode	b = 0.0251		b = 2	
	Btu	%	Btu	%
Sensible heat	36.0	1.6	2865.0	56.71
Latent heat	1075.5	48.4	1075.5	21.29
Convection	1111.5	50.0	1111.5	22.00
	2223.0	100.0	5052.0	100.00

Repeating the above calculation for  $M_e = 1$ : For  $b = 0.0261$  (or 0.0251),  $Q = 2.5$ ; for  $b = 2$ ,  $Q = 6.4$

$$\frac{1}{Q} = 0.4$$

Basis: 1 lb. H<sub>2</sub>O coming in

$$q_s'' = \frac{1111.5}{0.4} = 2778.75$$

Convection =  $2778.75 - 1111.5 = 1667.25$

Latent heat = 1075.5

Sensible heat = 36

$$\frac{1}{Q} = 0.156$$

Water coming in =  $\frac{2}{0.0251} = 79.68$  lb.

$$q_s'' = \frac{1111.5}{0.156} = 7125$$

Convection = 1667.25

Latent heat = 1075.5

Sensible heat = 4382.25

Appendix B-II  
Energy Balances

Hardy (16), Messenger (17) and others (18, 19) derived various equations relating surface temperature, anti-icing heat flow, and other variables. In this Appendix the problem is analyzed using the First Law of Thermodynamics for open systems. Both steady-state and unsteady conditions are analyzed. This analysis keeps clear the distinction between a "heat flow" and the effects of heat flows such as sensible heat and latent heat changes. The equations derived are somewhat more general than those previously presented since they recognize that part of the ice that forms and part of the remaining liquid both vaporize.

In any steady-state analysis it is assumed that there are equal mass flows in and out of the open system. This is valid when there is no freezing or when there is no adhesion of ice to the boundary surface of the system. However, when freezing does occur it is well known that the ice adheres to the surface and hence ice accumulates within the boundaries of the system. Consequently, one is dealing with a non-steady-state situation. For this reason, the author has applied the unsteady state open system First Law equation to this problem and derived relationships which apply more realistically.

Case 1. Steady Flow

Assuming steady state means that the combined flows of ice, liquid water and water vapor out equals the flow of liquid water in,  $\dot{m}_d$  and that temperatures, heat flows, and mass flows are constant.

System: open system inside indicated boundaries

$$\text{First Law: } Q - W_n = \Delta h + \frac{\Delta v_o^2}{2g_c} + g/g_c \Delta z \quad (I)$$

wherein

$Q$  = net heat flow,  $\Delta z$  = gravitational energy = 0

$W_n$  = shaft work = 0,  $\Delta v_o^2/2g_c = \dot{m}_d v_o^2/2g_c$

$Q = q_{IN} - h_c (t_w - t_a)$

$h_c$  = convective heat transfer coefficient

$t_w$  = temperature of system

- $t_r$  = recovery temperature of boundary layer
- $\Delta h = h_{IN} - h_{OUT}$
- $h$  = specific enthalpy (subscript indicates phase (l - liquid, I - ice, v - vapor))
- $n$  = fraction of incoming water which freezes
- $f_I$  = fraction of ice which vaporizes
- $f_L$  = fraction of remaining water which vaporizes
- $\dot{m}_d$  = water rate in per unit area
- $g_c$  = conversion factor
- $\dot{m}_v$  = total vaporization rate/unit area
- $\dot{m}_l$  = liquid water rate out/unit area
- $n$  = fraction of incoming water which freezes
- $t_\infty$  = temperature of free stream
- $t_{c\infty}$  = temperature of approaching water droplets
- $q_{IN}$  = anti-icing heat flux

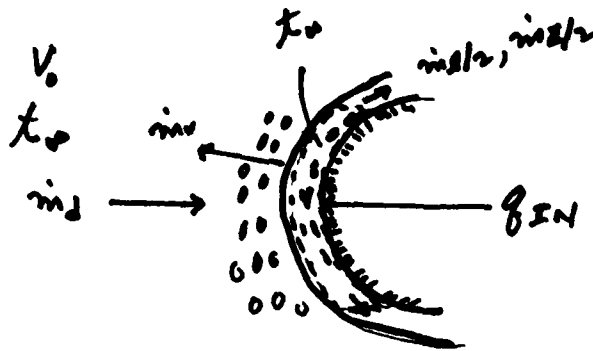


FIGURE B-II-1 - HEAT AND MASS FLOWS FOR A BODY UNDERGOING ICING

Looking at Figure B-II-1, we see that

$$h_{IN} = \dot{m}_d h_l (t_{c\infty}) + \dot{m}_d V_0^2 / 2g_c \quad (1)$$

$$h_{OUT} = \dot{m}_v h_v (t_w) + \dot{m}_I h_I (t_w) + \dot{m}_L h_L (t_w) \quad (11)$$

The following diagram is helpful in understanding the material balances:

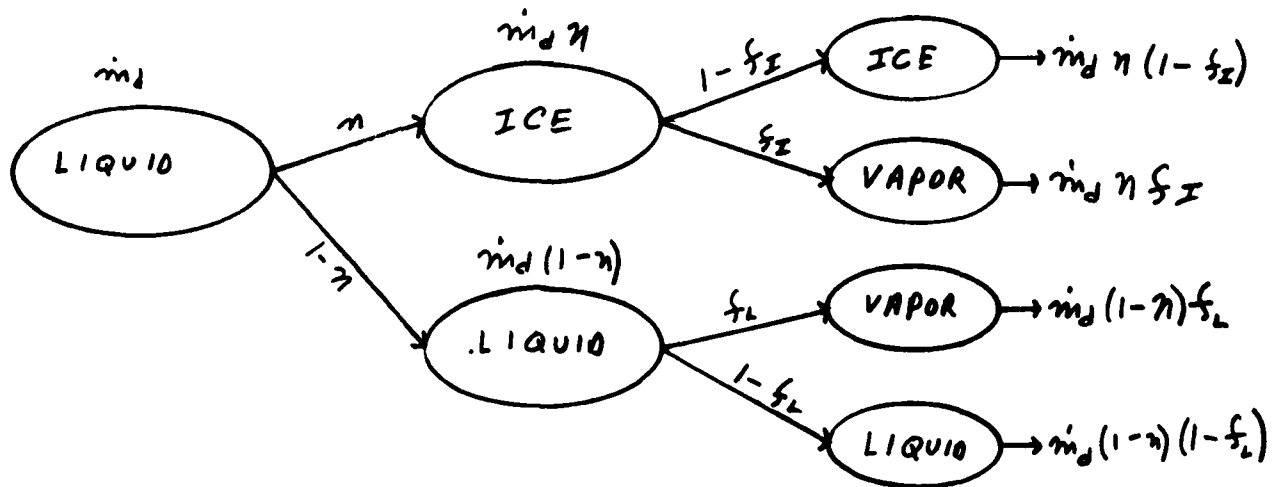


FIGURE B-II-2 - FLOWS OF WATER IN VARIOUS FORMS

From the above we can easily see that

$$\dot{m}_v = \dot{m}_d (n f_I + (1 - n) f_L) \quad (\text{iii})$$

$$\dot{m}_l = \dot{m}_d (1 - n) (1 - f_L) \quad (\text{iv})$$

$$\dot{m}_I = \dot{m}_d n (1 - f_I) \quad (\text{v})$$

Equation (I) combined with (i) and (ii) gives use to Equation (II) below:

$$q_{IN} = h_c (t_w - t_r) + \dot{m}_v h_v (t_w) + \dot{m}_I h_I (t_w) + \dot{m}_l h_l (t_w) - \dot{m}_d h_l (t_o) - \dot{m}_d \frac{v_o^2}{2g_c} \quad (\text{II})$$

Using (iii) - (v) , Equation (II) can be transformed into

$$q_{IN} = h_c (t_w - t_r) + \dot{m}_d (n f_I + (1 - n) f_L) h_v (t_w) + \dot{m}_d n (1 - f_I) h_I (t_w) + \dot{m}_d (1 - n) (1 - f_L) h_l (t_w) - \dot{m}_d h_l (t_{c\phi}) - \dot{m}_d \frac{v_o^2}{2g_c} \quad (\text{III})$$

Recognizing that

$$\dot{m}_d (h_l (t_w) - h_l (t_{c\phi})) = \text{sensible heat}$$

$$\dot{m}_d n (h_I (t_w) - h_I (t_w)) = \text{latent heat of fusion (-)}$$

$$\dot{m}_d n f_I (h_v (t_w) - h_I (t_w)) = \text{latent heat of sublimation}$$

$$\dot{m}_d (1 - n) f_L (h_v (t_w) - h_l (t_w)) = \text{latent heat of evaporation}$$

Equation (III) can be rearranged as follows:

$$\begin{aligned}
 q_{IN} = & h_c (t_w - t_r) + \dot{m}_d (h_1(t_w) - h_1(t_{c\phi})) + \dot{m}_d n (h_I(t_w) - h_1(t_w)) \\
 & + \dot{m}_d n f_I (h_v(t_w) - h_I(t_w)) + \dot{m}_d (1 - n) f_L (h_v(t_w) - h_1(t_w)) \\
 & - \frac{\dot{m}_d v_o^2}{2g_c}
 \end{aligned} \tag{IV}$$

One can ascribe the following meanings to the terms in Equation (IV):

$h_c (t_w - t_r)$  = convective heat transfer flux

$\dot{m}_d (h_1(t_w) - h_1(t_{c\phi}))$  = sensible heat effect = heat required to raise temperature of incoming water from  $t_{c\phi}$  to  $t_w$

$\dot{m}_d n (h_I(t_w) - h_1(t_w))$  = energy released when  $\dot{m}_d n$  of subcooled water freezes

$\dot{m}_d n f_I (h_v(t_w) - h_I(t_w))$  = energy required to vaporize  $\dot{m}_d n f_I$  ice at  $t_w$

$\dot{m}_d (1 - n) f_L (h_v(t_w) - h_1(t_w))$  = energy required to vaporize  $\dot{m}_d (1 - n) f_L$  liquid water at  $t_w$

$\dot{m}_d v_o^2 / 2g_c$  = Kinetic energy of impinging water droplets

Equation (IV) simplifies in various ways:

If  $n = 0$  (no freezing)

$$\begin{aligned}
 q_{IN} = & h_c (t_w - t_r) + \dot{m}_d (h_1(t_w) - h_1(t_{c\phi})) \\
 & + \dot{m}_d f_L (h_1(t_w) - h_1(t_w)) - \dot{m}_d \frac{v_o^2}{2g_c}
 \end{aligned} \tag{V}$$

Equation (V) is equivalent to Equation (10) above from Willbanks and Schulz (15).

If  $n = 1$  (total freezing)

$$\begin{aligned}
 q_{IN} = & h_c (t_w - t_r) + \dot{m}_d (h_1(t_w) - h_1(t_{c\phi})) + \dot{m}_d (h_I(t_w) - h_1(t_w)) \\
 & + \dot{m}_d f_I (h_v(t_w) - h_I(t_w)) - \dot{m}_d \frac{v_o^2}{2g_c}
 \end{aligned} \tag{VI}$$

Equations (IV), (V), or (VI) represent the energy balance for this situation.

The evaporative mass transfer rate can be correlated in terms of the product of a coefficient and a driving force.

For the case when  $n = 0$

$$\dot{m}_v = \dot{m}_d f_L = \frac{h_c (M, W, H_2O)}{C_{p,air} (M, W, Air) \left[ \frac{S_c}{P_r} \right]^{2/3}} \left( \frac{\bar{P}_w(t_w) - \bar{P}_o}{P} \right) \quad (VIII)$$

wherein

$\bar{P}_w(t_w)$  = partial pressure of water at  $t_w$   
 = vapor pressure of water at  $t_w$

$\bar{P}_o$  = partial pressure of water in air stream

$P$  = total pressure of air stream

$h_c$  = heat transfer coefficient

$S_c$  = Schmidt number

$P_r$  = Prandtl number

In Equation (VIII) the term in the square brackets can be considered the mass transfer coefficient and the driving force for the mass transfer is the partial pressure difference,  $(\bar{P}_w - \bar{P}_o)/P$ . Given constant values of  $t_w$  and  $\bar{P}_o$  the driving force remains constant. The mass transfer coefficient will be changed by a change in the fluid flow, i.e., a change in the Mach number or by a change in  $t_w$ .

For a fixed Mach number and fixed  $t_w$  (constant  $\bar{P}_w$ ) and  $\bar{P}_o$ ,  $\dot{m}_v$  will be fixed which implies that if  $\dot{m}_d$  is fixed,  $f_L$  will vary to accommodate the heat transfer and mass transfer.

For a given  $q_{IN}$ ,  $\dot{m}_d$ ,  $t_{c\checkmark}$ ,  $\bar{P}_o$ , Mach number  $t_w$  and  $f_L$  will adjust themselves so that equations (IV) and (VIII) are simultaneously satisfied.

For a given  $\dot{m}_d$ ,  $t_{c\checkmark}$ ,  $\bar{P}_o$ ,  $P$ , and Mach number ( $t_w$ ) as  $q_{IN}$  is increased  $t_w$  will increase which will simultaneously

- (a) increase convective heat transfer
- (b) increase sensible heat required

(c) increase driving force for mass transfer,  $(\bar{P}_w - \bar{P}_o)/P$ , and therefore

(d)  $f_L$  and heat required for evaporation

$q_{IN}$  can be fixed so that  $t_w$  has such a value that  $f_L = 1$ . In this case the surface is just maintained wet while all the incoming liquid vaporizes.  $q_{IN}$  can be increased without increasing  $t_w$  providing  $\dot{m}_d$  is simultaneously increased.

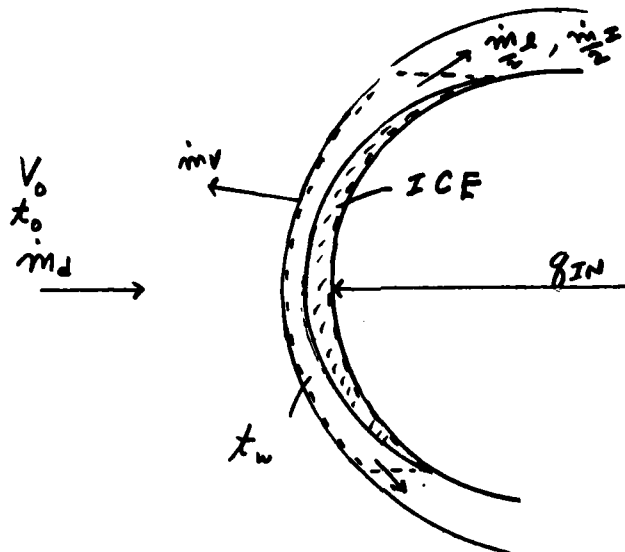
The procedure to be followed in the use of (V) and (VII) is as follows:

Known:  $t_r$ ,  $t_{c\heartsuit}$ ,  $h_c$ ,  $\dot{m}_d$ ,  $V_o^2$

- (1) Assume a  $t_w$
- (2) Calculate  $h_c (t_w - t_r)$ ,  $\dot{m}_d (h_1(t_w) - h_1(t_{c\heartsuit}))$
- (3) Calculate  $\dot{m}_v$  using (VII):  $\dot{m}_d f_L$
- (4) Calculate  $q_{IN}$  using (V)
- (5) Knowing  $\dot{m}_v$  and  $\dot{m}_d$ ,  $f_L$  can be calculated

Case 2. Unsteady State Situation

System: Non-constant mass system as shown in the Figure:



First Law Expression:

$$Q - W_n = U_2 - U_1 \pm \sum_i \left( h + \frac{v^2}{2g_c} + \frac{gZ}{g_c} \right) dm_i \quad (I)^*$$

wherein

$Q$  = heat transfer to or from system

$W_n$  = shaft work done by or on system

$U_1, U_2$  = internal energy of "parent system" (inside boundary) at start and at end of process, respectively

$h, \frac{v^2}{2g_c}, \frac{gZ}{g_c}$  = enthalpy, Kinetic energy and gravitational energy of streams flowing across boundaries of system. There is an integral for each stream. A plus sign is used with streams leaving the system and a negative sign with those entering.

\* See H. C. Weber and H. P. Meissner, Thermodynamics for Chemical Engineers 2nd edition, Wiley (1957).

All of the terms in the above equation have units of energy.

In this case  $W_n = 0$ ,  $g/g_c Z = 0$

$$Q = \int_0^{\tau} [q_{IN} - h_c (t_w - t_r)] d\theta$$

or, if  $q_{IN}$  and  $h_c (t_w - t_r)$  are constant with time,

$$Q = [q_{IN} - h_c (t_w - t_r)] \tau$$

wherein

$q_{IN}$  = anti-icing heat flux

$h_c$  = heat transfer coefficient

$t_w$  = temperature of system

$t_r$  = recovery temperature of air stream

$\tau$  = time period of experiment

$\dot{m}_d$  = flow rate of water droplets

$\dot{m}_v$  = flow rate of water being evaporated

$\dot{m}_l$  = flow rate of liquid water out of system

$\dot{m}_I$  = flow rate of ice out of system

Expanding Equation (I):

$$\begin{aligned} [q_{IN} - h_c (t_w - t_r)] \tau &= m_2 U_2 - m_1 U_1 - \dot{m}_d \tau \left( h (t_{cp}) + \frac{v_o^2}{2g_c} \right) \\ &+ \dot{m}_v \tau h_v (t_w) + \dot{m}_l \tau h_l (t_w) + \dot{m}_I \tau h_I (t_w) \end{aligned} \quad (II)$$

In Equation (II) it is assumed that  $\dot{m}_d$ ,  $\dot{m}_v$ ,  $\dot{m}_l$ ,  $\dot{m}_I$  are constant. The symbol  $h$  refers to the specific enthalpy of water, energy/unit mass. The subscript indicates the state involved. In (II)  $U_1$  and  $U_2$  are the specific internal energies of the ice at the start and end of process, hence  $U_1 = U_2 = U_i$ .  $m_1$  is the mass of the parent system at start,  $m_2$  at end.

Now, make a water balance over the period  $\tau$  :

$$\dot{m}_d = \dot{m}_v + \dot{m}_l + \dot{m}_I + \frac{m_2 - m_1}{\tau} \quad (III)$$

From (III):

$$m_2 - m_1 = (\dot{m}_d - \dot{m}_v - \dot{m}_e - \dot{m}_I) \tau \quad (IV)$$

Combining (II) and (IV) gives:

$$\begin{aligned} [q_{IN} - h_c (t_w - t_r)] \tau &= (\dot{m}_d - \dot{m}_v - \dot{m}_e - \dot{m}_I) \tau U_I \\ &- \dot{m}_d \tau \left( h_e (t_{c_e}) + \frac{v_o^2}{2g_c} \right) + \dot{m}_v \tau h_v (t_w) \\ &+ \dot{m}_e \tau h_e (t_w) + \dot{m}_I \tau h_I (t_w) \end{aligned} \quad (V)$$

It is quite reasonable in (V) to assume that  $\dot{m}_I = 0$

$$\begin{aligned} q_{IN} - h_c (t_w - t_r) &= (\dot{m}_d - \dot{m}_v - \dot{m}_e) U_I - \dot{m}_d \left( h_e (t_{c_e}) + \frac{v_o^2}{2g_c} \right) \\ &+ \dot{m}_v h_v (t_w) + \dot{m}_e h_e (t_w) \quad (VI) \\ &= \dot{m}_d \left( U_I - \left( h_e (t_{c_e}) + \frac{v_o^2}{2g_c} \right) \right) + \dot{m}_v \left( h_v (t_w) - U_I \right) \\ &+ \dot{m}_e \left( h_e (t_w) - U_I \right) \end{aligned}$$

1979 USAF - SCEE SUMMER FACULTY RESEARCH PROGRAM

Sponsored by the

AIR FORCE OFFICE OF SCIENTIFIC RESEARCH

Conducted by the

SOUTHEASTERN CENTER FOR ELECTRICAL ENGINEERING EDUCATION

FINAL REPORT

SHIPBOARD ANTENNA PLACEMENT OPTIMIZATION - (SAPO)

Prepared by:	Barry D. Bullard
Academic Rank:	Assistant Professor
Department and University:	Engineering Technology University of Central Florida
Research Location:	Air Force Eastern Test Range Ships Engineering Patrick AFB, FL
USAF Research Colleague:	Channing P. Hayes, Jr.
Date:	September 1, 1979
Contract No:	F49620-79-C-0038

## SHIPBOARD ANTENNA PLACEMENT OPTIMIZATION - (SAPO)

by

Barry D. Bullard

### ABSTRACT

A search was conducted to determine the most accurate and available means for optimum top-side antenna placement aboard Advanced Range Instrumentation Ships (ARIS). The goal of the search was to develop a user-oriented computer program of shipboard antenna placement optimization for use by TOEIS engineers at the Air Force Eastern Test Range. It was determined that for electromagnetic compatibility considerations (near-field), the computer algorithms PECAL/DECAL represented the bases for the best technique. The Numerical Electromagnetic Code (NEC) was determined to represent the best technique for the analytical calculation of antenna far-field radiation patterns in complex shipboard environment. Utilization of NEC in the determination of antenna placement for optimum far-field characteristics is discussed.

### ACKNOWLEDGEMENT

The author would like to extend thanks to the Air Force Systems Command, Air Force Office of Scientific Research, and the Southeastern Center for Electrical Engineering Education for granting him the opportunity to spend a most rewarding summer at Patrick Air Force Base.

Also, special thanks is due to Dr. Woodrow Everett, Mr. Bill Hayes, Lt. T. V. Marlar, and all the personnel of TOEIS for their helpful suggestions & guidance which provided an enjoyable and productive working atmosphere for the author to pursue research in the area of electromagnetics/antenna for Air Force Systems Command.

## I. INTRODUCTION:

The USNS General H. H. Arnold and the USNS General Hoyt S. Vandenberg are two Advanced Range Instrumentation Ships (ARIS) operated by the Air Force Systems Command. The ships' are mobile platforms designed to collect signature and metric measurement data on satellites and missile systems. ARIS instrumentation includes multiple high-performance radars, broad-band telemetry systems and extensive optical measurement equipment. Data handling, navigation/stabilization, timing, communication, meteorology and marine support equipments allow independent operation on optimum remote test positions on either the Air Force Eastern Test Range (ETR) or the Western Test Range (WTR). Figure No. 1 illustrates the ARIS topside and inboard profile. The problem addressed in this report concerns itself with two major areas applicable to ARIS: (1) the electromagnetic compatibility (EMC) of electronic systems were operating simultaneously, and (2) the electromagnetic (DM) radiation pattern distortion due to complex shipboard environment.

Typically, during a ballistic missile mission, an ARIS operates multiple radar and telemetry receiver/transmitters, two high-power HF transmitters, four HF receivers, and numerous VHF/UHF communications systems. With this high concentration of EM radiation, coupled with the close proximity of the antennas dictated by the ships structure, electromagnetic interference (EMI) among the electronic systems is inevitable. A possible solution to the EMI problem would be to optimize EMC via antenna location between simultaneously operating EM systems. Some technology has already been developed in this area,<sup>1</sup>

and is investigated further in this report.

Radio communications must be carried on in conditions of constant changes in the ships course, therefore, it is desirable that the EM radiation patterns of the antennas be omnidirectional or at least uniform in specified angular sectors. A possible solution is an optimum location of the antenna (or antennas) which give radiation pattern(s) as close to omnidirectional as is possible. If it is assumed that the probability of establishing communication with a station situated in a given direction is proportional to the square of the normalized radiation pattern value of a given antenna, an elementary loss due to reduction in the probability of establishing communication with a station lying in a given direction can be determined. By utilization of the above technique, and the Numerical Electromagnetic Code (NEC)<sup>2</sup> computer program for determining an antenna's radiation pattern in a complex shipboard environment, a possible solution exists to determine antenna location which realizes optimum omnidirectional EM radiation patterns.



## II. OBJECTIVES

The objectives of this project were:

(1) To determine the best means for which optimum antenna location aboard Advanced Range Instrumentation Ships could be analytically determined.

(2) To develop a user-oriented computer program of shipboard antenna placement optimization for the Air Force Eastern Test Range Advanced Range Instrumentation Ships for use by TOEIS\* engineers.

## III. LITERARY SEARCH:

An extensive search for research literature pertinent to the established objectives was conducted. Resources for the search included an interactive terminal at the University of Central Florida Library connected to the National Technical Information Service (NTIS), the Scientific and Technical Information Service - Patrick Air Force Base, and NASA Technical Library - Kennedy Space Center.

The NTIS search resulted in eight publications with direct concern to shipboard antenna radiation patterns and optimum antenna location. Table No. 1 represents a list of these publications. Towards the established objective of (2), the Pattern Handbook series utilizing the SCATRAN computer program was investigated further and results are discussed later in this report.

A classified search of pertinent literature was conducted by Scientific and Technical Information - U.S. Air Force, Patrick AFB

---

\*Technical-Operations-Engineering-Instrumentation-Ships

TABLE NO. 1

NTIS SEARCH

1. Pattern Handbook - Volume I: Far-Field Pattern for Shipboard Antenna, Ohio State University Antenna Lab.
2. Pattern Handbook - Volume II: Memorandum on Shipboard Antenna Far-Field Pattern Predication, Ohio State University, Antenna Lab.
3. Pattern Handbook - Volume III: Far-Field Patterns of a Linear Antenna Radiating in the Presence of Square Cylinders, Ohio State University, Antenna Lab.
4. Pattern Handbook - Volume IV: Far-Field Patterns of a Linear Antenna Radiating in the Presence of Rectangular Cylinders, Ohio State University, Antenna Lab.
5. Pattern Handbook - Volume V: Far-Field Patterns of a Linear Antenna Radiating in the Presence of Elliptical Cylinders, Ohio State University, Antenna Lab.
6. Pattern Handbook - Volume VI: Far-Field Patterns of a Linear Antenna Radiating in the Presence of Circular Cylinders, Ohio State University, Antenna Lab.
7. Shipboard VHF/UHF Antenna Design and Utilization Criteria, Naval Electronic Laboratory Center.
8. Ship Antennas, Naval Intelligence Support Center.

at the request of this researcher. The search incorporated all publications on file at the Defense Documentation Center - Alexandria, Virginia up to and including the classified level of SECRET. Results of the search provided the abstracts of approximately 900 publications with consideration to shipboard antennas. Review of the abstracts indicated ten candidates not revealed in the NTIS search usable toward the established objective (2). Table No. 2 represents a list of these publications.\* Of the ten candidates, the Shipboard Electromagnetic Compatibility Analysis (SEMCA) computer program was chosen for further investigation, and the results of that investigation are discussed later in this report.

The resources of the NASA Technical Library - Kennedy Space Center were utilized to acquire immediate acquisition of the SEMCA publications for review.

#### IV. SCATTRAN:

SCATTRAN represents an algorithm for approximating the far-field pattern in the horizontal plane of a thin vertical antenna near cylindrical scatterers of arbitrary cross-section whose physical heights are at least that of the antenna. The method is based on approximating the antenna with an infinite line source and the scatterer with an array of thin infinite wires<sup>3</sup>. Upon further investigation of SCATTRAN via its source (Naval Electronic Systems Command), it was discovered that an up-dated algorithm called the Numerical Electromagnetic Code (NEC) - Method of Moments exists. The NEC algorithm yields improved estimates of the performance of

---

\*All listed publications are UNCLASSIFIED

TABLE NO. 2

DDC SEARCH

1. Shipboard Electromagnetic Compatibility Analysis (SEMCA); Volume II, General Electric Co., Apollo Support Dept.
2. Shipboard Electromagnetic Compatibility Analysis (SEMCA); Volume III, General Electric Co., Apollo Support Dept.
3. Shipboard Electromagnetic Compatibility Analysis (SEMCA); Volume IXB, General Electric Co., Apollo Support Dept.
4. A Computer Method for Shipboard Siting of Antennas, Naval Research Lab.
5. Computer Study of the Performance of Shipboard High Frequency Antennas, Technology for Communications International.
6. Analytical Techniques for Predicting Electromagnetic Interference, Naval Weapons Lab.
7. HF Shipboard Antenna System Design and Utilization Criteria, Naval Electronics Lab.
8. Antenna Select Computer Program, Syracuse University.
9. Shipboard Antenna and Topside Arrangement Guidance, Naval Electronics Lab.
10. GRAPHANT: A FORTRAN Program for the Solution and Graphic Display of Gain and Patterns for Wire and Linear Antennas in the Presence of Lossy Ground, Naval Postgraduate School.

antennas mounted on shore stations, ships, aircraft, and spacecraft. NEC combines an integral equation for smooth surfaces with one for wires to provide convenient and accurate modeling of a wide range of structures (e.g. ships). The NEC program uses both an electric-field integral equation and a magnetic-field integral equation to model the electromagnetic response of general structure types<sup>4</sup>. After detailed review of NEC documentation, it was determined that NEC represented the most accurate and available means for the analytical calculation of antenna far-field radiation patterns in complex shipboard environment.

V. SEMCA:

The Shipboard Electromagnetic Compatibility Analysis (SEMCA) routine represents an algorithm for predicting electromagnetic compatibility among EM systems in shipboard environment. SEMCA utilizes two basic programs for predicting EMC; (1) the CULL Digital RFI program (CDRFI) provides a quick evaluation of the total interference situation at all frequency bands, and (2) the Scattering and Propagation Simulator program (SCAPS) is a more defined program for predicting interference in the region, accurately defining the interaction between closely coupled HF antennas and load effects at each antenna terminal<sup>5</sup>. The SEMCA program has the capability to evaluate:

- (a) Communication suit compatibility
- (b) Top-Side Antenna Arrangements
- (c) Optimum equipment arrangement for transmit and receive channels
- (d) Communication circuit performance between ships in a task force

(e) Equipment design problems (antenna tuner analysis)

(f) Frequency assignment and allocation

Figure No. 2 illustrates the SEMCA communication model.

With SEMCA having direct capability to determine optimum top-side antenna location based on EMC, investigation into the acquisition of the SEMCA program for use at the ETR was initiated. The following are the results of that investigation:

(1) General Electric Company-Daytona Beach, FL is the sole source of the SEMCA program.

(2) Mr. Raymond Bouchard is the Project Leader.

(3) The SEMCA program is the principal tool used for analysis by Naval Seas Systems Command.

(4) No documentation of the SEMCA program has been published since December 1974.

With no documentation of SEMCA published since 1974, it was the opinion of Mr. Bouchard that due to program changes and advancements since '74, utilization of SEMCA by any party other than the General Electric team was improbable. In consideration of Mr. Bouchard's comment, and since out-side contracting is beyond this project, use of the SEMCA program at the ETR was dismissed.

#### VI. ELECTROMAGNETIC COMPATIBILITY ANALYSIS CENTER:

Contact was made with the Electromagnetic Compatibility Analysis Center (ECAC) - Annapolis, Maryland, for the determination if ECAC had any information (publications, computer routine, etc.) which would realize goals toward the established objective (2). It was learned that the Naval Ocean Systems Center has tasked ECAC to

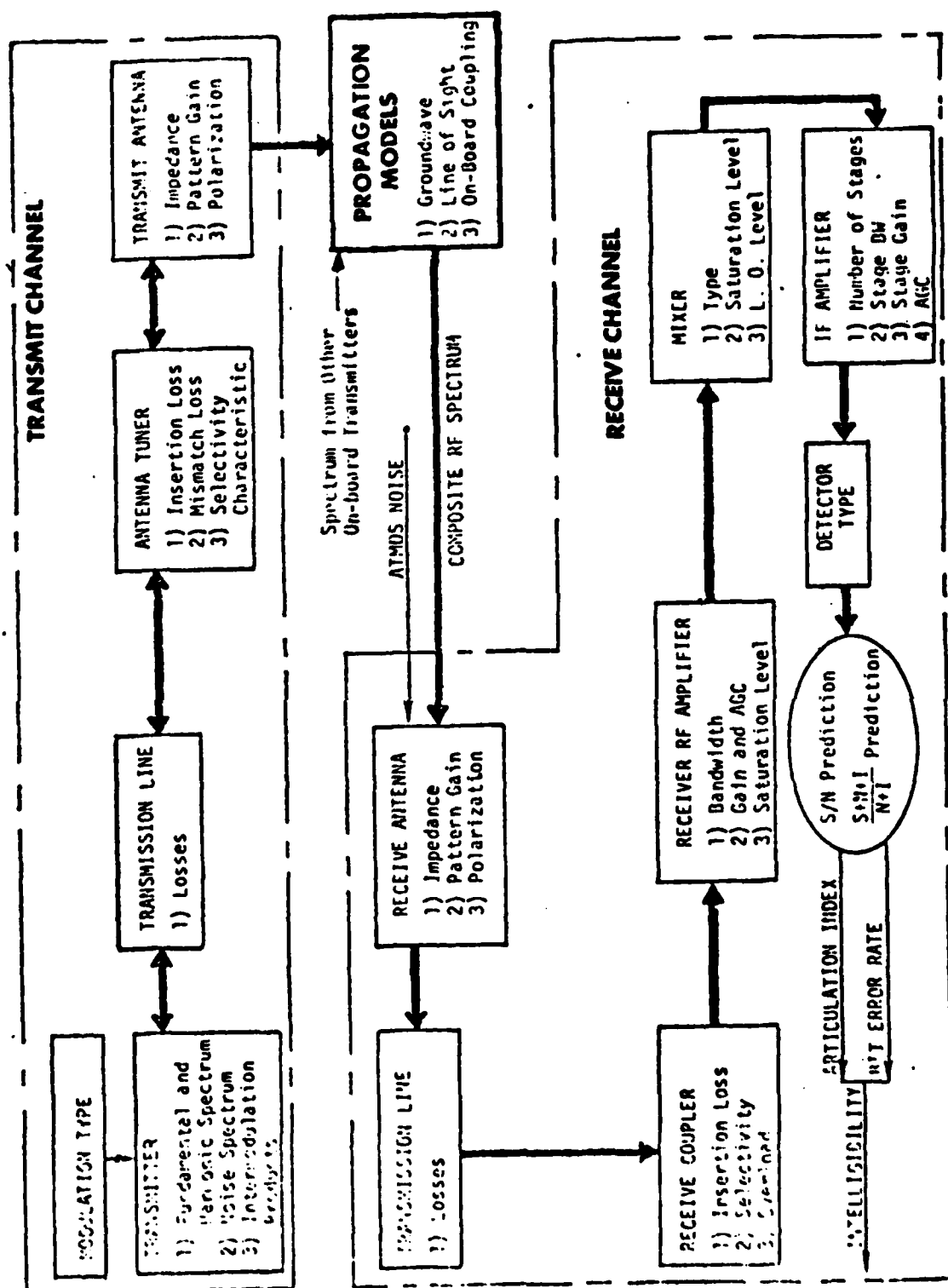


Figure No.2 SEMCA Communication Model

assist in the development of a computer analysis system to advance the goals of the Navy EMX\* program. Towards the above task, two computer algorithms were delivered to NOSC called the Design (Communications) Algorithm (DECAL), and Performance Evaluation (Communications) Algorithm (PECAL). DECAL is a quick-running interactive electromagnetic compatibility design algorithm for shipboard communication systems which operate between 2 and 400 MHz. PECAL is a longer-running statistical EMC performance evaluation algorithm for shipboard communication systems which operate between 2 and 400 MHz. The major purpose of these two programs is to predict and evaluate the EMC of specific trial arrangements of shipboard antenna locations for the various communication systems required by the ship<sup>1</sup>.

The procedure for using DECAL and PECAL to develop a topside design consists of iterations around two loops as shown in Figure No. 3. In loop 1 DECAL is used to quickly iterate through the various design changes to achieve an acceptable design. PECAL can then be exercised in the batch mode to determine a predicted measure of the performance of the proposed design. If the performance predicted by PECAL is unsatisfactory, further modifications to the design can be made using loops 2 and/or 1.<sup>6</sup>

Upon further investigation of the PECAL/DECAL computer algorithms, it was learned that sufficient and up-to-date documentation exist to allow the design engineer to load, execute and run the

---

\*EMX is a general classification which includes electromagnetic safety (EMSAF), electromagnetic noise (EMN), electromagnetic vulnerability (EMV), electromagnetic pulse (EMP), and electromagnetic compatibility (EMC).

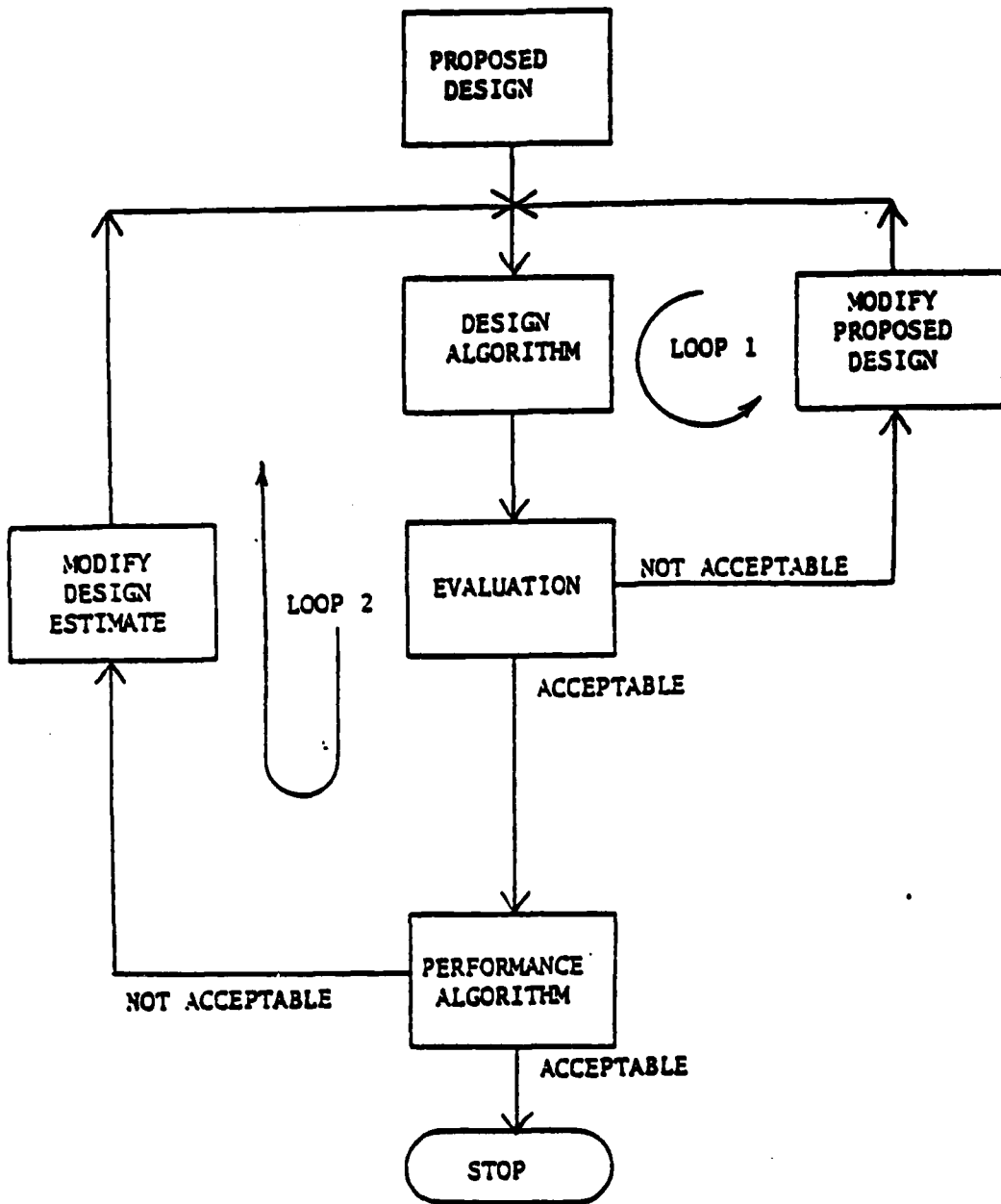


Figure No.3 PECCAL/DECAL Design Procedure

PECAL/DECAL algorithms.<sup>1,6,7,8,9,10</sup> After detailed review of PECAL/DECAL documentation, it was determined that PECAL/DECAL represented the most accurate and available means for the analytical calculation of optimum shipboard top-side antenna location based on EMC.

Investigation into the acquisition of the PECAL/DECAL computer programs for use at the ETR was initiated. The following are the results of the investigation:

(1) PECAL/DECAL could be supplied from ECAC at no cost to the ETR.

(2) PECAL/DECAL programs exist for the UNIVAC 1108 or 1110 computer and the IBM 360/370 computer.

(3) PECAL/DECAL represents approximately 10,000 cards of computer statements.

Computer availability at the ETR for this project was limited to the Control Data Corp. (CDC) Cyber 74 computer. Therefore, investigation into the feasibility of PECAL/DECAL being translated from UNIVAC (or IBM) to CDC was conducted.

Upon verbal communique with ECAC programmers at the request of this researcher, it was the opinion of the senior CDC resident programmer at the ETR that feasibility of translation from UNIVAC-to-CDC exist with approximately a one month task/effort. At the conclusion of this summer effort, a listing of PECAL/DECAL was on order from ECAC for further review by CDC programmers at the ETR.

#### VII. FAR-FIELD OPTIMIZATION - (NEC):

As stated earlier, "if it is assumed that the probability of establishing communication with a station situated in a given direction is proportional to the square of the normalized radiation

pattern value of a given antenna, an elementary loss due to reduction in the probability of establishing communication with a station lying in a given direction can be determined".<sup>11</sup> Mathematically, this can be expressed as;

$$dS(\phi) = [1 - F^2(\phi)] d\phi \quad (1)$$

If all directions are not of equal importance, a weight function  $m(\phi)$  is introduced. Elementary losses after the weight function has been taken into account can be expressed by the following relation;

$$dS(\phi) = m(\phi) [1 - F^2(\phi)] d\phi \quad (2)$$

Individual losses for the  $i$ -th antenna can be obtained by integrating expression (2) in the interval from  $0 - 2\pi$ ;

$$S_i = \int_0^{2\pi} dS_i(\phi) = \int_0^{2\pi} m_i(\phi) [1 - F^2(\phi)] d\phi \quad (3)$$

By utilizing the NEC computer algorithm to analytically determine the normalized radiation pattern (F) for a given antenna (S) in complex shipboard environment, antenna location which realizes the minimum value for expression (3) can be determined. This location would represent the top-side antenna placement which realizes optimum far-field characteristics.

#### VIII. RECOMMENDATIONS:

Recommendations generated by this research are as follows:

- (1) Translate PECAL/DECAL to CDC for use by the ETR. This could be done as a low-priority task at the ETR, thereby no additional expense would be incurred.

(2) Utilize PECAL/DECAL for optimum antenna placement aboard the Advanced Range Instrumentation Ships at the ETR.

(3) Modify DECAL so that an optimum antenna placement search could be made without "manual" location change of the antenna in question.

(4) Develop a computer algorithm which would realize far-field optimization as described in Section VII of this report.

## REFERENCES

1. Francis M. Kozivk, "Performance Evaluation (Communications) Algorithm (PECAL) User's Manual," IIT Research Institute, Consultative Report Contract F-19628-78-L-0006, August, 1978.
2. G. J. Burke, A. J. Poggio, "Numerical Electromagnetic Code (NEC)-Method of Moments," Part I: Program Description - Theory, Lawrence Livermore Laboratory, July, 1977.
3. Gray A. Thiele, "Pattern Handbook, Volume I: Far-Field Pattern Prediction for Shipboard Antennas, Ohio State University, Report No. 1522-11, March, 1965.
4. G. J. Burke, A. J. Poggio, "Numerical Electromagnetic Code (NEC)-Method of Moments," Part III: User's Guide, Lawrence Livermore Laboratory, July, 1977.
5. A. J. Heidrich, R. P. Bouchard, R. R. Raschke, J. T. Sterling, "Shipboard Electromagnetic Compatibility Analysis (SEMCA)," Volume IXB, Programmer's Reference Manual, General Electric Co., Apollo Support Dept., Contract N00024-70-C-1240, May, 1971.
6. W. Kowalyshyn, "Design (Communications) Algorithm (DECAL) User's Manual, IIT Research Institute, December, 1978.
7. F. M. Kozivk, "Performance Evaluation (Communications) Algorithm (DECAL) Code Manual," ECAC, Annapolis, MD, to be published.
8. P. C. Long, "Communication Systems Analysis Computer Algorithms Theory Manual, ECAC, Annapolis, MD, to be published.
9. W. Kowalyshyn, "Design (Communications) Algorithm (DECAL) Code Manual," ECAC-CR-78-067, ECAC, Annapolis, MD, September, 1978.
10. L. C. Minor, "Mathematical Models Which Can Be Used to Expand the Equipment Parameter File," IIT Research Institute, Final Report Contract F-19628-78-C-0006, November, 1978.
11. D. Bem, Z. Ianelli, "Compatible Localization of Stub Antennas on a Ship," IEEE Trans. Electromagnetic Compatability, pp. 327-330, June, 1977.

1979 USAF - SCEEE SUMMER FACULTY RESEARCH PROGRAM

Sponsored by the

AIR FORCE OFFICE OF SCIENTIFIC RESEARCH

Conducted by the

SOUTHEASTERN CENTER FOR ELECTRICAL ENGINEERING EDUCATION

FINAL REPORT

ARMA SPECTRAL ESTIMATION: AN EFFICIENT CLOSED-FORM APPROACH

Prepared by: Dr. James A. Cadzow

Academic Rank: Professor

Department and University: Department of Electrical Engineering  
Virginia Polytechnic Institute and State University

Research Location: Rome Air Development Center  
Surveillance Division  
Surveillance Technology Branch  
Signal Processing Section

USAF Research Colleague: Mr. Paul Van Etten

Date: August 22, 1979

Contract No.: F49620-79-C-0038

**ARMA SPECTRAL ESTIMATION:  
AN EFFICIENT CLOSED FORM PROCEDURE**

by  
James A. Cadzow

ABSTRACT

In this report, a method for generating an ARMA spectral estimate from a finite set of observations of a random time series is presented. The method's development is based upon a fundamental recursive relationship which characterizes the autocorrelation sequence of a time series that possesses a rational spectrum. When statistical estimates of the autocorrelation elements (obtained from the given time series observations) are substituted into this fundamental relationship, a set of equation errors results. The optimum ARMA spectral estimate is obtained by selecting relevant coefficients so as to minimize a quadratic functional of these equation errors. In examples treated to date, this ARMA spectral estimator has provided significantly superior performance when compared with the maximum entropy method.

#### ACKNOWLEDGEMENT

The author would like to thank the Air Force Systems Command, Air Force Office of Scientific Research, Rome Air Development Center, and the Southeastern Center for Electrical Engineer Education for providing the opportunity to carry out the research herein described. Special acknowledgement is made to Mr. Paul Van Etten of RADC, the effort's focal point, for his numerous discussions, guidance, and assistance which helped make the author's stay a most worthwhile and pleasurable experience. Appreciation is also due to Mr. Russell Brown, Mr. Clarence Silfer and Mr. John Huss, all of RADC, for their thoughtful assistance. Finally, he would like to thank Dr. Richard Miller of SCEEE for providing a well-organized program in which to participate.

## I. INTRODUCTION

There exist a variety of United States Air Force applications in which one seeks to obtain increased resolution capabilities over existing procedures. Some examples are detecting and identifying multiple targets from radar returns; tracking of low angle targets, high resolution imaging, synthetic aperture radar, spatial processing, and, enhanced angular resolution for both active and passive sensors in the micro, millimeter, infrared and optical bands. A procedure which has shown much promise in achieving increased resolution is that of spectral estimation. When applying spectral estimation to the above class of problems, one in essence converts the time (or spatial) domain data into the spectral (frequency) domain with the explicit objective of obtaining increased resolution. For purposes of presentation, the data to be transformed will hereafter be referred to as a time-series although in a specific situation it may be spatial in nature.

The inherent characteristics of a time series  $\{x(n)\}$  are often best displayed in the frequency domain. When the time series is deterministic in nature, this involves generating its discrete Fourier transform (DFT) as specified by

$$X(\omega) = \sum_{n=-\infty}^{\infty} x(n)e^{-j\omega n} \quad (1a)$$

On the other hand, in those situations where the time series is a wide-sense stationary random process, one must first generate the underlying autocorrelation sequence  $r_x(n)$  and then take its DFT to arrive at the power spectral density

$$S_x(\omega) = \sum_{n=-\infty}^{\infty} r_x(n)e^{-j\omega n} \quad (1b)$$

The autocorrelation sequence used in this power spectral density expression is formally given by

$$r_x(n) = E\{x(k) x(n + k)\} \quad (2)$$

where  $E$  denotes the expected value operator characterizing the wide sense stationary time series  $\{x(n)\}$ . Whether the time series is deterministic or nondeterministic, it is noted that a frequency (spectral) characterization

entails a complete knowledge of a deterministic sequence on the infinite extent interval  $-\infty < n < \infty$ . Unfortunately, this knowledge is generally not available in most practical applications.

In the discipline widely known as spectral estimation, one seeks to approximate the spectral content of a time series based upon an incomplete set of time series observations. Without loss of generality, this set of observations will be taken to be the contiguous set of  $N$  time series elements

$$x(1), x(2), \dots, x(N) \quad (3)$$

In the classical spectral estimation approach, the spectral content of the time series is estimated by suitably truncating the infinite extent summations (1) (e.g., see ref. 1). To be more specific, if the time series is taken to be deterministic, the classical spectral estimate generated from the incomplete time series observations would be given by

$$X(\omega) = \sum_{n=1}^N x(n)e^{-j\omega n} \quad (4a)$$

Using a similar approach, the classical spectral estimate of a random time series is typically determined from

$$S_x(\omega) = \sum_{n=-N+1}^{N-1} \hat{r}_x(n)e^{-j\omega n} \quad (4b)$$

where  $\hat{r}_x(n)$  denotes an autocorrelation estimate which is generated from the given time series observations (3). Upon comparing relationships (1) and (4), it is clear that the classical spectral estimation approach makes the implicit assumption that the time series is identically zero outside the observation window  $1 \leq n \leq N$ . In most relevant applications, this is a very unrealistic assumption and all too often results in poor spectral resolution performance.

In recognition of the classical method's shortcomings, a number of so-called modern spectral estimation procedures have evolved over the past decade. By in large, the typical modern spectral estimator seeks to model the underlying power spectrum as a rational function of the following form

$$S_x(\omega) = \left| \frac{b_0 + b_1 e^{-j\omega} + \dots + b_q e^{-jq\omega}}{1 + a_1 e^{-j\omega} + \dots + a_p e^{-jp\omega}} \right|^2 \quad (5)$$

This particular model will be shown to arise when a linear, time-invariant autoregressive-moving average (ARMA) system of order (p,q) is driven by a white noise excitation. The transfer function of this ARMA system is given by the rational function appearing in relationship (5). It is important to note that rational spectral models can be justified on the basis that any continuous power spectral density can be approximated arbitrarily closely by a rational function of sufficiently high order [2].

The various modern spectral estimation procedures distinguish themselves by the manner in which they estimate the rational models  $a_1$  and  $b_1$  coefficients from the given time series observations (3). The most widely used spectral estimation model is the so-called all-pole model in which all the  $b_1$  coefficients except  $b_0$  are taken to be zero. This particular model, known as the autoregressive (AR) model, has given rise to the essentially equivalent autoregressive, linear predictive coding, and maximum entropy methods of spectral estimation. A collection of papers treating these and other spectral estimation procedures is to be found in reference [3].

For an important class of time series, autoregressive spectral estimators have been found to produce superior spectral resolution performance when compared to the classical Fourier based methods. This behavior in conjunction with the resultant simplicity of the  $a_1$  coefficient selection has made the maximum entropy method a particular favorite tool of the practitioner. It must be noted, however, that in those cases where the spectrum is best approximated by a zero-pole model, the AR model can yield very poor spectral estimates. With this in mind, a number of methods for obtaining zero-pole spectral estimates (i.e., ARMA models) have been developed (e.g., see refs. [4]-[8]). Clearly, the ability to generate a zero-pole spectral estimation offers the potential of a more robust behavior and significantly better spectral estimate performance than its less general all-pole AR counterpart. This capability has been empirically demonstrated where it was found that an ARMA provided the best overall spectral estimations for a variety of problems [4].

The class of ARMA spectral estimators include those which utilize the so-called whitening filter concept (e.g., [4] & [5]). Unfortunately, these particular spectral estimator procedures are iterative in nature, and, typically require a relatively large number of time series observations to be effective. Another approach which makes use of the recursive nature of the time series autocorrelation sequence and does not share these liabilities was developed by Box and Jenkins [6]. A modification of this method involving a more efficient noniterative method for generating the moving average coefficients was recently proposed [7] and [8]. Although these noniterative methods are computationally efficient, their spectral estimation performance is often unsatisfactory.

## II. OBJECTIVES

The objectives of this project were:

- (i) to develop an effective and computationally efficient ARMA spectral estimator.
- (ii) empirically compare the performance of this estimator to the standard maximum entropy method.

A description of an ARMA spectral estimator which achieves objective (i) and has been found to yield a significantly better performance than the maximum entropy method will now be presented. This will entail a further discussion of the concept of a rational spectrum model.

### III. RATIONAL SPECTRUM MODEL

One of the most widely used models for spectral estimation is the rational model. The stochastic time series  $\{x(n)\}$  is said to have a rational power spectrum if its power spectral density can be expressed in the form

$$S_x(z) = H(z) H(z^{-1}) \sigma^2 \quad (6)$$

where  $\sigma^2$  is a positive constant and the characteristic rational function

$$H(z) = \frac{B(z)}{A(z)} = \frac{1 + b_1 z^{-1} + \dots + b_q z^{-q}}{1 + a_1 z^{-1} + \dots + a_p z^{-p}} \quad (7)$$

is composed of polynomials  $A(z)$  and  $B(z)$  which have real coefficients and have zeros wholly contained within the unit circle. The rational power spectral density (6) is said to have order  $(p,q)$  and its zeroes and poles are seen to occur in sets of complex conjugate reciprocals. For reasons which will be shortly made clear, we shall refer to the  $a_k$  and  $b_k$  coefficients as the autoregressive and moving average coefficients, respectively.

A particularly convenient interpretation on how a stochastic time series with rational spectrum may arise follows directly from the characteristic rational function. This entails treating the characteristic rational function (7) as being the transfer function of a causal, time-invariant linear system. It then follows that this system will be characterized by the recursive equation

$$x(n) = \sum_{i=0}^q b_i \varepsilon(n-i) - \sum_{i=1}^p a_i x(n-i) \quad (8)$$

where  $b_0 = 1$  and the time series  $\{\varepsilon(n)\}$  and  $\{x(n)\}$  are taken to be the excitation and response signals, respectively. It is well known that when this system is excited by a stationary white noise time series as statistically characterized by

$$E\{\varepsilon(n)\} = 0 \quad \text{and} \quad r_\varepsilon(n) = \sigma^2 \delta(n) \quad (9)$$

then the power spectral density of the response time series is given precisely by relationship (6).<sup>1</sup> Thus, a stationary random time series with rational power spectral density can be interpreted as being the response of a causal, time-invariant linear system to a white noise excitation. This linear system is then said to have colored the white noise excitation process (i.e.,  $S_{\epsilon}(z) = 1$ ) and for this reason it is commonly referred to as a coloring filter as suggestively depicted in Figure 1.

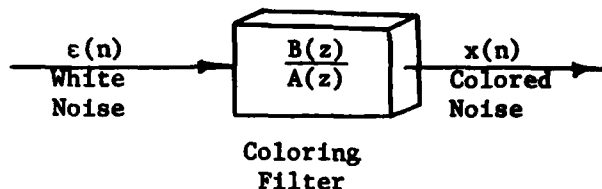


FIGURE 1: Model for a Rational Spectrum Generator

The general linear system (8) is commonly referred to as an autoregressive-moving average (ARMA) model in the spectral estimation literature. This ARMA model is said to be of order  $(p,q)$  and it gives rise to the rational spectrum (6) which possesses both zeros (via  $B(z)$ ) as well as poles (via  $A(z)$ ). The ARMA model is the most general of rational spectrum models possible and its  $a_k$  and  $b_k$  coefficients uniquely characterize the spectrum.

In the spectral estimation literature, the preponderance of activity has been directed towards the special class of ARMA models known as autoregressive (AR) models. An AR model is one in which the numerator polynomial  $B(z)$  is equal to the constant one (i.e.,  $b_k = 0$  for  $k \neq 0$ ). As such, the AR model is also referred to as an all-pole model since its transfer function is specified by

$$H(z) = \frac{1}{A(z)}$$

This all-pole model is the one most often used in spectral estimation primarily due to the ease with which one can compute the  $a_k$  coefficients

<sup>1</sup>The Kronecker delta sequence is defined by

$$\delta(n) = \begin{cases} 1 & n = 0 \\ 0 & \text{otherwise} \end{cases}$$

that correspond to a given finite set of time series observations. It should be noted that it is always possible to approximate a general ARMA model by an AR model in the following manner

$$H(z) = \frac{1}{A(z) \left[ \frac{1}{B(z)} \right]} = \frac{1}{A(z) A_1(z)}$$

whereby the polynomial  $A_1(z)$  is obtained by suitably truncating the power series  $1/B(z)$  as generated by long division. Clearly, the effectiveness of this approach is dependent on how quickly the coefficients of the long division  $1/B(z)$  converge to zero. If  $B(z)$  has a zero very close to the unit circle, this convergence rate will be extremely slow thereby making impractical the approximation of an ARMA model by a reasonably low order AR model. It can be conjectured that this is one of the main factors as to why AR models fail to yield satisfactory spectral estimates of time series composed of sinusoidal samples in a strong noisy environment (an ARMA process).

Another subclass of rational spectrum models which has received attention is the so-called moving average (MA) model as characterized by  $A(z) = 1$ . The transfer function of a MA model is given by  $B(z)$  and it is therefore also referred to as an all-zero model. With these thoughts in mind, it is apparent that a general ARMA model is composed of the cascading of an AR with an MA model. The rational spectrum associated with each of these models is displayed in Table 1.

MODEL	SPECTRUM
MA	$\sigma^2  B(e^{j\omega}) ^2$
AR	$\sigma^2 /  A(e^{j\omega}) ^2$
ARMA	$\sigma^2  B(e^{j\omega}) ^2 /  A(e^{j\omega}) ^2$

TABLE 1. Rational Spectrum Models

An examination of Table 1 reveals the greater flexibility which the ARMA model possesses in providing rational spectral estimates. This robustness was recently demonstrated in which the ARMA model was found to provide the overall best spectral estimates for a variety of problems [4]. Unless one has a priori knowledge which would indicate otherwise, it seems clear that the ARMA model is the one to utilize when seeking a rational spectrum model. Hereafter, we shall concern ourselves with the practical task of developing feasible procedures for determining the "optimum" coefficients of an ARMA model based on a finite set of time series measurements.

#### IV. FUNDAMENTAL AUTOCORRELATION RECURSIVE RELATIONSHIP

For reasons alluded to in the last section, there exists a basic incompatibility in generating an ARMA spectral model, which is most consistent with a given set of time series observations, when the number of observations is small. This incompatibility can be, to a large extent, alleviated by appealing to a fundamental recursive relationship characterizing ARMA time series. This relationship is obtained by analyzing the "causal image" of the autocorrelation sequence as defined by

$$r_x^+(n) = \begin{cases} r_x(n) & n \geq 0 \\ 0 & n < 0 \end{cases} \quad (10)$$

Since the autocorrelation sequence of a real valued time series is an even function of  $n$ , it is apparent that one can reconstruct the autocorrelation sequence from its causal image according to

$$r_x(n) = r_x^+(n) + r_x^+(-n) - r_x(0) \delta(n) \quad (11)$$

Upon taking the  $z$ -transform of this expression, the desired power spectral density is found, that is

$$S_x(z) = S_x^+(z) + S_x^+(z^{-1}) - r_x(0) \quad (12)$$

where the function  $S_x^+(z)$  denotes the  $z$ -transform of the causal image sequence (10). Thus, a power spectral density estimate may be equivalently accomplished by estimating the function  $S_x^+(z)$ . This will be the approach taken in this report.

When the underlying power spectral density is of the rational form (6), a little thought should convince oneself that the function  $S_x^+(z)$  must be of the specific rational form

$$S_x^+(z) = \frac{c_0 + c_1 z^{-1} + \dots + c_p z^{-p}}{1 + a_1 z^{-1} + \dots + a_p z^{-p}} \quad (13)$$

in which the denominator polynomial is identical to the  $A(z)$  polynomial that in part characterizes  $S_x(z)$ .<sup>1</sup> Upon multiplying both sides of this equation by the polynomial  $A(z)$  and then taking the inverse  $z$ -transform, one readily arrives at the following fundamental recursive relationship

$$r_x^+(n) = \sum_{i=0}^p c_i \delta(n-i) + \sum_{i=1}^p a_i r_x^+(n-i) \quad (14)$$

where the natural boundary conditions  $r_x^+(n) = 0$  for  $n < 0$  are imposed to reflect the causality of sequence  $r_x^+(n)$ . Thus, the causal image of an ARMA autocorrelation sequence of order  $(p,q)$  is seen to be governed by a linear difference equation of order  $p$ .

Upon examining fundamental relationship (14), it is apparent that a knowledge of the  $a_i, c_i$  coefficients will enable one to generate the entire autocorrelation sequence. If it were somehow possible to accurately estimate these coefficients from the given time series observations, a particularly effective method of spectral estimation is suggested. Namely, these coefficient estimates, when substituted into equation (13), will provide an estimate for  $S_x^+(z)$ . Using this estimate in relationship (12), the desired power spectral density estimate is then obtained

$$S_x(e^{j\omega}) = 2\text{Re} \left[ \sum_{k=0}^p c_k e^{-jk\omega} / \left[ 1 + \sum_{k=1}^p a_k e^{-jk\omega} \right] \right] - \hat{r}_x(0) \quad (15)$$

where use of the fact that  $S_x^+(e^{j\omega})$  and  $S_x^+(e^{-j\omega})$  are complex conjugates has been made. We shall now present a procedure for estimating the  $a_i, c_i$  coefficients with the ultimate goal of using relationship (15) for the spectral estimate.

---

<sup>1</sup>It is here assumed that the ARMA model of order  $(p,q)$  is such that  $p \geq q$ . When this is not the case, the degree of the numerator polynomial  $C(z)$  must be increased to  $q$ .

## V. ARMA MODEL COEFFICIENT SELECTION PROCEDURES

The most critical step of the proposed spectral estimation method involves estimating the  $a_1$  and  $c_1$  coefficients. In this section, the so-called direct and indirect procedures for accomplishing this task will be described. The direct approach makes explicit use of the fundamental autocorrelation relationship derived in the previous section. On the other hand, the more effective indirect approach uses an alternate approach which provides a solution procedure that is consistent with the fundamental autocorrelation relationship.

### Direct Method

In the direct method, one first generates estimates of the autocorrelation sequence from the given time series observations using some convenient method.<sup>1</sup> These estimates, denoted as  $\hat{r}_x(n)$ , are then substituted into fundamental relationship (14). In recognition that the autocorrelation estimates will be generally in error, and that the ARMA model order parameter  $p$  may be incorrect, it follows that this substitution will give rise to the following "equation error" sequence

$$e(n) = \hat{r}_x(n) + \sum_{i=1}^p a_i \hat{r}_x(n-i) - \sum_{i=0}^p c_i \delta(n-i) \quad 0 \leq n \leq N-1 \quad (16)$$

in which  $\hat{r}_x(n) = 0$  for  $n < 0$ .

Our objective will be that of selecting the models  $a_1, c_1$  coefficients so as to minimize these equation errors in some sense. For reasons of mathematical tractability and subsequently demonstrated effectiveness, the equation error criterion to be minimized is taken to be the quadratic functional

$$f(\underline{a}, \underline{c}) = \sum_{n=0}^{N-1} w(n) e^2(n) \quad (17)$$

---

<sup>1</sup>As an example, one might use the biased estimator.

$$\hat{r}_x(n) = \frac{1}{N} \sum_{k=1}^{N-n} x(k) x(k+n)$$

The nonnegative weights,  $w(n)$ , are usually selected to be monotonically nonincreasing (i.e.,  $w(n) \geq w(n+1)$ ) so as to reflect an anticipated degradation in equation error accuracy for increasing  $n$ . This degradation behavior arises primarily from a loss in autocorrelation estimate fidelity for increasing lags (i.e.,  $n$ ).

In minimizing this functional with respect to the  $c_1$  coefficients, it is apparent from relationship (16) that the  $c_1$  coefficients have no effect whatsoever on the  $e(n)$  for  $n > p$ . This being the case, it follows that the optimum  $c_1$  coefficients must be given by

$$c_n^0 = \hat{r}_x(n) + \sum_{i=1}^n a_i \hat{r}_x(n-i) \quad 0 \leq n \leq p \quad (18)$$

since such a selection will render the equation errors,  $e(n)$ , identically zero over  $0 \leq n \leq p$  for "any" choice of the  $a_1$  autoregressive coefficients. It then follows that the optimum autoregressive coefficients must render the remaining terms (i.e.,  $p < n < N$ ) of the quadratic functional a minimum. With this in mind, let us express these specific set of equation errors in the matrix format

$$\begin{bmatrix} e(p+1) \\ e(p+2) \\ \cdot \\ \cdot \\ e(N-1) \end{bmatrix} = \begin{bmatrix} \hat{r}_x(p) & \hat{r}_x(p-1) & \dots & \hat{r}_x(1) \\ \hat{r}_x(p+1) & \hat{r}_x(p) & \dots & \hat{r}_x(2) \\ \cdot & \cdot & \cdot & \cdot \\ \cdot & \cdot & \cdot & \cdot \\ \hat{r}_x(N-2) & \hat{r}_x(N-3) & \dots & \hat{r}_x(N-p-1) \end{bmatrix} \begin{bmatrix} a_1 \\ a_2 \\ \cdot \\ \cdot \\ a_p \end{bmatrix} + \begin{bmatrix} \hat{r}_x(p+1) \\ \hat{r}_x(p+2) \\ \cdot \\ \cdot \\ \hat{r}_x(N-1) \end{bmatrix} \quad (19a)$$

where use of relationship (16) for  $n > p$  has been made. This matrix system of equations can be conveniently expressed as

$$\underline{e} = \underline{R}\underline{a} + \underline{r} \quad (19b)$$

in which  $\underline{a}$  is the  $p \times 1$  autoregressive coefficient vector with elements  $a_n$ ,  $\underline{e}$  and  $\underline{r}$  are each  $(N-p-1) \times 1$  vectors with elements  $e(p+n)$  and  $\hat{r}_x(p+n)$ , respectively, and  $R$  is a  $(N-p-1) \times p$  Toeplitz matrix.

For the optimum  $c_1$  coefficient selection (18), it is apparent that the quadratic functional (17) may be expressed as

$$f(\underline{a}, \underline{c}^0) = [\underline{R}\underline{a} + \underline{r}]' W [\underline{R}\underline{a} + \underline{r}] \quad (20)$$

in which  $W$  is a positive semidefinite  $(N-p-1) \times (N-p-1)$  diagonal matrix whose diagonal elements are given by  $w_{nn} = w(p+n)$  for  $n=1, 2, \dots, N-p-1$ . The minimization of this quadratic functional with respect to the autoregressive coefficient vector is straightforwardly carried out and results in the following system of  $p$  linear equations for the required optimum autoregressive coefficient vector

$$[\hat{R}W\underline{R}] \underline{a}^0 = -\hat{R}' \underline{w} \quad (21)$$

One then solves this system of linear equations to obtain the desired optimum autoregressive coefficients. Upon substitution of these autoregressive coefficients into relationship (18), the optimum  $c_i^0$  coefficients are next determined. Finally, the desired power spectral density estimate is obtained by substituting these optimum  $a_i^0, c_i^0$  coefficients into relationship (15).

It is of interest to note that the system of equations for the autoregressive coefficients (21) reduces to the Box-Jenkins method for a weighting selection of  $w(n+p) = 1$  for  $1 \leq n \leq p$  and zero otherwise. Unfortunately, this particular weighting selection implicitly assumes that the equation errors  $e(n)$  for  $p+1 \leq n \leq 2p$  all have the same statistical behavior. More realistically, one would presume that the equation errors become more random as  $n$  increases. It is then conjectured that the primary reason as to why the Box-Jenkins method does not provide adequate spectral estimates for certain problems is due to this particular weighting choice and the fact that it makes no use of the fundamental autocorrelation relationship (14) for  $n > 2p$  whatsoever.

#### Indirect Method

Although the direct method has been found to provide satisfactory spectral estimation performance, the indirect approach to be now briefly described has yielded significantly better performance. Its development is based on the coloring filter's characteristic equation (8), and the fact that the random variables  $x(n)$  and  $\epsilon(m)$  are uncorrelated for  $m > n$ . To begin this development, we shall first replace the variable  $n$  appearing in relationship (8) by  $k$ . Next, each side of this characteristic equation

is multiplied by  $x(k-n)/(N-n)$  to obtain

$$x(k) \frac{x(k-n)}{N-n} = \left[ \sum_{i=0}^q b_i \varepsilon(k-i) - \sum_{i=1}^p a_i x(k-i) \right] \frac{x(k-n)}{N-n}$$

If both sides of this equality are then summed over the index range  $n < k \leq N$ , after rearrangement one obtains

$$\bar{e}(n) = \sum_{i=1}^p \left[ \frac{1}{N-n} \sum_{k=n+1}^N x(k-i) x(k-n) \right] a_i + \left[ \frac{1}{N-n} \sum_{k=n+1}^N x(k) x(k-n) \right] \quad (22)$$

for  $p < n < N$

where the pseudo equation error term is specified by

$$\bar{e}(n) = \sum_{i=0}^q b_i \left[ \frac{1}{N-n} \sum_{k=n+1}^N \varepsilon(k-i) x(k-n) \right] \quad p < n < N$$

Upon examination of this expression, it is clear that the expected value of the term  $\varepsilon(k-i) x(k-n)$  will be zero. This would indicate that the general pseudo equation error term  $\bar{e}(n)$  will itself tend to be close to zero (this is reinforced by the division by  $N-n$ ). With this in mind, a logical choice for the  $a_i$  coefficients used in expression (22) would be one which tended to minimize the pseudo equation error sequence.

If one compares the pseudo equation error relationship (22) with the equation error relationship (16), a similarity is in evidence. Namely, the elements within the brackets of expression (22) are recognized as unbiased autocorrelation estimates. If these estimates are substituted for the entries of matrix  $R$  and vector  $r$  in relationship (19), a new system of equations for the optimum autoregressive coefficients arises. These new systems of equations distinguish themselves from the former in that a genuinely different autocorrelation estimate formula is used for each equation. Once this modified system of equations have been solved for the  $a_i$  coefficients, the  $c_i$  coefficient estimates are obtained according to

$$c_n^o = \left[ \frac{1}{N-p} \sum_{k=p+1}^N x(k)x(k-n) \right] + \sum_{i=1}^n a_i \left[ \frac{1}{N-p} \sum_{k=p+1}^N x(k)x(k-n+1) \right] \quad (23)$$

for  $0 \leq n \leq p$

The required power spectral density estimate is then given by relationship (15).

## VI. NUMERICAL EXAMPLES

To test the effectiveness of the proposed ARMA spectral estimator method, the classical problem of detecting the presence of sinusoids in additive noise will be considered. In particular, we will investigate the specific case in which the time series observations are generated according to

$$x(n) = A_1 \cos(\pi f_1 n) + A_2 \cos(\pi f_2 n) + w(n) \quad 1 \leq n \leq N \quad (24)$$

where  $w(n)$  is a white Gaussian time series with variance one. This particular problem serves as an excellent vehicle for measuring a spectral estimator's performance relative to: (i) detecting the presence of sinusoids in a strong noisy background, and, (ii) resolving two sinusoids whose frequencies  $f_1$  and  $f_2$  are nearly equal. The individual sinusoidal signal-to-noise ratios (SNR) for the above signal are given by  $20 \log(A_k/\sqrt{2})$  for  $k = 1, 2$ . In order to consider the effectiveness of the proposed ARMA spectral estimator in different noise environments, we shall consider two cases. These cases have been examined in reference [9] where the performance of many modern spectral estimators are empirically compared.

$$\begin{aligned} \text{CASE I: } A_1 &= \sqrt{20}, f_1 = 0.4 \\ A_2 &= \sqrt{2}, f_2 = 0.426 \end{aligned}$$

In this example, we have two closely spaced (in frequency) sinusoids for which the stronger sinusoid has a SNR of 10 dB while the weaker sinusoid has a SNR of 0 dB. For this relatively low SNR case, the ability of a spectral estimator to resolve closely spaced sinusoids and identify their frequencies will be tested. Upon generating sequence (24) with the postulated parameters for a data length of  $N = 1024$ , spectral estimates

were obtained using a 15th order model with the indirect ARMA method ( $w(n) = (N-n)^3$ ), maximum entropy method, and the modified Box-Jenkins method incorporating biased autocorrelation estimates. In addition, a standard periodogram spectral estimate was obtained using the same data. The resultant spectral estimates are displayed in Figure 2 where a number of observations can be made

- (i) the indirect ARMA spectral estimate provides excellent results with two sharp peaks at  $\hat{f}_1 = 0.400$  and  $\hat{f}_2 = 0.427$ , and with the spectrum near 0 dB (the noise level) for most other frequencies.
- (ii) the maximum entropy and modified Box-Jenkins methods were unable to resolve the two sinusoids in the prevailing low SNR environment.
- (iii) although the periodogram is able to resolve the two sinusoids, the well-known random fluctuation behavior which characterizes the periodogram method is in evidence.

This example nicely demonstrates the potential capability of the herein developed indirect ARMA spectral estimation method relative to existing procedures.

In many practical problems, one does not have available exceedingly long data lengths upon which to make a spectral estimate. To demonstrate the ability of the indirect ARMA spectral estimator to perform in such situations, the first 64 samples of the data sequence in the above example were used to generate a spectral estimate. The resultant 15th order indirect ARMA spectral estimate obtained is shown in Figure 3 where the

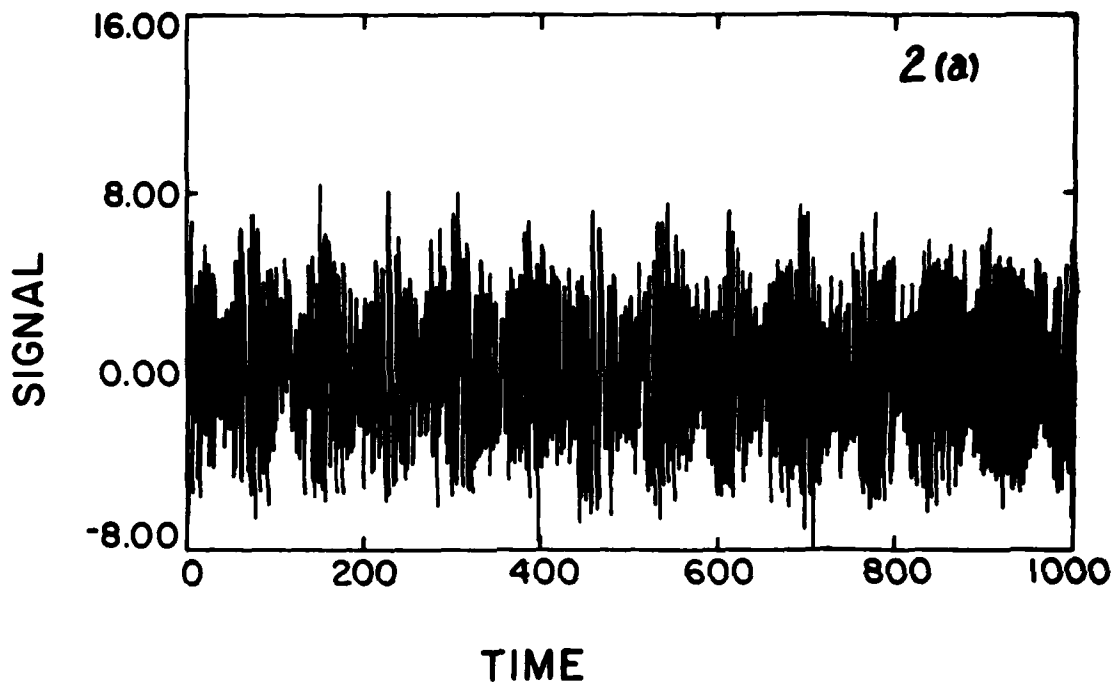


Fig. 2 Spectral estimates of the time series

$$x(n) = \sqrt{2} \cos(0.4\pi n) + 2 \cos(0.426\pi n) + w(n)$$

in which  $\{w(n)\}$  is a white Gaussian random process with variance one: (a) time series, and, spectral estimates given by the methods, (b) indirect ARMA, (c) Maximum entropy, (d) Box - Jenkins, (e) Periodogram

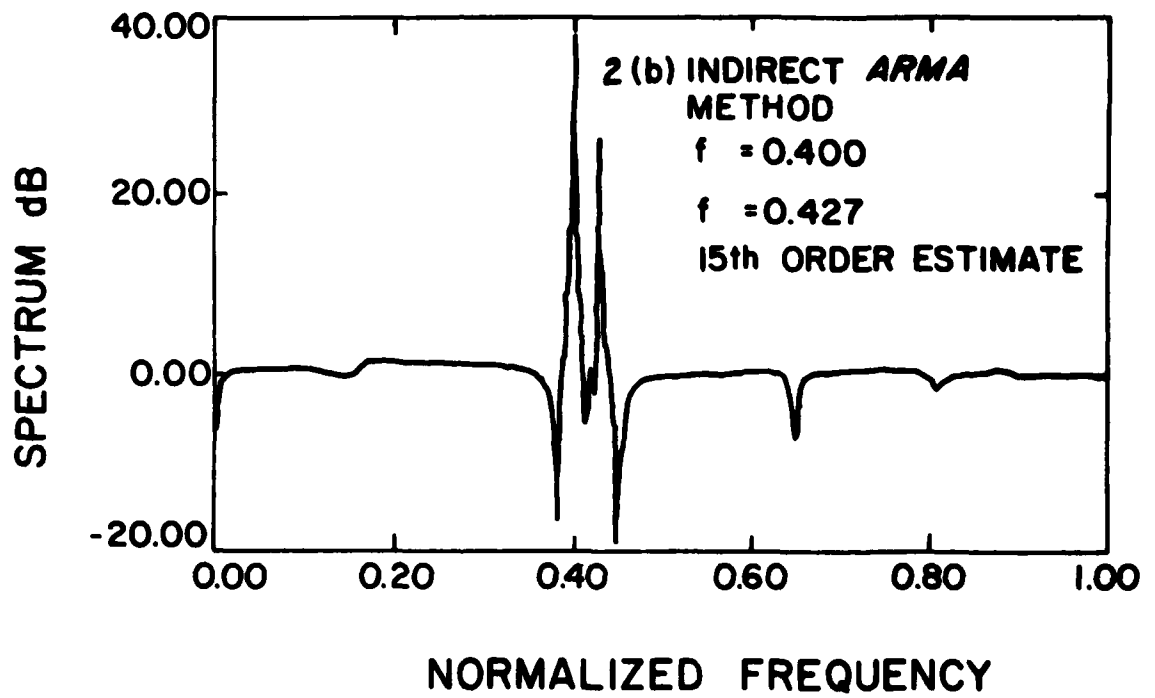


Figure 2b

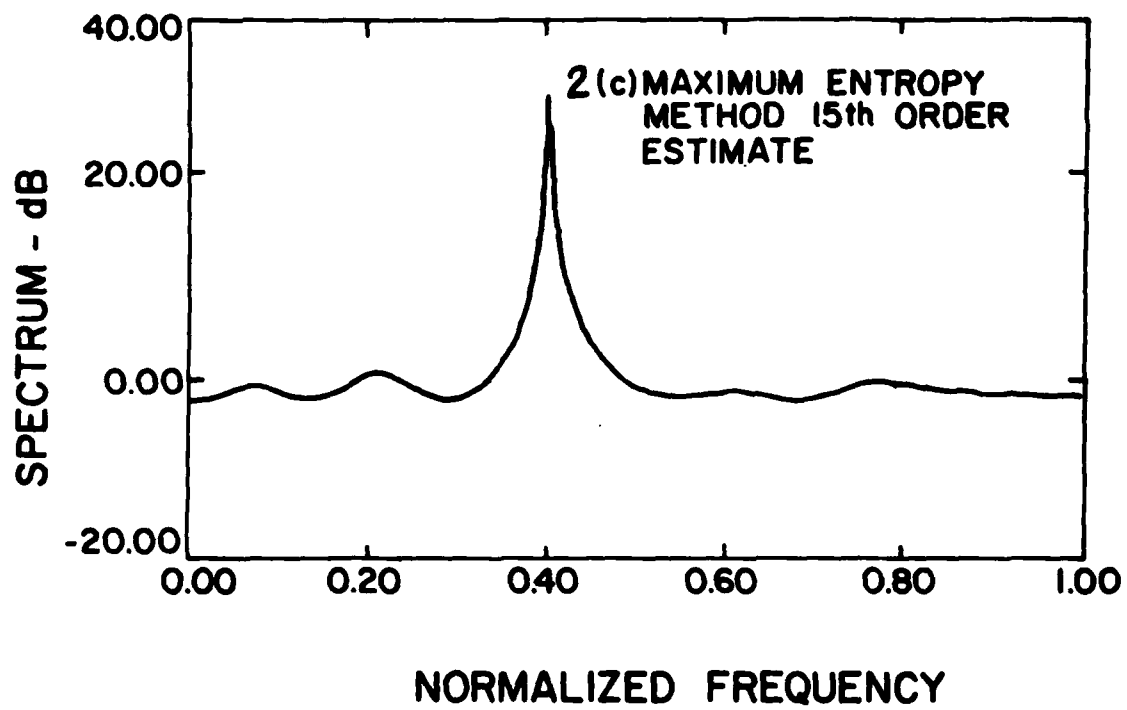


Figure 2c

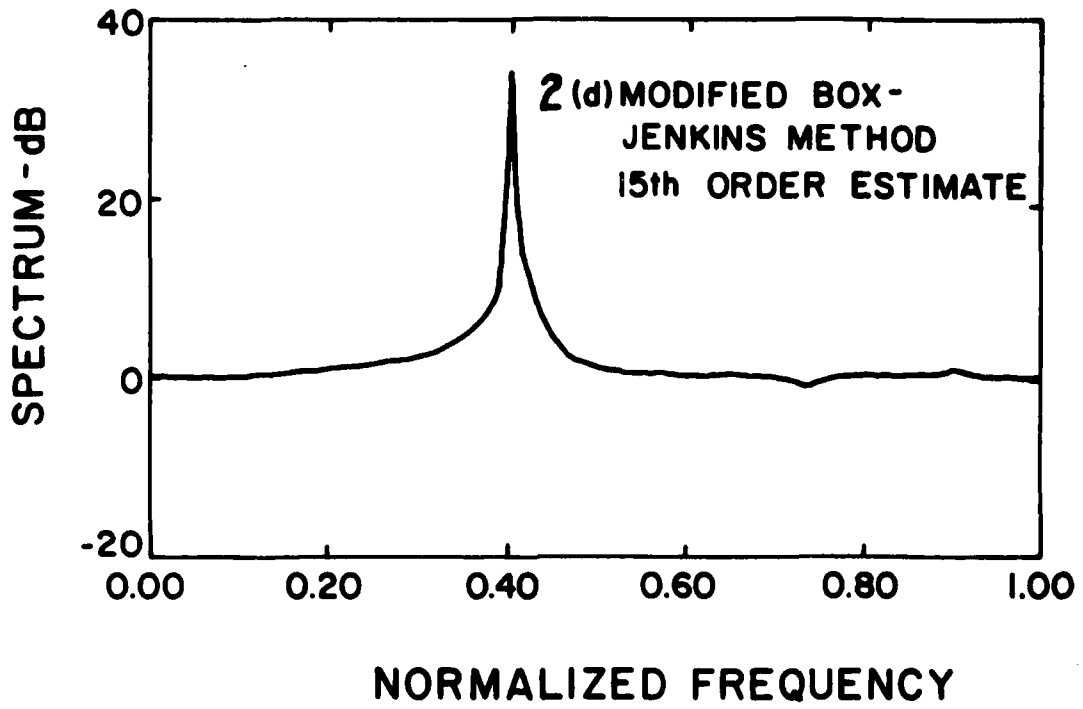


Figure 2d

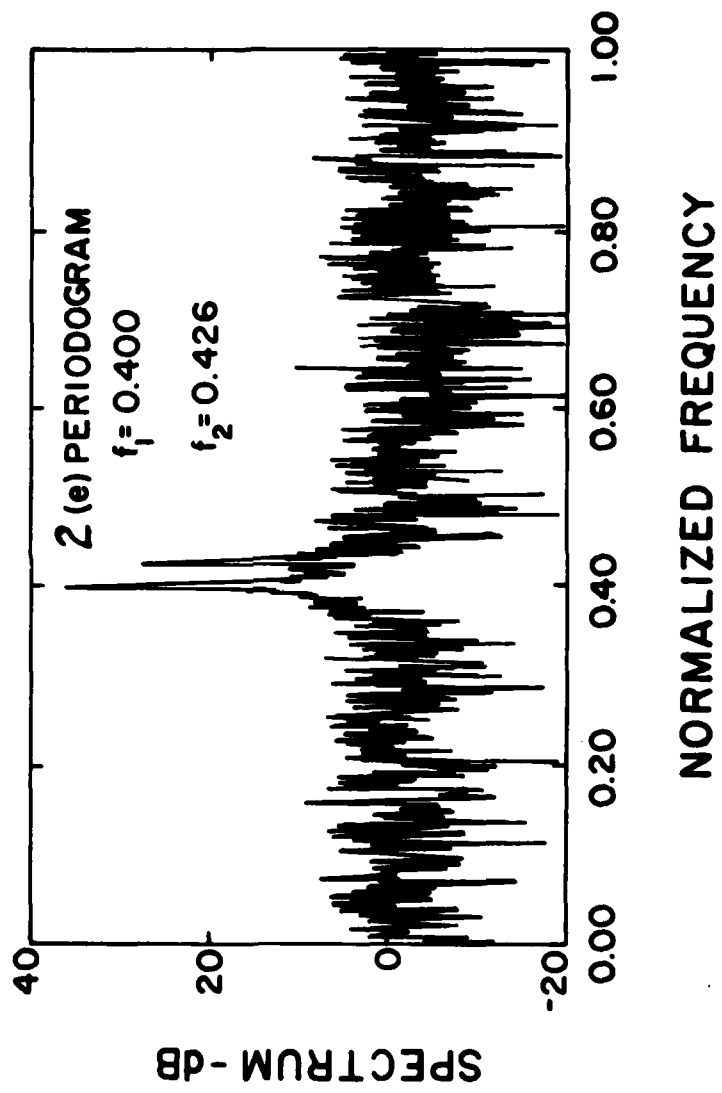


Figure 2e

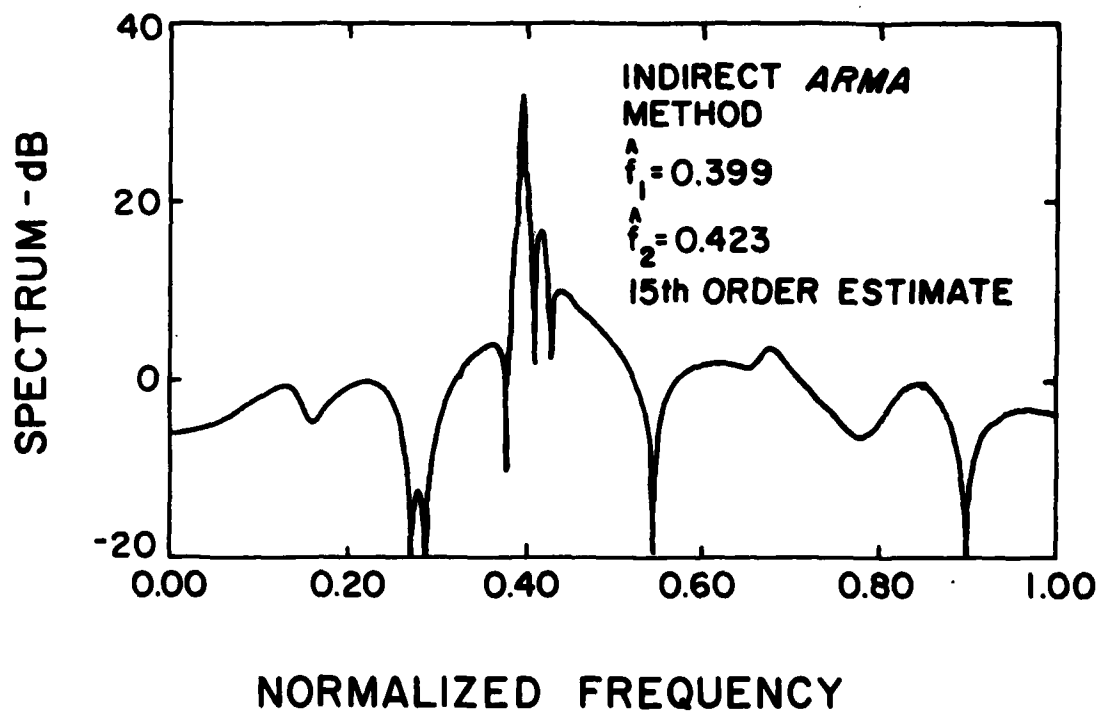


Fig. 3 Indirect ARMA spectral estimation obtained using the first 64 data points of Case I.

ability to resolve the two closely spaced sinusoids is again evident. The sinusoid's frequency estimates  $\hat{f}_1 = 0.399$  and  $\hat{f}_2 = 0.423$  are also of good quality in this low SNR environment.

$$\begin{aligned} \text{CASE II: } A_1 &= \sqrt{2}, f_1 = 0.32812 \\ A_2 &= \sqrt{2}, f_2 = 0.5 \end{aligned}$$

We are now examining the ability of the ARMA spectral estimator to detect sinusoids in a low SNR environment (i.e., 0 dB). For a selection of  $N = 64$ ,  $w(n) = (N-n)^3$  and  $p = 5$ , the resultant ARMA spectral estimation is displayed in Figure 4a. Clearly, one is able to detect the presence of the two sinusoids, and, the frequency estimates  $\hat{f}_1 = 0.3202$  and  $\hat{f}_2 = 0.5012$  are of good quality considering the prevailing SNR environment. A 15th order maximum entropy spectral estimator was then found to generate the spectral estimate displayed in Figure 4b. Although the two sinusoids were properly detected, a number of false peaks are in evidence.

#### Digital Filter Design

It is possible to use the proposed ARMA method for synthesizing digital filters. To illustrate the approach that is taken, let us consider the specific case of designing a low-pass filter of normalized, cutoff frequency  $f_c$ . One may readily show that the impulse response of an idealized version of this low pass filter is given by  $\sin[\pi f_c n]/\pi n$ . With this in mind, one then applies the herein developed ARMA procedure to the specific sequence

$$x(n) = \sin[\pi f_c (n-0.5N)]/\pi(n-0.5N) \quad 1 \leq n \leq N$$

The resultant ARMA model obtained in this manner will have the attenuation characteristics of the desired low-pass filter. To illustrate this, a 15th order ARMA spectral estimate of this sequence was made for  $f_c = 0.2$ ,  $N = 128$  and  $w(n) = [N-n]^2$ . The resultant filter's magnitude characteristics are displayed in Figure 5 where the low-pass characteristics are in evidence. In a paper now in preparation, a detailed description of this filter synthesis procedure will be made and compared to an alternate method [10].

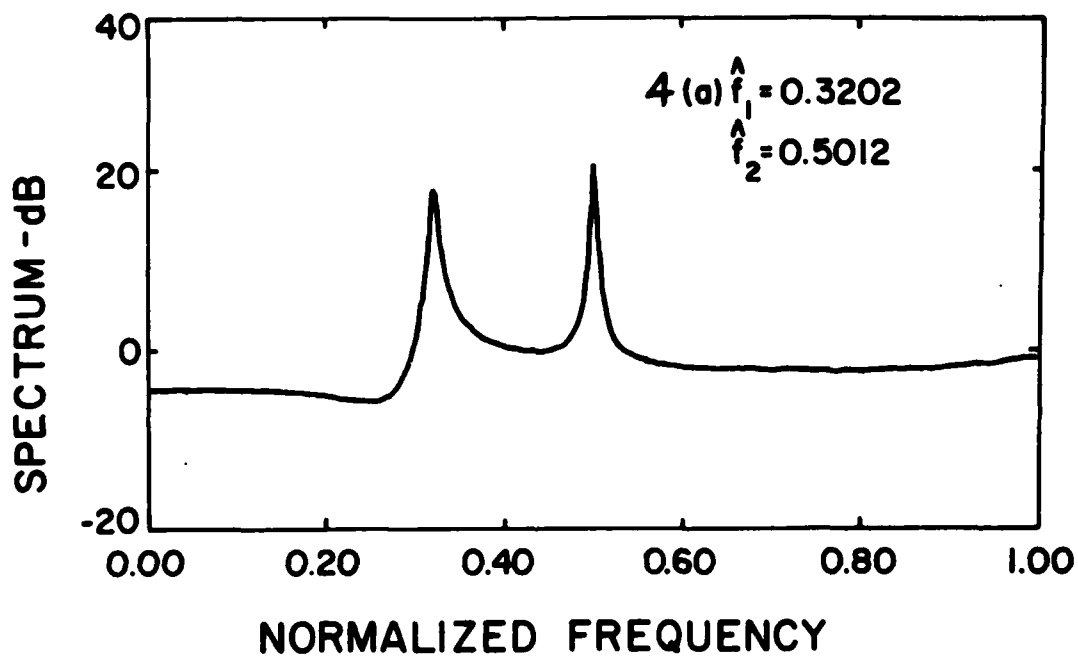


Fig. 4 Spectral estimates of the time series

$$x(n) = \sqrt{2} \cos(0.32812\pi n) + \sqrt{2} \cos(0.5\pi n) + w(n)$$

in which  $w(n)$  is a white Gaussian random process with variance one: (a) fifth order indirect ARMA method, (b) fifteenth order maximum entropy method.

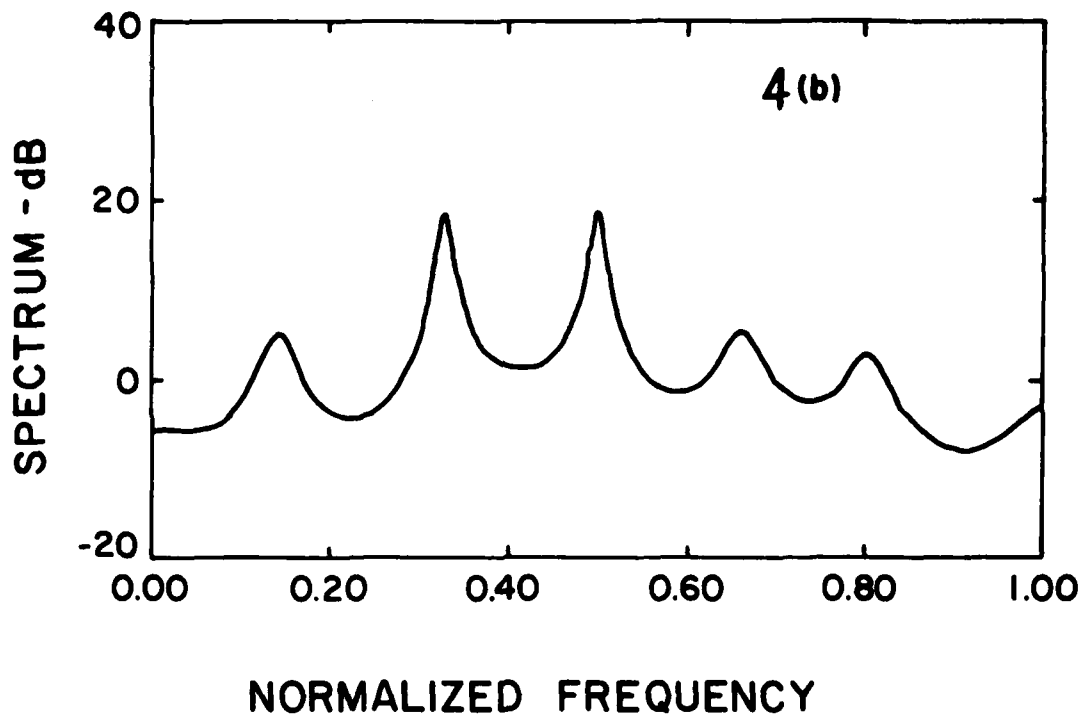


Figure 4b

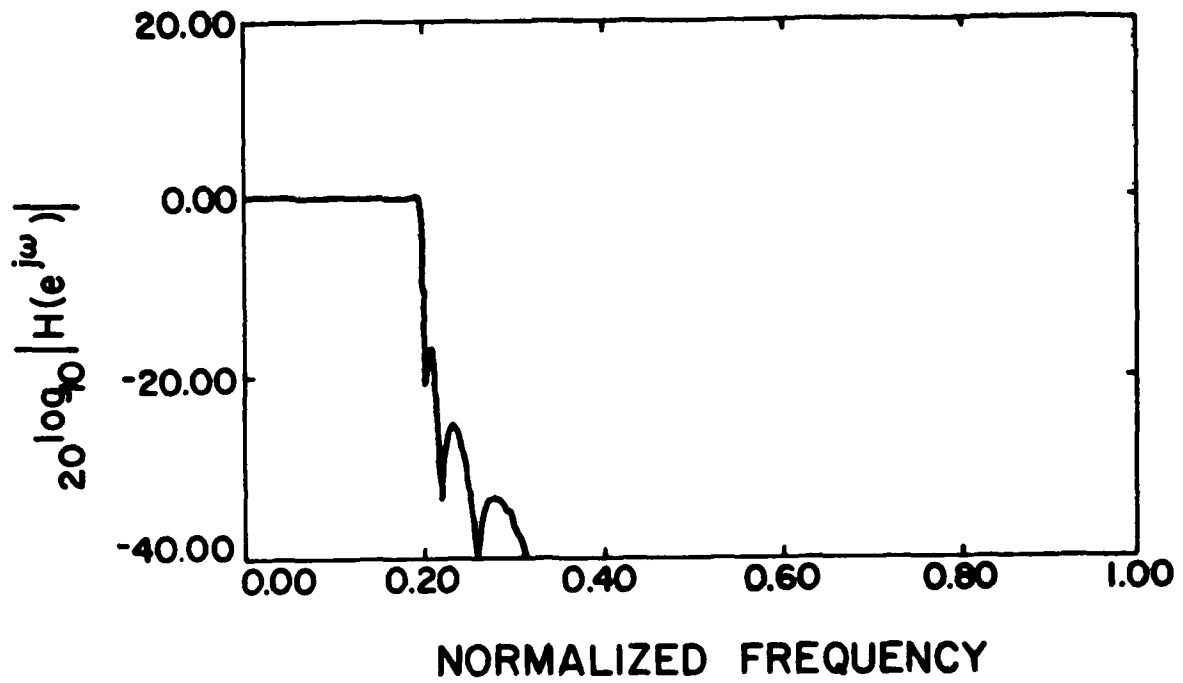


Fig. 5 Low-Pass Digital Filter Using a Fifteenth Order ARMA Model

## VII. RECOMMENDATIONS

A computationally efficient closed form method for generating ARMA spectral estimates has been presented. Conceptually, the method offers the promise of producing superior spectral estimation performance in comparison to such AR spectral estimators as the autoregressive, linear predictive coding, and maximum entropy methods. Empirical results have substantiated this conjecture.

In order for this method to achieve its full potential, a number of important considerations need further investigation. They include determination of the most effective autocorrelation estimation procedure to use since an inferior procedure will generally result in poor spectral estimations. Another important consideration is the choice of error weights. This weighting selection should reflect, in some manner, our growing lack of confidence in the autocorrelation estimates for increasing lags ( $n$ ). Since no statistical assumptions on the time series are being made (other than it is an ARMA time series), it is apparent that the weighting sequence should be data dependent. One further consideration is that of determining a procedure for obtaining the best choice of the ARMA ordering parameter  $p$ . As a final point, the possible use of the approach herein developed to two and higher dimensional signals should be explored.

VIII. REFERENCES

- [1] R. B. Blackman, and J. W. Tukey, THE MEASUREMENT OF POWER SPECTRA, Dover Publications, 1958.
- [2] L. H. Koopmans, THE SPECTRAL ANALYSIS OF TIME SERIES, Academic Press, New York, 1974.
- [3] D. G. Childers, MODERN SPECTRUM ANALYSIS, IEEE Press, 1978.
- [4] P. R. Gutowski, E. A. Robinson, and S. Treitel, "Spectral Estimation, Fact or Fiction," IEEE Trans. Geoscience Electronics, Vol. GE-16, No. 2, pp. 80-84, April 1978.
- [5] S. A. Tretter and K. Steiglitz, "Power-Spectrum Identification in Terms of Rational Models," IEEE Trans. Automatic Control, Vol. AC-12, pp. 185-188, April 1967.
- [6] G. Box and G. Jenkins, TIME SERIES ANALYSIS; FORECASTING AND CONTROL, Revised Edition, Holden-Day, San Francisco, 1976.
- [7] M. Kaveh, "High Resolution Spectral Estimation for Noisy Signals," IEEE Trans. Acoustics, Speech, and Signal Processing, Vol. ASSP-27, No. 3, pp. 286-287, June 1979.
- [8] J. F. Kinkel, J. Perl, L. Scharf, A. Stubberud, "A Note on Covariance-Invariant Digital Filter Design and Autoregressive Moving Average Spectrum Analysis," IEEE Trans. Acoustics, Speech, and Signal Processing, Vol. ASSP-27, No. 2, pp. 200-202, April 1979.
- [9] Y. M. Sullivan, O. L. Frost, J. R. Treichler, "High Resolution Signal Estimation," ARGO Systems Inc Tech Report, June 1978.
- [10] L. L. Scharf and J. C. Luby, "Statistical Design of Autoregressive-Moving Average Digital Filters," IEEE Trans. on Acoustics, Speech, and Signal Processing, Vol. ASSP-27, No. 3, pp. 240-247, June 1979.

1979 USAF - SCEE SUMMER FACULTY RESEARCH PROGRAM

Sponsored by the

AIR FORCE OFFICE OF SCIENTIFIC RESEARCH

Conducted by the

SOUTHEASTERN CENTER FOR ELECTRICAL ENGINEERING EDUCATION

FINAL REPORT

A STUDY OF TWO AVIONICS MULTIPLEX SIMULATION MODELS:

SNS and MUXSIM

Prepared by:	Malcolm D. Calhoun
Academic Rank:	Assistant Professor
Department and University:	Department of Electrical Engineering Mississippi State University
Research Location:	Air Force Avionics Laboratory System Avionics Division (AA) Avionic Systems Engineering Branch (AAA) System Design Group (AAA-1) Wright-Patterson Air Force Base, OH
USAF Research Colleague:	Robert L. Harris (AAA-1)
Date:	10 August 1979
Contract No.:	F49620-79-C-0038

A STUDY OF TWO AVIONICS MULTIPLEX SIMULATION MODELS: SNS AND MUXSIM

by

Malcolm D. Calhoun

ABSTRACT

Simulation is an invaluable aid in the development of Avionic Systems as required by the United States Air Force. To this end, the Air Force Avionics Laboratory (AFAL) at Wright-Patterson Air Force Base, Ohio has developed two simulation models to assist in the evaluation of multiplex avionics systems: (1) Multiplex Simulator (MUXSIM), and (2) System Network Simulator (SNS). A lack of utilization of these models led to the study reported herein. This paper describes the methods of use of these two simulators; also, attributes and deficiencies of the simulators are delineated. Included in the report is a literature survey of related simulation efforts. Since a major part of this study was devoted to utilization of MUXSIM and SNS, a User's Guide is included in the Appendix. Recommendations for further work on the simulators is included in the report.

#### ACKNOWLEDGEMENTS

The author wishes to express his gratitude to the Air Force Systems Command, Air Force Office of Scientific Research, and the Southeastern Center for Electrical Engineering Education for providing the opportunity to participate in the Summer Faculty Research Program. Credit is due to Dr. Richard N. Miller and his staff for their administration of the program. Special thanks go to Mr. Robert L. Harris, my effort focal point, for sharing his time and knowledge to assist me in this project. Thanks is extended to Lt Rick Butler and Mr. Robert Heuman for their timely and informative discussions regarding SNS and MUXSIM. Last, but not least, I wish to thank Mrs. Pam Grove for her assistance in the preparation of this report.

## I. INTRODUCTION

The advent of LSI and the microprocessor has led to integrated avionic systems in all types of Air Force aircraft. In conjunction with multiplexed data buses, microprocessors can be distributed both functionally and physically among various avionics subsystems. Simulation techniques provide the system design engineer with methods of evaluating complex avionic systems in the early design phase. Simulation allows system characteristics and operations to be varied and observed prior to the actual construction of hardware.

The avionics system engineer is confronted with the complex problem of designing the multiplex system to operate in an optimal fashion. For the case of several processors distributed along a multiplex bus, there is the problem of partitioning avionic tasks among the processors. For a data bus with one centralized controller, the problem is less complex but still requires modeling in terms of communication with remote terminals connected to the bus. At this point, simulation tools are employed to explore various system parameters such as bus architectures, message protocols, timing, and task partitioning.

To assist in the design and evaluation of avionic multiplex systems, the Air Force Avionics Laboratory (AFAL) has developed two simulation models, SNS and MUXSIM.<sup>1</sup> These simulators are resident in the DEC-10 Computer System at AFAL and are available for general use, yet the utilization of these models has been minimal since their development. The primary thrust of the summer research effort has been to utilize and document the two simulators to the extent that they may be useful to AFAL and contractor engineers.

## II. OBJECTIVES

The objectives of the summer research effort as specified in the Project Work Statement, Project AAA-14, were as follows:

- (1) To review available documentation on SNS and MUXSIM.
- (2) To prepare a user's manual for the two simulators giving information on the following:
  - (a) Types of problems appropriate to each simulation model.
  - (b) Input data requirements.
  - (c) Sources of input data.
  - (d) Evaluation of output data.

In addition to the objectives of the work statement, it was decided that a literature survey of multiplex simulation would be pertinent to this effort. Consequently, a literature search was performed and the results have been included in this report.

### III. SYSTEM NETWORK SIMULATOR (SNS)

SNS is a discrete event simulation program which allows the avionics system designer to evaluate various parameters of a distributed time-division multiplex system. The simulator provides a means of observing the transfer of digital information as a function of the topological configuration of the avionic system. Additionally, the effects of varying bus structure and protocol may be assessed by SNS.<sup>2</sup>

Presently, SNS resides in the DEC-10 computer system at AFAL. The simulator is encoded in ANSI FORTRAN and DEC-10 MACRO. Three versions of SNS allow some versatility in the evaluation of bus architecture; (1) MIL STD 1553A bus protocol with a central controller, (2) MIL STD 1553A protocol with control to terminal and terminal to terminal transfers, and (3) a round robin bus polling wherein bus control is passed sequentially from processor to processor. The simulation program may be run in batch mode or through an interactive terminal. A detailed description of the procedure for using SNS is contained in the Appendix. For specific information on the program, see reference [3].

The scheme of using SNS is outlined in flow chart form in Figure 1. The data base which is input to SNS may be a specific aircraft avionic system or it may be a generic type system. The SNS user is responsible

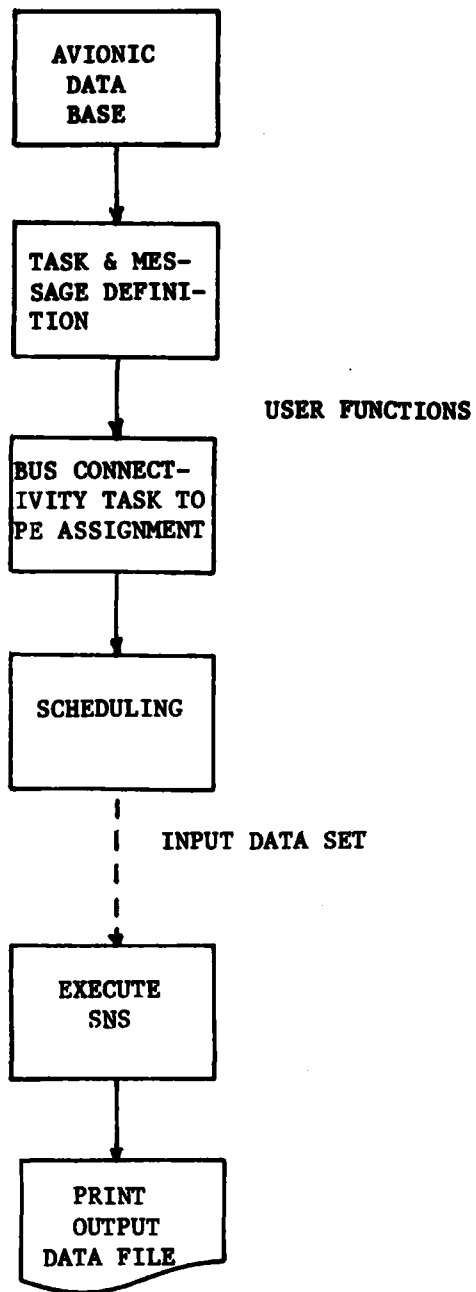


Figure 1. SNS INPUT/OUTPUT INTERFACES

for the assignment of tasks to be processed. Information regarding task start times, update rates, and execution times must be supplied. The input data file may be entered via punch cards, magnetic tape, or a time sharing terminal. An example of input data assignment along with information on executing SNS is contained in the Appendix.<sup>4</sup>

Capabilities and deficiencies of SNS are summarized below:

#### SNS Attributes

1. Evaluation of various architectures.
2. Ability to model a hierarchical system with global and local bus connectivities.
3. Verification of specific system design.
4. Evaluation of processor utilization and partitioning.
5. Output information,
  - (a) Discrete event summary
  - (b) Bus evaluation over a sample period
  - (c) Bus decomposition report
  - (d) Bus utilization summary
  - (e) Message transmission summary
  - (f) Processor utilization summary
6. Relative ease of varying input parameters and system architecture for comparative evaluations.

#### SNS Deficiencies

1. Provides for maximum of 16 processors.
2. Lack of software documentation makes modifications difficult.
3. Detail of defining tasks and messages, assigning tasks to processors, scheduling.
4. No provision for handling asynchronous messages.
5. No provisions for terminal or bus malfunctions or noise.
6. Executive processing overhead is not included in message summaries.
7. No provisions for fault tolerant simulation.

#### IV. MULTIPLEX SIMULATOR (MUXSIM)

The Multiplex Simulator (MUXSIM) simulates the transfer of digital avionics information on a single level, time-division multiplex bus.<sup>1</sup> The primary functions of MUXSIM are (1) analysis of bus loading and utilization, and (2) design aid for avionics systems.<sup>5</sup> As a design tool, MUXSIM aids the avionics engineer in the assignment and placement of subsystems and remote terminals. The primary capability of MUXSIM is the evaluation of data bus usage.

MUXSIM is coded in FORTRAN and resides in the AFAL DEC-10 Computer System. Additionally, MUXSIM is augmented with FORTRAN based GASP-IV.<sup>6</sup> The simulator's front-end routines are particularly useful in making assignments of subsystems to remote terminals, based on signal type and location. The MUXSIM user has the option of interactively modifying assignments of the system elements. A list of required inputs to MUXSIM is indicated in the Appendix.

The user has the responsibility for creating the input data files to MUXSIM. The large volume of input data to the program necessitates the use of punch cards or magnetic tapes. Subsequent to the data files being entered, MUXSIM operates on-line in an interactive mode, complete with a coaching text. The user has a choice of eight modes of operation of the multiplex data bus. The static and dynamic modes are listed in the Appendix. Figure 2 is a flow chart indicating user interaction with MUXSIM.

MUXSIM prints out a large number of reports, several of which are the input data lists sorted and reformatted. The bus analysis reports include (1) message bus loading and utilization, (2) data bus message structure list, and (3) bus schedule.

Some capabilities and deficiencies of MUXSIM are summarized below:

##### MUXSIM Attributes

1. Provision for reconfiguring task to processor assignment after initial input.
2. Provision for sorting, reformatting, and listing input data base.
3. Provisions for eight modes of bus control (see Appendix).

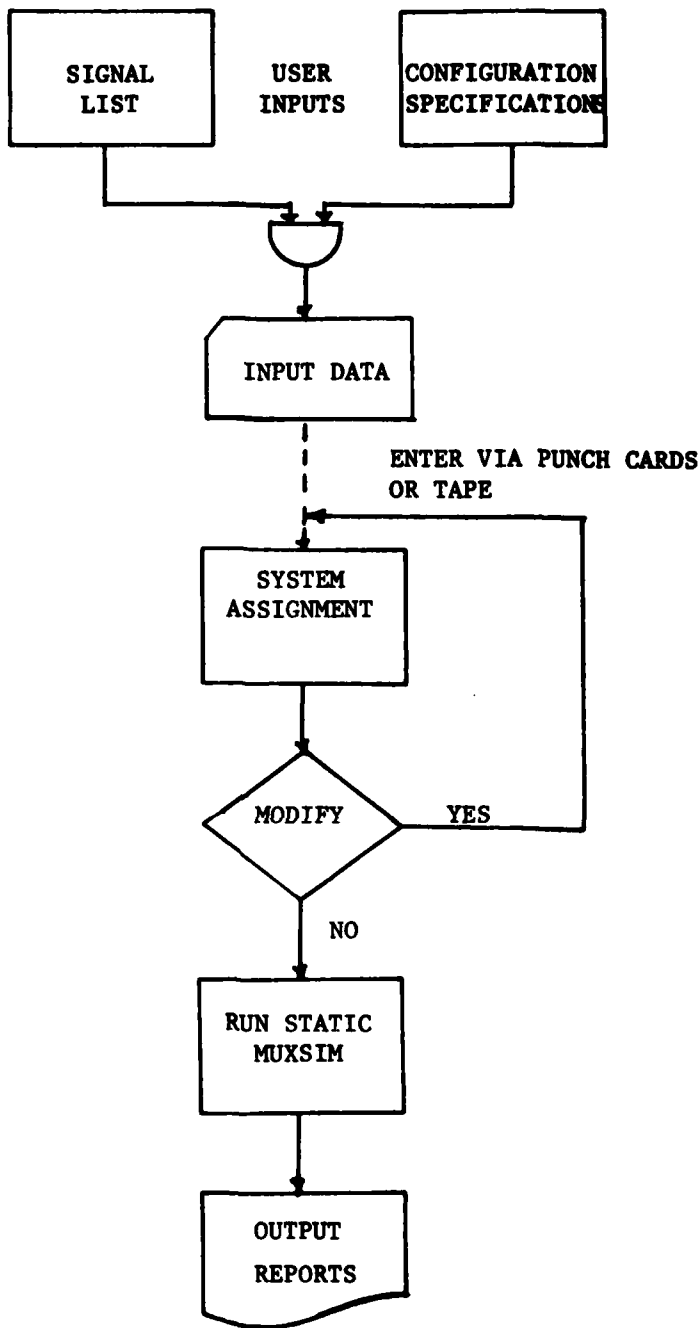


Figure 2. MUXSIM/USER INTERFACE

4. Provision for defining physical location of remote terminals in aircraft.
5. Provision for varying bus capacity.
6. Analyzes bus loading and scheduling.
7. Provision for simulating asynchronous messages, bus noise, and bus failures using GASP-IV (not directly through MUXSIM).

#### MUXSIM Deficiencies

1. Some input parameters not clearly defined in User's Manual.
2. Complex task of loading input signal list and dictionaries.
3. No provision for bus architecture above single level.
4. No provision for including executive processor overhead in message summary.
5. No provision for linking MUXSIM front-end with dynamic simulation.
6. No provisions for redundancy and fault-tolerant simulation.
7. Element memory, neither fixed nor dynamic, is considered.

#### V. SURVEY OF MULTIPLEX SIMULATION LITERATURE

As part of the research effort a literature survey of multiplex bus simulation was conducted. The search utilized the Lockheed Dialog data base, the Defense Documentation Center (DDC) data base, and the MASIS data bases. For convenient reference, the pertinent publications have been arranged categorically as follows:

- (A) Avionics Multiplex Simulation
- (B) MIL STD 1553 Data Bus Simulation
- (C) General Multiple Processor Systems
- (D) Other Multiplex Techniques

The references are listed alphabetically by author. The DDC AD number is given when available.

A. Avionics Multiplex Simulation

1. Brent, G. A., GASP-PL/1 Simulation of Integrated Avionic System Processor Architectures, NASA-CR-158244, Sept. 1978.

2. Husbands, C. R., A Comparison of Time Division Multiplex Data Bus Techniques Based on Data Transfer Performance, Mitre Corp., Bedford, Mass., Navy Contract F19628-77-C-0001.

3. Johnson, T. W., "Design of a Digital Flight Control System Using Area Multiplexing", Proceedings of the IEEE National Aerospace and Electronics Conference, Dayton, OH, May 1976.

4. Kearney, John J., A Computer Simulation Study of the General Purpose Multiplex System (GPMS) Applied to the Information Transfer Requirements of the A-7E Aircraft, Vol. I, Methodology and Results, Sencor, Inc., Mooristown, N.J., AD#787544, Oct. 1974.

5. Kieltyka, F. and J. K. Clema, "The Design and Management of AVSIM - A Real-Time Avionics System Simulator", Proceedings of the IEEE 1978 National Aerospace and Electronics Conference, Dayton, OH, May 1978.

6. Russell, Blinn W., A New Data Distribution System for Aircraft, AFAL-TR-73-133, July 1973.

7. Stovall, J. P., "RPV Simulation/Evaluation Program (RSEP)" IEEE Proceedings of the National Aerospace and Electronics Conference, Dayton, OH, June 1975.

B. MIL STD 1553 Data Bus Simulation

1. Balliet, L., Dalton, J. W., Earl, J. R. and Scott, W. W., Data Bus Network Simulation, IBM Federal System Division, Huntsville, AL, AFAL-TR-75-209, AD#A025115, March 1976.

2. Costa, R. A., Computer Simulation of MUX Bus Voltage Waveforms Under Steady State Conditions, Mitre Corp., Bedford, Mass., ESD-TR-75-67, June 1975.

3. Costa, R. A., "Computer Simulation of Multiple Subscriber TDM Networks", ACM Computer Science Conference, New York, NY, Feb 1975.

4. Mahler, B. B., Costa, R. A., and Boose, E. F., A Comparison of Time Division Multiplex Data Buses Based on Computer Simulation, Mitre Corp., Bedford, Mass., AD#A012305, May 1975.

#### C. General Purpose Multiple Processor Systems

1. Alexander, P., Digital Network Simulation System, Phase II, CNR Inc., DCA100-77-C-0041, March 1978.

2. Barbacci, Mario, et al, The Application of Multiple Processor Computer Systems to Digital Communications Networks, Carnegie-Mellon University, Pittsburgh, PA, AD#A049192, June 1976.

3. Hays, J. F., "Modeling an Experimental Computer Communication Network", IEEE Data Communications Symposium, St. Petersburg, Florida, Nov. 1973.

4. Hays, J. F., "Performance Models of an Experimental Computer Communication Network", Bell Systems Technical Journal, Vol. 53, No. 2, Feb. 1974.

5. Hoener, S. and W. Roehder, "Efficiency of a Multi-Processor System with Time-Shared Buses", Microprocessing and Microprogramming, Amsterdam, Netherlands, Oct. 1977.

6. McAuliffe, D. J., Switching Simulations, Rome Air Development Center, NY, RADC-4519-19-07, Oct. 1978.

7. Stickler, B. T., and P. M. Balisle, Data Distribution for Tactical Data Systems, Naval Post-Graduate School, Monterey, CA, AD#C004390L, Sept. 1975.

8. Warren, H. M., A General Computer Network Simulation Model, AFIT, WPAFB, OH, AD#A039772, March 1977.

#### D. Other Multiplex Techniques

1. Clark, A. P., "Synchronous Multiplexing of Digital Signals Using a Combination of Time-and-Code-Division Multiplexing (TDM and DCM)", Radio and Electronics Engineering (Great Britain), Vol. 42, No. 10, Oct. 1972.

2. Wing, P. A., "Code Division Multiplexing", Proceedings of the Institute of Radio and Electronics Engineering (Australia), Jan.-Feb., 1976.

## VI. CONCLUSIONS AND RECOMMENDATIONS

The primary strength of SNS is its ability to perform conceptual system architecture evaluations. From the user's point of view, SNS is easier to operate than MUXSIM because SNS requires less detail in the input data base. The major deficiencies of SNS are (1) the lack of adequate documentation for modification, and (2) its inability to simulate faults and recoveries.

The utility of the MUXSIM front-end in making subsystem and remote terminal assignments, and in mapping signals into messages, is a definite asset to the simulation process. MUXSIM also allows for several different modes of bus operation. A major negative feature of MUXSIM is the complex and laborious task of encoding a data base. One of the author's of MUXSIM estimated two to three man-months to encode the signal list and dictionaries for an avionics suite such as the F-16. Another weakness of MUXSIM is that its dynamic mode does not interface directly with the MUXSIM front-end.

In their present forms, SNS and MUXSIM are adequate as conceptual design tools within the constraints of the individual simulation programs. However, both simulators have serious deficiencies insofar as simulating advanced avionics systems such as multi-level architectures, distributed processors, and fault tolerant networks. It is felt that revision of these programs is not the approach to take at this time, but rather that new simulation tools should be assembled for the design and evaluation of advanced avionics systems. Consideration should be given to utilizing simulation languages such as SIMSCRIPT or ECSS II, or to higher order languages such as ADA.

Until new simulation routines are available, SNS and MUXSIM should be utilized to the fullest extent of their capabilities. Some possible revisions to enhance the value of MUXSIM are as follows:

- (1) Assemble a pre-processor for MUXSIM so that the user input is reduced to aircraft type, mission, and system configuration.
- (2) Link MUXSIM front-end with GASP-IV so that MUXSIM is truly a dynamic simulator.

VII. REFERENCES

1. AFAL/AA Handbook for Avionic System Analysis Tools, Systran Corp., Dayton, OH, Sept. 1978.
2. AFAL Simulation Facility/Capability Manual, Vol. I, AFAL-TR-77-118, June 1978.
3. Distributed Processor/Memory Architectures Design Program, AFAL-TR-75-80, Texas Instruments, Inc., Dallas, TX, Feb. 1975.
4. Butler, R., and System Consultants, Inc., System Network Simulator (SNS), User's Manual, AFAL, W-PAFB, OH, June 1977.
5. Multiplex Simulator Design Study, AFAL-TR-76-201, Harris Corp., Melbourne, Florida, Jan. 1977.
6. Pritsker, A. A. B., The GASP-IV Simulation Language, J. Wiley and Sons, New York, NY, 1974.
7. Multiplex System Simulator (MUXSIM) User's Manual, Contract AFAL F-33615-73-C-1172, Harris Corporation, Melbourne, Florida, June 1976.

APPENDIX

## USER'S GUIDE: SNS AND MUXSIM

### A.I. INTRODUCTION

The intent of the User's Guide is to provide the AFAL avionics systems engineer with sufficient information to utilize the simulators SNS and MUXSIM. Section A.II. contains information regarding the use of SNS, and Section A.III is devoted to MUXSIM.

### A.II. System Network Simulator (SNS)

#### 1. General Information

SNS is located on the AFAL DEC-10 Computer System. To conserve computer resources, SNS resides in executable form in disk area DSKG under project, programmer number (ppn) [275,316].

The FORTRAN source programs are stored on magnetic tape REELID 630, area [250,1322]. The procedure for copying the source coded files from tape to disk is given in Table A.1. A listing of FORTRAN coded SNS routines is found in reference [4]. Once SNS has been transferred into a disk area, the programs may be copied or modified as necessary.

```
.MOUNT MTA FAILSA/REEID:630
.DIR MTA <device number>:*..*[*,*]
.R FAILSA
*/W
*/A
*/J
*/L
*/T, <files to be transferred to disk>
.DISMOUNT FAILSA
```

TABLE A.1 SNS Tape Commands

Three executable forms of SNS are stored on the aforementioned tape and in DSKG [275,316]. For information on the three versions of SNS, refer to FILE.UND in area [275,316]. Briefly, the three executable versions of SNS are:

(1) TEST A.EXE - MIL STD 1553A bus protocol for a centralized bus controller allowing only terminal to controller and controller to terminal communications. All messages have a minimum length of 65 microseconds.

(2) TEST B.EXE - MIL STD 1553A bus protocol with C/T, T/C, and T/T data transfers. Messages numbered less than 100 are treated as T/C or C/T transfers with a minimum length of 65 microseconds. Messages numbered 100 or above in the data program are treated as T/T transfers with a minimum length of 110 microseconds.

(3) SNSY.SAV - Bus control is passed sequentially from one processor to the next in a round robin polling fashion. Data is treated as a 17 bit word with 3 bits of sync.

To run SNS, the user must create a data file which is linked to a disk assignment. Similarly, the output data file must be linked to an assigned element. After completion of the SNS execution and data printout, the temporary files FOR05.DAT, FOR06.DAT, and FOR10.DAT should be deleted.

The commands listed in Table A.2 are used to execute SNS from a TTY terminal. These commands cause test program SNSTES.NET to be copied into data file FOR05.DAT. Next, SNSY.SAV is executed and the output reports are displayed on the CRT terminal.

Since considerable time is required for execution of SNS, the user may elect to submit a batch job as outlined in Table A.3. This example control file was created under the name MC.CTL and executed by the command .SUBMIT MC.CTL.

.AS DSK:5  
.AS DSK:6  
.AS DSK:10  
.COPY FOR05.DAT=SNSTES.NET  
.RUN SNSY.SAV  
.TYPE FOR06.DAT  
.DELETE FOR05.DAT, FOR06.DAT, FOR10.DAT

TABLE A.2 SNS TTY Commands

.AS DSK:5  
.AS LPT:6  
.AS DSK:10  
.COPY FOR05.DAT=SNSTES.NET  
.RUN SNSY.SAV  
.DELETE FOR05.DAT, FOR10.DAT  
.K JOB

TABLE A.3 MC.CTL Control File

## 2. System Modeling for SNS

There are two primary considerations in modeling for SNS simulation. First, the avionics system should be laid out in flow graph form showing the relationship between subsystems and events. Secondly, avionics task scheduling must be considered with regard to (1) starting time, (2) execution time, (3) update rate, and (4) memory words required.

For illustration purposes, a simple avionics system consisting of five subsystems with six processors was used for test program SNSTES.NET. Figure A.1 illustrates the task assignments and message flow. Note that tasks numbered 1 through 20 are executive tasks and have no predecessors. Tasks numbered 41 through 69 have predecessors. On the flow chart, the number in the top of the circle indicates the task identification number. The number beside the ray indicates message number, and the quantity in parenthesis is the number of words in that particular message. Task 4 is a completion status and has no successor tasks.

For the same example program SNSTES.NET, Figure A.2 shows the processor bus connections thd the task to processor assignments. Note that processors 7 and 8 are shown with no bus connections. SNS requires a minimum of eight and a maximum of sixteen processors.

Concluding the example, start time RUNT, interation time ITER, and subfunction processor assignment SFPE are tabulated in Table A.4.

<u>TASK ID</u>	<u>RUNT</u>	<u>ITER</u>	<u>SFPE</u>
3	25000	31250	4
5	12600	31250	5
6	27500	31250	3
15	19000	31250	2
16	0	31250	6

TABLE A.4 Subfunction Schedule for SNSTES.NET

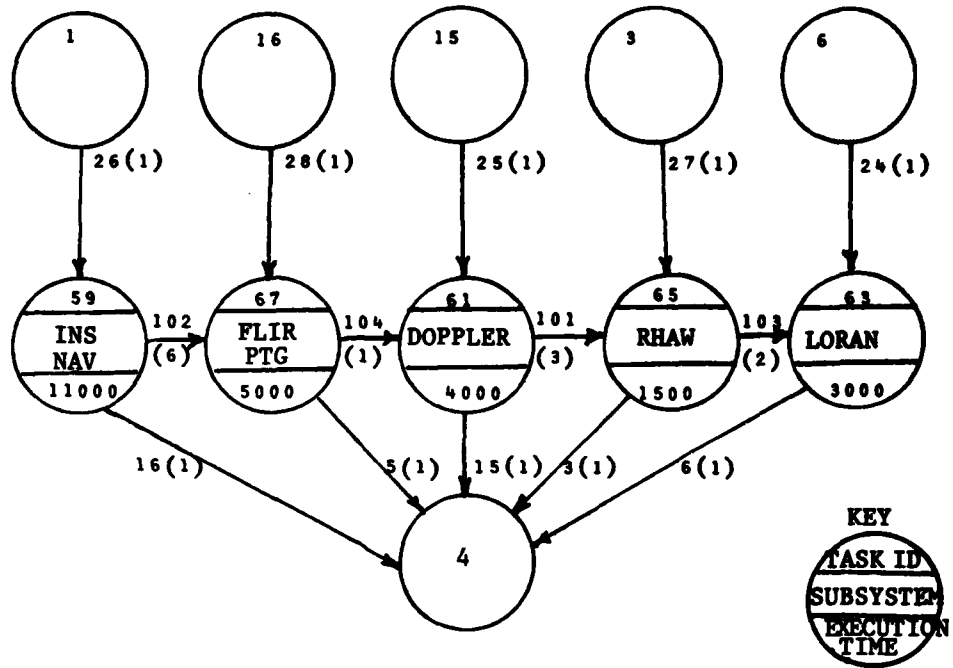


FIGURE A.1 Task Diagram for SNSTES.NET

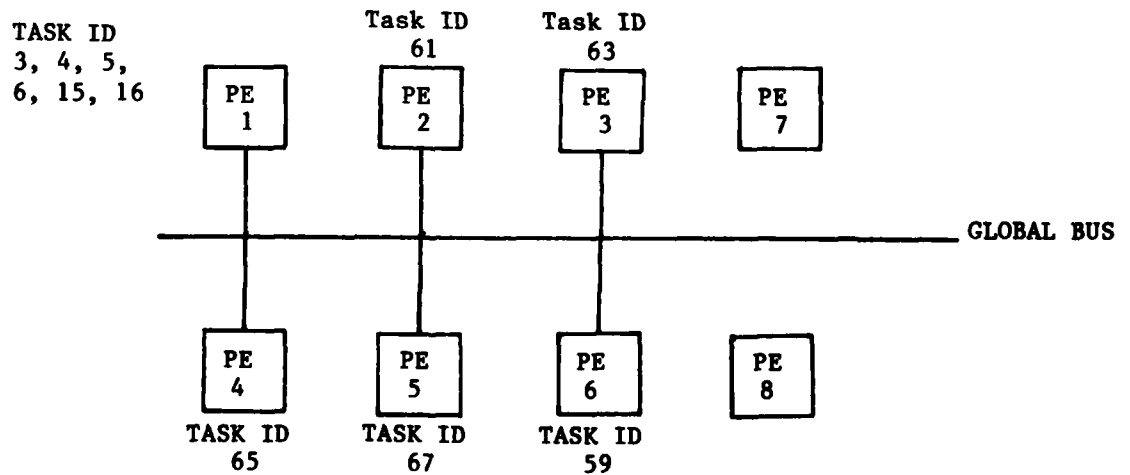


FIGURE A.2 Task to Processor Assignment for SNSTES.NET



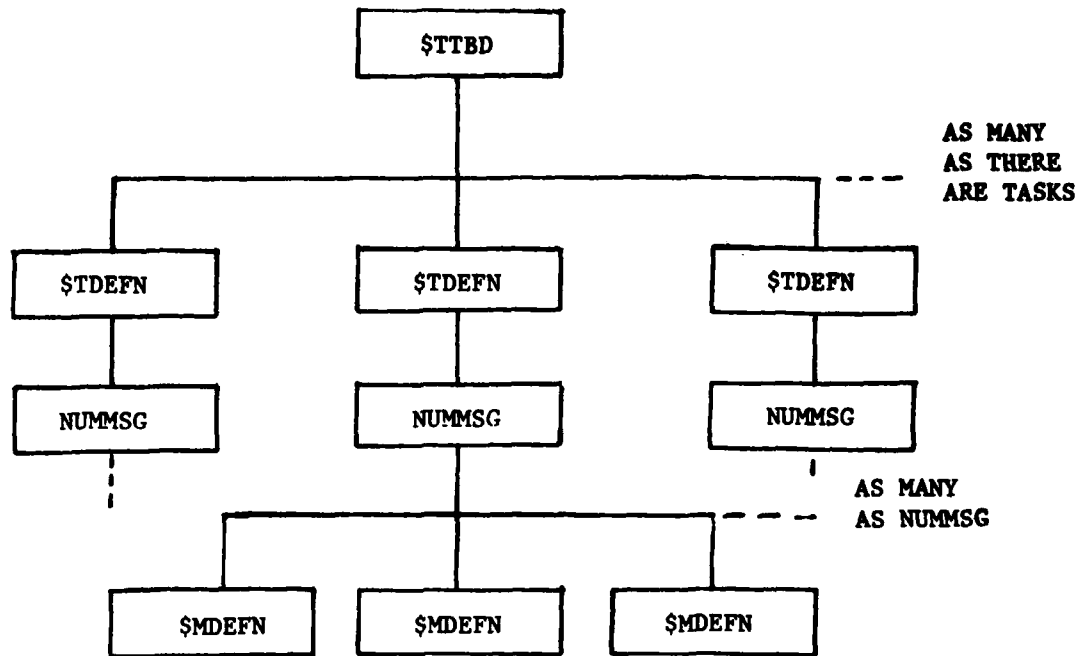


FIGURE A.4 Avionic Task Definition Structure

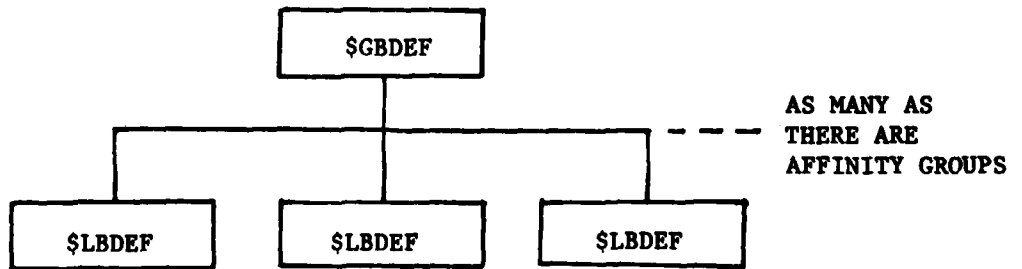


FIGURE A.5 Bus Connectivity Definition

<u>VARIABLE</u>	<u>DESCRIPTION</u>	<u>DEFAULT VALUE</u>
\$TTBD	Start NAMELIST	
WSIZE=	Bus data word length (μsec/bit)	20
BITPRD=	Bus bit period(μsec/bit)	1
MSYNC=	Message sync signal length (bits)	0
GAPTME=	Inter-message gap time (μsec)	5
\$END		

(As many of the following data sets are there are tasks\*)

\$TDEFN	Start NAMELIST data set descriptor	
LAST=	.True. If last task definition	
TASKID=	Task identification number	
NPRED=	Number of predecessors to task	0
DELTA=	Inverse of rep. rate (period)	$2^{32}-1$
NUMSUC=	Number of successor tasks	0
SRID=	List of successor tasks id's	
RTYPE=	16-bit words of memory used	
NUMBS=	Number of run time branch successors	0
BSID=	List of run time branch successors	
NIMSG=	Number of input messages required by task	0
IMTYPE=	List of input message types, pointer from TYPE	
XTIME=	Tasks' execution time in processor clocks	0
\$END	End NAMELIST data set	
\$MTBD	Start NAMELIST data set	
NUMMSG=	Number of output messages generated by task	
\$END	End NAMELIST data set	

As many of the following NAMELIST data sets as specified by NUMMSG

\$MDEFN	Start NAMELIST data set	
TYPE=	Message type, is a pointer to IMTYPE	0
LENGTH=	Message length in words exclusive of overhead	0
NUMDES=	Number of destination tasks	0
TASKID=	List of destination tasks	
PHASE=	Transmission time	0
PERIOD=	Period of message transmission	1
PRTY=	Priority of message	0
CCLEN=	Control length	20
SOURCE=	Source id	0
DENS=	Density	0
\$END	End NAMELIST data set	0

TABLE A.5 Avionic Task Definition

<u>VARIABLE</u>	<u>DESCRIPTION</u>	<u>DEFAULT VALUE</u>
\$GBDEF	Start NAMELIST data set descriptor	
TOTPE=	Total number of PEs in the system	
GBCL=	List of PE numbers that define the Global bus connectivity in the order for control to be passed, exclusive of Local connections.	
BLGTH=	Total number of elements in GBCL	
TLOCL=	Total number of local bus connections	0
PERTIME=	Period time for periodic reports	0
\$END		

(One set for each affinity group to be defined, if 15 processors, then 15 affinity groups are defined).

\$LBDEF	Start NAMELIST data set descriptor	
NUMPE=	Number of PEs in this affinity group	
PECON=	List of PE numbers that define the Local bus connectivity in the order for control to be passed.	
BLGTH=	Total number of elements in PECON	
LAST=	.TRUE. Use if last affinity group definition	
\$END		

TABLE A.6 Bus Connectivity Definition

<u>VARIABLE</u>	<u>DESCRIPTION</u>	<u>DEFAULT VALUE</u>
\$DEFINE	Start NAMELIST data set	
PEID=	ID of processor having tasks assigned to it	
NUMTSK=	Number of tasks assigned to processor	
TASKS=	List of tasks ID's assigned to the processor	
LAST=	.TRUE. If this is the last processor assigned	
\$END		

(One data set for each processor assignment defined)

TABLE A.7 Task to Processing Element Assignment

VARIABLE

DESCRIPTION

(As many of the following data sets as there are subfunctions)

\$FNDEFN	Start NAMELIST data set descriptor
RUNT=	Time at which subfunction gets first 'go' message
ITER=	Iteration period of subfunction
NUMPE=	Number of PEs with subfunction starting mode
SFPE=	ID of PEs with subfunction start mode
LAST=	.TRUE. If last subfunction definition
ID=	Numeric identity of subfunction
\$END	

TABLE A.8 SUBFUNCTION SCHEDULING DEFINITION

TASK	SRID		NIMSG	IMTYPE	SENT FROM TASKID	NUMMSG	TYPE	SENT TO TASKIDS
	BSID							
3						1	27	65
4						0		
5						1	28	67
6						1	24	63
15						1	25	61
16						1	26	59
59			1	26	16	2	102,16	67,4
61			2	25,104	15,67	2	101,15	65,4
63			2	24,103	6,65	1	6	4

TABLE A.9 Data for SNSTES.NET

TASK	SRID		NIMSG	IMTYPE	SENT FROM TASKID	NUMMSG	TYPE	SENT TO TASKIDS
	BSID							
65			2	27,101	3,61	2	103,3	63,4
67			2	28,102	5,59	2	104,5	61,4

TABLE A.9 (Continued) Data for SNSTES.NET

```

CONTROL 01  SNSTES.NET TEST CASE FOR DFM
CONTROL 02  SNS TEST PROGRAM
CONTROL 03  1111111111111111 1111111111111111 3333333
$TTBD
$END
$TDEFN
TASKID = 15
NPRD = 0
$END
$MTBD
NUMMSG = 1
$END
$MDEFN
TYPE = 25
LENGTH = 1,
NUMDES = 1,
TASKID = 61
$END
$TDEFN
TASKID = 16
NPRD = 0
$END
$NTBD
NUMMSG = 1
$END
$NDEFN
TYPE = 26
LENGTH = 1,
NUMDES = 1,
TASKID = 59
$END
$TDEFN
TASKID = 3
NPRD = 0
$END
$NTBD
NUMMSG = 1
$END
$TDEFN
TYPE = 27
LENGTH = 1,
NUMDES = 1,
TASKID = 65
$END
$TDEFN
TASKID=4
NPRD=1
$END
$NTBD
NUMMSG=0
$END

```

TABLE A.10 SNSTES.NET Listing

#### 4. SNS Output Data

The output reports generated by SNS occur at three levels: (1) event level, (2) at the completion of a sample period, and (3) at the completion of the simulation run. Event level reports occur at the completion of each event during the simulation. An example of an event level report is shown in Table A.11.

Sample period reports are generated every 50,000 microseconds or as specified by the user setting the parameter PERTIME. Evaluations are made of bus and processor performance over the sample interval. An example of a period report is shown in Table A.12.

Finally, SNS generates summary reports at the completion of the simulation. The summary reports include processor utilization summaries, bus utilization summaries, message transmission summaries, and a bus traffic decomposition report. An example of a summary report is given in Table A.13.

```

***** GOSIMX - BEGIN SIMULATION *****
*****
SDMD  INVOKED TRACEX AT CLOCK TIME          0 WITH ID VALUE OF          26
WAKEUP INVOKED TRACEX AT CLOCK TIME          0 WITH ID VALUE OF          25505
WAKEUP INVOKED TRACEX AT CLOCK TIME          0 WITH ID VALUE OF          24185
GETTTH INVOKED TRACEX AT CLOCK TIME          0 WITH ID VALUE OF          12222
GBUSCX INVOKED TRACEX AT CLOCK TIME          0 WITH ID VALUE OF           26
GBUSCR INVOKED TRACEX AT CLOCK TIME          65 WITH ID VALUE OF           26
WAKEUP INVOKED TRACEX AT CLOCK TIME          65 WITH ID VALUE OF          26681
IMSCAN INVOKED TRACEX AT CLOCK TIME          77 WITH ID VALUE OF           6
DECCNT INVOKED TRACEX AT CLOCK TIME          77 WITH ID VALUE OF          59
DISPIN INVOKED TRACEX AT CLOCK TIME          77 WITH ID VALUE OF          59
DISPCH INVOKED TRACEX AT CLOCK TIME          218 WITH ID VALUE OF           6
TSK19  INVOKED TRACEX AT CLOCK TIME          294 WITH ID VALUE OF          59
GETUP  INVOKED TRACEX AT CLOCK TIME          378 WITH ID VALUE OF          28705
WAKEUP INVOKED TRACEX AT CLOCK TIME          378 WITH ID VALUE OF          28577
IMSG   INVOKED TRACEX AT CLOCK TIME          384 WITH ID VALUE OF           0
DISPCH INVOKED TRACEX AT CLOCK TIME          594 WITH ID VALUE OF           1
TSK19E INVOKED TRACEX AT CLOCK TIME          11294 WITH ID VALUE OF          59
OMRGST INVOKED TRACEX AT CLOCK TIME          11294 WITH ID VALUE OF           8
SDMD   INVOKED TRACEX AT CLOCK TIME          11294 WITH ID VALUE OF          102
WAKEUP INVOKED TRACEX AT CLOCK TIME          11294 WITH ID VALUE OF          24681
WAKEUP INVOKED TRACEX AT CLOCK TIME          11294 WITH ID VALUE OF          24185
SDMD   INVOKED TRACEX AT CLOCK TIME          11294 WITH ID VALUE OF           16
WAKEUP INVOKED TRACEX AT CLOCK TIME          11294 WITH ID VALUE OF          24681
WAKEUP INVOKED TRACEX AT CLOCK TIME          11294 WITH ID VALUE OF          24185
GBUSCX INVOKED TRACEX AT CLOCK TIME          11322 WITH ID VALUE OF          102
GBUSCR INVOKED TRACEX AT CLOCK TIME          11435 WITH ID VALUE OF           59
SCHED  INVOKED TRACEX AT CLOCK TIME          11504 WITH ID VALUE OF           6
DISPCH INVOKED TRACEX AT CLOCK TIME          11504 WITH ID VALUE OF          102
GBUSCR INVOKED TRACEX AT CLOCK TIME          11504 WITH ID VALUE OF          27065
GBUSCX INVOKED TRACEX AT CLOCK TIME          11504 WITH ID VALUE OF           16
IMSCAN INVOKED TRACEX AT CLOCK TIME          11505 WITH ID VALUE OF           5
DECCNT INVOKED TRACEX AT CLOCK TIME          11505 WITH ID VALUE OF           67
GBUSCR INVOKED TRACEX AT CLOCK TIME          11569 WITH ID VALUE OF           16
WAKEUP INVOKED TRACEX AT CLOCK TIME          11569 WITH ID VALUE OF          28977
IMSG   INVOKED TRACEX AT CLOCK TIME          11583 WITH ID VALUE OF           0
IMSG   INVOKED TRACEX AT CLOCK TIME          11583 WITH ID VALUE OF           0

```

TABLE A.11 Event Level Report

```

*****
SNSTES.NET TEST CASE FOR DPM
PUS ACTIVITY REPORT FOR PUS NUMBER 99
MAJOR FRAME NUMBER 1 MINOR FRAME NUMBER 2
*****
MINOR FRAME START TIME = 0.050000
TOTAL PUS USAGE TIME = 0.001715
PERCENT OF MINOR FRAME UTILIZED = 3.43
*****
NUMBER OF MESSAGES TRANSMITTED = 23
MAXIMUM TIME ON OUTPUT QUEUE = 0.000165 FOR MESSAGE 16
MINIMUM TIME ON OUTPUT QUEUE = 0.000000 FOR MESSAGE 26
AVERAGE TIME ON OUTPUT QUEUE = 0.000026
LENGTH OF LONGEST MESSAGE TRANSMITTED = 160
LENGTH OF SHORTEST MESSAGE TRANSMITTED = 60
AVERAGE LENGTH OF MESSAGE TRANSMITTED = 69.00
*****
MESSAGE DESCRIPTOR FOR MESSAGE NUMBER 25
MESSAGE LENGTH = 60 ORIGIN = 1 DESTINATION = 2
RELATIVE TIME OF START = 0.000250 LENGTH OF TRANSMISSION = 0.000065
TIME ON OUTPUT QUEUE = 0.000000
*****
MESSAGE DESCRIPTOR FOR MESSAGE NUMBER 101
MESSAGE LENGTH = 100 ORIGIN = 2 DESTINATION = 4
RELATIVE TIME OF START = 0.004536 LENGTH OF TRANSMISSION = 0.000105
TIME ON OUTPUT QUEUE = 0.000000
*****
MESSAGE DESCRIPTOR FOR MESSAGE NUMBER 15
MESSAGE LENGTH = 60 ORIGIN = 2 DESTINATION = 1
RELATIVE TIME OF START = 0.004641 LENGTH OF TRANSMISSION = 0.000065
TIME ON OUTPUT QUEUE = 0.000105
*****
MESSAGE DESCRIPTOR FOR MESSAGE NUMBER 27
MESSAGE LENGTH = 60 ORIGIN = 1 DESTINATION = 4
RELATIVE TIME OF START = 0.000250 LENGTH OF TRANSMISSION = 0.000065
TIME ON OUTPUT QUEUE = 0.000000
*****

```

TABLE A.12 Sample Period Report



### A.III Multiplex Simulator (MUXSIM)

MUXSIM resides in the AFAL DEC-10 Computer System, area DSKG, ppn [275,311]. The MUXSIM routines in this area are encoded in FORTRAN as well as executable object code. MUXSIM is run from a remote terminal by typing .RU MS and following the coaching text.

In addition to its residence in disk, MUXSIM is stored on two magnetic tapes, REELID:587 and REELID:563. To copy files from tape 587, a routine called FAILSAFE is used. Table A.14 illustrates the method of copying the files from tape REELID:587, DSKH, ppn [171,7513] to disk area DSKF, ppn [242,363].

```
.MOUNT MTA FAILSA/REELID:587  
.R FAILSA  
*/W  
*/A  
*/L  
*/T, <files to be copied>  
.DISMOUNT FAILSA
```

TABLE A.14 FAILSAFE Example

The MUXSIM files stored on tape 563 were copied onto tape by use of a routine called FRS which is no longer in use on the DEC-10 System. For information on FRS, type on the remote terminal .TYPE DOC:FRS.DOC. To copy the MUXSIM files from tape 563 onto disk area DSKF, ppn [242,363], follow the procedure listed in Table A.15. Once the MUXSIM files have been copied into disk area DSKF, ppn [242,363], the user may modify or move files to other disk areas as necessary.

```
.MOUNT MTA FRS/REELID:563
.R FRS
*REW
*RESTORE DSKF:*.*[242,363]-DSKC:*.*[171,7513]=MTA#
.DISMOUNT FRS
```

TABLE A.15 FRS Example

An attempt has been made to consolidate all of the MUXSIM files onto one tape. The BACKUP routine was employed to store MUXSIM onto tape REELID:457. The procedure for copying files from tape 457 to a disk area is given in Table A.16.

```
.MOUNT MTA BACKUP/REELID:457
.R BACKUP
/REW
/FILES
/RESTORE DSKG: File name .ext[275,311]=DSKF: File name
        .ext [242,263]
.DISMOUNT BACKUP
```

TABLE A.16 BACKUP Example

In essence, MUXSIM front-end aids the user in modeling the avionic system being simulated. Subsequent to user input of the signal list and required dictionaries, MUXSIM allows interactive modification of the system until the user is satisfied with the design.

Input data required for MUXSIM engulfs the entire signal list of the avionic system, down to pin level. Other inputs include definitions and locations of various subsystem components and remote terminals. Static MUXSIM maps signals to appropriate remote terminals, allowing the user to make modifications as necessary. The detailed signal list and the following dictionaries are required inputs to MUXSIM:

- |     |            |                              |
|-----|------------|------------------------------|
| (1) | LRUNME.DIC | LRU Name                     |
| (2) | LRULOC.DIC | LRU Location/Remote Terminal |
| (3) | SGLADC.DIC | Signal Group/LRU Assignment  |
| (4) | LRUKMY.DIC | LRU Key Modification         |
| (5) | DRSMAP.DIC | Data Rate/Signal Map         |

Additionally, there is a dictionary input requirement for each of the two dynamic MUXSIM models.

The detailed signal list must be input as data; there are three lines of data to represent each signal. The format requirement for the signal list and the dictionaries is found in MUXSIM User's Manual, Section 5. The detailed signal list and the necessary dictionaries for the A7D avionic system are stored in the MUXSIM files on the DEC-10 Computer System.

There are eight static modes of operation of MUXSIM which are input through the STATIC subsystem Word Map and the Message Map programs.

- |     |          |  |
|-----|----------|--|
| (1) | Model SA | T/T data transfers   |
| (2) | Model SB | T/C/T data transfers   |
| (3) | Model SC | Digital T/T, Discrete T/C/T  |
| (4) | Model SD | Hybrid of SA and SB  |
| (5) | Model SE | T/T transfers with Bus Control Interface Unit (BCIU) Broadcast Reception |
| (6) | Model SF | T/C/T transfers with BCIU Broadcast Reception                            |
| (7) | Model SG | Hybrid of SE and SF  |
| (8) | Model SH | T/C/T transfers with word shuffling                                      |

In addition to the static models, there are two dynamic models; Model DA for demand access transfers and model DB for demand access transfers including fault-tolerant and redundancy schemes.

The output data from MUXSIM is as follows:

- (1) Corrected equipment list, signal list, and signal flow summary
- (2) Signal to remote terminal assignments
- (3) Signal to message assignments
- (4) Message bus loading and utilization
- (5) Dynamic model summary reports.

Documentation on the use of MUXSIM is available by typing .TYPE MUXSIM.DOC on the TTY terminal. More detailed information on the MUXSIM programs is found in MUXSIM User's Manual, reference [7]. With this documentation and the aid of MUXSIM coaching text, MUXSIM is relatively easy to run from an interactive terminal.

**1979 USAF - SCEEE SUMMER FACULTY RESEARCH PROGRAM**

**Sponsored by the**

**AIR FORCE OFFICE OF SCIENTIFIC RESEARCH**

**Conducted by the**

**SOUTHEASTERN CENTER FOR ELECTRICAL ENGINEERING EDUCATION**

**FINAL REPORT**

**LASER CANDIDATE AND ENERGETIC MATERIAL STUDIES**

**Prepared by:** William Robert Carper

**Academic Rank:** Professor

**Department and University:** Department of Chemistry, Wichita State University

**Research Location:** Frank J. Seiler Research Laboratory  
USAF Academy, Colorado

**USAF Research Colleague:** Capt William G. Thorpe  
Capt Larry P. Davis

**Date:** August 24, 1979

**Contract No:** F49620-79-C-0038

LASER CANDIDATE AND ENERGETIC MATERIAL STUDIES

by

William Robert Carper

ABSTRACT

The search for a chemical laser operating in the visible and ultraviolet spectral regions has been extended to SeF and TeF. The flame emission spectrum has been obtained and a vibrational analysis completed for both compounds. The spectroscopic analysis indicates that the internuclear distances vary considerably between the ground and excited states of SF, SeF and TeF. The results support the concept of SeF and TeF as potential laser candidates.

The energetic materials, RDX and HMX have been analyzed by mass spectral and ESR studies to determine their mode of thermal decomposition. The evidence supports the formation of gaseous free radical chains which are highly reactive and volatile. Future studies in this area are suggested.

### ACKNOWLEDGEMENTS

The author would like to thank the Air Force Systems Command, Air Force Office of Scientific Research, and the Southeastern Center for Electrical Engineering Education for providing him the opportunity to spend an educational and interesting summer at the Frank J. Seiler Research Laboratory, USAF Academy. Special thanks are due Dr. Richard N. Miller, Program Director of USAF - SCREE SFRP, whose efforts and advice (both written and oral) kept things well organized and running smoothly.

With regard to the research experience itself, I would first like to thank Lt Colonel Ben Loving, who made the original suggestion and helped to expedite various matters. Secondly, I would like to thank Captains Larry Davis, William Thorpe, and Henry Pugh for their enjoyable interaction with me in the laboratory along with Lt R. Cameron Dorey, Mr. Lloyd Pflug, and Mr. Fred Kibler. Finally, a special word of thanks to Colonel Bacon and Lt Colonel Siegenthaler for their encouragement and assistance and to Mrs. Betty Darcy who had to suffer with my handwriting.

I. INTRODUCTION: The research goals of this project are directly associated with two major concerns of the Air Force Systems Command: (1) the development of new chemical laser systems and (2) the characterization of decomposition mechanisms associated with energetic materials.

A. Chemical Lasers: Since the beginning of the laser era in 1960, the search has been in the direction of powerful chemical lasers. To date, only chemical lasers operating in the infrared have been produced. Chemical lasers operating in the visible and ultraviolet spectral region could offer lower atmospheric absorption, less beam divergence, and higher output power.<sup>1</sup> Thus the current interest in chemiluminescent reactions.

Chemiluminescence occurs when a chemical reaction leads directly to formation of an atom or molecule in an electronically excited state which can subsequently radiate light. The light emitted from most flames is thermal in origin.<sup>2</sup> However, the emission of formaldehyde bands<sup>3</sup> from "cool flames" of some hydrocarbons, ethers, and aldehydes can best be ascribed to chemiluminescence. Broida and coworkers<sup>4</sup> have studied the chemiluminescent reactions of the alkaline earth metals with the halogens, oxygen, and nitrous oxide. The reaction of barium atoms with nitrous oxide<sup>5</sup>, producing electronically excited BaO, was the first to give a radiative efficiency greater than 1%.

Sufficient information does not exist for effective screening of specific molecules as laser candidates.<sup>1,6</sup> One major difficulty to visible chemical lasers arises from the lack of known reactions in which the product species are partitioned efficiently into electronic states. Additional factors include the short radiative lifetimes ( $10^{-7}$  to  $10^{-9}$  sec) of most electronic excited states and insufficient kinetic information about reaction rates, quenching mechanisms, and deactivation cross sections.

The study of chemiluminescence gas phase reactions provides the means of determining energy levels and population distributions in ground and excited states. This method is useful for the screening of possible visible chemical laser systems and, ultimately, the formation of a realistic model describing the basic molecular requirements for laser action.

During a preliminary investigation, a cool green chemiluminescent flame resulted when selenium reacted with molecular fluorine.<sup>7</sup> The excited species responsible for the visible radiation is believed to be the SeF

radical. No optical spectroscopic study of SeF has been reported. Carrington<sup>8</sup> and Brown<sup>9</sup> produced SeF in an EPR cavity using COSe and F atoms (from CF<sub>4</sub>) as reactants. In most cases, their results compared favorably with the theoretical values calculated by O'Hare.<sup>10,11,12</sup> The analogous SF radical has been studied in more detail.<sup>13</sup> The presence of SF was confirmed by mass spectral data where COS was the sulfur source. Both radicals exist in a  $^2\Pi$  ground state. The absorption spectrum of the  $A^2\Pi - X^2\Pi$  transition at 330-400 nm indicated a non-degenerate ground state whose  $^2\Pi_{3/2}$  and  $^2\Pi_{1/2}$  levels were split by about 200 cm<sup>-1</sup>. Emission spectroscopy should produce a more detailed spectrum due to the expected population of higher vibrational states.<sup>14</sup>

B. Decomposition Studies of Energetic Materials: Chemical explosives have been used as weapons for centuries, however, systematic physical and chemical studies of energetic materials have been carried out only since World War II. Even then, we still do not have a detailed knowledge of the exact species in the reaction zone or the applicable kinetic and reaction products of a detonation.

Modern weapons are exposed to ever increasing severe environments such as aerodynamic heating and high shock pulses of extended duration in the msec range. Energetic materials capable of surviving this environment and functioning properly must be developed at a reasonable cost. Consequently, research is needed in thermal decomposition kinetics to understand the initiation process

In order to provide necessary shelf-life of energetic materials, we must develop the knowledge to predict the aging process of energetic materials under ambient conditions. This requires research in room temperature kinetics, and how the aging mechanism is affected by binders, etc. Models are needed for the interaction of energetic materials with non-energetic materials at ambient environmental conditions.

Non ideal energetic materials show a strong potential for sizeable gains in performance, based on a more efficient use of the available energy. However, before this concept can be applied to specific systems, a more detailed understanding of the non ideal explosive behavior must be acquired. This necessitates research in the following areas: (1) effects of molecular

weights on reaction products (2) identification and quantification of reaction products (3) reaction kinetics and controlling factors (4) determination of the state of the reaction products and (5) mathematical modeling of the non-ideal detonation phenomena.

A number of physical and chemical techniques have been employed in the decomposition studies of energetic materials. These include among others: (1) gas evolution analysis (2) product isolation and analysis (3) pressure studies and (4) isothermal differential scanning calorimetry (IDSC). The latter method (IDSC) measures the rate of energy evolution or absorption by the sample which is directly related to the rate of the reaction. While all of the above techniques are useful, none of them allows one to observe the change in concentration of an identifiable (directly observable) species versus time.

A useful technique which overcomes this problem is electron spin resonance (ESR) which allows one to observe the formation and disappearance of radicals and paramagnetic ions as a function of time.

Using ESR, Janzen<sup>15</sup> observed spontaneous free radical formation in the pyrolysis of a number of nitroaromatic compounds including TNT. He found that, if TNT was heated isothermally at 240°C, a concentration of approximately  $10^{-4}$  moles liter<sup>-1</sup> of free radicals was formed. In a more recent study, Guidry and Davis<sup>16</sup> used ESR to monitor the thermal decomposition kinetics of TNT in the pure liquid (neat). They were able to directly observe the intermediate and product species in the reaction mixture and to determine activation energies which agreed well with previously determined values obtained by other methods.

## II. OBJECTIVES:

The objectives of this project were:

- (1) The acquisition of the flame emission spectra of SeF and TeF.
- (2) A complete vibrational band analysis of SeF and TeF emission spectra.
- (3) The determination of spectroscopic constants associated with the species SeF and TeF.
- (4) ESR analysis and possible mass spectral identification of the products formed during the decomposition of RDX and HMX.

### III. RESULTS AND DISCUSSION:

A. SeF and TeF Spectral Studies: The flame emission spectra of both SeF and TeF were obtained by mixing microwave discharged  $F_2$  with either Se or Te Metal vapor at elevated temperatures. The burner/vacuum assembly is contained in an all stainless steel system consisting of a cross-shaped burner assembly with Quartz windows, a vacuum forepump, 150 cfm Kinney vacuum pump, and a scrubber exhausting to the intake of the duct system. The spectra were recorded using a half-meter McPherson scanning monochromator (300-1000 nm), a lock-in amplifier, light chopper, a photon counter and recorder system.

The spectrum of each diatomic molecule was recorded and the position of each bandhead determined in wavenumbers ( $cm^{-1}$ ). Deslandres tables<sup>17</sup> were first set up for SeF and the data computer analyzed to fit the general vibrational spectroscopic equation given below:

$$\gamma = \omega_e (v + 1/2) - \omega_e x_e (v + 1/2)^2 + \dots \quad (1)$$

Energy levels for small values of  $v$  are almost equally spaced by an amount  $\omega_e$ , however, as the  $\omega_e x_e$  term becomes more dominant, the spacing diminishes. Typical values of  $\omega_e$  and  $\omega_e x_e$  are 100-1000 and 0.1 - 10  $cm^{-1}$ , respectively.

The SeF spectrum consists of two band systems that could be analyzed. The major band system had an observed (0,0) transition at 15,416  $cm^{-1}$  and fitted the following equation to a high degree of accuracy:

$$\gamma = 15,413.5 + 437.46 (v') - 2.06 (v')^2 - 1108.01 (v'') + 1.34 (v'')^2 \quad (2)$$

$v'$  refers to the excited state vibrational level and  $v''$  the ground state vibrational level.

A secondary (weaker) band system was also observed for SeF. Its data was fitted to the following equation:

$$\gamma = 16,474 + 435.5 (v') - 3.0 (v')^2 + 1102 (v'') \quad (3)$$

The (0,0) transition was not observable and could only be estimated. The values of  $\omega_o'$  and  $\omega_o''$  calculated from equations (2) and (3) are:

	<u>Major Band</u>	<u>Minor Band</u>
	<u>System</u>	<u>System</u>
$\omega_o'$	436.2	435.5
$\omega_o''$	1105.7	1102

The two band systems represent the  ${}^2\Pi_{3/2} - {}^2\Pi_{3/2}$  and  ${}^2\Pi_{1/2} - {}^2\Pi_{1/2}$  subbands of the SeF doublet emission spectrum. The similarity in  $\omega_0'$  and  $\omega_0''$  supports this concept and a similar result was obtained by Di Lonardo and Trombetti for SF.<sup>13</sup>

The band spectrum of TeF also revealed at least two progressions, one major and one minor. The major progression was computer fitted to equation (4):

$$\gamma = 14,076 + 435.7 (v') - 1.763 (v')^2 - 615.56 (v'') + 3.093 (v'')^2 \quad (4)$$

Values of  $437.51 \text{ cm}^{-1}$  and  $618.65 \text{ cm}^{-1}$  for  $\omega_0'$  and  $\omega_0''$  were determined from equation (4). Since only eleven bands were discernable in the minor progression, it was impossible to computer fit the data to a polynomial similar to equation (1).

Analysis of the emission intensities of the major bands in SeF and TeF spectra indicates that there is a considerable difference between the internuclear distances in the ground and excited states of both molecules. The data on SF<sup>13</sup> also indicates a similar result. This conclusion was arrived at by observing the intensity data of the various Deslandres tables. A Condon parabola was drawn through the intensity maxima, and its apparent width observed. A wide parabola indicates that there is considerable difference between the internuclear distances of the ground and excited states. This is the case for the SeF, TeF and SF molecules.

One of the ways to identify a molecular species is to determine the isotopic shift both theoretically and experimentally. The shift ( $\Delta\gamma$ ) can be calculated from equation (6):

$$\Delta\gamma = (1 - \rho)[(v' + 1/2) \omega_e^1 - (v'' + 1/2) \omega_e''] \quad (6)$$

where  $\rho = (\mu/\mu_1)^{1/2}$  and  $\mu$  and  $\mu_1$  are atomic masses<sup>17</sup>.

Selenium contains the isotopes 74 (1%), 76 (9%), 77 (7.5%), 78 (24%), 80 (50%) and 82 (9%), whereas tellurium contains major isotopes at 126 (18.7%), 128 (32%) and 130(34.5%). Consequently, the isotope shifts are three times larger for Se than for Te. The net result is that although we have been able to verify the isotopic effect for a number of SeF transitions, we find that TeF isotopic shifts are only barely observable and almost equal to experimental error.

Finally, it was our intention to record lifetimes of SeF and TeF to aid us in evaluating the potential of these compounds as laser candidates.

This part of the project (the final phase) will be accomplished by Captain Thorpe with the assistance of Steve Davis at the Air Force Weapons Laboratory during the next few months.

B. RDX and HMX Decomposition Studies: RDX (cyclonite) and HMX are six and eight membered ring compounds containing alternating  $-\text{CH}_2 - \text{N}(-\text{NO}_2)-$  groups. RDX<sup>18</sup> usually contains 3-8% HMX as an impurity which can easily be removed by chromatographic techniques. HMX is synthesized in a relatively pure state, as contaminant RDX is destroyed during the latter stages of the HMX synthesis. RDX decomposes over the temperature range 213-299°C and HMX decomposes at a higher range of 271-314°C.<sup>18</sup>

The physical method of electron spin resonance is a sensitive one, and investigators in this area have occasionally studied reactions involving impurities rather than a reaction involving the compound of primary interest. A classic example involved the production of the naphthalene anion which was incorrectly analyzed as the solvated electron by a rather famous scientist. With the above in mind, a simple liquid chromatographic method was devised to purify and separate RDX and HMX. These two compounds are easily separated in acetonitrile -  $\text{CH}_2\text{Cl}_2$  mixtures by passing them through a silica column. The resulting fractions were collected and rotovaced to remove the solvents. The solids were then placed in quartz tubes, and the tubes placed in the ESR cavity. The compounds were heated separately up to approximately 20° below their decomposition temperature, at which point an ESR spectrum developed and was recorded for future analysis. The RDX and HMX spectra disappeared with time, and as the analysis indicates, are probably associated with the formation of a gas phase radical which is both volatile and highly reactive.

If the above conclusion is correct, then a mass spectral study of each compound should produce at least one fragment that corresponds to the hypothetical molecules deduced from the analysis of the ESR spectrum in each case. Consequently, a mass spectrum was obtained for the purified forms of RDX and HMX.<sup>19,20</sup> In both cases, only one mass spectral fragment (m/e ratio) was seen to correspond to the hypothesized structural formulas deduced from the ESR analysis.

A typical ESR spectra for a RDX melt is shown in Fig. 1. A computer program developed and generously provided by Dr. Ira Goldberg was used to

RDX

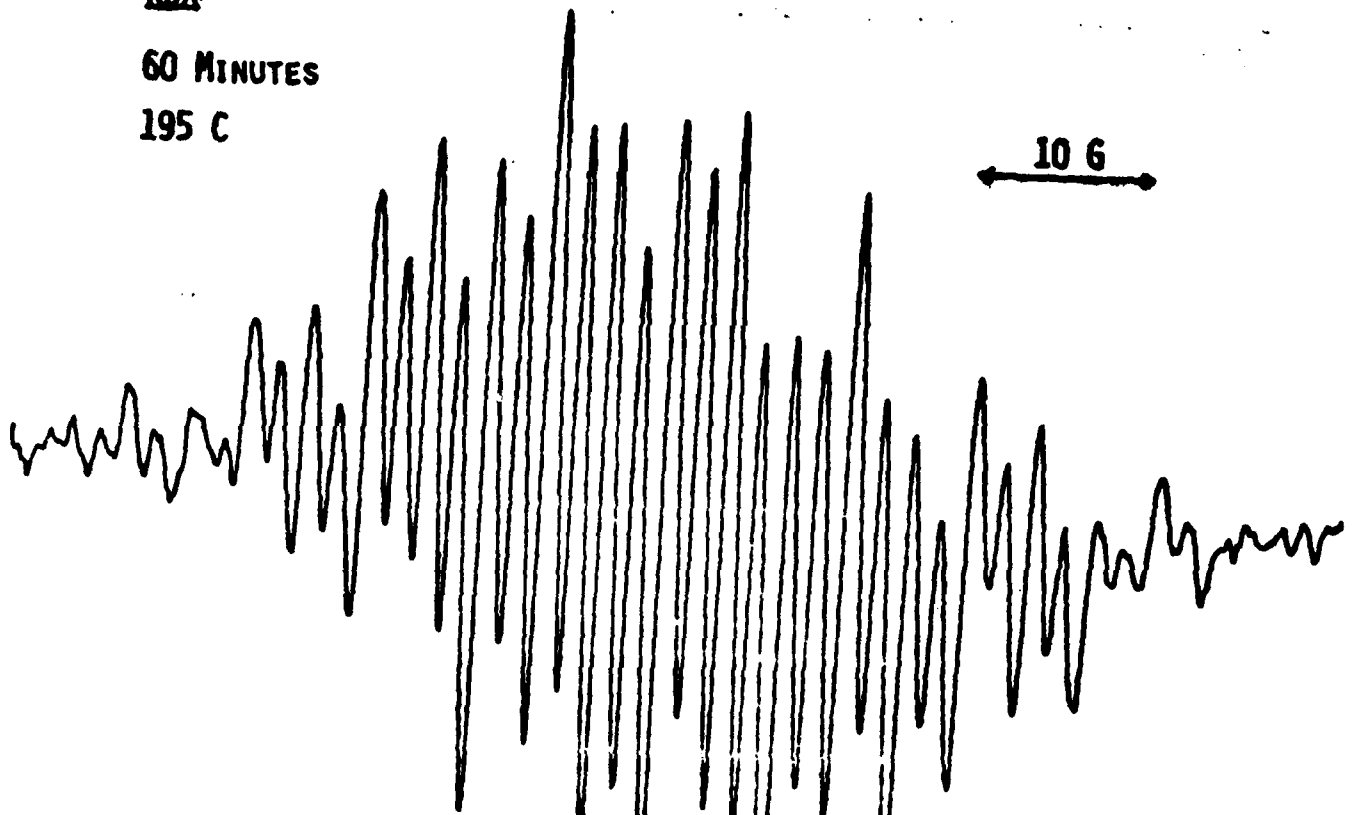
60 MINUTES

195 C

3259 G



10 G



RELATIVE INTENSITY  
(ARBITRARY UNITS)

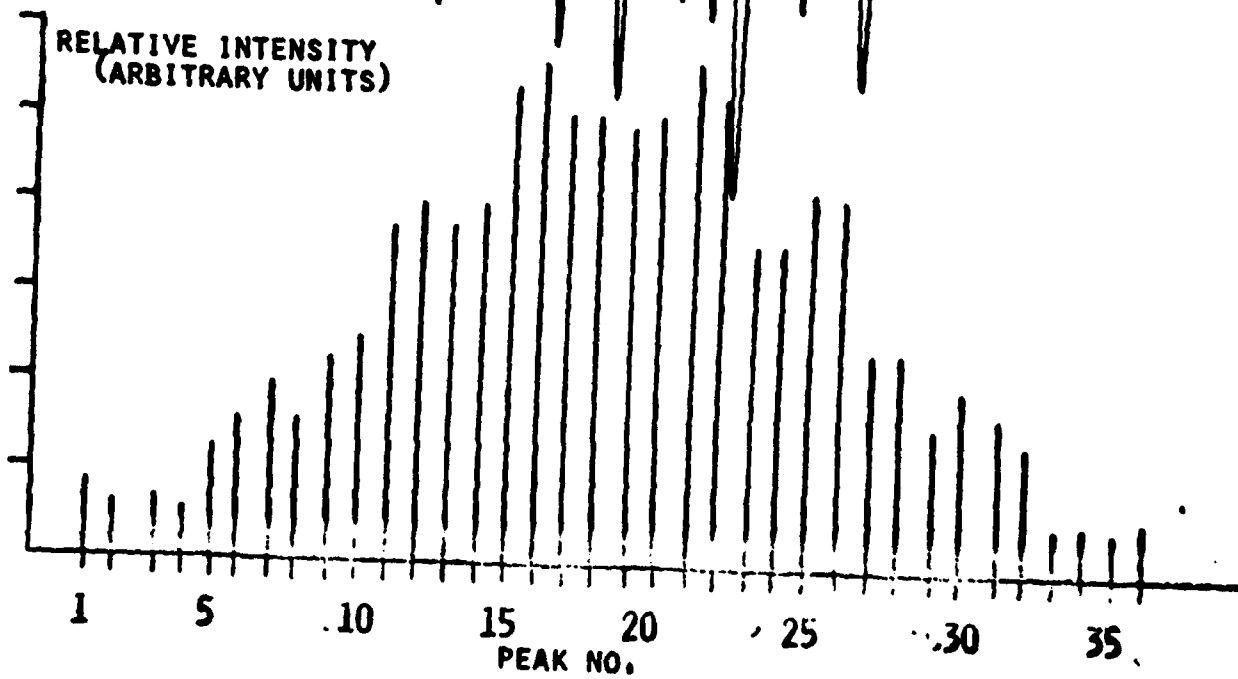
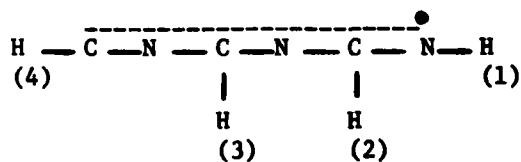
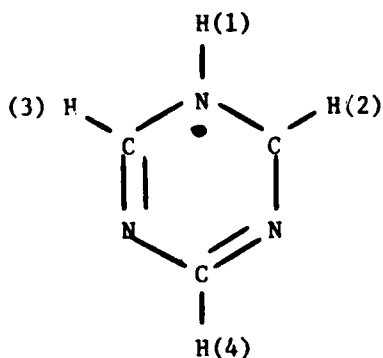


FIGURE 1 - RDX MELT

generate the simulated RDX ESR spectrum shown in Fig. 2. In simple homogeneous systems such as RDX and HMX melts, the relaxation processes are controlled by spin-lattice interactions. Consequently, the energy absorbed from the radiation field is distributed so that the spin system maintains thermal equilibrium throughout the resonance process and theory predicts a lorentzian<sup>21</sup> rather than a gaussian line shape. In the gaussian case, individual electrons find themselves in differing local fields so that resonances are not all simultaneous. In the case of RDX and HMX, a 80% lorentzian and 20% gaussian combination gave the best overall spectral representation.

The simulated RDX spectrum was generated with 3 equivalent nitrogen couplings ( $a_N$ ) of 6.8 gauss, and 3 non-equivalent hydrogen coupling constants ( $a_H$ ) of 13.8, 3.8 and 1.45 gauss. The possibility of the 3 equivalent nitrogens being replaced by 6 equivalent hydrogens was eliminated by intensity considerations.

The mass spectral analysis of RDX show a major fragment in m/e range 80, 81, 82 and 83, with 81 and 82 being the most predominant fragments. Since numerous nitrogen coupling constants range from 3 to 7 gauss<sup>22,23</sup> in varying situations, the following radical structures are proposed:



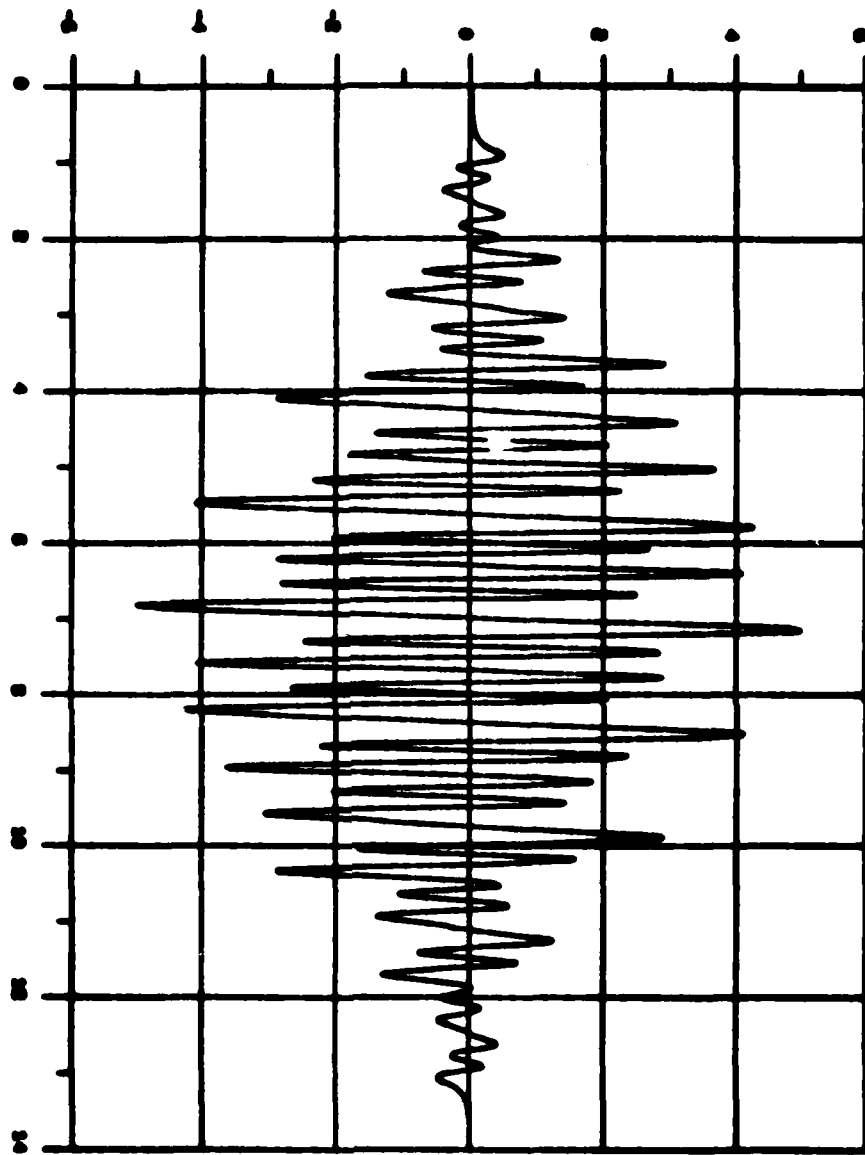
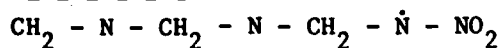


FIGURE 2 - SIMULATED RDX SPECTRUM

In both structures (a) and (b), the hydrogens are numbered such that  $a_H = 13.8$  gauss for H1,  $a_H = 3.8$  gauss for H2,  $a_H = 1.45$  gauss for H3, and  $a_H$  is less than 0.8 gauss (the measured linewidth) for H4. While either structure is a possibility, the observed fragmentation of RDX in the mass spectrometer suggests that ring rupture is more likely than ring stability, and therefore structure (b) is our first choice.

The HMX spectrum was obtained at 240°C and is shown in Fig. 3 along with the simulated version in Fig. 4. The spectrum was generated with 4 equivalent nitrogen coupling constants ( $a_N$ ) of 3.58 gauss, 1 nitrogen coupling constant of 12.9 gauss and 2 equivalent hydrogen coupling constants ( $a_H$ ) of 3.4 gauss. Other possibilities were eliminated through intensity or mass spectral considerations.<sup>19</sup>

The only HMX mass spectral fragments that correspond to such a system occur at m/e ratios of 157 and 158. The only logical radical is the chain compound given below:



The only possible ring structure is one that has a m/e ratio of less than 157, and there is no mass spectral evidence for such a radical.

In the final analysis, the preliminary evidence supports the formation of gas phase free radical chains as major products in the decomposition reactions of RDX and HMX. A possible fallacy in the analysis is that species other than those proposed, are the principal products observed by ESR. Such compounds might further react or decompose prior to the detection by the mass spectrometer. While such events may be unlikely, we cannot rule them out at this time.

#### IV. RECOMMENDATIONS:

A. Emission Spectroscopy of SeF and TeF. It is apparent from our initial studies that both of these compounds are potential laser candidates. However, until the lifetime studies are completed, it is impossible to properly evaluate their potential. Should the lifetime studies be favorable, then prototype laser design should begin immediately. An interesting possibility would be the coupling of SeF or TeF with another laser system to provide a wide-range tunable laser system.

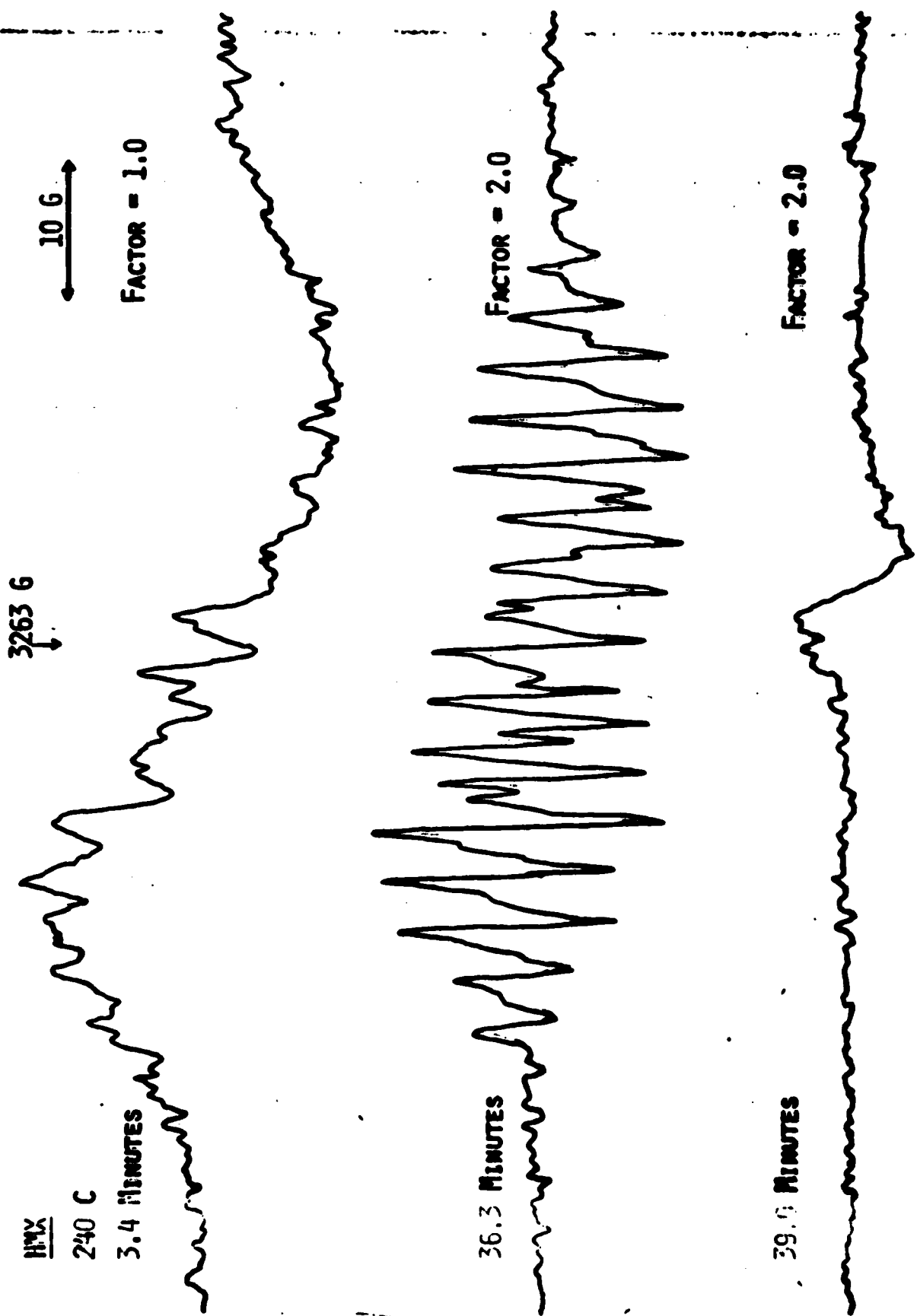


FIGURE 3 - HMX MELT

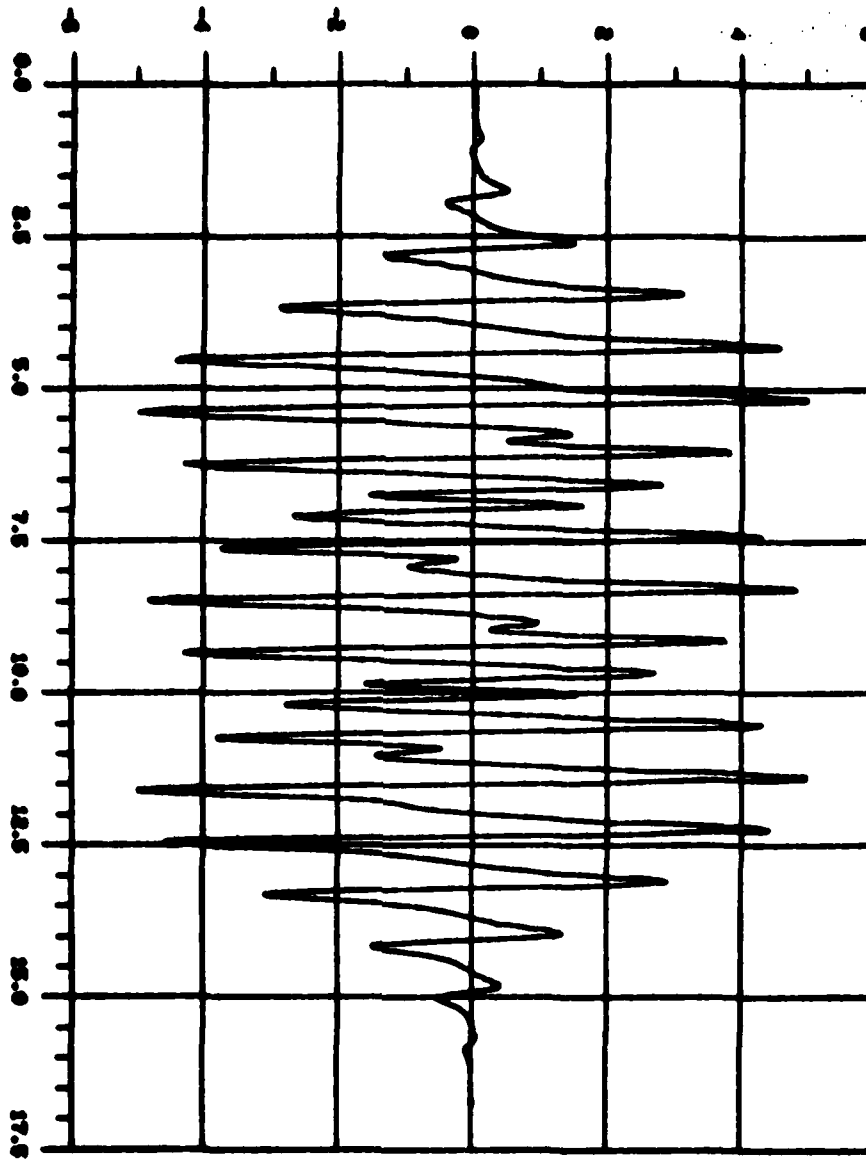


FIGURE 4 - SIMULATED HMX SPECTRUM

## B. Decomposition Studies of Energetic Materials.

(1) RDX and HMX - Our initial investigation of these compounds has resulted in a tentative identification of at least one major product (probably gaseous) in each case. There are several experiments that need to be performed before the species can be identified with certainty. These experiments are as follows: (a) An ESR study of the gaseous products released during the decomposition reaction of RDX and HMX. (b) Formation of radical cations and anion (in acetonitrile) by electrolysis in an ESR cell and (c) Use of a spin trapping agent<sup>24</sup> to physically and chemically identify any gaseous or liquid products of the decomposition reactions.

(2) TATB (triaminotrinitrobenzene) - Follow-on Research (subject of mini-grant proposal). This compound is a yellow solid with a melting point above 330°C<sup>18</sup>. TATB is a reasonably potent energetic material which is relatively insoluble in alcohol, ether, chloroform, benzene and acetic acid; and soluble in nitrobenzene and aniline.

Preliminary evidence has shown that TATB changes color from yellow to red at 280°C. Furthermore, TATB forms a charge-transfer complex with TCNQ, followed by the production of the radical anion, TCNQ<sup>-</sup>.

These results suggest that TATB and similar aminonitrobenzenes would be excellent subjects for a future study similar to that presently underway at the Frank J. Seiler Research Laboratory on RDX and HMX.

## REFERENCES

1. C. R. Jones and H. P. Broida, Laser Focus, March 1974, p. 37.
2. A. G. Gaydon and H. G. Wolfhard, Flames, Chapman and Hall LTD, 3rd ed. (1970), O. 211.
3. A. G. Gaydon, The Spectroscopy of Flames, Chapman and Hall, 2nd ed. (1974), p. 155.
4. R. S. Bradford, C. R. Jones, L. A. Southall, and H. P. Broida, J. Chem. Phys., 62, 2060 (1975).
5. C. R. Jones and H. P. Broida, J. Chem Phys., 59, 6677 (1973).
6. D. G. Sutton and S. N. Suchard, Applied Optics, 14, 1898 (1975).
7. S. J. Davis, Air Force Weapons Laboratory, unpublished results.
8. A. Carrington, G. Currie, T. A. Miller, J. Chem. Phys., 50, 2726 (1969).
9. J. M. Brown, C. R. Byfleet, B. J. Homard, and D. K. Russell, Mol. Phys., 23, 457 (1972).
10. P. A. G. O'Hare, J. Chem. Phys., 60, 4048 (1974).
11. P. A. G. O'Hare and A. C. Wahl, J. Chem. Phys., 53, 2834 (1970).
12. P. A. G. O'Hare, U. S. Atomic Energy Comm. Report #ANL-7315 (1968).
13. G. Di Lonardo and A. Trombetti, Trans. Faraday Soc., 66, 2694 (1970).
14. R. A. Young, J. Chem. Phys., 40, 1848 (1964).
15. E. G. Janzen, J. Amer. Chem. Soc., 87, 3531 (1965).
16. R. M. Guidry and L. P. Davis, Thermochimica Acta (in press).
17. G. Herzberg, Molecular Spectra and Molecular Structure, Van Nostrand Reinhold Co., 2nd ed. (1950).
18. Engineering Design Handbook, Explosive Series: Properties of Explosives of Military Interest, AMC Pamphlet, AMCP 706-177, March 1967.
19. L. Pflug, personal communication.
20. M. Farber and R. D. Srivastava, "A Mass Spectrophotometric Investigation of the Chemistry of Advanced Composite and Double Base Propellants", Space Sciences Inc. Ann. Tech. Rpt., Aug. 1978 (AD No. A058578).
21. R. S. Alger, Electron Paramagnetic Resonance, Interscience, New York, 1968.

22. M. Bersohn and J. C. Baird, An Introduction to Electron Paramagnetic Resonance, W. A. Benjamin, New York, 1966.
23. J. C. M. Henning, J. Chem. Phys., 44, 2139 (1966).
24. J. R. Harbour and M. L. Hair, Can. J. Chem., 57, 1150 (1979).

1979 USAF - SCEEER SUMMER FACULTY RESEARCH PROGRAM

Sponsored by the

AIR FORCE OFFICE OF SCIENTIFIC RESEARCH

Conducted by the

SOUTHEASTERN CENTER FOR ELECTRICAL ENGINEERING EDUCATION

FINAL REPORT

A NON-LINEAR MAXIMUM ENTROPY  
METHOD FOR SPECTRAL ESTIMATION

Prepared by:	Dr. Chi Hau Chen
Academic Rank:	Professor
Department and University:	Department of Electrical Engineering Southeastern Massachusetts University
Research Location:	Air Force Geophysics Laboratory Hanscom Air Force Base, MA
USAF Research Colleague:	Dr. Paul F. Fougere
Date:	August 17, 1979
Contract:	F49620-79-C-0038

A NON-LINEAR MAXIMUM  
ENTROPY METHOD FOR  
SPECTRAL ESTIMATION

by

C. H. Chen

ABSTRACT

The increased demand for high resolution spectral analysis makes it necessary to improve the popular Burg's maximum entropy method for spectral estimation. This report describes the computer implementation of a non-linear method proposed by P. F. Fougere for spectral estimation, which provides not only a much higher resolution than the Burg's method but also removes the line-splitting phenomenon for sinusoidal signals. Particular emphasis is placed on the complex signals as the real signals can be considered as a special case of complex signals. After a brief introduction of the method, computer results are presented which clearly illustrate the superiority of the non-linear method. The problems of parameter selection and computational complexity are examined. Suggestions for further research on this method are also given.

#### ACKNOWLEDGEMENT

The author would like to thank the Air Force Office of Scientific Research, and the Southeastern Center for Electrical Engineering Education for providing him the excellent opportunity to work at the Air Force Geophysics Lab. in the summer of 1979. Special acknowledgement is also due to Dr. Richard N. Miller, SFRP Director for a well-organized program.

Finally, he would like to thank Dr. Paul F. Fougere of Plasmas, Particles and Fields Branch, AFGL for numerous helpful discussions and guidance, and Dr. John Howard, Chief Scientist, AFGL for encouragements. Their efforts enabled the author to expand his horizons considerably in the area of advanced signal processing technology for Air Force needs.

## I. INTRODUCTION

In many geophysical problems the data records are short while an accurate spectral analysis is required. The conventional power spectrum estimation using smoothing and windowing procedures<sup>1</sup> provide poor resolution and undesired Gibbs phenomenon. The Burg's maximum entropy method<sup>2,3</sup> for spectrum analysis considerably improves the spectral resolution for short records. The method makes no assumption of data outside the time interval specified and is thus least committal on unavailable data. Generally speaking the method enhances the peaky component of the spectrum. However spectrum splitting and frequency shifting frequently occur especially for sinusoidal signals<sup>4,5</sup>. The Burg's maximum entropy method has now been well documented<sup>6</sup>. The method involves linear operations.

A new method was proposed by Fougere<sup>7,8</sup> which makes use of non-linear optimization procedure and provides the lowest possible prediction error power. In this project the computer implementation of this new non-linear method due to Fougere is considered. The new method is now fully operational and is suitable to provide an excellent spectral estimation for Air Force geophysical data.

## II. MATHEMATICAL PROCEDURES

The following is a brief description of mathematical procedures with the new method. Details are available in References 7 and 8. Given an n-point sample  $(x_1, x_2, \dots, x_n)$  of complex numbers  $x_i$ , which may be formed by real data from two different channels. Define an  $(m + 1)$  point prediction error filter (PEF)  $(1, g_{m1}, g_{m2}, \dots, g_{mm})$  where each  $g_{ij}$  is a complex variable, such that the kth prediction errors are:

$$\begin{aligned} E_{1k} &= \sum_{i=0}^m x_{k+m-i} g_{mi} \\ E_{2k} &= \sum_{i=0}^m x_{k+i} g_{mi}^* \end{aligned} \quad (1)$$

$k = 1, 2, 3, \dots, i-m$

where  $g_{mi}^*$  is the complex conjugate of  $g_{mi}$ ,  $g_{m0} = 1$ , and  $E_{1k}$  and  $E_{2k}$  are the forward and backward prediction errors, respectively.

Now the mean square prediction error, or mean error power, in both time directions is:

$$P_m = 0.5 (n - m)^{-1} \sum_{s=1}^2 \sum_{k=1}^{n-m} E_{sk} E_{sk}^* \quad (2)$$

If the PEF's (with leading "1" suppressed) of all orders 1,2, ---, m are gathered in one complex matrix  $G_m$ , we may write:

$$G_m = \begin{pmatrix} g_{11} & & & \\ g_{21} & g_{22} & & \\ \cdot & & & \\ \cdot & & & \\ g_{m1} & g_{m2} & \text{----} & g_{mm} \end{pmatrix} \quad (3)$$

The generalization of the Levinson recursion algorithm is given by,

$$g_{jk} = g_{j-1,k} + g_{jj} g_{j-1, j-k}^* \quad (4)$$

Burg has shown that if these diagonal elements (also called reflection coefficients) all lie in the range  $|g_{jj}| < 1$ , then the PEF is minimum phase, that is its Z-transform has all its zeros outside the unit circle.

In order to enforce this condition we can set

$$g_{jj} = U \tanh \theta_j \exp i \phi_j \quad (5)$$

for complex signals, where  $0 \leq \theta_j \leq \pi$ ,  $\theta_j$  and  $\phi_j$  are both real and U is a positive constant slightly less than unity. U is adjusted so that all of the roots of the Z-transform of the PEF all lie outside the unit circle and none lie on it. For real signals, we can set

$$g_{jj} = U \sin \theta_j \quad (6)$$

The non-linear optimization procedure starts with the expression for variations in  $\theta_j$ ,  $\phi_j$ ,

$$\begin{aligned} \theta_j &= \theta_j^0 + \Delta \theta_j \\ \phi_j &= \phi_j^0 + \Delta \phi_j \end{aligned} \quad (7)$$

and then expand the prediction error  $E_{sk}$  in a Taylor series about  $\theta_j^0$  and  $\phi_j^0$ , retaining only the first order terms. Then set  $\partial P_m / \partial \Delta \theta_j = 0$ ,  $\partial P_m / \partial \Delta \phi_j = 0$  to find the corrections  $\Delta \theta_j$  and  $\Delta \phi_j$ . The corrections are then substituted into (7) and the process is repeated until the corrections  $\Delta \theta_j$  and  $\Delta \phi_j$  become sufficiently small. The method of Fletcher and Powell<sup>11</sup> is utilized in the non-linear iterative procedure for error minimization. In the case of complex signals, error minimization procedure by the method of conjugate gradient<sup>12</sup> is also utilized.

### III. COMPUTER RESULTS

Both algorithms based on the non-linear method for real signals and for complex signals have been implemented at the CDC 6600 Computer at AFGL. For real signals of various levels of additive Gaussian noise, the cases considered include pure sinewave of various initial phases, the sum of two sinewaves of different frequencies, and the FSK signal consisting of two sinewaves of different frequencies occupying non-overlapped time intervals. The non-linear method consistently corrects the line-splitting and frequency shifting. Line-splitting is most evident when the initial phase of the sinewave is an odd multiple of  $45^\circ$ . Fig. 1 shows the power spectra of a 1 Hz 64-point sinewave with initial phase of  $45^\circ$  and 7 filter weights. The non-linear method due to Fougere clearly corrects the line-splitting in Burg's method and the line spectrum at 1 Hz is considerably sharper. The additive noise level has a noise power of 0.0002. As the noise power increases the line-splitting phenomenon gradually disappears but frequency shifting becomes more apparent. Again the non-linear method is superior as it corrects this problem also. For multiple equal-amplitude sinewaves the non-linear method always improves the resolution even though equal-amplitude spectral peaks cannot be guaranteed. For the FSK signal, the experimental results show that the non-linear method always provides correct locations of spectral peaks while the Burg's method often shows frequency shifting.

For the complex signals the two data sets provided by RADG for 1979 Spectral Estimation Workshop as well as a 16-point complex sinusoid are considered. Fig. 2 shows the two data records of 32 points each for the

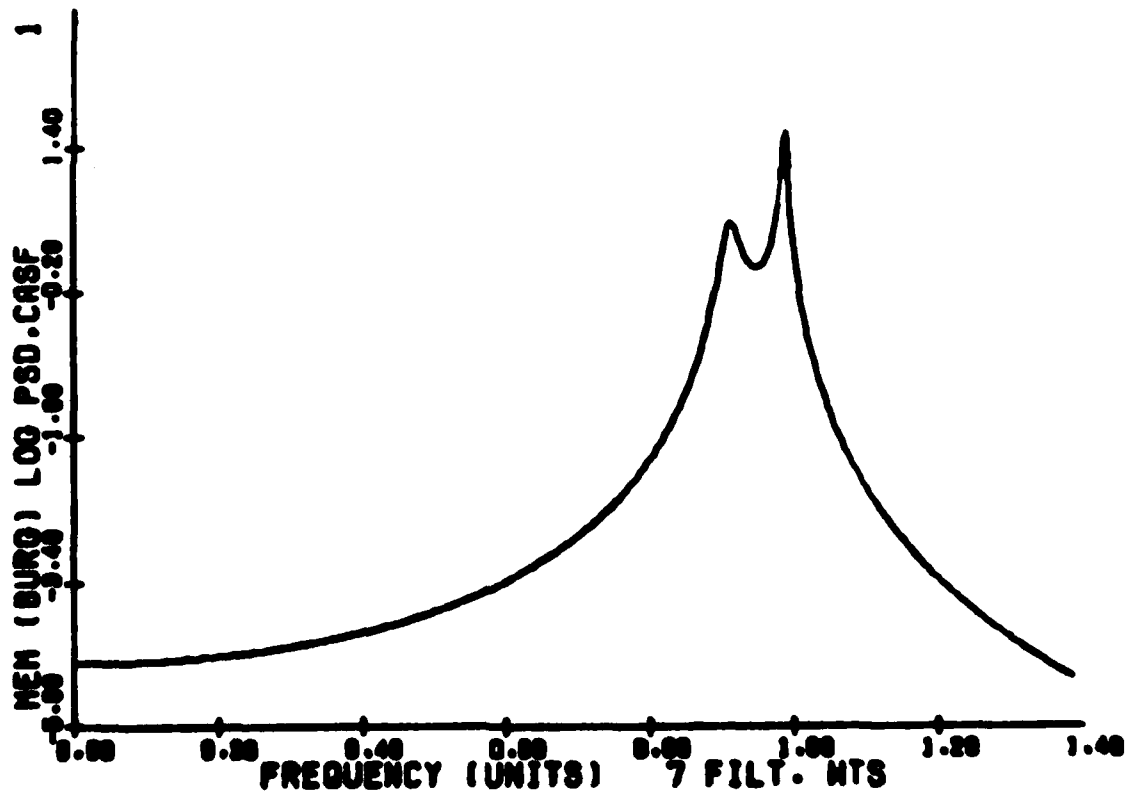
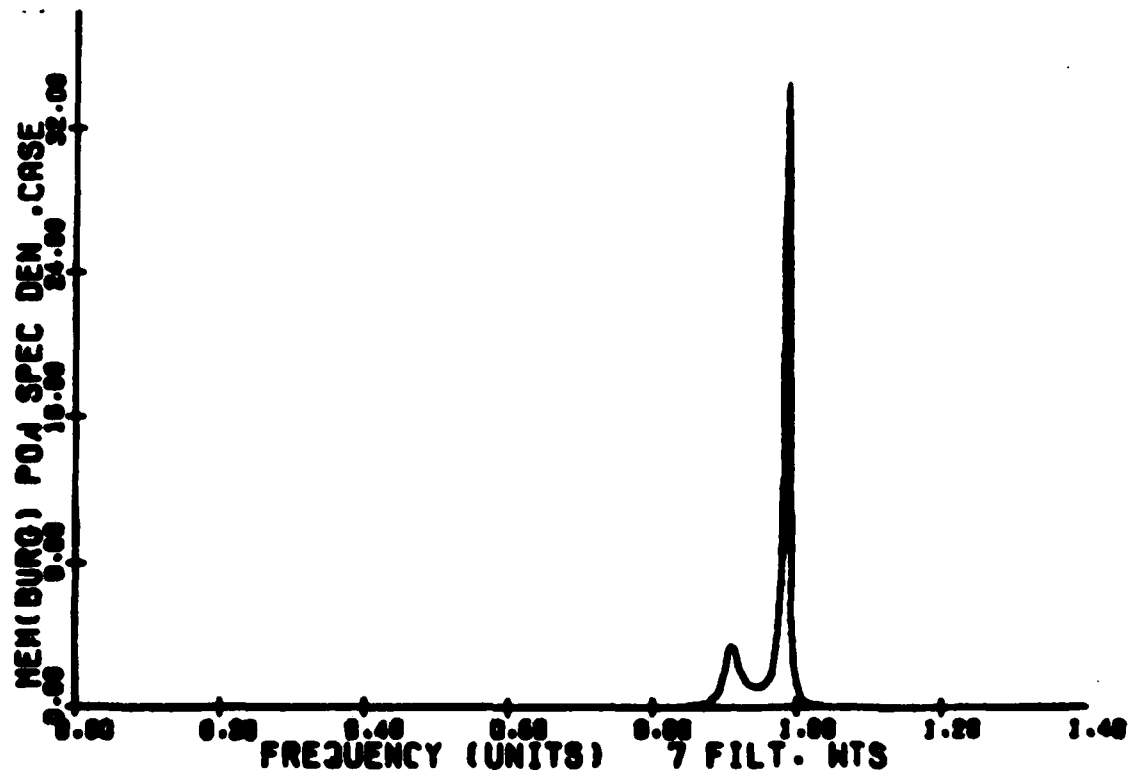


FIGURE 1

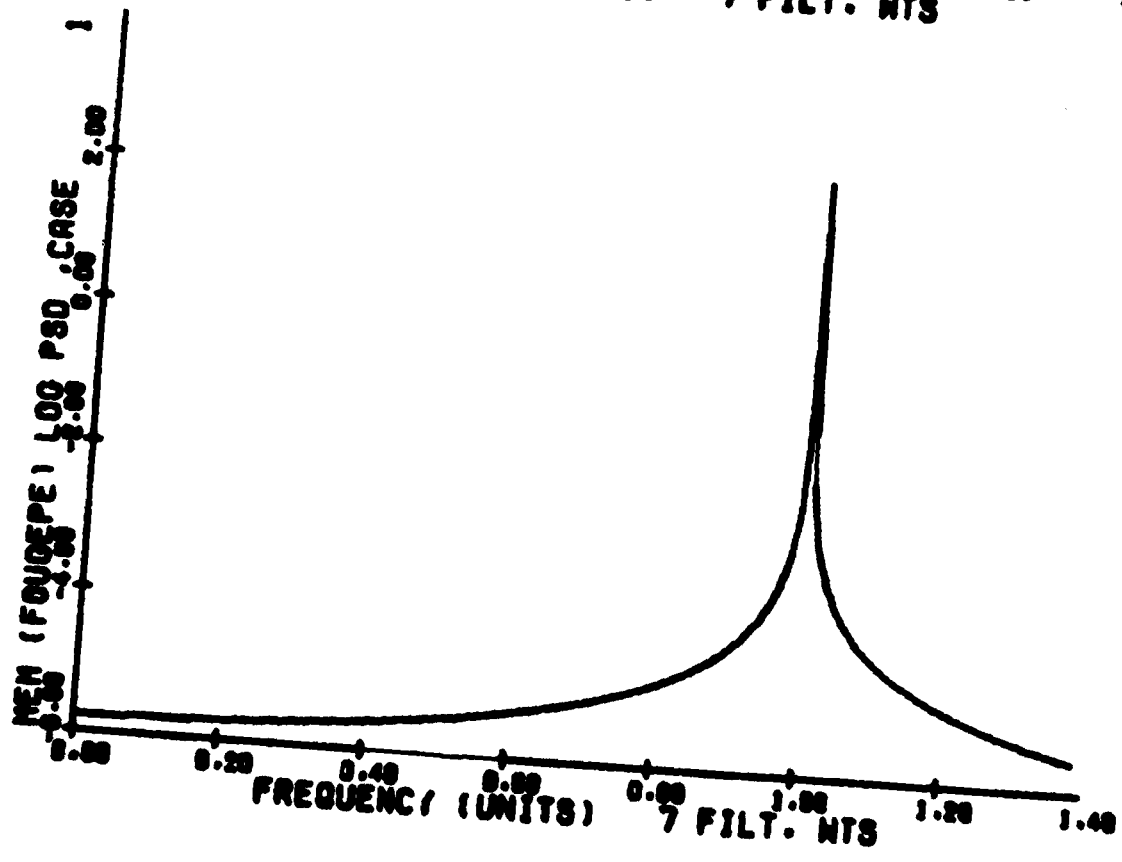
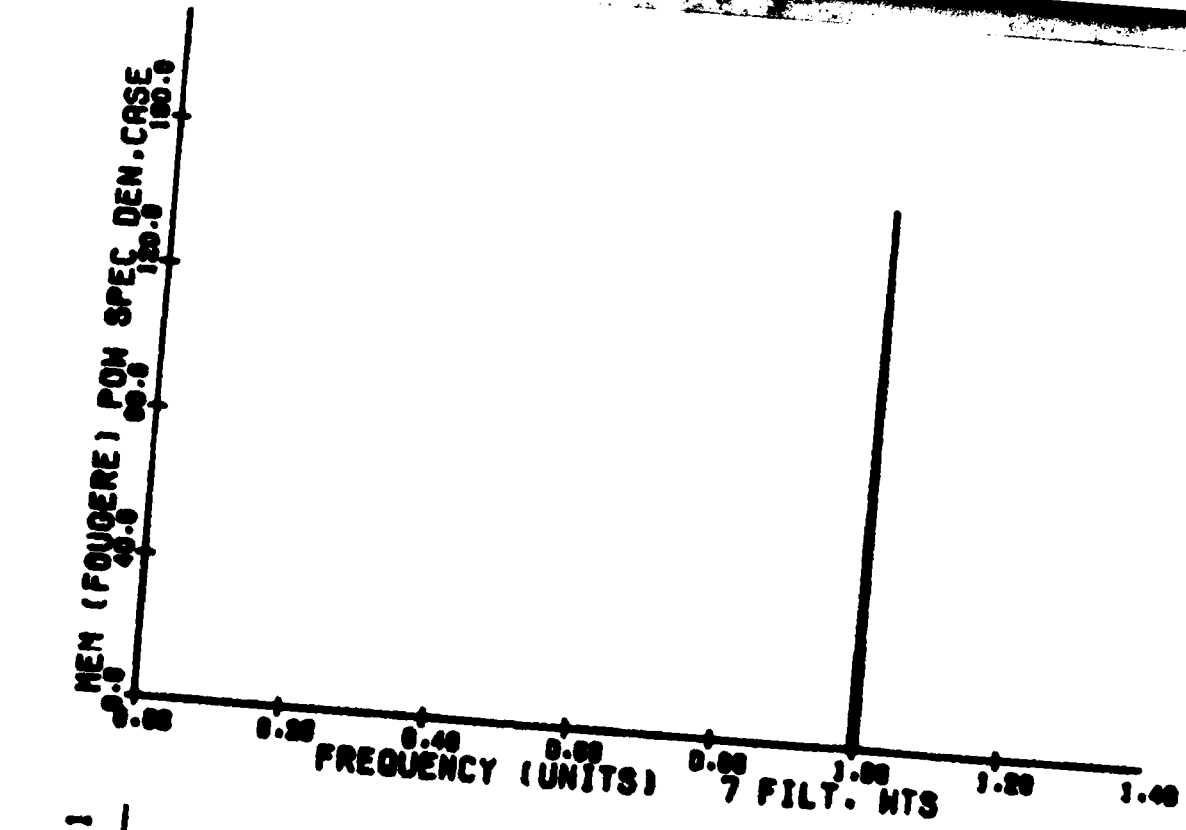


FIGURE 1 (continued)

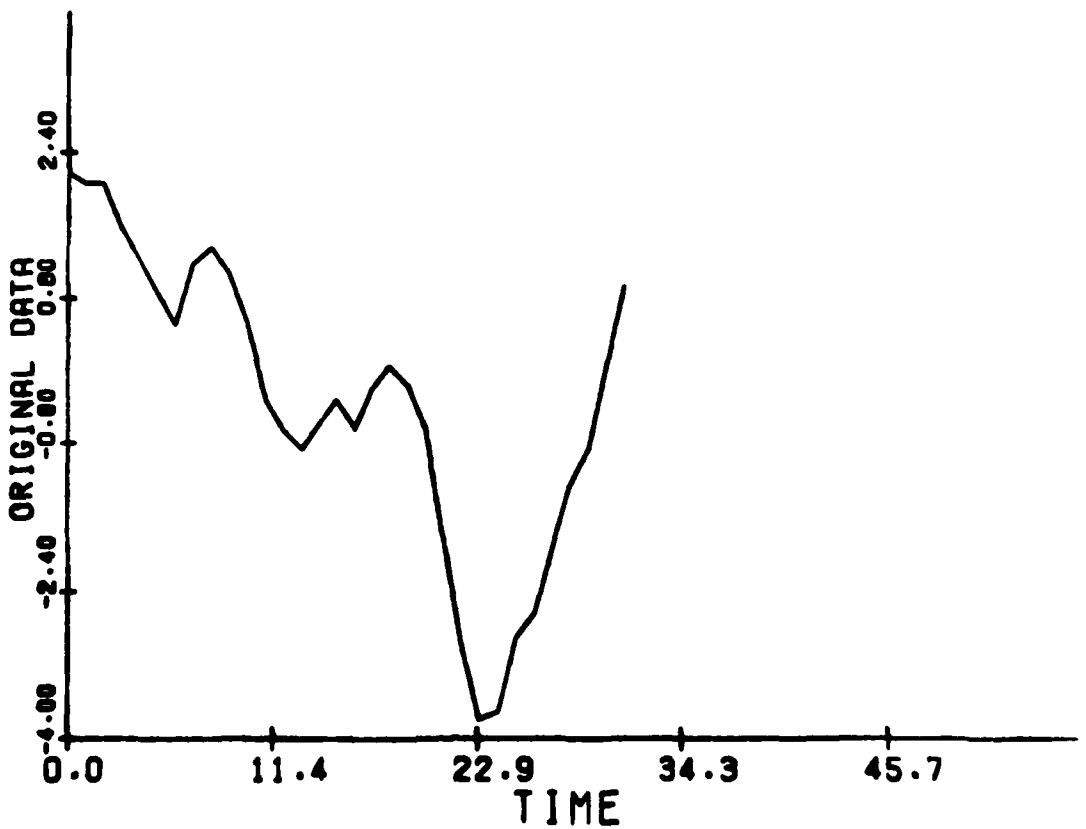
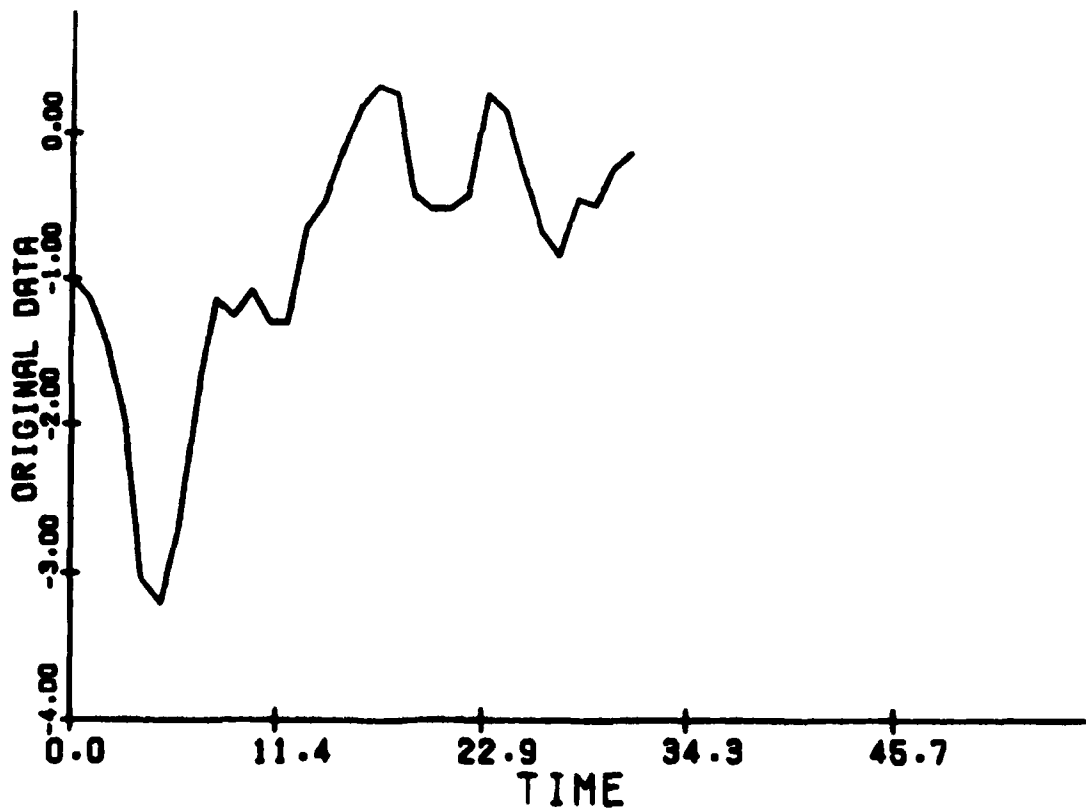


FIGURE 2 - DATA RECORDS OF CHANNEL 1 (Upper Curve) AND CHANNEL 2 (Lower Curve)

first RADC data set. For 3 filter weights, neither method is adequate to provide enough spectral resolution as shown by Fig. 3. For 11 filter weights, there are sufficient details in the spectra (Fig. 4). The ratio of first sidelobe with respect to the main peak is 0.639 for Burg's method and 0.572 for the non-linear method. For 16 filter weights, this ratio is considerably reduced and is equal 0.165 for Burg's method and 0.152 for the non-linear method (Fig. 5). Spectral contents of 11 and 16 filter weights are about the same. For the complex sinusoid, spectral splitting is not evident. However the non-linear method provides much sharper spectral peaks.

#### IV. RELATED PROBLEMS

Both the Burg's method and the non-linear method are well structured mathematical algorithms for maximum entropy spectral estimation. The amount of computation far exceeds the conventional power spectral analysis using fast algorithms. The non-linear method, furthermore, requires many times more computation as compared with the Burg's method. With the continued improvement in signal processing hardware, both methods will become practically feasible for real-time applications. At present the non-linear method can be computationally more efficient if started with previously optimized set of parameters. The present algorithm has incorporated such feature.

The next important problem is the choice of parameters such as the number of filter weights and the number of iterations in error minimization procedures. The optimum number of filter weights depends highly on the nature of data. Although the Akaike criterion does not consider the mean square errors in both time directions, it provides a useful rough estimate of the optimum number. The maximum number of filter weights should not exceed two-thirds of the total number of data points. The required computation increases approximately linearly with the increase in the number of filter weights.

The optimum numbers of iterations again depend on the data. There does not appear to have simple mathematical expressions for such parameters. Generally speaking, the more iterations the better. Some trial and error

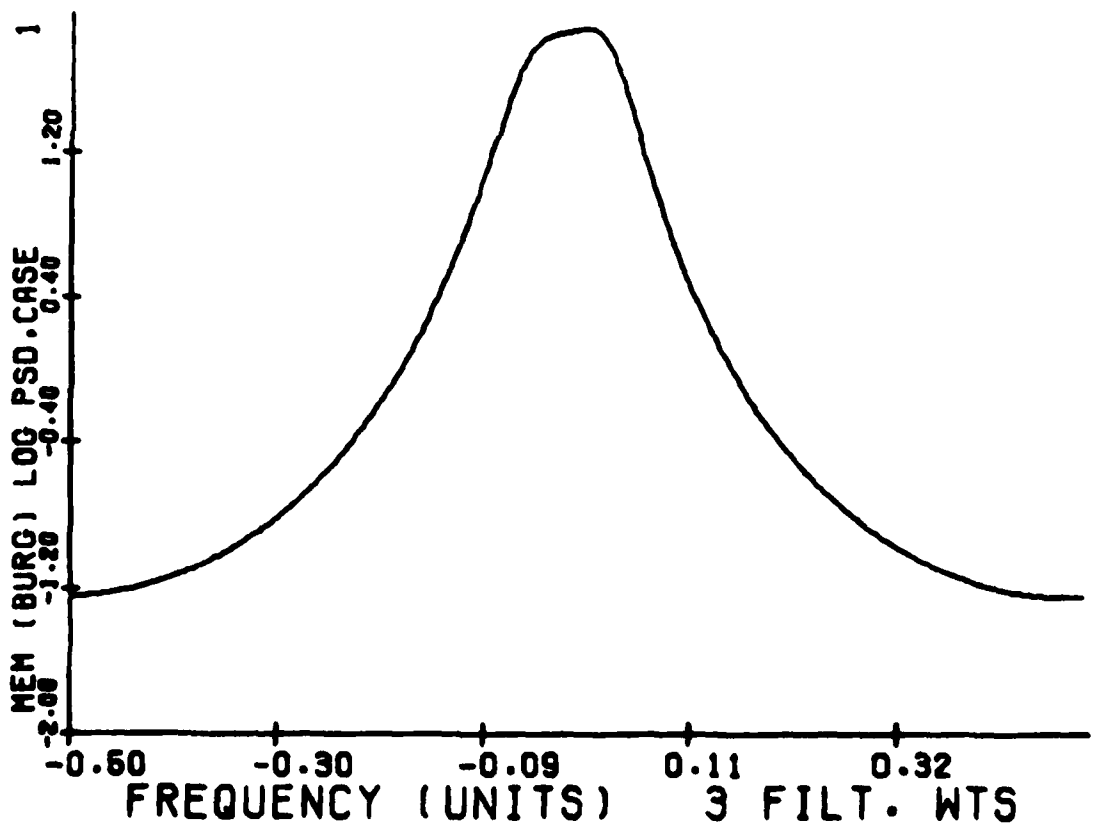
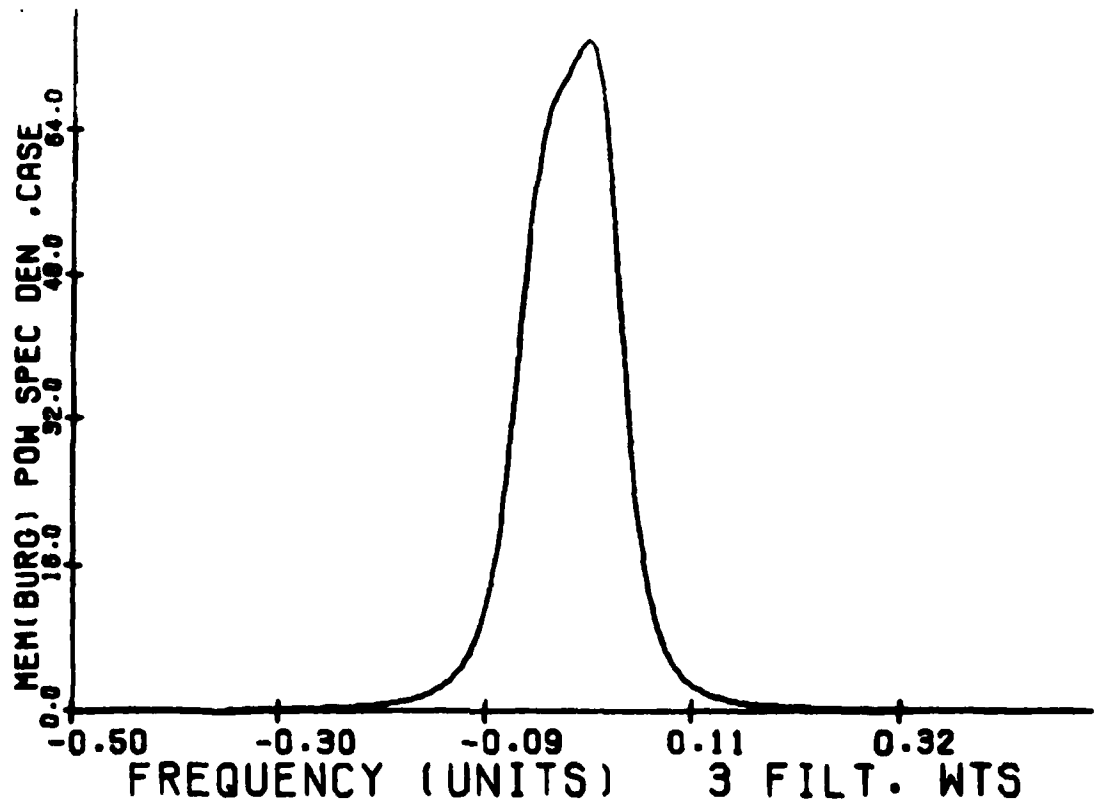


FIGURE 3

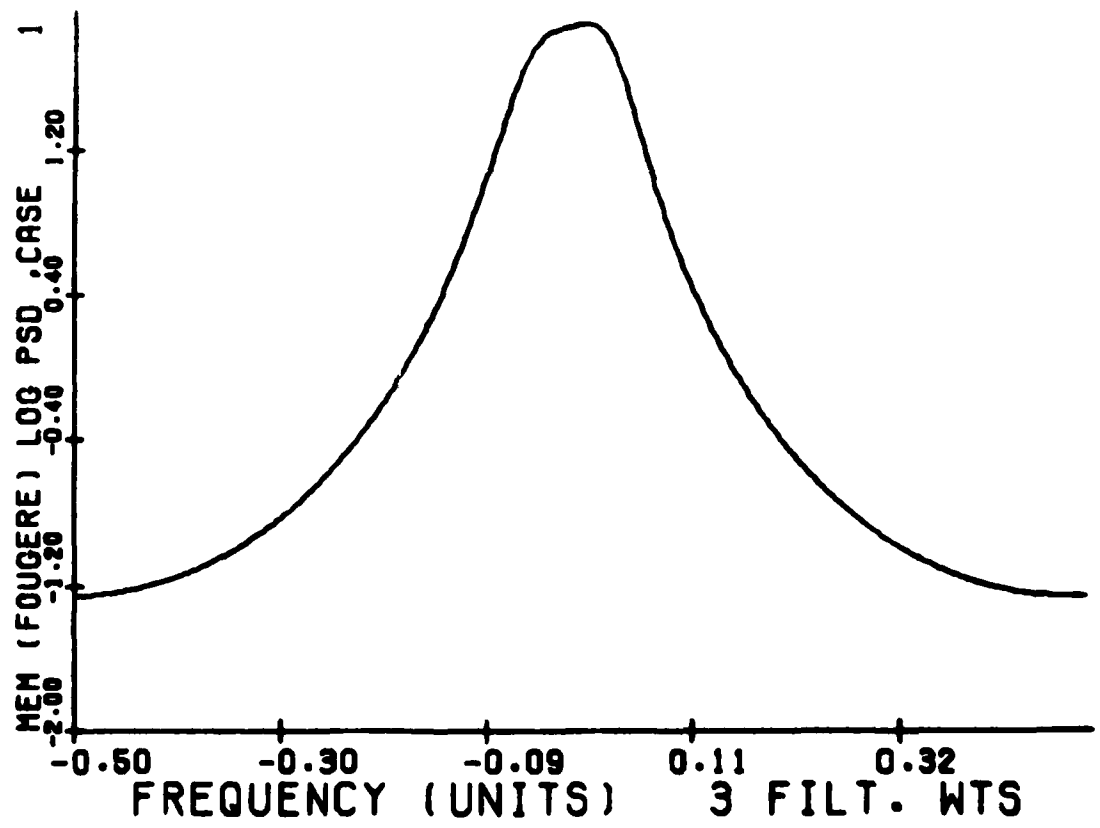
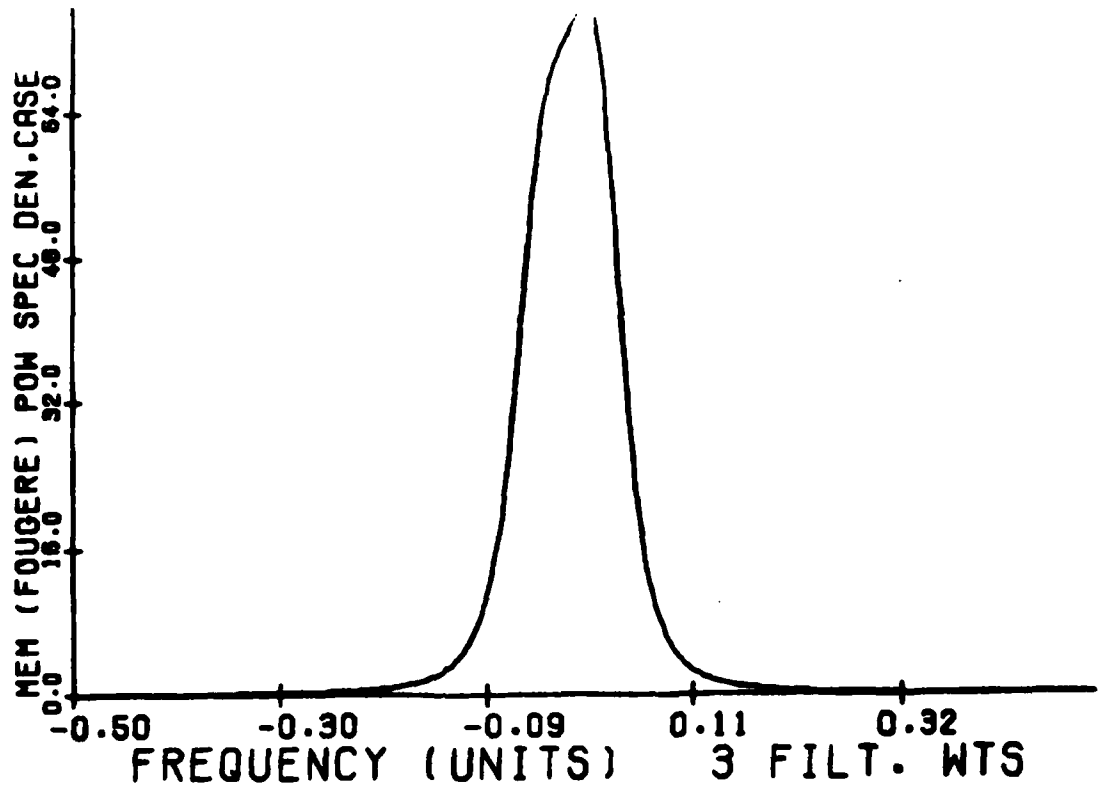


FIGURE 3 (Continued)

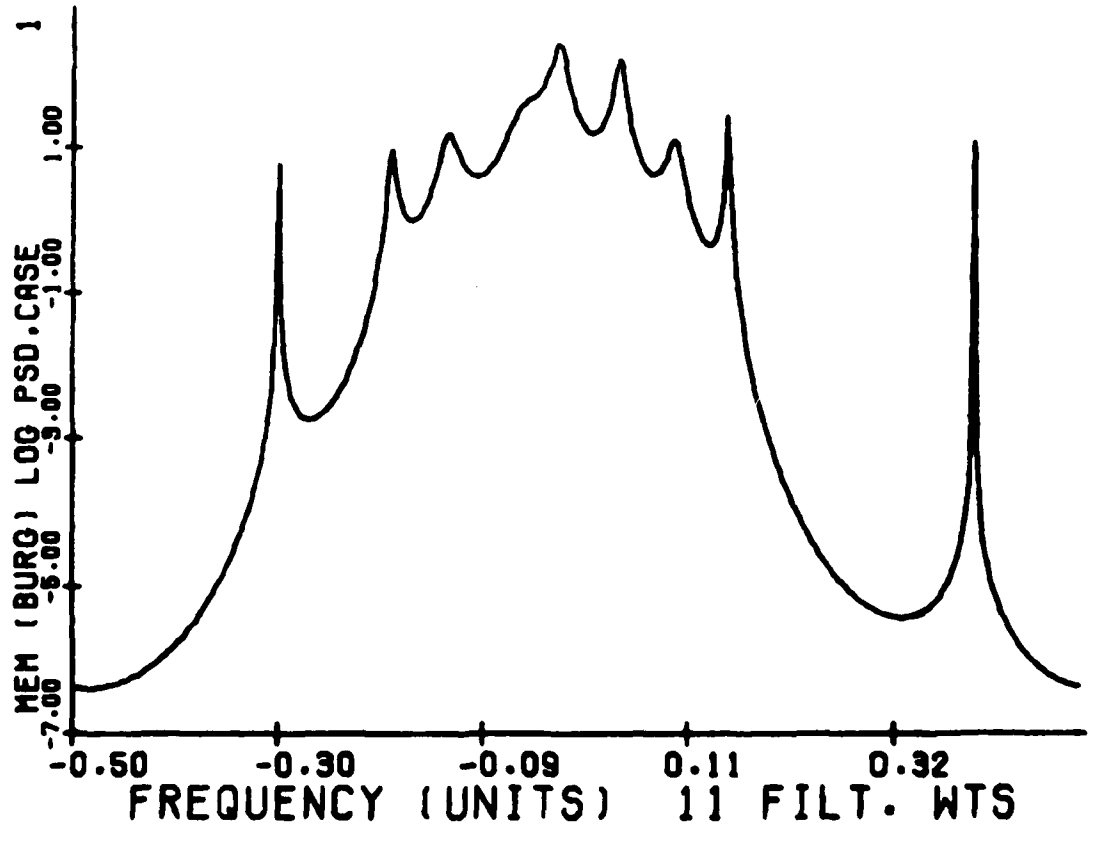
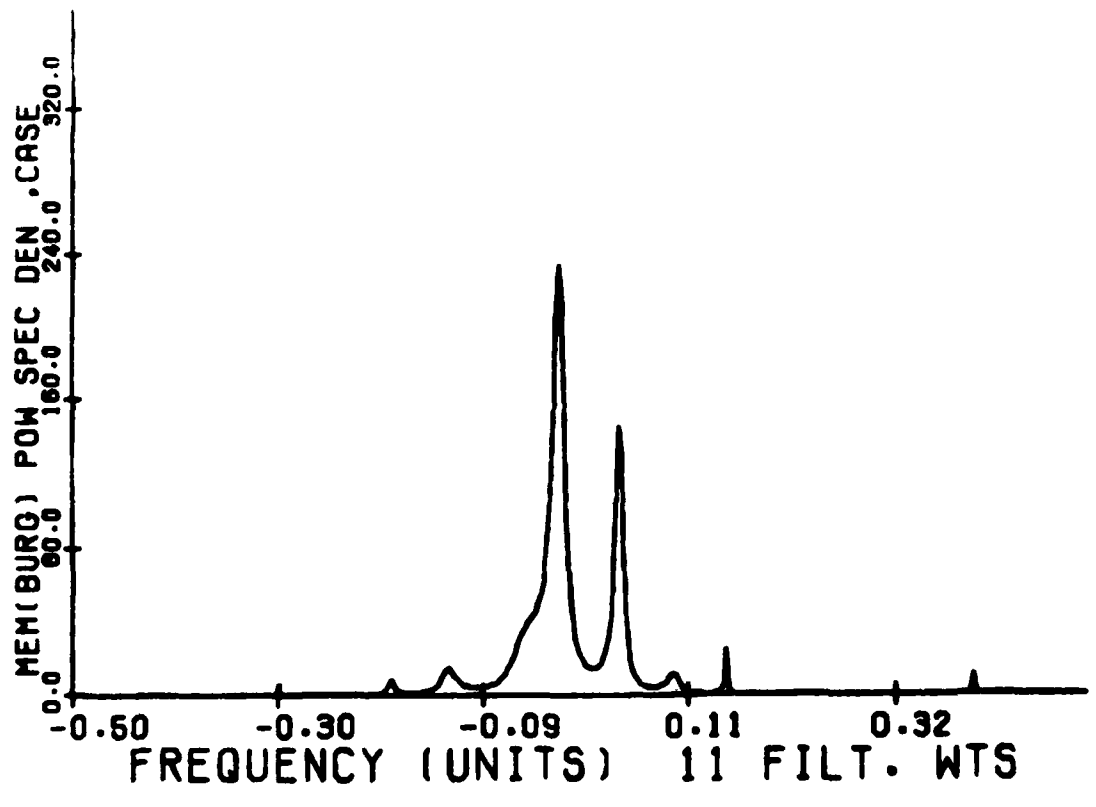


FIGURE 4

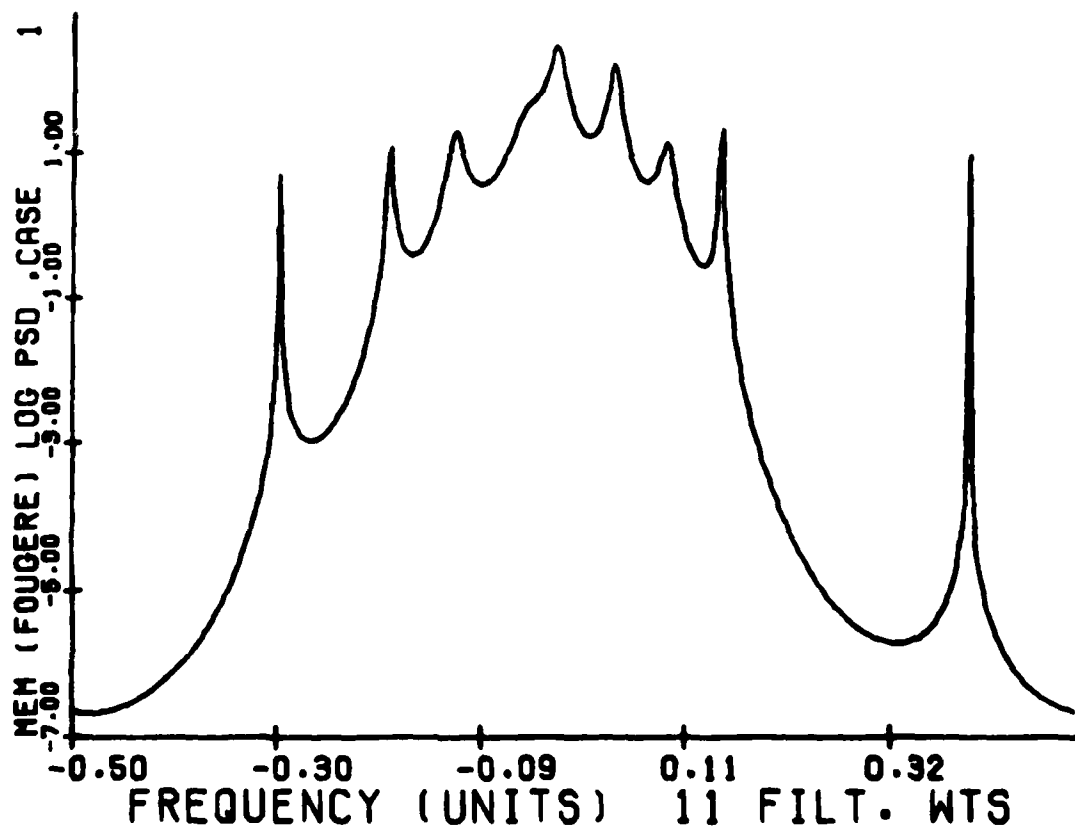
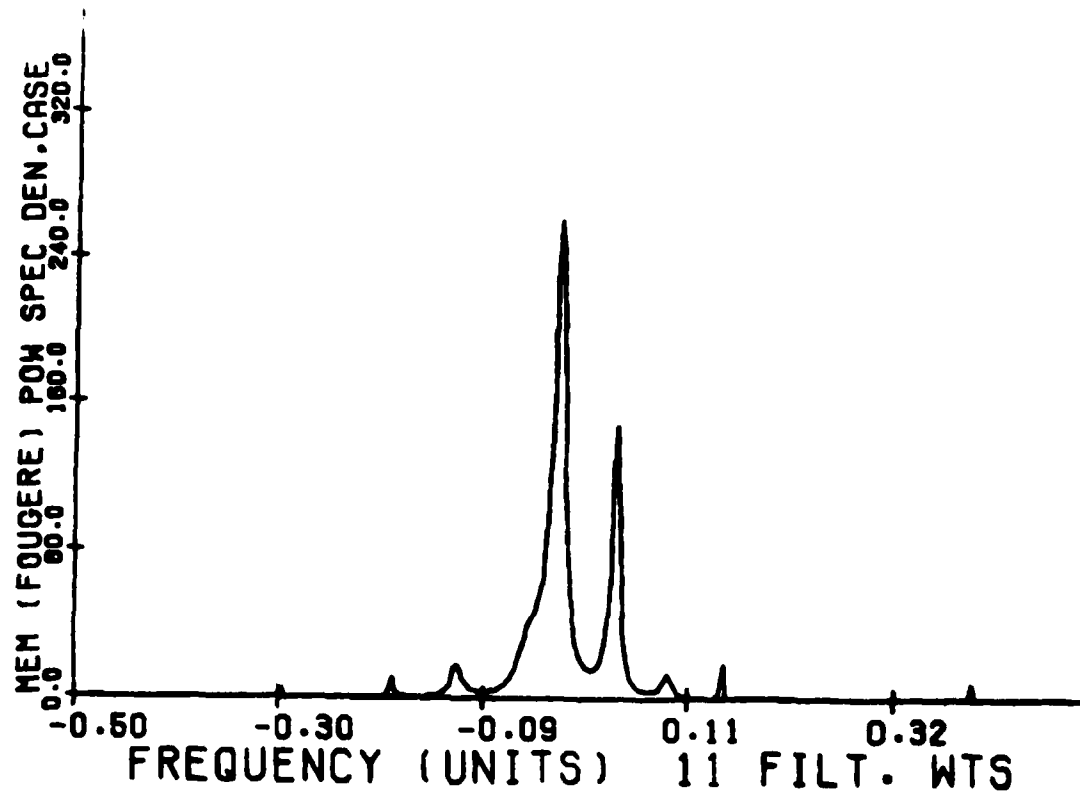


FIGURE 4 (Continued)

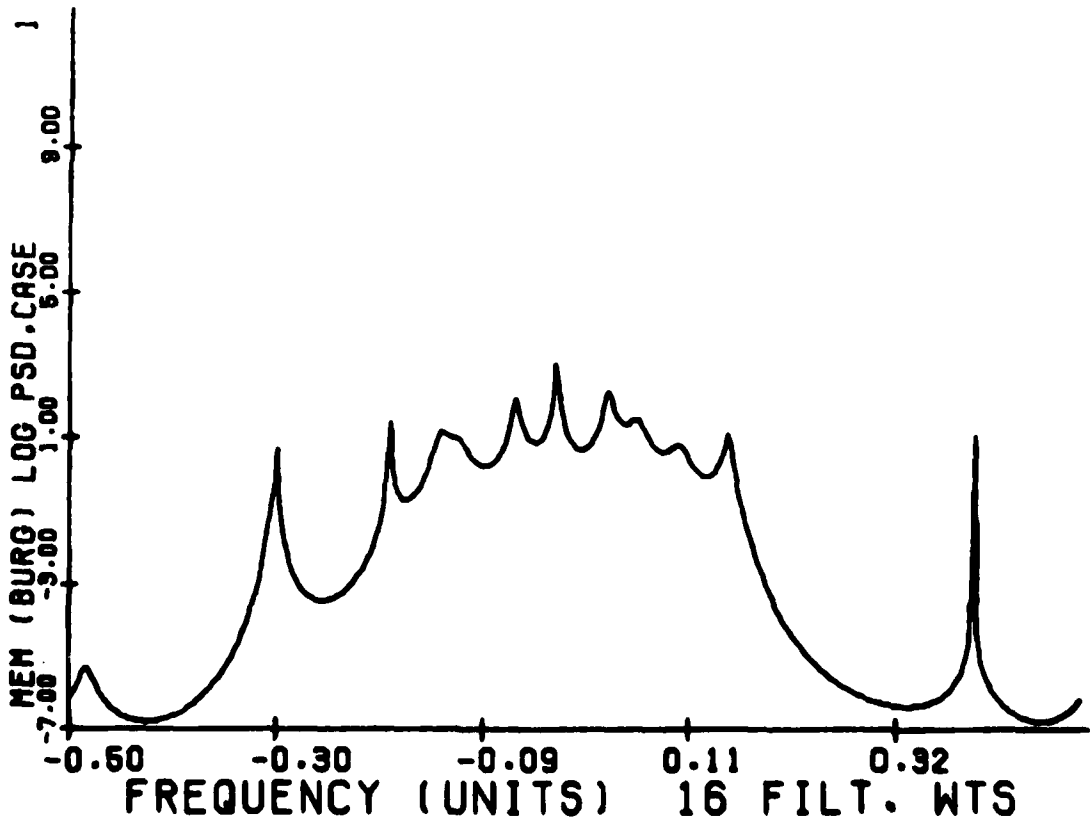
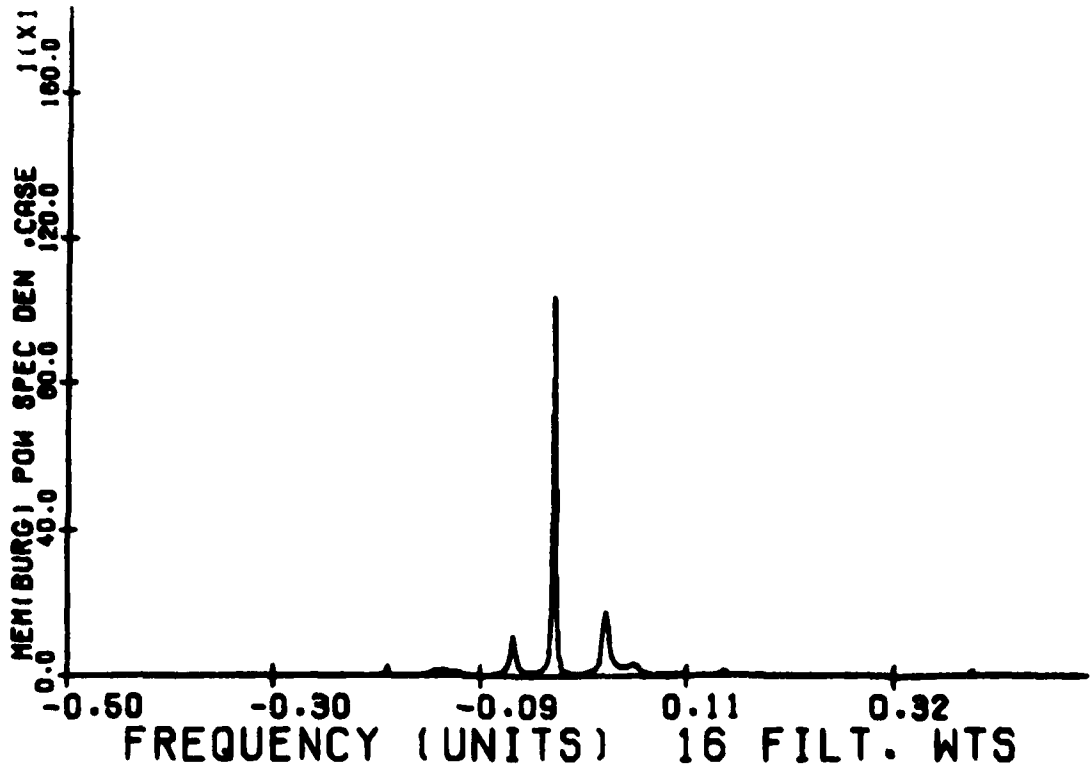


FIGURE 5

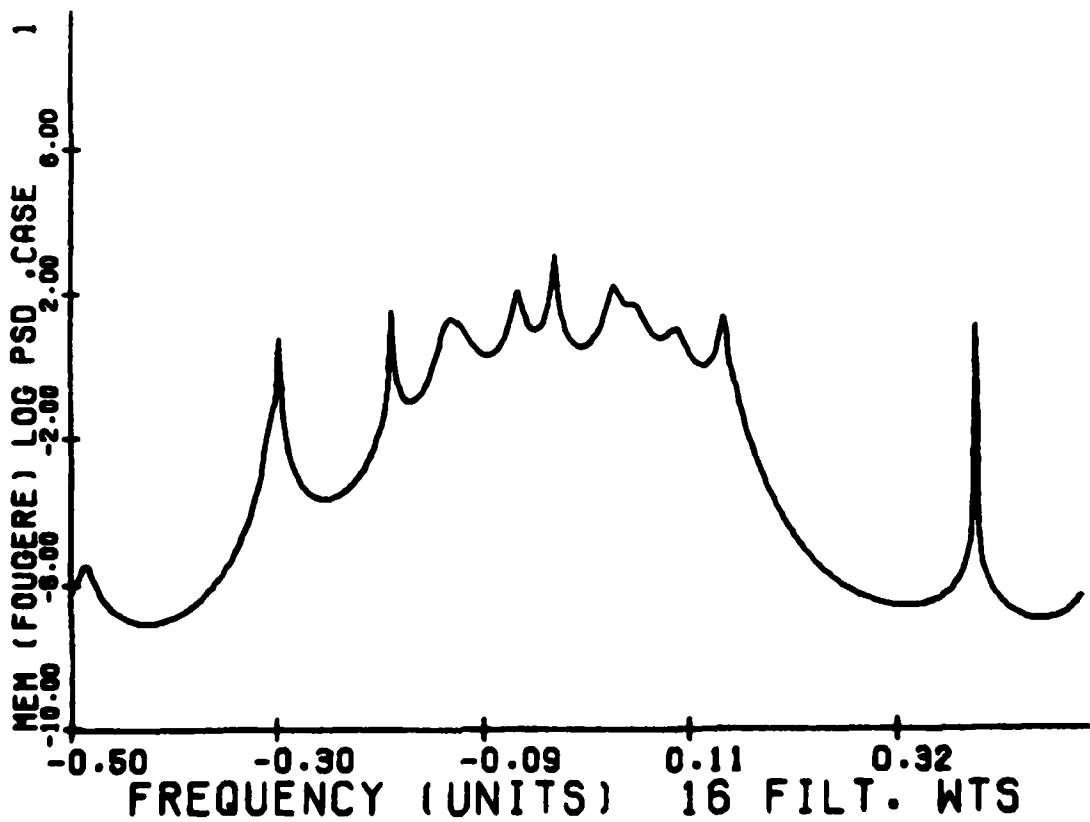
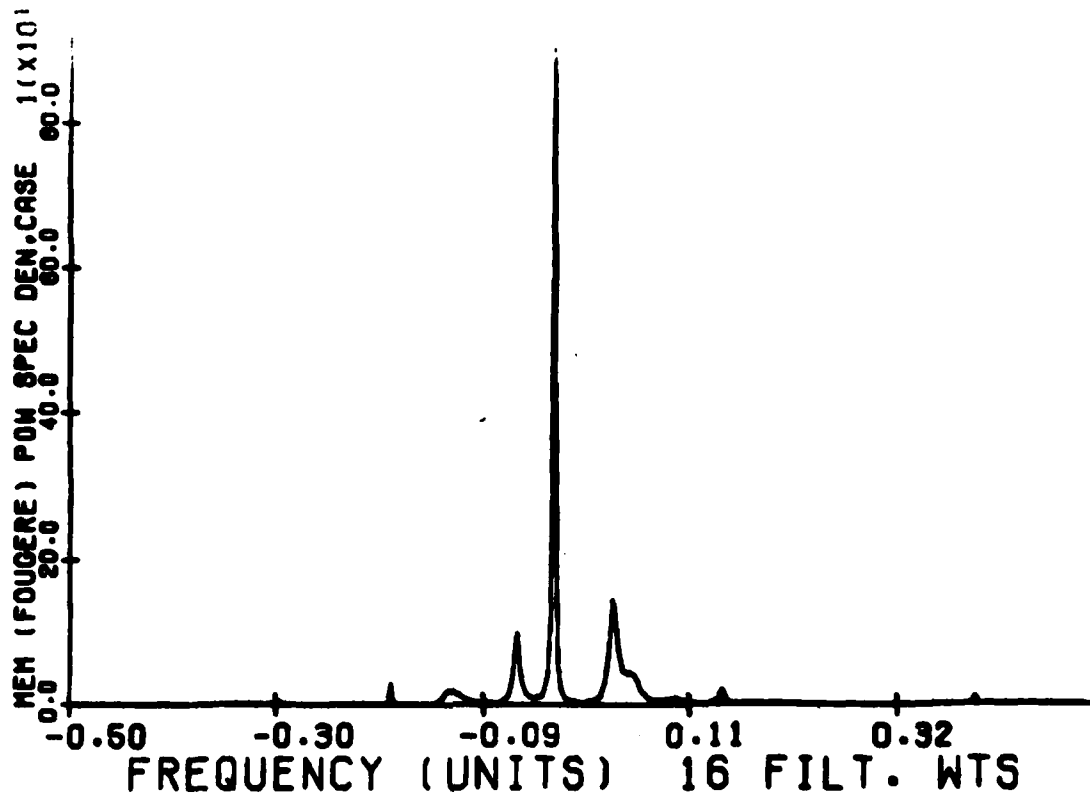


FIGURE 5 (Continued)

may be helpful to get an idea on the proper set of parameters. It is noted that the computation time increases slower than the linear relation as the numbers of iterations increases.

#### V. FURTHER WORK

A highly effective non-linear method of power spectrum estimation for real and complex signals has been successfully implemented on the CDC 6600 Computer. Several areas of further work are much needed and strongly recommended. They are:

- (1) Implementation of the method in a minicomputer such as PDP 11/45 which has smaller memory capacity and shorter word length. Some modification of the algorithms would be required in using the minicomputer. For example the round-off error may incorrectly place some roots of filter polynomial inside the unit circle.
- (2) Application to real data.
- (3) Empirical guideline for choice of parameters.
- (4) Extension to more than two channels of data based on the non-linear method.

## REFERENCES

1. A. V. Oppenheim and R. W. Schaffer, Digital Signal Processing, McGraw-Hill, Inc., N.Y., 1969.
2. J. P. Burg, "Maximum Entropy Spectral Analysis," presented at the Society of Exploration Geophysicists, Oklahoma City, Oklahoma, 1967.
3. J. P. Burg, "A New Analysis Technique for Time Series Data," presented at the NATO Advanced Study Institute on Signal Processing with Emphasis on Underwater Acoustics, Enschede, Netherlands, August 1968.
4. W. Y. Chen and G. R. Stegen, "Experiments with Maximum Entropy Power Spectra of Sinusoids," Journal of Geophysical Research, 79, No. 20, pp. 3019-3022, July 1974.
5. H. R. Radoski, P. F. Fougere, and E. J. Zawalick, "A Comparison of Power Spectral Estimates and Applications of the Maximum Entropy Method," Journal of Geophysical Research, 80, No. 4, pp. 619-625, February 1975.
6. D. G. Childers, editor, Modern Spectrum Analysis, IEEE Press, N.Y., 1978.
7. P. F. Fougere, E. J. Zawalick, and H. R. Radoski, "Spontaneous Line Splitting in Maximum Entropy Power Spectrum Analysis," Physics of the Earth and Planetary Interiors, vol. 12, pp. 201-207, 1976.
8. P. F. Fougere, "A Solution to the Problem of Complex Signals," Proceedings of the RADC Spectrum Estimation Workshop, May 24-26, 1978.
9. T. J. Ulrych and R. W. Clayton, "Time Series Modelling and Maximum Entropy," Physics of the Earth and Planetary Interiors, vol. 12, pp. 188-200, 1976.
10. J. P. Burg, "Maximum Entropy Spectral Analysis," Ph.D. thesis, Stanford University, Stanford, CA, 1975.
11. R. Fletcher and M. J. D. Powell, "A Rapid Descent Method for Minimization," Computer Journal, vol. 5, No. 2, pp. 163-168, 1963.
12. R. Fletcher and C. M. Reeves, "Function Minimization by Conjugate Gradients," Computer Journal, vol. 7, No. 2, pp. 149-154, 1964.

1979 USAF - SCEEE SUMMER FACULTY RESEARCH PROGRAM

Sponsored by the

AIR FORCE OFFICE OF SCIENTIFIC RESEARCH

Conducted by the

SOUTHEASTERN CENTER FOR ELECTRICAL ENGINEERING EDUCATION

FINAL REPORT

COMPUTER CODES APPLICABLE TO THE DETERMINATION

OF

EJECTION SEAT/MAN AERODYNAMIC PARAMETERS

Prepared by:	DONALD C. CHIANG
Academic Rank:	Professor
Department and University:	CIVIL AND MECHANICAL ENGINEERING DIVISION ROSE-HULMAN INSTITUTE OF TECHNOLOGY
Research Location:	AIR FORCE FLIGHT DYNAMICS LABORATORY/ VEHICLE EQUIPMENT DIVISION/ CREW ESCAPE AND SUBSYSTEMS BRANCH/ AIR CREW ESCAPE GROUP
USAF Research Colleagues:	LANNY A. JINES
Date:	August 10, 1979
Contract No:	F49620-79-C-0038

COMPUTER CODES APPLICABLE TO THE DETERMINATION

OF

EJECTION SEAT/MAN AERODYNAMIC PARAMETERS

by

DONALD C. CHIANG

ABSTRACT

A careful survey of computer codes applicable to the determination of ejection seat/man aerodynamic parameters was carried out. The current state of the art capability in computational aerodynamics was identified through an integration of several means including Defence Documentation Center (DDC) literature search, consultation with concerned industry and government agency, inputs from individuals interested in the subject as well as survey of research literature at large. Several computer program codes from government sources were found to be applicable. They range in scope from relatively simple to highly sophisticated, from an engineering tool to a research oriented program. But a considerable amount of preliminary work is required before these computer codes can be applied to the ejection seat/man configuration. Suggestions for further research in this area are also included.

### ACKNOWLEDGMENTS

The author would like to express his appreciation to the Air Force Systems Command, Air Force Office of Scientific Research and the Southeastern Center for Electrical Engineering Education for providing him an opportunity to work at the Air Force Flight Dynamics Laboratory, Wright-Patterson Air Force Base and with the members of the Air Crew Escape Group, Crew Escape and Subsystems Branch, Vehicle Equipment Division in particular.

Special thanks are due to Mr. Lanny A. Jines, the author's sponsor, for a well-organized program and many assistances rendered inside as well as outside the lab. He would also like to thank all the members of the Crew Escape and Subsystems Branch under the leadership of Mr. Edwin R. Schultz for providing a pleasant working atmosphere which enabled the author to expand his knowledge considerably in the area of air crew escape system in particular and computational aerodynamics in general.

## I. INTRODUCTION:

The idea of ejecting crews from disabled aircraft was advanced in the late 1920s. Ejecting air crews solves several escape problems. It permits air crews to leave aircraft that fly at high speeds or are in high deceleration spinning or tumbling motions. It protects the crew members during exit from contact with the aircraft and provides for safe escape from low speed ground level emergencies.

As soon as the first operational ejection seat was introduced near the end of World War II in the German night fighter, He 219, some general ejection seat aerodynamic problems were exposed. Adequate seat trajectory height was required to clear the tail of the aircraft. Stabilization of the seat in pitch and yaw was necessary immediately after ejection and proper man-seat separation afterward. When aircraft speeds increased in the early 1950s, protection of the air crews against certain consequences of wind blast, such as limb flailing and high "g" effect, became a problem.

That an unmodified ejection seat/man combination is aerodynamically unstable in pitch, yaw and roll is a well-known fact. But attempts at inherent aerodynamic stabilization so far have only been partially successful necessitating augmentation with drogue parachutes. This is an area more extensive research needs to be carried out. In this type of research work and many other works related to the air crew escape system such as performance verification, merit evaluation of conceptual design, etc., all require data concerning aerodynamic parameters in order to carry out the several tasks involved.

The aerodynamic data that are required include the three force components in the directions of three mutually perpendicular body axis

system and the three moment coefficients referred to the center of gravity of the seat/man system. There are two ways of acquiring the aerodynamic data: (1) wind tunnel test using mock-up system with scale model and dummy or real seat and dummy, or under special circumstances, real seat and real person, and (2) theoretical analysis of the flow field surrounding the seat/man configuration using digital computers. While the wind tunnel testing procedures and the test data reduction techniques have been fully developed and applied routinely to the study of ejection seat/man system, theoretical computation of the aerodynamic parameters of ejection seat/man system has not made appreciable progress so far in spite of the many brilliant advancements made in the electronic computer technology, hardware as well as software.

This lack of progress is not at all due to lack of interest but rather due primarily to the extremely complicated three-dimensional body surface the seat/man configuration presents (compared to the smooth and streamlined contour of the aircrafts, missiles, spacecrafts and other flying objects). (Fig. B1) Secondly, it is the transonic flow regime in which the system often operates. Mathematical theory concerning transonic flow has been slow in development because of many intrinsic difficulties of the problem. Many problems of practical importance exist today for which the aerodynamics are still not predictable mathematically, and there are flows that are still not very well understood in spite of their practical importance.

A breakthrough of sort which brought notable change in the situation occurred in the early seventies. A number of theoretical methods have been developed, yielding information that previously could have been

obtained only by experiment. Since then, the progress has been quite rapid, and interest in computational aerodynamics as a tool for design, development as well as research activities in those difficult areas have been revived. This includes the ejection seat/man configuration.

An effort was initiated, therefore, to survey the computational aerodynamic methods for determining body axis aerodynamic coefficients of geometrical shapes which are characteristic of that exhibited by the ejection seat/man configuration.

## II. OBJECTIVES OF THE RESEARCH EFFORT:

The objectives of this effort were:

(1) To survey the research literature in the area of subsonic/supersonic flow around three-dimensional, arbitrary body representative of an ejection seat/man combination.

(2) To survey the existing computer program codes that may be applicable, after appropriate modification or extension, to the aerodynamic problem posed by an ejection seat/man combination.

(3) To informally document the results of investigation for future in-house or contractual efforts.

### III. INPUT FROM COMPUTATIONAL AERODYNAMICS GROUP (AFFDL/FXM)

An informal discussion session was held with Dr. Joseph Shang, Aerospace Engineer of the Computational Aerodynamics Group, WPAFB, to find out the computational capabilities of the group to which he belongs and to solicit an expert opinion on matters related to the present effort. Dr. Shang summarized the situation as follows.

(1) There are working computer codes for solving two-dimensional and three-dimensional Navier-Stokes equations for both laminar and turbulent flows in his group at present. However, they do not have computer code for solving potential flow equations or Euler's equations, nor do they have computer capability for solving the boundary layer equations.

(2) Since aerodynamic forces (in contrast to viscous forces) are predominant in the ejection seat/man problem, fluid viscosity is of a secondary importance. Therefore, the flow field around the ejection seat/man configuration can be very well represented by Euler's equations and in some cases by the potential flow equations.

(3) Unsteady nature of the flow field around the ejection seat/man configuration needs a careful consideration. However, if the ejection seat/man configuration can be sufficiently stabilized, i.e., without violent tumbling motion, then treating the problem as a steady flow problem is well justified.

(4) Generally speaking there are four computational approaches to a three-dimensional flow problem such as that of ejection seat/man system:

- 1) Semi-empirical method using various pressure laws such as Newtonian impact theory, Unified pressure laws, etc. employed by the computer codes

GAC-HAPP and DAC-HABP. (These computer codes will be discussed later.)

- ii) Potential flow equations if the flow is inviscid and irrotational.
- iii) Euler's equations if the flow is inviscid, and
- iv) Navier-Stokes equations with no restrictions whatsoever.

While semi-empirical method is simple and easy to program, it will require a great deal of experience and insight in order to be successful. For example, for a complicated three-dimensional body such as ejection seat/man configuration, one must know what particular pressure law to apply on what portion of the body, etc. The success depends to some extent on the user's know-how. On the other hand, solution of full potential flow equations or Euler's equations will take much longer time to develop the computer program. But once the program is written the solution can be obtained more or less straight forward without guess work. Navier-Stokes equations are normally not necessary for this type of problem in which aerodynamic forces are of the primary interest.

#### IV. INPUT FROM INDUSTRY--GRUMMAN AEROSPACE CORPORATION

Grumman Aerospace Corporation is carrying out an investigation of MINIMUM-SIZED LOW PROFILE COCKPIT (MSLPC) AND CREW ESCAPE SYSTEM INTEGRATION under Air Force Contract No. F33615-78-C-3427. The aerodynamic data they needed in analyzing the conceptual escape system performance were generated by a computer code GAC-HAPP (Grumman High-Speed Aerodynamic Prediction Program) [1], in which they used a modified Newtonian pressure law together with a crude model and was able to obtain a set of aerodynamic data which correlated very well with the wind tunnel data published in Reference 2.

An informal discussion session was held with five scientist/engineers of the Grumman Aerospace Corporation, Bethpage, N.Y., led by Mr. Joseph Childs.\* Our discussion was centered around their computer code GAC-HAPP.\*\* The general consensus of the group was that, from an industrial point of view, an engineering tool such as GAC-HAPP is the only tool one should use in the trending study or design and development, because it is simple and economical. The program was originally designed for the evaluation of space shuttle performances in the supersonic/hypersonic flow regime. But successful experiences with the code in the low supersonic flow and even subsonic flow with Mach number as low as 0.6 [3] motivated Grumman to try to extend its range of application down to and including incompressible flow ( $M = 0$ ) by introducing appropriate new pressure laws and allowances for the lee-side pressure.

The group suggested that two things be included in the future wind tunnel test of ejection seat/man system: (i) measurement of static pressure at the representative locations of the ejection seat/man system, and (ii) measurement of some dynamic characteristic parameters such as damping coefficients, if possible. A knowledge of the static pressure distribution will help us understand the flow conditions around the body much better, and the dynamic parameters will help us understand the transient nature of the rapidly decelerating ejection seat/man system.

---

\* The name and phone number of each member are included in Appendix A.

\*\* See Appendix B for a brief description of the program.

V. INPUT FROM OTHER GOVERNMENT AGENCY--NASA AMES RESEARCH CENTER

This author was briefed by a group of scientist/engineers of NASA Ames Research Center, Moffett Field, CA, on the newest developments in computational fluid dynamics. Mr. Terry Holst, who was the author's point of contact, made arrangements for a meeting with three other scientists.\* Our discussion was centered around the advanced methods of solving full potential flow equations and Euler's equations. Mr. Holst summarized the state of the art as follows.

(1) Cost in CPU time: (Speaking in terms of applying the existing computer codes to a three-dimensional problem such as that of ejection seat/man configuration:) (i) Navier-Stokes equations (5 hours); (ii) Euler's equations (2 hours); and (iii) Full potential equations (10 minutes). The number of hours shown inside the parentheses indicate an estimated CPU time required to get a set of data (for one Mach number and one angle of attack). The dollar cost would be approximately \$1,000 per CPU hour. For unsteady flow problems, triple the amount of time quoted above.

(2) Time required to develop the computer program: The time required to modify an existing computer code to make it work for the ejection seat/man configuration would be from  $\frac{1}{2}$  to 1 year. The most efficient way to do it is to do it at NASA Ames Research Center where the expert advice is readily available. The person who undertakes this task should have a good background in fluid dynamics and, more preferably, in computational fluid dynamics (CFD).

(3) Level of impact: Somehow unclear because it is very difficult

\* The name and phone number of each member are included in Appendix A.

to make an assessment. A CFD code definitely cannot compete with an empirical approach such as GAC-HAPP with respect to cost and time involved. However, an improved accuracy can be obtained from CFD in general. But it is unclear how much accuracy can be obtained if, in order to hold down computer time and cost, a relatively crude model is employed in computation.

(4) Recommendations: (i) If the aerodynamic data desired is at the higher Mach numbers ( $M = 1.5$ ), Euler's equations should be used. On the other hand, if Mach numbers in the range of 0.6 to 1 are also equally important, then one should start out with the full potential equations. Because the computer code for the solution of full potential flow equations is simpler and less expensive. (ii) Another approach one might try is to solve the two-dimensional formulation of the problem on the symmetry plane of the system and empirically introduce allowances for the three-dimensional relief effect, because two-dimensional computer codes are much simpler than the corresponding three-dimensional computer codes. For example, two-dimensional computer code can solve full potential equations in approximately 30 seconds per case and Euler's equations in approximately 10 minutes per case.

#### VI. POTENTIAL COMPUTER PROGRAMS FROM GOVERNMENT SOURCES

A brief description of each potential computer program uncovered by the DDC literature search is given below.

(1) "THE MARK IV" SUPERSONIC-HYPERSONIC ARBITRARY-BODY PROGRAM [4]

This program was developed by the Douglas Aircraft Co. under Air Force contract. The program is also known by the code name "DAC-HABP." It is similar in scope to GAC-HAPP of Grumman. This program is by design

an engineering tool, usable by the designer in day-by-day design and development work, rather than a specialized research program requiring extensive knowledge for successful operation and large amounts of computer time. It places at the disposal of the user a collection of different aerodynamic analysis tools that he can use in attacking his particular problem. Therefore, the accuracy of the results achieved depends to a certain extent upon the user's knowledge of high speed aerodynamics and on how he decides to apply the program to his problem.

Although the program primarily uses local-slope pressure calculation methods that are most accurate at hypersonic speeds, its capabilities have been extended down into the supersonic speed range by the use of embedded flow field concepts. (See Appendix B for more detail.)

(2) "USSAERO" UNIFIED SUBSONIC-SUPERSONIC AERODYNAMIC PROGRAM [5]

This program was developed by the Analytical Methods Inc., under NASA contract. It employs the panel method for calculating steady, full potential flow about arbitrary three-dimensional body. The velocity components for the incompressible flow are determined first and the solutions are extended to the compressible flow by applying an extended Gothert's similarity rule in both subsonic and supersonic flow regimes.

The configuration surface is subdivided into a large number of panels each of which contains an aerodynamic singularity distribution. A constant source distribution is used on the body panels, and a vortex distribution having a linear variation in the streamwise direction is used on the wing and tail panels. The normal components of velocity induced at specified control points by each singularity distribution are

calculated and make up the coefficients of a system of linear equations relating the strengths of the singularities to the magnitude of the normal velocities.

A rapidly-convergent iteration scheme for solving large order system of equations is employed to find solution of the boundary condition equations. Once the singularity strengths are known the pressure coefficients are calculated and the forces and moments acting on the configuration are determined by numerical integration. (See Appendix C for more detail.)

(3) "AEDC PFP" THREE-DIMENSIONAL POTENTIAL FLOW PROGRAM [6]

This program was developed by the ARO, Inc., the contract operator of Arnold Engineering Development Center (AEDC) under the sponsorship of Air Force Systems Command. This program also uses the panel method for calculating steady potential flow about arbitrary three-dimensional body. However, the mathematical representation of an aerodynamic shape is normally made up of a series of loop or horse-shoe vortices. A control point is normally located at the center of each loop or horseshoe. The computer code is written to extend the incompressible flow solutions to the subsonic compressible flow by using Gothert's compressibility correction.

(4) "ATTACK" A COMPUTATION METHOD FOR TWO-DIMENSIONAL, AXISYMMETRIC, AND THREE-DIMENSIONAL BLUNT-BODY FLOWS [7]

This program was written by Capt. Ronald H. Aungier, USAF, under the sponsorship of Air Force Weapons Laboratory (AFWL). The computer

program was written specifically for axisymmetric body. This computer code solves the governing equations for unsteady, inviscid flow (Euler's equations) by the so-called time-dependent method.

An explicit finite difference scheme is used with stabilizing terms introduced into the governing equations for the unsteady flow. The shock points are treated with the quasi-one-dimensional unsteady characteristics scheme suggested by Morretti and Abbett [8]. A segmented solution procedure is employed to reduce computational time and storage requirements. It involves dividing the flow field into many discrete segments marching back along the body. The steady flow solution is obtained for each segment (starting with the blunt nose) before proceeding to the next segment. The downstream boundary solution at each segment is used as a constant upstream boundary solution for the next segment. (See Appendix D for more detail.)

(5) "STREET A IV" STRATEGIC REENTRY TECHNOLOGY PROGRAM [9]

This program was developed by the AVCO Systems Division under Air Force contract. This code is very similar in scope to ATTACK. It is used to calculate the three-dimensional perfect gas flow in the shock layer of a blunted circular or non-circular cone at an angle of attack. It employs a time-dependent finite difference technique for the subsonic nose region of the shock layer, and a steady finite difference technique for the supersonic after body flow region.

(6) "D3CSS" STEADY INVISCID THREE-DIMENSIONAL SUPERSONIC FLOW PROGRAM [10]

This program was written by members of the Mathematics and Engineering Analysis Branch of Naval Surface Weapons Center/White Oak Laboratory (NSWC/WOL). The initial code development was supported by the Naval Sea Systems Command and most of the final code development and documentation was supported by the Air Force Space and Missile System Organization (SAMSO).

The program computes the steady inviscid flow field in the supersonic region of the shock layer on arbitrarily shaped reentry body in pitch and yaw. The program also integrates the surface pressures to determine the aerodynamic forces and moments on the body.

The program uses second order accurate finite difference methods to solve numerically the inviscid flow equations in conservation form. The region of the shock layer in which the axial velocity component is supersonic is referred to as the supersonic region. In this region, the governing equations are of hyperbolic type with the  $s$ -axis (axial direction) as the time-like direction. An explicit finite difference method is used to advance the flow variables and the bow shock geometry to station  $s + \Delta s$  using the known quantities at station  $s$ . The calculation begins at some plane  $s = s_0$  in the supersonic region where all flow quantities and shock geometry are known.

A coordinate transformation is introduced to map the  $s = \text{constant}$  cross-section of the flow field into a rectangular domain having one of the sides representing the body surface. Computation is done in the rectangular computational plane and the solutions are transformed back

to the physical plane.

Codes of this type are sometimes referred to as the shock-capturing technique. The present code also incorporates special provisions which are used when certain discontinuities in body slope are encountered.

(See Appendix E for more detail.)

#### VII. OTHER ADVANCED COMPUTATIONAL TECHNIQUES

Some of the numerical techniques that were developed more recently and are, to this author's knowledge, relevant to the ejection seat/man problem are briefly described below.

(1) Higher-Order Panel Method for Nonlifting Three-Dimensional Potential Flow. [18]

For low speed flight (incompressible flow) potential equation reduces to Laplace's equation which is linear. Then the problem can be formulated as an integral equation for a certain singularity distribution over the surface of the body about which flow is to be computed. This procedure owes its efficiency to the fact that the domain of calculation can be restricted to the body surface, i.e., calculations need not be performed in the field of flow.

In three-dimensional problems, the numerical implementation of this procedure has represented the body surface by a large number of small four-sided surface elements or panels and thus come to be called panel method. In the Hess version these panels are placed on the actual body surface. This renders the method numerically exact and applicable to any arbitrary body.

On each panel a control point is selected where the boundary condition of zero normal velocity is to be applied and where surface velocities are ultimately calculated. A "matrix of influence coefficients" is then calculated. This consists of the computed set of velocities induced by the panels at each other's control points for unit strength of source or linearly varying strength of vorticity. On nonlifting portions of the configuration only source singularity is employed. On lifting portions both source and doublet singularities are used.

A lifting portion of the configuration is defined as one having a sharp trailing edge where Kutta condition is to be applied and from which issues a wake of trailing vorticity. Nonlifting portions are characterized by the absence of a sharp trailing edge and its associated vortex wake. The source strengths are adjusted to satisfy the zero normal velocity condition and the doublet parameters are adjusted to satisfy the Kutta condition.

Probably the principal disadvantage of any three-dimensional panel method is that each case is relatively expensive because a large number of panels means proportionately large amount of input data and computing time. This problem has been intensified by the very success of the method, because its success has led to its use in more and more challenging problems. There is an urgent need for an increase in speed of computation as well as accuracy.

The concept of the higher-order approach was first put forward by Hess who has shown that the effect of surface curvature and the effect of the variation of surface singularity strength are of the same order of

magnitude. Thus inclusion of one without the other is inconsistent and, in general, does not lead to an improvement in accuracy over the base method (such as one used in "USSAERO"). The consistent approximations in ascending order of accuracy are: (i) flat-panel with constant-source (base method), (ii) paraboloidal-panel with linear source, and (iii) cubic-panel with quadratic-source. In other words, a consistent approach uses a source polynomial one degree less than the panel polynomial. The last one was felt to be too complicated to be feasible and the "higher-order" procedure adopted was the paraboloidal-panel with linear-source.

The essence of constructing a higher-order panel method consists of generating altered "matrix of influence coefficients." The formulas that in the base method give the velocity induced at arbitrary control point by a flat panel with a constant singularity strength must be replaced in a higher-order method by formulas that give the velocity induced at an arbitrary control point by a curved panel with a variable singularity strength.

(2) Numerical Calculation of Transonic Potential Flow about Wing-Body Combinations. [19]

One of the major complications of treating the full potential equation results from the need to treat the boundary conditions accurately. This can be done, in general, (i) by analytically transforming the equation to a boundary-conforming coordinate system so that the boundary conditions can be applied easily on the body surface itself, or (ii) the boundary conditions are satisfied by interpolating on a regular Cartesian mesh. The complexity of the finite difference code of implementing the first

approach grows rapidly with increasing geometrical complexity, so that application of this method to geometries more complicated than a wing-cylinder combination seems unlikely.

An alternate method proposed here is based upon the particularly simple form the quasilinear potential equation takes under a completely arbitrary coordinate transformation when the velocity is expressed in terms of its contravariant components. The coordinate transformation generating each mesh cell is considered to be independent of the others, and is determined numerically at each step in the calculation from the Cartesian coordinates of the mesh points.

An arbitrary (nonsingular) transformation is used to transform the potential equation. The new equation involves  $U$ ,  $V$ , and  $W$ , the contravariant components of the velocity vector  $(u,v,w)$ , in the new coordinate system  $(X,Y,Z)$ . A finite difference approximation to the equation is constructed using centered differences everywhere. An explicit artificial viscosity is then added to the equation at points where the flow is locally supersonic. Finally an iterative procedure based on an equivalent time-dependent process is constructed to solve the resulting difference equations.

Treatment of geometry: The geometry is first normalized by an appropriate transformation. A final transformation and suitable stretching transformations reduce the geometry to a finite rectangular box. A uniform rectangular mesh in this domain is then mapped back to the physical domain to give the Cartesian coordinates of the grid points.

### (3) Implicit Approximate Factorization Technique (AF) [20]

There are basically three formulations for inviscid transonic flows:

(i) transonic small-disturbance potential equation (TSD), (ii) full potential equation (FP), and (iii) Euler's equations (exact inviscid formulation). The FP formulation is the most efficient of the three formulations in terms of accuracy-to-cost ratio for a wide range of inviscid transonic flow applications.

A general form for two-level solution procedure for solving an equation of the form  $L\phi^n = 0$  is given by  $NC^n + wR^n = 0$ , where  $C^n = \phi^{n+1} - \phi^n$  is the correction,  $R^n = (L\phi^n)$  is the residual and  $w$  is the relaxation parameter. The operator  $N$  determines the type of iterative procedure and, therefore, determines the rate at which the solution procedure converges.

In the approximate factorization approach,  $N$  is chosen as a product of two or more factors indicated by  $N = N_1 N_2$ . The factors  $N_1$  and  $N_2$  are chosen so that (i) their product is an approximation to  $L$ , (ii) only simple matrix operations are required, and (iii) the overall scheme is stable.

Different iteration procedures result from different choice of  $N$ . For example: (i) successive line overrelaxation (SLOR), the standard transonic flow solution procedure, (ii) alternating direction implicit (ADI), one type of implicit approximate factorisation scheme sometimes referred to as AF1, and (iii) AF2, another type of implicit approximate factorization used in Reference 20.

### VIII. RECOMMENDATIONS

Computational aerodynamics is capable of producing the aerodynamic data that are required for dynamic analysis of the ejection seat/man combination. Several potential computer programs from the government sources were found to be applicable in one way or another, but none of them is applicable to the ejection seat/man configuration without further modification and adaptation, nor is any single computer code applicable to the entire performance envelop of the modern high performance air crew escape systems.

#### Recommendations:

(1) Develop MARK IV as an engineering tool to be used in day-by-day design and development work. The major and primary effort involved in adapting this code to the ejection seat/man configuration is modeling and inputting the geometric data into the computer. The second phase of the effort would be to develop a system of matching various pressure laws with various flow regions surrounding the ejection seat/man combination by correlating the data obtained from computation with the data obtained from wind tunnel test.

(2) Develop USSAERO as an engineering/research tool to obtain aerodynamic data based on potential flow assumption. With modeling technique already developed in the previous effort, adaptation of this computer code to the ejection seat/man combination can be expected to progress smoothly. The emphasis here would be in the area of improving the modeling technique to achieve accuracy of results and reduction of cost.

(3) Develop a preliminary research program patterned after ATTACK and DJCSS. The emphasis here would be adaptation of the time-dependent technique and the shock-capturing technique to the solution of the flow field inside the shock layer.

(4) Develop research oriented computer program by incorporating whatever advanced techniques that may be available at the moment for solving full potential equations and Euler's equations.

Research tools today, engineering tools tomorrow.

APPENDIX A

The name and phone number of each member with whom this author met and discussed matters pertaining to the ejection seat/man problem as part of his effort are shown below.

(1) Grumman Aerospace Co., Bethpage, N.Y.

Joseph Childs	(516) 575-3671
Gianky Daformo	(516) 575-3662
Hing Lam	(516) 575-5722
Rudy Meyer	(516) 575-8860
Herbert Watman	(516) 575-2790

(2) NASA Ames Research Center, Moffett Field, CA

Terry Holst	(415) 965-6415
Robert Warning	(415) 965-5215
Unmeal B. Mehta	(415) 965-5548
Peter Goorjian	(415) 965-6329

## APPENDIX B

(1) Excerpts from several Grumman Reports [1, 15, 16, 17] are included here to illustrate various features of the computer code GAC-HAPP.

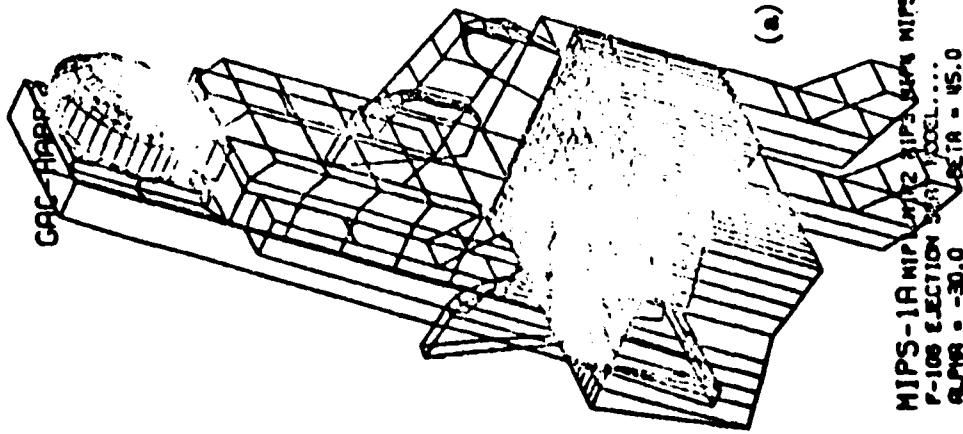
1. The GAC-HAPP is a versatile computer tool for the prediction of all-axis supersonic to hypersonic force and moment coefficients, static and dynamic derivatives, loads, and detailed surface pressures for arbitrary shapes arbitrarily oriented in the flow. (Fig. B1)

2. The following features are incorporated in the program:

- o An all-attitude arbitrary shape interference shielding option.
- o An all-attitude graphics.
- o A viscous effects option.
- o A modular configuration build-up capability.
- o A geometric routine for pertinent area/volume computation.
- o A punched-card output.
- o Control effectiveness prediction.

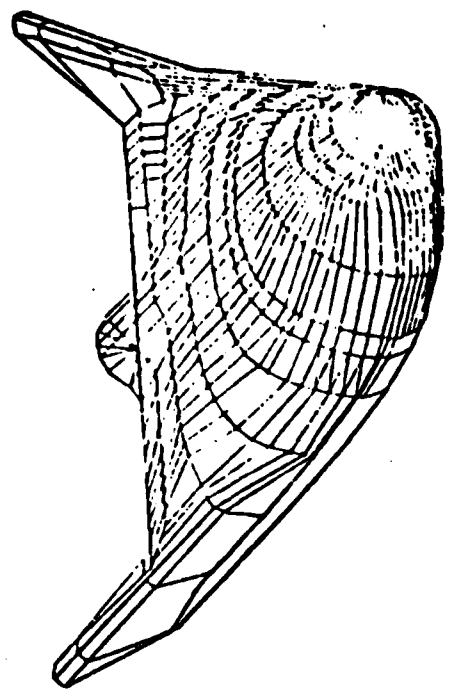
3. Machine processing of one flight point (mach, altitude, angle of attack, yaw angle) takes an average of 1/10 to 1 minute, depending upon the complexity of the computation and vehicle geometry. Turnaround time from preliminary lines to aerodynamic data is 24 hours.

4. The vehicle geometry must possess a plane (usually vertical) of symmetry. A triangular faceted description of the vehicle surface is employed. Incremental and total area, volume and centroid-of-area characteristics for each module and the total configuration are calculated. If the surface pressure and other elemental data are requested by the user, the program also calculates the centroids of the several



(a)

MIPS-1A MIPS-1A2 MIPS-3A4 MIPS-5A6 MIPS-6A7 MIPS-7A8 MIPS-8A9 MIPS-9A10 MIPS-10A  
 F-108 EJECTION SEAT MODEL...  
 ALPHA = -30.0 BETA = 45.0 SCALE = 3.067 /IN



NASA HL-10

(b)

Fig. B1 Computer modeling of (a) ejection seat/man combination and (b) more conventional flying object by CAC-HAPP.

thousand triangular surface elements.

5. The pressure coefficient for each triangular surface element, a function of its orientation in the stream, and its contribution to the vehicle forces and moments are computed and integrated over the vehicle surface.
6. Various pressure laws that are available include Newtonian, modified Newtonian, Unified, Tangent-sedge, Tangent-cone, and Prandtl-Meyer.
7. The viscid procedure, based on Eckert's reference enthalpy method, has options for normal or oblique shock edge flow properties, and laminar turbulent, or transitional boundary layers.
8. Computing time for complex geometries in graphics routine is about the same as that required for aerodynamic analysis. For a vertically symmetric shape requiring 1,000 input coordinate points and including self-shielding, for example, the processing time is approximately 10 seconds for one picture. For an average out-of-the-pitch-plane picture, the time involved can be up to one minute.

(2) The major features of MARK IV computer code include the following capabilities. [3]

1. Analyze completely arbitrary three-dimensional shapes.
2. Build up a vehicle from many components, each of which may be of arbitrary shape.
3. Include a number of force analysis methods so that the program would have the widest possible application to various vehicle shapes and flight conditions.
4. Provide engineering methods to account for the effect of the flow

field generated by one component on the characteristics of another component.

5. Provide for convenient storage of data between program components.

6. A total analysis system frame work that is adaptable to continued improvement and expansion.

7. Program runs either on CDC or IBM computers with a minimum of effort required to convert from one to the other.

8. A summary of the basic pressure calculation methods employed by MARK IV is given below.

Impact Flow

Modified Newtonian  
Modified Newtonian + Prandtl-Meyer  
Tangent-wedge  
Tangent-wedge empirical  
Tangent-cone  
Inclined cone  
Van Dyke Unified  
Blunt-body shear force  
Shock-expansion  
Free molecular flow  
Input pressure coefficient  
Hankey flat-surface empirical  
Delta wing empirical  
Modified Dahlem-Buck  
Blast wave

Shadow Flow

Newtonian ( $C_p = 0$ )  
Modified Newtonian + Prandtl-Meyer  
Prandtl-Meyer from free-stream  
Inclined cone  
Van Dyke Unified  
High Mach base pressure  
Shock-expansion  
Input pressure coefficient  
Free molecular flow

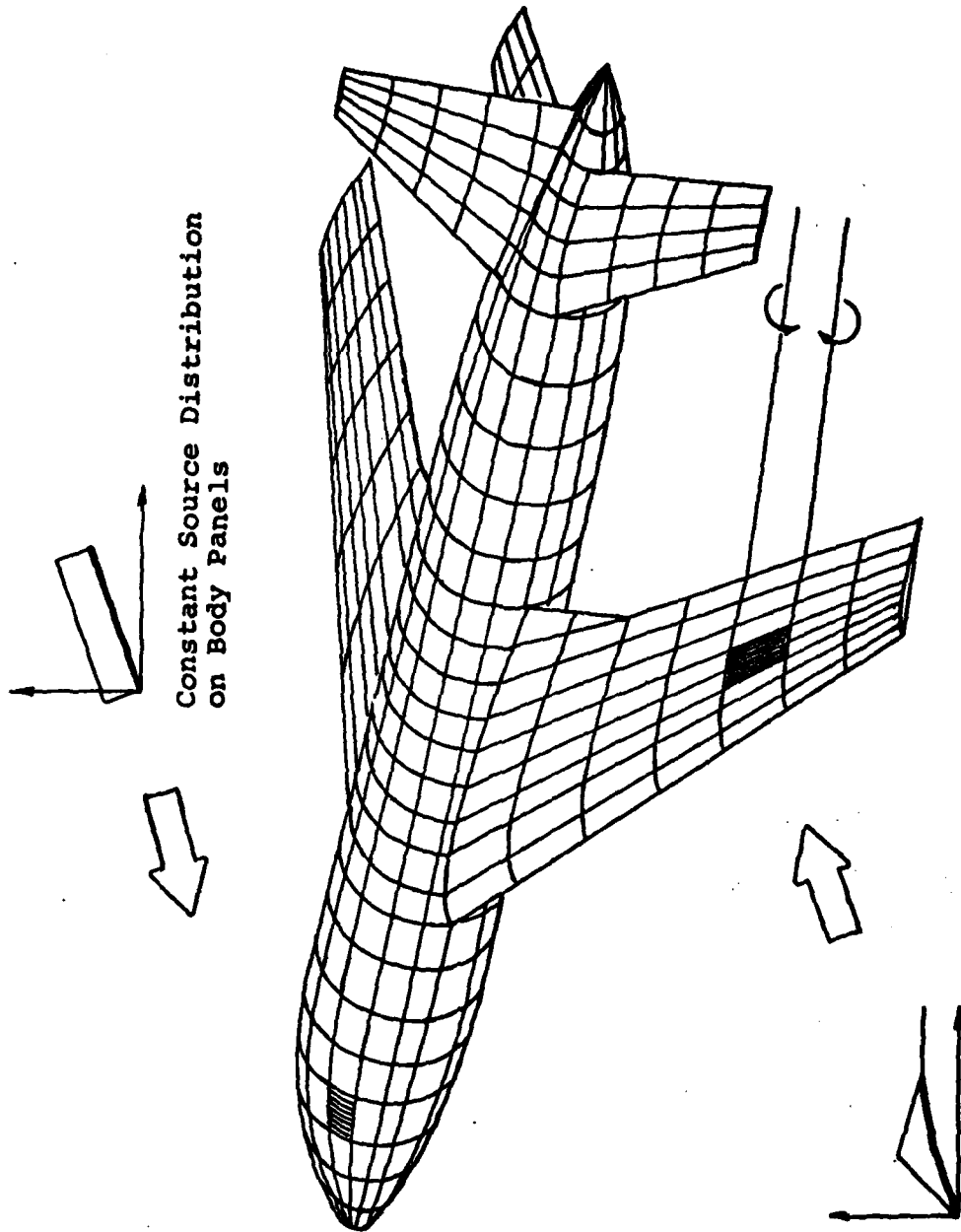
## APPENDIX C

### (1) The Panel Method [5]

The governing equation for a steady, irrotational, inviscid and incompressible (low speed) flow of a perfect gas is Laplace's equation which is linear. Then the problem can be formulated as an integral equation for a certain singularity distribution over the surface of the body about which flow is to be computed.

In three-dimensional problems the numerical implementation of this procedure has represented the body surface by a large number of small four-sided surface elements or panels. On each panel a control point is selected where the boundary condition of zero normal velocity is to be applied and where the surface velocities are ultimately calculated. (Fig. C1) On nonlifting portions of the configuration only source singularity is employed. On lifting portions a vortex distribution having a linear variation in the streamwise direction is used.

Analytical expressions are derived for the perturbation velocity field induced by each panel singularity distribution. These expressions are used to calculate the coefficients of a system of linear equations relating the magnitude of the normal velocities at the panel control points to the unknown singularity strengths. The singularity strengths which satisfy the boundary condition of tangential flow at the control points for a given Mach number and angle of attack are determined by solving this system of equations by an iterative procedure. The pressure coefficients at panel control points are then calculated in terms of the velocity components, and the forces and moments acting on the configuration obtained



Constant Source Distribution  
on Body Panels

Linear Vortex Distribution  
on Wing and Tail Panels

Fig. C1 Aerodynamic representation of three-dimensional body.

by numerical integration.

(2) The Compressible Flow Velocity Components

The compressible flow velocity components induced by the source and vortex distributions are obtained by applying an extended Gothert's similarity rule which applies to both subsonic and supersonic flows. The extended rule states that the velocity components  $u$ ,  $v$ , and  $w$  at point  $P(x,y,z)$  in a compressible flow are equal to the real parts of  $u_1$ ,  $\beta v_1$ , and  $\beta w_1$  where  $u_1$ ,  $v_1$ , and  $w_1$  are the incompressible velocity components evaluated at point  $P(x, \beta y, \beta z)$  and  $\beta = (1 - M^2)^{\frac{1}{2}}$  where  $M$  represents the Mach number.

In subsonic flow, this rule agrees exactly with that given by Gothert originally if each of the compressible velocity components are divided by the constant  $\beta^2$ .

## APPENDIX D

### The Time-Dependent Method for Solving Steady Euler Equations

#### 1. Introduction:

This method is based on the principle that correct steady-state solution is obtainable as the limit for large time of a transient solution.

The presence of time derivatives in the Euler equations of motion makes the system hyperbolic; hence the initial value problem is well posed. This means that for any given freestream values of velocity, density and pressure, the equations can be integrated forward in time until the flow field no longer changes.

For this procedure to be successful, the finite difference scheme which is to be used must have the following two properties: (i) it must be valid across any discontinuity, i.e., it should prevent the occurrence of infinite derivatives at the shock wave, and (ii) it must satisfy the Rankine-Hugoniot conditions across any shocks that may develop inside the flow field. [11]

Most difficulties in treating initial-boundary-value problems are encountered not in solving the differential equations, but in attempting to satisfy the boundary conditions. Therefore, a body oriented coordinate system is often adopted to simplify the latter task. The ease with which the boundary conditions can be satisfied far outweighs whatever complications adoption of such coordinate system may bring. [12]

#### 2. Implementation of the time-dependent method by "ATTACK" [7]

A body oriented coordinate system is used to optimize the nodal point

distribution and to improve the wall boundary conditions. The  $s$ -coordinate surface is parallel to the body surface while the  $n$ -coordinate surface is normal to the body surface. The  $\beta$ -coordinate is the standard azimuthal coordinate in a cylindrical system. (Fig. D1)

For spatial derivatives, either central, forward, or backward differences are employed. The partial derivatives in time will always be expressed as forward differences.

Since the explicit finite difference scheme for the unsteady flow equations is unstable, stabilizing terms are introduced into the equation. These stabilizing terms are proportional to the local flow properties and to the time step used. Therefore, the magnitude of the stabilizing terms can be reduced as much as is desired by reducing the magnitude of  $\Delta t$ .

The shock points are treated with the quasi-one-dimensional unsteady characteristics scheme suggested by Morreti and Abbett [8]. This scheme is based on the assumption that the variation of physical variables along the direction normal to the shock are the relevant parameters for determining the shock behavior.

A computational procedure developed in Reference 13 which was referred to as the segmented solution procedure is employed here. It involves dividing the flow field into many discrete segments marching back along the body. (Fig. D2) The steady flow solution is obtained for each segment, starting with the blunt nose where the flow is subsonic, before proceeding to the next segment. The downstream boundary solution at each segment is used as a constant upstream boundary solution for the next segment.

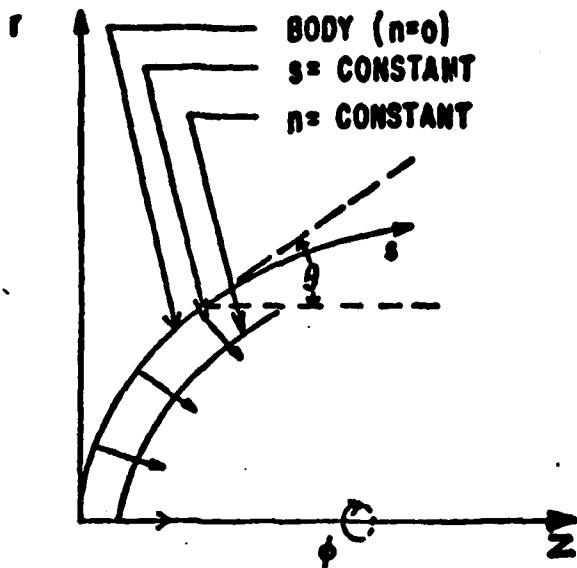


Fig. D1 Body-oriented coordinate system

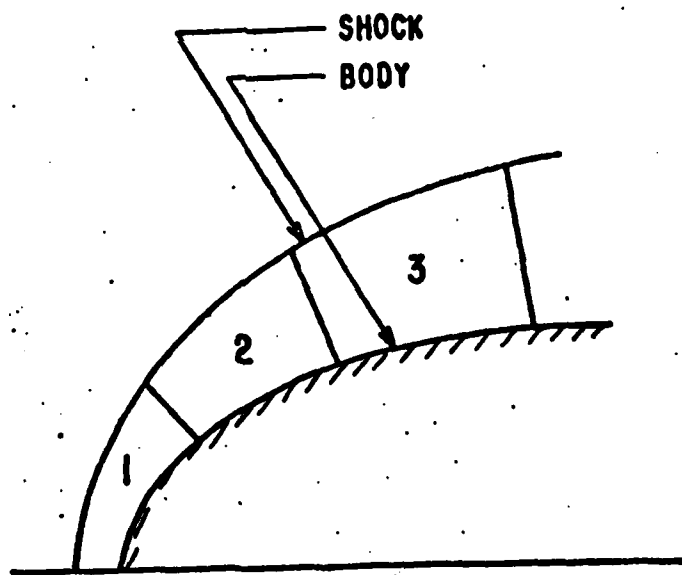


Fig. D2 Segmented solution procedure

## APPENDIX E

### The Shock-Capturing Method for Solving Steady Euler's Equations in the Supersonic Flow Region

#### 1. Introduction:

The conventional sharp shock theories (those that isolate a shock and apply the Rankine-Hugoniot shock relations across it) are limited in their capability of handling the shock-shock interaction problem and the formation of all embedded shock waves. Another approach in tackling this complex problem is to use a shock-capturing technique (SCT) which is capable of numerically predicting the location and intensity of all predominant shock waves without the explicit use of any shock fitting procedures.

The implementation of the numerical solution is greatly simplified if it is carried out in terms of a nonorthogonal coordinate system in which both body and shock are coordinate surfaces, rather than in terms of the original physical coordinate system.

The ability of an SCT to accurately predict the location and intensity of all shock waves in addition to the continuous portion of the flowfield depends in part on the finite difference scheme used. [14]

#### 2. Implementation of Shock-capturing Method by "D3CSS" [10]

Conservation of mass and momentum equations for a steady, inviscid flow are to be solved in the supersonic region of the shock layer bounded by the bow shock and the body surface. (Fig. E1)

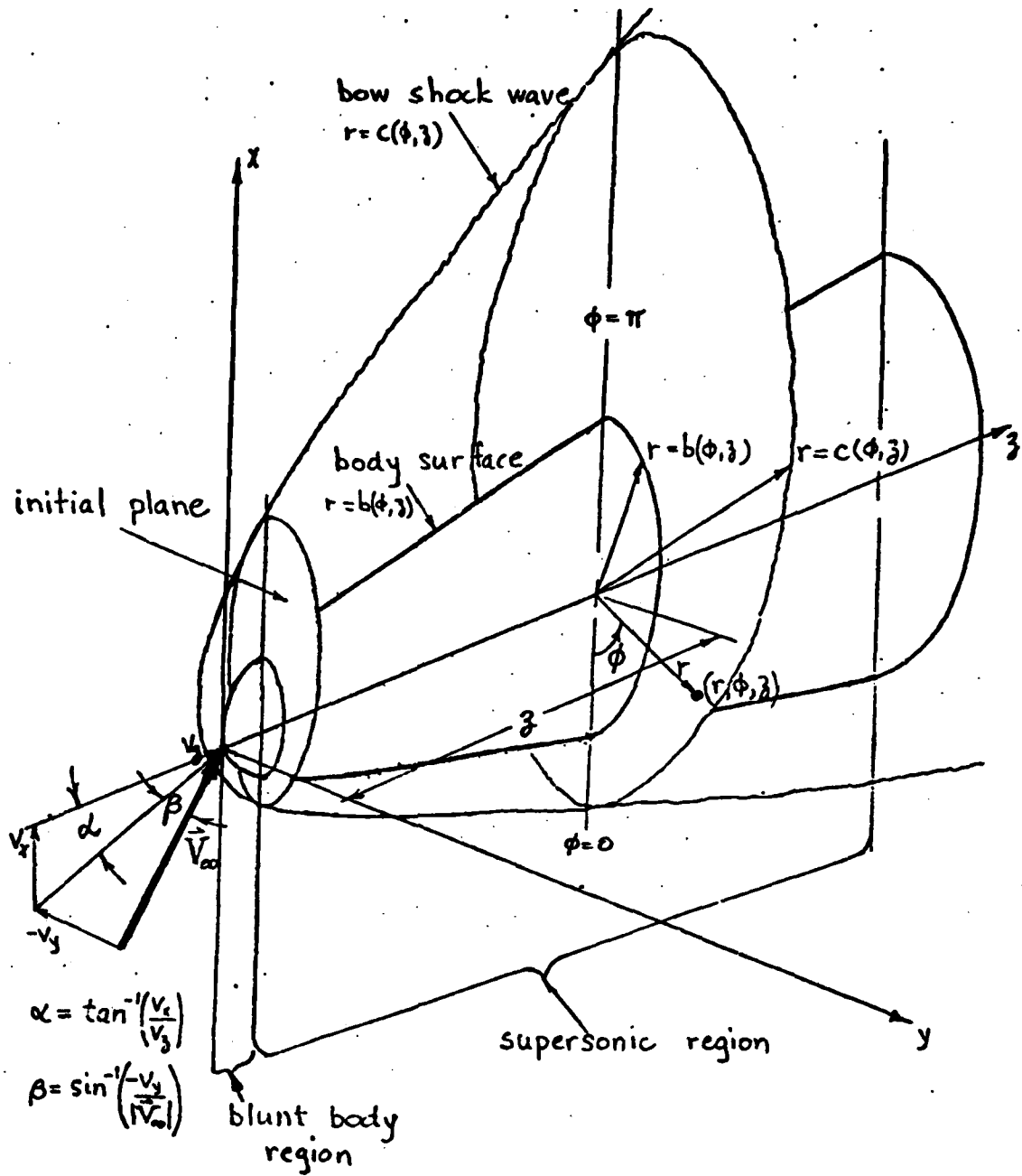


Fig. E1 Computational regions of D3CSS

The governing equations in cylindrical coordinates with  $z$ -axis along the axis of the body in the supersonic flow region (the velocity component in the  $z$ -direction is supersonic) is of hyperbolic type with  $z$ -axis as the time-like direction.

A nonorthogonal coordinate transformation is introduced which normalizes the distance between the body and the outer boundary. A second mapping maps this region one-to-one onto itself. The reason for doing this is to cluster computational points in the shock layer by choosing the mapping functions appropriately. This is an added feature of this computer code.

The system of partial differential equations is discretized and solved numerically in the computational space. (Fig. E2) For all points, the solution is advanced using predictor-corrector finite difference methods. Namely, the known solution at  $z = Z$ , say, is used to determine temporary (predicted) values at  $z = Z + \Delta Z$ ; then the predicted values are used to determine the final solution (corrected) values at  $z = Z + \Delta Z$ .

At the bow shock boundary, the Rankine-Hugoniot relations must be satisfied. These relations give the flow variables at the shock in terms of the shock geometry parameters (which are unknowns) and the free stream quantities. A special system of equations for the shock geometry parameters is numerically solved using a second-order accurate predictor-corrector method to advance the shock geometry.

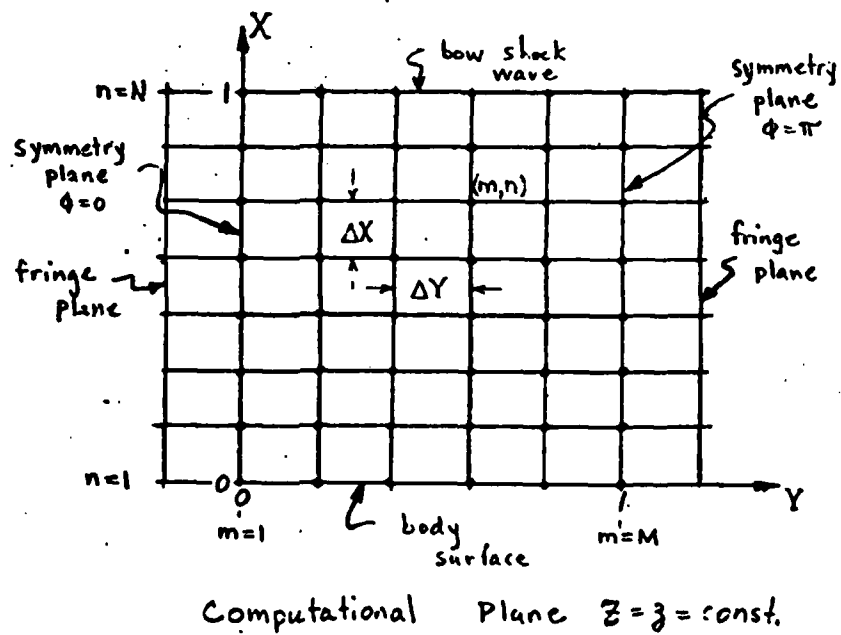
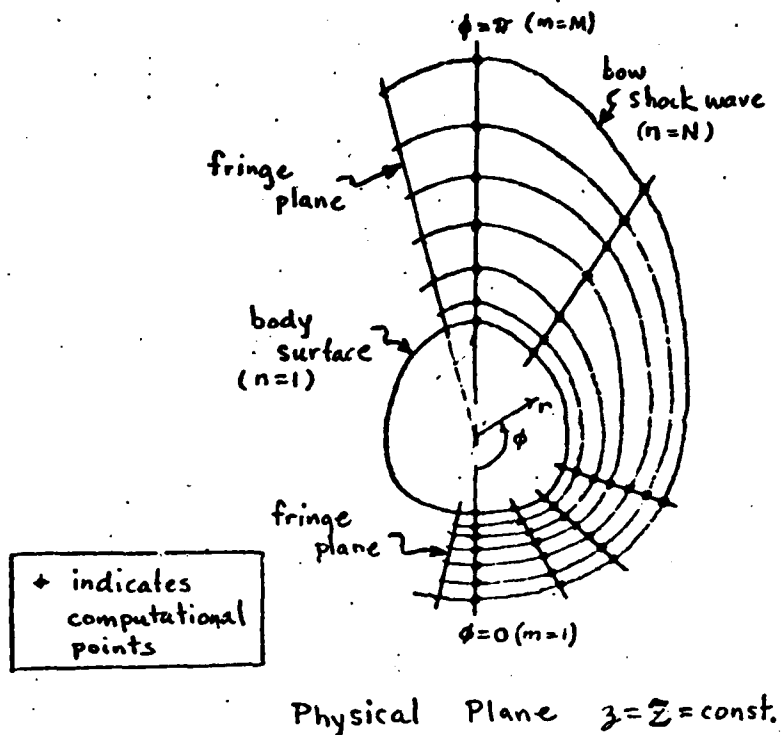


Fig. E2 Computational plane and corresponding physical plane for D3CSS

#### REFERENCES

1. H. Watman and R. Meyer, "Grumman High-Speed Aerodynamic Prediction Program," ADR 01-03-74.3, March, 1974.
2. B. J. White, "Aeromechanical Properties of Ejection Seat Escape System," Technical Report AFFDL-TR-74-57, April, 1974.
3. H. Lam, "A Refined Modeling of F-106 Ejection Seat/man Configuration," Grumman Report No. 392-79-01 (Proprietary), June, 1979.
4. A. E. Gentry, D. N. Smyth and W. R. Oliver, "The Mark IV Supersonic-Hypersonic Arbitrary-Body Program, Vol. I - User's Manual, Vol. II - Program Formulation, Vol. III - Program Listings," AFFDL-TR-73-159, November, 1973.
5. F. A. Woodward, "An Improved Method for the Aerodynamic Analysis of Wing-Body-Tail Configurations in Subsonic and Supersonic Flow, Program USSAERO, Part I - Theory and Application, Part II - Computer Program Description," NASA CR-2228, May, 1973.
6. R. L. Palko, "The AEDC Three-Dimensional Potential Flow Computer Program (FPF), Vol. I - Method and Computer Program, Vol. II - Mathematical Modeling, Application, and Verification," AEDC-TR-75-75, February, 1976.
7. A. H. Aungier, "A Computational Method for Two-Dimensional, Axisymmetric and Three-Dimensional, Blunt-Body Flows, (Program ATTACK)," AFWL-TR-70-124, February, 1971.
8. G. Morretti and M. Abbett, "A Time Dependent Computational Method for Blunt Body Flows," AIAA J., 4, pp. 2136-2141, 1966.
9. T. M. Liu, "Strategic Reentry Technology Program (STREET A IV), Vol. II - Three-dimensional Inviscid Flow Analysis, User's Guide for the Three-dimensional Blunt Cone Program," SAMSO TR-75-52, December, 1974.
10. J. M. Solomon, M. Ciment, R. E. Ferguson, J. B. Bell and A. B. Wardlaw, "A Program for Computing Steady Inviscid Three-Dimensional Supersonic Flow on Reentry Vehicles, Vol. I - Analysis and Programming, Vol. II - User's Manual," NSWL/WOL/TR-77-28/32, May, 1977.
11. I. O. Bohachevsky and E. L. Rubin, "A Direct Method for Computation of Nonequilibrium Flows with Detached Shock Waves," AIAA J., 4, pp. 600-607, 1966.
12. I. O. Bohachevsky and R. E. Mates, "A Direct Method for Calculation of Flow about an Axisymmetric Blunt Body at Angle of Attack," AIAA J., 4, pp. 776-782, 1966.

13. R. H. Aungier, "A Computational Method for Exact, Direct and Unified Solutions for Axisymmetric Flow Over Blunt Bodies of Arbitrary Shape (Program BLUNT)," AFWL-TR-70-16, July, 1970.
14. P. Kutler, R. F. Warming and H. Lomax, "Computation of Space Shuttle Flowfields Using Noncentered Finite-Difference Schemes," AIAA J. 11, pp. 196-204, February, 1973.
15. H. Watman, V. Seredinsky and J. Pastoral, "The Newtonian Aerodynamic Characteristics of Vertically Symmetric Configurations at Combined Angles of Attack and Sideslip," ADR 01-07-65.1, December, 1965.
16. H. Watman, "Assessment of the Unified Approach for Predicting the Hypersonic Characteristics of A High L/D Reentry Glider," ADR 22-02-73.4, February, 1973.
17. R. Meyer and H. watman, "Survey of GAC-HAPP Capabilities," ADR 01-01-73.2, June, 1973.
18. J. L. Hess, "Status of A Higher-Order Panel Method for Nonlifting Three-Dimensional Potential Flow," NADC-76118-30, or MDC J7714-01, August, 1977.
19. D. A. Caughey and A. Jameson, "Numerical Calculation of Transonic Potential Flow about Wing-Body Combinations," AIAA J. 17, pp. 175-181, February, 1979.
20. T. L. Holst and W. F. Ballhaus, "Fast, Conservative Schemes for the Full Potential Equation Applied to Transonic Flows," AIAA J. 17, pp. 145-152, February, 1979.

1979 USAF - SCEEE SUMMER FACULTY RESEARCH PROGRAM

Sponsored by the

AIR FORCE OFFICE OF SCIENTIFIC RESEARCH

Conducted by the

SOUTHEASTERN CENTER FOR ELECTRICAL ENGINEERING EDUCATION

FINAL REPORT

PETRI NET-RELATED MODELS FOR AVIONIC SYSTEMS

Prepared by: Aaron S. Collins

Academic Rank: Assistant Professor

Department and University: Electrical Engineering  
Tennessee Technological University

Research Location: Wright Patterson Air Force Base, Avionics  
Laboratory, Avionic Systems Engineering Branch

USAF Research Colleague: Lt. Barry Baxley

Date: August 17, 1979

Contract No: F49620-79-C-0038

## PETRI NET-RELATED MODELS FOR AVIONIC SYSTEMS

by

Aaron S. Collins

### ABSTRACT

Avionic systems are evolving toward concurrent processing computer architectures, and digital technology is becoming more functional in structure as very large scale integration continues to progress. Petri nets and Petri net-related models have been proposed as functional models for the design, simulation, and analysis of integrated hardware-software systems, particularly those which involve concurrent processing. Petri nets, LOGOS, the SARA Graphic Model of Behavior (GMB), Evaluation nets, and colored Petri nets were studied and compared, and an avionic subsystem was partially modelled. It was concluded that the combination of the GMB format restricted to LOGOS primitive structure would be of more general use than any of the individual models studied.

#### ACKNOWLEDGEMENT

The author would like to thank the Air Force Systems Command, the Air Force Office of Scientific Research, and the Southeastern Center for Electrical Engineering Education for the opportunity to spend a very useful and interesting summer at the Air Force Avionics Laboratory. I have learned a great deal which will benefit me in my future research efforts and which hopefully will also benefit the Air Force.

I would especially like to thank Colonel Raymond Siferd, Lieutenant Colonel Eugene Jones, Capt Greg Jolda, and Lieutenant Barry Baxley for providing strong support and an excellent working environment throughout the summer. The entire Avionics Laboratory administration was quite supportive. Also, Mrs Betty Hoover was conscientious and provided clerical work of high quality.

## I. INTRODUCTION:

In selecting the computer architecture for the next generation of avionic systems, the Air Force will have the opportunity to employ a reconfigurable, fault-tolerant multi-processor design. Also, with the rapid progress which is continuing in semiconductor technology, it is becoming possible to integrate more and more functions onto a single chip. The result is that functions which are currently conceived as multi-device subsystems will shift their hardware-software boundary in the near future. In addition, chips are becoming so complex that comprehensive testing and analysis may be replaced in some designs by functional testing and analysis.

These and other trends lead to a need for a common hardware-software language for describing systems. Such a language would model systems on the functional level with no clear delineation of hardware-software boundaries and would serve as a communication medium between hardware designers, software designers, reliability analysts, and simulation professionals. This would support the comparison of potential avionic computer architectures on a common basis and would aid in the design, analysis, simulation process for proposed integrated subsystems. Use of functional models is particularly appropriate for future system design efforts in view of the fact that higher levels of chip integration leads to a hardware design which is functional in structure.

The need for better tools for the design and analysis of fault-tolerant digital systems became evident to this researcher during the 1973-76 during the development of a computerized protection system for a nuclear power plant. It became clear that the reliability and capability of digital systems is limited, not just by manufacturing technology or cost, but by our ability to design, analyze, and verify complex systems. With a research background in simulation and computer-aided design, a project whose goal is to develop a better tool for the design and analysis of fault-tolerant systems has great appeal.

## II. OBJECTIVES:

The computer architectures being considered for future avionic system use involve concurrent processing, and Petri net models along with derivations of Petri nets appear to be the most promising approach to modelling concurrent processes. The initial research goal for this project was to determine the strengths and limitations of Petri net-like models for modelling concurrent processes and fault-tolerant systems for design, simulation, fault analysis, and as a common language among specialists. This goal was pursued using a four stage effort:

- (1) Perform a literature search to identify previous related work and models.
- (2) Compare the analytical and simulation properties of selected model formulations.
- (3) Model some example systems to obtain an ergonomic comparison and to classify useful hierarchy levels for avionic applications.
- (4) Draw conclusions and make recommendations for modelling and simulation of fault-tolerant, multi-processor avionic systems.

As the summer progressed, the literature survey was expanded to include some investigation of fault tolerant computer architectures and simulation of digital systems in order to facilitate a direct, realistic application of Petri net-like modelling during the follow-up phase of this investigation.

## III. LITERATURE SURVEY:

Computer literature searches (DDC and NTIS data bases) led to a consideration of the following models for concurrent processing models:

- (1) Petri nets
- (2) LOGOS
- (3) Graphic Model of Behavior
- (4) Evaluation Nets
- (5) Colored Petri nets

Petri nets (11, 13) were introduced by Carl Petri as a marked graph model for concurrent processes. Karp and Miller (5) developed the properties of a Vector Addition System which is equivalent to Petri nets, but is more amenable to numerical manipulation and analysis. A good overview of this early work is given in Peterson (11). LOGOS (19-29) was

developed at Case Western Reserve University and retains the VAS logic structure of Petri nets but adds the ability to model data structure and data access. This is needed for determinant analysis of concurrent processes. Evaluation nets (17) are a Petri net-like simulation tool, but they do not explicitly model data structure. The Graphic Model of Behavior (30-36) was developed at UCLA and is a simulation model which handles data structure in a manner similar to LOGOS, but does not adhere to Vector Addition System constructs. Colored Petri nets handle data, but also do not handle data structure. All these modelling systems evolved from Petri nets.

A description and comparison of these models is provided in the following section, and reference material is indicated in the partially annotated bibliography.

The fault-tolerant system literature (37-55) was selected based on its applicability to avionic systems and/or general historical value.

Functional fault analysis (56-58) is motivated by the same factors which lead to a need for a common language for modelling concurrent hardware/software systems . . . the increasing complexity of digital systems. It is hoped the functional modelling, design, and simulation will prove complementary to functional fault analysis.

The simulation references (59-62) represent a tiny sample from the vast simulation literature. Petri net-like models have potential application to analytic simulation during the early design stages and to operational simulation during advanced stages of design. Applications include fault simulation, reliability prediction, performance evaluation, and a number of other design and analysis facets.

The reliability references (63-65) are included as recognition that there exists a need for better reliability modelling and analysis tools for reconfigurable systems.

The multiple processor references (66-72) include some early considerations of multiple processor concepts.

The ADA references (73-76) are included since the preliminary definition of ADA contains some parallel process communication capability (called tasking in ADA). In the spirit of functional structure for hardware, it is probable that some future computer systems will implement some of the ADA

capabilities in hardware, including parallel process communications. As a consequence, it is wise to consider the capability of a concurrent process model to handle ADA constructs. Also, the language is so well thought out and has so much potential as a standard and better computer language that it is worthwhile to take this opportunity to encourage close monitoring of the progress of the ADA effort. Cost, reliability and software portability are closely entwined with the structure and capability of the computer language used.

The Remote Link Unit (77-78) is a proposed DAIS improvement which is still in the preliminary design stage. As such, it provided a convenient vehicle for evaluating the feasibility of introducing Petri net-like models early in the design stage as a common language between designers and design evaluators in an effort to speed up the evaluation process.

#### IV. COMPARISON OF PETRI NET-LIKE MODELS:

Petri nets were developed by Carl Petri as a marked graph model for concurrent processes. Much of the early work was quite theoretical in nature and does not have direct application to physical systems at this time. Of interest in later developments in Petri net applications are the conclusions drawn by Karp and Miller for Vector Addition Systems and by Gostelow (34) regarding proper termination. Bradshaw (20) develops relevant points which lead to a model which is amenable to analysis.

Figure 1D shows a simple Petri net model. If tokens are present at  $C_1$ ,  $C_2$ , and  $C_3$ , the transition is enabled to fire, and tokens will disappear at  $C_1$ ,  $C_2$  and  $C_3$  and will appear at  $C_4$  and  $C_5$ . Such simple sequencing of events is possible with Petri nets, but no consideration is given to time or to data transformations. All the remaining models in Figure 1 are essentially equivalent to the Petri net model. Notice that the E-net model could not handle three inputs to a single transition.

Figure 2 shows the LOGOS, VAS 'OR' operation. As is shown by the Vector Addition System computation, only one token is removed from the input places by a single transition firing. This constraint is necessary if tokens represent resources (such as jobs in a batch stream); it avoids losing resources. VAS logic is built into the LOGOS system and can be

enforced for the Graphic Model of Behavior. Tokens may reside on either arcs or control nodes (circles) in GMB models. The '+' in the dotted ellipse of the GMB model indicates that a token on either arc  $C_1$  or arc  $C_2$  will initiate the process associated with the control node. The '\*' indicates that upon termination of the process (after a specified delay), tokens will appear on both arc  $C_3$  and arc  $C_4$ . The E-net model allows the specification of a resolution procedure at each transition to determine which input node will fire first or which output node will receive a token. Since Petri nets fire only whenever all input places for a transition contain tokens ('AND' logic), two transitions are required to implement 'OR' logic.

Figure 3 shows the LOGOS Predicate Operator and approximate equivalents. The GMB Data Graph is shown in Figure 3B and illustrates the association of a processor (hexagon) with a control node (circle). Whenever a token resides in the control node, the associated processor is enabled. This processor may be a computer subroutine or hardwired logic. The token will move from the control node to one of the output arcs after a specified delay. The processor in Figure 3B may read data cells A and B and may write data cell C. The data cell  $C_T$  is included to indicate that LOGOS logic can be implemented using GMB structure. The LOGOS token exits to either  $C_2$  or  $C_3$  based on the value of the logical data variable,  $C_T$ . Also, LOGOS supports a data graph identical to that of the GMB system but does not incorporate a time delay. Data access information is indicated by the directed arcs (arrows) in the data graph and is required for analysis of concurrent processes (discussed later). The E-net model incorporates a resolution procedure to determine whether the token moves to  $C_2$  or  $C_3$  and assigns attributes to tokens to model data. Also, time is associated with each E-net transition. No data structure is included in the E-net model, however. Of special interest in this figure is the fact that the Petri net model chooses to send the token to  $C_2$  or  $C_3$  randomly. Rarely is such indiscriminate behavior allowable in real systems, and this represents an inherent limitation of Petri net models. The flow chart is included to indicate that software can be modelled using these constructs.

The GMB system is part of a larger SARA (System Architects Apprentice) system which includes structural constraints and checks for developing structured software and systems. Petri nets have no data handling capability, therefore offer a control flow only model of software (Item 8).

The concepts of determinacy, safeness, and deadlock are discussed by Peterson (11). The Vector Addition System of Karp and Miller and Proper Termination analysis of Gostelow, et-al, offer a mechanism for analysis of marked graphs for these important properties. Bradshaw developed this analysis for the LOGOS system. E-nets are always safe (never have more than one token in a location), but give up considerable modelling power to achieve this. Also, since they do not support data structure definition, they are not analyzable for determinacy. GMB models can be analyzed for these properties only if model structures are restricted. No significant loss in modelling power results from such restrictions, however.

Item 13 indicates that E-nets and the GMB system are both easily applied as simulation models. The GMB model is more flexible, however, and has the advantage of modelling data structure. LOGOS suffers from the lack of a mechanism for modelling time.

#### V. EXAMPLE SYSTEM (RLU) MODELS:

To determine the feasibility of using Petri net-like models as a common language between specialists, a proposed DAIS subsystem which is now in the preliminary design stage was partially modelled. The primary reason for a partial model is that the proposed system, the Remote Link Unit (RLU) (77,78) is not yet completely specified.

The RLU is an intelligent unit which links DAIS to subsystems in such a way as to make subsystem differences somewhat transparent to DAIS. The advantages of the RLU concept are discussed in the referenced documents.

The RLU system includes some memory and logic capability associated with each subsystem. This small unit or Nameplate is specified in some detail in the Preliminary Functional Design of the Subsystem/RLU Interface (77) referenced above. Figure 5-3 of that document describes the Nameplate Architecture and Figure 5-4 is the associated State Diagram and Timing Diagram. These figures are reproduced in this report for reference purposes

Table 1 is a subjective and informal comparison of the properties of Petri net-like models of concurrent systems. The various models were developed with different goals in mind and at different times in the evolution of concurrent process and Petri net theory. As a consequence, their structure and properties vary. The next several paragraphs discuss Table 1.

Item 1 indicates that all the models were intended for use in analysis of concurrent processes, but that Petri nets were formulated as a theoretical analysis tool. E-nets were intended primarily as a simulation model, and LOGOS was developed as a design and analysis aid. The GMB system was intended as a comprehensive design and simulation tool with analysis also possible. Since the GMB system does not necessarily restrict itself to the VAS constructs for token flow, LOGOS has the advantage of allowing VAS analysis.

A graphical package (Item 2) may have been developed for all the systems by this time. Item 4 indicates that E-nets, GMB, and LOGOS either require or may require conditions on output locations prior to firing a transition. As a result, this internal logic is not visible in the graphic model as it is in a Petri net model. Requiring output locations to be empty prior to transition firing aids in assuring a 'safe' net in that no multiple or lost tokens are generated due to placing one token in the same place as another.

Item 5 indicates that Petri nets allow transitions to fire only if all input places contain tokens. E-nets and LOGOS allow 'OR' firings, but tokens are conserved by allowing only one input token to be removed by a single firing. The GMB system allows any logic, but should be restricted to LOGOS type firing logic if a determinant, safe, analyzable net is desired.

Data modelling is necessary to support analysis of a system for determinancy. If process A reads and writes a memory location, then process B reads and writes the same location, a particular result will ensue. If it is possible for the order in which process A and process B access the location to be reversed, then the result is indeterminant. Data flow modelling is therefore necessary to handle determinancy analysis (Item 10).

as Figures 11 and 12, respectively.

Figure 4 shows a GMB form for the RLU Nameplate Model. The Control Graph on the left is connected with the Data Graph on the right by the dotted lines which connect associated Control Nodes and Data Processors. The presence of a token on the 'start' arc indicates that power is on, and the system is ready for operation. No clock pulses occur between messages sent to the Nameplate, so the first clock pulse to arrive indicates that a transmission is beginning. Nodes CN1 and CN1.5 model the UART which converts the serial bits transmitted to the Nameplate by the RLU to a parallel word. The word is decoded and control is transferred to the 'execute' processor, CN2/P2, or to the 'wait for command gap' processor, CN5/P5, depending on whether the command is addressed to this Nameplate or to another one. CN3 is activated only if the command does references memory. CN2 would be expanded into much greater detail if the system simulation were intended to allow execution of specific instructions.

The pins or data/control lines connected to the Nameplate are all modelled as data except the first clock pulse in a transmission which is treated as a control marker or token, and subsequent clock pulses which are implicitly modelled as time delays associated with each control node. Several other compromises are possible, but if the initial clock pulse is treated as data, the initial node must have a loop associated with it to enable processor, P0, to continuously check for the presence of a clock pulse. Such a model would be inefficient in terms of CPU time required for simulation.

Figure 5 shows a Petri net model for the RLU Nameplate. The key items to note here are that there exists no mechanism for determining which of two enabled transitions, such as the three transitions following the 'wait and decode' node or the two transitions following the 'execute' node, will fire. This randomness limits the usefulness of Petri nets in their purest form. Also, no data values are associated with this graph.

Figure 6 shows a LOGOS model for the RLU Nameplate control flow. The LOGOS model requires the three way decision following the 'wait and decode' node to be broken into two two-way decisions. Also, the LOGOS control graph employs nineteen primitives (blocks) of four types whereas

the GMB control graph employs seven primitives (circles) of a single type. From an ergonomic viewpoint, the GMB model has clear advantages over LOGOS. This is especially clear when it is observed that the State Diagram drawn by the RLU designer at the top of Figure 12 is almost equivalent to the GMB control graph.

The E-net model in Figure 7 employs resolution procedures to make control flow decisions, and like the LOGOS model, must break the three-way decision into two two-way decisions. The E-net model requires twenty individual blocks of two types, so it also does not fare well in an ergonomic comparison.

Note that this GMB functional model contains essentially enough structural information for simulation of the Nameplate functions. Some additional details need to be specified, however. The model could be merged with DAIS and RLU models to yield a complete RLU functional model with the Nameplate model as a subsystem. Reference to the description of the GMB simulation language, PLIP, as described by Razouk and Estrin (35), indicates how easily the control graph and data graph can be converted into simulation language. About twenty lines of PLIP code would be sufficient to describe the information in Figure 4. An additional subroutine would be required to describe operations for each of the seven data processors.

Figure 8 shows the Interface Configuration Adapter (ICA) to Subsystem processing for a Serial Input Operation - Refresh Mode. This operation is described in Section 4.3.3 and Figure 4-11 (a) of the Preliminary Functional Design of the Subsystem/RLU Interface (77). Both local data storage and bus data are represented in the data graphs.

Figure 9 shows RLU Asynchronous Message Operation as described in Figure 3-3 of the Preliminary Functional Design of the DAIS/RLU Interface (78). The three processors could be simulated individually with communication linkage essentially equivalent to hardware linkage, or the entire net shown in Figure 9 could be simulated as an entity. Clearly, any individual control note can be replaced by a detailed subgraph if a more detailed simulation is needed. This particular graph represents data as virtual data without consideration of multiplexing of data lines.

Figure 10 shows the control graph for the first few blocks of the Initialization Sequence defined in Figure 3-4 of the Preliminary Functional Design of the Subsystem/RLU Interface. The communication through shared memory which is involved in this sequence was modelled by a data graph, but the data graph was found to be somewhat cluttered due to the number of data words involved in the sequence. It would be sufficient and easy to model such data linkage directly in the PLIP language mentioned earlier. That language shows the data structure clearly and explicitly.

#### VI. CONCLUSIONS AND RECOMMENDATIONS:

Either the GMB, the E-net, or the LOGOS model could be modified to serve as a common language between hardware, software, fault analysis, and simulation specialists. Varying degrees of effort and success would result, however, depending on which model is chosen.

The E-net model suffers from primitives which are too restrictive. This makes the analysis of E-net models easier, but limits their modelling power. As a consequence, modelling with E-net is sometimes clumsy and artificial. Also, the gains in ease of safety analysis are offset by the lack of a model for data structure. The E-net approach has its place in the evolution of Petri net concepts, but even from an ergonomic standpoint are somewhat undesirable as system models. It is not likely that any of the specialists listed above will develop a fondness for E-nets if exposed to GMB.

The LOGOS model is quite adequate as a representation of both control and data structure. It, however, lacks a mechanism for handling time so it needs substantial modification to serve as a simulation model. It results in a cluttered model, as was observed for the Nameplate model, and flunks the ergonomic appeal test. Also, LOGOS is implemented in SAIL which means that all users must learn a new language. Its strongest appeal is its adherence to vector addition system control structure and the large amount of analysis software already developed in the LOGOS system.

The Graphic Model of Behavior system could be used with its control structure limited to LOGOS constructs. This would result in a one-to-one correspondence between GMB and LOGOS models, and would allow LOGOS analysis

of GMB simulation models or vice versa. GMB is the only model considered which handles both time and data structure. In addition, the SARA system has some additional tools for support of structured design. The SARA system is implemented in PL/1 which is more widely used than SAIL. Finally, the GMB model is ergonomically appealing. Only control nodes stand out on the control graph, and as a result the ratio of information to data is higher for the GMB model than for other models. Also, since the GMB model looks essentially like a state diagram, it should be more readily accepted by all computer people than by the other, more radical, models.

Petri net models need time, decision power, and data structure added in order to conveniently represent real systems. If this is done, the result will be similar to GMB or LOGOS.

The overall conclusion to be drawn from this study is that the GMB formulation is applicable to functional design, simulation, and use as a common language between specialists. In addition, it appears that it can also be used for fault studies.

The partial modelling of the RLU lead to the conclusion that the designer could easily develop GMB models for hardware/software systems, and that he would not find the models strange. This could greatly speed up the simulation and evaluation process. Also, it would result in a more complete and consistent design specification. The designer would not need to do just a partial model as was done in this report; he could easily fit all the pieces together into a hierarchy of models which would completely describe the system. One of the major advantages of simulating a system is that the process of developing a simulation model is very enlightening. Why not have the designer develop the model and fill in all the missing gaps in the specification instead of waiting for someone downstream of the designer to need missing information?

It is recommended that the GMB model be used to model a fault-tolerant, reconfigurable computer architecture which is specified adequately to allow performance analysis in order to determine the validity and usefulness of this approach for comparison of competing architectures. The GMB control structures should be limited to LOGOS constructs.

It would be instructive to develop a complete GMB model for an avionic subsystem and obtain an evaluation of its usefulness from key simulation and fault analysis personnel. Fault analysis and reliability applications have not been adequately addressed by this study.

Decisions relating to further development of GMB/LOGOS type models should be based on the slope of the trend toward functional hardware structure and functional testing and analysis.

The progress of the development of the ADA language should be closely monitored. If a GMB/LOGOS tool is to be used widely, it may be advantageous to develop an integrated tool in ADA.

PARTIALLY ANNOTATED BIBLIOGRAPHY

Petri nets

1. Ayache, J.M., P. Azema, M. Diaz, "Observer - A Concept for On-Line Detection of Control Errors in Concurrent Systems," FTCS-9, 1979.

A Petri-net run time observer to monitor the control structure of concurrent processes is proposed.

2. Han, Y.W. and W.L. Heimerdinger, "Transformation a Petri Net-Like Labelled Graph to a Directed Graph for Graph Error Detection." FTCS-7, 1977.
3. Holt, A.W., "Research on Information System Specification," N00014-76-C-0781, Aug 1977.
4. Hopcroft, J. and J. Pansiot, "On the Reachability Problem for 5-Dimensional Vector Addition," N00014-67-A-0077-0021, June 1976.
5. Karp, R.M. and R.E. Miller, "Parallel Program Schemata," J. Computer and Systems Science, 3,4 May 1969.
6. Keller, Robert M., "Formal Verification of Parallel Programs," C M, July 1976.

Deadlock and determinacy are treated in a theoretical manner using proof of assertions.

7. Miller, Raymond E., "A Comparison of Some Theoretical Models of Parallel Computation," IEEE Trans. on Computers, Aug 1973.

Petri nets, computational graphs, and parallel program schemata are compared as theoretical models for parallel computation.

8. Miller, R.E., "Talk Notes on Mathematical Studies of Parallel Computation," N00014-75-C-0752, Oct 1976.
9. Misunas, David, "Petri nets and Speed Independent Design," Comm. of ACM, Aug 1973.

Some elementary systems are modelled using Petri nets.

10. Peterson, James L., "Computation Sequence Sets," Journal of Computer and System Sciences, 13, 1-24, 1976.

Formal (theoretical) consideration of CSS language which is based on generalized Petri nets.

11. Peterson, James L., "Petri Nets," Computing Surveys, Vol. 9, No. 3, Sept 1977.

An excellent survey of Petri net theory, but does not address data structure, time, or other considerations required for general application of Petri nets.

12. Peterson, W.W. and A. Lew, "An Investigation of Computer System Problems," ARO-11944, 16-M, Apr 1977.
13. Petri, C.A., Translation is supplement to T.R. RADC-TR-65-337, Vol. 1, Griffis Air Force Base, N.Y., 1965.
14. Zervos, C.R. and K.B. Irani, "Colored Petri Nets: Their Properties and Applications," RADC-TR-77-246, Aug 1977.

#### E-Nets

15. Murato, T., "State Equations for E-Net Interpreted Marked Graphs," 19th Midwest Symposium on Circuits and Systems, U. of Wisconsin, 1976.
16. Murato, Tadao and Tasvir Shah, "On Liveness, Deadlock, and Reachability of E-nets," 14th Annual Allerton Conference on Circuits and System Theory, U. of Illinois, Oct 1976.
17. Noe, Jerre D. and Gary J. Nutt, "Macro E-Nets for Representation of Parallel Systems," IEEE Trans. on Computers, Aug 1973.

A good brief introduction to E-Nets. (Nutt's Thesis is a better definition of E-net capabilities and limitations).

18. Nutt, G.J., "Evaluation Nets for Computer Performance," FJCC, 1972.

#### LOGOS

19. Bradshaw, F.T., "Some Structural Ideas for Computer Systems," CWRU, Oct 1971.
20. Bradshaw, F.T., "Structure and Representation of Digital Computer Systems," Ph.D. Thesis, CWRU, Jan 1971.
21. Glaser, E.L., "Introduction and Overview of The LOGOS Project," CWRU, Oct 1971.
22. Heath, F.G. and C.W. Rose, "The Case for Integrated Hardware/Software Design, with CAD Implications," CWRU, Oct 1971.
23. Heath, F.G., "Project LOGOS - A Computer-Aided Design System for Integrated Hardware and Software," CWRU, Oct 1971.
24. Katzke, S.W., "A Graph Oriented Data Structure Language," Ph.D. Thesis, CWRU, June 1973.

25. "LOGOS Implementation Note 10, Capabilities of LOGOS 1.5," Report to AFAL, Contract No. F33615-76-C-1208, Aug 1976.
26. Plinor, M.S. and C.W. Rose, "A Primitive Data Base Management System for an Integrated Computer Aided Design Facility," CRWU, Oct 1971.
27. Rose, C.W., "A System of Representation for General Purpose Digital Computer Systems," Ph.D. Thesis, CWRU, Sept 1970.
28. Rose, C.W. and F.T. Bradshaw, "The LOGOS Representation System," CWRU, Oct 1971.
29. Torson, J.M., "Deadlock Prevention and Analysis of Control Flow Behavior in Digital Computer Systems." Report to Advanced Research Projects Agency, Contract No. DAAB-03-70-C-0024, July 1973.

SARA (GMB)

30. Campos, Ivan M. and Gerald Estrin, "Specialization of SARA for Software Synthesis," Proceedings of SDAM, 1977, Palo Alto.
31. Estrin, Gerald, "Modeling for Synthesis - The Gap Between Intent and Behavior," Proceedings of Symposium on Design Automation and Microprocessors, Feb 24-25, 1977, Palo Alto, CA.

This paper defines the SARA primitives.

32. Gardner, Robert I., "Multi-level Modelling in SARA," Proceedings of SDAM, 1977, Palo Alto.

Discusses nested structure capabilities of SARA.

33. Gardner, Robert I., "State of the Implementation of SARA," Proceedings of SDAM, 1977, Palo Alto.

A discussion of how the SARA subsystems fit together.

34. Gostelow, K.P., V.G. Cerf, and G. Estrin, "Proper Termination of Flow of Control in Programs Involving Concurrent Processes," Proceedings of the ACM Annual Conference, Aug 1972.

35. Razouk, Rami R. and Gerald Estrin, "The Graph Model of Behavior Simulation," Proceedings of SDAM, 1977, Palo Alto.

A good explanation of GMB with examples. Includes discussion and examples of modeling language.

36. Overman, William T. and Gerald Estrin, "Developing a SARA Building Block - The 8080," Proceedings of SDAM, 1977, Palo Alto.

An enlightening chip model based on timing diagram and state transitions.

### Fault-Tolerant Systems

37. Avizienis, Algirdas, "Architecture of Fault-Tolerant Computing Systems," FTCS-5, 1975.

A classic paper introducing the contrasting terms, fault-intolerance vs. fault-tolerance.

38. Avizienis, Algirdas and Liming Chen, "N-Version Programming: A Fault-Tolerance Approach to Reliability of Software Operation," FTCS-8, 1978.

39. Goldberg, Jack, "New problems in Fault-Tolerant Computing," FTCS-5, 1975.

An overview of problems which need solutions.

40. Han, Y.W. and W.L. Heimerdinger, "Theory of Fault Tolerance - 1977 Final Report," ONR Contract No. N00014-75-C-0011, Dec 1977.

41. Heimerdinger, W.L., et-al, "A Fault Tolerant Assessment of DAIS," Final Report, AFAL contract.

42. Heimerdinger, W.L. and L.A. Jack, "A Graph Theoretic Approach to Fault Tolerant Computing," AFOSR-TR-76-0506, Mur. 1976.

43. Heimerdinger, W.L., Y.W. Han, and L.A. Jack, "Theory of Fault Tolerance Volume 1, 1976 Final Report," N00014-75-C-0011, Dec 1976.

44. Heimerdinger, W.L. and Y.W. Han, "A Graph Theoretic Approach to Fault Tolerant Computing," F44620-75-C-0053, Sept 1977.

45. Hopkins, Albert L., Jr., "Design Foundations for Survivable Integrated On-Board Computation and Control," JACC, 1977.

A brief survey with identification of areas in which further development is needed.

46. Jack, L.A., "Theory of Fault Tolerance, Volume 2," N00014-75-C-0011, Dec 1976.

47. Jack, L.A., W.L. Heimerdinger, and M.D. Johnson, "Theory of Fault Tolerance - 1974-75 Final Report," Sept 1975.

48. Kurzhals, Peter R. and Richard Deloach, "Integrity in Flight Control Systems," JACC, 1977.

Brief NASA summary of flight control system evolution.

49. Meyer, J.F., D.G. Furchtgott, and L.T. Wu, "Performability Evaluation of the SIFT Computer," FTCS-9, 1979.

50. Rennels, David A., Algirdas Avizienis, and Milos Ercegovac, "A Study of Standard Building Blocks for the Design of Fault-Tolerant Distributed Computer Systems," FTCS-8, 1978.

51. Saheban, F., L. Simoncini, and A.D. Friedman, "Concurrent Computation and Diagnosis in Multiprocessor Systems," FTCS-9, 1979.

Formal consideration of concurrent computation/  
diagnosis by parallel processors.

52. Siewiorek, D., M. Canepa, and S. Clark, "C.VMP: Analysis, Architecture, and Implementation," AFOSR-TR-77-0449, Dec 1976.
53. Weinstock, Charles B. and Jack Goldberg, "SIFT: Software Implement Fault-Tolerance," Ninth Annual International Symposium on Fault-Tolerant Computing, FTCS-9, IEEE Computer Society, 1979.

A brief summary of SIFT concepts.

54. Westermeier, T.F., "Redundancy Management of Digital Fly-By-Wire Systems," JACC, 1977.

McDonnell Aircraft, a brief theoretical treatment of  
FBW.

55. Ultrasystems, Inc., "Definition and Trade-off Study of Reconfigurable Airborne Digital Computer System Organization," NASA Final Report, Nov 1974.

#### Functional Fault Concepts

56. Han, Y.W. and W.L. Heimerdinger, "Theory of Fault Tolerance, 1977 Final Report," Honeywell Report, Contract No N00014-75-C-0011 (ONR).
57. Jack, L.A., "Functional Faults," Special Sessions on Fault Tolerant Computing of 1976 Johns Hopkins Conference on Information Sciences and Systems, April 1976.
58. Thatte, Satish M. and Jacob A. Abraham, "A Methodology for Functional Level Testing of Microprocessors," FTCS-8, 1978.

#### Simulation Applications in Fault Tolerant Systems

59. Crowley, C.P. and J.D. Noe, "Interactive Graphical Simulation Using Modified Petri Nets," Symposium on Simulation of Computer Systems, NBS, Aug 1975.
60. Hong, Se June, "Fault Simulation Strategy for Combinational Logic Networks," FTCS-8, 1978.
61. Iwata, H.Y. and M.M. Cutler, "CSPII - A Universal Computer Architecture Simulation System for Performance Evaluation," SSCS, Nat. Bureau of Standards, Aug 1975.
62. Levy, H. Oliver and Ralph B. Conn, "A Simulation Program for Reliability Prediction of Fault Tolerant Systems," FTCS-5, 1975.

### Reliability

63. Avizienis, A. and Ying-Wah Ng, "A Reliability Model for Gracefully Degrading and Repairable Fault-Tolerant Systems," FTCS-7, 1977.
64. Hecht, Linda O. and Joseph R. Fragola, "Reliability Data Bases - A Review," Joint Automatic Controls Conference, 1977.

Attempts to identify and classify sources of information on component reliability statistics.

65. Ingle, Ashok D. and Daniel P. Siewiorek, "Reliability Models for Multiprocessor Systems With and Without Periodic Maintenance," FTCS-7, 1977.

### Multiple Processor Systems

66. Baer, J.L., "A Survey of Some Theoretical Aspects of Multiprocessing," Computing Surveys, March 1973.

Broad and extensive survey of concepts models, and simulation of multi-processor systems.

67. Bernstein, A.J., "Analysis of Programs for Parallel Processing," IEEE Trans. on Electronic Computers, Oct 1966.
68. Dijkstra, E.W., "The Structure of "THE" - Multiprogramming System," CACM, May 1968.
69. "Distributed Systems," Infotech State of the Art Report, 1976.

Includes an annotated bibliography as well as a broad overview of concurrent processing. 'Distributed systems' is loosely interpreted so that most concurrent processing topics are allowed in the report.

70. Habermann, A.N., "Prevention of System Deadlocks," Communications of the ACM, July 1969.
71. Habermann, A.N. and D.L. Parnas, "Comment on Deadlock Prevention Method." CACM, Sept 1972.
72. Hold, Richard C., "Comments on Prevention of System Deadlocks," CACM, Jan 1971.

### ADA

73. A Tutorial: An Informal Introduction to ADA, Apr 1979.

The opening four examples provide a quick introduction to ADA concepts.

74. Rationale for the Design of the ADA Programming Language, ACM, Sigplan Notices, June 1979.

Recommended reading for all computer professionals. Comprehensive discussion of Programming Language features and why they are important. Chapter 11, Tasking, discusses communication between parallel processes.

75. Set of Sample Problems for ADA, Apr 1979.

Ten well-selected problems are formulated, programmed in ADA, and discussed. Illustrates the power of ADA.

76. Preliminary ADA Reference Manual, ACM, Sigplan Notices, June 1979.

A more concise and complete definition of ADA.

Remote Link Unit

77. Tavora, C.J., et-al, "Preliminary Functional Design of the Subsystem/RLU Interface," University of Houston for USAFSC, May 1979.
78. Tavora, C.J., et-al, "Preliminary Functional Design of the DAIS/RLU Interface."

TABLE 1 INFORMAL COMPARISON OF PROPERTIES OF PETRI NET-LIKE MODELS

<u>ITEM</u>	<u>EVALUATION CRITERIA</u>	<u>PETRI NETS</u>	<u>E-NETS</u>	<u>GMB (SARA)</u>	<u>LOGOS</u>
1	Modelling System Goals	Analysis Tool	Simulation Tool, Analysis Tool	Simulation Tool, Analysis Tool, Design Tool	Analysis Tool Design Tool
2	Graphical Package	TBD	TBD	TBD	Yes
3	High Level System Definition Language (Control and Data) Defined and Implemented	TBD	Partially Defined (Control Only)	Yes	Yes
4	Feedback Structure Visible in Model (Pipeline, etc.)	Yes	No	No	No
5	Logic Capabilities	'AND' Only	'AND', 'OR', with Conservation	Any Logic	'AND', 'OR' with Conservation
6	Data Modelling	None	Ad Hoc	Structure is Part of Graph	Structure is Part of Graph
7	Implementation Language, Portability	TBD	TBD	PL1 + Special Functions	SAIL + Special Functions
8	Software Structure Enforced in Model	TBD	TBD	Substantial Structural Constraints Available and Programmed into the System	TBD

TABLE 1 INFORMAL COMPARISON OF PROPERTIES OF PETRI NET-LIKE MODELS (Cont'd)

ITEM	EVALUATION CRITERIA	PETRI NETS	E-NETS	GMB (SARA)	LOGOS
9	Modelling of Hardware and Software	No Algorithmic (Software) Capability	Can Model Both Hardware and Software	Can Model Both Hardware and Software	Can Model Both Hardware and Software, Software Capability Limited
10	Can Analyze for Determinancy and Structure to be Determinant	Not Practical: One Location can Feed Two Transitions, No Data Constraints	No Data Constraints or Models (Needs Data Structure to Support Proper Termination Analysis)	Yes	Yes
11	Can Analyze for 'Safe' Property	Reachability Tree	Can Be Forced without Analysis	Yes (Needs Some Additional Primitive Structure)	Yes
12	Can Analyze for Deadlock Freeness and Design to Avoid Deadlock Freeness	Not Practical, Deadlocked Model Likely for Concurrent Sys.	No: Proper Termination Requires Data Structure	Yes	Yes
13	System Simulation	Flow of Control Only	Flow of Control and Real Time Simulation of Algorithms	Flow of Control and Real Time Simulation of Algorithms	Flow of Control only (Needs Time + Simulation Capabilities Added)
14	Can Support a Hierarchy of Models	Yes	Yes	Yes, and Structure for Multi-Level Interface is Defined	Yes

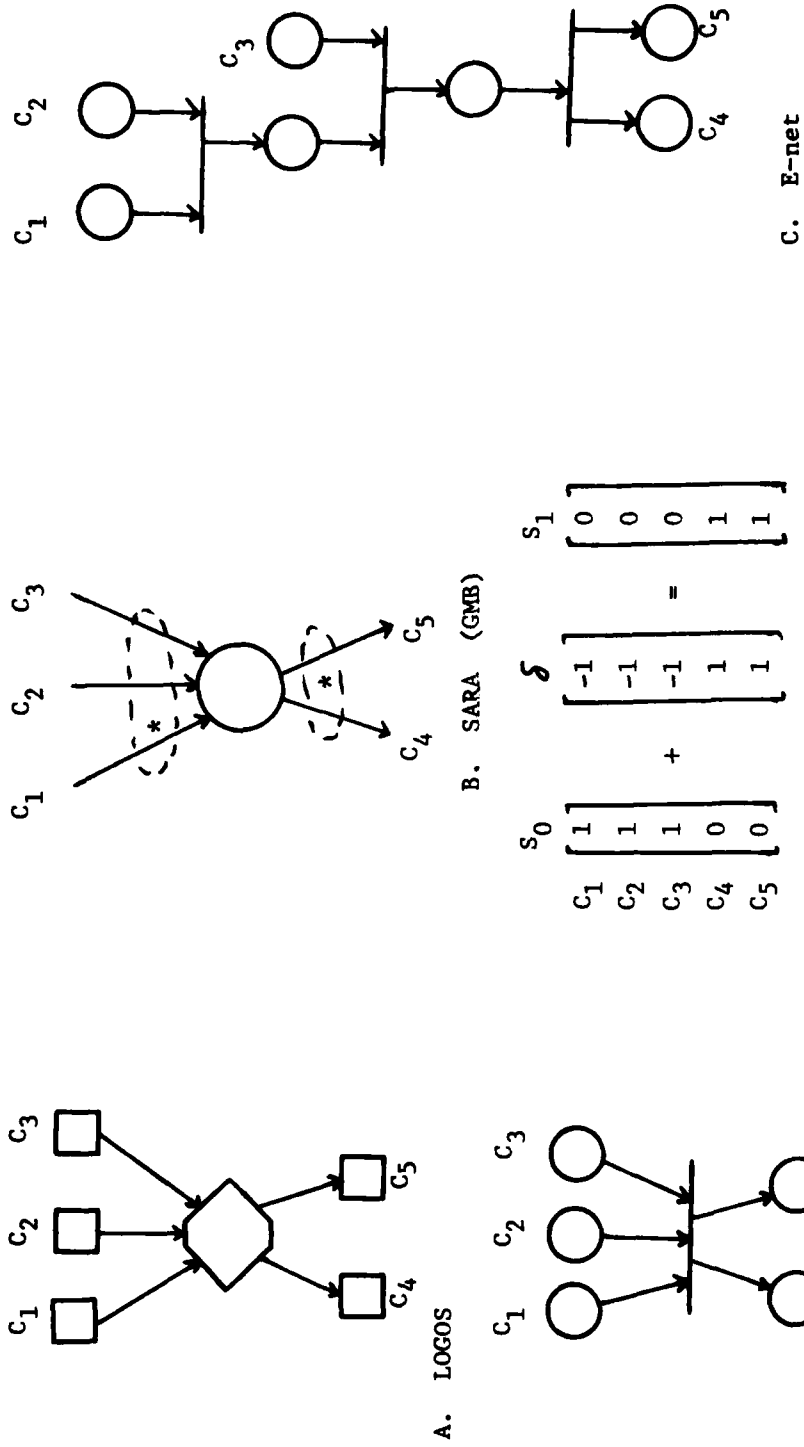


Figure 1. LOGOS 'AND' OPERATOR CELL WITH EQUIVALENT MODELS.

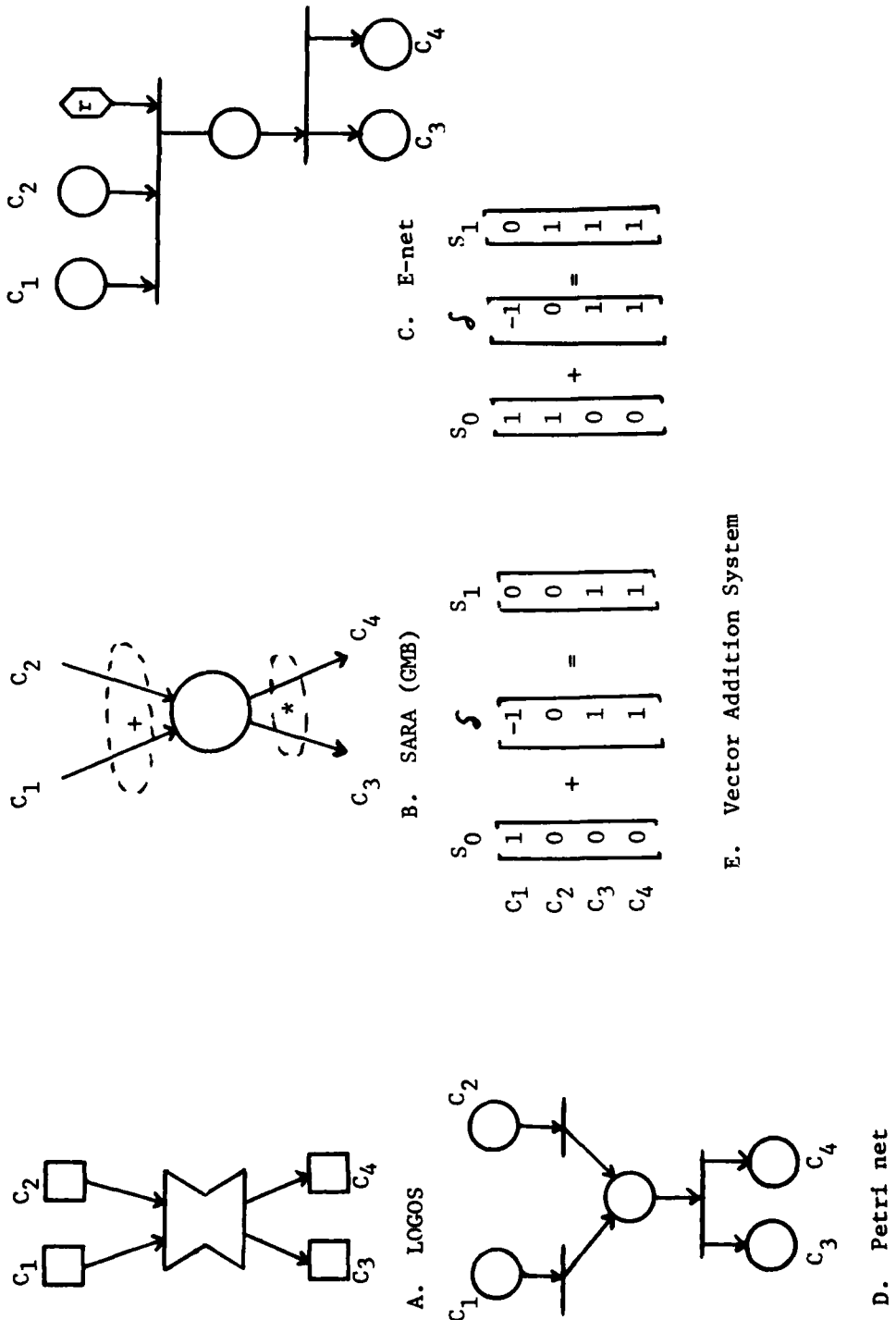
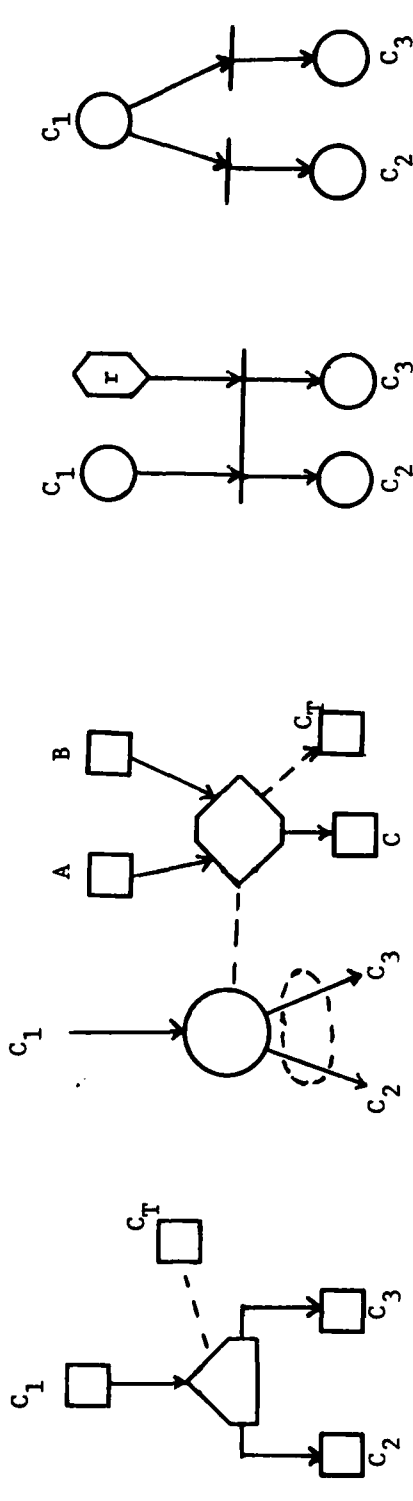


Figure 2. Modelling Equivalents of LOGOS Primitive, OR.

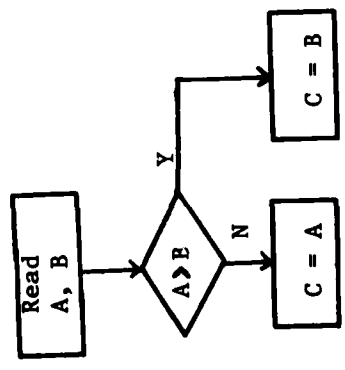


A. LOGOS

B. SARA (GMB)

C. E-net

D. Petri net



E. Flow Chart

$$\begin{matrix} C_1 \\ C_2 \\ C_3 \\ C_T \end{matrix} \quad S_0 \begin{bmatrix} 1 \\ 0 \\ 0 \\ 1 \end{bmatrix} + \delta \begin{bmatrix} -1 \\ 1 \\ 0 \\ 0 \end{bmatrix} = S_1 \begin{bmatrix} 0 \\ 1 \\ 0 \\ 1 \end{bmatrix}$$

F. Vector Addition System

Figure 3. Modelling Equivalents of LOGOS Primitive, Predicate Operator

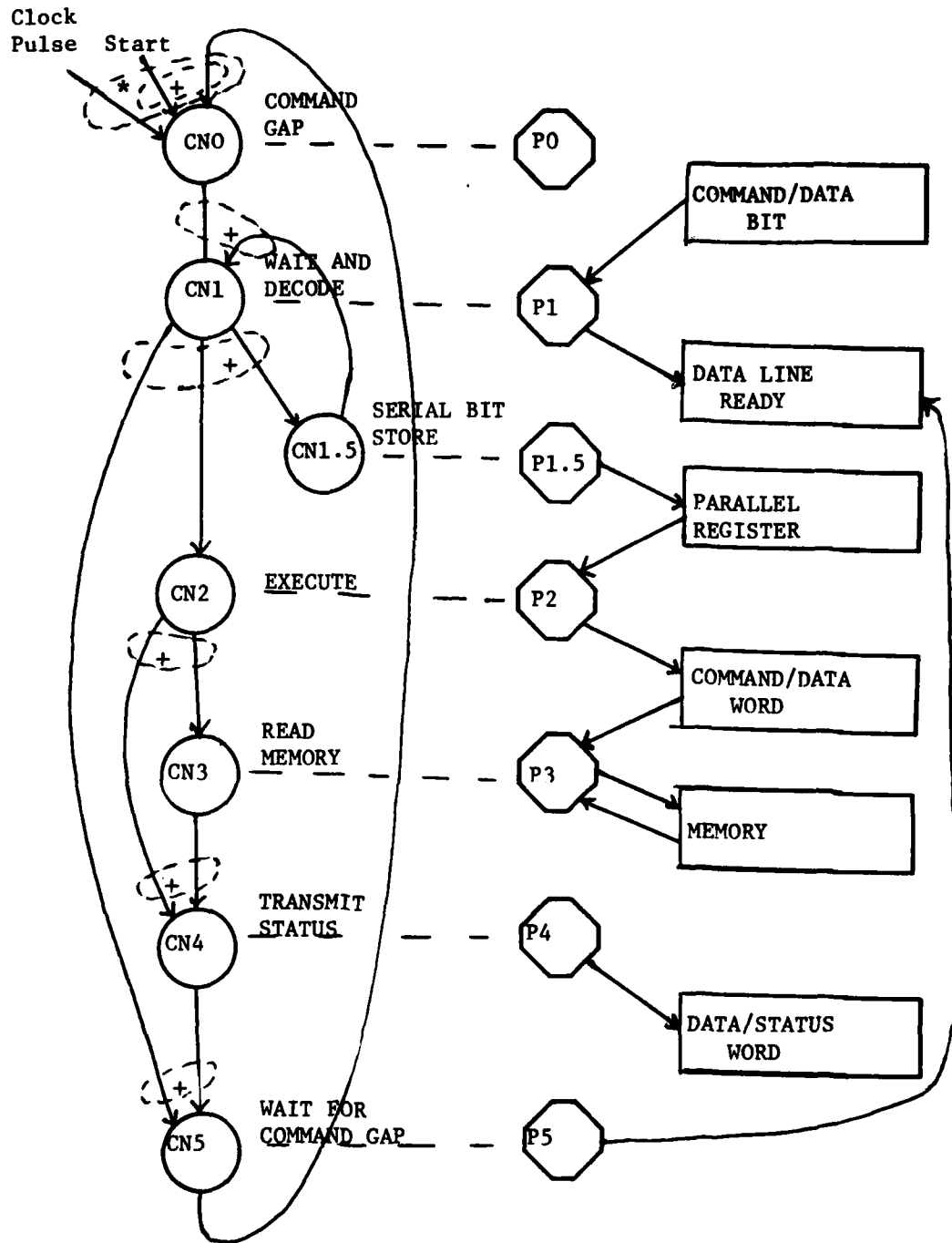
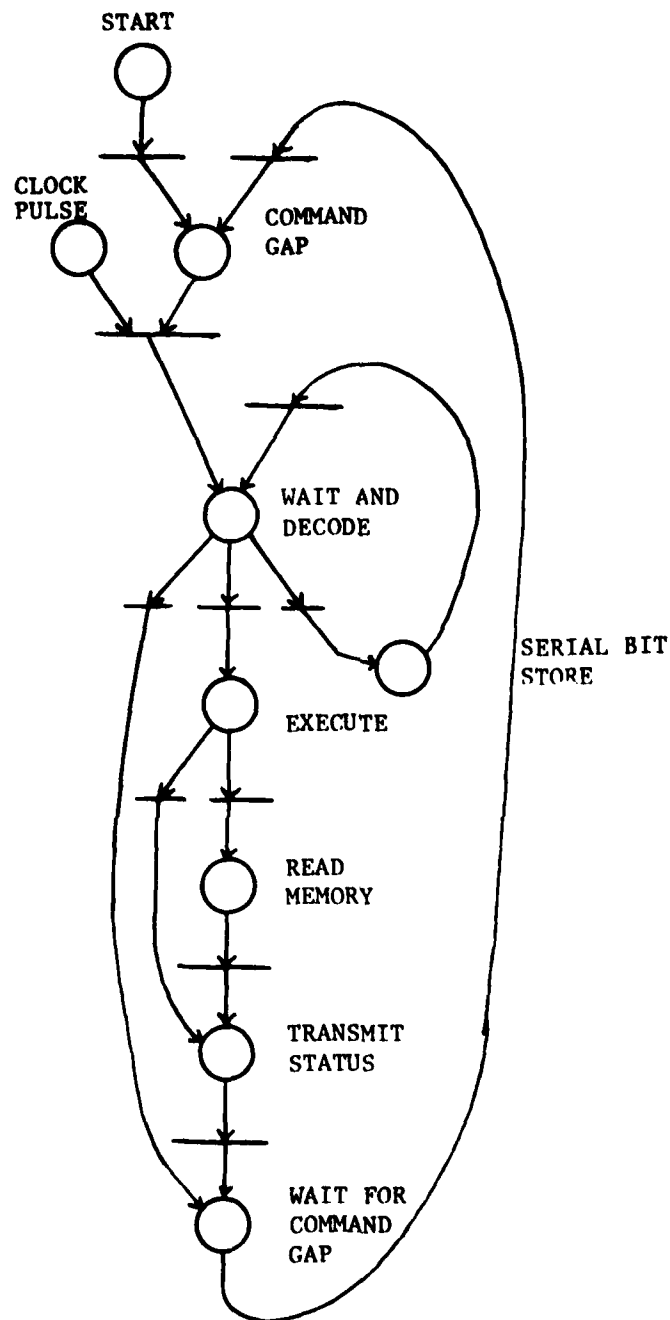
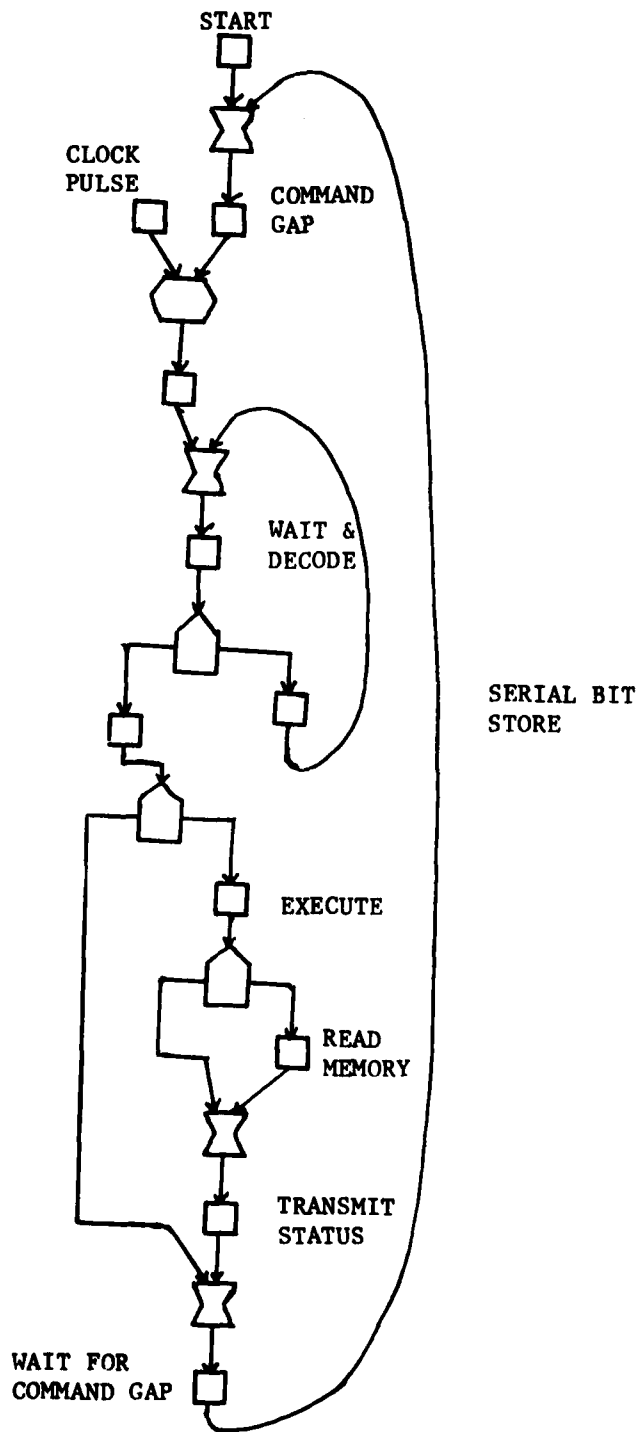


Figure 4. RLU NAMEPLATE MODEL (GMB).



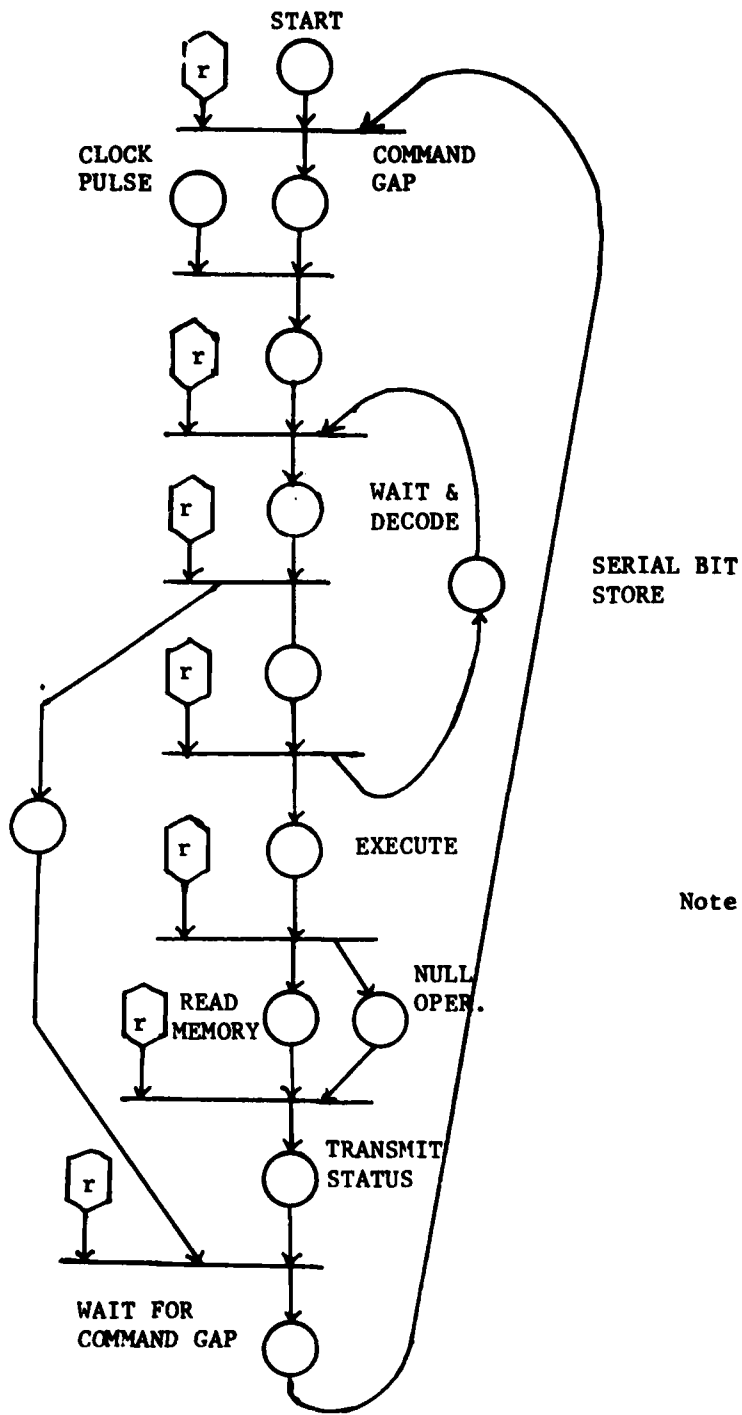
NOTE: No Data Graph is associated with the Petri net model.

Figure 5. Petri net Model of RLU Nameplate



Note: Data Graph is the same as Figure 4.

Figure 6. LOGOS Model of RLU Nameplate



Note: No Data Graph is associated with the E-net Model.

Figure 7. E-net Model of the RLU Nameplate

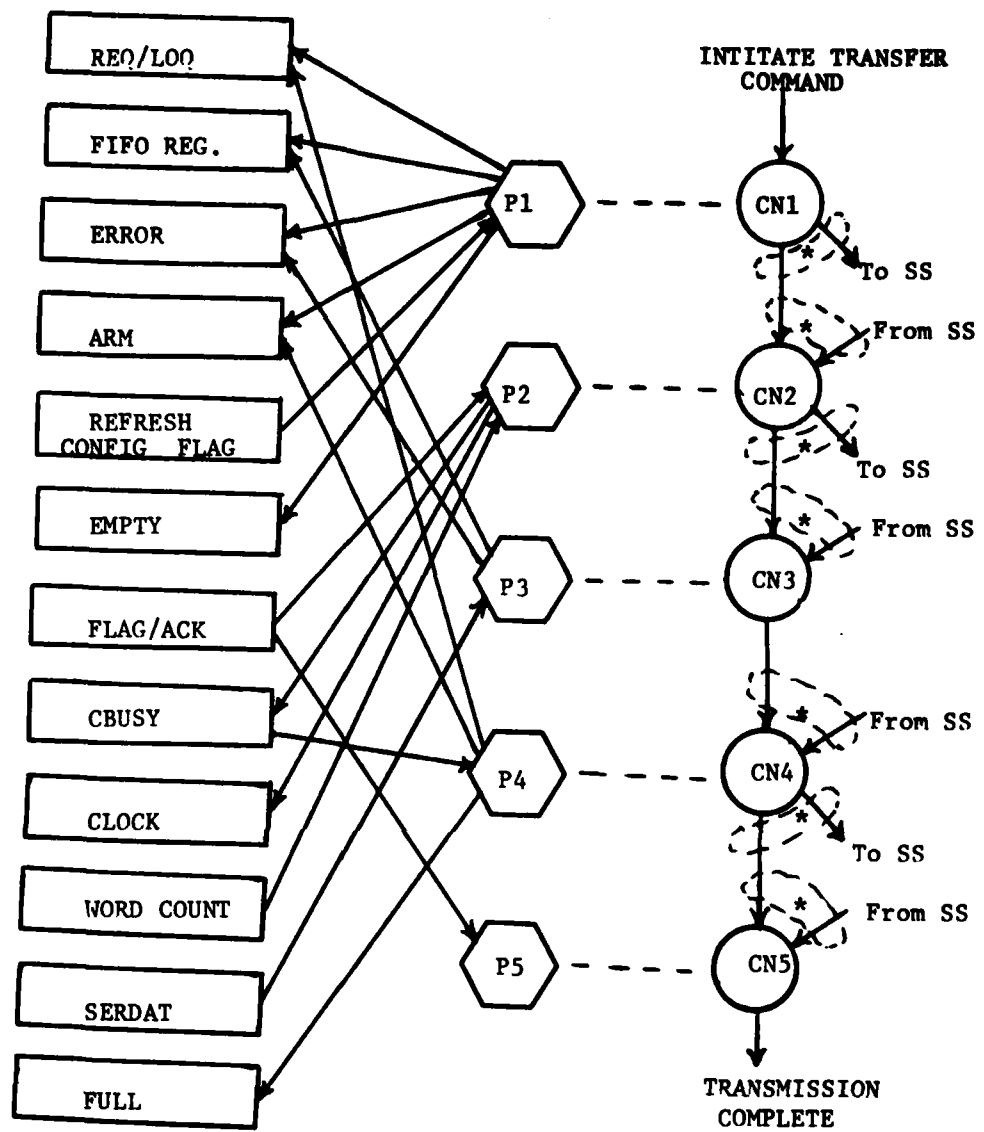


Figure 8A. RLU-ICA Serial Input - Refresh Mode, ICA Processing.

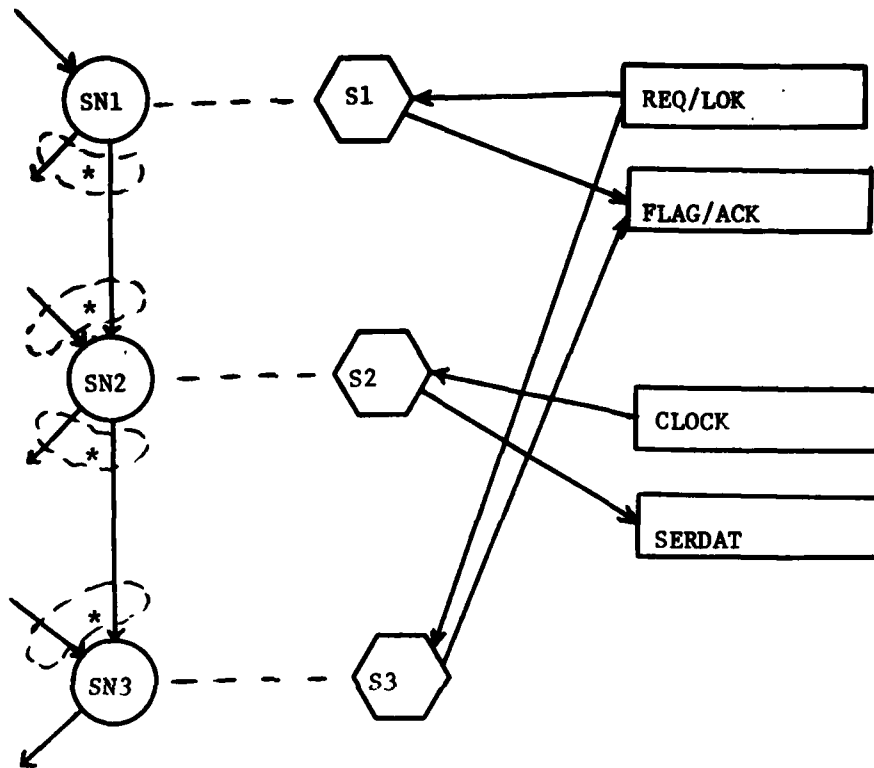


Figure 8B. RLU-ICA Serial Input - Refresh Mode, Subsystem Processing.

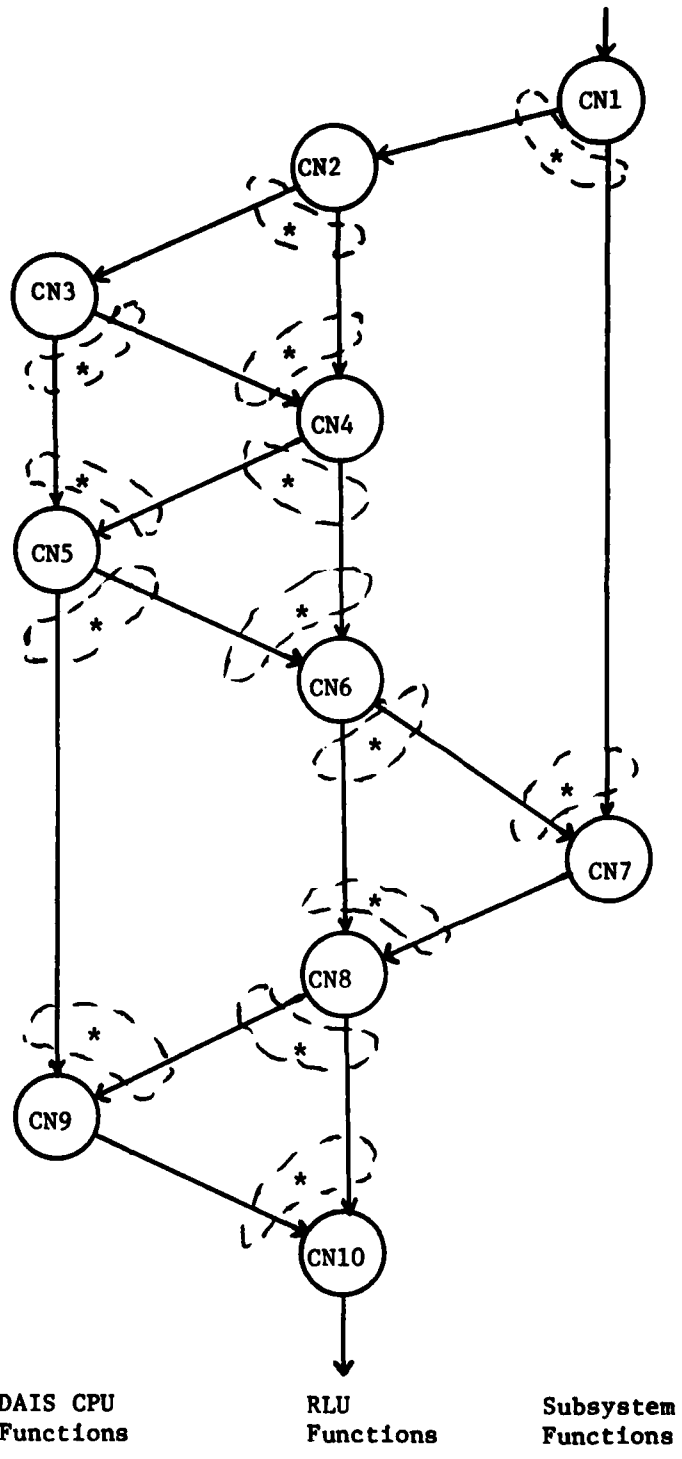


Figure 9A. Control Graph For RLU Asynchronous Message Operation.

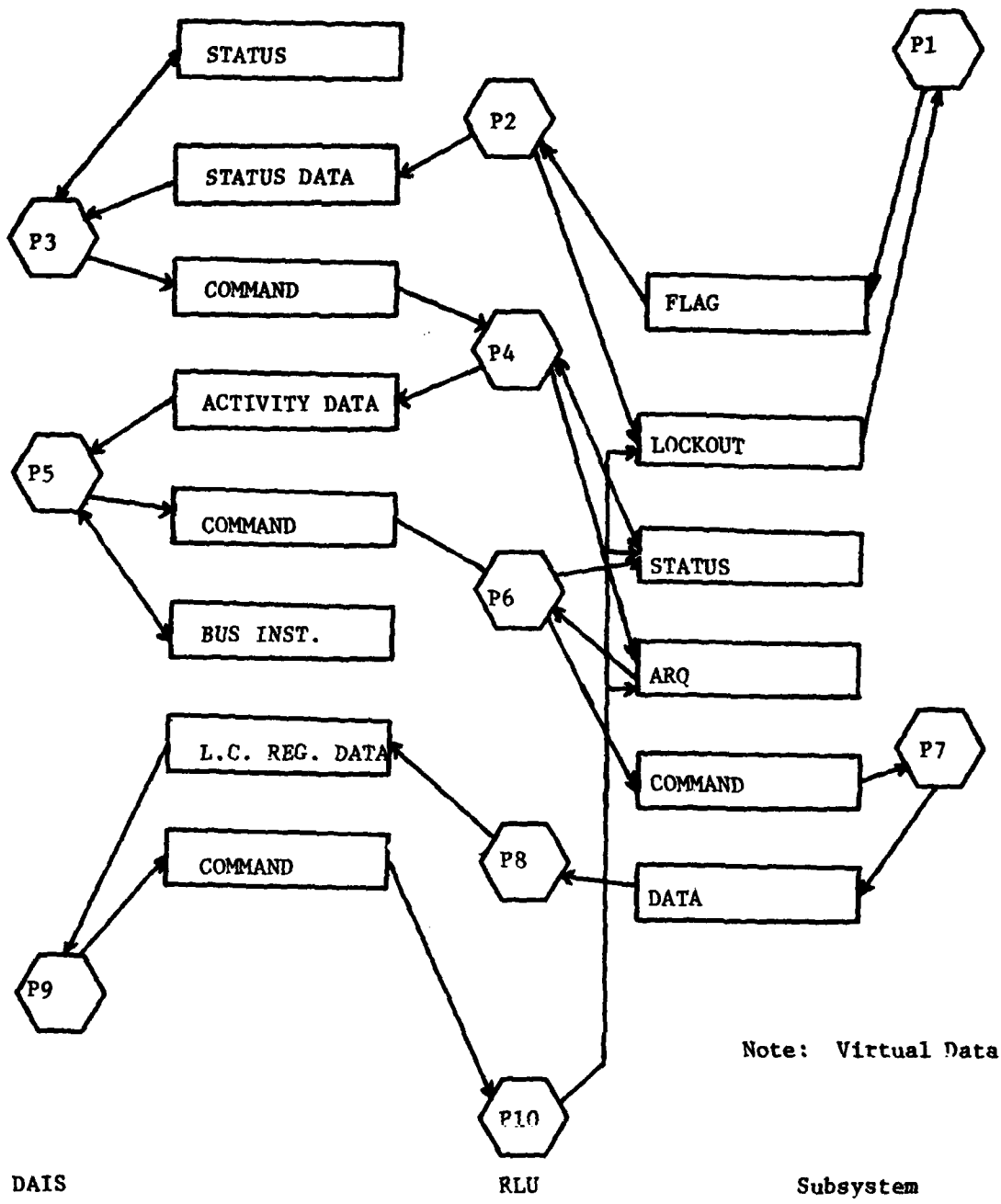


Figure 9B. Data Graph for RLU Asynchronous Message Operation.

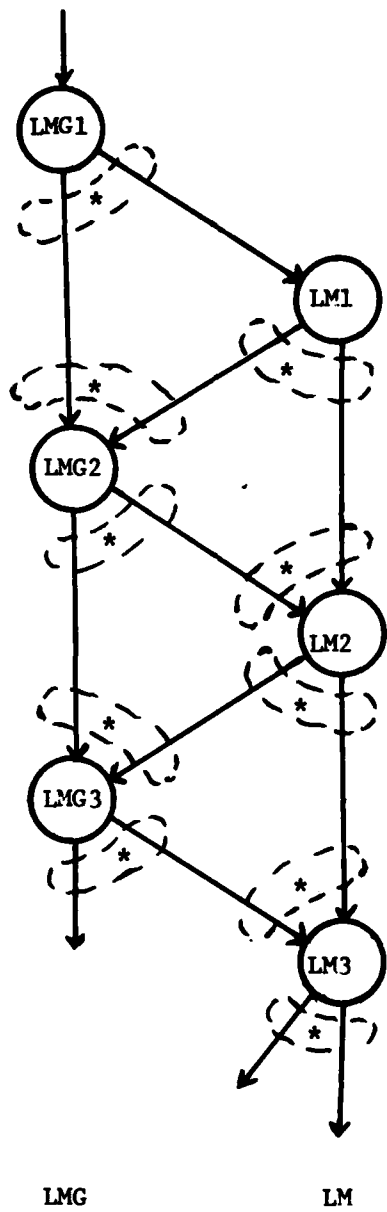


Figure 10. RLU Initialization Sequence.

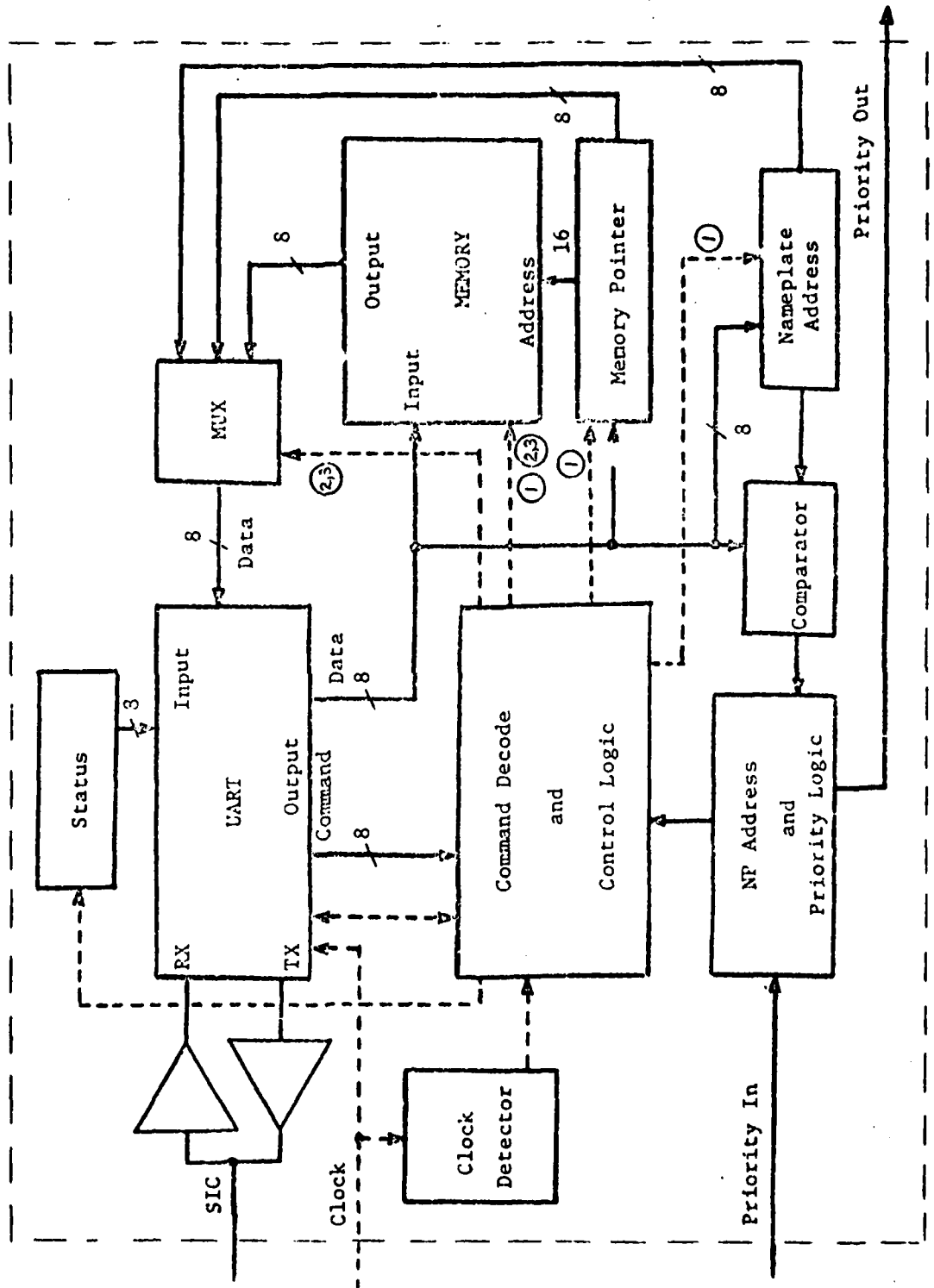


Figure 11 Nameplate Architecture .

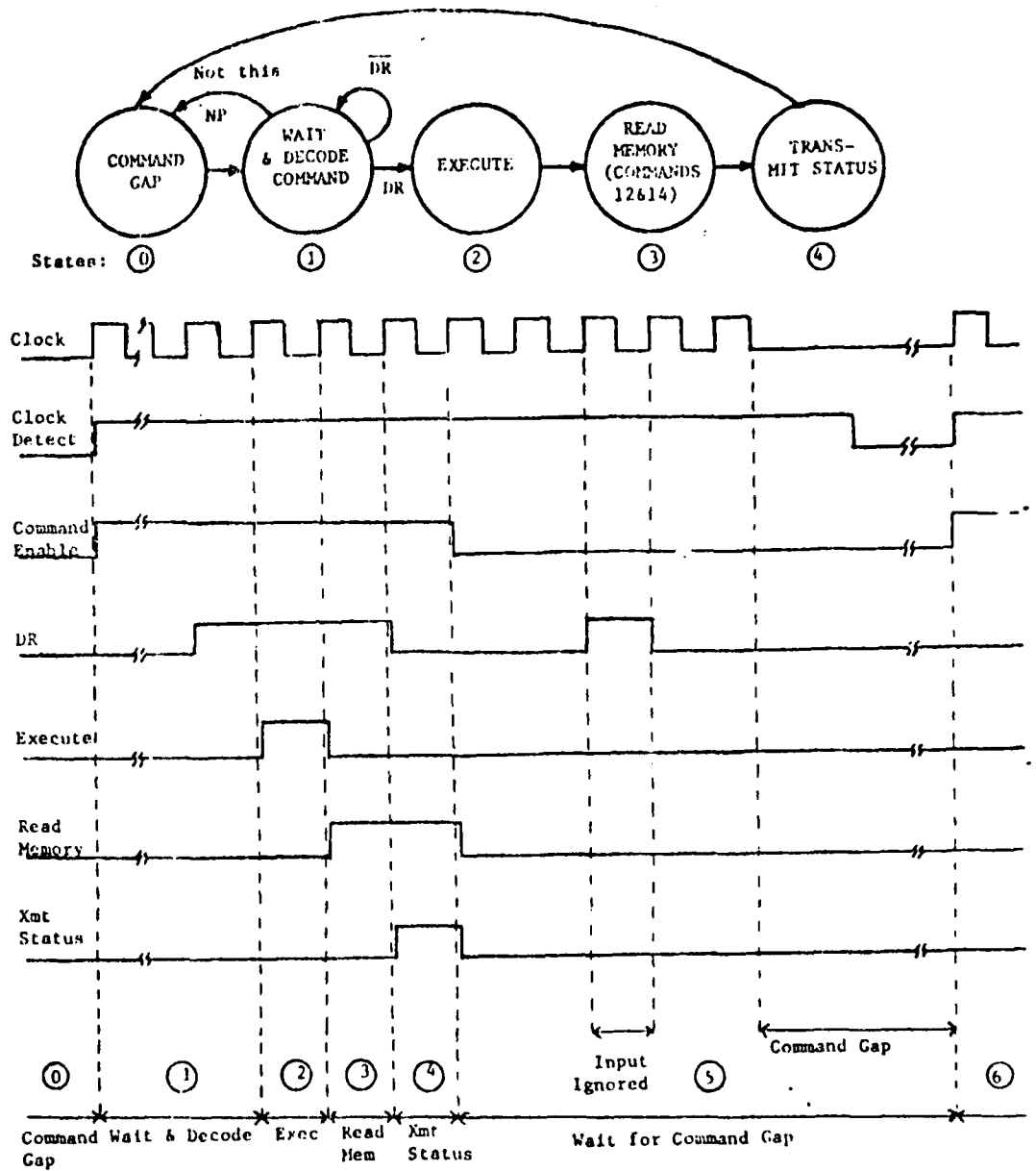


Figure 12 State Diagram and Timing Diagram

1979 USAF - SCEEE SUMMER FACULTY RESEARCH PROGRAM

Sponsored by the

AIR FORCE OFFICE OF SCIENTIFIC RESEARCH

Conducted by the

SOUTHEASTERN CENTER FOR ELECTRICAL ENGINEERING EDUCATION

FINAL REPORT

BOUNDING SIGNAL LEVELS AT WIRE TERMINATIONS BEHIND APERTURES

Prepared by:	Dr. William A. Davis
Academic Rank:	Assistant Professor
Department and University:	Electrical Engineering Department Virginia Polytechnic Institute and State University
Research Location:	Technology Branch Electromagnetics Division Air Force Weapons Laboratory Kirtland AFB, NM 87117
USAF Research Colleague:	Dr. J. Philip Castillo
Date:	20 August 1979
Contract No:	F49620-79-C-0038

BOUNDING SIGNAL LEVELS AT WIRE TERMINATIONS BEHIND APERTURES

by

William A. Davis

ABSTRACT

This report develops techniques for bounding the voltages and currents at terminations on a wire which is excited by incident electromagnetic energy coupled through an aperture. The internal interaction and coupling problems are considered. The theory of aperture coupling for low frequencies is reviewed and the quasi-static aperture problem is modeled by dipole moments and the corresponding polarizabilities. Bounding methods are considered and the bound of an inscribing ellipse is chosen. The interaction with a wire and modifications to the coupling are developed using spatial approximations. The analysis identifies a new capacitive term in the aperture loading. Bounds are developed for the power waves launched on the wire structure and the termination signal levels bound with a term included for multiple reflections. Tighter bounds are obtained by separating the incident field into individual parts typically characterized by poles in the complex frequency domain.

#### ACKNOWLEDGEMENTS

The author would like to thank the sponsor of this research, Air Force Systems Command, Air Force Office of Scientific Research, for enabling him to develop a friendly and working association with the people at the Air Force Weapons Laboratory and the opportunity to learn more about the mission of this organization. A special thanks to Dr. R. Miller of SCEEE and Dr. W. Blackwell of VPI&SU for making this opportunity known to me and encouraging me to participate.

I would like to thank Drs. J. P. Castillo, my research associate, K. Chen, and C. Baum of the Air Force Weapons Laboratory Electromagnetics Division for many useful discussions. I would also like to thank Dr. C. Taylor of Mississippi State University, who was a summer colleague, for proposing the topic and making helpful suggestions.

## I. INTRODUCTION:

The past two decades have involved a substantial effort in the analysis and measurement of electromagnetic pulse (EMP) effects. The interest has centered on the electromagnetic effects resulting from nuclear explosions, particularly high altitude blasts, with a lesser effort in lightening strike effects. The Air Force is primarily interested in the survivability of aircraft and weapon systems when exposed to an electromagnetic pulse environment.

An EMP problem is typically broken into three separate problems: external interaction, coupling, and internal interaction. Since coupling effects are often minimal, it is not uncommon to neglect the coupling effect on external interaction and also to neglect the internal interaction effect on coupling. The knowledge of currents coupled to equipment inside of aircraft due to incident electromagnetic energy is of vital importance to assessing the survivability of aircraft exposed to high level electromagnetic energy. The coupling problem is further broken into three classes: direct coupling to antennas and similar structures, aperture coupling, and diffusion through the skin. The objective of this investigation was to develop a method for obtaining bounds on the signal levels at terminations resulting from energy coupled to a wire behind an aperture. A more definitive statement of the objectives is given in Section II.

Numerous authors have contributed a wealth of information to the subject of interaction and coupling of electromagnetic energy with structures. The external interaction problem often involves computation or measurement of the currents and charges on an approximate structure geometry. [1,2] This often involves simple stick or pipe models of aircraft. [3] The resultant current and charge is the short-circuit current and charge used in the aperture coupling problem. The theory of coupling by small apertures [4-7] is reviewed in Section III. The intent was to provide a complete development with standard notation for a small aperture in a plane. The well-known solutions for the circle and ellipse are given which provide the basis for bounds obtained in the following sections.

Section IV provides the development for the interaction of a wire with the aperture. For a thin wire at least one aperture dimension

from the aperture, it is shown that the interaction can be modeled by a voltage and a current source on a transmission line. A new capacitive term arising from the discharge of the aperture region by outgoing currents has been identified for a wire close to the aperture. Comparison of the sources is made to those obtained for aperture coupling through a coaxial sheath. This comparison suggests the planar problem bounds above the coupling to a wire by an aperture in a shield given the same short circuit aperture fields from the external interaction problem.

Using the planar problem as a bound for aperture coupling, bounds are developed in Section V for the planar problem and thus for shield problems. The planar bounds involve two steps: First, current methods of bounding the aperture polarizabilities are reviewed and a bound for the aperture polarizabilities is given. Secondly, bounds for signals launched on the wire structure are developed along with bounds for the resultant currents and voltages. The results are generalized with the power wave concept to account for geometrical variations along the wire. These bounds are applied to a simple problem in Section VI. The results of the example suggest the separation of transient incident fields into several pieces as might be characterized by a series of complex exponentials; summing the bounds obtained for each separate part of the incident field. Measured data are also considered.

Section VII summarizes the results and provides recommendations for further work.

## II. OBJECTIVES:

The prime objective of this project was to develop a technique for bounding above the magnitudes of currents and voltages in terminations of wires. In particular, these wires are located behind an aperture in a perfectly electric conducting plane. The following sub-objectives were chosen to accomplish the task:

- (1) To review quasi-static theory for coupling by small apertures.
- (2) To bound the aperture polarizabilities above.
- (3) To develop the spatial approximation theory for aperture coupling to a thin wire.
- (4) To develop upper bounds for the power or voltage waves launched on the wire and for the resultant voltages and currents at the terminations.

Due to the nature of EMP, the objectives were restricted to small apertures. To make the problem tractable for the given time period, the wire was assumed to be thin and to be sufficiently far from the aperture for the aperture polarizability approximation to be valid. The sponsor expressed minimal concern for cavity effects, resulting in its exclusion from the theoretical treatment of such as part of the task.

### III. APERTURE COUPLING:

Coupling through an aperture in an infinite plane is generally cast in the context of a diffraction problem. To determine the coupled or diffracted fields, we must determine the perturbed fields in the aperture and on the plane from which the diffracted fields may be computed. For the problem at hand, the computation may be limited to the electric field intensity in the aperture of the plane by image theory or an appropriate dyadic Green's function. The diffracted fields of a small aperture are typically computed from two equivalent dipoles which approximate the aperture field expansion. [8]

Following the development of Butler, et al [7], we consider the aperture shown in Fig. 1 cut in a perfect electric conductor (PEC) with sources on both sides of the plane. We write the total fields

$$\bar{E}^{\pm} = \bar{E}^{SC\pm} + \bar{E}^{D\pm} \quad (1)$$

and

$$\bar{H}^{\pm} = \bar{H}^{SC\pm} + \bar{H}^{D\pm} \quad (2)$$

where  $\pm$  designates  $z \gtrless 0$ , SC designates the fields with the aperture A shorted, and D designates the diffracted fields. Incorporating image theory in the basic boundary value expressions for the electromagnetic fields we may write [9] ( $e^{j\omega t}$  convention)

$$\bar{E}^{D\pm} = \pm 2 \int_A [\nabla' G(\bar{r}, \bar{r}') \times (-\hat{z} \times \bar{E}(\bar{r}))] ds' \quad (3)$$

and

$$\bar{H}^{D\pm} = \pm \frac{2}{j\omega\mu} \int_A [k^2 G(-\hat{z} \times \bar{E}) - \nabla'_s \cdot (-\hat{z} \times \bar{E}) \nabla' G] ds' \quad (4)$$

where  $G$  is the free space scalar Green's function

$$G(\bar{r}, \bar{r}') = \frac{e^{-jk|\bar{r}-\bar{r}'|}}{4\pi|\bar{r}-\bar{r}'|} \quad (5)$$

with  $k = \omega\sqrt{\mu\epsilon}$ . Since  $\hat{z} \times \bar{E}^{SC\pm} = 0$  at the PEC,  $\bar{E}$  may be replaced by  $\bar{E}^{D+}$  or  $\bar{E}^{D-}$  in the integrals of (3) and (4) if desired.

The boundary conditions at the aperture require the continuity of

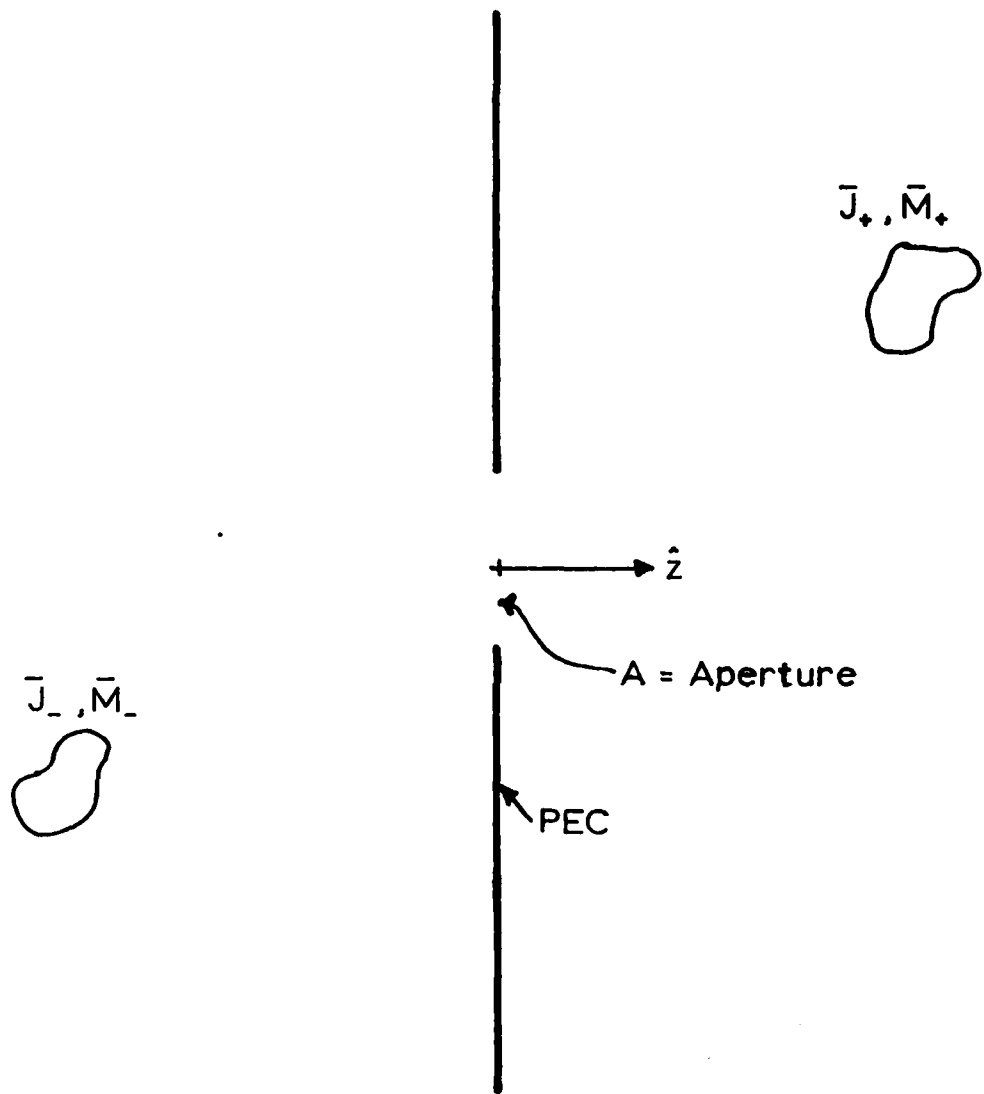


Figure 1. Source locations for aperture coupling through a planar perfect electric conductor.

$\bar{E}$  and  $\bar{H}$ . Taking the limits of (3) and (4) from both the left and right and imposing field continuity in the aperture we obtain

$$\hat{z} \cdot (\bar{E}^{SC-} - \bar{E}^{SC+}) = 4\hat{z} \cdot \int_A [\nabla'G \times \bar{M}] ds' \quad (6)$$

and

$$\hat{z} \times (\bar{H}^{SC-} - \bar{H}^{SC+}) = \frac{4}{j\omega\mu} \hat{z} \times \int_A [k^2G\bar{M} - (\nabla' \cdot \bar{M}) \nabla'G] ds' \quad (7)$$

where

$$\bar{M} = -\hat{z} \times \bar{E}(\bar{r}), \quad \bar{r} \in A$$

is the equivalent magnetic surface current in A, the - through the integral denotes the Cauchy principal value, and the surface  $\nabla'_g$  is replaced by  $\nabla'$  without ambiguity. Since the tangential components of  $\bar{E}^{SC\pm}$  and the normal components of  $\bar{H}^{SC\pm}$  are zero by interaction with the PEC, the tangential  $\bar{E}$  and normal  $\bar{H}$  continuity of Eqs. (1) thru (4) are automatically satisfied.

Two observations may be made about (6) and (7) as they stand. First we note that (6) may be obtained from the divergence of (7), implying that (7) is sufficient for non-zero frequencies. Second, due to the existence of edges with an aperture, we must impose an edge constraint on  $\bar{M}$ . From energy considerations this constraint may be written in two parts as

$$\hat{n}_e \cdot \bar{M} = O(\rho^{1/2}), \quad \rho \rightarrow 0 \quad (8a)$$

and

$$\hat{n}_e \times \bar{M} = O(\rho^{-1/2}), \quad \rho \rightarrow 0 \quad (8b)$$

for  $\hat{n}_e$  the normal to the edge in the plane,  $\rho$  the distance to the edge, and  $O(x)$  read order of  $x$ . Eq. (7) has been solved numerically by Graves, et al [10]. A modified form of these equations for the dual problem of the disk were proposed by Mittra, et al [11], and subsequently solved numerically by Rahmat-Samii [12] for apertures up to about three wavelength dimensions. However, our interest is in expanding (6) and (7) for low frequency coupling rather than obtain a complete current description.

Lord Rayleigh [13] proposed the use of a series in  $k$  to obtain

equations for the dominant quasi-static terms in aperture coupling. Bouwkamp [4] used this idea to solve some canonical apertures analytically in the low frequency region. More recently, De Meulenaere and Van Bladel [14] have treated the quasi-static problem of several shapes numerically. We now proceed with a review of this quasi-static theory.

Using a Rayleigh series, we expand all field quantities  $\bar{F}(\bar{r}, k)$  as

$$\bar{F} = \bar{F}_0 + jk\bar{F}_1 + \dots + (jk)^n \bar{F}_n + \dots \quad (9)$$

where we have assumed analytic fields in  $k$  for the low frequency region. We also expand the free space Green's function as

$$G(\bar{r}, \bar{r}') = G_0 + jkG_1 + \dots + (jk)^n G_n + \dots \quad (10)$$

where  $G_0 = 1/4\pi R$ , the static free space Green's function, and  $R = |\bar{r} - \bar{r}'|$ . Substituting (9) and (10) into (6) and (7) we obtain

$$\hat{z} \cdot (\bar{E}_N^{SC-} - \bar{E}_N^{SC+}) = 4\hat{z} \cdot \sum_{n=0}^N \int_A [\nabla' G_n \times \bar{M}_{N-n}] ds' \quad (11)$$

and

$$\hat{z} \times (\bar{H}_N^{SC-} - \bar{H}_N^{SC+}) = \frac{4}{\eta} \hat{z} \times \sum_{n=0}^{N+1} \int_A [-G_n \bar{M}_{N-n-1} - (\nabla' \cdot \bar{M}_{N+1-n}) \nabla' G_n] ds' \quad (12)$$

where  $\bar{M}_{-1} = \bar{M}_{-2} = 0$ ,  $\eta = \sqrt{\mu/\epsilon}$ , and

$$\int_A [\nabla' G_0 (\nabla' \cdot \bar{M}_0)] ds' = 0. \quad (13)$$

Integrating (13) we have

$$\int_A [G_0 (\nabla' \cdot \bar{M}_0)] ds' = A = \text{constant} \quad (14)$$

with a solution [12] for a circle of radius  $a$  given by

$$\nabla' \cdot \bar{M}_0 = A/(\pi\sqrt{a^2 - \rho'^2}). \quad (15)$$

The surface integral of (15) is

$$2\pi a M_{0\rho}(a) = 2aA$$

or

$$A = \pi M_{0\rho} (a)$$

which requires A to be zero upon imposing the edge constraint of (8a). Assuming that we may generalize this result for the circle to arbitrary apertures, we take the solution to (13) to be

$$\nabla' \cdot \bar{M}_0 = 0. \quad (16)$$

It is interesting to note that if (13) had been interpreted as a finite part integral, the solution in (15) would have contained terms  $O[(a - \rho')^{-n/2}]$  corresponding to the multiplicity of solutions to Maxwell's equations in the vicinity of an edge with no physical edge constraints imposed [15].

It is straight forward to show that the divergence of (12) for N gives (11) for N-1. However our general interest is in N=0 for both (11) and (12) to solve for  $\bar{M}_0$  and the divergence of  $\bar{M}_1$  or  $m_0$ , the zeroth order magnetic charge. The use of (12) for N=1 would provide the further complication of adding the unknown divergence of  $\bar{M}_2$  and still require the solution of (11).

To summarize, the quasi-static equations for the magnetic current and charge in the aperture are

$$(E_{0z}^{SC+} - E_{0z}^{SC-}) = 4\hat{z} \cdot \nabla \times \int_A \bar{M}_0 G_0 ds', \quad (17)$$

$$\hat{z} \times (\bar{H}_0^{SC+} - \bar{H}_0^{SC-}) = \frac{4}{\mu} \hat{z} \times \nabla \int_A m_0 G_0 ds', \quad (18)$$

and

$$\nabla' \cdot \bar{M}_0 = 0 \quad (16)$$

where  $m_0$  is given by  $(-\nabla' \cdot \bar{M}_1) / \sqrt{\mu\epsilon}$ . The importance of using both  $\bar{M}_0$  and  $m_0$  may be observed by rewriting (3) and (4) as

$$\bar{E}^{D\pm} = \pm 2\nabla \times \left( - \int_A \bar{M} G ds' \right) \quad (19)$$

and

$$\bar{H}^{D\pm} = \pm 2 \left[ - \frac{1}{\eta} \int_A \bar{M} G ds' - \frac{1}{\mu} \nabla \int_A m G ds' \right] \quad (20)$$

where  $\eta = \sqrt{\mu/\epsilon}$ . The near electric fields are dominated by the zero

order magnetic current where as the near magnetic fields are dominated by the zero order magnetic charge requiring both terms for distances less than one wavelength. This requirement can also be shown to be valid in the far field of the aperture (distances greater than one wavelength).

It is more common to describe the fields in the distant region of the aperture (distances > maximum aperture dimension) which extends the far field expansion into the near field region. From (19) we define the magnetic vector potential by

$$\vec{F}(\vec{r}) = \int_A \vec{M}(\vec{r}') G(\vec{r}, \vec{r}') ds' \quad (21)$$

For  $r \gg r'$ , we may expand  $G$  to obtain

$$G(\vec{r}, \vec{r}') \sim G(\vec{r}, 0) \left[ 1 + (\hat{r} \cdot \vec{r}') \frac{1 + jkr}{r} \right].$$

Substituting into (21) we have

$$\vec{F}(\vec{r}) \sim G(\vec{r}, 0) \int_A \vec{M}(\vec{r}') \left[ 1 + (\hat{r} \cdot \vec{r}') \frac{1 + jkr}{r} \right] ds' \quad (22)$$

The first integral is given by

$$\int_A \vec{M} ds' = \int_A [\vec{M} - \nabla' \cdot (\vec{M} \vec{r}')] ds'$$

using the constraint (8a) and the surface form of the divergence theorem.

Expanding the dyadic divergence we obtain

$$\begin{aligned} \int_A \vec{M} ds' &= - \int_A \vec{r}' (\nabla' \cdot \vec{M}) ds' \\ &= j\omega \int_A \vec{r}' m ds' \end{aligned} \quad (23)$$

The second integral may be expanded as

$$\int_A (\hat{r} \cdot \vec{r}') \vec{M} ds' = \frac{1}{2} \int_A \{ \hat{r} \times (\vec{M} \times \vec{r}') + [(\hat{r} \cdot \vec{r}') \vec{M} + \vec{r}' (\hat{r} \cdot \vec{M})] \} ds'$$

The last two terms may be written in dyadic form as

$$\vec{M} \cdot \nabla' (\vec{r}' (\hat{r} \cdot \vec{r}')).$$

Subtracting the divergence of  $(\vec{M} \vec{r}' (\hat{r} \cdot \vec{r}'))$  which integrates to zero due to (8a), we obtain

$$\int_A (\hat{r} \cdot \bar{r}') \bar{M} ds' = \frac{1}{2} \int_A [\hat{r} \times (\bar{M} \times \bar{r}') + j\omega(\hat{r} \cdot \bar{r}') \bar{r}'_m] ds' \quad (24)$$

Substituting (23) and (24) into (22)

$$\begin{aligned} \bar{F} &\sim j\omega G(\bar{r}, 0) \int_A \bar{r}'_m ds' \\ &- \nabla G(\bar{r}, 0) \times \frac{1}{2} \int_A (\bar{M} \times \bar{r}') ds' \\ &- j\omega \nabla G(\bar{r}, 0) \cdot \frac{1}{2} \int_A \bar{r}' \bar{r}'_m ds' \end{aligned} \quad (25)$$

with the magnetic vector potential composed of a magnetic dipole, an electric dipole, and a magnetic quadrupole given respectively by

$$\bar{p}_m = \frac{1}{\mu} \int_A \bar{r}'_m ds' \quad (26a)$$

$$\bar{p}_e = \frac{\epsilon}{2} \int_A (\bar{M} \times \bar{r}') ds' \quad (26b)$$

and

$$\bar{q}_m = \frac{1}{\mu} \int_A \bar{r}' \bar{r}'_m ds'. \quad (26c)$$

The diffracted fields may thus be written

$$\bar{E}^{D\pm} = \pm \left[ -\frac{2}{\epsilon} \nabla \times (\bar{p}_e \times \nabla G) + 2j\omega\mu \bar{p}_m \times \nabla G + j\omega\mu \nabla \times (\bar{q}_m \times \nabla G) \right] \quad (27)$$

and

$$\bar{H}^{D\pm} = \pm \left[ -2 \nabla \times (\bar{p}_m \times \nabla G) - 2j\omega \bar{p}_e \times \nabla G - \nabla \times \nabla \times (\bar{q}_m \times G) \right]. \quad (28)$$

Usually the quadrupole term is small and therefore neglected. In fact  $\bar{q}_{m0}$  is zero for a circular aperture in the quasi-static problem.

The short-circuited fields in (17) and (18) are nearly constant for small apertures sufficiently far from the sources such that

$$\bar{p}_e = \epsilon \alpha_e \hat{z} \hat{z} \cdot (\bar{E}^{SC-} - \bar{E}^{SC+}) \quad (29a)$$

and

$$\bar{p}_m = -\bar{\alpha}_m \cdot (\bar{H}^{SC-} - \bar{H}^{SC+}) \quad (29b)$$

where  $\bar{\alpha}_m$  has no z components and  $\bar{p}_e$  and  $\bar{p}_m$  have been approximated by the

zero order current and charge. The neglected quadrupole term would be represented by a triad term if it were to be used. The quantities  $\alpha_e$  and  $\alpha_m$  are called the aperture electric and magnetic polarizabilities respectively.

Equations (16) to (18) have been solved analytically for the circle and ellipse [4,6,16] with the resultant polarizabilities of Table I.  $K$  and  $E$  represent the complete elliptic integrals of the first and second kind respectively and the ellipse major axis of length  $l$  is along  $x$ . The polarizabilities of several other shapes have been obtained numerically by De Meulenaere and Van Bladel [14].

To use these results for aperture coupling into aircraft cavities, one obviously becomes concerned with the effects of nearby conductors and surface curvature on the coupling dipole moments. Latham [17] has shown that surface radii of curvature and distance to nearby conductors of at least the linear dimensions of the aperture cause less than one percent variation in the aperture polarizabilities. I defer the discussion on the dipole moment effects to Section IV.

Table I

APERTURE POLARIZABILITIES

Shape	$\alpha_e$	$\alpha_{max}$	$\alpha_{myy}$
Circle (a = radius)	$\frac{2}{3} a^3$	$\frac{4}{3} a^3$	$\frac{4}{3} a^3$
Ellipse (e = eccentricity)	$\frac{\pi \ell^3 (1 - e^2)}{3E(e)}$	$\frac{\pi \ell^3 e^2}{3[K(e) - E(e)]}$	$\frac{\pi \ell^3 e^2}{3[E(e)/(1-e) - K(e)]}$
Narrow Ellipse (e = 1)	$\frac{\pi \ell^3 (1 - e^2)}{3}$	$\frac{2\pi \ell^3}{3[\ln(16/(1-e^2)) - 2]}$	$\frac{\pi \ell^3 (1 - e^2)}{3}$

$$e = \left[ 1 - \left( \frac{\text{major axis}}{\text{minor axis}} \right)^2 \right]^{\frac{1}{2}}$$

#### IV. WIRE BEHIND APERTURE:

Coupling to a wire behind an aperture has been treated in a variety of ways. Kajfez [18] derived the equivalent sources using both mode-matching and reciprocity, but neglected the loading effects of the aperture on the wire. Lee and Yang [19] developed the same sources using transform approximations and added the effects of the loading in order to discuss the effects of a wire close to the aperture. The problem has also been cast in numerical form by Butler and Umashankar [20]. The following development is spatially equivalent to the transform method of Lee and Yang, but identifies an additional capacitance not included in the previous development. Under the problem constraints, it will be shown that only the sources are needed and are equivalent to those obtained by Kajfez. If the wire approaches the aperture, then the lumped elements must be included and the new capacitance becomes of importance.

The geometry of interest is shown in Fig. 2 with the constraints as follows: the wire of radius  $a$  is considered to be thin and the distance  $\rho_0$  is greater than or equal to the maximum aperture dimension. Two simultaneous boundary value problems are involved in this development. The aperture problem may be considered solved in terms of the polarizabilities of the aperture once the short circuit fields of the incident field and wire have been computed. The remaining problem is to determine the wire current from the dipole moments by requiring the electric field on the wire to be zero.

The electric field along the wire due to the aperture is obtained from (27) and (28) as

$$E_x^A = 2 \left[ p_e / \epsilon \frac{\partial^2 G}{\partial x \partial z} + j \omega \mu p_{my} \frac{\partial G}{\partial z} \right]. \quad (30)$$

The electric field due to the x-directed wire current and its image is

$$E_x^W = \frac{1}{j \omega \epsilon} \left( k^2 + \frac{\partial^2}{\partial x^2} \right) \int_{-\infty}^{\infty} I(x') \left[ \frac{e^{-jk\sqrt{(x-x')^2+a^2}}}{4\pi\sqrt{(x-x')^2+a^2}} - \frac{e^{-jk\sqrt{(x-x')^2+4d^2}}}{4\pi\sqrt{(x-x')^2+4d^2}} \right] dx'. \quad (31)$$

Since the kernel of (31) is approximately zero for  $|x-x'| > 2d$ , we integrate (31) as though  $I(x')$  were constant to obtain

$$E_x^W \approx \frac{Z_0}{jk} \left( k^2 + \frac{d^2}{dx^2} \right) I(x) \quad (32)$$

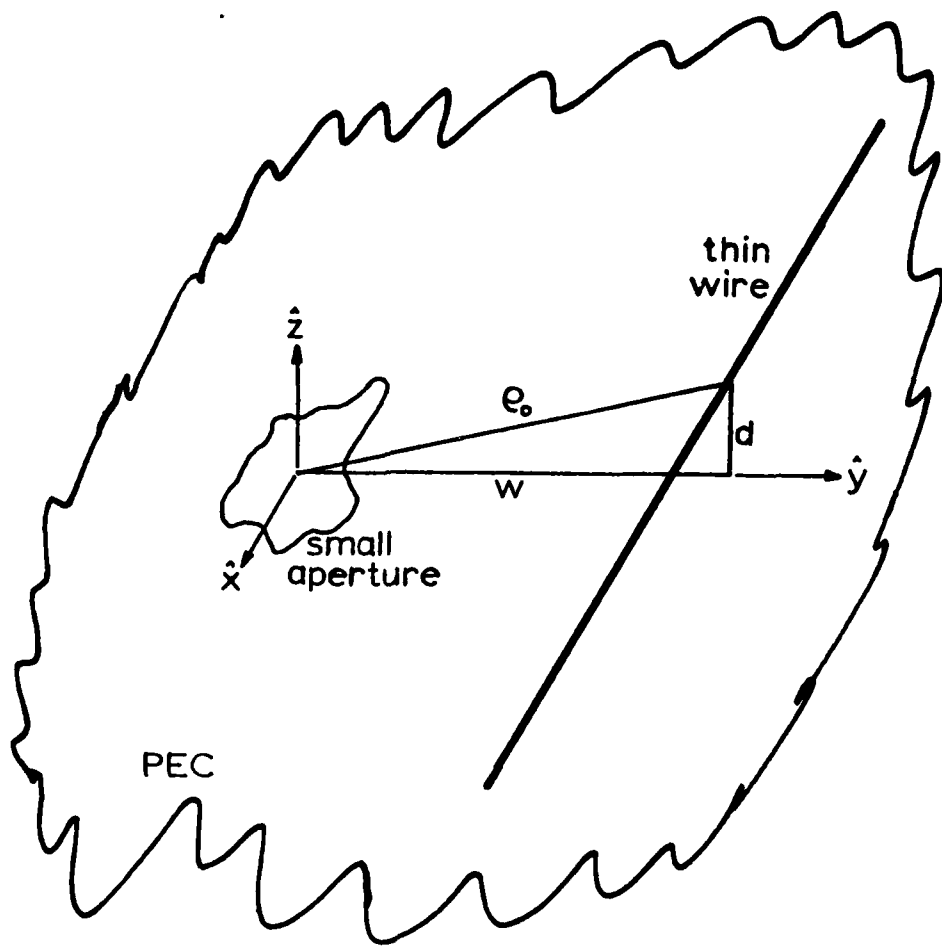


Figure 2. Wire geometry for aperture coupling through a planar perfect electric conductor.

where the impedance of a thin wire over a conducting plane  $Z_0$  given by  $\eta \ln(2d/a)/2\pi$  has been used.

To obtain the current, we set (32) equal to the negative of (30) and invert the differential operator to obtain

$$I(x) = \frac{1}{Z_0} \int_{-\infty}^{\infty} e^{-jk|x-x'|} \left[ p_e/\epsilon \frac{\partial^2 G}{\partial x' \partial z'} + j\omega\mu p_{my} \frac{\partial G}{\partial z'} \right] dx' + A e^{-jkx} + B e^{jkx}$$

which may be approximated due to the peaked nature of  $\frac{\partial G}{\partial z'}$  by

$$\begin{aligned} I(x) &= \frac{e^{-jk|x|}}{Z_0} [jk p_e/\epsilon \operatorname{sgn}(x) - j\omega\mu p_{my}] \left(\frac{d}{2\pi\rho_0^2}\right) \\ &\quad + A e^{-jkx} + B e^{jkx} \\ &= A e^{-jkx} + B e^{jkx} + C \operatorname{sgn}(x) e^{-jk|x|} + D e^{-jk|x|} \end{aligned} \quad (33)$$

Computing the average short circuit fields in the aperture we obtain

$$p_{my} = -[\hat{y} \cdot \bar{\alpha}_m \cdot \bar{H}^{SC-} - \frac{d\alpha_{myy}}{\pi\rho_0^2} (A + B + D)] \quad (34a)$$

and

$$p_e = \epsilon\alpha_e \left[ \hat{z} \cdot \bar{E}^{SC-} + \frac{\eta d}{\pi\rho_0^2} \left( A - B + C - \frac{C}{jk\rho_0} \right) \right]. \quad (34b)$$

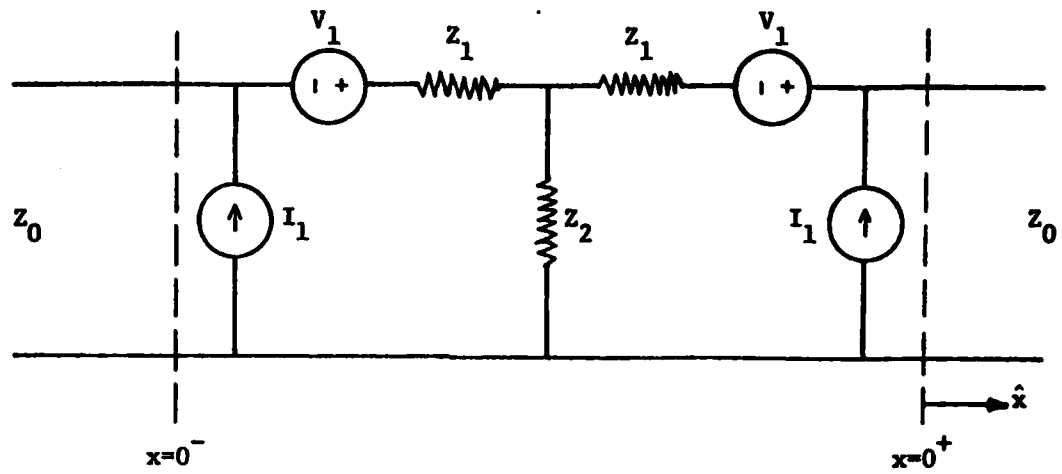
The last term in (34b) accounting for the capacitive discharge of the aperture region by the outgoing current was not obtained by Lee and Yang. As  $\rho_0$  becomes small, this new capacitive term will dominate the capacitance of the aperture region. Substituting (34) into (33) and solving for C and D we obtain

$$C = j\omega\epsilon\alpha_e \frac{\eta}{Z_0} \left(\frac{d}{2\pi\rho_0^2}\right) \frac{[(\hat{z} \cdot \bar{E}^{SC-}) + \eta(\frac{d}{\pi\rho_0^2})(A-B)]}{1 + \frac{jk\eta\alpha_e}{2Z_0} \left(\frac{d}{\pi\rho_0^2}\right)^2 \left(\frac{1}{jk\rho_0} - 1\right)} \quad (35a)$$

and

$$D = \frac{j\omega\mu}{Z_0} \left(\frac{d}{2\pi\rho_0^2}\right) \frac{[\hat{y} \cdot \bar{\alpha}_m \cdot \bar{H}^{SC-} - \alpha_{myy} \left(\frac{d}{\pi\rho_0^2}\right)(A+B)]}{1 + \frac{jk\eta\alpha_{myy}}{2Z_0} \left(\frac{d}{\pi\rho_0^2}\right)^2} \quad (35b)$$

We may model the equations of (33) and (35) by the transmission line model of Fig. 3. For the dimensional constraints chosen, it is



$$V_1 = j\omega\mu \left(\frac{d}{2\pi\rho_0}\right) (\hat{y} \cdot \bar{\alpha}_m \cdot \bar{H}^{SC-})$$

$$I_1 = j\omega\epsilon \frac{\eta}{Z_0} \left(\frac{d}{2\pi\rho_0}\right) \alpha_e (\hat{z} \cdot \bar{E}^{SC-}) \left[1 + \frac{\eta\alpha_e}{2Z_0\rho_0} \left(\frac{d}{\pi\rho_0}\right)^2\right]^{-1}$$

$$Z_1 = j\omega L_1 = j\omega \left[\mu \frac{\alpha_{yy}}{2} \left(\frac{d}{\pi\rho_0}\right)^2\right]$$

$$Z_2 = 1/j\omega C_2 + j\omega L_2$$

$$= -\frac{Z_0}{j\omega\epsilon\eta} \left(\frac{1}{2\rho_0} + \frac{Z_0}{\eta\alpha_e \left(\frac{d}{\pi\rho_0}\right)^2}\right) - j\omega L_1/2$$

Figure 3. General source and impedance model for the aperture region of a wire behind a planar conductor.

easily shown that  $Z_1$  and  $Z_2$  may be neglected compared to  $Z_0$  as may the bracket in the  $I_1$  expression. What remains is the two source model of Kajfez [18]. We observe that as long as the conductor is at least an aperture dimension away, the dipole moments depend only on the exterior short-circuited fields. We would suspect this to also be true for a coax.

We may obtain the sources for a coax given by Latham [17] simply by replacing  $Z_0$  by the coax impedance  $\eta \ln(b/a)/2\pi$  [21] and  $(2d/\rho_0^2)$  by  $1/b$  where  $b$  is the radius of the coaxial outer sheath. From the general form of Latham and the results presented, one might hypothesize that  $V_1$  and  $I_1$  may be obtained for any concave geometry by letting  $Z_0$  be the line impedance and  $d/\pi\rho_0^2$  be replaced by the ratio of the short-circuit aperture current density to the total current on the line. For  $b=d$ , the coaxial sources are approximately one-half those for the planar case. This is reasonable in the sense that the more confined coaxial region causes fewer coupled magnetic field lines to cut the wire and fewer coupled electric flux lines to interact with the line charge. This suggests a bound similar to that of Harrison [22] for the exterior problem. It is reasonable to claim that in the time domain, the signals coupled to wires behind apertures irrespective of cavities are bound by the signals coupled to a wire behind an aperture in a plane given the same dipole moments determined from the exterior interaction problem.

Taking the planar problem as bounding aperture coupling, we model the equivalent transmission problem as shown in Fig. 4. In the Laplacian frequency domain we may write the voltage and current at  $Z_4$  as

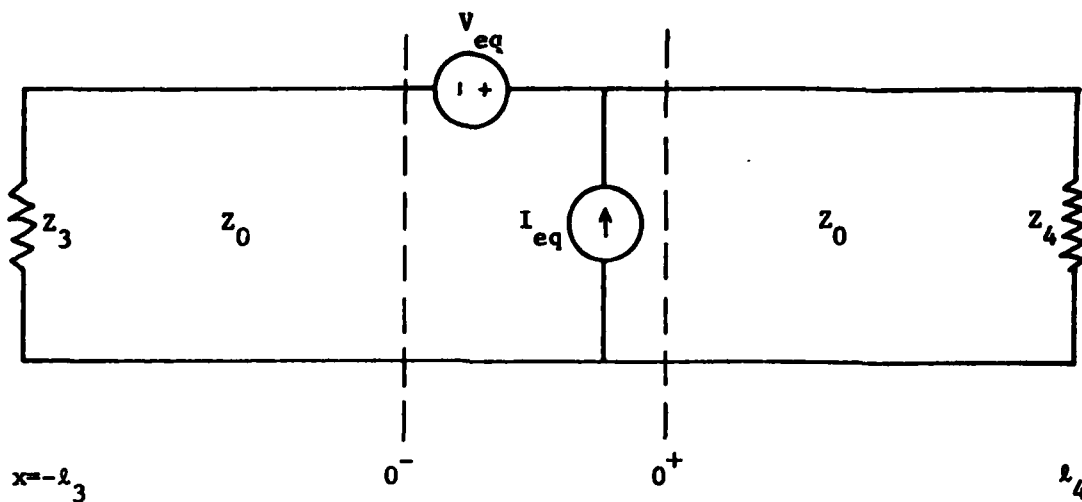
$$V_4 = \frac{-e^{-s\tau_4}}{1-\Gamma_3\Gamma_4} \frac{e^{-2s\tau_T} [(I_{eq} Z_0 + V_{eq}) + \Gamma_3 (I_{eq} Z_0 - V_{eq}) e^{-2s\tau_3}] \frac{Z_4}{Z_0 + Z_4}}{e^{-2s\tau_T}} \quad (36)$$

and

$$I_4 = V_4 / Z_4 \quad (37)$$

where  $\tau_3$ ,  $\tau_4$ , and  $\tau_T$  represent the time delays of  $l_3/c$ ,  $l_4/c$ , and  $(l_3+l_4)/c$  respectively ( $c$  - the speed of light). These equations will be the basis for our discussion of the bounds in the next section.

Before we proceed with the bounding problem, it is interesting to



$$V_{eq} = j\omega\mu R (\hat{y} \cdot \vec{a}_m \cdot \vec{H}^{SC-})$$

$$Z_0 I_{eq} = j\omega\epsilon\eta R \alpha_e (\hat{z} \cdot \vec{E}^{SC-})$$

$$Z_0 = \eta \ln(2d/a) / 2\pi$$

$$R = \frac{J_{Aperture}^{SC}}{I(0)} = \frac{d}{\pi\rho_0^2}$$

Figure 4. Simplified transmission line model for aperture coupling to a wire behind a planar conductor.

note some power relationships for aperture coupling. The average power transmitted by a small aperture to a half-space is given by

$$P_{\frac{1}{2}} = \frac{k^4}{6\pi\eta} [|\frac{P_e}{\epsilon}|^2 + |\eta\bar{p}_m|^2].$$

The average power launched on the wire structure is

$$P_W = \frac{k^2}{Z_0} (\frac{d}{\pi\rho_0}) [|\frac{P_e}{\epsilon}|^2 + |\eta p_{my}|^2].$$

Neglecting  $p_{mx}$ , which is unrelated to the wire problem, we have

$$P_W/P_{\frac{1}{2}} = \frac{3}{\pi^2 \ln(2d/a)} (\frac{\lambda d}{\rho_0})^2.$$

For many problems of interest,  $d$  is on the order of  $\rho_0$ . Since  $\rho_0$  has been required to be much less than  $\lambda$ , one wavelength, the power launched on the wire is much greater than that transmitted into the half-space. This increase in power is due to the higher field strength in the region of the aperture due to the presence of the wire. This is easier to visualize for the coaxial structure in which power is coupled to the TEM mode of the coax. Without the wire, the structure is simply a cutoff waveguide.

## V. BOUNDS:

In the previous sections we have developed the relations for low frequency aperture coupling to a wire. We have suggested that such coupling may be bounded above by a wire behind an aperture in a plane. This suggestion was based on comparison of the planar and coaxial problems and the physical mechanisms bounding the coaxial problem above by the planar problem. Hence, the first step in bounding the signals at terminations is to replace the given wire structure with a wire situated behind an aperture in a planar perfect electric conductor.

The second step is to bound the aperture polarizabilities and thus the sources in the transmission line model. For circles and ellipses, no bounds are required since exact formulae are available. However, other structures, which in general must be treated numerically, are not readily amenable to analysis and thus suggest the use of a bound.

Fikhmanas and Fridberg [23] have developed variational methods for bounding the polarizabilities. Unfortunately these methods still require a fair amount of computation. Papas and Jaggard [24,25,26] have considered bounds which depend only on the area and perimeter of the aperture and are based on symmetrization of isoperimetric variational analysis. The primary disadvantage of their results is exclusion of the aperture eccentricity which causes the magnetic polarizabilities not to be bounded as given, but which requires an averaging of the components of the magnetic polarizability. In fact, the bounds that are presented may be classed more as estimates since they do reasonably estimate the polarizabilities in many cases and do not bound the polarizabilities in several other cases.

Since our prime interest is in an absolute upper bound, I suggest that the aperture of interest be bounded by an elliptical aperture of minimum area circumscribing the given aperture. This bound would exceed that of constant perimeter for concave objects as is suggested by Papas, [24], but is less than the bound of Papas for many convex objects. Comparing this bound to the results of De Meulenaere and Van Bladel [14] for the polarizabilities of several shapes, we find the ellipse to bound the rectangle and diamond by a factor of

approximately 1.8. The rounded-off rectangle is also bounded by about 1.8 for eccentricities approaching unity and is equal to the ellipse for small eccentricity. In a similar manner, the circle bounds the polarizabilities of the cross.

In those cases when it is undesirable to compute the ellipse dimensions and bounds, a less tight bound may be obtained with a circle circumscribing the aperture. In this instance the polarizabilities are

$$\alpha_e = \frac{2}{3} (\text{radius})^3$$

and

$$\alpha_{\text{max}} = \alpha_{\text{myy}} = \frac{4}{3} (\text{radius})^3.$$

These polarizabilities and those of an ellipse with an x-directed major axis are tabulated in Table I of Section III.

Having bound the original problem by the planar problem and developed bounds for the aperture polarizability, we may complete the problem by determining the termination signal levels from the model of Fig. 4. The appropriate equations for this problem are (36) and (37). In many instances the geometry is known, but  $Z_3$  and  $Z_4$  are not. Let us consider several cases of interest. If the terminations are matched, then  $\Gamma_3$  and  $\Gamma_4$  are zero and  $V_4$  and  $I_4$  are

$$\begin{aligned} |V_4| &= |I_{\text{eq}} Z_0 + V_{\text{eq}}| / 2 \\ &\leq (|I_{\text{eq}} Z_0| + |V_{\text{eq}}|) / 2 \end{aligned}$$

and

$$|I_4| = |V_4| / Z_0$$

where we neglect phase cancellations that may occur between  $I_{\text{eq}}$  and  $V_{\text{eq}}$  represented by the previously discussed bounds.

Absolute bounds may be obtained by considering open and short circuit terminations along with a multiple reflection decay constant. In the time domain, (36) may be written for resistive terminations as

$$\begin{aligned} v_4(t) = & - \frac{Z_4}{Z_0 + Z_4} \sum_{n=0}^{\infty} \Gamma_3^n \Gamma_4^n [Z_0 i_{\text{eq}}(t - \tau_4 - 2n\tau_T) + v_{\text{eq}}(t - \tau_4 - 2n\tau_T) \\ & + \Gamma_3 Z_0 i_{\text{eq}}(t + \tau_4 - 2(n+1)\tau_T) - \Gamma_3 v_{\text{eq}}(t + \tau_4 - 2(n+1)\tau_T)]. \end{aligned} \quad (38)$$

The simplest bound of (38) is to neglect all multiple-reflection phase cancellations, set  $Z_4$  to infinity and let  $l_3$  tend to zero to obtain

$$|v_4(t)| \leq \sum_{n=0}^{\infty} 2e^{-\sigma n} \max\{Z_0 |i_{eq}(t-2n\tau_T)|, |v_{eq}(t-2n\tau_T)|\}$$

where the overall time delay has been neglected and  $\sigma$  represents the attenuation of the reflections and the power loss of the line if any.

This may be written as a bound on  $|v_4|$

$$|v_4|_{\max} \leq 2 \frac{\max\{Z_0 |i_{eq}|_{\max}, |v_{eq}|_{\max}\}}{1 - e^{-(\sigma+2\alpha\tau_T)}} \quad (39)$$

where  $\alpha$  is the exponential decay bound on the sources.

To bound the current, the only modification is to let  $Z_3$  and  $Z_4$  be short circuits to obtain

$$|i_4|_{\max} \leq |v_4|_{\max} / Z_0 \quad (40)$$

In the rare case of oscillations in the exterior fields at multiple frequencies, it might possibly be required to remove the maximum operator in the bounds and replace it by a sum. We shall neglect this case here and consider an alternative in the next section. If the phase delay of  $\Gamma_3$  and  $\Gamma_4$  are known to combine with twice the line length delay to cancel over the frequency range of interest, the denominators of (39) and (40) may be set to unity giving the bounds in terms of the maximum time derivative of the incident signal.

Current transmission line measurement and analysis techniques make use of power waves [27].  $Z_0 i_{eq}$  and  $v_{eq}$  need only be divided by  $2\sqrt{Z_0}$  to be normalized in the power wave sense. Thus we may bound the voltage and current at terminations with a local geometry characterized by  $Z_L$  as

$$|v_4|_{\max} \leq 2\sqrt{\frac{Z_L}{Z_0}} \frac{\max\{Z_0 |i_{eq}|_{\max}, |v_{eq}|_{\max}\}}{1 - e^{-(\sigma+2\alpha\tau_T)}} \quad (41a)$$

and

$$|i_4|_{\max} \leq |v_4|_{\max} / Z_L \quad (41b)$$

where  $\tau_T$  is proportional to the minimum distance between significant obstructions on the line one might encounter, such as the ribbing inside an aircraft.

VI. EXAMPLES:

To obtain a feeling for the capabilities of the developed bounds we consider the case analyzed by Kajfez [18]. He considered a circular aperture problem with the following parameters:

aperture radius	10 mm
w (y distance to wire)	20 mm
a (wire radius)	1 mm
d (wire height)	10 mm
$l_4$	2.1 m
$l_3$	3.0 m
$\phi$	TM incident wave direction
$\theta$	
	90°

and an incident time behavior of a double exponential

$$F(t) = A_0 (e^{-\alpha t} - e^{-\beta t}) u(t).$$

The incident parameters used were

$$\begin{aligned} A_0 &= 100 \text{ kV/m} \\ \alpha &= 3 \times 10^6 \text{ s}^{-1} \\ \beta &= 10^8 \text{ s}^{-1}. \end{aligned}$$

The time domain equivalent sources may be obtained from Fig. 4 as

$$Z_0 i_{eq} = 2.001 \times 10^{-14} \times \frac{\partial F}{\partial t}$$

and

$$v_{eq} = 4.902 \times 10^{-14} \times \frac{\partial F}{\partial t}.$$

The maximum of  $\frac{\partial F}{\partial t}$  occurs at  $t=0$  and is  $10^{13}$  V/m-s. For  $Z_L = Z_0$  and the  $\alpha$  of (41) the same as in  $F(t)$ , we have

$$\begin{aligned} |v_4|_{\max} &\leq .98 / (1 - .903) \text{ V} \\ &= 10.1 \text{ V}. \end{aligned} \tag{42}$$

Kajfez chose  $Z_4$  as  $10 \text{ k}\Omega$  and  $Z_3$  as  $10\Omega$  to obtain a peak voltage of approximately 0.5 volts occurring before reflections. Later voltages were of lesser value. Noticing that  $\Gamma_3$  and  $\Gamma_4$  provide phase cancellation with the line length for the frequencies of interest, we may neglect the denominator in (42) to obtain

$$|v_4|_{\max} \leq .98 \text{ V}$$

which is a reasonable bound.

It may be of interest to obtain a better bound without neglecting the denominator. In the problem given, the early time behavior has a decay constant of  $\beta$  and not  $\alpha$ . One method of improving the bound is to bound the response to each pole term of the incident field separately and add the results. To do this we write

$$F(t) = A_0 [(1 - e^{-\beta t}) - (1 - e^{-\alpha t})] u(t)$$

to obtain the bounds

$$|v_4^\alpha|_{\max} = .303 \text{ V}$$

and

$$|v_4^\beta|_{\max} = 1.014 \text{ V}$$

which sum to bound  $v_4$  at 1.317 V. By treating the poles separately we obtain a reasonable bound and do not have to be concerned with multiple modes requiring the maximum function of (41) to be replaced by a sum in some instances as suggested in Section V.

An interesting observation may be made by comparison with the measured data of Lin, et al [28], for a circular aperture of radius 18 in. with a wire centered 3.5 in. behind the aperture and 24 in. long. The low frequency data obtained for a parallel plate short circuit field incident from the x-direction has the same frequency behavior obtained from (36). (Constant for  $Z_3 = \infty$  and proportional to  $f$  for  $Z_3 = 0$ ) However, (36) overestimates the levels for  $Z_4$  infinity and both open- and short-circuited  $Z_3$  by approximately 20 dB. In addition, (36) has been used where the constraints on its derivation are no longer valid due to both the aperture interaction and the polarizability approximation. One might conjecture from these results that (36) and (37) bound problems for wires close to the aperture. Further study is required to support this conclusion.

## VII. CONCLUSIONS AND RECOMMENDATIONS:

This report has presented the results of an investigation on bounding signal levels coupled to wire termination behind apertures. The theory of small aperture coupling has been reviewed and interaction with wires developed in the spatial domain. The latter development has identified a capacitance not found in previous developments. This capacitance results from the discharge of the aperture region by currents launched on the wire and is of importance if the wire is sufficiently close to the aperture.

Bounds were developed for the signal levels at terminations with the following results: A wire behind an aperture in a plane bounds the problem of a wire behind an aperture in an enclosing structure for the same external short circuit fields; The aperture polarizabilities may be bound above by the polarizabilities of either a circumscribing ellipse of minimum area or less tightly bound by an circumscribing circle; Bounds on the power waves launched on the wire may be obtained from the aperture bounds using proportionalities related to the geometry in the vicinity of the aperture; Bounding multiple reflections with a decay constant, bounds on the termination voltages and currents are proportional to the power waves and a multiple reflection function; For phase cancelling multiple reflections, only the power waves need be considered, neglecting the multiple reflections; and To obtain a tight bound with multiple reflections, the bounds for the separate parts of the incident field should be summed if the field is separable into different time functions. These results follow a step-by-step form for obtaining bounds to the signals at desired terminations.

There are several recommendations for further work. It would be desirable to review the work of Lee and Yang [19] for wires close to an aperture to include the capacitive term that was not included in their work. It would also be desirable to extend this work to include larger apertures for applications in conformal antenna design. In some instances, the currents on wires in a bundle have been found to be larger than expected (greater than the bulk current). Hence it is desirable to consider the coupling to thick wires, wire bundles, and the associated differential mode currents in wire bundles.

Though the bounds appear to be reasonable when compared to computation, it would be worthwhile to set up measurements of several canonical problems for both aperture polarizability and wire coupling. With the importance of direct coupling, it would also be useful to develop the theory of coupling by wires passing through apertures between the interior and exterior regions. This coupling might involve either antenna structures or control cables, the latter often covered by composite panels and excited by diffusion. From a theory for such coupling, similar bounds may be developed as in this report for apertures.

## REFERENCES

1. C. D. Taylor, "External interaction of the nuclear EMP with aircraft and missiles," IEEE Trans. Ant. Prop., AP-26, 64-76, Jan. 1978.
2. V. V. Liepa, "Surface field measurements of scale model EC-135 aircraft," AFWL Interaction Application Memo 15, Aug. 1977.
3. G. Bedrosian, "Stick-model characterization of the natural frequencies and natural modes of aircraft," AFWL Interaction Note 326, Sept. 1977.
4. C. J. Bouwkamp, "Diffraction theory," Rep. Prog. Phys., 17, 35-100, 1954.
5. C. J. Bouwkamp, "Theoretical and numerical treatment of diffraction through a circular aperture," IEEE Trans. Ant. Prop., AP-18, 152-176, Mar. 1970.
6. H. A. Bethe, "Theory of diffraction by small holes," Phys. Rev., 66, 163-182, 1944.
7. C. M. Butler, Y. Rahmat-Samii, and R. Mittra, "Electromagnetic penetration through apertures in conducting surfaces," IEEE Trans. Ant. Prop., AP-26, 82-93, Jan. 1978.
8. C. M. Butler, "A review of electromagnetic diffraction by small apertures in conducting surfaces," Invited paper, IEE 1978 Int'l Symp. on EMC, June 20-22, 1978, Atlanta, pp 86-91.
9. W. A. Davis, "Numerical solutions to the problems of electromagnetic radiation and scattering by a finite hollow cylinder," Ph.D. dissertation, University of Illinois, Champaign-Urbana, 1974.
10. B. D. Graves, T. T. Crow, and C. D. Taylor, "On the electromagnetic field penetration through apertures," AFWL Interaction Note 199, 1974.
11. R. Mittra, Y. Rahmat-Samii, D. V. Jamejad, and W. A. Davis, "A new look at the thin-plate scattering problem," Radio Sci., 8, 869-875, 1973.
12. Y. Rahmat-Samii and R. Mittra, "Electromagnetic coupling through small apertures in a conducting screen," IEEE Trans. Ant. Prop., AP-25, 180-187, Mar. 1977.
13. Lord Rayleigh, "On the passage of waves through apertures in plane screens," Philos. Mag., 43, 259-272, 1897.
14. F. De Meulenaere and J. Van Bladel, "Polarizability of some small apertures," IEEE Trans. Ant. Prop., AP-25, Mar. 1977.

15. D. F. Hanson, "The current source-function technique solution of electromagnetic scattering from a half plane," Radio Sci., 13, 49-58, Jan. 1978.
16. R. E. Collin, Field Theory of Guided Waves, McGraw-Hill, NY, 1960, pp 294ff.
17. R. W. Latham, "Small holes in cable shields," AFWL Interaction Note 118, Sept. 1972.
18. D. Kajfez, "Excitation of a terminated TEM transmission line through a small aperture," AFWL Interaction Note 215, July 1974.
19. K. S. H. Lee and F. C. Yang, "A wire passing by a circular aperture in an infinite ground plane," AFWL Interaction Note 317, Feb. 1977.
20. C. M. Butler and K. R. Umashankar, "Electromagnetic excitation of a wire through an aperture-perforated conducting screen," IEEE Trans. Ant. Prop., AP-24, 456-462, July, 1976.
21. ———, Reference Data for Radio Engineers, International Telephone and Telegraph Corporation, NY, Dec. 1967.
22. C. W. Harrison, "Bounds on the load currents of exposed one- and two-conductor transmission lines electromagnetically coupled to a rocket," IEEE Trans. EM Comp., EMC-14, 4-9, Feb. 1972.
23. R. F. Fikhmanas and P. Sh. Fridberg, "Theory of diffraction at small apertures. Computation of upper and lower boundaries of the polarizability coefficients," Radio Eng. Electron. Physcs. (USSR), 18, 824-829, 1973.
24. C. H. Papas, "An application of symmetrization to EMP penetration through apertures," AFWL Interaction Note 299, Dec, 1976.
25. D. L. Jaggard and C. H. Papas, "On the application of symmetrization to the transmission of electromagnetic waves through small convex apertures of arbitrary shape," AFWL Interaction Note 324, Oct. 1977.
26. C. L. Jaggard, "Transmission through one or more small apertures of arbitrary shape," AFWL-TR-77-173, Dec. 1977.
27. ———, "S-parameter techniques for faster, more accurate network design," HP Appl. Note 95-1, Hewlett-Packard, Calif.
28. J.-L. Lin, W.L. Curtis, and M. C. Vincent, "Electromagnetic coupling to a cable through apertures," IEEE Trans. Ant. Prop., AP-24, 198-202, Mar. 1976.

1979 USAF - SCEEE SUMMER FACULTY RESEARCH PROGRAM

Sponsored by the

AIR FORCE OFFICE OF SCIENTIFIC RESEARCH

Conducted by the

SOUTHEASTERN CENTER FOR ELECTRICAL ENGINEERING EDUCATION

FINAL REPORT

PHOTOCONDUCTIVITY OF EXTRINSIC SILICON

Prepared by: Alan S. Edelstein

Academic Rank: Associate Professor

Department and University: Department of Physics, University of Illinois at Chicago Circle

Research Location: Air Force Materials Laboratory  
Laser & Optical Materials Branch  
Electromagnetic Materials Division  
Wright-Patterson Air Force Base, Ohio 45433

USAF Research Colleague: Robert J. Spry

Date: August 17, 1979

Contract No: F49620-79-C-0038

PHOTOCONDUCTIVITY OF EXTRINSIC SILICON

by

Alan S. Edelstein

ABSTRACT

As part of a materials characterization program on extrinsic Si we have developed a photoconductivity apparatus. We have tested the system by measuring the temperature dependence of the photocurrent and ionization energy of the holes in In doped Si for In at 20K and found that the long wavelength cut off occurs at  $8.37 \pm 0.3 \mu\text{m}$ . This technique has the advantage of being very sensitive and can be applied to both the donor and acceptor levels. Another possible application of the technique is given.

#### ACKNOWLEDGEMENT

The author would like to thank the Air Force Office of Scientific Research and the Southeastern Center for Electrical Engineering Education for providing him with the opportunity to spend a stimulating and worthwhile summer at Wright-Patterson Air Force Base. Special acknowledgement is due Dr. Richard N. Miller of the Operations Office of the Southeastern Center for Electrical Engineering Education, Florida Technological University for a well-organized program.

The author wishes to thank Drs. P. M. Hemenger, M. C. Ohmer, D. L. Reynolds, and R. J. Spry for useful discussions, worthwhile advice and kind hospitality. The technical assistance of Lt. T. C. Chandler and E. Soltis is gratefully acknowledged.

## I. INTRODUCTION

As part of an Air Force program on infrared detectors there is a need for sample characterization. In order to optimize detector performance it is essential to identify the dopants present, measure their concentrations, quantum efficiencies, and their recombination times. Photoconductivity experiments can play an important role in this sample characterization process. This report describes the development of a photoconductivity facility at Wright-Patterson AFB and the applications that can be made with this facility.

One application which will be made is in the characterization of extrinsic silicon samples. Extrinsic silicon is a useful material for the fabrication of infrared detectors and is particularly well suited for the fabrication of low cost detector arrays. A suitable dopant in the 3-5  $\mu\text{m}$  wavelength band is In while a suitable dopant in the 8-14  $\mu\text{m}$  wavelength band is Ga.<sup>1</sup> Compared to intrinsic detectors, extrinsic silicon detectors require lower operating temperatures before they are limited by the radiation background. This disadvantage is mitigated in the development of detector arrays by the possibility of combining these arrays with silicon signal processors on the same chip.

The photoconductivity facility is being established as part of a larger characterization program at Wright-Patterson AFB which includes Hall effect, absorption, and luminescence measurements. Photoconductivity as a sample characterization technique has several useful properties: 1. It is sensitive 2. It can identify both majority and minority dopants. 3. It allows one to make reasonable estimates of the impurity ratios. 4. The sample is used in the configuration that it will be used as a detector. In addition to these fundamental advantages, the method also has certain practical advantages, such as the measurements are relatively easy to make, and sample size and shape are not critical. In combination with absorption measurements photoconductivity measurements can determine the probability that an electron (hole) which is excited from the ground state to an excited state by a photon will reach the conduction (valence) band. The method has already been discussed extensively.<sup>2-4</sup>

## II. OBJECTIVES

The objectives of this project were:

1. To develop a facility for making photoconductivity measurements on extrinsic silicon.
2. To apply this facility to certain characterization problems of extrinsic silicon samples. In particular we had planned to apply the facility to study neutron transmutation doping, NTD, of silicon with phosphorous.

## III. PHOTOCONDUCTIVITY FACILITY

The basic processes utilized in the case of an acceptor impurity in the photoconductivity facility is illustrated in Fig. 1. A hole can be

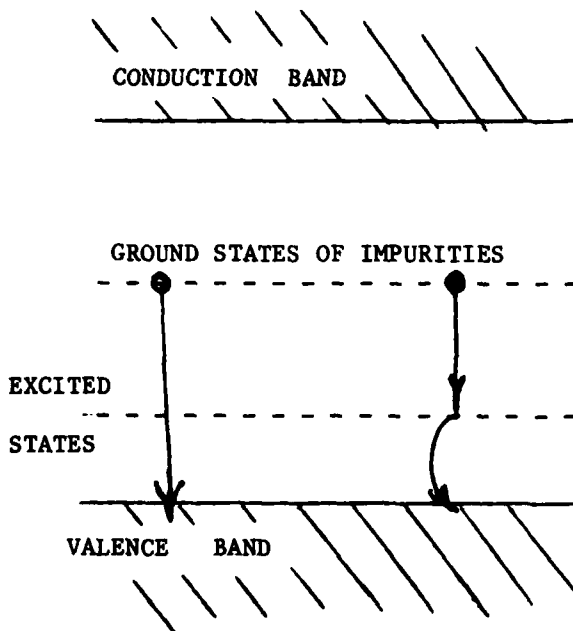


FIGURE 1- PROCESSES FOR THE PRODUCTION OF HOLES IN THE VALENCE BAND

excited directly from the ground state of the acceptor to the valence band by the absorption of a photon as illustrated by the process in the left side of Fig. 1. Alternatively the hole can be raised to an excited state by the absorption of a photon and then thermally excited to the valence band as illustrated by the process in the right side of Fig. 1. Thus at higher temperature one can observe excited states.

The facility that was put into operation this summer is illustrated in Fig. 2. Nearly all the components for this system

were already available. During the summer the remaining components were fabricated and the facility made operational. Below we summarize the basic operation of this system.<sup>5</sup> Light from the light source, a Nernst glower, passes through a

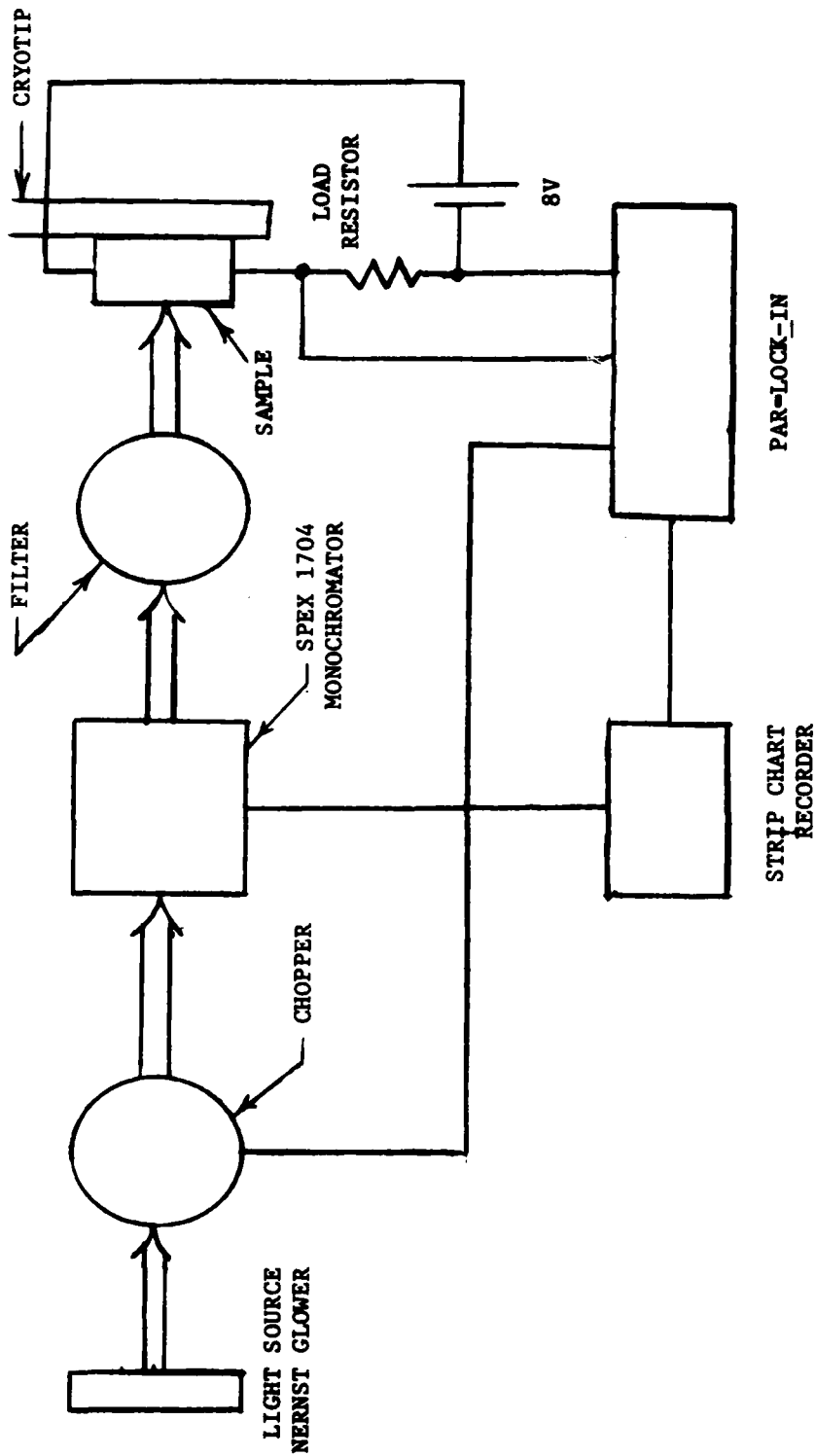


FIGURE 2- SCHEMATIC OF THE PHOTOCONDUCTIVITY FACILITY

chopper, then through a monochromator, a filter, and then on to the sample. This causes an increase in the sample's conductance. The chopper which was driven at frequencies from 50 to 200 Hz is used to drive the lock-in amplifier. The lock-in amplifier, PAR Model 124, was used with a PAR model 116 preamplifier in the differential mode. It is necessary to purge the optical system with nitrogen to avoid atmospheric absorption.

#### IV. TEST RESULTS

Our first test was to utilize a white light source. The light from this source was sent through the chopper, a germanium filter and then onto the sample. The signal generated in this way is given by

$$V_R = \frac{r^2 \Delta g I_0 R}{r + R + i\omega C r R} \quad (1)$$

where  $V_R$  is the voltage across the load  $R$ ,  $r$  is the sample resistance,  $\omega$  is the chopper frequency,  $I_0$  is the DC current,  $C$  a parasitic capacitance in parallel with the load, and  $\Delta g$  is the change in the conductance of the sample. In the derivation of Eq. (1), it is assumed that  $\Delta g \ll 1/r$ .

In this experiment and the subsequent tests reported on here a Si sample doped with  $2.5 \times 10^{16}$  atoms of In/cc was employed. The load resistance was 1K. At high temperatures,  $T \gg 100K$ , most of the In holes are ionized. Hence the photons have little effect,  $\Delta g$  in Eq.(1) is small, and the photo current is small. At low temperatures,  $T \ll 40K$ , the holes are not ionized and photons can give rise to a large  $\Delta g$ . Thus we expect the photocurrent to be a strong function of temperature. Figure 3 shows a plot of the signal voltage as function of temperature. We varied the chopper frequency between 200 and 1200 Hz and observed 10% decrease in signal amplitude which was proportional to the square of the chopper frequency. On subsequent runs we observed that improving the thermal shielding decreased the lowest temperature we could attain to 11K.

We then tested the full system shown in Fig. 2. The load resistance was 100K. The spectra we observed are somewhat contaminated by water vapor lines. Our results taken at 20°K are shown in Fig. 4 and should be compared with the

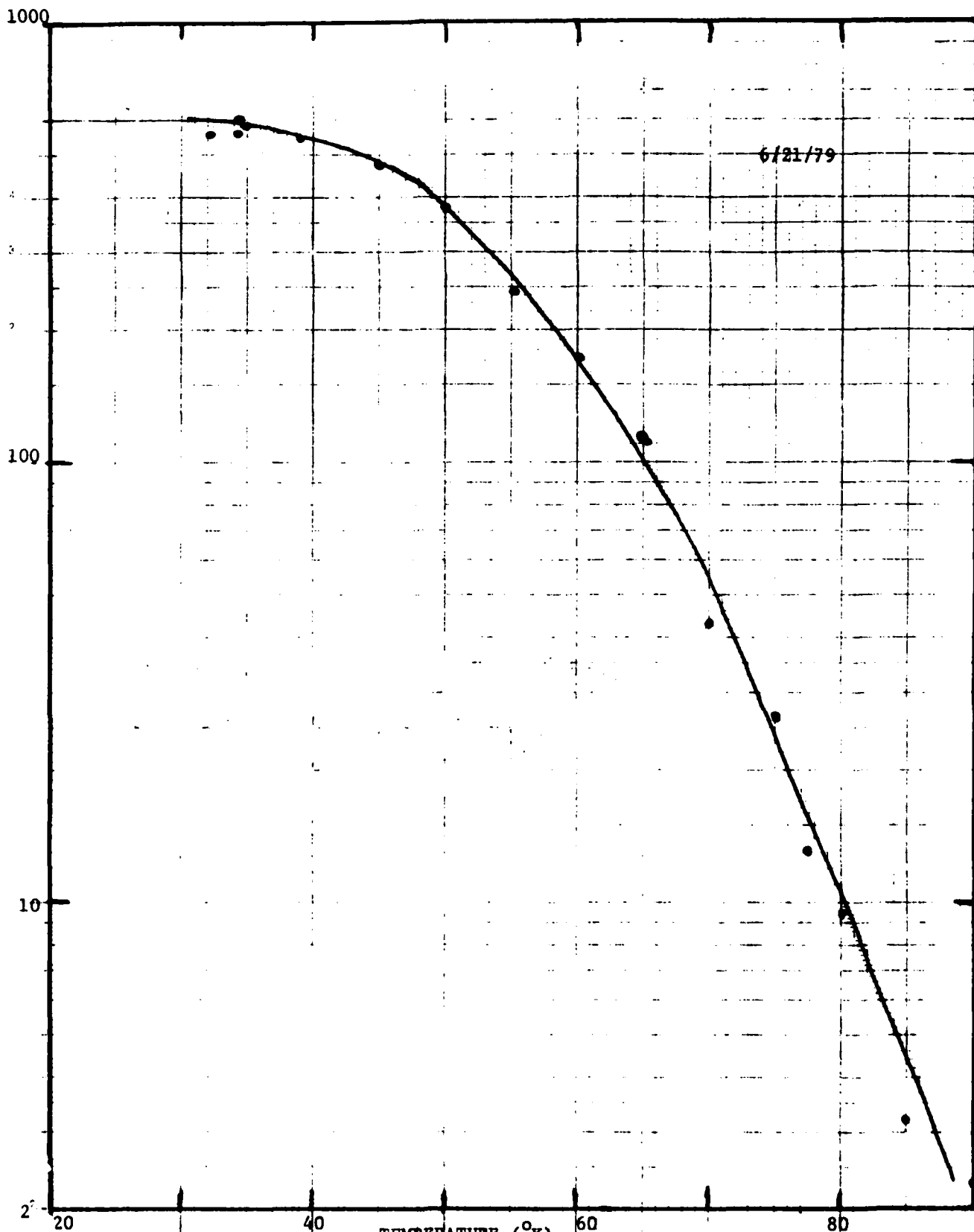


FIGURE 3 - PHOTOCURRENT USING GE FILTER. SAMPLE: SI:IN 061-194-0075  
 THE CURRENT IS PLOTTED IN RELATIVE UNITS ON A SEMILOG PLOT

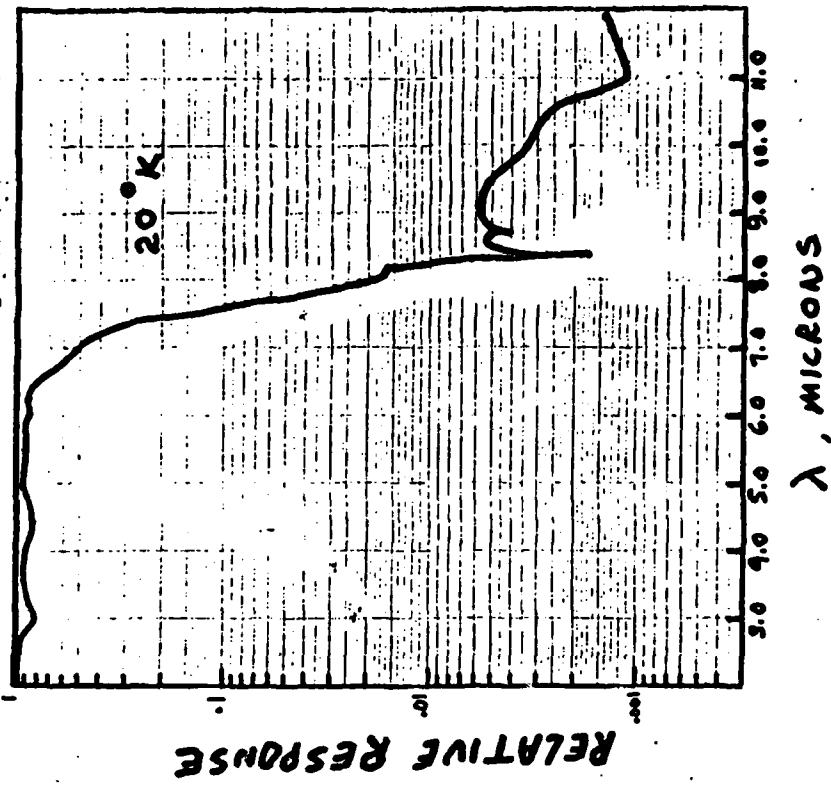


FIGURE 5 - SPECTRUM OF SI:IN SHOWING THE ONSET OF IONIZATION. DATA TAKEN FROM REF. 6.

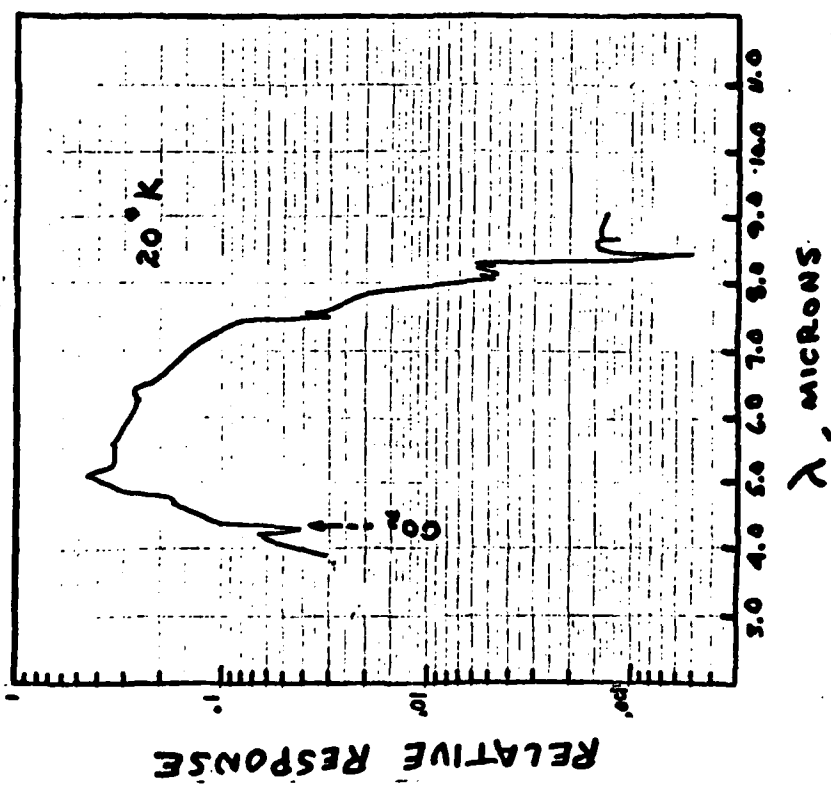


FIGURE 4 - SPECTRUM OF SI:IN SHOWING THE ONSET OF IONIZATION. DATA TAKEN WITH PHOTOIONIZATION FACILITY.

data of Baron et al.<sup>6</sup> shown in Fig. 5. One sees the good general agreement of the two sets of data. The sharp increase with decreasing wavelength was reproducible on subsequent runs and agrees with the results of Baron et al. The increase occurs at  $8.37 \pm .03 \mu\text{m}$ , i.e. .148 eV. This energy is less than the ionization energy of In in Si of .155 eV. The reason for this difference may be that the temperature was sufficiently high, 20°K, that the holes that are excited to high level excited states become thermally excited into the valence band. We have found it difficult to observe the excited states in this sample.

#### CONCLUSION AND SUGGESTIONS

We have established the facility. In the near future a computer will be interfaced to the system for automatic data acquisition. I accomplished the first of the two goals I initially set. We ran into equipment difficulties with the light source which slowed our progress and prevented us from reaching the second goal. Future work at the Materials Laboratory with the facility is planned which include attaining the second goal, i.e. studying NTD silicon samples.

I plan to submit a proposal to AFOSR to study the X-levels<sup>6</sup> in silicon using photoconductivity measurements in a magnetic field. These measurements will directly determine the multiplicity and symmetry of the X-levels.

#### REFERENCES

1. N. Sclar, "Survey of Dopants in Silicon for 2-2.7 and 3-5  $\mu$ m Infrared Detector Applications" *Infrared Physics*, Vol. 17, pp 71-82, 1977.
2. Sh. M. Kogan and T. M. Lifshits, "Photoelectric Spectroscopy - A New Method of Analysis of Impurities in Semiconductors" *Phys. Stat. Sol.* Vol. 39, pp 11-39, 1977.
3. E. M. Bykova, T. M. Lifshits, and V. I. Sidorov, "Photoelectric Spectroscopy as a Means for Complete Qualitative Analysis of Residual Impurities in a Semiconductor". *Sov. Phys. Semicond.* Vol. 7, No. 5 pp 671-672, 1973.
4. G. E. Stillman, C. M. Wolfe, and J. O. Dimmock "Far-Infrared Photoconductivity in High Purity GaAs," Chap. 4 in Vol. 12 *Semiconductors and Semimetals* ed. by R. K. Willardson and A. C. Been, Academic Press, New York (1977).
5. Details can be found in a) S. M. Ryvkin "Photoelectric Effects in Semiconductors" Consultants Bureau, New York, 1964.  
b) A. Rose "Concepts in Photoconductivity and Allied Problems", *Interscience Tracts on Physics and Astronomy* Number 19, Interscience a Div. of John Wiley and Sons, New York, 1963.
6. R. Baron, M. H. Young, J. K. Neeland, and O. J. Marsh, "A New Acceptor Level in Indium-Doped Silicon", *Appl. Phys. Letters*, Vol 30, No. 11 pp 594-596, 1977.

1979 USAF - SCEEE SUMMER FACULTY RESEARCH PROGRAM

Sponsored by the

AIR FORCE OFFICE OF SCIENTIFIC RESEARCH

Conducted by the

SOUTHEASTERN CENTER FOR ELECTRICAL ENGINEERING EDUCATION

FINAL REPORT

SYSTEM ANALYSIS OF THE

ENVIRONMENTAL TECHNICAL INFORMATION SYSTEM (ETIS)

Prepared by:	Willard Fey
Academic Rank:	Associate Professor
Department and University:	School of Industrial and Systems Engineering Georgia Institute of Technology
Research Location:	Air Force Engineering and Services Center Directorate of Environmental Planning Community Planning Group Tyndall Air Force Base
USAF Research Colleague:	John E. Palmer
Date:	August 13, 1979
Contract No:	F49620-79-C-0038

SYSTEM ANALYSIS OF THE  
ENVIRONMENTAL TECHNICAL INFORMATION SYSTEM (ETIS)

by

Willard Fey

ABSTRACT

The Environmental Technical Information System (ETIS) was developed to assist planners and base engineers in complying with the National Environmental Policy Act and the Air Force and Army regulations relating to it. As an on-line, efficient, simplified-format guide, it is effective in supporting environmental impact assessment and reporting. As the system's usage expands and its capabilities are broadened to include pollution abatement reporting, the experimental, non-standard format of the system becomes less acceptable. This report attempts to evaluate the present ETIS configuration and to review its future possibilities. Recommendations are then made to encourage lower development and operating costs, greater task effectiveness, and broader utilization. A multiservice, consolidated environmental data management and analysis system is suggested. Its operation would be similar to that of ETIS, but would be written in a military standard language, be located to utilize computer communications network connections, and be operated within the military with data management support from professional groups. The consolidated system would be developed in small self-sustaining increments over a five year period to avoid disruptive changes, major expenditures and impractical operations.

The consolidated environmental system could then provide environmental data and analyses inputs to an Air Force comprehensive planning assistance program. This would relate and evaluate the environmental, financial, energy, personnel and facilities resources and constraints so that base project and command realignment proposals could be compared and their feasibility tested on-line. The comprehensive planning system requirements could serve to clarify and unify the objectives and activities of the AF Engineering and Services Center divisions which presently analyse many aspects of planning and operations.

## ACKNOWLEDGMENTS

The author wishes to express his appreciation to the many organizations and individuals who have encouraged him and assisted in his research. Special appreciation goes to the Air Force Systems Command and the Air Force Office of Scientific Research that sponsored this excellent program of Summer Faculty Fellowships and to Dr. Richard Miller of the Southeastern Center for Electrical Engineering and Lt. Col. James Morrow, program coordinator at Tyndall Air Force Base, who so ably administered this program for me.

The Directorate of Environmental Planning (DEV) of the Air Force Engineering and Services Center at Tyndall Air Force Base provided an exceptionally pleasant, helpful and effective work environment. Colonel Sterling Schultz, Directorate Commander, and Mr. John Palmer, my research colleague, were particularly capable, helpful and supportive. Their help was indispensable to the success of this project. Others in DEV and its data processing group who provided much guidance and information included Major Gary Clendenen, Captain Ronald Hawkins, Captain Robert Kunselman, Mr. Allen Nixon and Mr. Zane Spitzer. Mrs. Carol Matthews patiently and efficiently handled the details of travel arrangements and typing.

Mr. Charles Hudson, Chief of the Air Force Base Planning and Development Branch of the Headquarters Air Force Environmental Planning Division, was most informative and gracious in providing an excellent broad perspective on military environmental activities and attitudes and in permitting me to use his office while visiting the Pentagon.

The very capable staff of the Army Construction Engineering Research Laboratory (CERL) that pioneered in interactive environmental programming was most kind and helpful. Dr. Ravinder Jain, Chief of the Environmental Division, and his team chiefs, Dr. Edward Novak and Mr. Walter Mikucki, provided many ideas and much information. The author extends particular appreciation to his principal contact at CERL, Mr. Ronald Webster, Chief of the Environmental Systems Team, who kindly shared his broad knowledge of all facets of environmental programming.

Others who were most generous with their time and knowledge included

Dr. Carl Ferguson, University of Alabama; Dr. Alton P. Jensen, Ms. Edith Martin, and Dr. Lawrence Gallaher, Georgia Institute of Technology; Mr. David Brown, Naval Coastal Systems Laboratory; Ms. Natalie Shaw, Naval Environmental Support Office; Mr. Charles Imel, Naval Civil Engineering Laboratory; Mr. Philip Rockwell, Naval Facilities Support Office; Mr. Lawrence Isley, Western Electric Company; Mr. William Webster, Air Force Armament Development Test Center; Mr. William Carlson, Defense Advanced Research Projects Agency; and Ms. Elizabeth Feinler, SRI International.

SYSTEM ANALYSIS OF THE  
ENVIRONMENTAL TECHNICAL INFORMATION SYSTEM (ETIS)

CONTENTS

ABSTRACT

ACKNOWLEDGMENTS

CONTENTS

- I. INTRODUCTION
- II. OBJECTIVES OF THE RESEARCH EFFORT
- III. RESEARCH APPROACH
- IV. THE EXISTING ENVIRONMENTAL TECHNICAL INFORMATION SYSTEM
- V. PRESENT AND PROSPECTIVE USES AND USERS
- VI. ALTERNATIVE SYSTEMS STRUCTURES FOR ENVIRONMENTAL COMPLIANCE
  - Multiservice collaboration
  - Program consolidation
  - Programming language
  - Computer hardware
  - Data base format and management
  - Communications network
  - User-to-computer interface format
  - Output formats
- VII. RECOMMENDATIONS
  - Consolidated multiservice environmental data management and analysis system
  - Conservative step-by-step development
  - User development
  - Air Force comprehensive planning system
  - Preparation for computer assistance in planning
  - AFESC coordination

## I. INTRODUCTION

Air Force bases and other facilities are located in environments that have ecological, geophysical and human influences and dependencies. Normal base activities and changes in base staff levels or physical status have impacts on the natural and human surroundings. In the past such impacts had little influence on Air Force decisions. However, since the passage of the National Environmental Policy Act (NEPA) in 1969, all agencies of the Federal Government have been required to evaluate and limit the environmental impacts of their proposed projects before they are undertaken and to regulate their ongoing activities. In the last ten years additional federal, state and local regulations have extended the requirements for reporting and control of both anticipated and existing environmental impacts. Substantially more regulation is expected in the future.

Two general areas of environmental concern have developed. The first, biophysical impacts, relates to ecological conditions, air and water quality, noise and radiation levels and the creation and storage of hazardous and solid wastes. The other involves socioeconomic impacts on human populations, employment, income, housing, schools, business, etc. Violations of the laws or even of "reasonable limits" are subject to judicial action. Several suits have been filed against each of the services. In May 1979 a Colorado judge issued an injunction to prevent the transfer of Air Defense Command personnel to other locations pending further analysis. The Air Force had failed to assess adequately the environmental impact of the transfer. The transfer was eventually permitted, but not without a long delay and considerable expense.

In order adequately to determine the impacts of activities and changes, the services have set up internal groups to gather environmental data of many types, to perform analyses to assess or forecast the impacts, to issue reports to the designated agencies, to keep adequate documentation to protect themselves against legal actions and to guide and assist operations people in the control of activities. An important group in the Air Force is the Directorate of Environmental Planning (DEV) in the Engineering and Services Center (AFESC). DEV's function is to develop and disseminate programs and procedures to facilitate Air Force compliance with the environmental rules and regulations.

Compliance involves data gathering, analysis, report writing and operational implementation of the appropriate decisions. Many of these activities are laborious and expensive when done manually. Computers have been used by the services to do some of these tasks more rapidly and less expensively than by hand. One computer-based assessment aid used by the Air Force is the Environmental Technical Information System (ETIS). It was developed and is operated by the Army Construction Engineering Research Laboratory (CERL). This program has three major parts (EICS, EIFS, CELDS to be discussed later) written in C language for time sharing execution under the UNIX operating system of a PDP 11/50 computer at the University of Illinois. It is used via commercial telephone lines by base civil engineers and community planners, military mission planners at the major commands and Headquarters Air Force and the analysts at DEV.

Several other environmental programs written in FORTRAN for other computers are maintained by DEV. Many other programs for required reporting are being planned. The Army and Navy also have programs and plans for compliance with the same environmental laws. A complete systems analysis of ETIS and its relationship to other DEV programs and other service programs seemed desirable as the result of uncertainties about a) the availability of Air Force access to the Illinois computer and Army programming, b) the apparent desirability, but questionable implementability, of multiservice environmental collaboration, c) continued operation with non-military-standard programming languages and computers, d) the complexities and expense of effective data base management and of an efficient communications system, and e) the format to be used for future programs.

The author was selected to assist with the analysis of ETIS and the planning for future programs because he was perceived to be independent and unbiased and his background seemed to be appropriate for the task. The capabilities required for this evaluation include a general familiarity with military, particularly Air Force, procedures; an understanding of the biophysical environment; an understanding of economic analysis; a familiarity with computers and their use; experience with scientific methodologies, systems analysis, benefit/cost analysis and dynamic

modeling; an awareness of legal procedures; and experience in implementing recommendations in large, complex organizations.

The author acquired his military background as a consultant with the MITRE Corporation, 1963-68. There he developed dynamic mathematical models of logistics, limited war and missile defense systems for Air Force contractors. Though he is not a biologist, the author has supervised ecological modeling for water quality, marine ecology and terrestrial ecosystem succession studies. He is co-author of a book, ECOSYSTEM SUCCESSION, to be published by MIT Press in late 1979. The author obtained his economics training as a doctoral student in the Economics Department at MIT. Before transferring to MIT's Sloan School of Management for dissertation work, he passed comprehensive doctoral examinations in the major fields of micro and macro economics, statistics, operations research and system dynamics. He has also performed and supervised dynamic modeling and analyses of companies, cities and national economics. The author has used computers for over twenty years and has programmed them using assembly languages, general purpose compilers (FORTRAN, COBOL) and special purpose simulation languages (DYNAMO, GASP) on a variety of computers including the first large scale electronic computer (Whirlwind I at MIT), many IBM computers, the Burroughs 5500, UNIVAC 1108 and CDC 6600/6400. He has a Master of Science in Electrical Engineering degree (MIT 1961) with a specialty in feedback control theory. The courses that he now teaches in the School of Industrial and Systems Engineering at Georgia Tech (feedback dynamics, systems engineering, engineering economy, and simulation) focus on systems analysis, benefit/cost analysis and dynamic system modeling using the computer as an important tool. The author's familiarity with legal procedures was obtained through his development of a special complete management curriculum (the Undergraduate Systems Program) while he was an Assistant Professor of Management at MIT (1964-67). As a consultant the author has implemented policy recommendations for large and small corporations and a city. He has also written papers and given talks on the problems of implementation.

## II. OBJECTIVES OF THE RESEARCH EFFORT

There are two general objectives of this research, one related to short run decisions and the other involving long run planning. The first goal is to analyse and evaluate the existing Environmental Technical Information System and the way it is used by the Air Force and then to identify and evaluate alternative systems and other ways to structure and use the present system, so that specific recommendations can be made to indicate whether the Air Force should continue to use ETIS. If continued use is desirable, the computer hardware type and location, programming language, communication network, data management procedures, and relationship to other Air Force environmental programs should be specified. If continued use is not desirable, alternative methods for environmental compliance assistance should be proposed. Results of this part of the research focus on decisions and actions to be taken by the Air Force within the next six to twelve months.

The second objective is to help with the planning for the long run development of Air Force programs and procedures for compliance with environmental law and effective environmental utilization and preservation. Environmental impact and pollution abatement laws are still being written and interpreted. It is an infant field that inevitably will expand and change. Many programs will be required in the future to respond to new and modified requirements. Many of these needs are already known, though the laws are not yet in effect. Therefore, planning for these needed programs and their relationship to existing programs can be done now. In addition as understanding of ecological system functioning expands, opportunities will be revealed for environmental utilization that will benefit both the Air Force and the environment. Planning for the research that will clarify beneficial intervention strategies and integrate these into the over all environmental data management and control process is essential. Compliance programming and intervention research should be planned for the next five to ten years. In that way proper directions can be established for all current activities and long run budgeting and staffing can be specified.

### III. RESEARCH APPROACH

A series of activities were required to perform this systems analysis of the Environmental Technical Information System. These included the identification of the detailed structure and use of the existing system, the determination of alternative structures and uses and the specification of the criteria to be used for evaluation. Then the alternatives were evaluated and compared. The result was a set of recommendations for changes in the system and suggestions for ways to implement the recommendations. For long run planning purposes, a list of future program needs and uses was developed based on estimates of future regulations and requirements by experienced environmental analysts. These requirements were then arranged in a logical time sequence.

The system identification, determination of alternatives and specification of criteria involved an extensive investigation that included a review of all the available material written about the system, personal use of the system and observation of those using it, and interviews with users, the developers of the system, and those who advocate or operate alternative systems or operating parts. Many of those who were interviewed are identified in the Acknowledgements. A benefit/cost analysis with constraints was used to evaluate and compare the alternatives. There was not enough time in the ten week summer program to thoroughly evaluate all alternatives for all the elements of the system. Therefore, some of the recommendations suggest future studies.

#### IV. THE EXISTING ENVIRONMENTAL TECHNICAL INFORMATION SYSTEM

The Environmental Technical Information System (ETIS) is a group of computer programs that have a common interactive format and access procedure designed to provide information necessary to assess the environmental impact of proposed base projects and to answer many of the questions required for an environmental impact statement. There are three major parts of this system, the Environmental Impact Computer System (EICS), the Economic Impact Forecast System (EIFS) and the Computer-aided Environmental Legislative Data System (CELDS). Other smaller parts include the Clearinghouse Information System (CHIS) and the Interagency Intergovernmental Coordination of Environmental Programs System (IICEPS).

These programs are used on-line over telephone connections by users throughout the United States. The programs are written in C language and run under the UNIX operating system on a Digital Equipment Corporation PDP-11/50 computer located at the University of Illinois in Champaign, IL. ETIS was written by the Army Construction Engineering Research Laboratory (CERL) over a period of six years, at a cost of more than \$4,000,000. The original version was written in FORTRAN under System 2000 and run on a CDC machine. This configuration produced programming difficulties and expensive maintenance, so a change was made several years ago to the C/UNIX/PDP arrangement. This is much more effective and less expensive, but it is not an Air Force or military standard structure. CERL has modified various of these programs for Air Force use and maintains the system in its various forms for all users. The PDP computer is leased for this purpose by CERL (also located in Champaign, IL) from the University of Illinois. The biophysical, socio-economic and legislative data bases are maintained by CERL with assistance from the Library Research Service of the University of Illinois.

The Environmental Impact Computer System is a program that takes information provided by a user about a specific proposed project (e.g., construction of a runway or barracks) and the physical and biological characteristics of the proposed site and provides in a matrix format the types and possible severity of environmental interferences that may be expected to occur and for which an impact statement may be required. If an EIS is necessary, the program provides the description to be used to

specify the impact of the project and the procedures and precautions to be used to minimize adverse effects. The program does not make the assessment nor write the environmental impact statement. It simply provides much of the information needed in a format that is easily understood and easily obtained by a base civil engineer who is not a computer programmer.

The Economic Impact Forecast System provides information about socioeconomic conditions (population, income, housing, etc.) for all United States counties. It also includes an economic model that predicts the changes in these conditions that might occur if a change were made in a base's activities. This information is necessary both for environmental impact statements and for personnel realignment proposal evaluations.

The Computer-aided Environmental Legislative Data System provides abstracts of federal and state environmental legislation and regulations. These indicate to the user the legal constraints that must be considered in the design of base projects. Many keyword categories are provided to enable the user to obtain the needed information quickly. A few local law abstracts have been added recently and more are proposed because the local laws sometimes are the most stringent.

While this system is used by only a small percentage of Air Force bases (and Army bases), it has been found to be effective and easy to use by most users, and its use is growing. Air Force [ 5, p. 1] and Navy [ 6, p. 45] studies have recognized its usefulness and recommended continued, expanded utilization. AFR 19-2 requires the use of ETIS.

There are other programs, not associated with ETIS, that perform other environmental tasks. The Air Force DEV maintains programs that plot noise intensities around bases and perform simple pollution abatement reporting. These are written in FORTRAN and run on the CDC 6600 computer at Eglin AFB. The Naval Environmental Support Office at Port Hueneme, CA maintains several programs for pollution abatement reporting. These are written in COBOL and run on an IBM 370 machine. Neither the Air Force or the Navy systems are interactive. Measurements of noise, air, water, and solid waste variables are provided by the user and these programs in a batch mode provide hard copy plots or reports at a later time. There are other smaller activities in each of the services that provide environ-

mental support. I did not have time this summer to review them all. However, each has its own program or programs written in its own language and run on a different machine. The activities are not coordinated, so there may be some functional overlap and use is limited.

Each of the groups in the services is planning new programs that will be needed to respond to the greater demands of recent and expected legislation. At this time the different programs in the services perform different tasks. There is relatively little repetition. However, in the next two or three years, there will be much overlap as all the services will be forced to respond to the same laws. If collaboration is to be effective in preventing repetition of effort it must be started now.

## V. PRESENT AND PROSPECTIVE USES AND USERS

At present ETIS is used as a source of information and simple analyses by planners and engineers at headquarters, command and base levels who need to assess, report and/or mitigate the impacts of proposed base projects and realignments on the socio-economic and/or biophysical environments. The program does not write reports, make decisions or control operations, but it does provide important information in a form needed by those who do.

The characteristic that sets ETIS apart from the other environmental programs that perform analyses or write reports is its consolidated, interactive, user oriented format. As the environmental laws become more stringent and expand to affect more aspects of base operations, planning at all levels will become much more complex and reporting and control activities will become more burdensome and difficult. Computerized assistance will be essential. But separate programming on a different computer in a different language for each report and task will soon be inadequate.

Project planners will need to quickly relate and compare the effects of a proposed project on different aspects of the base's environment. The evaluation of personnel transfers from one or more bases to others will require the simultaneous estimation of the economic distress in the declining bases' communities, the extra strains on the biophysical environments of the expanding bases and the advantages and costs of the transfers. These will then be compared for the different possible ways that the realignments can be made. To be manageable such a task requires a single source for the estimates, rapid interaction, and simple user-oriented formats for planners or commanders who are not likely to be programmers themselves.

Environmental impact assessing and statement writing; air, water, hazardous waste, noise, radiation, etc. pollution reporting; and abatement control can all be done by hand or using separate computer programs. But the consolidation of computer programs in a single place with a common format and access procedure would greatly simplify the activity, reduce errors and lower the skill level required for base engineers. Since the planning effort will require consolidated data sources and interaction anyway and such a format would greatly reduce the compliance and abatement effort, it would seem that a consolidated data base which can be

interactively accessed by non-experts to relate and compare various environmental aspects at several bases should be the long run goal.

These observations may seem far fetched, idealistic or unnecessary to some, but I suspect that the severity of the long run impact of environmental laws on military activities has not been fully recognized. Actually it is not just environmental legislation that will change the military command and control structure. Three clearly visible forces will all arise in the next five years to greatly alter operations. These are environmental regulation, economic recession and energy restriction. The general effect of these will be to impose simultaneously multiple major constraints on activities. Bases' freedom to negatively influence their socio-economic and biophysical environments will be curtailed at the same time that budgets are reduced and energy use is restrained. Planning and operation are relatively easy when one is reasonably free to do whatever ones mission requires. As constraints are added planning and operation become much more difficult and the adverse consequences of errors in either one are greatly increased. In order to avoid greatly reduced activities, planning will have to be done with great care and with a longer time horizon into the future. Activities that were separate and independent will become dependent. Priorities will be revised. The greater centralization, greater accountability, greater dependence on planning altered goals and longer run perspective that come with more constraints will require both expanded computer assistance and the learning of new skills by commanders, planners, and operating personnel. Therefore, the following sections discuss the training required to prepare people for these difficulties and the nature of a consolidated computerized environmental system which could be constructed a piece at a time over the next five years and could serve as a part of a broader planning system.

## VI. ALTERNATIVE SYSTEM STRUCTURES FOR ENVIRONMENTAL COMPLIANCE

Environmental regulations have become so numerous and complex that computer assistance for compliance procedures appears to be the only way to maintain costs and personnel effort at reasonable levels and to avoid the need for a staff of environmental experts and economists at every base. Therefore, the growth in computer use for this purpose is understandable, perhaps unavoidable, and undoubtedly will continue. The problem is to determine what computer systems should be developed to maximize effectiveness and minimize cost. This section deals with the specification of criteria for judging alternative computer configurations and programs, the definition of the characteristics of systems and programs that are important, and the identification and evaluation of alternative ways of obtaining systems with these characteristics.

A computer system or systems for assistance with environmental compliance must be easy and rapid for base engineers, staff analysts, planners, and commanders to access from their operating environments. It must be easy to use and understand by non-programmers. It must be capable of performing the designated tasks more effectively than by hand at lower cost within the existing protocol of the Air Force command and control system. Therefore, to be effective any system must have all of these characteristics -- accessibility, usability, capability, frugality, and acceptability. The following alternatives will be considered relative to these criteria.

There are several important aspects of the computer system or systems for environmental compliance. These aspects include the degree of multi-service collaboration in program development and use, the extent of consolidation of the programs for different environmental tasks, the programming language to be used, the time sharing/batch processing configuration, the type and location of computer hardware, the format of the data bases, the nature of the communication network, the style of the interaction between user and machine, and the output formats. Further judgements are needed to determine which people or organizations should maintain the operating system(s), program the tasks required, and update the data bases. While each of these will be discussed in a separate section, appropriate references will be made when one aspect is dependent

on another.

Multiservice collaboration seems to have many advantages in environmental impact and base realignment assessments, forecastings and reporting. Standard triservice procedures, programs and models would lead to service-wide uniformity in evaluations. This would enhance understanding and confidence at all command levels, prevent contradictions that could lead to legal difficulties, and maintain credibility for the DoD effort. Collaboration would lead to only one programming effort instead of several, require the maintenance of one data base instead of several, and incorporate the best ideas of all the services in one system. Therefore, a higher quality program would be obtained at a much lower cost.

The desirability of triservice collaboration in this area seems to be universally accepted. It has been endorsed, even directed, by DoD and the services. No one with whom I have spoken opposes it, perhaps, because its benefits are so large and obvious or because it is the stated policy. Nevertheless, collaboration has been limited. An equally universal opinion is that it will not happen in practice. Therefore, the question is not whether the services should collaborate in environmental matters, they obviously should; but rather it is, how can it be accomplished?

For greatest benefit collaboration should occur at the conceptualization, planning, system development, use and upgrading stages. Before any joint program is written to do any common tasks, all three services (often represented at several levels) should specify their needs and understand the needs of others. All should participate in the conceptualization of a procedure, algorithm, data display and/or analysis that would meet the needs and be usable and effective in the organizational and human contexts within which the needs arise. Services do not always do this for their own activities, so the collaboration sometimes would improve their processes. All should participate in planning the development and use of each program and its relationship to other programs. While all services need not participate in the computer programming, all should participate in debugging and testing the programs. After development and testing, all should use the working programs and contribute to their continued improvement.

Collaboration has been difficult to achieve. A triservice committee

for environmental matters was created. It held several annual meetings and subcommittees were formed to study particular issues. The subcommittees never met. Some limited cooperation is occurring. The Army has written some special programs and modified some Army programs which the Air Force uses through Army supported facilities. Since collaboration did not occur at the conceptualization stage of the Army's programs, expensive Air Force modifications were required and dissatisfaction still exists with one part of the system. On occasion some Air Force bases use some of the Navy's environment programs maintained at Port Hueneme. The Naval Civil Engineering Laboratory occasionally uses the Army's ETIS program. There has been an attempt to obtain a standard socioeconomic impact analysis methodology for base realignment evaluations. Unfortunately, a collaborative conceptualization effort was not undertaken. Therefore, there are several methodologies that are candidates to be the standard. Each is advocated by its originator with no one being so clearly superior that it cannot be challenged. A confrontation may or may not occur and a standard economic impact methodology may or may not be mandated; but even if one is selected, there is certain to be continued controversy and implementation difficulty.

Problems in achieving collaboration are understandable. Military people by nature are and must be strong, self-assured and self-reliant, since they must be ready and able to repulse a national enemy. For many years there have been interservice differences over limited funds and the maintenance of self-identity. The services' command structures themselves are based on authority, not collaboration. Therefore, collaboration will be difficult to achieve.

There are several approaches to collaboration that either have not worked or could be expected not to work. A general directive to collaborate from the upper levels of DoD or the services has not worked. Even if the procedures for collaboration had been clearly specified and appropriate rewards and punishments had been devised, it would probably not have succeeded. It is philosophically inconsistent and in practice almost unenforceable to force people to collaborate. The creation of multiservice committees to foster collaboration will not work unless many of the people are strongly motivated to collaborate. They rarely are. In addition

such committees are usually composed of high level people, but to be effective the collaboration is required at the working levels. Designation of one service or a group in one of the services to take the lead in encouraging collaboration or in creating the standard systems inevitably leads to conflict because it sets one service above the others. Finally, collaboration seldom arises spontaneously in a large organization unless there is so great a crisis which so clearly points to collaboration as the only means to survival that it is unavoidable. Therefore, one should not wait for it to happen by itself.

If collaboration cannot be forced or lead and will not arise spontaneously, how can it be achieved? The only possibility that occurs to me is the use of dedicated personal initiative. This would involve a small group of people headed by a civilian with no commitment to any one service and funded by DoD. They would have only one objective to which they were strongly personally committed -- to have a standard multiservice environmental analysis system created and operated that works effectively and is used widely.

They would go to the operating and planning people in the services at headquarters, command and base levels with the service's staff people and help the potential users determine what they need, what they could and would use and how they would use it. This presumes a thorough knowledge of the environmental laws, precedents and expected developments. Therefore, they would also work closely with EPA and other agencies. There are existing programs at each service that might be used in whole or part with or without reprogramming that would have to be reviewed. Engineering and support groups in the services would be encouraged to share their research, programs and knowledge and to direct their efforts toward significant problems that everyone is facing. The catalyst group would encourage contacts between operating counterparts in the services to exchange ideas and problems. They would encourage the drafting of concept proposals for future programs based on their knowledge of common problems. These would be critiqued individually and jointly by operating and staff people in the services. They would involve the appropriate service people in the detailed planning for each program that must fit into the general system. Common computer interaction and output formats

would be developed collaboratively for the programs. Much of the system usage would be through a central computer location with wide, easy, inexpensive access. The group would help to set up a facility or use an existing one. The capability for decentralized (on site) use in some cases should probably be provided. Through time new programs would be developed and old ones improved through the same close cooperation.

The catalyst group would have to take the initiative to make the contacts, do much of the legwork, follow up on ideas and activities started in the services and maintain uniform, triservice usability. If the group did its work well, the resulting standard programs would be so useful, so well-known, so accessible, and so acceptable that widespread use would be difficult to prevent.

The success of such an activity would be strongly dependent upon the capabilities and personalities of the people. They would have to be exceptionally capable, impartial, motivated, diplomatic, persuasive, persistent, tolerant of criticism and unselfish. Clearly, the most difficult task would be to find the right people. If they could be found, success would be quite likely and the benefits would be very great. Without the right people such an effort would fail, even if it were properly organized and the philosophy and tasks were clearly communicated to the people that were chosen.

Program consolidation refers to the combining of the various environmental impact and pollution abatement programs into a single large program that is written in one computer language and run on one computer which services all users. ETIS is a partly consolidated program in that several programs (EICS, EIFS, CELDS, CHIS, etc.) are grouped together in a single place with a common format. However, there are many others operated by different groups in the services that are not associated with ETIS or each other.

There are advantages and disadvantages to consolidation. The advantages include convenience, efficiency, comparability of information about different environmental variables. If all programs are in the same place with the same use format a user must learn only one set of access and use procedures. An interaction format can be designed to simplify use so that the engineer need not be a programmer and can understand information

about all types of environmental characteristics. Information about all areas can readily be compared because the data are all in one place and format. Complex interactive programs are too expensive to write several times, so separate programs would not have as many capabilities as a consolidated one. Where the same data base is used by several programs the consolidated format is more efficient because several forms of the same data need not be stored and updated.

The two major disadvantages are the possible failure of a consolidated program to deal with all the necessary details of every local situation and lost efficiency when all programs are written in one language. Proper conceptualization of the consolidated program can avoid the former problem. A small specialized program can be programmed in a language that is particularly efficient for that application. The Air Force standard languages, FORTRAN and COBOL, were selected to efficiently program scientific (computation intensive) and data handling problems, respectively. Neither is suited to an interrogative user-to-machine interface, so the language of the consolidated system would not be either of these, if possible. The proposed military standard language, Ada, appears to do both scientific and data handling problems well and also handles interfacing. A benchmark study of ETIS is scheduled for fall, 1979 to test that statement in detail. If Ada is better in all ways, it will be a strong candidate for the consolidated system language and will eliminate the second disadvantage.

The consolidated system seems to be a desirable choice if a military standard language that equals FORTRAN and COBOL in their specialties can be found and if a broad, collaborative conceptualization procedure can be found to precede the writing of programs in the consolidated system.

Programming language selection has four important aspects -- military standardization, portability, capability and efficiency. There are two major standard military languages, FORTRAN and COBOL. Programs written in other languages cannot be run on military computers. There are a few exceptions to this, but they are not relevant to environmental programming. Portability refers to the ability to run a program on a variety of different computers. Capability and efficiency are often related in the sense that most high order languages such as FORTRAN or COBOL have the capability

to perform most tasks, but they may be very inefficient in doing some things. Efficiency refers both to the ease with which the tasks are programmed and to the operating efficiency of doing the task.

ETIS is written in C language, a non-standard, non-portable, highly capable and efficient language. Other environmental programs are written in FORTRAN and COBOL both of which are standard and portable. FORTRAN is capable and fairly efficient for scientific applications and COBOL is effective for file handling problems. Neither handles very well the interrogative user-to-machine interaction employed by ETIS.

There are several reasons for writing these programs in a military standard language. Programs written in non-standard languages cannot be run on military computers. Should these programs need to run on Air Force machines, reprogramming would be required. Programs written in non-standard languages are perceived to be experimental by users and are not taken as seriously as standard programs. Pressure to standardize is imposed by service computer people and higher level officers on the operators of widely used non-standard programs. It is the accepted way to do important tasks. A multiservice environmental system would almost have to be written in a standard language.

There also are reasons to write portable programs. Machines and people change. When such changes occur portable programs usually need only minor adjustments to run on other computers. Very few programs are perfectly portable and require no modifications. But major reprogramming is not needed. Professional managers of computer systems rarely permit non-portable software. C language programs are not portable because currently only PDP 1100 series computers support them.

ETIS was converted from FORTRAN to C to obtain a substantial improvement in capability and efficiency. It is not clear how much improvement has been obtained, but a benchmark study is planned to determine this. However, in the opinion of the programmers at CERL and other programmers at the University of Alabama and Georgia Tech with whom I have spoken the difference is "substantial." It is for that reason that CERL has been so reluctant to reprogram despite great pressures to standardize. The Air Force and Navy programs, written in FORTRAN and COBOL, respectively, are probably (I have not examined them in detail) efficient because they

are written in appropriate languages. However, they have no interactive capabilities.

There may be another alternative language called Ada. Ada is a proposed military standard language that was developed for the Military Computer Family (MCF). Ada is much like PASCAL and C, so it includes many features necessary to create interactive programs. If Ada were accepted as a military standard language and if it were substantially better than FORTRAN or COBOL for this application, then ETIS could be reprogrammed in Ada. The result would be an efficient, standard, portable program. The benchmark study is designed to include an evaluation of Ada.

Computer hardware refers to the machinery used to operate the programs. Computer selection is based on cost, efficiency and capability of the machine to operate the programs. Further considerations relate to the location and management of the host machine(s).

ETIS requires a computer that stores and transfers large data files efficiently, has an effective time-sharing capability and supports C language. Only PDP 1100 series mini computers support C. If ETIS were reprogrammed in FORTRAN or COBOL most large main-frame and mini computers could do the task. Mini computers seem to handle the large data handling, small computation, time-shared programs better than the large machines which were designed for massive computation. The C/PDP configuration is so effective, because an efficient language is run on an efficient mini computer. The Air Force standard machines are the Burroughs 3500/3900/4700's (to be replaced in 1982 under the Phase IV program) at bases, the Honeywell 6000 machines used by the commands, the CDC 6600's at Eglin AFB and the headquarters unclassified machines in the Pentagon which are being replaced next spring by computers that have not yet been announced. Any of these could run ETIS, if it were written in FORTRAN or COBOL, but a mini computer would probably be less expensive [see analyses in 10]. The benchmark test should somewhat clarify these judgments.

The Military Computer Family development has identified a standard hardware (instruction architecture) as well as a standard language. Most existing machines that conform to the standard are mini computers. Of these, two PDP versions, the 11/70 and the 11/780 VAX, are included. The VAX is a much more powerful machine than the 11/70. It has greater core

and disk storage capabilities; greater time-sharing terminal capacity; and uses a 16 bit instead of an 8 bit word length. The 16 bit word provides greater flexibility and programming efficiency. If a substantially expanded program size and usage is anticipated in the future for ETIS, the VAX is the logical computer choice. If little change is anticipated, the present PDP 11/50 is adequate.

Location and management are also important. Since ETIS is a centrally serviced facility, the computer must be easy and inexpensive to access. The present machine is located in Champaign, IL. It is reached via commercial telephone lines with two 800 level lines to be available soon. It is not connected to any military or civilian computer networks such as ARPANET or TELENET. Other commercial, university, or military machines may be more advantageously located, but I have not had time to investigate the alternatives thoroughly.

The present ETIS computer is operated by a university (Illinois) and leased through the Army Construction Engineering Research Laboratory. Some concern has been expressed that the machine is not an Air Force or even a military machine. Therefore, availability is dependent upon decisions and actions of organizations outside the Air Force. For occasionally-used or experimental applications this may be acceptable. However, this vulnerability may not be acceptable when ETIS is widely used on a regular basis.

Data base format and management are important for any data intensive system such as ETIS. There are 50-70 megabytes of data and abstracts associated with the current version. These are divided between biophysical, socioeconomic and legal/reference information categories. The biophysical data base includes a list of endangered species, information about the environmental impacts for different types of projects and site characteristics, and mitigation procedures. The socioeconomic data base includes recent values for variables such as population, income, housing, employment, etc. for all continental United States counties. The legal/reference data base contains abstracts of state and federal laws and regulations pertaining to environmental matters and lists of contacts for information and interpretations about environmental considerations.

Updating of the computer data files is done by CERL. The biophysical

information is relatively fixed so little update is required. If bio-physical data for each base were included, the updating effort would be substantial. Eventually base specific data will be required. At that time an organization should be selected to supervise the data gathering, formatting and filing.

Socioeconomic data comes largely from Bureau of the Census tapes. There are other data sources in other federal agencies which may be used in the future. People at CERL obtain the data tapes and transfer the information to disk storage. There is no direct access to data source computer files. In the distant future direct data transfer from source to ETIS file will be feasible and desirable. Until then an organization will have to obtain tapes and transfer data. Full time, experienced data management organizations exist for this purpose. One effective group is the Center for Business and Economic Research (CBER) at the University of Alabama. It would probably be better to have such a group manage the data than CERL because CERL's forte is programming and they are already understaffed. Therefore, the burden of data management should be removed so they can more effectively perform the critical programming function. The one weakness of CBER is its localized experience. It is an Alabama data center and does not now have national data in its files. Nor does it have experienced with national data. If national data centers exist, they may be better candidates than CBER, but I have not discovered them.

Legal abstracting for the legal data base is now done by the University of Illinois Library Research Center. CERL compiles contact and reference lists. Effort should be given to the evaluation of these activities and the search for alternatives. The reference updating should probably be transferred elsewhere to relieve some of the non-programming load on CERL.

The communications network is a vital part of ETIS. Much effort was devoted to the design of an effective on-line interface between the computer and users. This on-line interface is dependent upon the communications link between the user's terminal and the machine. Presently, ordinary commercial telephone lines are used, though two 800 level lines are being ordered and DEV has a data quality FEX line from Tyndall AFB

to Champaign. The two problems with telephone usage are high cost and low quality. High quality lines would be essential if graphics displays were used because high speed transmission is required (minimum of 1200 baud and preferably 9600 baud compared to the usual telephone 300 baud).

One alternative is the location of the computer at a center that has access to computer networks to which the users could be connected. ARPANET, SAMNET, and TELENET are possibilities. Unfortunately, no one has determined the availability of network access to the base, command and headquarters users. I have not had time to thoroughly investigate the network and base configurations, but it is a necessary task since improvements in operating cost and quality associated with network use can be substantial. The University of Illinois PDP 11/50 is not connected to any network. There would be a \$70,000 charge to attach the machine to the ARPANET connection in Champaign.

The user-to-computer interface format of ETIS has been developed with considerable thought and effort. The objective is to have the computer ask the pertinent questions and provide the pertinent answers in ordinary English on-line. Therefore, users who know nothing about computer programming can use the system easily. Users who are not aware of all environment impact statement requirements are provided with necessary information that they may have forgotten or of which they were not aware. The direct on-line interaction enables the environmental impact statement user to finish his task quickly all at one time while he is concentrating on it. It enables command and base planners to evaluate alternative projects and realignments quickly while they are thinking about the choices. The speed, flexibility and effectiveness of such a format encourages use and is much more task effective than batch access using FORTRAN or COBOL notation.

The superiority of the ETIS interaction format suggests the desirability of its use in future environmental applications. The difficulty is programming. It takes a great deal of programming skill and effort to build in this simplified interrogation capability. The structures of FORTRAN and COBOL are not conducive to this type of format. That is one major reason for the use of C language. The programming difficulty suggests that if this format is to be used, a single consolidated environmental

computer system should be developed to incorporate all the impact and abatement programs. That will avoid duplication of this difficult task. However, it also extends dependence on the non-standard C/UNIX/PDP configuration. It is to be hoped that Ada can be used as a capable, standard alternative to C.

Output formats that are pertinent and understandable greatly encourage effective system use. ETIS has a normal line-by-line printout format with sentences, lists of clearly identified data numbers, a matrix of impact characteristics to consider, and several bar charts for population distributions. There are no time history plots or maps. The Air Force has a NOISEMAP program (batch operated) that plots on a separate plotter base noise contours on a simple base map. The Navy's pollution abatement programs produce hard copy, 8 1/2 x 11 reports for submission to the appropriate monitoring agencies. ETIS has no hard copy report outputs.

Another output format for future consideration is computer graphics. Use of graphics would permit maps with superimposed characteristics to be presented on-line. It would make possible the drawing of time histories of environmental variables and the superimposing of different characteristics for one base or the same characteristic for several bases on the same graph for comparison and trend analysis. It would seem desirable in the long run to have all of these output formats available in one program with one additional capability. That is the ability to transfer data directly to monitoring agency computer files and microfiche without the need to produce paper copies. In order to provide these output capabilities, the files of ETIS would have to be restructured to facilitate the programming of hard copy, graphics and direct transfer modes.

## VII. RECOMMENDATIONS

The Environmental Technical Information System is an effective program whose use should be extended as much as possible. Recommendations for the system pertain to its scope of use and the details of its structure. It should be noted that it has been and is effective in its present form. Therefore, the recommendations focus on ways to broaden its use, reduce its cost and increase its effectiveness to make it an even more successful system and to prepare it to encompass additional environmental capabilities as needs arise in the future.

The characteristics of ETIS as enumerated in the previous sections cannot be taken separately for individual recommendations. The parts depend on each other so the system must be considered as a whole. Therefore, the primary recommendation, that the Environmental Technical Information System should be developed over a period of five years to become the consolidated multiservice environmental data management and analysis system, sets the context for recommendations related to hardware, software, communications, etc. Figure 1 shows a diagram of this proposed system as it might look when completed in 1984. The advantages of program consolidation and multiservice use are discussed above. The elimination of effort duplication to reduce costs and the collaborative development to improve effectiveness are obvious. However, the difficulties associated with implementation are substantial. Assistance, guidance, and support are essential in a helpful, nonthreatening style. Detailed suggestions for accomplishing this liaison are offered above. Other ways may appear as development proceeds.

The broad multiservice context can only succeed in the long run if the program is written in a military standard computer language. The three alternatives are FORTRAN, COBOL, and Ada. A superficial comparison suggests that Ada will be more efficient and more portable in the long run than FORTRAN or COBOL. The efficiency should be researched or benchmarked to be certain. A detailed program evaluation is beyond the scope of this study. Since Ada is a future military standard language with compilers not scheduled for completion for a year or more, reprogramming from C to Ada would not be done for several years. Fortunately, C and

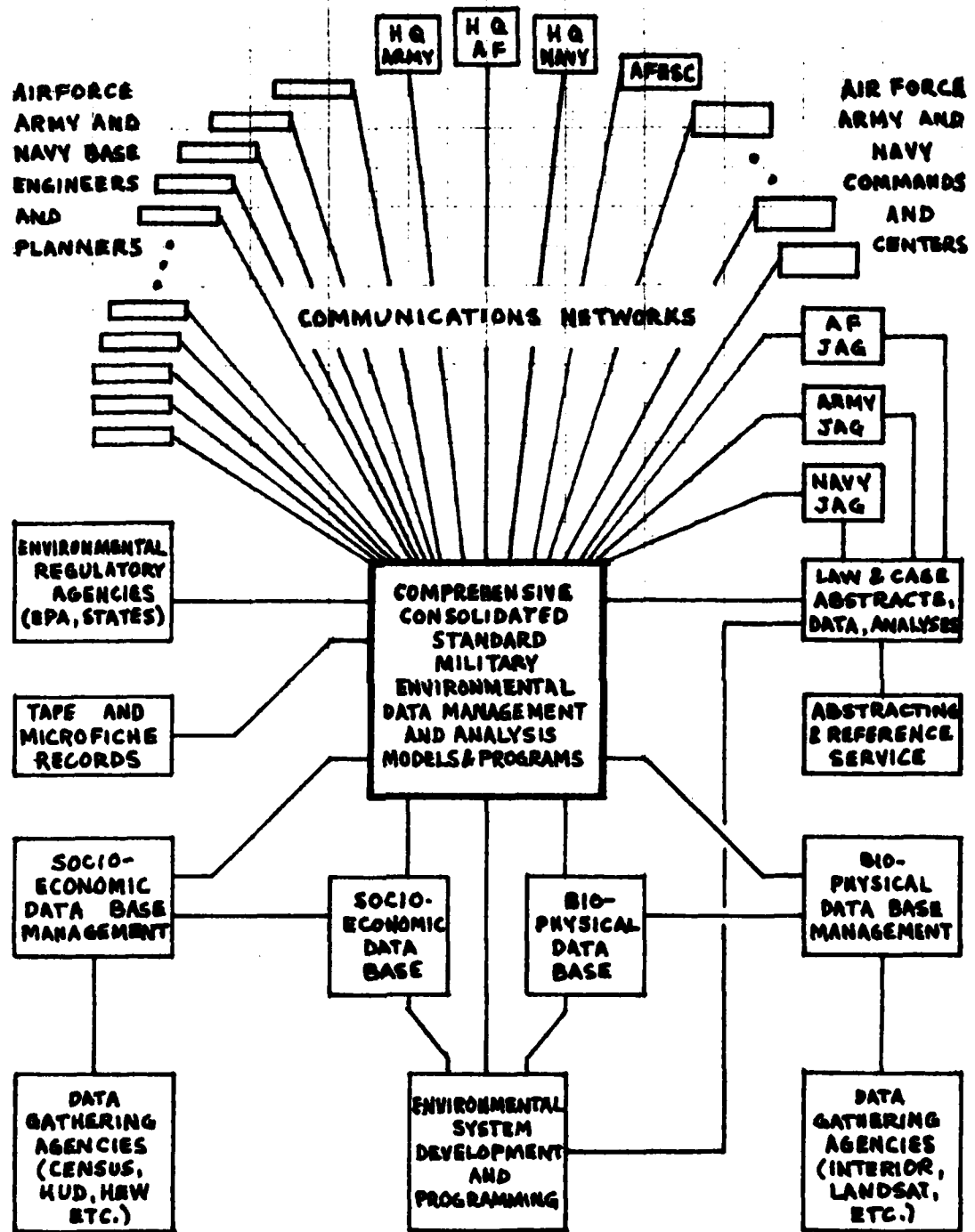


FIGURE 1. RECOMMENDED OPERATING STRUCTURE FOR A COMPREHENSIVE, CONSOLIDATED STANDARD MILITARY ENVIRONMENTAL DATA MANAGEMENT AND ANALYSIS COMPUTER SYSTEM TO BE FINISHED ABOUT FY 1984.

Ada come from the same general family of languages, so conversion or reprogramming ought to be relatively simple, while C-to-FORTRAN or C-to-COBOL reprogramming would be expensive and time consuming. It is assumed that the eventual standard operating system for Ada will be similar to or compatible with UNIX, the present operating system. Much of the capability and efficiency of the present configuration is associated with UNIX. Since the programming language and the operating system cannot be separated, the benchmark study mentioned above should consider the relevant combinations.

Unfortunately, any program's efficiency will also depend on the computer on which the operating system and language are run. A C/UNIX program run on a PDP 11/50 will not necessarily perform in exactly the same way as the same C/UNIX program run on a PDP 11/780 VAX. Therefore, the benchmark should also consider several hardware alternatives. The most-likely candidate is the VAX. It is one of the better military standard instruction set architectures associated with Ada. A major advantage is its compatibility with the existing ETIS. Therefore, a VAX machine could be obtained in a year or two to simultaneously run the existing C system and support the development of the Ada upgrade. Other possibilities use the CDC 6600 at Eglin AFB or one of the Honeywell 6000 series machines used by the AF Commands. Base and headquarters level computers are being replaced. When the replacements are known, they could be considered also. The only specific hardware recommendation is that the PDP 11/50 at the University of Illinois that now run ETIS be upgraded to a PDP 11/780 VAX. That will be an inexpensive way (about \$50,000) to provide expanded capability for the present system and prepare for the future configuration. Even if the consolidated system is not undertaken, this upgrade is worthwhile for the present system.

Data base management will become a major activity as the pollution abatement programs are added to ETIS. It is recommended that professional data base management organizations be used for economic and biophysical data updating. The programmers at CERL are too scarce and valuable for their programming skills to be used to maintain the data bases. The Center of Business and Economic Research at the University of Alabama

is a capable group, but is not set up for national economic data management. If no national economic data management organization can be found, CBER would be an excellent choice.

A communications network to link base, command and headquarters users from all the services to the consolidated system should be considered carefully. The locations of all potential users and their proximity to connection points for ARPANET, SAMNET, TELENET and other networks should be researched. The use of standard telephone lines is very expensive and of low quality. Modems can be installed to improve quality, but the cost remains high. 800 level lines help to reduce the cost. However, the study suggested above may reveal a location at the intersection of several nets. Then the computer could be located there and enable many users to access ETIS through existing low cost, high quality networks.

The on-line, simple, interrogative interaction format is a valuable part of the present system. It should be used for all programs as they are added to the ETIS package. A hard copy report-writing capability should be added (in time). The Navy has written effective report-writing programs that are not on-line. With the Navy's help these and other programs can be introduced into the ETIS on-line configuration. Thought should be given to the file structures and processing necessary for direct data and report transfer to EPA and other agency computer files. Eventually, paper copies may be eliminated. Data will be transferred from military to agency computer files and hard records will be kept on microfiche.

Display formats are also important. Computer graphics capabilities are available which, display graphs, charts and maps with superimposed overlays of data for various characteristics. For example, the basic display of a base map could have overlays for noise contours, vegetation types, surrounding community population densities, etc. Both planners at all levels and base personnel who monitor and control environmental factors will find such a capability extremely useful. Within a year or two a study of graphics capabilities and their potential uses should be done to prepare for the addition of a graphics capability to ETIS. The CERL researchers are already experimenting with graphics systems, so some of the capabilities and limitations will be known before the study is begun.

The preceding recommendations refer to a consolidated multiservice environmental computer system as it could exist in five years. The actions necessary to achieve it should be taken slowly, one at a time in such a way that each step will be small enough to be budgetted easily and will be justified on the basis of its immediate contribution to the system in operation at the time. Therefore, there should be no major changes, no large expenditures, no disruption of operating systems and no unpleasant, unnecessary conflicts as the capabilities required for the consolidated system are gradually assembled. The necessities are a clear goal, patience and persistence. Figure 1 shows the goal, the future system. Figure 2 provides a milestone chart for many, but not all of the required activities. The times in the milestone chart are not rigidly fixed nor is the sequence of actions always required as shown. Not all required tasks are included in this outline. As time passes and some of the tasks are finished the chart should be revised. It is meant to be a general guide, not an inflexible rule.

The justification for and benefits from this system are based on its use by engineers, planners, and officers. The tasks with which the system assists are required by law. Use of the system enables those tasks to be done faster and better with less personnel effort. The personnel time saved and the more effective compliance that avoids litigation constitutes the economic benefit. The more widely the system is used, the greater will be the benefits. ETIS and other environmental programs are not used widely enough. Less than one quarter of the Air Force bases use it regularly. The Army is not much better and the Navy does not use it at all. A kind of marketing campaign is needed. Engineers and planners who do not use it should be encouraged and assisted. If equipment inadequacies limit accessibility, they should be resolved. One common problem is that the computer terminal available to some base civil engineers is hard wired to the base Burroughs computer. It cannot be used for off base telephone connections. Relatively minor modifications can resolve this problem. However, initiative must be exercised by capable staff people to discover and correct the particular problems at each user site. This may require the designation of one or two people to travel to or at least contact by telephone each potential user.

TIME	HARDWARE & COMMUN	SOFTWARE	PROGRAMS	SOCIO ECON DATA BASE	BIO-PHYS DATA BASE	LEGAL DATA BASE	COLLAB. & TRAINING	
4 Q FY 79	CONTINUE MULTIPLE	AGREE TO STANDARD.	CONTINUE EXISTING	CONTINUE EXISTING	CONTINUE EXISTING	CONTINUE EXISTING		
1 Q FY 80	OPERATE VAX AT UOI	LANGUAGE BENCHMARK	TO BE DEVELOPED IN C/C++ IN ORDER OF PRIORITY	STUDY DATA BASE MANAGERS	HAZARDOUS WASTE NEEDS		JOINT WORKSHOP HAZ. WASTE	
2 Q FY 80	ACCESS NET STUDY					STUDY JAG/DATA NEEDS		
3 Q FY 80		SELECT LANGUAGE	POLLUTION ABATEMENT	SELECT DATA BASE MANAGERS	STUDY L-R DATA NEEDS		STUDY EXPANDED USE CONTACT CECOS	
4 Q FY 80	VAX/NET DAR	IF ADA, DEMONSTRAT. PROGRAM	HAZARDOUS WASTE	STUDY L-R DATA NEEDS	STUDY DATA BASE MANAGERS	STUDY DATA BASE MANAGERS		
1 Q FY 81			STD/AUTO TAB A-1		SELECT DATA BASE MANAGERS		EXPAND USE STRATEGY	
2 Q FY 81	TERMINAL NEEDS STUDY	STUDY PROGRAM FILES REVISION	IMPROVED SRI	SELECT DATA SOURCES AS NEEDED	SELECT DATA SOURCES	SELECT DATA BASE MANAGER	TRAIN BASES TO COLLECT SOC-EC DATA	
3 Q FY 81			IMPROVED EWS		AS NEEDED		TRAIN BASES TO COLLECT BIO-PH. DATA	
4 Q FY 81	TERMINAL DAR	BEGIN REPROGRAM	BIO-PHYSICAL MODELS	BEGIN BASE DATA COLLECT.				
1 Q FY 82					BEGIN BASE DATA COLLECT.			
2 Q FY 82	RECEIVE VAX/NET							
3 Q FY 82								
4 Q FY 82	.....	BEGIN GRAPHICS	CONSOLIDATED SYSTEM IN OPERATION					
1 Q FY 83								
2 Q FY 83	RECEIVE TERMINALS							
3 Q FY 83								
4 Q FY 83								
1 Q FY 84								
2 Q FY 84								
3 Q FY 84								
4 Q FY 84	MAJOR DATA GATHERING AND PROGRAM DEVELOPMENT COMPLETE							

FIGURE 2. TIME TABLE TO ACHIEVE CONSOLIDATED ENVIRONMENTAL SYSTEM BY ABOUT FY 1984.

Questionnaires are not enough. Engineers and planners are busy people who have developed ways of doing their job over the years. Changing those old procedures in a context of many other pressures requires substantial skill and effort.

The last group of recommendations relates to planning, rather than legal compliance. Major constraints are now being imposed on Air Force operations. In all probability these will intensify as the 1980's progress. The environmental constraints both socio-economic and biophysical are discussed at length above. The energy and financial constraints have not been mentioned as extensively. The energy problems are obvious. National regulations are being imposed on public energy use. Buildings cannot be kept as warm in winter or cool in summer as before. Car pooling is being imposed. Gas Rationing has been proposed. In time the number of AF aircraft flights and vehicle miles may be limited. The country is also entering an economic recession which may last for some time. In recession times budgets are restricted and staffs are reduced. All but the essential activities are cut back.

Under such conditions planning and careful control become much more important than in unconstrained times. It is suggested that the concept of computer assistance could and perhaps will have to be extended to comprehensive planning at the various levels of command. It is extremely difficult for people to remember, relate and analyze the simultaneous effects of many constraints on actual operations and proposed changes. The computer is uniquely suited to that type of evaluation. Even now ETIS is used by some command and base planners. A more complete computer planning assistance program could enumerate, relate and evaluate, financial, energy, environmental, personnel, facilities, and mission requirement factors for present conditions and proposed projects and realignments. The computer could do analyses in a matter of minutes that people could only do in days or weeks.

The consolidated environmental system as recommended above could provide the environmental data and analysis input to this broader planning system. But the planning program should be separate from the environmental program because the other inputs (financial, mission, facilities including weapons, etc.) are service specific and in some instances, classified.

A conceptualization of this separate planning system is shown in Figure 3. To be effective it should be developed in the same format as the consolidated environmental system, but it should be operated within the Air Force. The same slow, step-by-step development should be used. Since it will be similar in structure and operation to the environmental system, the ideas and capabilities developed there should be usable for the planning system.

One problem with such a system is that its use will be unfamiliar to the planners and officers who have learned other approaches to their tasks. Many people distrust, dislike, or fear computers. That is understandable. In fact, I dislike them myself and use them as little as possible. However, their great speed, capacity and accuracy make possible many things that could not be done without them. It appears that effective Air Force comprehensive planning in an era of multiple service constraints is one activity that will need computer assistance. Therefore, thought should be given to the preparation of people and operations for this likely necessity.

Since the planning system would not be in operation for four or five years even if its development went smoothly, there is time for people to become accustomed to computer assistance and to be trained in the use of the system. An effort could be undertaken to encourage planners and officers to use existing computer programs more frequently. Planning seminars and computer familiarization programs could be developed. Several universities have special Masters programs (usually in engineering fields) for military officers. Courses in planning with computer assistance could be added to these curricula. The National Defense University and the Air Force Institute of Technology could develop programs related to this need. Opportunities for the development of planning skills which utilize computer assistance are widespread and should be considered carefully. Planning for planning is as essential as planning for environmental compliance.

Many of the factors that must be considered in comprehensive planning activities are being analysed by specialists in the AF Engineering and Services Center. The environmental area that is the primary focus of this report is one. Energy is another. A comprehensive planning

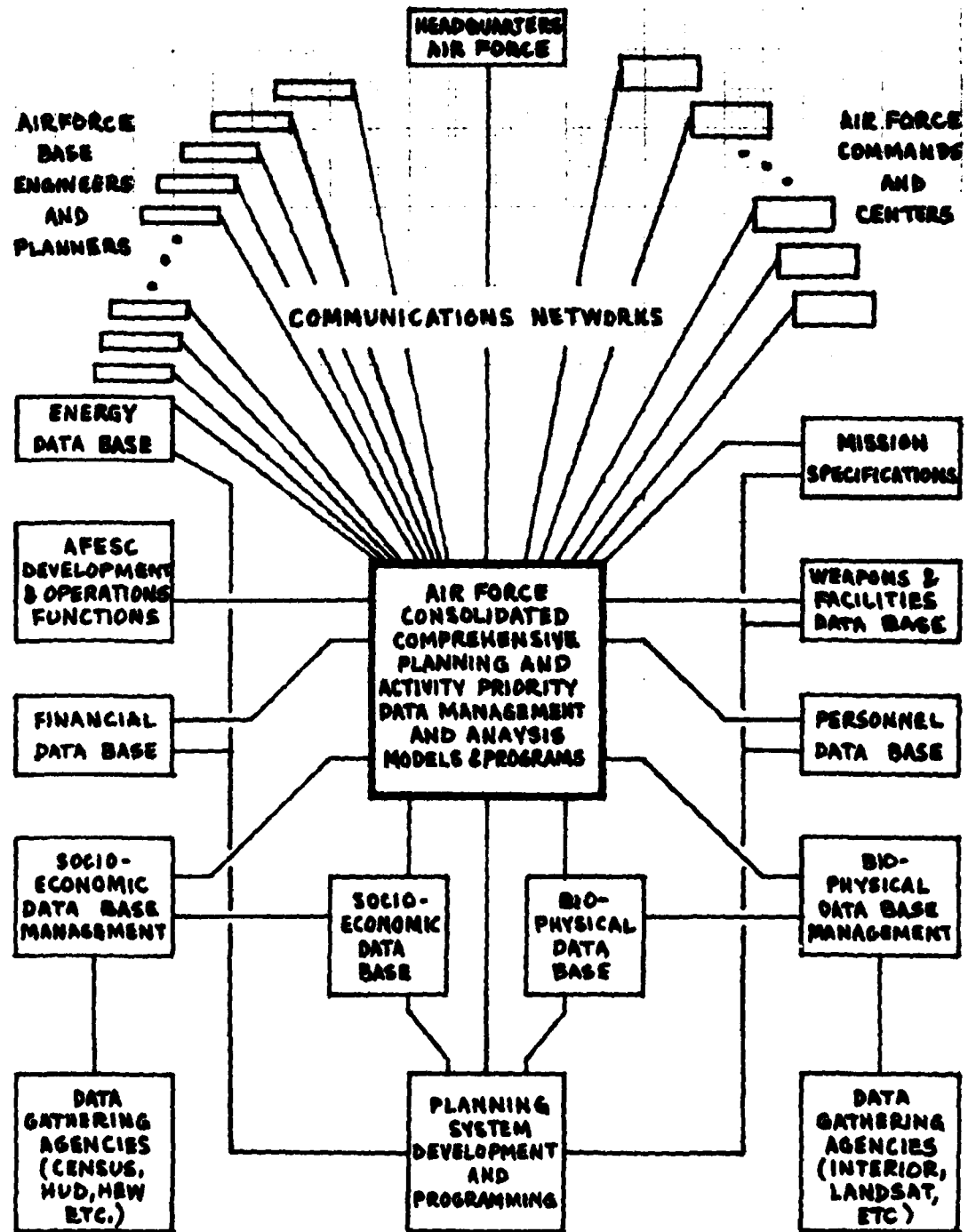


FIGURE 3. RECOMMENDED OPERATING STRUCTURE FOR A CONSOLIDATED AIR FORCE COMPREHENSIVE PLANNING AND ACTIVITY PRIORITY DATA MANAGEMENT AND ANALYSIS COMPUTER SYSTEM TO BE FINISHED ABOUT FY 1984.

assistance program of the type described above could only be developed with the close collaboration of the different divisions of AFESC. Perhaps the comprehensive planning need could serve to clarify the relationships between the various AFESC activities and to promote unified objectives and collaborative operations.

## REFERENCES

1. E. Lieblein and E. W. Martin, "The Military Computer Family Part V: Software for Embedded Computers," Military Electronics/Countermeasures, July, 1979.
2. E. W. Martin, "The Military Computer Family Part I: A Documentary," Military Electronics/Countermeasures, March, 1979.
3. E. W. Martin, "The Military Computer Family Part II: The Approach," Military Electronics/Countermeasures, April, 1979.
4. E. W. Martin, "The Military Computer Family Part III: The Issues," Military Electronics/Countermeasures, May, 1979.
5. J. R. Sculley, "Development and Implementation of the Environmental Technical Information System for Air Force Use," Summer Faculty Research Report, Air Force Office of Scientific Research, 11 August, 1978.
6. F. A. Skove and C. L. Cockran, Bridging the Gap between Environmental Data Systems and Potential Users, Report No. USNA-EPRD-36 Naval Facilities Engineering Command, Alexandria, VA, 1 March, 1977.
7. "Data Automation Requirement for Obtaining an Air Force Operated Environmental Technical Information System," Air Force Engineering and Services Center, Directorate of Environmental Planning, 9 November, 1978.
8. Directory of Federal Contacts on Environmental Protection, Report No. NESO 20.2-001B, Naval Environmental Protection Support Service, Port Hueneme, CA, May 1979.
9. "Preliminary Ada Reference Manual," Sigplan Notices, Vol. 14, No. 6, June, 1979.
10. System Overview: Environmental Technical Information System, Army Construction Engineering Research Laboratory, Champaign, IL, Revised 18 December, 1978.

1979 USAF - SCEEE SUMMER FACULTY RESEARCH PROGRAM

Sponsored by the

AIR FORCE OFFICE OF SCIENTIFIC RESEARCH

Conducted by the

SOUTHEASTERN CENTER FOR ELECTRICAL ENGINEERING EDUCATION

FINAL REPORT

THE UNIQUENESS OF PHASE RETRIEVAL FROM INTENSITY MEASUREMENTS

Prepared by: Dr. John T. Foley  
Academic Rank: Assistant Professor  
Department and University: Department of Physics  
Mississippi State University  
Research Location: Air Force Weapons Laboratory, Advanced Beam  
Control Division, Advanced Laser Optics Branch  
USAF Research Colleague: Dr. R. Russell Butts  
Date: September 7, 1979  
Contract No: F49620-79-C-0038

THE UNIQUENESS OF PHASE RETRIEVAL

FROM INTENSITY MEASUREMENTS

by

John T. Foley

ABSTRACT

The question of the uniqueness of the determination of the phase of a wavefield from the knowledge of its intensity in the aperture plane and focal plane of a thin lens is investigated. It is shown that if the wavefield intensity across the lens is uniform and the phase is represented by means of the nine lowest order Zernike polynomials, that the phase can be determined uniquely (except for the well-known twin solution ambiguity) from its focal plane intensity. The twin ambiguity is discussed in physical terms which allow one to eliminate it. Similar results are obtained for a Gaussian distribution of intensity in the aperture. Suggestions for further research in this area are offered.

### Acknowledgement

The author would like to thank the Air Force Systems Command, the Air Force Office of Scientific Research and the Southeastern Center for Electrical Engineering Education for providing him with the opportunity to spend a very worthwhile and interesting summer at the Air Force Weapons Laboratory, Kirtland AFB, N.M. He would like to acknowledge the laboratory, in particular the Advanced Laser Optics branch, for its hospitality and excellent working conditions.

Finally, he would like to thank Dr. R. Russell Butts for suggesting this area of research and for his collaboration and guidance, and he would like to acknowledge many helpful discussions with Dr. Gregory Dente and Capt. Stan Lewantowicz.

## I. INTRODUCTION:

The determination of the phase of an optical wavefield is a very fundamental and extremely important problem. For the Air Force in particular, the extraction of phase information from an incoming optical signal is a central part of most tracking devices and beam control systems.

The present project is concerned with a particular method of phase determination, namely the deduction of the phase of the complex amplitude of a scalar monochromatic wavefield from a knowledge of the intensity of the field in two planes: the aperture plane and focal plane of a thin lens. More precisely, let the field in the aperture plane of the lens (which we take to be the plane  $z = 0$ ) be written as

$$\begin{aligned} V(\underline{\rho}_0, t) &= \text{Re} \{ U_a(\underline{\rho}_0) e^{-i\omega t} \}, \\ &= \text{Re} \{ |U_a(\underline{\rho}_0)| e^{i\phi_a(\underline{\rho}_0)} e^{-i\omega t} \} \end{aligned} \quad (1)$$

where  $\underline{\rho}_0 = (x_0, y_0)$  is the two-dimensional position vector in the aperture plane,  $U_a(\underline{\rho}_0)$  is the complex amplitude of the field in that plane,  $\omega$  is the temporal frequency of the field and  $\text{Re}$  denotes that the real part is to be taken. The method in question strives to determine the phase  $\phi_a(\underline{\rho}_0)$  from the knowledge of the aperture plane intensity,  $|U_a(\underline{\rho}_0)|^2$ , and the focal plane intensity,  $|U_f(\underline{\rho})|^2$ .  $\underline{\rho}$  is the position vector in the focal plane. From here on  $|U|$  will be referred to as the amplitude of the field.

The motivation for such an approach is twofold. First, if the source of the wavefield is a large distance from the lens and the medium through which the field propagates does not introduce significant amplitude distortion, the amplitude (and hence the intensity) of the field will be approximately constant (as a function of its spatial variables) in the aperture plane of the lens. Therefore, a single intensity measurement in the focal plane of the lens would give us the necessary information to pursue this method of phase retrieval. This method has the advantage of being extremely straightforward and, more importantly, it is the most efficient way of using the energy available, since it does not require expansion or splitting of the incident

field, as interferometric techniques do. The second source of motivation is that for cases where the amplitude is not constant across the aperture of the lens, we can still use this approach by making intensity measurements in two planes.

Numerical experiments which successfully retrieve the phase from aperture plane and focal plane intensities have been performed. Gon-salves<sup>1</sup> treated the one-dimensional focusing problem. He found, for several test cases, that his algorithm always converged to either the correct phase or its "twin" (the twin solution will be explained in Sec. IV). Southwell<sup>2</sup> treated exactly the problem described in the previous paragraph: phase retrieval when the intensity in the aper-ture plane is a constant and the intensity in the focal plane is measured. He found, for several test cases, that his algorithm pro-duced the correct phase, but he overlooked completely the possibility of the twin solution.

Neither of these papers made a definitive statement about the general problem of uniqueness, i.e., about whether or not there is only one possible phase function consistent with the two known inten-sities. Until this point is clarified, one cannot be confident that the phase one calculates is the one occurring physically. In the one-dimensional problem, some interesting results on the question of uniqueness have been obtained.<sup>3,4,5,6</sup> However, the two dimensional problem is not a straightforward extension, because physical wave-functions can not, in general, be subjected to the method of separation of variables and, furthermore, lenses have circular apertures, not square ones. Indeed, very recently the question of uniqueness for the problem we have described above has been debated in the literature.<sup>7,8</sup> Aspects of references 5 and 6 will be commented upon in the final section of this report.

## II. OBJECTIVES

The main objective of this project was to investigate the question of the uniqueness of the phase retrieval method discussed above. We did not attempt to solve the general problem, i.e., we did not try to treat arbitrary types of aperture fields. Instead, we treated the

simplest (and most practical) cases, leaving the more complicated cases for later investigations. Our specific objectives were:

- (1) To determine a criterion for choosing between the two "twin" solutions that occur when the aperture intensity is symmetric.
- (2) To determine the uniqueness or possible ambiguities in the problem Southwell treated: uniform aperture intensity and a phase function which can be expanded in terms of the first nine Zernike polynomials.
- (3) To extend Southwell's problem to the case of a Gaussian intensity distribution in the aperture plane.

It should be noted at this point that the restriction on the phase (expansion in terms of the first nine Zernike polynomials) is not a severe one. The Zernike expansion is a very practical way of describing the phase and nine terms do a good job of describing most wavefields.

### III. PRECISE MATHEMATICAL STATEMENT OF THE UNIQUENESS PROBLEM

Before presenting the methods used and results obtained, it is necessary to state the uniqueness problem in precise mathematical terms. The physical situation is pictured in Figure 1 below.

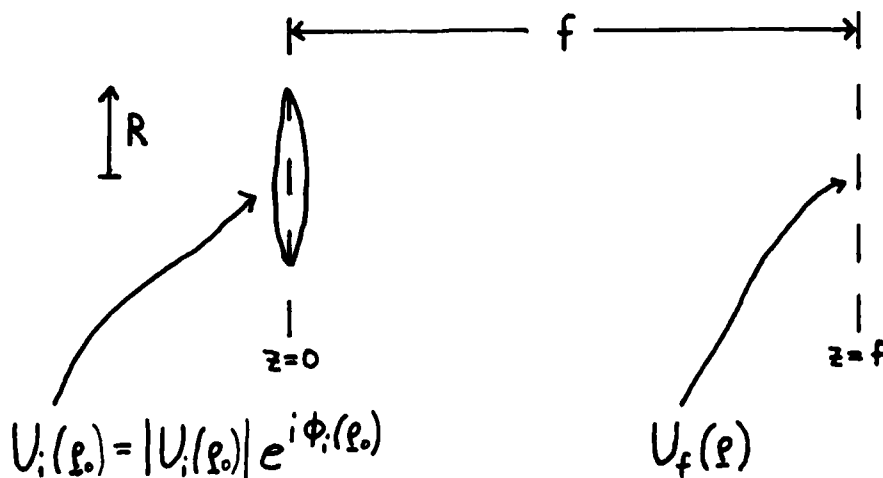


FIGURE 1 - THIN LENS GEOMETRY

The field

$$U_i(\rho_0) = |U_i(\rho_0)| e^{i\phi_i(\rho_0)} \quad (2)$$

is incident upon a thin lens of focal length  $f$  and radius  $R$ . The lens is surrounded by a stop, therefore the field in the aperture plane ( $z = 0$ ) is

$$\begin{aligned} U_a(\rho_0) &= U_i(\rho_0) \text{circ}(|\rho_0|/R), \\ &\equiv |U_a(\rho_0)| e^{i\phi_a(\rho_0)}, \end{aligned} \quad (3)$$

where

$$\text{circ}(|\rho_0|/R) = \begin{cases} 1, & |\rho_0| \leq R \\ 0, & |\rho_0| > R \end{cases}. \quad (4)$$

The resultant field in the focal plane is  $U_f(\rho)$ .

In words the uniqueness problem can be stated as: is it possible for two (or more) aperture plane fields to have equal  $|U_a(\rho_0)|$  for all  $\rho_0$ , produce equal  $|U_f(\rho)|$  for all  $\rho$  and yet have different aperture plane phases,  $\phi_a(\rho_0)$ ? This can be rephrased in precise mathematical terms if we recall one of the basic results of Fourier optics.

For the situation described above it is well-known<sup>9</sup> that the focal plane field is determined by the Fourier transform of the aperture plane field:

$$U_f(\rho) = \frac{1}{i\lambda f} \exp\left(-\frac{ik\rho^2}{2f}\right) \widetilde{U}_a(\rho/\lambda f), \quad (5)$$

where  $\lambda$  is the wavelength of the light and

$$\widetilde{U}_a(\rho/\lambda f) = \iint_{-\infty}^{\infty} U_a(\rho_0) \exp\left(-\frac{2\pi i}{\lambda f} \rho \cdot \rho_0\right) d^2\rho_0. \quad (6)$$

Therefore

$$|U_f(\rho)| = \frac{1}{\lambda f} |\widetilde{U}_a(\rho/\lambda f)| \quad (7)$$

and we can rephrase our uniqueness question as: is it possible for two (or more) aperture plane fields to have equal  $|U_a(\rho_0)|$  for all  $\rho_0$  and equal  $|\widetilde{U}_a(\rho/\lambda f)|$  for all  $\rho$  and yet have different aperture plane phases,  $\phi_a(\rho_0)$ ?

#### IV. TWIN SOLUTIONS

It is well-known<sup>1,3,10</sup> that if the aperture plane amplitude is symmetric, i.e.,

$$|U_a(-\rho_0)| = |U_a(\rho_0)|, \text{ for all } \rho_0, \quad (8)$$

then the answer to the above question is yes: there are at least two fields that behave in the prescribed manner. They are the so-called twin solutions:

$$\begin{aligned} U_{a1}(\rho_0) &= |U_a(\rho_0)| e^{i\phi_a(\rho_0)}, \\ U_{a2}(\rho_0) &= |U_a(\rho_0)| e^{-i\phi_a(-\rho_0)}. \end{aligned} \quad (9)$$

By definition  $|U_{a1}(\rho_0)| = |U_{a2}(\rho_0)|$  and it is a straightforward exercise to show that

$$\widetilde{U}_{a2}(\rho/\lambda f) = [\widetilde{U}_{a1}(\rho/\lambda f)]^*,$$

where the asterik denotes the complex conjugate. Therefore, the two fields have equal intensities in both planes.

To distinguish between these two solutions we represented the first phase in an expansion in Zernike polynomials \*

---

\* In this expression and in all our work, we do not include the constant phase term. Clearly phase retrieval via intensity measurements will not allow one to determine the constant term in the phase. This loss is of no consequence since physically we are always interested in phase differences.

Furthermore, we have terminated our Zernike expansion after nine terms in order to correlate our results with Sec. V. The results of Sec. IV can be simply extended to an arbitrary number of terms.

$$\phi_{a1}(\rho_0) = \phi_a(\rho_0) = \sum_{j=1}^9 a_j Z_j(\rho_0, \theta_0), \quad (10)$$

where the  $a_j$ 's are constants and

$$Z_1 = \rho_0 \cos \theta_0,$$

$$Z_2 = \rho_0 \sin \theta_0,$$

$$Z_3 = 2\rho_0^2 - 1,$$

$$Z_4 = \rho_0^2 \cos 2\theta_0,$$

$$Z_5 = \rho_0^2 \sin 2\theta_0,$$

$$Z_6 = (3\rho_0^2 - 2) \rho_0 \cos \theta_0,$$

$$Z_7 = (3\rho_0^2 - 2) \rho_0 \sin \theta_0,$$

$$Z_8 = \rho_0^3 \cos 3\theta_0,$$

$$Z_9 = \rho_0^3 \sin 3\theta_0.$$

The second phase function is therefore

$$\begin{aligned} \phi_{a2}(\rho_0) &= -\phi_a(-\rho_0) \\ &= \sum_{j=1}^2 a_j Z_j(\rho_0, \theta_0) - \sum_{j=3}^5 a_j Z_j(\rho_0, \theta_0) + \sum_{j=6}^9 a_j Z_j(\rho_0, \theta_0). \end{aligned} \quad (11)$$

Each of the terms in the Zernike expansion has a physical interpretation.  $a_1$  and  $a_2$  measure the tilt in the x and y directions, respectively.  $a_3$  measures the defocus,  $a_4$  the  $0^\circ$  astigmatism,  $a_5$  the  $45^\circ$  astigmatism, and  $a_6$  through  $a_9$  the coma. Therefore, by comparing (10) and (11), we found that: the twin solutions have the same tilt and coma and their defocus and astigmatisms are exactly the negatives of each other. Hence,

all we need in order to decide between the two is one piece of additional information, e.g., the sign of the defocus or astigmatism.

#### V. UNIFORM OR GAUSSIAN INTENSITY IN THE APERTURE PLANE

If the aperture plane field has uniform intensity, it can be written as

$$U_a(\rho_0) = U_0 e^{i\phi_a(\rho_0)} \text{circ}(|\rho_0|/R), \quad (12)$$

where  $U_0$  is a constant. The phase retrieval from intensity problem obviously is not completely unique, since we get the twin solutions in this case. However, since we can handle the twin solution ambiguity, we now ask the question: is this the only nonuniqueness?

The answer is yes and we proved it in the following way. Consider two different aperture plane fields,

$$\begin{aligned} U_{aA}(\rho_0) &= U_0 e^{i\phi_A(\rho_0)} \text{circ}(|\rho_0|/R), \\ U_{aB}(\rho_0) &= U_0 e^{i\phi_B(\rho_0)} \text{circ}(|\rho_0|/R), \end{aligned} \quad (13)$$

where  $U_0 = \text{constant}$ ,

$$\begin{aligned} \phi_A(\rho_0) &= \sum_{j=1}^9 a_j Z_j(\rho_0, \theta_0), \\ \phi_B(\rho_0) &= \sum_{j=1}^9 b_j Z_j(\rho_0, \theta_0). \end{aligned} \quad (14)$$

If they produce the same focal plane intensities, it follows from Eq. (7) that

$$|\tilde{U}_{aA}(\rho/\lambda f)|^2 = |\tilde{U}_{aB}(\rho/\lambda f)|^2, \text{ for all } \rho. \quad (15)$$

It then follows from the convolution theorem that the autocorrelation functions of the two aperture plane fields must be equal, i.e.,

$$\gamma_A(\underline{s}) = \gamma_B(\underline{s}), \text{ for all } \underline{s}. \quad (16)$$

where

$$\gamma(\underline{s}) = \iint_{-\infty}^{\infty} U_a(\rho_0) U_a^*(\rho_0 - \underline{s}) d^2 \rho_0 . \quad (17)$$

By substituting Eqs. (13) and (14) into Eq. (16), performing a Hopkins rotation<sup>11</sup> and then making a small  $|\underline{s}|$  expansion, one can show (see reference 12 for details) that only two possible solutions to Eq. (16) exist:

$$a_j = b_j \quad (j = 1, 2, \dots, 9) \quad (18)$$

or

$$a_j = b_j \quad (j = 1, 2, 6, 7, 8, 9), \quad (19)$$

$$a_j = -b_j \quad (j = 3, 4, 5).$$

These are the twin solutions of Sec. IV, therefore the twin solution is the only possible nonuniqueness for the problem.

If the aperture plane field has a Gaussian intensity distribution, we obtained exactly the same results: phase retrieval from intensity measurements is unique except for the possibility of the twin solution.

#### VI. RECOMMENDATIONS

At this point let us put our results in a practical perspective. Consider Southwell's problem: the intensity across the aperture,  $I_a(\rho_0)$ , is a constant, the focal plane intensity,  $I_f(\rho)$ , is measured and then  $\phi_a(\rho_0)$  is calculated. We have shown that if you know  $I_f(\rho)$  for all  $\rho$ , then the Zernike coefficients can be uniquely determined (except for the twin ambiguity).

However, in practice we do not know  $I_f(\rho)$  for all  $\rho$ , we know it only over a set of sample points. Our results show that if you sample on a fine enough grid you should be able to determine the actual Zernicke coefficients.

The fact that in practice we are dealing with a sampled intensity brings up the next problem that should be treated in this research area,

that of resolution. If the sampling rate in the focal plane is too slow, an incorrect set of Zernike coefficients will be obtained, e.g., a phase with a small tilt will look like a phase with no tilt, a small amount of coma may look like a tilt, etc. Therefore, it is important to determine the resolution possible in phase retrieval from intensity measurements, i.e., how fast must one sample to be able to determine the Zernike coefficients accurately?

I propose to do this by investigating the effect of sampling on Eqs. (15) through (17). In particular, the fact that  $I_a(\rho_0)$  is a constant and that  $I_f(\rho)$  is bandlimited should make the resolution problem tractable. Indeed, the former fact should help us avoid the kinds of problems that references 5 and 6 experienced (they sampled in both planes).

A second recommendation for follow-on research is to treat, using the methods of the present work, the case where the amplitude is more general (i.e., not a simple function such as a constant or a Gaussian). For non-symmetric amplitudes, there should be no possibility of a twin solution.

#### REFERENCES

1. R. A. Gonsalves, "Phase Retrieval from Modulus Data," J. Opt. Soc. Am., Vol. 66, pp. 961-964, 1976.
2. W. H. Southwell, "Wave-front Analyzer Using a Maximum Likelihood Algorithm," J. Opt. Soc. Am., Vol. 67, pp. 396-399, 1976.
3. A. M. J. Huiser, A. J. J. Drenth and H. A. Ferwerda, "On Phase Retrieval in Electron Microscopy from Image and Diffraction Pattern," Optik, Vol. 45, pp. 303-316, 1976.
4. A. M. J. Huiser, "On the Problem of Phase Retrieval in Electron Microscopy from Image and Diffraction Pattern. II. On the Uniqueness and Stability," Optik, Vol. 46, pp. 407-420, 1976.
5. V. P. Schiske, "Ein- und Mehrdeutigkeit der Phasenbestimmung aus Bild und Beugungsfigur," Optik, Vol. 40, pp. 261-275 (1974).
6. W. J. Dallas, "Digital Computation of Image Complex Amplitude from Image - and Diffraction - Intensity: An Alternative to Holography," Optik, Vol. 41, pp. 45-59 (1975).
7. Stanley R. Robinson, "On the Problem of Phase from Intensity Measurements," J. Opt. Soc. Am., Vol. 68, pp. 87-92, 1978.
8. A. J. Devaney and R. Chidlaw, "On the Uniqueness Question in the Problem of Phase Retrieval from Intensity Measurements," J. Opt. Soc. Am., Vol. 68, pp. 1352-1354.
9. Joseph W. Goodman, Introduction to Fourier Optics, (McGraw-Hill, New York, 1968), p. 85.
10. B. J. Hoenders, "On the Solution of the Phase Retrieval Problem," J. Math. Phys., Vol. 16, pp. 1719-1725, 1975.
11. H. H. Hopkins, "The Frequency Response of a Defocused Optical System," Proc. Roy. Soc. A, Vol. 231, pp. 91-103, 1955.
12. John T. Foley and R. Russell Butts, "The Uniqueness of Phase Retrieval from Intensity Measurements," to be submitted to J. Opt. Soc. Am.

1979 USAF - SCEEE SUMMER FACULTY RESEARCH PROGRAM

Sponsored by the

AIR FORCE OFFICE OF SCIENTIFIC RESEARCH

Conducted by the

SOUTHEASTERN CENTER FOR ELECTRICAL ENGINEERING EDUCATION

FINAL REPORT

HIGH SPEED ELECTROMAGNETIC TRANSIENTS

ON SUPERCONDUCTING COIL

Prepared by:	G. J. Gabriel, Ph.D.
Academic Rank:	Visiting Professor
Department and University:	Department of Electrical Engineering Old Dominion University
Research Location:	Aero Propulsion Laboratory Wright-Patterson AFB, Ohio
USAF Research Colleague:	Dr. Charles E. Oberly
Date:	September 14, 1979
Contract No:	F49620-79-C-0038

HIGH SPEED ELECTROMAGNETIC TRANSIENTS

ON SUPERCONDUCTING COILS

by

G. J. Gabriel

ABSTRACT

Superconducting coils are prime candidates for energy storage in pulsed high power applications, where electromagnetic transients play an important role. An investigation of such transients on a Nb-Ti coil at 10°K, 77°K and room temperature were carried out utilizing reflections when the coil is excited by low power pulses having 10 nsec duration. While the theoretical and experimental results are preliminary, they verify the role of turn-to-turn coupling and suggest the need for further investigations on a more refined and elaborate scale. The experimental data tentatively support the viewpoint of a coil as a multi-conductor coupled transmission line.

#### ACKNOWLEDGEMENT

The author takes pleasure in thanking the Air Force Systems Command, Air Force Office of Scientific Research, and the South Eastern Center for Electrical Engineering Education for providing him with the opportunity to work on a scientifically interesting problem.

He extends a special note of thanks to Dr. Charles E. Oberly, Air Force Aero Propulsion Laboratory, for his active support of the effort and for providing an atmosphere conducive to intellectual inquiry. The assistance of Dr. James Ho, Senior Investigator for SCEEE, and of Mr. Price Thomas of AFAPL in the conduct of the experiments is gratefully acknowledged.

## I. INTRODUCTION:

The effort undertaken in this project consists of an investigation of electromagnetic transients on superconducting helical coils on the nanosecond time scale. It is a preliminary step toward the broader objective of understanding the general behavior of electromagnetic disturbances in the neighborhood of superconducting boundaries, such as filamentary coils and cavity resonators. Superconducting coils and resonators<sup>1</sup> are prime candidates as light weight energy storage elements in high power pulse sources, which by nature involve rapid electromagnetic transients. The U. S. Air Force's interest in superconductivity is largely motivated by the need for light weight power sources for airborne applications among others<sup>2</sup>.

In large coils, the travel time of electromagnetic disturbances along the wire becomes a significant parameter so that their behavior cannot be adequately described by the lumped inductors of circuit theory<sup>3</sup>. Owing to the spacial distribution of transients throughout a coil, a field theoretic approach for analysis is essential. Electromagnetic transients on superconducting coils are generally a source of trouble where protection of the coil against breakdown is of concern. The author had been involved in theoretical and experimental investigations of such transients, it being maintained that an understanding of these holds the key to suppressing them in any protection schemes. It soon became apparent that the opposite might also serve a purpose<sup>4</sup>. That is, by controlled initiation of transients, bursts of high frequency energy might be extracted from a dc magnet. Since the bulk of the previous work was done on coils at room temperature, where damping is problematic, the need for data on at least a cryogenic

coil, if not a superconducting one, was apparent. Hence, acquisition of data on transients on such coils is the primary target. However, due to limitations of the apparatus available at the time, the experiments were designed to be compatible with the frequency bandwidth (or rise time) characteristics of the apparatus. Consequently, the results obtained thus far are preliminary in nature, serving to point the direction which future, more refined experiments might take. The experiments also served as a guide for the theoretical analysis undertaken in this project.

## II. OBJECTIVES OF RESEARCH EFFORT:

The specific goals of the project reported here was confined to an investigation of some aspects of electromagnetic transients on superconducting helical coils, both in theoretical and experimental terms. As a theoretical framework for the description of such transients, the approach adopted was that of viewing coils as coupled multi-conductor transmission lines. In view of the scarcity of data on electromagnetic transients at cryogenic temperatures, an experiment was proposed and executed for the purpose of providing insights and direction to the theory. Within limitations of apparatus available at the time, the goals of the experiment as a preliminary step were defined to be

- a) An appraisal of the adopted theoretical viewpoint;
- b) An appraisal of the role of turn-to-turn coupling;
- c) A determination of the effects of temperature;
- d) An estimate of unforeseen problems and the refinements needed for future experiments.

This report gives only a brief outline of experimental results and theoretical analysis, leaving the details of the theory to a later publication.

### III. EXPERIMENTAL METHOD AND RESULTS:

The experimental method consisted of observation of reflection patterns from a Nb-Ti coil immersed in a dewar and excited with a low voltage pulse train. This was achieved by the configuration shown schematically in Figure 1. A matched resistive splitter divides the incoming pulse, sending equal portions to the oscilloscope and the coil. The split pulse reaching the oscilloscope establishes the reference time. A reflected pulse from the coil also divides at the splitter, a portion returning to the source where it is absorbed and the remainder going to the oscilloscope as the principal datum. If one were to view the coil as a single conventional transmission line, the configuration is analogous to connecting the generator between the receiving and sending ends of the line.<sup>3</sup>

The coil was constructed from Nb-Ti wire, 5 mils in diameter, wound on a form 24" in diameter with a pitch of 0.2". Seven turns were used, corresponding approximately to 54 nanosecond pulse travel time around the entire coil. This choice of dimensions and number of turns represents a compromise dictated by the physical size of the dewar, the bandwidth characteristics of available electronic instrumentation, and the desired time resolution.

Typical oscilloscope traces are shown in Figures 2 and 3. The time interval of about 80 nsec between the main peaks in the reflection patterns of Figures 3a and b correlate well with the estimated travel time of 76 nsec for the coil and lead wire combination, thus indicating multiple reflections from end to end. The duration of the fine structure, on the other hand, is approximately 15 nsec corresponding to twice the travel time around a single turn. Existence of this fine structure is

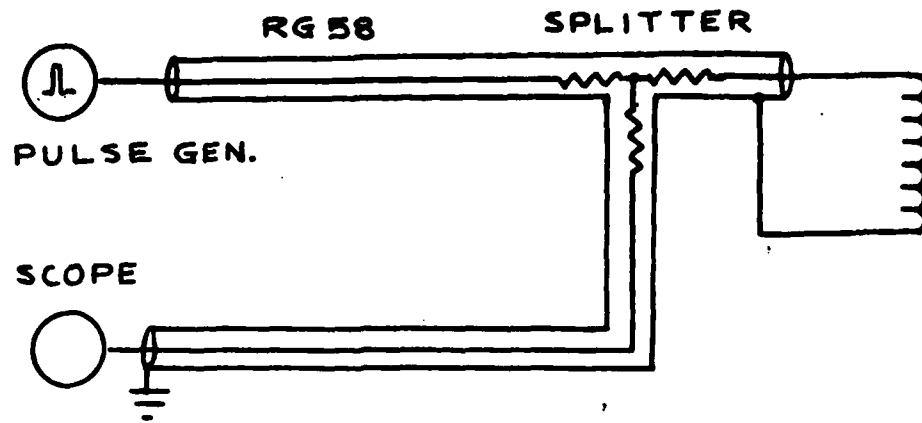


Figure 1: Schematic diagram of configuration of Experiment.  
 Signal Source: HP8012B  
 Oscilloscope: Teletronix 2904 with 7A19.

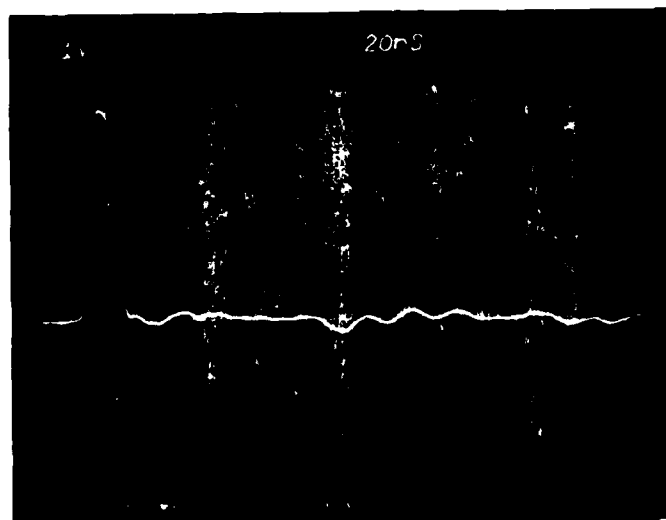
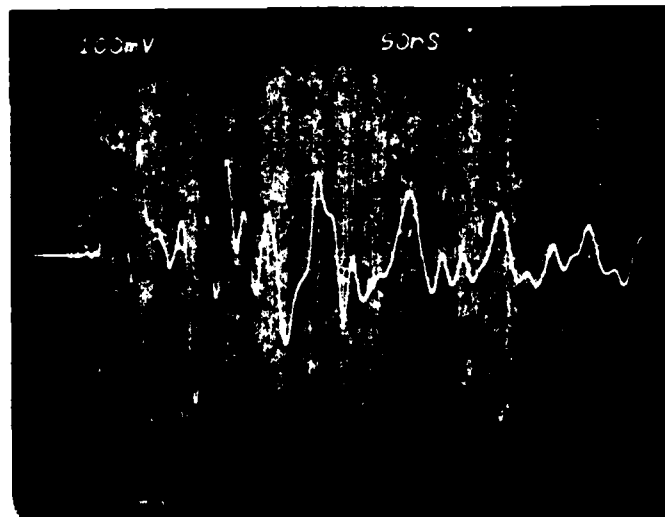


Figure 2: Trace of input pulse.



(a)



(b)

**Figure 3: Reflection patterns from coil.**  
(a) At room temperature.  
(b) At approximately 10° K.

indicative of turn-to-turn coupling.

The traces taken at room temperature and at 10°K clearly illustrate the effect of reduced damping at the lower temperature, but, as to be expected, no significant change in propagation time is discernible. However, since the superconducting state was not achieved in these experiments, the results are not conclusive as to what might happen in that state.

#### IV. OUTLINE OF THEORETICAL APPROACH:

One of the important questions essential to any experiment concerns the identification of what is being observed and how it is related to the theory. In the case of electromagnetic transients on helical wires, the significance of voltage and current as understood in the ordinary sense is obscured. However, analysis indicates that the quantities that are manifested on instruments such as oscilloscopes are appropriately related to the charge and current density distributions along the coil. Further, owing to the propagation of electromagnetic disturbances and the physical proximity of wires in a helix, the charge and current densities in a differential length element on one turn of wire are expected to be coupled to the densities on all other turns, the degree of coupling being as yet undetermined. On the basis of this reasoning, the electromagnetic field around an  $n$ th turn is characterized by a function  $v_n(x,t)$  related to the charge, which we call "voltage," and another function  $i_n(x,t)$  corresponding to the current at a point on the  $n$ th turn. With some justification from the field integrals, the set of equations governing the behavior of the coil are postulated to be

$$\frac{\partial}{\partial x} v_m (x, t) = - \sum_n L_{mn} \frac{\partial}{\partial t} i_n (x, t) \quad (1)$$

$$\frac{\partial}{\partial x} i_m (x, t) = - \sum_n C_{mn} \frac{\partial}{\partial t} v_n (x, t) \quad (2)$$

where  $x$  is the arc distance along a turn, and  $L_{mn}$  and  $C_{mn}$  are elements of coupling matrices having the property

$$\sum_n L_{mn} C_{nk} = \frac{1}{c^2} \delta_{mk} \quad (3)$$

and  $c$  is the speed of propagation on a straight wire.

Equations (1) and (2), which are well known in the theory of straight coupled transmission lines, are far from giving a complete picture of the complicated behavior of a superconducting coil. However, they provide a promising start, since their exact solutions for two and three turn coils are in agreement with qualitative observations on normal conductors. In the context of the experiments described above, the appearance of a fine structure in the reflection pattern is strongly suggestive of the presence of turn-to-turn coupling. For, in the absence of such coupling, resulting in diagonal matrices, the theoretical reflection pattern would consist of only the major peaks separated by time intervals corresponding to the overall length of the coil and leads. Significantly, the observed fine structure is not clearly evident at room temperature but it becomes progressively more prominent as the damping is diminished with reduced temperature. As mentioned in Section I, the bulk of the earlier work on transients had been done at room temperature. Thus, the results at cryogenic temperatures reported here, though very limited in scope, do suggest that the theoretical viewpoint in terms of coupled lines is evolving in the right direction.

V. RECOMMENDATION:

The theory and experiments outlined above are preliminary and far from being conclusive. What has been achieved is essentially a better understanding of the sort of problems involved. For deeper insights, it is desirable that similar experiments be repeated, but with refinements in the electronic instrumentation. Shorter pulses combined with faster instruments would permit a more detailed analysis of coils with fewer turns than was possible at present. Comparison of theory with experiment is substantially facilitated as the number of turns is diminished especially where the question of coupling is concerned. Further, since it was not possible to achieve superconductivity in the present experiments, it is essential that transient be investigated in the superconducting state in the near future.

Finally, one of the questions deserving very serious deliberations concerns the current distribution throughout the wire cross section. Given the typical configuration of copper-clad superconductor fibers, it is quite certain from the Maxwell theory that the current due to an externally induced disturbance in an uncharged coil resides on the outer surface of the copper substrate. It is not clear, however, how a large current initially confined within the superconducting fibers would distribute itself when it is suddenly disturbed in the neighborhood of the associated high magnetic field. This question is central to the overall problem of electrodynamic transients on superconducting wire especially where practical utilization of the effects is of prime consideration.

#### REFERENCES

1. D. Brix, G. J. Dick, J. E. Mercereau, D. J. Scalapino, "Microwave Power Gain Utilizing Superconducting Resonant Energy Storage," Applied Physics Letters, vol. 32(1), pp. 68-70, 1978.
2. C. E. Oberly, "Air Force Applications of Light Weight Superconducting Machinery," IEEE Transactions on Magnetics, MAG-13, No. 1, pp. 260-268, 1977.
3. G. J. Gabriel, J. A. Burkhart, "Potential Damage to DC Superconducting Magnets Due to High Frequency Electromagnetic Waves," Proceedings IEEE Seventh Symposium on Engineering Problems in Fusion Research, Knoxville, Tennessee, October, 1977, pp. 741-745.
4. C. E. Oberly, Private Communication.
5. G. J. Gabriel, "Theory of Electromagnetic Transmission Structure, Part I: Relativistic Foundations and Network Formalisms," Proceedings of IEEE (to appear in 1979-80).

1979 USAF-SCEEE SUMMER FACULTY RESEARCH PROGRAM

Sponsored by the

AIR FORCE OFFICE OF SCIENTIFIC RESEARCH

Conducted by the

SOUTHEASTERN CENTER FOR ELECTRICAL ENGINEERING EDUCATION

FINAL REPORT

PART I. EFFECTS OF DEHYDRATION AND  
HEAT ON ACCELERATION RESPONSE IN MAN

PART II. RELATIONSHIPS BETWEEN TOTAL BODY  
SWEATING RATE AND LOCALIZED SWEATING RATE

Prepared by:	James A. Gessaman
Academic Rank:	Associate Professor
Department and University:	Biology, Utah State University
Research Location:	Crew Protection Branch, USAF School of Aerospace Medicine, Brooks AFB, TX 78235
USAF Research Colleague:	Sarah A. Nunneley
Date:	September 13, 1979
Contract No:	F49620-79-C-0038

PART I: EFFECTS OF DEHYDRATION AND  
HEAT ON ACCELERATION RESPONSE IN MAN

by

J. A. Gessaman

ABSTRACT

The G-tolerance of two subjects was tested at air temperatures of 18°C and 40°C under normal hydration and 3% dehydration conditions. Two centrifuge acceleration stress profiles were employed: 1. A gradual onset of 1 G/15 sec without an anti-G suit and 2. a SACM II profile with an anti-G suit. In the absence of dehydration both subjects performed better at 40°C than at 18°C on the SACM II profile. Both subjects were significantly less tolerant to G stress when dehydrated.

#### ACKNOWLEDGEMENTS

Sarah Nunnely was especially helpful as a research colleague and consultant. I wish to thank Thomas Crosby, Richard Reyna, and Mary Ann Orzech and the staffs of E Chamber and the Human Contrifuge for their assistance. I gratefully acknowledge the time, dedication, and fortitude contributed by the volunteer centrifuge subjects, Brent Richey and Kevin Adams. This work was made possible by a faculty summer fellowship from Air Force Systems Command, Air Force Office of Scientific Research.

## I. INTRODUCTION:

Nunneley and Stribley (1979), my research colleagues in the thermal stress laboratory (Division of Crew Protection) of the School of Aerospace Medicine reported that dehydration and heat stress lower the G tolerance of male subjects. In their studies the subjects sat in an aircraft seat within a centrifuge capsule preheated to 38°C for a 20-minute equilibration period. This was followed by a series of three relaxed runs: 2G X 1 minute, 3G X 1 minute and a gradual onset of 1G/15 sec tolerance limit. The subjects remained in place while the capsule cooled to 20°C and the three relaxed runs were then repeated. For the final run, 7G X 1 minute, the anti-G suit was activated and the subject strained as needed to maintain vision.

Heat lowered relaxed G tolerance by .3G; dehydration tended to lower G tolerance and increase the variability of response to heat. Heat-induced tolerance loss appeared to be similar for gradual--and rapid-onset centrifuge profiles. In contrast, dehydration effects were greater in rapid-onset runs.

My research effort at the thermal stress laboratory was aimed at investigating the G-tolerance of dehydrated subjects to an acceleration profile which is more similar to that experienced by fighter pilots in an aerial combat maneuver, viz., the SACM II profile: 4.5G X 15 sec and 7.0G X 15 sec repeated to the limit of tolerance.

## II. OBJECTIVES:

To investigate the effect of 3% dehydration and cockpit air temperatures of 18°C and 40°C on G-tolerance to a gradual onset profile of 1G/15 sec and to the SACM II acceleration profile.

## III. METHODS:

Subjects were two male volunteers (subjects A and B) both age 23 with the following characteristics: Height (A=173.2 cm, B=167.6 cm) and weight (A=66.1 kg, B=90.2 kg). Each man was a veteran member of the human centrifuge subject panel and had learned to ride the centrifuge in two different ways 1. relaxed, without any voluntary muscle contraction and 2. using the valsalva-like "M-1" straining maneuver to maximize G tolerance.

Subjects were studied at one dehydration level, 3% body weight loss. Experiments on a given subject were separated by one week. Subjects were instructed to avoid strenuous activity, alcohol and extremes of fluid

intake for 24 hours preceding each experiment.

I employed the method described by Nunneley and Stribley (1979) to dehydrate the subjects. Subjects were dehydrated between 0900 and 1200h.

Acceleration runs took place between 1300 and 1600h. The subject was instrumented with ECG leads and then dressed in summer flight clothing and an anti-G suit. The centrifuge capsule was either preheated to 40°C or cooled to 18°C. The subject then sat in an aircraft seat (back angle 13° behind the vertical) in the capsule for a 20 to 30 minute equilibration period. This was followed by three acceleration runs, a 3G X 15 sec (a warm-up run), a gradual onset acceleration of 1G/15 sec up to 7G or to a tolerance limit below 7G without the anti-G suit on and finally the SACM II acceleration profile with the anti-G suit turned on. All three runs were separated by five-minute rest periods.

#### IV. RESULTS:

During the dehydration phase subjects lost weight at an average rate of (A=0.95±.01 kg/hr, B=1.02±.11 kg/hr). The fluid needed to replace excess losses was 0.38±.16 kg for A and 0.19±.09 kg for B.

In the absence of dehydration both subjects performed better at 40°C than at 18°C on the SACM II profile. (Table 1.) Subject A also was more tolerant of the gradual onset acceleration at 40°C. Subject B rode to 7G at both 18°C and 40°C.

Both subjects were significantly less tolerant to G stress when dehydrated. Subject A rode the SACM II profile more than twice as long at 40°C than at 18°C whereas the ride duration for Subject B was identical at both temperatures.

Heart rate increased during the SACM II accelerations in both subjects (Figure 1) and plateaued at 192 BPM in Subject A in three trials and 186 BPM in one trial. In contrast the heart rate of Subject B plateaued at 120 BPM during the control runs and at higher rates during the dehydration runs.

Table 1.

	CONTROL		3% DEHYDRATION	
	18°C	40°C	18°C	40°C
G-tolerance of 1G/15 sec gradual onset				
Subject A	6.0G	6.7G	5.4G	5.3G
Subject B	7.0G	7.0G	4.8G	5.1G
Tolerance of SACM II (min:sec)				
Subject A	7'13"	7'47"	3'11"	6'36"
Subject B	6'11"	8'37"	2'17"	2'17"

Table 1. The effect of 3% dehydration and temperatures of 18°C and 40°C on the G-tolerance of two subjects during a 1G/15 sec gradual onset profile ending at 7.0 G and on their tolerance of a simulated aerial combat maneuver profile (SACM II--a repetitive series of fluctuations between 4.5G X 15 sec and 7.0G X 15 sec) measured by the duration of the ride.

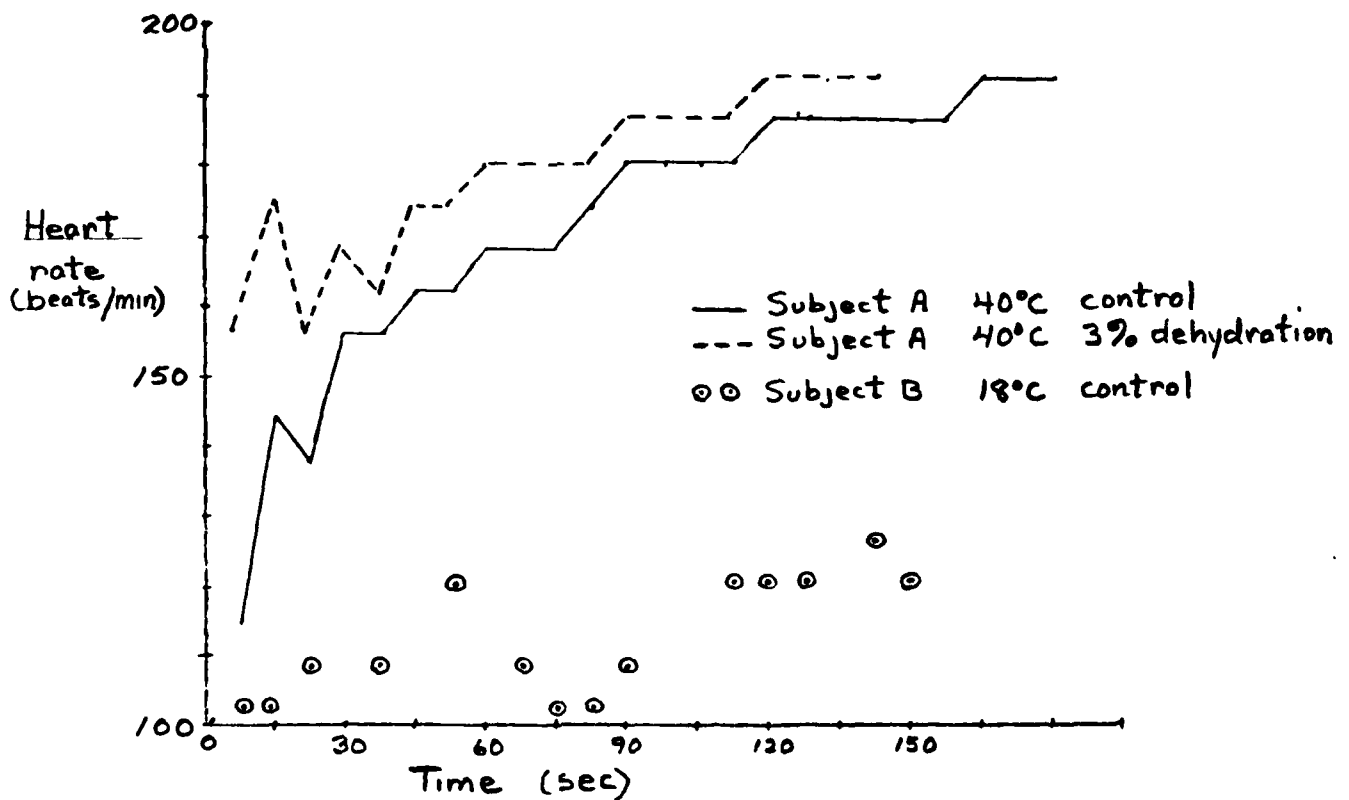


Fig. 1 - Heart rate of subject A & B during 3 trials of the SACM II acceleration profile.

V. RECOMMENDATIONS:

This research on two subjects went very well. I do not have any specific recommendations for improving the experimental methodology or design of the project.

The sample size was obviously too small from which to draw conclusions which would be acceptable to the scientific community. The inavailability of four or more trained centrifuge riders during the Summer made a larger sample size impossible. A minimum of four or more subjects is needed to complete the study. Since Utah State University does not have a human centrifuge it will be impossible for me to continue this investigation during the next 12 months. Dr. Sarah Nunneley, my research colleague in the Division of Crew Protection plans to continue this project this Fall and Winter. We will then publish the combined results under joint authorship.

#### REFERENCES

S. A. Nunneley and R. F. Stribley, "Heat and Acute Dehydration Effects on Acceleration Response in Man," J. Appl. Physiol., Vol. 47, pp. 197-200, 1979.

PART II: RELATIONSHIPS BETWEEN TOTAL  
BODY SWEATING RATE AND LOCALIZED SWEATING RATE

by

J. A. Gessaman

ABSTRACT

Water loss by sweating in hot environments is a useful index of heat stress. Nude weight loss is the most direct method of measuring water loss but is an impractical method in many aerospace environments. I evaluated the accuracy of predicting whole body sweat rates from local sweat rates measured on the forearm, forehead, chest, thigh and leg during exercise and at rest. During exercise the observed values averaged 15% more than the predicted and at rest the observed values averaged 37 % more. The factors contributing to these discrepancies is discussed.

ACKNOWLEDGEMENTS

I want to thank Thomas Crosby, Richard Reyna and Richard Stribley for their technical assistance and dedication as subjects. I am grateful to Sarah Nunnely, Donald Tucker, Loren Myhre and the staff of E Chamber for their help in various aspects of the study. This work was made possible by a faculty summer fellowship from Air Force Systems Command, Air Force Office of Scientific Research.

## I. INTRODUCTION:

Thermal conditions in the cockpit of the A10, F104E, F11A and F-15 fighter aircraft during flights in desert and tropical conditions and physiological indicators of heat stress of the pilots of these aircraft have been studied by the heat stress laboratory of the USAF School of Aerospace Medicine (Nunneley and James, 1977; Nunneley and Myhre, 1976). These physiological indicators have included rectal temperature, skin temperature and heart rate.

The rate of water loss by sweating in hot environments is another index of heat stress which workers at the heat stress laboratory would like to measure in future investigations. Nude weight loss is the most direct method of measuring water loss, however, repeated measurements of the nude body weight of pilots or other workers in many aerospace environments is impractical.

In these situations an indirect measure of total body sweating rate is necessary. Tam et al (1976) have shown that hygrometric measurements of sweating rate using sweat collection capsules at five locations on the body can predict (within  $\pm 5\%$ ) the real sweat secretion rate from the whole body. The predicted value which they called mean sweating rate (MSR) was calculated by weighing the local sweating rates (LSR) with the corresponding skin area factors, i.e.,

$$\begin{aligned} \text{MSR} = & 0.11 \text{ LSR}_{\text{forehead}} + 0.29 \text{ LSR}_{\text{chest}} + 0.14 \text{ LSR}_{\text{forearm}} + 0.22 \text{ LSR}_{\text{thigh}} \\ & + 0.24 \text{ LSR}_{\text{calf}} \end{aligned} \quad (1)$$

The equations which they derived are applicable to subjects dressed in swimming suits who are resting in a  $25 \pm 5\%$  relative humidity environment with a slow air movement. Since sweat collection capsules containing filter paper are more practical to use in a cockpit or under chemical protective clothing than capsules equipped with hygrometric sensors, there is a need to evaluate the accuracy of predicting total body sweat rate from localized sweat rates measured with sweat collection capsules containing filter paper.

## II. OBJECTIVE:

Evaluate the accuracy of predicting total body sweating rate from local sweating rates measured at five locations on the body by sweat collection capsules containing filter paper.

## III. METHODS:

Subjects were four male volunteers aged 21-39 with the following

characteristics, height= $174.9 \pm 5.5$  cm and weight= $75.9 \pm 14.6$  kg.

Two methods were used to induce and maintain sweating. One, the subject walked on a treadmill until sweating commenced and he then began three rest/walk (5 min/15 min) cycles at an air temperature of  $40^{\circ}\text{C}$ . In the other method the subject was immersed in a bath at  $40^{\circ}\text{C}$  for 20 min. Sweat was collected in the first method during each 15 min. walk and in the second method during the 15 min. of rest outside the bath.

Sweat was collected in capsules strapped on five locations of the body with elastic bands 1. midforehead, 2. superiorflexor side of the left forearm, 3. right pectoralis major, 4. medial midsection of left thigh and, 5. upper medial side of left calf. A sweat capsule has two parts as shown in Figure 1--a metal capsule which houses filter paper discs (4.25 cm, Whatman #541) and a metal cap containing an O-ring seal.

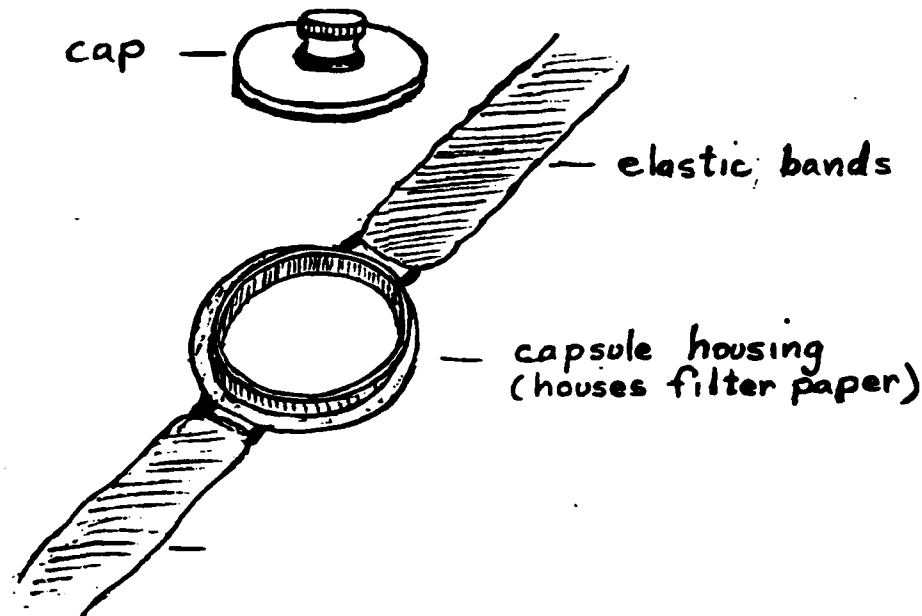


Fig. 1 - Sweat collection capsule.

In the first four weeks of measurement the capsule housings (capsule minus the cap and filter paper) were removed from the subject's body during the 10 minute rest period (between treadmill walks) before he was weighed. Weighings took place about five minutes before the filter papers were inserted into the capsules and five minutes after they were removed. In the last week of the study the capsule housings were left in place on the body during weighing, thereby reducing the delay between weighings and insertion or removal of filter paper to three minutes.

Weight loss of subjects was measured by a platform balance with an accuracy of  $\pm 10g$ . Loss in weight was due to sweat evaporation, respiration and insensible perspiration. Assuming oxygen consumption is proportional to the volumetric ventilation rate, the rate of weight losses due to respiratory evaporation ( $\dot{M}_e$ ) and  $CO_2-O_2$  exchange ( $\dot{M}_r$ ) were estimated by using the following equation, respectively  $\dot{M}_e = 0.019 \dot{V}_{O_2}(44 - P_a)$   $\dot{M}_r = \dot{V}_{O_2}(R p_{CO_2} - p_{O_2})$ , where  $\dot{V}_{O_2}$  is the oxygen consumption in l/min STPD,  $P_a$  is the ambient water vapor pressure (mm Hg), R is the ratio of moles of  $CO_2$  eliminated to moles of  $O_2$  taken up, a value of 0.82 was chosen as the resting ratio and  $p_{CO_2}$  and  $p_{O_2}$  are the densities of carbon dioxide and oxygen at STPD.  $\dot{V}_{O_2}$  was estimated according to the age and sex of the subject using a modified Du Bois standard (Boothby et al, 1936). Temperature corrections on  $\dot{V}_{O_2}$  were made at a scale of 13% rise per degree in rectal temperature.

The rates of weight loss  $\dot{M}_e$  and  $\dot{M}_r$  were subtracted from the total rate of weight loss observed from the platform balance to give a weight loss due to sweat secretion alone.

The total surface area ( $S_A$  in cm) of the subject was estimated from height and weight using the nomogram of Sendroy and Collison (1960). Mean sweating rate (MSR) was calculated by weighting the local sweating rates (LSR in mg/min) with the corresponding skin area factors.

$$MSR = (0.11 S_A LSR_{forehead} + 0.39 S_A LSR_{chest} + 0.14 S_A LSR_{forearm} + 0.18 S_A LSR_{thigh} + 0.18 S_A LSR_{calf}) / 15.067^* \quad (2)$$

\* The surface area of the sweat collection capsules is  $15.067 \text{ cm}^2$ .

#### IV. RESULTS:

In six trials the actual sweat loss of two subjects running on a treadmill was on the average 15.2% greater than that predicted by equation 2 from local sweating rates. In two of three trials on a third subject the actual sweating rate was less than predicted (Table 1). In 13 of 14 trials on three subjects where sweating was induced by immersion in a water bath at 40°C, actual sweat loss was 36.6±18.1% less than that predicted by equation 2 (Table 2).

#### IV. RECOMMENDATIONS:

The results clearly suggest that equation (2), in general, predicts a value which is less than the actual value both at rest and during exercise and that it is less accurate as a predictor when the subject is at rest. These results may reflect the problems inherent in evaluating the method rather than the accuracy of the method itself.

I believe that the second observation above is a result of the differences in procedures used during the trials involving the treadmill and the water bath and that the accuracy of equation (2) during rest can be significantly improved. The major difference between the trials at rest and during exercise is that the time between weighings of a subject was 25 to 30 minutes in the former and 18 to 21 minutes in the latter whereas the sweat capsules measured local sweating rate for only 15 minutes within these longer periods in both kinds of trials.

Ideally the measurement of whole body sweating rate should coincide exact with that of local sweating rates, i.e., the subject should be weighed immediately before and after the filter papers are inserted and removed, respectively, from the capsules.

This was neither accomplished in the treadmill nor the water bath trials, but it was more nearly accomplished in the former. For example, the delay between weighing the subject and inserting the filter paper in the capsules was about eight minutes in the water bath trials but only about four minutes in the treadmill trials. If sweating rate had been constant throughout the time between weighings, this disparity would not have been a problem, but this was probably not the case. Sweating rate of the subject was probably greater during the first 10 minutes after the subject stepped from the water bath therefore the average

<u>Subject</u>	<u>Trial</u>	<u>Whole Body Sweat Rate</u> (mg/min)		$\frac{A-B}{A} \times 100$
		<u>Observed</u> (A)	<u>Predicted</u> (B)	
1	1	12114	10618	12.3
	2	11135	10476	5.9
	3	11956	9235	22.8
	4	11086	8696	21.6
2	1	8055	6944	13.8
	2	7242	6131	15.3
3	1	9341	8736	6.5
	2	6747	9351	-38.6
	3	9445	10708	-13.4

Table 1. A comparison of actual whole body sweat rate with that predicted by Equation 2 from measurements of five local sweat rates during exercise on a treadmill at 40°C.

<u>Subject</u>	<u>Trial</u>	<u>Whole Body Sweat Rate</u> (mg/min)		$\frac{A-B}{A} \times 100$
		<u>Observed</u> (A)	<u>Predicted</u> (B)	
1	1	9000.3000	6678.4900	25.7970
	2	10370.2000	8358.6000	19.3979
	3	8998.4000	6378.2500	29.1179
	4	11964.3000	6749.1300	43.5894
	5	8593.7000	11885.8000	-38.3080
	6	11768.6000	5385.0900	54.2419
	7	8958.5000	8515.9000	4.9406
	8	10651.4000	8950.0400	15.9732
2	1	7961.5200	3819.6400	52.0237
	2	9000.3200	4027.7100	55.2492
	3	7130.4800	3880.0400	45.5852
3	1	9687.5000	3847.8900	60.2798
	2	8476.9500	4237.6700	50.0095
	3	7790.3000	6293.6200	19.2122

Table 2. A comparison of actual whole body sweat rate with that predicted by Equation 2 from measurements of five local sweat rates during rest at 40°C. Sweat was induced by immersion in a bath at 40°C.

sweating rate (per minute) calculated from the difference in body weight was more than predicted from local sweating rates and the disparity should increase as the delay between weighing the subject and insertion of the filter paper increases.

The inaccuracy of the platform balance was another source of error. When two consecutive weighings of the subject indicated a loss of 300g (a typical value) the error of this measurement may have been as large as 6.7% since the balance had an accuracy of  $\pm 20$ g.

Undoubtedly another source of error was the use of inappropriate weighting factors for the five body areas in equation (2). I intend to apply for a mini-grant and to investigate the weighting factor problem further. This approach toward estimating whole body sweating rate is scientifically sound and I would like to work on improving the methods of evaluating it with the help of a mini-grant.

#### REFERENCES

W. M. Boothby, J Berkson and H. L. Dunn. "Studies of the Energy Metabolism of Normal Individuals: A Standard for Basal Metabolism, With a Nomogram for Clinical Application." Am. J. Physiol., Vol. 116, pp. 468-484, 1936.

S. A. Nunneley and L. G. Myhre, "Physiological Effects of Solar Heat Load in a Fighter Cockpit," Aviation, Space and Environmental Medicine, Vol. 49, pp. 969-973, 1976.

S. A. Nunneley and G. R. James, "Cockpit Thermal Conditions and Crew Skin Temperatures Measured in Flight," Aviation, Space and Environmental Medicine, Vol. 48, pp. 44-47, 1977.

J. Sendroy and H. A. Collison, "Nomogram for Determination of Human Body Surface Area From Height and Weight." J. Appl. Physiol., Vol. 15, pp. 958-959, 1960.

H. Tam, R. C. Darling, J. A. Downey and H. Cheh, "Relationship Between Evaporation Rate of Sweat and Mean Sweating Rate," J. Appl. Physiol., Vol. 41, pp. 777-780, 1976.

1979 USAF - SCEEE SUMMER FACULTY RESEARCH PROGRAM

Sponsored by the  
AIR FORCE OFFICE OF SCIENTIFIC RESEARCH

Conducted by the  
SOUTHEASTERN CENTER FOR ELECTRICAL ENGINEERING EDUCATION

FINAL REPORT

THE UTILIZATION OF GEOTHERMAL RESOURCES  
AT UNITED STATES AIR FORCE BASES

Prepared By  
Paul K. Grogger, Associate Professor  
Department of Geology and Applied Earth Sciences  
University of Colorado  
Colorado Springs, Colorado

Air Force Engineering and Services Center  
Energy Group  
Tyndall Air Force Base, Florida

USAF Research Colleague  
Bruce MacDonald

4 June to 10 August 1979

Contract No.:  
F49620-79-C-0038

THE UTILIZATION OF GEOTHERMAL RESOURCES  
AT UNITED STATES AIR FORCE BASES

by  
P. K. Grogger

ABSTRACT

The use of geothermal energy is one of the few energy sources which may be an answer to our present and future energy crisis.

The Air Force installations on the continental United States as well as Alaska and Hawaii, were evaluated as to the possibility of utilizing geothermal energy to develop electricity, produce process steam, or heat and/or cool buildings. Twenty-five bases have suspected geothermal resources available. Because of either need and available technology seven installations were rated priority I, six were rated priority II and priority III and IV totaled ten.

Geological and geophysical data indicate further investigation of the priority I installations, Saylor Creek Range, Idaho, Ellsworth AFB, South Dakota, Charleston AFB, South Carolina, Kirtland AFB, New Mexico, Vandenberg AFB, California, Luke AFB, Arizona, and Williams AFB, Arizona, should be accomplished as soon as possible.

The use of geothermal energy will decrease the need for fossil fuels by the USAF and during times of short supply allow such fuels to be used for the Air Force's primary mission, military defense.

## ACKNOWLEDGEMENTS

The author would like to thank the Air Force Office of Scientific Research and the Southeastern Center for Electrical Engineering Education (SCEEE) for providing him the opportunity to spend a most worthwhile and interesting summer at Tyndall Air Force Base, Florida.

The Air Force Engineering and Services Center (AFESC) and its Energy Group deserve special thanks for their interest and constant assistance. Dr. Richard N. Miller of SCEEE and Major Fred Morrow of AFESC were especially helpful and were responsible for a well-organized program.

Finally, he would like to thank Mr. Bruce MacDonald for many helpful discussions, in assisting the author in procuring needed materials, and taking a sincere interest in the utilization of geothermal energy by the United States Air Force.

## INTRODUCTION

Within the next few decades, if not earlier, an energy famine will occur (1,2,3). At present the only alternative resource that can be developed in time to stave off such an occurrence and with a great enough capacity to insure our quality of life is geothermal energy.

The heat of the interior of the earth is one of the largest energy resources available to the human race. In fact, when the volume ( $1,097 \times 10^9$  cubic kilometers) of the earth's interior and the specific heat of rock are taken into account, it becomes evident that this geothermal heat is by far the largest reservoir of energy that is now available.

The amount of heat increases with depth but the rate of increase varies considerably. If an area is not technically active, the values will usually range between  $10^\circ$  and  $50^\circ\text{C}/\text{km}$ . The average temperature gradient of the earth indicates a loss of heat by conduction at a rate of about 1.5 micro-calories/cm<sup>2</sup> which equals 1.5 heat flow units (hfu) or about  $60\text{w}/\text{km}^2$ . Because the surface area of the earth is  $5.1 \times 10^{18}\text{cm}^2$  the total geothermal heat flux is  $8 \times 10^{17}\text{Btu}/\text{yr}$ . This amount of energy is far larger than the energy available from all of the uranium and thorium combined when using breeder reactors. It is also important to realize that the heat already exists; therefore, it is not necessary to burn other fuels to produce the required heat. However, the size of the resource is not the only significant factor. While the natural heat flow from the center of the earth is too diffuse and presently not economical to be utilized, there are many areas in the world where pockets of geothermal heat found close to the surface have been developed and put to beneficial use for present technology and related economics make it possible to utilize geothermal energy only when the hfu's are greater than 2.0. This is the specific reason the following definition of geothermal energy is correct at this time: a localized deposit of geothermal heat concentrated at attainable depths, in

adequate volumes, and at temperatures sufficient for exploration (4). Usually at these locations the process of convection dominates. This takes place due to volcanism and thermal activity which causes transporting fluids to move along fractures in the rock formations.

The heat is primarily due to heat released by radioactive decay of unstable elements, chiefly uranium and thorium (80 percent) and the other 20 percent is stored heat left from the formation of the earth.

Until now the human race has not even scratched the surface of the potential of geothermal energy. Although sources of geothermal energy have been known and exploited for many years for medical and other purposes, notably in Iceland, Italy, and New Zealand, interest in the possibility of finding and developing new sources in the United States has only recently become viable due to the passage of the Federal Steam Act of 1970. The increase in geothermal utilization over the past 15 years has occurred at concentrated geothermal areas. These areas and others like them are capable of much greater production. In the near future many other areas will be able to become productive as new science and technological discoveries allow geothermal fields to be created where none exists now.

It has been 75 years since the Larderello, Italy, fields produced electricity from natural steam. During these years only 1,500MW of geothermal energy have been developed. Why? The technology of the past allowed only a few fields to be developed and many of the plausible fields were too remote from potential energy markets. Also other fields are located in countries with abundant cheap alternative energy sources that could be developed without the need for new techniques and the risk of unconventional engineering. There has also been the initial high cost of verifying high internal heat by drilling which will not be spent if an alternative energy source is obtainable without risk. Finally, there has been the psychological factor that the public utilities, with their conservatism, are unwilling to regard geothermal energy as a

viable alternative due to its newness.

Even with these problems the installed electrical capacity of geothermal energy grew at a 5.22 percent annual rate from 1942 to 1958. Since that time the annual increase has grown at an even faster rate (Table 1). However, even with this increase, geothermal energy's total contribution to the coverage of the world's energy demand corresponds to about only 0.2 percent (5) of the world's total oil consumption. There is very little doubt that this percentage as well as the actual total energy use of geothermal resources will increase in the future. This is true for several reasons: higher cost of fossil fuels due to inflation and scarcity; governmental incentives; technological improvements in prospecting techniques so more immediately usable geothermal reservoirs will be discovered; the development of improved drilling systems and equipment so production costs will decrease and deeper reservoirs will become economic and accessible; solving the chemical problems associated with relatively concentrated hot brines; the development of two-fluid generating systems so lower temperature geothermal reservoirs will be usable for electrical generation; non-electrical uses of the heat from geothermal waters so an increase in such applications as domestic and industrial heating and cooling will occur; desalination of water; distillation of domestic and industrial wastes; recovery of minerals; and more efficient physical and chemical processing.

TABLE 1  
GROWTH OF INSTALLED GEOTHERMAL POWER CAPACITY

<u>Year</u>	<u>Average Annual Compound Growth Rate</u>	<u>Geothermal MW Installed</u>
1904		0
1942		130
1958	5.22% (1942-1958)	203
1961		420
1963		536
1970	7.20% (1958-1970)	675
1976	12.42% (1970-1976)	1362
1981	15.74% (1976-1981)*	2828*

\*Estimated  
Modified from Reference 5

For too long, geothermal resources have only been thought of as being a source for electrical generation. This is due to several factors: (1) electricity is a very marketable commodity, (2) electrical applications are versatile, and (3) the geothermal areas which were being noticed provided transfer mediums at high temperatures. However, it is now evident that the geothermal areas with high enough temperatures for electrical production are much less numerous than areas of lower temperatures (less than 150°C). More use of lower temperature fluids will occur as the needed techniques are developed and the quantity will make up for what is lacked in quality. Also, these fluids will usually contain less dissolved solids and gases than fluids at higher temperatures which will lessen corrosion problems.

Air Force lands are dominated by low temperature fluids and the two principal problems of using such fluids, larger land area needed and possible subsidence problems, should be less of a problem on an Air Force base if proper planning takes place. It is also possible, due to the makeup of most bases in the Air Force, that the Air Force could be one of the first to establish dual or multi-purpose plants. By developing and utilizing low temperature geothermal resources or by initiating multi-purpose plants in the United States, the Air Force will be in the forefront of geothermal energy development. This type of position would be very important for the United States as approximately 40 percent of the United States energy requirements could be provided by geothermal energy once the techniques of utilization are developed and the geothermal resources are located.

LOCATION AND EVALUATION OF POSSIBLE GEOTHERMAL  
AREAS ON AIR FORCE PROPERTY

PREVIOUS STUDIES

Industrial, academic, and private studies have investigated possible geothermal areas in or near the following United States Air Force Bases: Dover AFB, Dover, Delaware; Mountain Home AFB, Mountain Home, Idaho; Kingsley AFB, Klamath Falls, Oregon; Bellows AFB, Waimanalo, Oahu, Hawaii; and Williams AFB, Chandler, Arizona. Of the five locations, two were recognized geothermal areas, the Mountain Home and Kingsley AFBs.

Since the mid-70's and the 1973 embargo on fossil fuels by OPEC the United States Air Force (USAF) has become increasingly interested in developing alternative energy resources and lessening their dependence on unstable and decreasing energy sources.

In 1978 two reports, the Technology Assessment-Geothermal report by W. A. Tolbert (6) and the report concerning the Geothermal Potential at USAF Bases by C. F. Austin and J. A. Whelan (7), were released after two, one-year independent studies were completed. Both reports attempted to determine the geothermal utilization possibilities of Air Force lands. Both reports listed five bases as being the best geothermal candidates. As can be observed in Table 2, the report agreed on four of the bases, Ellsworth AFB, Rapid City, South Dakota; Hill AFB, Ogden, Utah; Mountain Home AFB and Saylor Creek Range, Mountain Home, Idaho; and Williams AFB, Chandler, Arizona. The Austin report included Keesler AFB, Biloxi, Mississippi as its fifth base, whereas Tolbert determined that Dover AFB, Dover, Delaware was a better possibility. Both studies were generalized and their estimates relied on varying degrees of accuracy and differences in study needs as well as the expertise of the authors. Although the table of geothermal potential included at the end of the Austin report is often of questionable accuracy, it was the first attempt to catalog nearly all of the USAF bases as to their geothermal possibilities.

TABLE 2. A TIME REVIEW OF THE DETERMINATION OF THE POSSIBLE UTILIZATION OF GEOTHERMAL RESOURCES AT UNITED STATES AIR FORCE BASES

Initial Lists		China Lake Report (Nov 78)	This report's Initial List (May 79)	General Geologic Review (Jun 1 79)	Intensive Geologic Research (Jun 25 79)	After Further Earth Science Review, Phone Calls & Visits (Jul 1 79)	After Base Energy Consumption & Utilization Review (Aug 1 79)	Comments
AFSC/DEB List (Aug 78)	Dover				S <sup>1</sup>	L <sup>5</sup>	No	Too far from energy source
	Ellsworth Hill	Ellsworth Hill		S <sub>2</sub>	P <sup>2</sup>	G (heating)	P <sup>1,6</sup>	80-90% certainty
	Mtn Home	Mtn Home		S		M (heating)	P	Data needed, geophysical & geochemical
	Saylor Creek	Saylor Creek		P		M (electricity)	P <sup>6</sup>	One of top seven
	Williams	Williams		P <sup>3</sup>		G (electric/cooling)	P <sup>6</sup>	90 to 95% certainty
	Kessler			S		L	S <sup>4</sup>	Edge of resources, expensive
		Beale		S		L	No	Poor economics
		Cannon		No				
		Davis-Monahan		P		M (cooling)	P	More data needed, good economics
		Edwards		P		H (heating), M (cooling)	P	Data needed, good economics
		Elmendorf Fairchild						
		George	No	S		L	S	Low possibility, low economics
		Hickam		P		M (cooling)	S	Good geology data needed, economics ok
		Holloman		P		L	No	Negative data
		Kingsley		P		M (cooling)	P	Geology moderate, economics ok
				P		H (heating)	S	Present energy sources less expensive

Kirtland		P	G (cooling)	P <sup>6</sup>	Geology high to moderate good economics
Malmstrom	No				
March		S <sup>4</sup>	M (cooling)	S	Geology moderate, need low
McClellan/ Mather		No			
Nellis		S	M (cooling)		Lack of geology data Economics ok
Norton					
Pease	No				
Peterson		No			
Travis		No			
Vandenberg		P	M (cooling)	P <sup>6</sup>	Lack of data, but indications are good, great need
Warren	No				
Wheeler		S	M (cooling)	S	Possible, but lack of data, need great
	Langley	P	M (heating)	S	Poor economics, edge of resource
	Charleston	P	H (cooling)	P <sup>6</sup>	Good possibility, more data needed
	Andrews	No			
	Ellington		H (electric) <sup>4</sup>	No	Too far from source
	Little Rock		L	P <sup>6</sup>	Good indications, need is high
	Luke		H (cooling)		Economics very good, lack of data, but good possibilities
	Bellows		H (electric)	P	On the edge of a high heat flow zone
	Offutt		M (heating)	S	

1 S = Secondary Prospect  
P = Primary Prospect

2 Geophysical & geochemical investigations completed;  
exploration drilling started, early October  
completion date.

3 Geological, geophysical & geochemical investi-  
gations completed; funding for drilling  
is being determined.

4 Geopressed system possibility; questionable  
economics.

5 H = High possibility; M = Moderate possibility;  
L = Low possibility.

6 One of top seven possibilities as of 10 August 1979.

## PRESENT STUDY

Using Austin's table, previous knowledge of potential areas, and the Known Geothermal Resource Area's (KGRA) of the United States Geological Survey (USGS) a first initial list of air bases that needed to be geologically evaluated was developed (Table 2). An initial geologic review of the areas included on the initial list eliminated four bases as well as adding three. By using the USGS geologic research libraries at Denver, Colorado and Reston, Virginia, the geothermal potential of the remaining bases were evaluated as to whether they were of primary or secondary importance. Five more bases were added for evaluation and five bases were eliminated due to this research. A final period of geologic evaluation separated the bases remaining into their potential as to electricity, cooling, or heating and each of these categories were classified as to being an area of high possibility, moderate possibility, or low possibility.

The final analysis of the geothermal potential of USAF bases included an energy consumption and utilization review as well as a general economic evaluation. From this final analysis the remaining bases were again classified as to being a primary or a secondary prospect. Using this methodology, seven installations were considered to have a high possibility for utilizing geothermal resources in one or more ways: Ellsworth AFB, South Dakota; Saylor Creek Range, Idaho; Williams AFB, Arizona; Kirtland AFB, Albuquerque, New Mexico; Vandenberg AFB, Lompoc, California; Charleston AFB, Charleston, South Carolina; and Luke AFB, Phoenix, Arizona. Three of these bases were included by one or both of the two original reports, Ellsworth AFB, Williams AFB, and Mountain Home AFB. Two bases, Hill AFB and Williams AFB are already having exploration techniques used to determine their actual geothermal resource. Hill AFB has had a geophysical and geochemical evaluation completed and an exploration well is to be drilled by early October, 1979. The Williams AFB geophysical and geochemical

study is completed and funding for a production well is now being sought. It is very possible that temperatures for space heating utilization will be located for Hill AFB and temperatures for space cooling and/or electrical production will be available at Williams AFB.

Further geologic investigation, remote sensing as well as initial geophysical and geochemical studies of seven of the eight high possibility bases, excluding Williams AFB, listed in Table 2, will be attempted during the 1979-80 period, if funding for such research is obtained. If enough funding is obtained, six other bases will also be investigated further: Mountain Home AFB; McClelland/Mather AFB's, Sacramento, California; Davis-Monthan AFB, Tucson, Arizona; Edwards AFB, Rosamond, California; Holloman AFB, Alamogordo, New Mexico; and Bellows AFB and Wheeler AFB, Hawaii.

Specific data obtained, references used, economic feasibility, and the type of geothermal resource(s) available are listed in Table 3. During the time this report was written, no magma or vapor-dominated geothermal systems have been positively identified; Keesler AFB, Mississippi and Ellington AFB, Genoa, Texas, are located above geopressed systems. McClellan and Mather AFBs, Sacramento, California may be located on a geopressed system. The seven possible hot dry rock systems are indicated in Table 3. To develop the hot dry type of geothermal resource, assistance from the Department of Energy's Hot Dry Rock section at Los Alamos Scientific Laboratories will be necessary. The primary geothermal system found at USAF bases is the water-dominated system with fourteen of the twenty-five bases having a strong possibility of such a system being utilized.

Electrical production may be possible at five bases: Saylor Creek, Davis-Monthan, Bellows, Luke, and Williams AFBs. With further technological advances the possibility of electrical productions at six other bases could become reality: Charleston, Kirtland, Edwards, Vandenberg, Kessler, and Ellington AFB's.

TABLE 3. FACTORS CONSIDERED IN DETERMINING THE POSSIBILITY OF GEOTHERMAL UTILIZATION AT US AIR FORCE BASES

Air Base	Location	Command	Type of Geothermal Resource <sup>1,2</sup>			Economics		Type of Fuel and amount of energy used <sup>3,6</sup>						
			Vapor-dominated	Water-dominated	Hot dry rock	Economic	Marginal	Submarginal	Not Economic	Electricity	Fuel oil	Natural gas	Propane	Coal
1. Hts Home/Creek	Idaho	TAC	Possible	100°C at 4m 100°C to 200°C at 4m					572,704	155,016	57,844		336,216	
2. Saylor	Dover, DE	MAC		48°C at 1km (21)					583,004	121,573	5,930		324,564	
3. Brevard	Mad City	SAC		40°C at 1km (17)					699,352	698,256				
4. Ellsworth	Elmsh	ABC		30°C at 1km					801,478	754,429	883,473	398		
5. Kingsley	Falls, OR	TAC		126°C at 1km					200,435	17,314	889,941	0	105,139	
6. Davis	Tucson, AZ	PACF							190,565	9,148			52,511	
7. Hickam	Honolulu, HI	PACF							877,575	6,679	348,754			
8. Wheeler	Omaha, NE	PACF							963,508	7,992	301,613			
9. Bellows	Omaha, NE	PACF							1,690,526	64,471				
10. Langley	Washington, DC	TAC		41°C/700m (21)					1,611,658	26,108				
11. Charleston	Charleston, SC	MAC		60°C at 1km										
12. Holloman	Alamogordo, NM	TAC		32°C at 500m										
13. Kirtland	Albuquerque, NM	MAC												
14. Edwards	Boonville, MO	AFSC		85°C-90°C at 3m	Possible				1,019,488	652,623	87,266		1,185	
15. George	Victorville, CA	TAC		30°C	Possible				1,227,036	653,140	102,421		1,286	
16. McChellum	San Ramon, CA	ARLZ/ATC							583,421	499,034	103,205		17	
17. March	Riverside, CA	SAC							685,444	279,070	117,100		14	
18. Norton	San Bernardino, CA	MAC							697,457	624	596,459		4,426	
19. Vandenberg	Lawrenceville, GA	SAC							750,137	334	605,148		2,062	
20. Beeler	Biloxi, MS	ATC							7,184,940	24,390	920,259		9,384	
21. Ellington	Genoa, TN	ATC							1,007,480	16,712	775,271		6,074	
22. Laha	Phenix, AZ	TAC							1,270,327	72,779	222,012		12,259	
23. Offutt	Omaha, NE	SAC							1,321,668	23,157	592,484		6,200	
24. Williams	Chandler, AZ	ATC							481,189	4,937	485,108		1,316	

<sup>1</sup> Temperature/depth is given if known or can be estimated.  
<sup>2</sup> Margins is not listed as it is not known on any bases.  
<sup>3</sup> Use is listed.  
<sup>4</sup> If resource is available.  
<sup>5</sup> Figures are in MBTU's.  
<sup>6</sup> Upper figure is for 1975; lower is for 1978.  
<sup>7</sup> Mountain Home & Saylor Creek fuel amounts are totaled together.  
<sup>8</sup> Fuel amounts for all three bases in Maui are totaled and presented as Hickam AFB energy use.

Type of data obtained concerning geothermal resources of particular air bases & number of reference/s cited		Surface Phenomena		Well data		Geochemical		Geophysical		Geothermal Gradient																		
Regional Geology	Local Geology	12, 15	12	16	12, 19, 20	21, 28, 29, 30	33, 37, 38, 39, 40, 41	49, 61, 62, 63, 64, 65	67, 68, 69, 70, 71	84, 85, 86, 87, 88	105, 106, 107, 108	105, 106, 107, 108	105, 106, 107, 108, 114, 115	89, 128, 129, 130, 131, 132, 133	89, 128, 129, 130, 131, 132, 147, 148	167, 168, 169	171	171	173, 175	173, 175	179	176, 188	179, 182	186	176, 183, 186, 188	8.5°C/100m		
1. 8, 9, 10	14, 15, 16	12, 15	12	16	12, 19, 20	21, 28, 29, 30	33, 37, 38, 39, 40, 41	49, 61, 62, 63, 64, 65	67, 68, 69, 70, 71	84, 85, 86, 87, 88	105, 106, 107, 108	105, 106, 107, 108	105, 106, 107, 108, 114, 115	89, 128, 129, 130, 131, 132, 133	89, 128, 129, 130, 131, 132, 147, 148	167, 168, 169	171	171	173, 175	173, 175	179	176, 188	179, 182	186	176, 183, 186, 188	8.5°C/100m		
2. 11, 12, 13	17, 18																											
3. 22, 23	26																											
4. 31, 32, 33, 34	32, 35, 36	18	27	36	21, 28, 29, 30	33, 37, 38, 39, 40, 41	49, 61, 62, 63, 64, 65	67, 68, 69, 70, 71	84, 85, 86, 87, 88	105, 106, 107, 108	105, 106, 107, 108	105, 106, 107, 108, 114, 115	89, 128, 129, 130, 131, 132, 133	89, 128, 129, 130, 131, 132, 147, 148	167, 168, 169	171	171	173, 175	173, 175	179	176, 188	179, 182	186	176, 183, 186, 188	8.5°C/100m			
5. 42, 43, 44, 45, 46, 47	44, 45, 46, 47, 48, 49, 50, 51, 52, 53, 54, 55, 56																											
6. 73, 74, 75, 76, 77, 78, 89	79, 80, 81																											
7. 91, 92	92, 93, 94, 96, 97																											
8. 91, 92	92, 94, 96, 97, 109, 110, 111																											
9. 91, 92	92, 94, 96, 97, 112																											
10. 22																												
11. 22																												
12. 116, 117, 118	119, 120, 121, 122, 123, 124																											
13. 116, 118, 135	136, 137, 138, 139, 140, 141, 142, 143, 144, 145, 146																											
14. 149, 150	150, 151, 152, 153, 154																											
15. 156, 157	158, 159, 160, 161																											
16. 162, 163, 164, 165	165, 166																											
17. 150	170																											
18. 150, 153	153																											
19. 153, 172, 173	153, 172																											
20. 173	173, 174																											
21. 173	173, 174																											
22. 178, 180, 189	177, 187																											
23.																												
24. 178, 180, 189	177, 184, 185, 187																											

The final rating of priority for further investigation of Air Force installations is illustrated in Table 4 and Figure 2. The priority listing is based on geothermal resource data and the need for geothermal utilization.

TABLE 4  
RELATIVE PRIORITIES FOR EXPLORATION AND  
UTILIZATION OF AIR FORCE LANDS

Air Base	Resource Temp °C	Thermal Grad °C/Km	Depth to Prod Km	Need	Assessed, <sup>1</sup> Priority
Mtn Home	100	4-60	4	Low	II
Saylor Creek Range	100-200	50-90	3	Low	I
Dover	48	38	1	Moderate	IV
Ellsworth	50	31-45	1.35	High	I
Kingsley	30	UK	1	Very Low	IV
Davis-Monthan	130 <sup>2</sup>	50	1	Moderate	II
Hawaiian bases	UK <sup>2</sup>	UK	UK	High	II/III
Langley	41	41	.07	High	III
Charleston	60	60	1	Moderate	I
Holloman	40	32	3	High	II
Kirtland	60	80	1	Very High	I
Edwards	85-90	45	2	Very High	II
George	30	UK	UK	Moderate	III
McClellan/ Mather	UK	UK	UK	Very High	II
March	UK	UK	UK	Moderate	IV
Norton	35	UK	UK	High	III
Vandenberg	25-35	40	2	Very High	I
Keesler	100	30	4	Very High	III
Ellington	200	35	5	Very Low	IV
Luke	150-200	60	3	High	I
Offutt	35	35	1	Very High	III
Williams	200	85	3	Moderate	I

<sup>1</sup> I (highest priority) - - IV (lowest priority)

<sup>2</sup> UK = Unknown

Figure 1. Location of U.S. Air Force installation with possible geothermal resources. Geothermal resources are categorized.

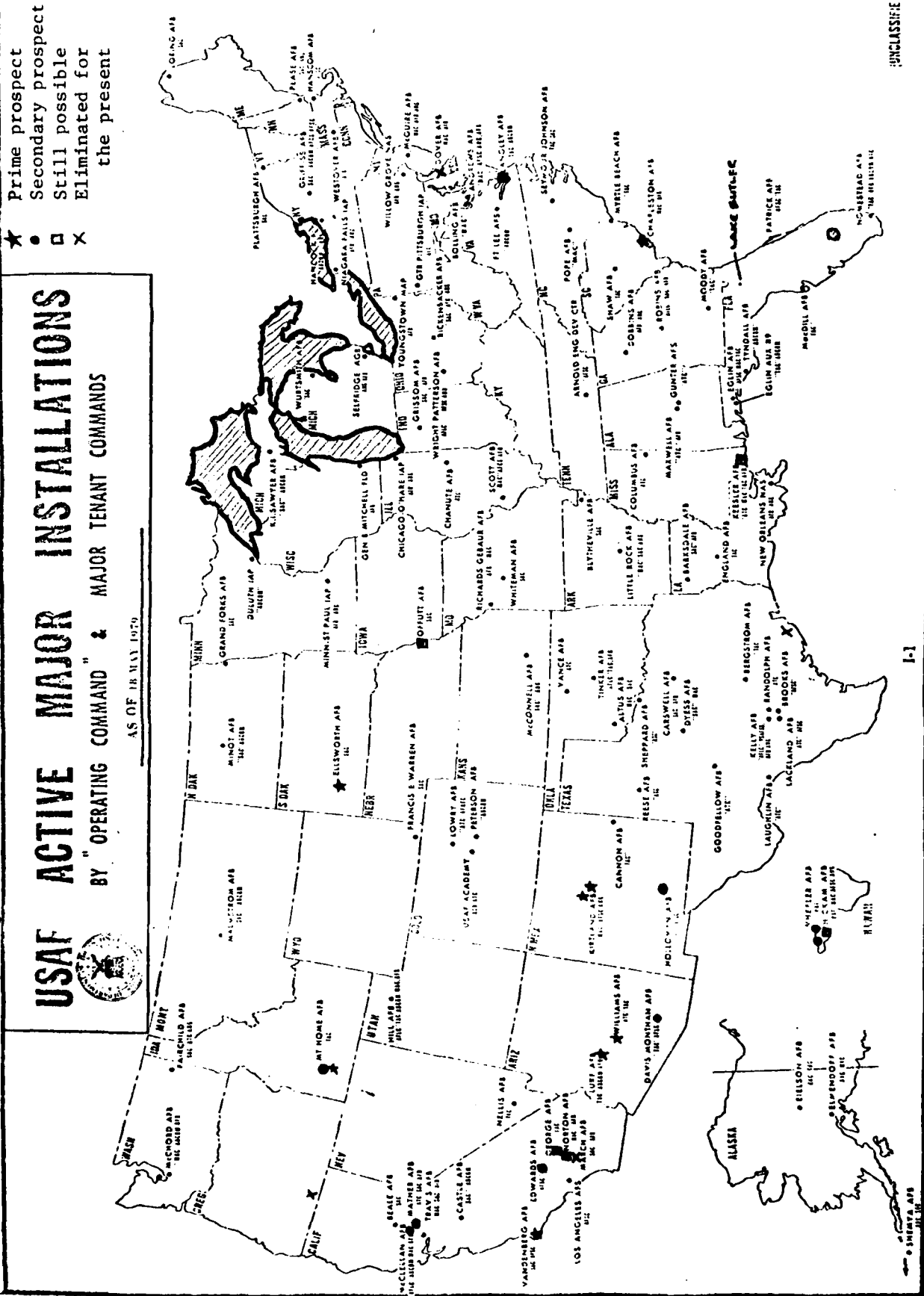
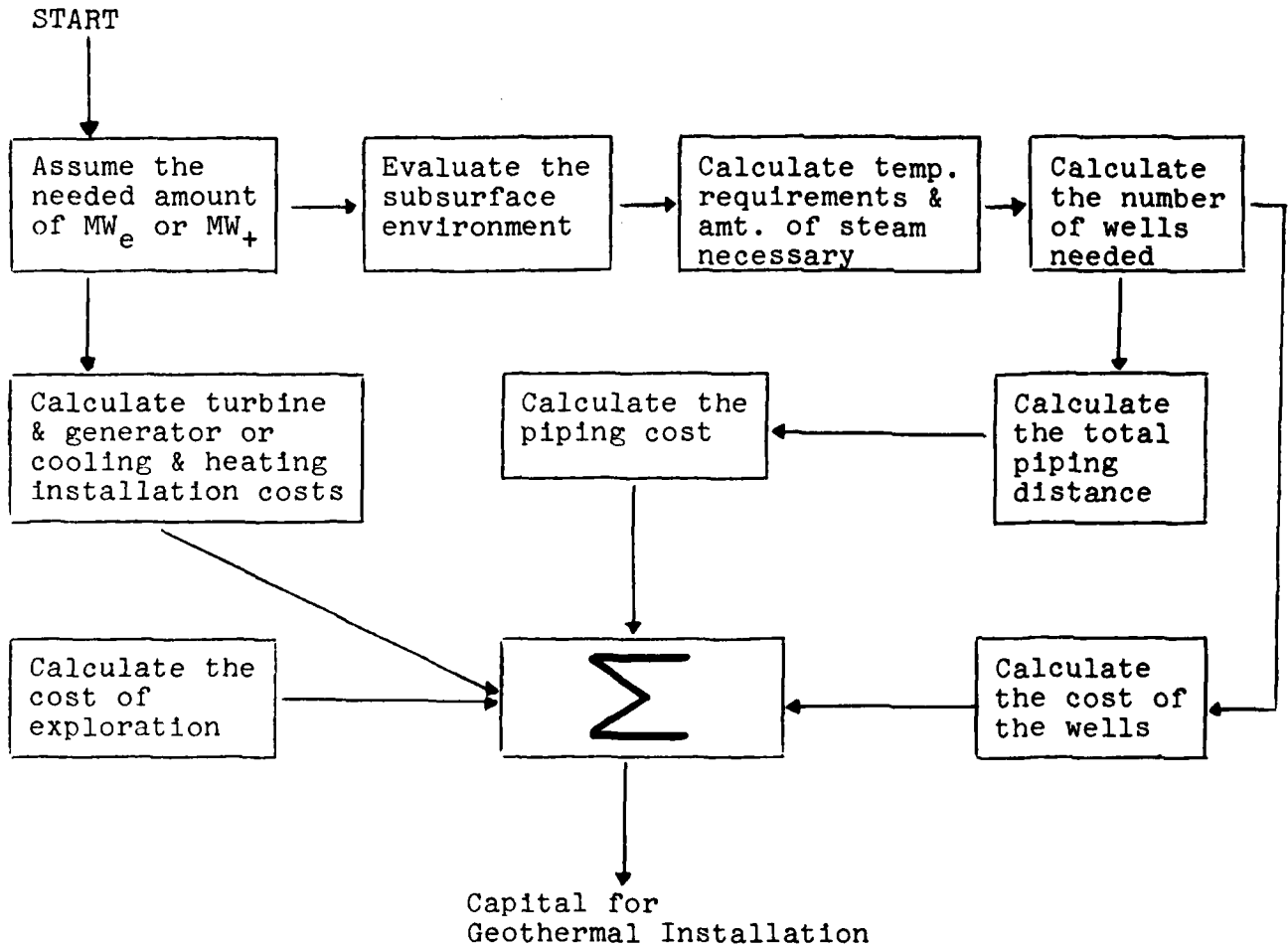


Figure 2. Flow model of determining the capital cost of any needed geothermal installation.



## GENERAL ECONOMIC ANALYSIS OF A U.S. AIR FORCE GEOTHERMAL PROGRAM

### INTRODUCTION

To assess the cost of a geothermal installation, whether it is to be used for electrical production or heating and cooling of buildings, four factors must be considered: (1) data related to the subsurface environment (geothermal gradient, pressure gradient, reservoir flow capacity, and reservoir rock characteristics) must be developed; (2) a technically feasible design must be chosen; (3) the cost for each expenditure category must be determined; and (4) the actual cost of generating power must be determined, usually by using a model for the surface environment and system design (design of production and disposal wells and the gathering system and the design of the utilization plant, whether for electricity, heating, cooling, and/or process steam)(189).

The above factors can be observed in Figure 2 as a flow model which starts with the known amount and type of energy needed and continues until the final capital cost is determined.

### ELECTRICAL PRODUCTION

The actual categories of expense needed to be determined when developing the total capital cost estimate for a geothermal power plant are (the percent figure indicates the approximate percentage of the total capital cost that category includes): (1) engineering design - 15%; plant equipment - 46% including heat exchangers, condensers, turbine-generator, main feed pump turbine, cooling tower, pumps and drives, auxiliary systems, and electrical equipment; bulk plant materials - 29%, including concrete and earthwork, electrical, piping, insulation, and valves, instrumentation, site improvements; control and turbine buildings - 6%; and other engineering and construction support - 4% (190).

The cost of utilizing geothermal resources varies with the quality and quantity of the specific site. However, assuming

a normal situation (20 percent rate of return, current tax policy, plant availability factor of 0.75, 200°C temperature, 65Kg/s, 3.9MW<sub>e</sub>) an estimated price of electricity at busbar will be 30 mills/kWh. The importance of this estimate can be understood by observing Table 5. It is readily seen that the average geothermal electrical facility, especially steam, is presently economical in comparison to other power systems. As the cost of the fossil fuel power plants continue to escalate geothermal electrical production will become even more economical.

The low range figures will not be applicable for most geothermal power plants located at Air Force installations. The primary reason for a higher cost is the smaller generation capacity, 10 to 25 MW<sub>e</sub> power plants. The unit cost of a 10MW<sub>e</sub> development has been estimated (195) to be 25 to 35 percent higher than the corresponding cost for a 50 MW<sub>e</sub> power plant. Even so, the cost of the geothermal produced electrical power will normally be competitive with all other power sources except hydroelectric because the other agency sources costs are escalating at a faster rate than geothermal.

The actual cost of small geothermal installations for each of the four types of geothermal resources now technologically capable of being built is listed in Table 6.

As can be observed, vapor-dominated systems are the most economical but only two air bases have a possible success rate ratio of 1:4. Depending on the reservoir temperature, water-dominated and hot dry rock systems will be the next lowest price electrical producer. At the present time electrical production from such systems are marginal; however, in the next five years both systems should become economical due to the increased price of alternative fuels and advancements in geothermal technology. Only the geopressured system is not economical at present nor will it become economical before 1985.

TABLE 5

COMPARISON OF COSTS FOR FUTURE GENERATING  
 FACILITIES IN CONSTANT 1976 DOLLARS  
 (Refs. 191,192,193,194)

Type	Estimated Total Capital Investment (\$/KW <sub>e</sub> )	Estimated Price of Electricity at Bursbar (Mills KWh)
Coal-fired Power Plant	570-600	28-33
Nuclear Power Plant (LWR)	720-830	29-38
Breeder Reactor Power Plant	800-1100	35-50
Conventional Oil-Fired Power Plant (low-sulfur oil)	350-400	34-42
Combined Cycle (oil-fired) Power Plant (low-sulfur oil)	275-350	32-40
Geothermal Power Plant		
Steam	250-280	18-25
Hot Water		
Flash cycle	400-800	25-55
Binary cycle	500-700	30-42
Hot dry rock	350 and higher	28 and higher
Geopressured	700-2000	30 and higher

TABLE 6

Cost of Small, 10 to 25 MW<sub>e</sub>, Geothermal Electrical  
Power Plants at U.S. Air Force Installations

Type of Geothermal Resource Ssystem	Size of Power (MW <sub>e</sub> )	Estimated Cost (\$ x 10 <sup>6</sup> )	Reference
Vapor-dominated	100	20-30	453
	50	15-20	
	25	10-15	
	10	8-12	
Water-dominated			
Binary	50	28-33	449
Flash	50	26-35	
Hybrid	50	35-40	
Binary	10	18	
Rankine cycle	10	23	
Hot dry Rock			
300°C reservoir temp	100	30-35	
175°C reservoir temp	100	40-50	
250°C reservoir temp	25	20-25	
Geopressured			
Two-stage flash steam	50	60-80	452
Two-stage flash steam	25	30-40	452

## HEATING AND COOLING

The cost of heating and cooling buildings varies greatly depending on the type of fuel used. By 1985 natural gas will cost from \$4 to 5/GJ, heating oil from \$5 to 7/GJ and electrical heating will vary from \$9 to 11/GJ. These costs can be compared to geothermal costs of \$2 to 4/GJ at the well head (196). The actual cost of geothermal energy supply will be determined by several characteristics: the size of the energy demand, the maximum temperature of utilization, the effective temperature range of utilization, the impacts of seasonal factors and plant operating schedule on the load factor, and the distance of transmission. By locating production wells close to the site of utilization, heating by geothermal energy will be able to be used at any base where reservoir temperatures of 50°C can be acquired and in some cases temperatures as low as 30°C will be able to be used.

For any given geothermal heat plant the following formula can be used to determine the production costs (in \$ per gigacalorie) of geothermal heat:

$$S = \frac{1}{N} \left[ \left( \frac{i^n S_n (1+i)^n}{(1+i)^{n-1}} \right) + S_{n+1} \right]$$

where N is the total amount of gigacalories per year; i is the annual interest rate,  $S_n$  is the cost for the components of the plant,  $S_{n+1}$  is the annual operating cost and n is the amortization periods in years (197).

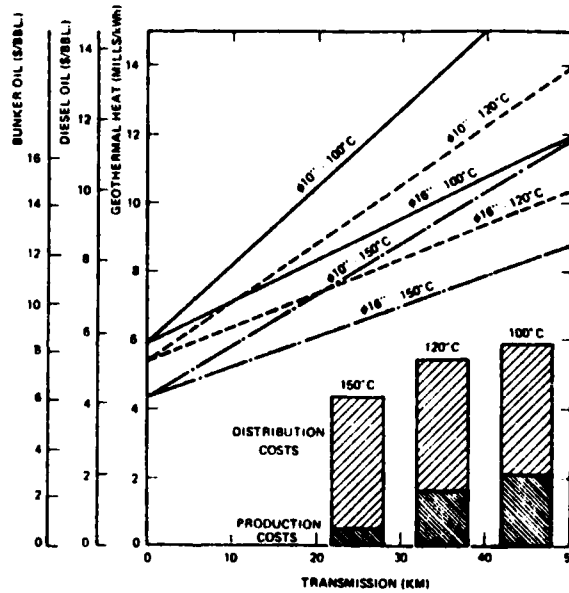
Just as with electrical power, geothermal heating of buildings is economic at present, depending on the distance the heat must be transported. Under two kilometers geothermal heat is normally the least expensive heat source (Figure 3).

Depending on the size of the heating and cooling needs; the cost of the installed facility, not including exploration and well costs, will range from \$4.5x10<sup>6</sup> at Williams AFB to approximately \$4-6x10<sup>6</sup> at Charleston AFB for cooling and \$2x10<sup>6</sup>

at Mountain Home to  $\$5 \times 10^6$  at Offutt or Langley AFB's for heating.

The approximate cost of the geothermal scenario developed in the following section is as follows for a 1980 initiative:

Figure 3. Total cost of geothermal heat in relation to the distance of transmission and other parameters as well as a cost comparison with petroleum (198).



<u>Type of Utilization</u>	<u>Possible Location</u>	<u>Exploration &amp; Facility Cost</u> <u>(\$ x 10<sup>6</sup>)</u>
<b>Electrical Power Plants</b>		
10MW <sub>e</sub>	Williams AFB	18- 22
15MW <sub>e</sub>	Luke AFB or Saylor Creek	25- 30
25MW <sub>e</sub>	Saylor Creek or Luke AFB	40- 45
	Subtotal	<u>83- 97</u>
<b>Cooling Plants</b>		
	Williams AFB	7- 9
	Luke AFB	9- 11
	Charleston AFB	11- 13
	Subtotal	<u>27- 33</u>
<b>Heating Plants</b>		
	Mountain Home AFB	2- 4
	Hill AFB	3- 5
	Ellsworth AFB	4- 6
	Kirtland AFB	5- 7
	Offutt AFB or Langley AFB	5- 7
	Subtotal	<u>19- 29</u>
	Total	<u>129-159</u>

Costs are approximate and may vary by as much as +50 percent to -20 percent. There are just too many unknowns at this time for a more exact cost estimate. The length of time to payback the cost will vary with each project but will average between eight and fifteen years. A more exact cost analysis will be completed after Phase II is finished (Table 7).

TABLE 7

GEOTHERMAL PLANT DEVELOPMENT MODEL TIMELINE  
(modified from 191,199,200,201)

TIME IN YEARS	0 to 0.5	0.5 to 1	1.0 to 2.5	2 to 4	3 to 5
PHASE I: Feasibility and Need Studies			Determination of type & amount of fuels presently used Determination of energy replacement by geothermal sources Preliminary geological investigation Technology availability		
Decision Point			Decision to Perform Geothermal Exploration		
PHASE II: Identify Prospect					
a. Recognition of Probable Resource Areas			Secondary Geological Investigation Geochemical and Initial Geophysical Investigation		
b. Identification of Sites			Secondary Geophysical Investigation Airborne infrared Shallow wells and/or slimhole drilling		
Decision Point			Evaluation of data to choose specific sites		
PHASE III: Evaluation of Specific Site/s as to Resource Quality and Potential				Obtain permits if any are necessary Process pertinent environmental studies Deep drilling Evaluate resource	
Decision Point				Evaluation of data to determine type of use	
PHASE IV: Development of Resource					
a. Site selection				Obtain necessary permits Process pertinent environmental studies Perform site selection study	
b. Design and Development				Developmental drilling Preliminary plant designs	

Equipment Fabrication  
Detailed Plant Designs

Decide on appropriate plant

Clear and grade location  
Foundation poured  
Install plant equipment  
Install transmission and/or  
transportation equipment

Check and make necessary equipment  
adjustments

Start up

Decision Point

PHASE V:

Construction

Decision Point

PHASE VI

Production

GENERAL SCENARIO FOR GEOTHERMAL UTILIZATION  
BY THE U.S. AIR FORCE

Three steps must be completed before a general scenario of geothermal exploration, development, construction, and utilization can be proposed. First, identify the principal prospects based on an estimated potential, exploration, and development activities. Second, both resource quality (temperature, permeability, and water) and resource potential need to be established. The quality of the resource data ranges from quite good where extensive drilling has occurred to quite speculative where little data exists. Third, the year that a power plant can be on-line is determined and based on current needs and/or an assessment of current development status, technology availability, and the considerations of marketability, such as resource quality and magnitude, estimated costs, transmission line availability and demonstrated industrial interest, and environmental sensitivity.

Table 7 can be used as a scenario guide for the development of an individual site, a combination of several sites, or for an analysis of all possible sites. As of September 1979, all Air Force installations within the fifty states of the United States have been evaluated through Phase I. Twenty-two bases are classified as primary (greater than 60 percent chance of geothermal utilization) or secondary (60 to 30 percent chance of geothermal utilization); eleven primary and eleven secondary. Depending on available funding the eleven primary sites will have Phase II completed by August 1980. Thirteen Air Force installations have been eliminated at this time due to a possible lack of resource (less than 30 percent chance of geothermal utilization), favorable economic situation and/or technology.

One base, Hill AFB, is presently in Phase III with exploration wells being drilled. The third decision point will need to be decided in the near future, once the reservoir quality and quantity is determined from the data received due to the completion of the exploratory drilling.

Another base, Williams AFB, is either at the end of Phase II or waiting for a decision point at the end of Phase III. The reason for this uncertainty in determining its position on the geothermal scenario phase chart is the unusual condition of this geothermal field. Two exploration wells were drilled by private industry in 1973. High temperatures are a fact (200°C); in the short distance, approximately two miles, from the two wells to the planned site for the Williams AFB well the temperature will not change appreciably. Because of the high known temperatures, exploration drilling to quantify the resource is not necessary so most of Phase III is not needed. It is this unusual situation that is causing a problem in starting Phase IV. Presently, the Department of Energy (DOE) will not drill a production well; however, the USAF still considers the drilling as exploratory due to the unknown permeability of the production zone. This problem may be solved in the near future because DOE is giving a high degree of assurance that if the reservoir has permeability problems they will fund a well-stimulation effect, whether hydro-logic, chemical, explosive, or a combination of the three, to initiate production from the geothermal field (202).

If further funding becomes available Phase II, a and b will be completed for the twenty-two Air Force bases previously discussed and listed in Table 2 by September 1981. With a normal exploration success rate, three electrical plants of 10 to 25MW<sub>e</sub> capacity, three cooling plants producing 4,000 to 7,000 tons of cooling, and five heating plants of 15 to 50 MW<sub>t</sub> capacity could be on-line at Air Force installations by the beginning of 1985. The controlling limitation will be the funding availability for the geothermal program. The resource is there, the technology is available for most uses, the economics are favorable, the money for exploration, development, and construction must be found.

## RECOMMENDATIONS

The geothermal community recognizes only one member of the Department of Defense (DOD) as being seriously interested in geothermal energy, the United States Navy. This is due to the work completed during the investigation of the Coso Springs geothermal area of California. The development of this area has been much slower than originally planned because of several factors concerning resource quality and quantity as well as managerial problems.

It is an appropriate time for the United States Air Force to take the lead in geothermal research and development within DOD. The large variety of and the potential for geothermal resources available for USAF utilization is the greatest for any of the United States military agencies. The following recommendations will assist the USAF in the goal of investigating, developing and utilizing geothermal resources.

1. Develop funding for geothermal research and development. This can be accomplished by (a) continuing to use the Engineering Assistance Program of DOE as has been accomplished for initial investigations of Hill and Williams AFB's; (b) contacting state agencies for assistance such as has been done with the State of Arizona; (3) use academicians through the Air Force Office of Scientific Research (AFOSR) to research topics of use to the Air Force and the development of geothermal energy; (d) front-end load funds into the geothermal resource program so money is available for the infrastructure building phase of geothermal development. This will assist private contractors in the early stages of development and help them gain the necessary expertise for future Air Force needs; (e) protect geothermal money in the Air Force budgeting process. Whenever a decision to cut either hardware or energy money occurs, energy loses. Normally this is the proper decision but one fact must be considered seriously . . . without energy the hardware will not be useable and as energy shortages become more common, the likelihood of national security problems

being created and mission capability crippled becomes more possible.

2. Make the geothermal community aware of the Air Force's interest in geothermal resource utilization. This can be accomplished by (a) joining the Interagency Geothermal Coordinating Council (IGCC) of the Federal government. Not only will this make the other members of the IGCC (National Science Foundation, Dept. of Agriculture, Environmental Protection Agency, Dept. of the Treasury, Dept. of the Interior, and the Dept. of Energy) aware of USAF's interest but the likelihood of increased geothermal knowledge and expertise being made available to the Air Force increases; (b) further visibility can occur by joining the Geothermal Resources Council composed of members from the academic world, private industry, government and research organizations; (c) the Air Force should also increase the manpower committed to geothermal energy. Full-time personnel is necessary if an on-going, serious geothermal program is to develop. The personnel involved would plan, implement, and coordinate the program and stay in contact and keep an active dialogue with individuals and groups involved in geothermal energy outside the Air Force, especially in private industry and with the Department of Energy. Such personnel could be assigned to AFESC/DEB at Tyndall AFB, Florida.

3. Make the United States public aware of the Air Force's interest in geothermal energy. In recruitment advertising show the need for energy awareness and the possibility of learning about energy and the career possibilities in energy fields.

4. Use the information presented in this report to develop a specific timetable for a geothermal energy program. The author of this report is applying for further funding to complete Phase II of the development plan illustrated in Table 6. After Phase II is completed the development of geothermal installations should occur on a regular basis.

5. New legislation dealing with geothermal energy in the Congress should be followed carefully and comments made to the appropriate members to enhance the Air Force's geothermal program.

6. Air Force/DOD should plan for eventual tie-in to existing power grids in order to wheel power from an Air Force/DOD geothermal-electric plant to other installations. The assumption is made that one or more DOD installations will eventually be producing geothermal-electric power excess to local base facility energy needs. To provide the most economical use of the excess capacity, arrangements could be made for feeding power into existing power grids for wheeling to other DOD installations.

7. Development and construction of the geothermal resources at Williams AFB should occur as soon as possible. The definite capability for cooling and the strong possibility of electrical production should be utilized as quickly as budgetary problems can be overcome. Each month that passes by makes the project more expensive and is a waste of money.

## REFERENCES CITED

1. Hubbert, M.K., 1962, Energy resources: National Academy of Sciences, National Research Council, Publication 1000-D, 141p.
2. Odum, H.T., 1971, Environment, Power, and Society: Wiley Interscience, New York,
3. Ehrlich, P. and Ehrlich, A., 1972, Population, resources, environment: 2nd ed., W.H. Freeman and Co., San Francisco.
4. Wylie, P.J., 1971, The dynamic earth: textbook in geosciences; John Wiley and Sons, N.Y., 416p.
5. Armstead, H.C.H., 1978, Geothermal Energy: E. & F.N Spon Ltd., London, 357p.

6. Tolbert, W.A., 1978, Technology assessment-geothermal: USAF, Air Force Systems Command, Civil and Environmental Engineering Development Office, Civil and Engineering Development Office, Tyndall AFB, Florida.
7. Austin, C.F. and Wheland, J.A., 1978, Geothermal Potential at US Air Force Bases, USAF Civil and Environmental Engineering Development Office Report-78-47, Tyndall AFB, Florida.
8. Malde, H.E., 1959, Fault zone along northern boundary of western Snake River plain, Idaho: Science, v.130, p.272.
9. Bonini, W.E. and Lavin, P.M., 1957, Gravity anomalies in Southern Idaho and southwestern Montana: Geol. Soc. America Bull., v.68, p.1702.
10. Brott, C.A., Blackwell, D.B., and Mitchell, J.C., 1977, Regional heat flow and the geothermal character of the Snake River plain, Idaho: Geothermal Resources Council, Transactions, v.1, p.31-32.
11. Warner, M.M., 1972, Geothermal resources of Idaho: in Geothermal Overviews of the Western United States, Anderseo, D.N. and Aztell, L.H., eds., Geothermal Resources Council, Sp.
12. Ross, S.H., 1971, Geothermal potential of Idaho: Idaho Bureau of Mines of Geology, Pamphlet No. 150, Moscow, Idaho, 72p.
13. Warner, M.M., 1975, Special aspects of Cenozoic history of southern Idaho and their geothermal implications: 2nd U.N. Symposium, Development and Use of Geothermal Resources, San Francisco, v.I, p.653-663.
14. Rightmire, C.T., Young, H.W., and Whitehead, R.L., 1976, Isotopic and geochemical analyses of water from the Bruneau-Grand View and Weisis Areas, Southwest Idaho, in Geothermal Investigations in Idaho, Idaho Dept. of Water Resources, Water Inf. Bull., No. 30, part 4, 28p.
15. Malde, H.E., Powers, H.A., and Marshall, C.H., 1963, Reconnaissance geologic map of west-central Snake River Plain, Idaho: U.S. Geol. Survey Misc. Geol. Inv. Map 1-373, 1 sheet.
16. Ralston, D.R. and Chapman, S.L., 1968, Ground water resource of the Mountain Home area, Elmore County, Idaho, Idaho Dept. of Reclamation, Water Inf. Bull. no.4, Boise, Idaho, 63p.

17. Young, H.W. and Mitchell, J.C., 1973, Geochemical and geologic setting of selected thermal waters: in Geothermal Investigations in Idaho, Idaho Dept. of Water Administration, Water Inf. Bull. No.30, part 1, Boise, Idaho, p.12-33.
18. Waring, G.A., 1965, Thermal springs of the United States and other countries of the world - a summary: U.S. Geological Survey, Prof. Paper 492, U.S. Gov't Printing Office, 383p.
19. Hill, D.P., Baldwin, L.H., Jr., and Pakiser, L.C., 1961, Gravity, volcanism, and crustal deformation in the Snake River plain, Idaho: Geological Survey Research 1961, p.B-248 to B-250.
20. Mabey, D.R., Peterson, D.L., and Wilson, C.W., 1974, Preliminary gravity map of southern Idaho: U.S. Geological Survey, 1-500,000.
21. Costain, J.K., 1979, Unpublished material.
22. Costain, J.K., 1979, Geothermal resources of the Atlantic Coast plain: in Energy Technology VI, Hill, R.F., ed., Proc. of the Sixth Energy Technology Conf., Washington, DC, p.878-880.
23. Jordan, R.R., 1962, Stratigraphy of the sedimentary rocks of Delaware: Delaware Geological Survey Bull. No.9, 51p.
24. Marine, I.W. and Rasmussen, W.D., 1955, Preliminary report on the geology and ground-water resources of Delaware: Delaware Geol. Survey Bull. No.4, 336 p.
25. Schlee, J.C. and others, 1976, Regional geologic framework of northeastern United States: Am. Assoc. Pet. Geol. Bull., v.60, no.6, p.926-951.
26. Whelan, J.A., 1978, Geothermal potential of Dover AFB, Delaware: report for CEEDO, Tyndall AFB, Florida, 7p.
27. Rasmussen, W.C., Groot, J.J., and Depman, A.J., 1958, High-capacity test well developed at the Air Force Base: Delaware Geological Survey, Rept. of Investigations No.2, 36p.
28. Woodruff, K.D., 1977, Preliminary results of seismic and magnetic surveys off Delaware's coast: Delaware Geological Survey, Open file rept. no.10, 19p.

29. Jordan, R.R., Woodruff, K.D., and Pickett, T.E., 1974, Earthquake history and geology of northern Delaware: in Papers Presented by Staff Members of the Delaware Geological Survey at the Baltimore Mtg. of the North-eastern Section of G.S.A., Delaware Geological Survey, Open file report, no.4, p.1-8.
30. Jordan, R.R., Pickett, T.E., Woodruff, K.D., et al., 1974, Delaware-New Jersey-Pennsylvania earthquake of February 28, 1973: Delaware Geological Survey, Open file report, no.4, p-9-13.
31. Combs, J. and Simmons, G., 1973, Terrestrial heat flow determinations in the north central United States: Jr. of Geophysical REsearch, v.78, no.2, p.441-461.
32. Schoon, R.A. and McGregor, D.J., 1974, Geothermal potentiails in South Dakota: Geothermal Energy, Sept., p.19-29.
33. Norton, J.J., 1975, Geology: in Mineral and Water Resources of South Dakota, McGregor, D.J., ed., U.S. Geological Survey, no.16, p.13-55.
34. McGregor, D.J., 1972, Geologic map of the Black Hills: South Dakota Geological Survey, Educational Series, Map 5.
35. Darton, N.H., 1909, Geology and water resources of the northern portion of the Black Hills and adjoining areas: U.S. Geological Survey, Prof. Paper no. 65, U.S. Gov't Printing Office, Washington, DC, 105p.
36. Gries, J.P., 1978, Geothermal applications of the Madison (Papasapa) aquifer system in South Dakota: Proc. of the Distirct Utilization of Geothermal Energy - A Symposium, p. 61-65.
37. Lum, 1961, Gravity measurements east of the Black Hills and along a line from Rapid City to Souix Falls, South Dakota: State Geological Survey, Rept. of Investigations, no.88, 26p.
38. Tullis, E.L., 1964, Gravity survey in southwestern South Dakota: State Geological Survey, Rept. of Investigations, no.94, 10p.
39. Petsch, B.C. and Carlson, L.A., 1950, Magnetic observations in South Dakota: State Geological Survey, Rept. of Investigations, no.66, 35p.

40. Hyde, J. and Whelan, J.A., 1978, Geothermal potential of Ellsworth Air Force Base, South Dakota: rept. for CEEDO, Tyndall AFB, Florida, 6p.
41. Norton, J.J., Kleinkopf, M.D., Redden, J.A., and Allcott, G.H., 1975, Geophysics and geochemistry: in Mineral and Water Resources of South Dakota, McGregor, D.J., ed., U.S. Geological Survey, no.16, p.57-70.
42. Groh, E.A., 1966, Geothermal energy potential in Oregon: The Ore Bin, v.28, no.7, p.125-135.
43. Wells, F.G. and Peck, D.L., 1961, Geologic map of Oregon west of the 121st meridian: U.S. Geol. Survey Misc., Geol. Invest. I-325.
44. Peterson, N.W. and McIntyre, J.R., 1970, The reconnaissance geology and mineral resources of eastern Klamath county and western Lake county, Oregon: Dept. of Geology and Mineral Industries, Bull. no.66, 70p.
45. Peck, D.L., and others, 1964, Geology of the central and northern parts of the western Cascade Range in Oregon: U.S. Geol. Survey, Prof. Paper 449, 56p.
46. Bowen, R.G. and Peterson, N.V., 1970, Thermal springs and wells, Oregon: Oregon Dept. Geology and Mineral Industries Misc. Paper 14.
47. Christiansen, R.L. and Lipman, P.W., 1972, Cenozoic volcanism and plate-tectonic evolution of the western United States - II, late Cenozoic: Royal Soc. London Philos. Trans., A271, p.249-284.
48. Lund, J.W., Culver, G.G., and Svanevik, L.S., 1975, Utilization of intermediate-temperature geothermal water in Klamath Falls, Oregon: 2nd U.N. Symposium, Development and Use of Geothermal Resources, San Francisco, v.2, p.2147-2154.
49. Stark, M., Goldstein, N., Wollenberg, H., Strisower, B., Hege, H., and Wilt, M., 1979, Geothermal exploration assessment and interpretation, Klamath basin, Oregon-Swan Lake and Klamath Hills area: Lawrence Berkeley Labs., Cont. No. W-7405-ENG-48, 75p.
50. Peterson, N.V. and Groh, E.A., 1967, Geothermal Potential of the Klamath Falls area, Oregon - A preliminary study: The Ore Bin, v.29, no.11, p.209-231.

51. Karr, D.J., 1977, Geothermal energy and water resources: Oregon State Univ., Water Resources Res. Inst., Cowallis, Oregon, 121p.
52. Sammel, D.A., 1976, Hydrologic reconnaissance of the Geothermal area near Klamath Falls, Oregon: U.S. Geol. Survey Open File Report, WRI 76-127, 129p.
53. Walker, G.W., 1963, Reconnaissance geologic map of the eastern half of the Klamath Falls (AMS) quadrangle, Lake and Klamath Counties, Oregon: U.S. Geol. Survey Map MF-260.
54. Merewether, E.A., 1953, Geology of the lower Sprague River area, Klamath county, Oregon: Univ. of Oregon master's thesis, unpub., 62p.
55. Fuller, R.E. and Waters, A.C., 1929, The nature and origin of the horst and graben structure of southern Oregon: Jr. Geology, v.37, no.3, p.204-238.
56. Johnson, D.W., 1918, Block faulting in the Klamath Lakes region, Oregon: Jr. Geology, v.26, p.229-236.
57. Newcomb, R.C. and Hart, D.H., 1958, Preliminary report on the groundwater resources of the Klamath River basin, Oregon: U.S. Geol. Survey Open-file report.
58. Matlick, J.S., III and Buseck, P.R., 1975, Exploration for geothermal areas using mercury: a new geochemical technique: 2nd U.N. Symposium, Development and Use of Geothermal Resources, San Francisco, v.1, p.785-792.
59. Bowen, R.G., 1968, Geochemical sampling data, Klamath and Lake Counties, Oregon: Oregon Rept. Geology and Mineral Industries Open-file report, unpub.
60. Mariner, R.H., Rapp, J.B., Willey, L.M., and Presser, T.S., 1974, The chemical composition and estimated minimum thermal reservoir temperatures of selected hot springs in Oregon: U.S. Geol. Survey Open-file Report, 27p.
61. Bodvarsson, G., Couch, R.W., MacFarlane, W.T., Tank, R.W., and Whitsett, R.M., 1974, Telluric current exploration for geothermal anomalies in Oregon: The Ore Bin, v.36, no.6, p.93-107.
62. Thiruvathukal, J.V., Berg, J.W., Jr., and Heinrichs, D.F., 1970, Regional gravity of Oregon: Geol. Soc. America Bull., v.81, p.725-738.

63. Blank, R.H., Jr., 1966, General features of the Bouguer gravity field in southwestern Oregon: U.S. Geol. Survey Prof. Paper 550-C, p.C113.
64. Donath, F.A. and Kuo, J.T., 1962, Seismic-refraction study of block faulting, south-central Oregon: Geol. Soc. America Bull., v.73, no.4, p.429-434.
65. Berg, J.W., Jr. and Thiruvathukal, J.W., 1967, Complete Bouguer gravity anomaly map of Oregon: Oregon Dept. Geology and Mineral Industries Map GMS 4-b.
66. van Deusen, J.E., 1978, Mapping geothermal anomalies in the Klamath Falls, Oregon region using gravity and aeromagnetic data: masters thesis, Univ. of Oregon, Eugene.
67. Sass, J.H. and Sammel, E.A., 1976, Heat-flow data and their relation to observed geothermal phenomena near Klamath Falls, Oregon: Jr. Geophys. Research, v.81, no.26, p.4863-4868.
68. Hull, D.A., Blackwell, D.D., Boyen, R.G., Peterson, N.V., and Black, G.L., 1977, Geothermal gradient data: Oregon Dept. Geol. and Mineral Indust., Open-file report, 0-77-2, 135p.
69. Bowen, R.G., 1975, Geothermal gradient data: Oregon Dept. of Geology and Mineral Indust., Open-file report, 0-75-3, 133p.
70. Senterfit, R.M. and Bedinger, G.M., 1976, Audio-magneto-telluric data log and station location map for Klamath Falls Known geothermal resource area, Oregon: U.S. Geol. Survey Open-file report, 76-320, p.1-6.
71. Bowen, R.G., Blackwell, H.D., and Hull, D.A., 1975, Geothermal studies and exploration in Oregon: Oregon Dept. of Geol. and Mineral Indust., Open-file report, 0-75-7, 65p.
72. McKee, E.D., 1951, Sedimentary basins of Arizona and adjoining areas: Geol. Soc. America, Bull. v.62, p.481-506.
73. Reeside, J.B., 1944, Thickness and general character of the Cretaceous deposits in the western interior of the United States: U.S. Geol. Survey, Oil and Gas Invest., Prelim. Map 10.
74. Cooley, M.E., 1967, The geologic history of Arizona on Arizona Highway Geologic Map: Arizona Geol. Soc., Tucson.

75. Darton, N.H., 1925, A resume of Arizona geology: Arizona Bur. Mines Bull. 119, 298p.
76. Wilson, E.D., 1962, a resume of the geology of Arizona: Arizona Bur. Mines Bull. 171, 140p.
77. Titley, S.R., ed., 1968, Southern Arizona guidebook III: Arizona Geol. Soc., Tuscon, 354p.
78. Drewes, H., 1971, Geologic map of the Mount Wrighton quadrangle, southeast of Tucson, Santa Cruz and Pima Counties, Arizona: U.S. Geol. Survey Misc. Invest. Map I-614.
79. Drewes, H., 1971, Geologic map of the Sahuarita quadrangle, southeast of Tucson, Pima County, Arizona: U.S. Geol. Survey Misc. Invest. Map I-613.
80. Cooper, J.R., 1973, Geologic map of the Twin Buttes quadrangle, southwest of Tuscon, Pima County, Arizona: U.S. Geol. Survey Misc. Invest. Map I-745.
81. Swanberg, C.A., Morgan, P., Stoyer, C.H., and Witcher, J.C., 1977, An appraisal study of the geothermal resources of Arizona and adjacent areas in New Mexico and Utah and their value for desalination and other uses: New Mexcio Energy Institute, New Mexico State Univ., 88p.
82. Drewes, H., 1970, Structural control of geochemical anomalies in the Greaterville mining district, southeast of Tucson, Arizona: U.S. Geol. Survey Bul. no. 1312-A, p.A1-A49.
83. Peterson, D.L., 1968, Bouger gravity map of parts of Maricopa, Pima, Pinal, and Yuma Counties, Arizona: U.S. Geol. Survey Geophysical Invest. Map GP-615.
84. Am. Assoc. of Petroleum Geologists, 1975, Geothermal gradient map of Arizona and western New Mexico: port-folio map area no.18, Geothermal Survey of North America.
85. Gerlach, T., Norton, D., DeCook, K.J., and Summer, J.S., 1975, Geothermal water resources in Arizona: Feasibility Study: Project Completion Rept., U.S. Dept. Int., Office Water Resources Research Project A-054-Ariz., Washington, DC, 36p.
86. Blackwell, D.D. and Chapman, D.S., 1977, Interpretation of geothermal gradient and heat flow data for Basin and Range geothermal systems: Geothermal Resources Council, Transactions, v.1, p.19-20.

87. Sauck, W.A., and Sumner, J.S., 1970, Residual aeromagnetic map of Arizona: Dept. Geosciences, Univ. of Arizona, Tucson, Arizona.
88. Warren, R.E., Sclather, J.G., Vacquier, V., and Roy, R.F., 1969, A comparison of terrestrial heat flow and transient geomagnetic fluctuations in the southwestern United States: Geophysics, v.34, no.3, p.463-478.
89. West, R.W., and Sumner, J.S., 1973, Bouguer gravity anomaly map of Arizona: Lab. Geophys., Dept. Geosciences, Univ. of Arizona, Tucson, Arizona.
90. Stearns, H.T., 1946, Geology of the Hawaiian Islands: Hawaii Division of Hydrography, Bull. no.8, 106p; reprinted with supplement, 1967, 112p.
91. MacDonald, G.A. and Abbott, A.T., 1971, Volcanoes in the sea: The geology of Hawaii: Univ. of Hawaii Press, Honolulu, Hawaii, 441p.
92. Wentworth, C.K., 1951, Geology and ground-water resources of the Honolulu-Pearl Harbor area, Oahu, Hawaii: Board of Water Supply, Honolulu, Hawaii, 111p.
93. Winchell, H., 1947, Honolulu Series, Oahu, Hawaii: Geol. Soc. America Bull., v.58, p.1-48.
94. Wentworth, C.K. and Winchell, H., 1947, Loolau basalt series, Oahu, Hawaii: Geol. Soc. America Bull., v.58, p.49-78.
95. Stearns, H.T., 1939, Geologic map and guide of the island of Oahu, Hawaii: Hawaii Div. of Hydrography, Bull. no.2, 75p.
96. Stearns, H.T., 1940, Supplement to the geology and ground-water resources of the island of Oahu, Hawaii: Hawaii Division of Hydrography, Bull.5, p.3-55.
97. Mink, J.F., 1964, Groundwater temperatures in a tropical island environment: Jr. of Geophysical Research, v.69, p.5225-5230.
98. Stearns, H.T. and Chamberlain, T.K., 1967, Deep cores of Oahu, Hawaii and their bearings on the geologic history of the central Pacific basin: Pacific Science, v.21, p.153-165.
99. Visher, F.N. and Mink, J.F., 1964, Ground-water resources in southern Oahu, Hawaii: U.S. Geol. Survey, Water Supply Paper 1778, 133p.

100. Yoder, H.S., Jr. and Tilley, C.E., 1962, Origin of basalt magmas: An experimental study of natural and synthetic rock systems: *Jr. of Petology*, v.3, p.342-352.
101. MacDonald, G.A., 1968, Composition and origin of Hawaiian lavas: *Geol. Soc. America, Memoir* 116, p.477-522.
102. MacDonald, G.A. and Katsura, T., 1964, Chemical composition of Hawaiian lavas: *Jr. of Petology*, v.5, p.82-133.
103. Powers, H.A., 1955, Composition and origin of basaltic magma of the Hawaiian Islands: *Geochimica et Cosmochimica Acta*, v.7, p.77-107.
104. Strange, W.E., Machevsky, L.F., and Wollard, G.P., 1965, A gravity survey of the island of Oahu, Hawaii: *Pacific Science*, v.19, p.350-353.
105. Malahoff, A. and Woollard, G.P., 1966, Magnetic surveys over the Hawaiian Islands and their geologic implications: *Pacific Science*, v.20, p.265-311.
106. Malahoff, A. and Wollard, G.P., 1968, Magnetic and tectonic trends over the Hawaiian Ridge: In *Crust and Upper Mantle of the Pacific Area*, Knopoff, L., Drake, C.L., and Hart, P.J., eds., *Geophys. Mono.* 12, Am. Geophys. Union, Washington DC, p.241-276.
107. Jackson, e.D., 1968, The character of the lower crust and upper mantle beneath the Hawaiian Islands: *XXIII Internat. Geological Congress Rept.*, v.1, p.135-150.
108. Bryan, W.A., 1915, Evidence of deep subsidence of the Waianae Mountains, Oahu: in *Thrum's Hawaiian Annual for 1916*, Honolulu, p.95-125.
109. MacDonald, G.A., 1940, Petrography of the Waianae Range, Oahu: *Hawaii Div. of Hydrography, Bull.* no.5, p.63-91.
110. Palmer, H.S., 1946, The geology of the Honolulu ground water supply: *Board of Water Supply, Honolulu, Hawaii*, 55p.
111. Wentworth, C.K. and Jones, A.E., 1940, Intrusive rocks of the leeward slope of the Koolau Range, Oahu, *Jr. of Geology*, v.48, p.975-1006.

112. Palmer, H.S., 1967, Origin and diffusion of the Hergberg principle with especial reference to Hawaii: Pacific Science, v.11, p.181-189.
113. Adams, W.M. and Furumoto, A.S., 1965, A seismic refraction study of the Koolau volcanic plug: Pacific Science, v.19, p.296-305.
114. Helsley, C.E., 1977, Geothermal potential for Hawaii in light to HGP-A: Geothermal Resources Council, Transactions, v.1, p.137-138.
115. Dane, C.H. and Bachman, G.O., 1965, Geologic map of New Mexico: New Mexico Bur. Mines and Mineral Resources, Socorro, N.M.
116. Renault, J., 1970, Major-element variations in the Potrillo, Carrizozo, and McCartys basalt fields, New Mexico: State Bureau of Mines and Mineral Resources, Socorro, N.M., Cir. 113, 22p.
117. Hunt, C.B., 1977, Surficial geology of southeast New Mexico: New Mexico Bureau of Mines and Mineral Resources, Geologic map 41.
118. Kelley, V.C. and Thompson, T.B., 1914, Tectonics and general geology of th Ruidoso-Carrizozo region, central New Mexico: in Guidebook of the Ruidoso country, N. Mex. Geol. Soc., Guidebook, 15th Field Conf., p.110-121.
119. Pray, L.C., 1954, Outline of the stratigraphy and structure of the Sacramento Mountain escarpment: in Guidebook of Southeastern New Mexico, N. Mex. Geol. Soc., Guidebook, 5th Field Conf., p.92-107.
120. Sandeen, W.M., 1954, Geology of the Tularosa Basin, New Mexico: in Guidebook of Southeastern New Mexico, N. Mex., Geol. Soc., Guidebook, 5th Field Conf., p.81-88.
121. Jerome, S.E., Campbell, D.D., Wright, J.S., and Vitz, H.E., 1965, Geology and ore deposits of the Sacramento (High Rolls) Mining District, Otero County, New Mexico: State Bureau of Mines and Mineral Resources, Bull. 36, 30p.
122. Pray, L.C., 1961, Geology of the Sacramento Mountains escarpment, Otero County, New Mexico: State Bureau of Mines and Mineral Resources, Bull.35, 144p.

123. Otte, C., Jr., 1959, Late Pennsylvanian and Early Permian Stratigraphy of the northern Sacramento Mountains, Otero County, New Mexico: State Bureau of Mines and Mineral Resources, Bull.50, 11p.
124. Hood, J.W. and Kister, L.R., 1962, Saline-water resources of New Mexico: U.S. Geol. Survey, Water-Supply Paper 1601, 70p.
125. Summers, W.K., 1976, Catalogue of thermal waters in New Mexico: New Mexico Bur. Mines and Mineral Resources, Hydrologic Rept.4, 80p.
126. Summers, W.K., 1965, Chemical characteristics of New Mexico's thermal water - a critique: New Mexico Bur. Mines and Mineral Resources, circ.83, 27p.
127. Reiter, M., Edwards, C.L., and Weidman, C., 1973, Heat-flow studies of New Mexico and neighboring areas of the southwest United States: Geol. Soc. America, Abstracts with Programs, v.5, no.7, p779.
128. Reiter, M., Hartman, C.L., and Weidman, C., 1975, Terrestrial heat flow along the Rio Grande Rift, New Mexico and southern Colorado: GEol. Soc. Am. Bull., v.86, p.811-818.
129. Sanford, A.R., and Cash, D.J., 1969, An instrumental study of New Mexico earthquakes: New Mexico Bur. Mines and Mineral Resources, Circ. 102, 7p.
130. Sanford, A.R., Budding, A.J., Hoffman, J.P., Alptekin, O.S., Rush, C.A., and Topozada, T.R., 1972, Seismicity of the Rio Grande Rift in New Mexico: New Mexico Bur. Mines and Mineral Resources, Cir. 120, 19p.
131. Edwards, C.L., Reiter, M., and Weidman, C., 1973, Geothermal studies in New Mexico and southern Colorado: Am. Geophys. Union Trans., v.54, no.4, p.463.
132. Topozada, T.R., 1973, Crustal structure in central New Mexico: Am. Geophys. Union Trans., v.54, no.11, p.1141.
133. Reiter, M., Edwards, C.L., Hartman, H., and Weidman, C., 1975, Terrestrial heat flow along the Rio Grande Rift: Geol. Soc. America Bull., v.86, no.7, p.811-818.
134. Hunt, C.B., 1978, Surficial geology of northwest New Mexico: New Mexico Bur. Mines and Mineral Resources, Geologic map 43.

135. Kelley, V.C., 1963, Geologic map of the Sandia Mountains and vicinity, New Mexico: New Mexico Bur. of Mines and Mineral Resources, Geologic map 18.
136. Anonymous, 1961, Structural problems of the Rio Grande trough in Albuquerque country: in Guidebook of Albuquerque Country, N. Mex. Geol. Soc., Guidebook, 12th Field Conf., p.144-147.
137. Titus, F.B., Jr., 1961, Ground-water geology of the Rio Grande trough in north-central New Mexico, with sections on the Jemez caldera and the Lucero uplift: in Guidebook of Albuquerque Country, N. Mex. Geol. Soc., Guidebook, 12th Field Conf., p.186-192.
138. Kelley, V.C. and Northrop, S.A., 1975, Geology of Sandia Mountains and vicinity, New Mexico: New Mexico Bur. Mines and Mineral Resources, Memoir 29, 135p.
139. Kelley, V.C., 1977, Geology of Albuquerque Basin, New Mexico: New Mexico Bur. Mines and Mineral Resources, Memoir 33, 59p.
140. Caprio, E.R., 1960, Water resources of the western slopes of the Sandia Mountains, Bernalillo and Sandoval Counties, New Mexico: Master's thesis, Univ. of New Mexico, 176p.
141. Campbell, J.A., 1967, Geology and structure of a portion of the Rio Puerco fault belt, western Bernalillo County, New Mexico: Master's thesis, Univ. New Mexico, 89p.
142. Chapin, C.E., 1971, The Rio Grande rift, Pt.I: modifications and additions: New Mexico Geol. Soc., Guidebook, 22nd Field Conf., p.191-202.
143. Cordell, L.E. and Kottowski, F.E., 1975, Geology of the Rio Grande graben: Geology, v.3, p.420-424.
144. Kelley, V.C. and Kudo, A.M., 1978, Volcanoes and related basaltic rocks of the Albuquerque-Belen Basin, New Mexico: New Mexico Bur. Mines and Mineral Resources, Circ. 156.
145. Lambert, P.W., 1968, Quaternary stratigraphy of the Albuquerque area, New Mexico: Doctor's dissertation, Univ. New Mexico, 329p.
146. Cordell, L.E., Joesting, H.R., and Case, J.E., 1973, Gravity map of Albuquerque-Grants area: U.S. Geol. Survey, Open-file map.

147. Budding, J.A., Sanford, A.R., and Topozada, T.M.R., 1971, Seismicity and tectonics of the Rio Grande rift zone in central New Mexico: Geol. Soc. America, Abstracts with Programs, v.3, no.7, p.515-516.
148. Hewett, D.F., 1954, General geology of the Mojave Desert region, California: in Geology of southern California: California Div. Mines Bull. 170, p.5-20.
149. Campbell, I., 1969, Geologic map of California, Los Angeles: Division of Mines and Geology, San Francisco, 1:250,000.
150. Hill, M.L. and Dibblee, T.W., Jr., 1953, San Andreas, Garlock, and Big Pine faults, California: Geol. Soc. America Bull., v.64, p.443-468.
151. Simpson, E.C., 1934, Geology and mineral deposits of the Elizabeth Lake quadrangle, California: California Jr. Mines and Geology, v.30, p.371-415.
152. Bailey, T.L., and Jahns, R.H., 1954, Geology of the Transverse Range province, southern California: in Geology of southern California: California Div. Mines Bull. 170, Chap.II, contr.6, p.83-106.
153. Crowell, J.C., 1954, Strike-slip displacement of the San Gabriel fault, southern California: in Geology of Southern California: California Div. Mines Bull.170, Chap.IV, contr.6, p.49-52.
154. Austin, C.F., 1978, Memo about geothermal potential of Edwards Air Force Base: CEEDO, Tyndall Air Force Base, Florida.
155. Campbell, I., 1969, Geologic Map of California, San Bernardino: Division of Mines and Geology, San Francisco, 1:250,000.
156. Bowen, E.E., Jr., 1954, Geology and mineral deposits of Barstow quadrangel, San Bernardino County, California: California Div. of Mines, Bull. no.115, 185p.
157. Troxel, B.W. and Gunderson, J.N., 1970, Geology of the Shadow Mountains and northern part of the Shadow Mountains southeast quadrangles, western San Bernardino County, California: Div. of Mines and Geology, Preliminary Rept. 12.
158. Bowen, O.E., Jr. and ver Planck, W.E., 1965, Stratigraphy, structure, and mineral deposits in the Oro Grande series near Victorville, California: Calif. Div. of Mines and Geology, Spec. Rept. 84, 41p.

159. Miller, W.J., 1944, Geology of parts of the Barstow quadrangle, San Bernardino, County, California: Calif. Jr. Mines and Geol., v.40, no.1, p.72-112.
160. Dibblee, T.W., Jr., 1960, Preliminary geologic map of the Victorville quadrangle, California: U.S. Geol. Survey Map Sheet MF-229.
161. Olmsted, F.H. and Davis, G.H., 1961, Geologic features and ground-water storage capacity of the Sacramento Valley, California: U.S. Geol. Survey Water-Supply Paper 1497, 241p.
162. Lachenbruch, M.C., 1962, Geology of the west side of the Sacramento Valley, California: California Div. Mines and Geology Bull.181, p.53-66.
163. Hackel, O., 1960, Summary of the geology of the Great Valley: in Geology of Northern California, California Div. Mines and Geology Bull.190, p.217-238.
164. Campbell, I., 1966, Geologic map of California, Sacramento sheet: California Div. Mines and Geology, San Francisco, 1:250,000.
165. Bryan, K., 1923, Geology and ground-water resources of Sacramento Valley, California: U.S. Geol. Survey Water-Supply Paper 495, 285p.
166. Chapman, r.H., 1966, The California Division of Mines and Geology gravity base station network: California Div. of Mines and Geology, Spec. Rept. 90, 49p.
167. Griscom, A., 1966, Magnetic data and regional structure in northern California: in Geology of northern California, Bailey, E.H., ed., California Div. Mines and Geology Bull. 190, p.407-417.
168. Meuschke, J.L., Pitking, J.A., and Smith, C.W., 1966, Aeromagnetic map of Sacramento and vicinity, California: U.S. Geol. Survey Gephysical Invest. Map GP-574.
169. Larsen, E.S., 1951, Crystalline rocks of the Corons, Elsinore, and San Luis Rey quadrangles, southern California: California Div. Mines and Geology Bull. 159, p.7-50.
170. Richter, C.F. and Gutenberg, B., , Seismicity of southern California: in Geology of southern California: Div. Mines Bull. 170, p.19-25.

171. Anonymous, 1959, Geologic map of California, Santa Maria sheet: California Div. Mines, San Francisco, 1:250,000.
172. Jones, P.H., 1975, Geothermal and hydrocarbon regimes, northern Gulf of Mexico basin: Geopressured-geothermal energy conference, 1st, Austin, Texas, June 2-4, 1975, Center for Energy Studies, Univ. Texas at Austin, Proc., p.15-89.
173. Jones P.H. and Wallace, R.H., Jr., 1974, Hydrogeologic aspects of structural deformation in the northern Gulf of Mexico basin, Jr. of Research, U.S. Geol. Survey, Sept-Oct, 1974, p.511-517.
174. Jones, P.H., 1975, Geothermal and hydrodynamic regimes in the northern Gulf of Mexico basin: 2nd U.N. Symposium, Development and Use of Geothermal Resources, San Francisco, v.I, p.429-440.
175. Aiken, C., 1977, Residual bouguer gravity anomaly analysis of Arizona and hot dry rock exploration: in Exploration Methods for Hot Dry Rock, West, F.G. and Shankland, T.J., eds., p.28-31.
176. Cooley, M.E., 1973, Map showing distribution and estimated thickness of alluvial deposits in the Phoenix area, Arizona: U.S. Geological Survey, Miscellaneous Investigations, Map I-845-C.
177. Eberly, L.D. and Stanley, T.B., 1978, Cenozoic stratigraphy and geologic history of southwestern Arizona: Geol. Soc. Am. Bull., v.89, p.921-940.
178. Osterkamp, W.R., 1973, Map showing depth to water wells in Phoenix area, Arizona: U.S. Geological Survey, Misc. Investigations, Map I-845-D.
179. Scarborough, R.B. and Peirce, H.W., 1978, late Cenozoic basins of Arizona: New Mexico Geol. Soc. Guidebook, Land of Cochise, p.253-259.
180. Hahman, W.R., 1979, Hot-water irrigation wells near Luke AFB, Arizona: to be published in Geothermal Magazine.
181. Amstrat, Inc., 1976, Logs of wells GKI No.1 and 2; Logs No. D-4113 and D-4335.
182. Peterson, D.L., 1968, Bouguer gravity amp of parts of Maricopa, Pima, Pinal, and Yuma counties, Arizona: U.S. Geological Survey, Map GP-615.

183. Sheridan, M.F., 1978, The Superstition cauldron complex: Guidebook to the Geology of Central Arizona, Special Paper No. 2, Bureau of Geology and Mineral Technology, Tucson, Arizona, P.85-96.
184. Stucless, J.S. and Sheridan, 1971, Tertiary volcanic stratigraphy in the Goldfield and Superstition Mountains, Arizona: Geol. Soc. Am. Bull., v.82, no.11, p.3235-3240.
185. Gertsch, W.D., Keller, J.G., Hahman, W.R., Sr., and Ruschmann, D., 1979, The potential for using geothermal energy for space cooling at Williams Air Force Base, Arizona: U.S. Dept. Energy, Idaho Operations Office, 67p.
186. Goff, F.W., 1979, "Wet" Geothermal potential of the Kingman-Williams region, Arizona: Los Alamos Scientific Laboratory, LA-7757-MS, UC-66a, 26p.
187. Aiken, C.L.V., 1976, Analysis of the gravity anomalies of Arizona: Ph.D. dissertation, Univ. Arizona, Tucson, Arizona.
188. Hahman, W.R., Stone, C., and Witcher, J.C., 1978, Preliminary map geothermal energy resources of Arizona: Geothermal Map No. 1, Bureau of Geology and Mineral Technology, Univ. Arizona, Tucson, Arizona.
189. Sapre, A.A. and Schoepfel, R.J., 1975, Technological and Economic assessment of electric power generation from geothermal hot water: 2nd U.N. Symposium, Development and Use of Geothermal Resources, San Francisco, v.3, p.2343-2350.
190. Hankin, J.W., Beaulaurier, L.O., and Comprelli, F.O., 1975, Conceptual design and cost estimate for a 10-MW (Net) generating unit and experimental facility using geothermal brine resources: 2nd U.N. Symposium, Development and Utilization of Geothermal Resources, San Francisco, v.2, p.1985-1996.
191. Frederickson, D.D., 1977, Analysis of requirements for accelerating the development of geothermal energy resources in California: Jet Propulsion Laboratories and the California Institute of Technology, JPL-PUB-77-63.
192. Ramachandru, G.R., 1977, Economic analysis of geothermal energy development in California: The Stanford Research Institute, Stanford University.

193. Trehan, R.K., Leigh, J.G., Williams, F., and Pond, S., 1976, Analysis of geothermal energy development scenarios: Mitre Tech. Rept. MTR-7220, Contract No. E(49-18)-2268, 133p.
194. Wilson, J.S., Shepherd, B.P., and Kaufman, S., 1975, An analysis of the potential use of geopressed geothermal energy for power generation: 2nd U.N. Symposium, Development and Use of Geothermal Resources, San Francisco, v.2, p.1865-1869.
195. Swanberg, C.A., 1975, Physical aspects of pollution related to geothermal energy development: 2nd U.N. Symposium, Development and Use of Geothermal Resources, San Francisco, v.2., p.1435-1443.
196. Bloomster, C.H., Fassbender, L.L., and McDonald, C.L., 1977, Geothermal energy potential for district and process heating applications in the U.S. - An economic analysis: Battelle Pacific Northwest Laboratories, Dept. of Energy.
197. Delisle, G., Kappelmeyer, O., and Haenel, R., 1975, Prospects for geothermal energy for space heating in low-enthalpy areas: 2nd U.N. Symposium, Development and Use of Geothermal Resources, San Francisco, v.3, p.2283-2289.
198. Einarsson, S.S., 1975, Geothermal space heating and cooling: 2nd U.N. Symposium, Development and Use of Geothermal Resources, San Francisco, v.2, p.2117-2126.
199. Jet Propulsion Laboratories, 1976, Geothermal energy resources in California: Status Report, Jet Propulsion Laboratories and the California Institute of Technology, JPL Doc. 5040-25.
200. Hankin, J.W., Beaulaurier, L.O., and Comprelli, F.O., 1975, Conceptual design and cost estimate for a 10-MW<sup>e</sup> (Net) generating unit and experimental facility using geothermal brine resources: 2nd U.N. Symposium, Development and Utilization of Geothermal Resources, San Francisco, v.2, p.1985-1996.
201. Hersam, D.E., Dan, F.J., Kho, S.K., and Krumland, L.R., 1975, Development of a typical generating unit at The Geysers geothermal project - A case study: 2nd U.N. Symposium, Development and Utilization of Geothermal Resources, San Francisco, v.2, p.1949-1958.
202. Overton, H.L. and Hanold, R.J., 1977, Geothermal reservoir categorization and stimulation study: Los Alamos Scientific Laboratory, LA-6889-M5, 62p.

1979 USAF - SCEEE SUMMER FACULTY RESEARCH PROGRAM

Sponsored by the

AIR FORCE OFFICE OF SCIENTIFIC RESEARCH

Conducted by the

SOUTHEASTERN CENTER FOR ELECTRICAL ENGINEERING EDUCATION

FINAL REPORT

A CRITICAL EVALUATION OF THE USAF METHODOLOGY FOR ASSESSING  
THE SOCIOECONOMIC IMPACT OF PROPOSED BASE REALIGNMENTS

Prepared by:	William D. Gunther
Academic Rank:	Professor of Economics
Department and University:	Economics, Finance and Legal Studies Program, The University of Alabama
Research Location:	Air Force Engineering Service Center, Directorate of Environmental Planning (AFESC/DEV), Tyndall AFB, Florida
USAF Research Colleague:	Mr. W. Allan Nixon
Date:	August 21, 1979
Contract No.	F49620-79-C-0038

A CRITICAL EVALUATION OF THE USAF METHODOLOGY FOR ASSESSING  
THE SOCIOECONOMIC IMPACT OF PROPOSED BASE REALIGNMENTS

by

William D. Gunther

ABSTRACT

The Air Force Engineering Services Center is considering the adoption of a computer-based socioeconomic impact model for all their impact statements. This model, developed by SRI International analyzes both "loser" and "gainer" installations and evaluates employment, income, population, and housing attributes. Additional attributes are evaluated in a series of hand calculations, but these are not part of the computer based model.

This paper critically evaluates the "loser" portion of the proposed methodology and makes a series of recommendations. The objective of each recommendation is to provide either documentation for a particular approach taken, or to restructure a section which in the researcher's view, is questionable.

### ACKNOWLEDGMENTS

The author would like to express appreciation to the Air Force Systems Command, Air Force Office of Scientific Research, and Directorate of Environmental Planning, Air Force Engineering Service Center at Tyndall Air Force Base, Florida, for the opportunity to participate in the summer faculty research program. Special acknowledgments are due to Col. Sterling J. Schultz, Director of the Directorate of Environmental Planning, for support of my efforts during the summer, and to Mr. W. Allan Nixon, Economist in the Directorate of Environmental Planning, for many useful and stimulating discussions.

The author also wishes to acknowledge the many hours of useful discussions with his wife, Irene, on the technical aspects of the computer model. Her years of computer experience proved invaluable to an economist who believes in the principle of comparative advantage.

Finally, the author hopes that his efforts will be useful to the USAF in improving their socioeconomic impact forecasts.

## I. INTRODUCTION:

The Engineering Services Center at Tyndall AFB, is considering the adoption of a computer model developed by SRI International for all of its economic impact analysis statements.<sup>1</sup> This model has evolved from earlier work by SRI for the Center and may be considered for adoption by other agencies as well.<sup>2</sup> The need for a critical evaluation of a model which has the potential use being suggested for the SRI model is obvious.

## II. OBJECTIVES OF THE RESEARCH EFFORT:

As originally developed, the QRSAS model yielded output in terms of the size of the realignment that could occur without tripping a determined "threshold" level. For example, while the model calculated projections for income and employment, it only printed the size of the realignment that could occur before population and income threshold were exceeded.

Recognizing the need for more definitive information on proposed realignments, the AF requested that SRI rewrite QRSAS to project proposed socioeconomic impacts. The resultant model, which is somewhat different from the QRSAS model, is referred to as the SRI or "Proposed Air Force Methodology." While the QRSAS model was documented in a report, no such detail was provided for the SRI model. Although the two models are closely related, there are sufficient differences between them to warrant the development of a methodological text to accompany the SRI model.

The proposed Air Force methodology contains two basic models, one for "loser" installations and one for "gainer" installations. In addition, each model contains four sectors, (1) unemployment, (2) income, (3) population, and (4) housing. Although many of the algorithms of the model have been computer programmed, there are a number of hand calculations remaining.

The objective of this research effort was to critically evaluate the computer programmed algorithm of the "loser" model. This model was selected because more realignments involve loser installations than gainer ones. Hand calculations were excluded from analysis for

reasons of time. Certainly both the "gainer" model and all hand calculations need critical review before all can be integrated into a single document supporting the Air Force methodology for assessing socioeconomic impacts.

### III. AN OVERVIEW OF THE SRI MODEL:

As it is currently programmed, the SRI model can be classified as an "economic base" model. This general class of models divide the local economies into two sectors: (1) a sector where firms and individuals serve strictly local markets; and (2) a sector where firms and individuals serve external, or "export" markets. The driving force of local economic growth is assumed to be export activity, with local activities assumed to service the export oriented activities. If employment in the export serving market rises or falls, employment in local serving activities is expected to move in the same direction. Additionally, base models typically assume that the ratio of export to service employment will remain constant. Thus an increase in employment in the export sector will cause an increase in service sector employment by the proportion of export to non-export employment. This ratio of export or basic employment to service or non-basic employment is the economic base multiplier. Once a multiplier is established, a change in export employment can be translated into a change in total employment via the multiplier. An alternative multiplier can be found using income data rather than employment data. The same basic assumptions are made regarding basic and non-basic income.

The SRI model utilizes an income multiplier to determine the total lost income attributed only to base employment in the study area. This lost income is then translated into lost secondary employment in the region of analysis. Once an estimate of total secondary employment losses are obtained, the lost income is estimated by determining the average wage in the relevant sectors of those lost jobs. By summing the direct income losses and the secondary income losses, an estimate of the total income loss can be obtained.

The remaining two sectors of the model (population and housing) are tied to the estimated employment losses. Figure 1 indicates the general flow of calculations in the model.

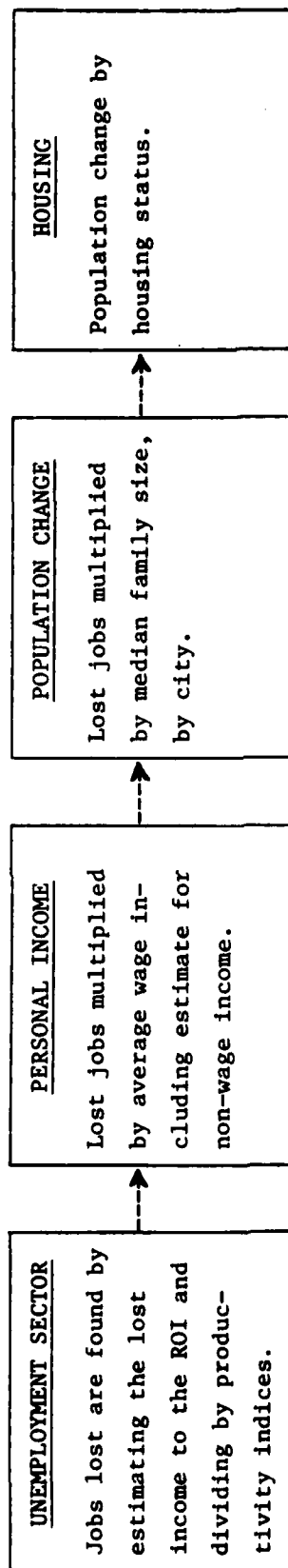


FIGURE 1 - RELATIONSHIP OF MAJOR SECTORS OF SRI MODEL

Unemployment Sector. The estimated change in unemployment associated with a proposed action is found by summing the direct and indirect (secondary) job losses. The estimate of secondary job losses is found by dividing the primary income loss (including the multiplier effect) by an estimated "productivity" index. This index is an estimate of the sales per employee in the relevant sectors. With sales income reduced by the proposed action, there is assumed to be a reduced need for employees in those sectors. In the direct employment change, allowance is made for the fact that many of the job holders will transfer and thus will not affect the unemployment situation in the region.

The model then estimates the size of the labor force at a post-action date, the total unemployed at that date, and the unemployment rate at that date. Once the total unemployed at a post-action date is determined, the model estimates the number of people who would have to leave the region to keep the unemployment rate from exceeding an established bench mark. Figure 2 illustrates the general flow of calculations in this sector.

Personal Income. The estimate of total income losses to a region is found by using estimated average wages and estimated non-wage income in connection with employment changes. Allowances are made for taxes, savings, and income which is spent outside the region of analysis.

An estimate of total personal income that would exist without the proposed action is obtained by extrapolating recent per capita income and multiplying by an estimated population at  $t_2$ .

The model then calculates the estimated percentage change in total personal income in the region of analysis. This change is then compared to a bench mark historic change which allows the reader to assess the relative magnitude of the expected change. Figure 3 illustrates the direction of flow of the major calculations in this sector.

Population. This sector estimates the total population affected by the proposed action by obtaining those likely to leave the region and multiplying by an average family size. An estimate of the population growth rate that would exist during the realignment period is made. Figure 4 illustrates the general flow of calculations.

Housing. Once an estimate of the expected population change is made, estimates of the proportions of these families who own their own

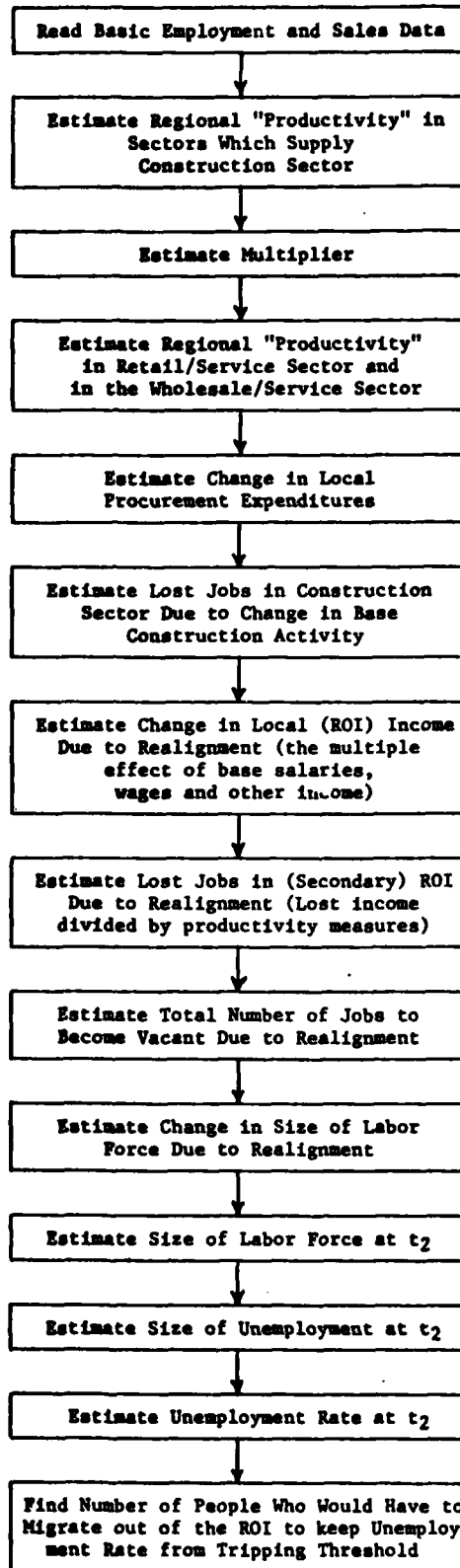


FIGURE 2 - FLOW OF CALCULATIONS IN UNEMPLOYMENT SECTOR

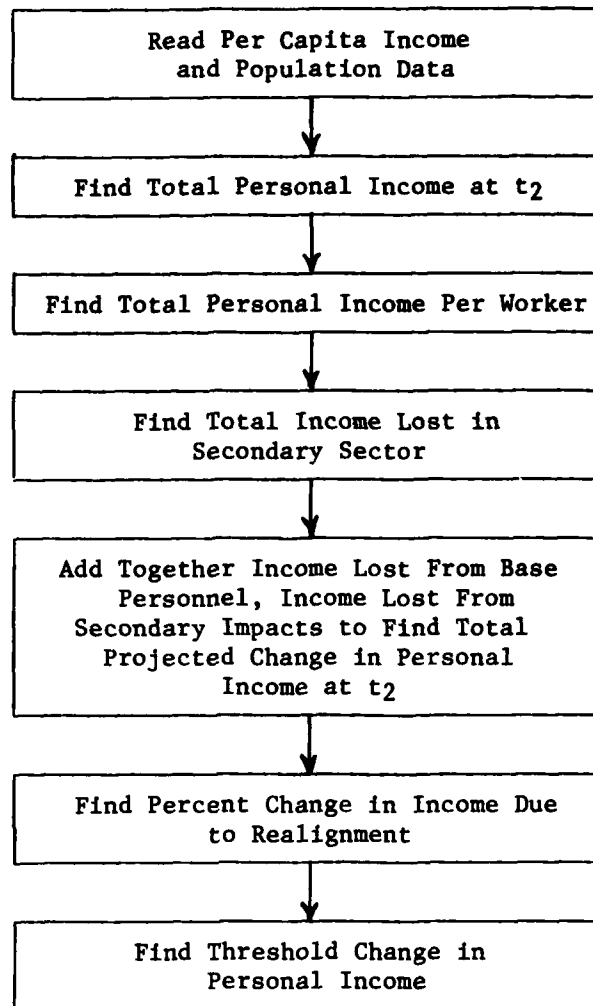


FIGURE 3 - FLOW OF CALCULATION IN PERSONAL INCOME SECTOR

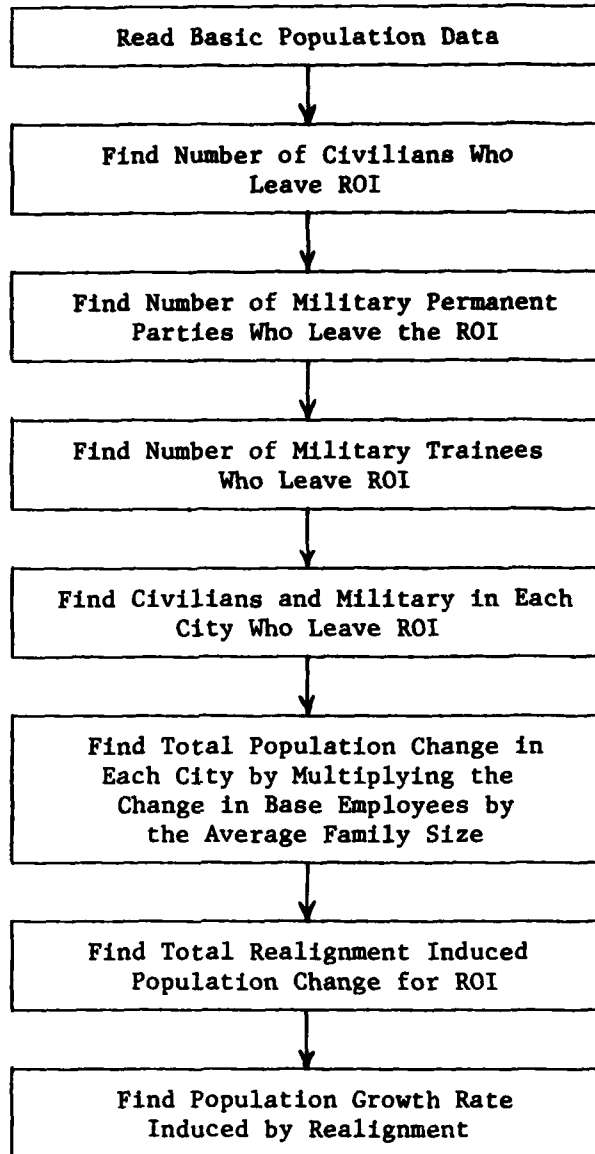


FIGURE 4 - FLOW OF CALCULATIONS IN POPULATION CALCULATIONS

homes and those who rent is made. These estimates are compared against the estimated housing stocks at  $t_2$  to obtain a projection of the change in vacancy rates that would likely accompany the proposed action. Finally, the projected total vacancy rate that would exist following the action is compared against a bench mark rate based upon historic HUD statistics and what is considered "healthy" vacancy rates. Figure 5 illustrates the general flow of calculations.

Order of Operation of the Proposed Model. To operate the proposed methodology, a number of tasks must be performed prior to implementing the computer analysis.

Step 1. Identify the Geographic Area(s):

The initial step prior to data collection is to identify the geographic impact area. Depending upon the variables analyzed, and the available data, the geographic areas are:

- (a) The "region of influence," on ROI. This area is normally equivalent to the SMSA or the county in which the base is located. It may, however, be a smaller area, such as the labor market area.
- (b) The study area or maximum commute area (MCA). This area is defined as the area in which approximately 90% of the affected base personnel reside.
- (c) Cities. In housing and population calculations, impacts are estimated for each of the cities in which a substantial number of affected base personnel reside. City 1 always includes the base and the last city is usually defined as the balance of residents in the ROI not identified by specific city.

Step 2. Define Multipliers to be Inputed:

The model currently calculates a multiplier based upon the estimated population size of the region of influence. This multiplier is based upon the "minimum requirements approach" and follows closely the procedures established by Ulman and Dacey. In addition, the model allows for externally inputing a multiplier.\*

---

\*It is current policy to input a multiplier derived from an alternative source.

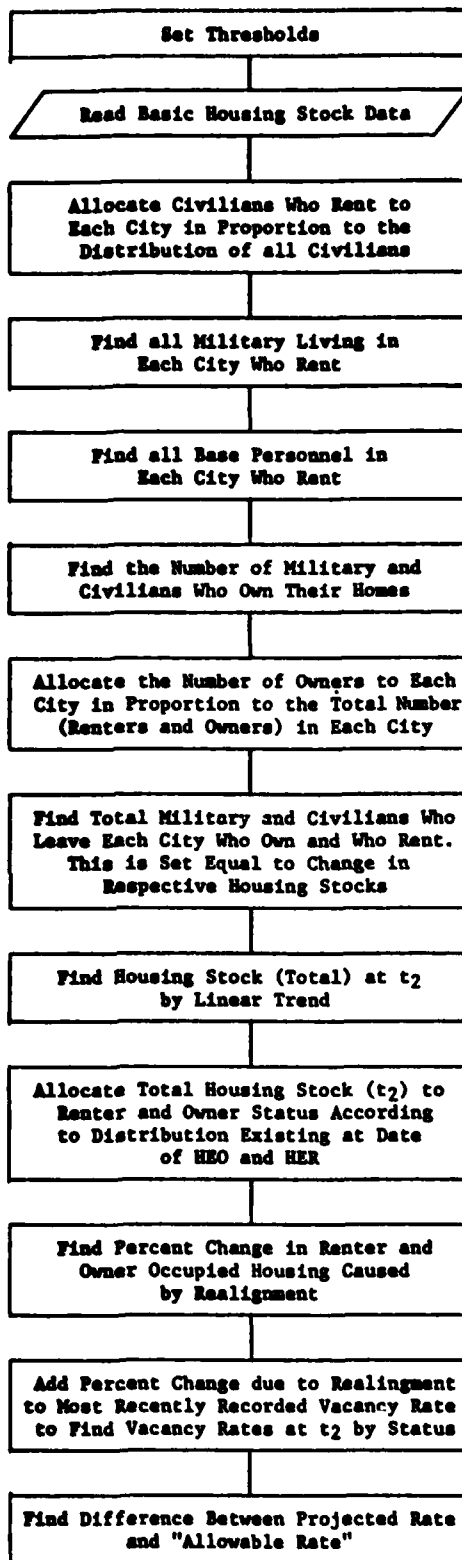


FIGURE 5 - FLOW OF CALCULATIONS IN HOUSING SECTOR

Step 3. Collect Input Data Identified on the Sample Data Input Sheet (Appendix A):

The sample data input sheet identifies all the data which must be collected by the user.

Step 4. Run the Model and Obtain Intermediate and Final Outputs:

Some of the output of the model is considered final and can be used directly. Other outputs are used as intermediate values and are used in hand-calculation.

Step 5. Verify All Data Inputs and Sources:

The user should verify all data inputs on the data sheet as to their correctness. The data should then be verified as to the correctness of the inputted value.

This section has provided a very brief overview of the model and its major sectors. The next section will dwell at greater length with each equation in the program. Prior to beginning the evaluations, a list of all variables and their definitions was developed. This list is contained in Appendix B.

#### IV. ALGORITHMS:

This section of the report list all the major equations used in the proposed Air Force methodology and comments, where appropriate, on the implicit methodology. Criticisms, where applicable, are included in the comments following each equation. The equations are listed in order of their appearance in the computer program.

##### Unemployment Calculations

(1) Solve for  $PT_4$  where:

$$PT_4 = YT_4/ET_4$$

where

$PT_4$  = Productivity in the national labor force

$YT_4$  = National output in  $t_4$

$ET_4$  = National employment in  $t_4$

Measures the dollar value of output associated with each worker in the U.S. in  $t_4$ .

(2) Solve for  $PT_6$  where:

$$PT_6 = YT_6/ET_6$$

where:

$PT_6$  = Productivity in the national labor force

YT6 = National output in  $t_6$

ET6 = National employment in  $t_6$

Measures the dollar value of output associated with each worker in the U.S. in  $t_6$ .

(3) Solve for NU where:

$$NU = NU + MU(K)$$

where:

NU = Fraction of output from new construction that goes to the purchase of material in other sectors.

MU(K) = Fraction of output from new construction that goes to the purchase of material in each of K sectors.

This equation sums the K values to arrive at a total fraction of output from new construction that goes to the purchase of materials in other sectors.

(4) Solve for GAM where:

$$GAM = GAM + GAMB + GAMN$$

where:

GAM = The fraction of output from new construction that goes to wages and salaries.

GAMB = The fraction of output from new construction that goes to employees compensation.

GAMN = Fraction of output from new construction that goes to property income.

This equation estimates that portion of construction expenditure that flow into the local economy as wages, salaries and property income.

(5) Solve for PGAM where:

$$PGAM = PGAM + PT4 * SJT6(K) * 1.000 * MU(K) / (PT6 * EJT6(K) * NU)$$

where:

PGAM = Regional labor productivity in the sectors that supply the construction sector.

SJT6(K) = National output for  $t_6$  in each of K(5) sectors (Mfg., Transportation, Trade, Finance, and Services).

PT4 = Productivity of the national labor force in  $t_4$

MU(K) = The fraction of output from new construction that goes to the purchase of materials in each of the K sectors (Mfg., Transportation, Trade, Finance, and Services).

PT6 = Productivity of the national labor force in  $t_4$

EJT6(K) = National employment for  $t_6$  in each of K  
sector (Mfg., Transportation, Trade, Finance,  
and Services)

NU = Fraction of output from new construction that goes  
to the purchase of materials in other sectors

This equation calculates a weighted average productivity  
index for the five sectors that supply the construction  
sector.

(6) Solve for YKST4 where:

$$YKST4 = SKST5 * PDCT4 / PDCT5$$

where:

YKST4 = Total state output for the construction sector  
in  $t_4$

SKST5 = State construction sector receipts for the most  
recently recorded year ( $t_5$ )

PDCT4 = Price deflator, construction sector,  $t_4$

PDCT5 = Price deflator, construction sector,  $t_5$

This equation inflates the sales estimate for year  $t_5$  to  
the year  $t_4$ . Thus it simply allows for the same real out-  
put in  $t_4$  as existed in  $t_5$ .

(7) Solve for PKS where:

$$PKS = YKST4 / EKST5$$

where:

PKS = Regional labor productivity in the construction  
sector

EKST5 = Total state employment in the construction  
sector at  $t_5$

YKST4 = Total state output for the construction sector  
in  $t_4$

This equation calculates the average sales per employee in  
the construction sector for  $t$ . It assumes the same real  
productivity per worker in year  $t_5$ , which needs verifica-  
tion if constant real productivity is to be assumed.

(8) Solve for P2 where:

$$P2 = (((RPBZ - RPAZ) * (T2 - TRPAZ)) / (TRPBZ - TRPAZ)) + RPAZ$$

where:

P2 = Population of the ROI at  $t_2$  excluding the effects  
of the action

RPAZ = The population of the ROI at  $t_{1-y}$  or  $t_0$   
RPBZ = The population of the ROI at  $t_{2+x}$  or  $t_{1-y}$   
T2 = The date of completion of the action.  
TRPAZ = The date of RPAZ data  
TRPBZ = The date of RPBZ data

This equation solves for the expected population at the date of completion of the action as if the action did not occur. The equation interpolates linearly between two points, one preceding the action and one extending beyond the date of completion of the action.

(9) Solve for UD where:

$$UD = .1 * \text{ALOG10}(P2) - .1$$

where:

UD = Ulman-Dacey Factor (fraction of income spent locally)

ALOG10 = Common logarithm

The UD (Ulman-Dacey) factor is based upon a study which related the fraction of income spent locally to the population size of cities. This equation simply summarizes that study and allows the model to calculate the UD factor for any size (P2) area.

(10) Solve for M where:

$$M = 1 / (1 - UD) - 1$$

where:

M = Net income multiplier

Input alternative multiplier if desired. Currently, AF procedure is to input the EIFS income multiplier. This is a questionable procedure for several reasons. First, it mixes the methodological support of two models, which may involve internal conflicts. Secondly, it creates potential conflicts of output, such as the employment impacts. If the AF selects the income multiplier from EIFS, which is derived from employment data, why not utilize the employment multiplier as well? Why utilize the proposed AF methodology at all then? What about conflicts in wage data used in determination of the income multiplier and wage data used in the proposed AF methodology? It is not

advisable to utilize EIFS without carefully examining these questions.

(11) Solve for YWST4 where:

$$YWST4 = SWST3 * PDWT4 / PDWT3$$

where:

YWST4 = Total regional output or sales for the wholesale sector in  $t_4$

SWST3 = Total regional output or sales for the most recently recorded year

PDWT4 = Price deflator index for the wholesale trade sector for  $t_4$

PDWT3 = Price deflator index for the wholesale trade sector for  $t_3$

Wholesale sector data at  $t_3$  is inflated to obtain an estimate of wholesale sales at  $t_4$ .

(12) Solve for YRST4 where:

$$YRST4 = SRST3 * PDRT4 / PDRT3$$

where:

YRST4 = Total regional output or sales for the retail sector at  $t_4$

SRST3 = Total regional output or sales for the retail sector at  $t_3$

PDRT4 = Price deflator index for the retail sector for  $t_4$

PDRT3 = Price deflator index for the retail sector for  $t_3$

Retail sales data at  $t_3$  is inflated to obtain an estimate of retail sales at  $t_4$ .

(13) Solve for YSST4 where:

$$YSST4 = SSST3 * PDST4 / PDST3$$

where

YSST4 = Total regional output or sales for the service sector in  $t_4$

SSST3 = Total regional output or sales for the service sector in  $t_3$

PDST4 = Price deflator for the service sector  $t_4$

PDST3 = Price deflator for the service sector  $t_3$

Service sector sales data at  $t_3$  is inflated to obtain an estimate of service sector sales at  $t_4$ .

(14) Solve for PWS where:

$$PWS = (YWST4 + YSST4) / (EWST3 + ESST3)$$

where:

PWS = Productivity in the wholesale trade and service sectors in the ROI

EWST3 = Total regional employment in the wholesale sector at  $t_3$

ESST3 = Total regional employment in the service sector at  $t_3$

Measures the dollar value of sales associated with each employee.

(15) Solve for PRS where:

$$PRS = (YRST4 + YSST4) / (ERST3 + ESST3)$$

where:

PRS = The productivity in the retail trade sector in the ROI

ERST3 = Total regional employment in the retail sector in  $t_3$

Measures the dollar value of sales per employee in the retail trade sector.

(16) Solve for LI where:

$$IF(LI.EQ.0.0) GO TO 21$$

where:

LI = The total number of persons employed by and assigned to the base

This equation is designed to skip the next equation if direct data exists for YPG.

(17) Solve for YPG where:

$$YPG = (YPI - YQ) * RL / LI$$

where:

YPG = The change in USAF procurement expenditures in the ROI due to the realignment

YPI = Total amount of procurement expenditure in ROI

YQ = Total amount of procurement expenditures in ROI commissary and BX goods purchased by retirees

RL = Total size of the realignment

This equation estimates the procurement expenditures lost to the ROI by assuming a per person procurement expenditure.

Retirees are taken out of the calculation since it is assumed they will remain in the ROI and thus someone else will be purchasing the goods to satisfy this demand in the ROI. If direct data exists for YPG, it can be inputted directly and the estimation procedure skipped.

(18) Solve for ALC where:

$$ALC = ALT + ALRC + ALSP + ALP$$

where:

ALC = Fraction of positions terminated or relocated held by civilians

ALT = Fraction of positions terminated or relocated held by civilians who will transfer with the realignment

ALRC = Fraction of positions terminated or relocated held by civilians who retire

ALSP = Fraction of positions terminated or relocated held by civilians who separate from the USAF

ALP = Fraction of positions terminated or relocated held by civilians who will be placed elsewhere

This equation summarizes the fraction of all the civilians who are expected to be affected by the proposed action.

(19) Solve for ALMS where:

$$ALMS = ALMP + ALRM$$

where:

ALMS = Fraction of positions terminated or relocated held by military permanent parties

ALMP = Fraction of positions terminated or relocated held by military permanent parties who transfer

ALRM = Fraction of positions terminated or relocated held by military permanent parties who retire

This equation summarizes the fraction of all military who are expected to be affected by the action.

(20) Solve for EK where:

$$EK = YKG / (PKS + M * \text{TAU} * \text{SIGMA} * \text{GAM} * YKG / \text{PRS} + \text{NU} * YKG / \text{PGAM})$$

where:

EK = The change in the number employed due to the change in base construction expenditures caused by the USAF action. Includes construction and secondary jobs lost

- M = Net regional income multiplier
- PKS = Regional labor productivity in the construction sector
- TAU = Fraction of wages remaining after taxes
- SIGMA = Fraction of after-tax wages remaining after savings
- GAM = The fraction of output from new construction that goes to wages and income
- YKG = Change in construction expenditures because of the action
- PRS = The productivity of workers in the retail trade and service sectors in the ROI
- NU = Fraction of output from new construction that goes to the purchase of materials in other sectors
- PGAM = Regional labor productivity in the sectors that supply the construction sector

This equation estimates the lost jobs associated with the construction sector by summing three components: (1) the lost direct construction jobs, (2) the lost retail-service jobs due to lost income to construction workers, and (3) lost jobs in those sectors that supply the construction industry.

(21) Solve for  $K_1$  where:

$$K_1 = Y(K)/YL(K)+K_1$$

where:

$K_1$  = The sum of the ratio of total personal income to wage and salary income for ROI for past KY years

Y = Total personal income for ROI for each of KY years

YL = Total wage and salary income for ROI for each of KY years

This equation finds the sum over the past KY years, of the ratio of total personal income to wage and salary income.

(22) Solve for  $K_1$  where:

$$K_1 = K_1/KY$$

where:

$K_1$  = The sum of the ratio of total personal income to wage and salary income for ROI for past KY years

KY = Number of observations (years) of data on Y and YL

This equation finds the average ratio of total personal income to wage and salary income for the ROI over the past KY years.

(23) Solve for K2 where:

$$IF (K2.LE.0.0)K2=(K1-1.0)/2.0$$

where:

K2 = Ratio of non-wage and salary income to wage and salary income for ROI

K1 = Ratio of total personal income to wage and salary income for ROI

This statement reads the inputted value of K2 and if it is 0 (no data exists), assumes K2 equal to one half the ratio implied in K1. No evidence exists for such an approach.

(24) Solve for WMP where:

$$WMP = RL*ALMS*WWMP*(K2+1)$$

where:

WMP = Total personal income of military permanent parties affected by the action

RL = Total size of the realignment

ALMS = Fraction of positions terminated or relocated held by military permanent parties

WWMP = The average wage of military permanent parties affected by the action

K2 = Ratio of non-wage and salary income to wage and salary income

This equation estimates the total personal income of military permanent parties who will be affected by the action. The assumption is made that each person affected by the action had additional income (beyond military income) equal to K2 percent of wage and salary income.

(25) Solve for WMT where:

$$WMT = RL*ALMT*WWMT$$

where:

WMT = Total personal income of military trainees affected by the action

RL = Total size of the realignment

ALMT = Fraction of positions terminated or relocated held by military trainees who transfer

WWMT = Average wage of military trainees affected by the action

This equation estimates the total personal income of military trainees affected by the action. The assumption is made that military trainees have no other source of personal income except their military wage. It seems reasonable to assume that there should be a difference between military trainees and others in terms of supplemental income. However, it is not clear if the assumption that they have no supplemental income is the most realistic assumption.

(26) Solve for WC where:

$$WC = RL*ALC*WWC*K1$$

where:

WC = Total personal income of civilians affected by the action

RL = Total size of the realignment

ALC = Fraction of positions terminated or relocated held by civilians

WWC = Average wage of civilians personal affected by the action

K1 = Ratio of total personal income to wage and salary income

This equation estimates the total personal income of civilians affected by the action. The assumption is made that each civilian affected by the action has additional non-wage income equal to (K1-1) percent of wage and salary income. There is no apparent reason why (K1-1) for civilians should be different from K2 for military permanent parties.

(27) Solve for YMP where:

$$YMP = WMP*OMMP*TAU*SIGMA$$

where:

YMP = Disposable total personal income in ROI associated with military permanent parties who are affected by the action

WMP = Total personal income of military permanent parties affected by the action

OMMP = Fraction of disposable total personal income of military permanent parties spent in the ROI, exclusive of on-base expenditures

TAU = Fraction of total personal income remaining after taxes

SIGMA = Fraction of after tax total personal income remaining after savings

This equation estimates the disposable income flowing into the ROI from military permanent parties. The two terms, TAU and SIGMA are assumed to be constant for military permanent parties, military trainees, and civilians. It appears however that they would be different for different classes and income levels, and different for different ROI's.

(28) Solve for YMT where:

$$YMT = WMT * OMMT * TAU * SIGMA$$

where:

YMT = Disposable total personal income in ROI associated with military trainees who are affected by the action

WMT = Total personal income of military trainees affected by the action

OMMT = Fraction of disposable total personal income of military trainees spent in the ROI exclusive of on-base expenditures

TAU = Fraction of total personal income remaining after taxes

SIGMA = Fraction of after tax total personal income remaining after savings

This equation estimates the disposable income flowing into the ROI from military trainees. The same assumptions are made here as in YMP.

(29) Solve for YC where:

$$YC = WC * OMC * TAU * SIGMA$$

where:

YC = Disposable total personal income in ROI associated with civilians affected by the action

WC = Total personal income of civilians affected by the action

OMC = Fraction of disposable total personal income of civilians spent in the ROI

TAU = Fraction of total personal income remaining after taxes

SIGMA = Fraction of after tax total personal income remaining after savings

This equation estimates the disposable income flowing into the ROI from civilians. The same assumptions are made here as in YMP and YMT.

(30) Solve for YIG where:

$$YIG = YC + YMT + YMP$$

where:

YIG = Total disposable income spent in the ROI from all military and civilian parties affected by the action

YC = Disposable total personal income in ROI associated with civilians affected by the action

YMT = Disposable total personal income in ROI associated with military trainees who are affected by the action

YMP = Disposable total personal income in ROI associated with military permanent parties who are affected by the action

This equation estimates the income flowing into the ROI from all base employees affected by the action.

(31) Solve for ES where:

$$ES = M * YIG / PRS + M * YPG / PWS + EK$$

where:

ES = The total number of secondary jobs estimated to be lost as a direct result of the action

M = Net regional income multiplier

YIG = Total disposable income spent in the ROI from all military and civilian parties affected by the action

PRS = The productivity (sales per employee) in the retail trade and personal service sectors in the ROI

YPG = The change in USAF procurement expenditures in the ROI due to the realignment

PWS = The productivity (sales per employee) in the wholesale and service sectors in the ROI

EK = The change in the number of persons employed due to the change in construction expenditures.

This equation estimates the total number of jobs to be lost in the combined retail, wholesale, and construction sectors.

The assumptions that jobs will be lost in direct proportion to the lost income (YPG/PWS for example) probably results in an overestimate of the economic impact of a proposed action. The value of the income multiplier is critical in this equation in estimating jobs lost.

(32) Solve for ET where:

$$ET = ALT*RL$$

where:

ET = The number of civilian personnel who transfer with the realignment

ALT = Fraction of positions terminated or relocated held by civilians who will transfer with the realignment

RL = Total size of realignment

This equation estimates the total number of civilians who will transfer with the realignment. ALT will vary with the ROI and the potential relocation site.

(33) Solve for EMP where:

$$EMP = ALMP*RL$$

where:

EMP = Number of military permanent parties who transfer

ALMP = Fraction of positions terminated or relocated held by military permanent parties who transfer

RL = Total size of the realignment

This equation estimates the total number of military permanent parties that will transfer with the realignment.

(34) Solve for EMT where:

$$EMT = ALMT*RL$$

where:

EMT = Number of military trainees who transfer

ALMT = Fraction of positions terminated or relocated held by military trainees who transfer

RL = Total size of the realignment

This equation estimates the total number of military trainees who transfer with the realignment.

(35) Solve for ERM where:

$$ERM = ALRM*RL$$

where:

ERM = Number of military permanent parties who retire

ALRM = Fraction of positions terminated or relocated held by military permanent parties who retire

RL = Total size of realignment

This equation estimates the total number of military permanent parties who retire.

(36) Solve for EP where:

$$EP = ALP * RL$$

where:

EP = Number of civilians personnel who are placed by DOD in other positions

ALP = Fraction of positions terminated or relocated held by civilians who will be placed elsewhere

RL = Total size of the realignment

This evaluation estimates the number of civilians who will be placed in DOD jobs elsewhere. It would seem reasonable to assume that this number would vary with the ROI.

(37) Solve for ESP where:

$$ESP = ALSP * RL$$

where:

ESP = Number of civilians personnel who separate from the USAF

ALSP = Fraction of positions terminated or relocated held by civilians who will separate from the USAF

RL = Total size of the realignment

This equation estimates the total number of civilians who separate from the USAF.

(38) Solve for ERC where:

$$ERC = ALRC * RL$$

where:

ERC = The number of civilian personnel who retire

ALRC = Fraction of positions terminated or relocated held by civilian personnel who retire

RL = Total size of the realignment

This equation estimates the total number of civilian personnel who retire. This number should vary with the ROI and

the age distribution of each base's civilian employees. As the population becomes older, this number should increase (long run trend).

(39) Solve for ESJ where:

$$ESJ = (ET+PIP*EP)*RHOSJC+EMP*RHOSJM$$

where:

- ESJ = The number of personnel who leave the ROI who hold second jobs
- ET = The number of civilian personnel who transfer
- PIP = The fraction of civilians placed by DOD in positions outside the ROI
- EP = Number of civilians personnel who are placed by DOD in other positions
- RHOSJC = The fraction of USAF civilian personnel in ROI who hold a second job
- EMP = Number of military permanent parties who transfer
- RHOSJM = The fraction of military permanent parties who transfer who held a second job

This equation estimates the total number of secondary jobs held in the ROI by military permanent parties and civilians. It is assumed that no secondary jobs are held by military trainees.

(40) Solve for EWD where:

$$EWD = (ET+PIP*EP)*RHOWDC+EMP*RHOWDM$$

where:

- EWD = Number of dependents of USAF personnel who are employed
- ET = The number of civilian personnel who transfer with the realignment
- PIP = The fraction of civilians placed by DOD in positions outside the ROI
- EP = Number of civilian personnel who are placed by DOD in other positions
- RHOWDC = The fraction of USAF civilian personnel in the ROI who have dependents who are employed
- EMP = Number of military permanent parties who transfer
- RHOWDM = The fraction of military permanent parties who transfer who have dependents who are employed

This equation estimates the number of jobs held by dependents of employees who leave the ROI. It is assumed that military trainees have no dependents who are employed. Since RHOWDC and RHOWDM would normally be less than one, it is also assumed that there could not be more than one dependent per employee who hold jobs. This may need rethinking.

(41) Solve for UAF where:

$$\text{UAF} = (1-\text{PIRC})\text{ERC} + (1-\text{PIRM})\text{ERM} + \text{PIBP}\text{ESP} - \text{ZETSJ}\text{ESJ} - \text{ZETWD}\text{EWD} - \text{ES}$$

where:

- UAF = The change in the number of unemployed as a result of the USAF action
- PIRC = The fraction of civilian retirees who leave the ROI labor force (i.e., retire from work or leave the retion)
- ERC = Number of civilian personnel who retire
- PIRM = The fraction of military retirees who do not enter the ROI labor force
- ERM = Number of military permanent parties who retire
- PISP = The fraction of USAF personnel that separate who do not become employed elsewhere before  $t_2$
- ESP = Number of civilian personnel that separate from the USAF
- ZETSJ = Second job full-time employment equivalency factor
- ESJ = The number of personnel who leave the ROI who hold second jobs
- ZETWD = Working dependent full-time employment equivalency factor
- EWD = Number of dependents of USAF personnel who are employed
- ES = The number of secondary jobs (indirect and induced)

This equation estimates the number of unemployed caused by the action by summing the following:

- (a) The number of civilians who retire from USAF, but remain in labor force in ROI.
- (b) The number of military permanent parties who retire from USAF, but remain in the labor force in the ROI.
- (c) The number of civilians who separate from the USAF, but remain in the labor force in the ROI.

(d) The total number of secondary jobs estimated to be lost as a direct result of the action.

Then subtract the following:

(e) The full-time equivalent number of secondary jobs held by employees who transfer.

(f) The full-time equivalent number of working dependent jobs held by those who will transfer.

This equation assumes that all secondary jobs held by military and civilians and all working dependent jobs will be absorbed by the local labor force. Thus they will not create additional unemployment.

(42) Solve for EAF where:

$$EAF = -ET - PIRC * ERC - PIP * EP - ZETWD * EWD + (1 - PIRM) * ERM$$

where:

EAF = The change in the size of the labor force due to the USAF action

ET = The number of civilian personnel who transfer with the realignment

PIRC = The fraction of civilian retirees who leave the ROI labor force (i.e., retire from work or leave the ROI)

ERC = Number of civilian personnel who retire

PIP = The fraction of civilians placed by DOD in positions outside the ROI

EP = The number of civilian personnel who are placed by DOD in other positions

ZETWD = Working dependent full-time employment equivalency factor

EWD = Number of dependents of USAF personnel who are employed

PIRM = The fraction of military retirees who do not enter the ROI labor force

ERM = Number of military permanent parties who retire

This equation estimates the total number of individuals who leave the labor force in the ROI.

(43) Solve for L2 where:

$$L2 = (LBZ - LAZ) * (T2 - TLAZ) / (TLBZ - TLAZ) + LAZ$$

where:

L2 = The size of the labor force in the ROI at t<sub>2</sub>

LBZ = The size of the labor force at  $t_{2+x}$  or  $t_{1-y}$   
 LAZ = The size of the labor force at  $t_{1-y}$  or  $t_{70}$   
 T2 = Date of completion of the action  
 TLAZ = Date of LAZ data  
 TLBZ = Date of LBZ data

This equation estimates the size of the labor force at T2 by a linear interpolation between two points. The accuracy of this procedure depends upon the assumptions made in the forecast of LBZ, which is normally secondary data.

(44) Solve for G2ROI where:

$$G2ROI = (RPBZ - RPAZ) / (RPAZ * (TRPBZ - TRPAZ))$$

where:

G2ROI = The average annual population growth rate of the ROI before the action  
 RPBZ = The projected population of the region at  $t_{2+x}$  or  $t_{1-t}$   
 RPAZ = The population of the region at  $t_{1-y}$  or  $t_{70}$   
 TRPAZ = Date of RPAZ data  
 TRPBZ = Date of RPBZ data

This equation calculates the average annual percentage change in the population by a linear interpolation of forecasts.

(45) Solve for TLBZ where:

$$IF(TLBZ.LT.T2) GO TO 27$$

where:

TLBZ = Date of LBZ data

This equation selects an alternative methodology for estimating the size of the labor force if projected labor force data does not exist. This alternative (explained in 46-48) is based upon population projections.

(46) Solve for RPLBZ where:

$$RPLBZ = (RPAZ * G2ROI * (TLBZ - TRPAZ)) + RPAZ$$

where:

RPLBZ = The projected total population at some date as labor force (LBZ)  
 RPAZ = The population of the region at  $t_{1-y}$  or  $t_{70}$

G2ROI = The average annual population growth rate of the ROI before the action

TLBZ = Date of LBZ data

TRPAZ = Date of RPAZ data

This equation estimates the size of the population of the ROI at the same date as LBZ data. The equation takes the population at a given date and increases this number at the growth rate, G2ROI.

(47) Solve for PRTLZ where:

$$PRTLZ = LBZ/RPLBZ$$

where:

PRTLZ = The calculated labor force participation rate of the civilian labor force at BZ

LBZ = The size of the labor force at  $t_{1-y}$

RPLBZ = The projected population at date of LBZ

This equation calculates the estimated labor force participation rate at a date prior to the date of completion of the action. This equation assumes the labor force participation is the same (a constant) at  $t_{BZ}$  or  $t_{1-y}$  as it is at  $t_{az}$ .

(48) Solve for LPRT2 where:

$$LPRT2 = PRTLZ + (PRTLZ * 0.007 * (T2 - TLBZ))$$

where:

LPRT2 = Labor force participation rate at  $t_2$

PRTLZ = Labor force participation rate of the civilian labor force at BZ

T2 = Date of completion of the action

TLBZ = Date of LBZ data

This equation estimates the labor force participation rate at  $t_2$  as equal to that which existed (estimated) at BZ plus .7 percent per year growth. The major assumptions are that the labor force participation rate grows at a constant rate (i.e., there are no significant year-to-year fluctuations) and that the rate of growth is best approximated by the constant term, .007.

(49) Solve for L2 where:

$$L2 = LPRT2 * P2$$

where:

L2 = The size of the labor force in the ROI at  $t_2$

LPRT2 = Labor force participation rate at  $t_2$

P2 = Population of region at  $t_2$

This equation estimates the size of the labor force at the date of completion of action, excluding the action based upon population and labor force participation projections.

(50) Solve for U2 where:

$$U2 = L2 * E2$$

where

U2 = The estimated number of unemployed in the ROI at  $t_2$  excluding the effects of the USAF action

E2 = The unemployment rate at  $t_2$  excluding the effects of the USAF action

This equation estimates the likely number of unemployed at  $t_2$  by assuming the unemployment rate at  $t_2$  is equal to the most recently recorded unemployment rate in the ROI. E2 will be either a (1) forecasted rate available from secondary sources, or (2) equal to the most recently recorded rate. If the most recently recorded rate is used, it is important that the date be reasonably close to  $t_2$  and the general economic conditions remain the same.

(51) Solve for E where:

$$E = (U2 + UAF) / (L2 + EAF)$$

where:

E = Unemployment rate at  $t_2$ , including the effects of the USAF action

U2 = The estimated number of unemployed in the ROI at  $t_2$  excluding the effects of the USAF action

UAF = The change in the number of unemployed as a result of the USAF action

L2 = The size of the labor force in the ROI at  $t_2$

EAF = The change in the size of the labor force due to the USAF action

This equation estimates the new unemployment rate that would likely exist after the USAF action.

(52) Unemployment Thresholds

Threshold determinations have not been evaluated at this time.

Personal Income Calculations

- (1) Solve for EPSIH where:

$$\text{EPSIH} = \text{CPIT}_4 / \text{CPITH}$$

where:

EPSIH = Per capita income adjustment factor for  $t_h$

CPIT<sub>4</sub> = Consumer price index for  $t_4$

CPITH = Consumer price index for  $t_h$

This equation develops a ratio of price indices to apply to per capita income.

- (2) Solve for Y2 where:

$$Y_2 = YH * \text{EPSIH} * P_2$$

where:

Y<sub>2</sub> = Total regional personal income at  $t_2$

YH = Regional per capita income for the most recently recorded year,  $t_h$

EPSIH = Wage adjustment factor for  $t_h$

P<sub>2</sub> = Population of the ROI at  $t_2$

This equation estimates total personal income of the ROI by inflating a base year ( $t_h$ ) per capita income estimate and multiplying by an estimate of the total population. This equation assumes a constant real per capita income between  $t_h$  and  $t_2$ . It is also assumed that the consumer price index is an adequate predictor of per capita income movements.

- (3) Solve for YY2 where:

$$YY_2 = YH * \text{EPSIH}$$

where:

YY<sub>2</sub> = The per capita personal income at  $t_2$

YH = Regional per capita income for the most recently recorded year,  $t_h$

EPSIH = Per capita income adjustment factor

This equation estimates a per capita income estimate for the ROI at  $t_2$  by inflating data for  $t_h$  by the adjustment

factor, EPSIH. In fact, the estimate is for  $t_4$ . If one assumes that per capita income is constant in current dollars, then the estimate for  $t_2$  is correct. Otherwise, the equation needs rethinking.

- (4) Solve for EPSIF where:

$$\text{EPSIF} = \text{CPIT4}/\text{CPITF}$$

where:

EPSIF = Wage adjustment factor

CPIT4 = Consumer price index for  $t_4$

CPITF = Consumer price index for  $t_f$

This equation develops a rate of price indices to apply to wage data below.

- (5) Solve for WNU where:

$$\text{WNU} = (\text{YK} + \text{YM} + \text{YN}) * \text{EPSIF} / \text{ENU}$$

where:

WNU = Total personal income per employed worker at  $t_f$

YK = National personal income from other labor income in  $t_f$

YM = National personal income from wages and salaries

YN = National personal income of proprietors

EPSIF = Wage adjustment factor

ENU = Total national employment for  $t_f$

This equation estimates an average total personal income per worker to be used in later calculations. The implicit assumption made is that each worker has income from three sources in the same proportion as the U.S. averages. This assumption is unrealistic and significantly overestimates the lost income to a ROI.

- (6) Solve for EPSIT3 where:

$$\text{EPSIT3} = \text{CPIT4}/\text{CPIT3}$$

where:

EPSIT3 = Wage adjustment factor for  $t_3$

CPIT4 = Consumer price index for  $t_4$

CPIT3 = Consumer price index for  $t_3$

This equation develops a ratio of price indices to apply to wage data.

(7) Solve for WWS where:

$$WWS = (WWST3+WSST3)*EPS1T3/(EWST3+ESST3)$$

where:

WWS = Average gross wage per worker in wholesale and service sector

WWST3 = Total regional wages in the wholesale sector in  $t_3$

WSST3 = Total regional wages in the service sector in  $t_3$

EPS1T3 = Wage adjustment sector

EWST3 = Total regional employment in the wholesale sector in  $t_3$

ESST3 = Total regional employment in the service sector in  $t_3$

This equation estimates the average wage received by employees in the wholesale and service sectors. The wage is for  $t_4$  (but the same real wage as  $t_3$ ), and is assumed the same for  $t_2$ . This is questionable and needs closer examination.

(8) Solve for WRS where:

$$WRS = (WRST3+WSST3)*EPSIT3/ERST3+ESST3$$

where:

WRS = The average wage in the regions retail trade and personal services sector

WRST3 = The total regional wage in the retail sector in  $t_3$

WSST3 = The total regional wage in the service sector in  $t_3$

EPSIT3 = Wage adjustment factor

ERST3 = Total regional employment in the retail trade sector in  $t_3$

ESST3 = Total regional employment in the service sector in  $t_3$

This equation estimates the average wage received by employees in the retail trade and service sector. The equation will assume a constant real wage equal to  $t_3$  and use this as an estimate for  $t_2$ . This is a questionable assumption and needs closer examination.

(9) Solve for YS where:

$$YS = \frac{WRS * M * YIG}{PRS + WWS * M * YPG} / \frac{PWS + GAM * YKG + WRS * M * SIGMA * TAU * GAM * YKG}{PRS + WNU * NU * YKG / PGAM}$$

where:

- YS = The total personal income of people holding secondary jobs (induced and indirect jobs)
- WRS = The average wage in the regions retail trade and personal services sector
- M = Net regional income multiplier
- YIG = The change in total amount spent by military and civilian personnel in the ROI due to the realignment
- PRS = The productivity (sales per employee) in the retail trade and personal service sectors in the ROI
- WWS = Average gross wage per worker in wholesale and services sector at  $t_4$
- YPG = The change in USAF procurement expenditures in the ROI due to the realignment
- PWS = Productivity in the wholesale trade and services sectors in the ROI
- GAM = The fraction of output from new construction that goes to wages and income
- YKG = Change in construction expenditures because of the action
- SIGMA = Fraction of after-tax total personal income remaining after savings
- TAU = Fraction of total personal income remaining after taxes
- WNU = Total personal income per employed worker at  $t_f$
- NU = Fraction of output from new construction that goes to the purchase of materials in other sectors
- PGAM = Regional labor productivity in the sectors that supply the construction sector

This equation estimates the number of jobs to be lost (secondary) by dividing lost incomes by productivity indices. The assumption that jobs would be lost in proportion to the productivity index is perhaps too liberal.

(10) Solve for YW where:

$$YW = WC + WMP + WMT$$

where:

YW = Total personal income of USAF personnel involved in the realignment

WC = Total personal income of civilian personnel affected by the action

WMP = Total personal income of military permanent parties affected by the action

WMT = Total personal income of military trainees affected by the action

An estimate of total income associated with personnel affected by the realignment.

(11) Solve for YSNW where:

$$YSNW = (K1-1.) * YS$$

where:

YSNW = Non-wage income associated with secondary job estimate

K1 = Average of the time series for the ratio of personal income to labor income

YS = The total personal income of people holding secondary jobs (induced and indirect jobs affected by unemployment)

This equation estimates the addition income (non-wage) associated with secondary job holders who are affected by the action. The estimate is far too high because it attributes non-wage income to all workers at an excessive proportion.

(12) Solve for YAF where:

$$YAF = YW + YS + YSNW$$

where:

YAF = The total change in personal income resulting from the action

YW = The total personal income of USAF personnel involved in realignment

YS = The total personal income of people holding secondary jobs affected by the realignment

YSNW = Non-wage income associated with secondary job holders affected by the action

This equation estimates the total lost income to the ROI associated with the proposed realignment. There is an assumption that non-wage income will be lost, as well as wage income, which needs to be verified or altered.

(13) Solve for YDELTA where:

$$YDELTA = YAF/Y2$$

where:

YDELTA = Percentage change in total personal income in the ROI resulting from the realignment

YAF = The total change in personal income resulting from the action

Y2 = Total personal income at  $t_2$

This equation estimates the likely percentage change in total personal income to the ROI as a result of the proposed realignment.

#### Personal Income Thresholds

Thresholds have not been evaluated at this time.

#### Population and Housing for ROI Calculations

(1) Solve for DLMT where:

$$DLMT = LMT * FOMT$$

where:

DLMT = The number of dwelling units occupied (beds) by military trainees living on-base

LMT = The number of military trainees currently assigned to the installation

FOMT = The fraction of military trainees who live on-base

This equation estimates the number of on-base beds occupied by military trainees.

(2) Solve for DLMP where:

$$DLMP = LMP * FOMP$$

where:

DLMP = The number of dwelling units occupied by military permanent parties living on-base

LMP = The number of military permanent parties currently assigned to the base

FOMP = The fraction of military permanent parties living on-base

This equation estimates the number of on-base military permanent parties.

(3) Solve for DKMD where:

$$DKMD = DLMP + DLMT - DKMF$$

where:

DKMD = The number of on-base dormitory units occupied at  $t_1$

DLMP = The number of military permanent parties living on-base

DLMT = The number of military trainees living on-base

DKMF = The number of on-base family housing units occupied at  $t_1$

The number of occupied on-base dormitory beds occupied is found by adding together the number of military trainees and permanent parties living on-base and subtracting the number of on-base family units occupied.

(4) Solve for DKMD where:

$$IF(DKMD.LT.0.0)DKMD=0$$

where:

DKMD = The number of on-base dormitory units occupied at  $t_1$

This equation tests for negative answers and if found sets them equal to zero.

(5) Solve for DMP where:

$$DMP = LMP - DLMP$$

where:

DMP = Number of military permanent parties living off base at  $t_1$

LMP = The number of military permanent parties currently assigned to the base

DLMP = The number of military permanent parties living on-base

This equation finds the number of military permanent parties living off-base as the difference between total military permanent parties and those living on-base.

(6) Solve for DMT where:

$$DMT = LMT - DLMT$$

where:

DMT = The number of military trainees living off-base at  $t_1$

LMT = The number of military trainees currently assigned to the base

DLMT = The number of military trainees living on-base

This equation finds the number of military trainees living off-base as the difference between total military trainees and those living on-base.

(7) Solve for DMT where:

$$\text{IF}(\text{DMT.LT.O.O})\text{DMT}=0$$

where:

DMT = Number of military trainees living off-base at  $t_1$

This equation tests for negative answers and if found sets them equal to zero.

(8) Solve for XIMT where:

$$\text{XIMT} = \text{DMT}/(\text{DMT}+\text{DMP})$$

where:

XIMT = The fraction of military who live off-base who are trainees

DMT = The number of military trainees living off-base at  $t_1$

DMP = The number of military permanent parties living off-base at  $t_1$

This equation calculates the fraction of military who live off-base who are trainees.

(9) Solve for XIMP where:

$$\text{XIMP} = 1.-\text{XIMT}$$

where:

XIMP = The fraction of military who live off-base who are permanent parties

XIMT = The fraction of military who live off-base who are trainees

This equation finds the fraction of military who live off-base who are permanent parties.

(10) Solve for RLC where:

$$\text{RLC} = \text{ET}+\text{LRC}*\text{ERC}+\text{LP}*EP$$

where:

RLC = Total number of civilian personnel who will leave the region

ET = The number of civilian personnel who transfer with the realignment

LRC = The fraction of civilian retirees who leave the region

ERC = Number of civilian personnel who retire

LP = The fraction of civilians placed by DOD outside the region

EP = Number of civilian personnel who are placed by DOD in other positions

This equation estimates the total number of civilian personnel who leave the region as the sum of those who transfer, those who retire and leave, and those who are placed in other regions by DOD.

(11) Solve for RLMT where:

$$RLMT = EMT$$

where:

RLMT = The number of military trainees who will leave the region as a result of the realignment

EMT = Number of military trainees who transfer

This equation estimates the number of military trainees who transfer as being equal to the total military trainees who transfer.

(12) Solve for RLMP where:

$$RLMP = EMP + LRM * ERM$$

where:

RLMP = The number of military permanent parties who will leave the region as a result of the realignment

EMP = Number of military permanent parties who transfer

LRM = The fraction of military retirees who leave the region

ERM = Number of military permanent parties who retire

This equation estimates the number of military permanent parties who leave the ROI as a result of the action. It is the sum of those who transfer with the realignment and those retirees who leave the ROI.

(13) Solve for NT where:

$$NT = 0.0$$

where:

NT = Total number of civilians assigned to the base

$$M = 0$$

where:

MT = Total number of military personnel assigned to the base

These two equations set the initial value of accumulators to zero.

(14) Solve for NT where:

$$NT = NT + NC(K)$$

where:

NT = The total number of civilians assigned to the base

NC = The number of civilians residing in city  $i$  where  $i=1, K$ .

This equation sums the value for each city to find a value for the region.

(15) Solve for MT where:

$$MT = MT + MC(K)$$

where:

MT = The total number of military personnel residing in the ROI

MC = Total number of military personnel residing in city being analyzed. (Note city 1 must include military on base)

This equation sums the value for each city to find a value for the region.

(16) Solve for FL where:

$$FL = (FT*ALT + FMP*ALMP + FMT*ALMT + FT*ALRC + FMP*ALRM) / (ALT + ALMP) + ALMT + ALRC + ALRM$$

where:

FL = The average family size of the personnel affected by the action

ALT = Fraction of positions terminated or relocated held by civilians who will transfer with the realignment

FMP = Median number of persons per household of military permanent parties

ALMP = Fraction of positions terminated or relocated held by military permanent parties who transfer

FMT = Median number of persons per household of military trainees

- ALMT = Fraction of positions terminated or relocated held by military trainees who transfer
- FT = Median number of persons per household of USAF civilian transferees
- ALRC = Fraction of positions terminated or relocated held by civilians who retire.
- ALRM = Fraction of positions terminated or relocated held by military permanent parties who retire
- ALT = Fraction of positions terminated or relocated held by civilians who will transfer with the realignment

This equation calculated a weighted average family size. The use of medians, rather than means, imply the distribution of family sizes is normal. This needs verification.

(17) Solve for PAF where:

$$PAF = (RLC + RLMT + RLMP) * FL$$

where:

- PAF = The total population associated with base employees
- RLC = The number of civilian personnel who will leave the region
- RLMT = The number of military trainees who will leave the region as a result of the realignment
- RLMP = The number of military permanent parties who will leave the region as a result of the realignment
- RL = The average family size of the personnel affected by the action

This equation estimates the total population associated with all base personnel.

(18) Solve for BETCR where:

$$BETCR = 1 - BETCO$$

where:

- BETCR = Fraction of civilian personnel who rent
- BETCO = Fraction of civilian personnel who own their own homes

This equation estimates the fraction of civilians who rent as being equal to 1 minus the fraction who own.

(19) Solve for BETMPR where:

$$BETMPR = 1 - BETMPO$$

where:

BETMPR = Fraction of military permanent parties who rent  
(for city 1, this will include the military who  
live on base)

BETMPO = Fraction of military permanent parties who own  
their own home

This equation estimates the fraction of military permanent  
parties who rent as being equal to 1 minus the fraction who  
own.

(20) Solve for BETMTR where:

$$\text{BETMTR} = 1 - \text{BETMTO}$$

where:

BETMTR = Fraction of military trainees who rent housing

BETMTO = Fraction of military trainees who own their own  
home

This equation estimates the fraction of military trainees who  
own their own homes as being equal to 1 minus the fraction  
who rent.

(21) Solve for MPRL where:

$$\text{MPRL} = \text{BETMPR} * \text{RLMP}$$

where:

MPRL = Total military permanent parties who were rent-  
ing who leave the region

BETMPR = Fraction of military permanent parties who  
rent

RLMP = The number of military permanent parties who  
will leave the region as a result of the re-  
alignment

This equation estimates the number of military permanent  
parties who were renting who will leave the ROI.

(22) Solve for MTRL where:

$$\text{MTRL} = \text{BETMTR} * \text{RLMT}$$

where:

MTRL = Number of military trainees who rent who leave  
the region

BETMTR = Fraction of military trainees who rent

RLMT = The number of military trainees who will leave  
the region as a result of the realignment

This equation estimates the total number of military  
trainees who rent who will leave the region.

(23) Solve for CRL where:

$$CRL = BETCR * RLC$$

where:

CRL = The number of civilian personnel who rent who leave the region

BETCR = Fraction of civilian personnel who rent

RLC = The total number of civilian personnel who will leave the region

This equation estimates the total number of civilian personnel who rent housing.

(24) Solve for GAF where:

$$GAF = PAF * (THETA / ((T2 - T1) * P2))$$

where:

GAF = Annualized percentage change in population associated with USAF action

THETA = The fraction of USAF personnel who currently reside in the ROI

T2 = Date of completion of the action

T1 = Date of initiation of the action

P2 = Total population at  $t_2$  excluding the action

This equation expresses the percentage change in population caused by the realignment in annual rates. This is not a very clear way in which to express this change.

(25) Solve for GHAT where:

$$GHAT = G2ROI - GAF$$

where:

GHAT = Projected growth rate including realignment

G2ROI = The average annual population growth rate in the ROI

GAF = Annualized percentage change in population associated with USAF action

This equation attempts to explain the new population growth rate following the realignment. Unfortunately, it is not clear that there is much logic to the equation.

(26) Solve for P2CI where:

$$P2CI = (((PBZ - PAZ) * (T2 - TPAZ)) / (TPBZ - TPAZ)) + PAZ$$

where:

P2CI = Population of city 1 at t<sub>2</sub>  
PBZ = Population of city 1 at b<sub>2</sub>  
PAZ = Population of city 1 at a<sub>2</sub>  
T2 = Date of completion of action  
TPAZ = Date of PAZ data  
TPBZ = Date of PBZ data

This equation estimates the total population loss to each city using a linear interpolation of data inputted into the model.

(27) Solve for THETAC where:

$$\text{THETAC} = (\text{NC(K)} + \text{MC(K)}) / (\text{MT} + \text{NT})$$

where:

THETAC = The fraction of USAF personnel who currently reside in the city being analyzed  
NC = The number of civilians residing in city 1  
MC = The number of military personnel residing in city 1  
MT = The total number of military personnel  
NT = The total number of civilian personnel

This equation calculates the fractions of total employment who live in each of "K" cities. It is important that military on base be included in city one and that any personnel not falling into a defined "city" be placed together as the last "city."

(28) Solve for PAFC where:

$$\text{PAFC} = \text{THETAC} * \text{PAF}$$

where:

PAFC = The total population associated with base employees who reside in city 1  
THETAC = The fraction of USAF personnel who currently reside in the city being analyzed  
PAF = The total population associated with base employees

This equation allocated the estimated total population associated with the realignment to each city. The assumption made is that the population is distributed in the same fashion as employees, or that all communities are

identical in their ability to attract married personnel and those with families.

(29) Solve for GAF where:

$$GAF = PAFC / (T2 - T1) * P2CI$$

where:

GAF = Annualized percentage change in population associated with the USAF action

PAFC = The total population associated with base employees who reside in city 1

T2 = Date of completion of the action

T1 = Date of initiation of the action

P2CI = Population of city 1 at  $t_2$

This equation expresses the estimated percentage change in population in the city being analyzed.

(30) Solve for G2 where:

$$G2 = (PBZ - PAZ) / (PAZ * (TBZ - TPAZ))$$

where:

G2 = The population growth rate for city 1

PBZ = Population of city at  $t_{bz}$

PAZ = Population of city at  $t_{az}$

TBZ = Date of TBZ data

TPAZ = Date of TPAZ data

This equation calculates the simple rate of growth in the population between two points,  $T_{BZ}$  and TBAZ

(31) Solve for GHAT where:

$$GHAT = G2 - GAF$$

where:

GHAT = Projected growth rate including realignment

G2 = The average annual population growth rate at  $t_2$  excluding realignment

GAF = Annualized percentage change in population associated with USAF action

This equation attempts to explain the new population growth rate following the realignment. Unfortunately, this equation suffers from an absence of logic.

(32) Solve for P2AFC where:

$$P2AFC = P2CI - PAFC$$

where:

P2AFC = Population of city i after the effect of the realignment

P2CI = Population of city i at  $t_2$  (before action)

PAFC = The total population associated with base employees who live in city i

This equation solves for the new population of city i following the realignment.

#### Population Thresholds Calculations

Population threshold calculations have not been evaluated at this time.

#### Housing Calculations

(1) Solve for CRLC where:

$$CRLC = CRL * NC(K) / NT$$

where:

CRLC = The number of civilian personnel who rent in city i who leave the city

CRL = The number of civilian personnel who rent who leave the region

NC(K) = The number of civilian personnel residing in city being analyzed

NT = The total number of civilians assigned to the base affected by the realignment

This equation allocates civilian to renter status in each city by assuming that the distribution of civilians who rent is the same as the total (renter and owner) distribution of civilian by city. If cities tend to be "specialized," that is, tend to be more renter oriented, then the allocative methodology will not accurately predict the number of renters who leave a particular city. Additional work on this equation is needed to support or refine the relationship modeled.

(2) Solve for K where:

$$IF(K.GT.1.0) GO TO 95$$

where:

K = Counts the number of cities being analyzed

This equation selects the next two equations for the first city only.

(3) Solve for MPRLC where:

$$\text{MPRLC} = \text{MPRL} * \text{MC}(K) / \text{MT} - \text{DLMP} * \text{RL} * (\text{ALMP} + \text{ALRM}) / \text{LMP}$$

where:

- MPRLC = The total number of military permanent parties who rent in city i who will leave the city
- MPRL = The total number of military permanent parties who rent who leave the region (includes on-base military permanent parties)
- MC(K) = The number of military personnel residing in city i. (Note: city 1 must include military on-base.)
- MT = The total number of military personnel assigned to the base
- DLMP = The number of military permanent parties living on-base
- RL = Total size of the realignment
- ALMP = Fraction of positions terminated or relocated held by military permanent parties who transfer
- ALRM = Fraction of positions terminated or relocated held by military permanent parties who retire
- LMP = The number of military permanent parties currently assigned to the base

This equation estimates the number of military permanent parties who were renting who will leave city i. It allocates military permanent parties who rent (total) to each city in the same proportion as the distribution of all military permanent parties (renter and owner) by city. Each city is thus assumed to have the same share of renter and owner occupied housing by military permanent parties as the region. If cities in fact tend to specialize in renter or owner occupied housing, then the allocative methodology will not accurately model the situation.

This equation also adjusts the number of military permanent parties who rent in city i for the number of military permanent parties on base. This adjustment is necessary because MC(K) includes all military permanent parties living in city 1 including on-base. MPRL also includes military permanent parties on-base.

(4) Solve for LMT where:

IF(LMT.EQ.0.0) GO TO 96

where:

LMT = The number of military trainees currently assigned to the base

This equation will allow for the omission of the next step when no military trainees are assigned to the base.

(5) Solve for MTRLC where:

$$\text{MTRLC} = \text{MTRL} * \text{MC}(K) / \text{MT} - \text{DLMT} * \text{RL} * \text{ALMT} / \text{LMT}$$

where:

MTRLC = The number of military trainees who rent in city i who leave the region

MTRL = The total number of military trainees who rent in the region (including those living on base)

MC(K) = The number of military personnel residing in city i (note: city 1 must include military on base)

MT = The total number of military personnel assigned to the base

DLMT = The number of military trainees living on base

RL = The size of the realignment

ALMT = Fraction of position terminated or relocated held by military trainees who transfer

LMT = The number of military trainees currently assigned to the base

This equation estimates the number of military trainees who were renting in city i. It allocates military trainees who rent to each city in the same proportions as the distribution, by city, of all military trainees (renter and owner). This methodology assumes each city will have the same renter-owner distribution as the region. If the cities tend to be more specialized in providing housing, the methodology will not predict accurately.

The equation adjusts for military trainees who live on-base which have been included in city 1.

(6) Solve for MPRLC where:

$$\text{MPRLC} = \text{MPRL} * \text{MC}(K) / \text{MT}$$

where:

MPRLC = The total number of military permanent parties who rent in city i who will leave the city

MPRL = The total number of military permanent parties who rent who leave the region

MC(K) = The number of military personnel residing in city i

MT = The total number of military personnel residing in region

This equation allocates the remaining (after city 1) military permanent parties who rent to the remaining n cities. The same comments regarding the distribution of owner-renter status across cities made in statement 3 and 5 apply here as well.

(7) Solve for MTRLC where:

$$\text{MTRLC} = \text{MTRL} * \text{MC}(K) / \text{MT}$$

where:

MTRLC = The number of military trainees who rent in city being analyzed

MTRL = The total number of military trainees who rent in the region

MC(K) = The number of military personnel residing in city i

MT = The total number of military personnel residing in region

This equation allocates the remaining (after city 1) military trainees who rent to the remaining n cities. The same comments regarding the distribution of owner-renter status across cities made in statements 3 and 5 above apply here as well.

(8) Solve for RLRC where:

$$\text{RLRC} = \text{CRLC} + \text{MPRLC} + \text{MTRLC}$$

where:

RLRC = Total number of off-case personnel who were renting who will leave the city

CRLC = The number of civilian personnel who rent in city i who leave the city

MPRLC = The total number of military permanent parties who rent in city i who leave the city

MTRLC = The total number of military trainees who rent in city i who will leave the region

This equation sums the three categories of renter status personnel who will leave each city.

(9) Solve for MPOL where:

$$\text{MPOL} = \text{BETMPO} * \text{RLMP}$$

where:

MPOL = Military permanent parties who own their own home who leave the region

BETMPO = Fraction of military permanent parties who own their own homes

RLMP = The number of military permanent parties who will leave the region as a result of the realignment

This equation estimates the total number of military permanent parties who own their own homes who leave the region.

(10) Solve for MTOL where:

$$\text{MTOL} = \text{BETMTO} * \text{RLMT}$$

where:

MTOL = The number of military trainees who own their own homes

BETMTO = The fraction of military trainees who own their own homes

RLMT = The number of military trainees who will leave the region as a result of the realignment

This equation estimates the total number of military trainees who own their own homes who leave the region.

(11) Solve for COL where:

$$\text{COL} = \text{BETCO} * \text{RLC}$$

where:

COL = The number of civilians who own their own homes who will leave the region

BETCO = Fraction of civilian personnel who own their own home

RLC = Total number of civilian personnel who will leave the region

This equation estimates the total number of civilians who own their own homes who leave the region.

(12) Solve for COLC where:

$$\text{COLC} = \text{COL} * \text{NC}(K) / \text{NT}$$

where:

COLC = The number of civilians who own their own home who will leave city i

COL = The number of civilians who own their own home who leave the region

NC(K) = Number of civilian personnel residing in city i

NT = Total number of civilians assigned to the base

This equation allocates the number of civilians who own their own homes among the n cities. The methodology used assumes that each city has the same proportion of owner-renter housing as distributions of total civilian personnel. If cities tend to be specialized in owner or renter housing, the methodology will breakdown. Further research into this area is needed.

(13) Solve for MOLC where:

$$\text{MOLC} = (\text{MPOL} + \text{MTOL}) * \text{MC}(K) / \text{MT}$$

where:

MOLC = Total number of military personnel who own their own homes in city i who leave the city

MPOL = Military permanent parties who own their own homes who leave the region

MTOL = Number of military trainees who own their own homes who leave the region

MC(K) = The number of military personnel residing in city i. (Note: city 1 must include military on-base)

MT = The total number of military personnel assigned to the base

This equation estimates the total number of military personnel who own their own homes who leave the city. The allocative methodology assumes that owner occupied housing is distributed among the various cities in the same proportion as the distribution of all military (renter and owner) by city.

Note that since MC(K) where K=1 includes military on base, MOLC for city 1 will be very high. This needs critical evaluation.

(14) Solve for RLOC where:

$$\text{RLOC} = \text{MOLC} + \text{COLC}$$

where:

RLOC = Total number of base personnel who own their own homes who will leave the city

MOLC = Total number of military personnel who own their own homes who will leave the city

COLC = The number of civilians who own their own home who leave the city

This equation sums the number of military and civilian who own their own homes who leave city i.

(15) Solve for RLTC where:

$$RLTC = (RLMP+RLMT)*MC(K)/MT+RLC*NC(K)/NT$$

where:

RLTC = Total number of military and civilians who will leave the city (not city 1)

RLMP = The number of military permanent parties who will leave the region as a result of the realignment

RLMT = The number of military trainees who will leave the region as a result of the realignment

MC(K) = The number of military personnel residing in city i (Note: city 1 must include military on-base)

MT = The total number of military personnel assigned to the base

RLC = Total number of civilian personnel who will leave the region

NC(K) = Number of civilian personnel residing in city i

NT = Total number of civilians assigned to the base

This equation estimates the total number of personnel who will leave each city. The allocative methodology assumes that those involved in the realignment have residential patterns in the same proportions as the distribution of total base personnel.

(16) Solve for RLTC where:

$$RLTC = RLTC-DLMP*RL*(ALMP+ALRM)/LMP-DLMT*RL*ALMT/LMT$$

where:

RLTC = Total number of military and civilians who will leave city i

DLMP = The number of military permanent parties living on-base

RL = Total size of the realignment

ALMP = Fraction of positions terminated or relocated held by military permanent parties who transfer

ALRM = Fraction of positions terminated or relocated held by military permanent parties who retire

LMP = The number of military permanent parties currently assigned to the base

DLMT = The number of military trainees living on base

ALMT = Fraction of positions terminated or relocated held by military trainees who transfer

LMT = The number of military trainees currently assigned to the base

This equation estimates the total number of civilians and military personnel who leave city 1 as a result of the realignment.

(17) Solve for DHAT2 where:

$$\text{DHAT2} = \text{RLTC}$$

where:

DHAT2 = Change in total housing vacancies in city i caused by the realignment

RLTC = Total number of military and civilians who will leave city i

This equation sets housing vacancies equal to the number of personnel who leave city i. This assumes that every individual seeks separate housing in the city.

(18) Solve for DHAT2R where:

$$\text{DHAT2R} = \text{RLRC}$$

where:

DHAT2R = Change in renter housing vacancies in city i caused by the realignment

RLRC = Total number of off-base personnel who were renting who will leave city i

This equation sets renter housing vacancies equal to the number of personnel who leave city i. This assumes that every renter in the city seeks separate rental housing.

(19) Solve for DHAT20 where:

$$\text{DHAT20} = \text{RLOC}$$

where:

DHAT20 = Change in owner housing vacancies in city i caused by the realignment

RLOC = Total number of base personnel who own their own homes who leave the city

This equation sets owner housing vacancies in city i equal to the number of personnel who own their own home who leave

the area. The equation assumes all base personnel who own their own home in city 1 seek separate housing.

(20) Solve for H2 where:

$$H2 = (HBZ-HAZ)*(T2-THAZ)/(THBZ-THAZ)+HAZ$$

where:

H2 = The total number of year-round housing units at  $t_2$

HBZ = The size of the housing stock at  $t_{2+x}$  (or  $t_{1-y}$  if projections are not available)

HAZ = The size of the housing stock at  $t_{1-y}$  (or  $t_{70}$  if no projections are available)

T2 = Date of completion of the action

THAZ = Date of HAZ data

THBZ = Date of HBZ data

This equation estimates the number of housing units available at  $t_2$  in the city. The methodology interpolates between two numbers, or if not available, extrapolates to find the value at  $t_2$ .

(21) Solve for VE where:

IF(VE.GT.0.0) GO TO 93

where:

VE = The most recently recorded total housing stock vacancy rate

This equation selects equations for estimating total housing vacancies when detail on owner and renter vacancy rates does not exist.

(22) Solve for PSIO where:

$$PSIO = HEO/(HEO+HER)$$

where:

PSIO = The fraction of the  $t_2$  housing stock that is owner-occupied or for sale

HEO = The most recently recorded number of housing units that are owner-occupied or for sale

HER = The most recently recorded number of housing units that are renter-occupied or for rent

This equation calculates the fraction of total stock that is owner occupied or for sale in a given year. If census data is used, this fraction is for 1970. Later this fraction is used to allocate projected housing stock between owner and

renter type. This is a questionable technique and needs further research.

(23) Solve for PSIR where:

$$PSIR = HER / (HER + HEO)$$

where:

PSIR = The fraction of the  $t_2$  housing stock that is renter-occupied or for rent

HER = The most recently recorded number of housing units that are renter-occupied or for rent

HEO = The most recently recorded number of housing units that are owner-occupied or for sale

This equation calculates the fraction of total housing stock that is renter-occupied or for rent in a given year. The same comments made above apply to this equation as well.

(24) Solve for H20 where:

$$H20 = PSIO * H2$$

where:

H20 = The total number of year round owner-occupied or for sale housing units at  $t_2$

PSIO = Fraction of the  $t_2$  housing stock that is owner-occupied or for sale

H2 = The total number of year round housing units at  $t_2$

This equation estimates the total housing stock that is owner-occupied at  $t_2$  by assuming the distribution that existed at the date of HEO and HER is the same at  $t_2$ . Depending upon the time span between the date of HEO and HER and  $t_2$ , this could present problems in forecasting housing stock at  $t_2$

(25) Solve for H2R where:

$$H2R = PSIR * H2$$

where:

H2R = The total number of year-round renter-occupied or for rent housing units at  $t_2$

PSIR = Fraction of the  $t_2$  housing stock that is renter-occupied or for rent

H2 = The total number of year-round housing units at  $t_2$

This equation estimates the total housing stock that is

renter-occupied or for rent at  $t_2$  by assuming the distribution that existed at the date of HEO and HER is the same at  $t_2$ . The same comments made on statement 24 applies to this statement as well.

(26) Solve for VHAT20 where:

$$\text{VHAT20} = \text{DHAT20}/\text{H20}$$

where:

VHAT20 = Percentage change in the number of owner-occupied housing units which will become vacant

DHAT20 = Change in owner housing vacancies in city 1 caused by the realignment

H20 = The total number of year-round owner-occupied or for sale housing units at  $t_2$

This equation calculates the percentage change in the number of owner-occupied housing units which become vacant as a result of the realignment.

(27) Solve for VHAT2R where:

$$\text{VHAT2R} = \text{DHAT2R}/\text{H2R}$$

where:

VHAT2R = Percentage change in the number of renter-occupied housing units which will become vacant

DHAT2R = Change in renter housing vacancies in city 1 caused by the realignment

H2R = The total number of year-round renter-occupied if for rent at  $t_2$

This equation calculates the percentage change in the number of renter-occupied housing units which become vacant as a result of the realignment.

(28) Solve for VO where:

$$\text{VO} = \text{VHAT20} + \text{VEO}$$

where:

VO = The new (post-closure) owner-occupied vacancy rate

VHAT20 = Percentage change in the number of owner-occupied housing units which will become vacant

VEO = The most recently recorded owner-occupied housing vacancy rate

This equation estimates the new owner-occupied vacancy rate.

(29) Solve for VR where:

$$VR = VHAT2R + VER$$

where:

VR = The new (post-closure) renter-occupied vacancy rate

VHAR2R = Percentage change in the number of renter-occupied housing units which will become vacant

VER = The most recently recorded renter-occupied housing vacancy rate

This equation estimates the new renter-occupied vacancy rate.

(30)  $VDIFO = VO - VMAXO$

(31)  $VDIFR = VR = VMAXR$

These two equations are used to calculate thresholds, which have not yet been examined.

(32) Solve for VHAT2 where:

$$VHAT2 = DHAT2 / H2$$

where:

VHAT2 = Percentage change in the number of total housing units which will become vacant

DHAT2 = Change in total housing vacancies caused by realignment

H2 = The total number of year-round housing units at  $t_2$

This equation calculates the percentage change in the number of housing units, both renter and owner occupied, which will become vacant. This equation is used if detail on renter and owner-occupied housing is not available.

(33) Solve for V where:

$$V = VE + VHAT2$$

where:

V = New (post-closure) housing vacancy rate

VE = The most recently recorded total housing stock vacancy rate

VHAT2 = Percentage change in the number of total housing units which will become vacant

This equation calculates the new vacancy rate when detail on renter and owner status is not available.

- (34)  $V_{MAX} = H700 * V_{MAXO} + H70R * V_{MAXR}$
- (35)  $H70 = H700 + H70R$
- (36)  $V_{MAX} = V_{MAX} / H70$
- (37)  $VOIF = V - V_{MAX}$

The above four equations relate to housing thresholds and have not been critically evaluated at this time.

#### V. RECOMMENDATIONS:

This review has led to a number of discoveries and resultant recommendations. These recommendations are divided into two classes, those that can be accomplished immediately and those that require further study. Line number in parentheses refer to statement number in the program listing in Appendix C.

##### For Immediate Consideration or Change

1. The models output is burdensome and requires attention if it is to be time saving rather than time consuming.
2. (Line 34). Delete "1,000" from equation and instruct user to input either whole number or input in scientific notation. Input sheet should be changed.
3. (Lines 64-65). Where "alpha" values are read into the model, it would be easier to build the methodology into the model. It appears that the same basic data for finding alpha's is used in all studies. Thus the work of finding "alphas" can be standardized.
4. (Line 100). Statement 100 is redundant and should be eliminated.
5. (Line 262). Model has been changed to reflect new methodology for finding BETCR, BETMPR and BETMTR. Delete the read statement for these variables only. Also change the input sheet to reflect this change.
6. (Line 241). Term CPIT4/CPI(K) is correct only if input sheet is altered to read "CPIT4 = Consumer price index at  $t_4$ ," or change all to a ratio of PDR's.
7. (Line 303). The use of "median" household size in this equation is justifiable only if it is reasonable to assume that the median equals the mean. Recommend the immediate use of mean size to avoid the problem of assuming normal distribution of household size.

8. (Line 14, 54). Change PDIVT3 to PDWT3.
9. (Line 14, 54). Change PDIVT4 to PDWT4.
10. (Line 8). Delete "YT." It is not used.
11. (Line 10). Delete "LAMBCC" and "LAMBMC." They are not used.
12. (Line 285). Delete write statement for DKMD. It is written twice.
13. (Line 269). Since it is not possible for DKMD to be less than 0 without the number of on-base family housing units occupied being greater than the number of military living on-base (permanent party and trainee), the statement is redundant and should be deleted.
14. (Line 59). This IF statement selects an allocation methodology for determining local procurement expenditures. However, the variable "LI" in the "if" statement will always exist and thus the model will always select the allocative methodology even if data exists. Care should be exercised on the input sheet so that if YPG is inputted, LI should be set equal to "0." Perhaps to avoid confusion, the "IF" statement should be re-written with a different control variable.
15. I recommend deletion of the "worst-case" philosophy or justification for particular inputs or algorithms. This approach does not allow one to say, "this is what we believe will happen," but rather must say, "if the worst of all things occur, this will happen." I believe that the obligation of economic forecasts is to attempt to project the likely future. Planners can react to that. How can they react to statements that "this is the worst that will happen"?
16. The model contains two variables with the same variable code (ES). This could result in errors if not corrected.
17. (Lines 83, 168). The variable EPSIH is printed twice. The second write statement should be deleted.
18. In the estimation of OMMP and OMMT, care should be exercised to avoid including that portion of income spent at the BX as part of income being spent in the region. Thus, both parameters should reflect only that portion of income which are spent in the ROI (excluding on-base expenditures).

### For Further Research

1. Multiplier Analysis (Lines 39-40). The SRI model currently allows for the calculation of the Ulman-Dacey multiplier or the inputting of a multiplier from outside the model. Currently, the EIFS income multiplier is inputted and is used in completing the LECS.

While there has been some suggestion that any multiplier can be inputted into the SRI model, that in fact is not the case. The SRI model uses as current input sufficient data to calculate an implicit "Keynesian-type" regional multiplier. Thus while it is true that any multiplier can be inputted into the model, if it is significantly different from the "implicit" multiplier, a question arises about the value of the selected inputs used to calculate the implicit multiplier and other attributes in the model. These variables are  $omc$ ,  $\tau$ , and  $\sigma$ .

If data can be found which would allow for regional specific values of  $omc$ ,  $\tau$  and  $\sigma$  to be used, then regionally specific income multipliers can be developed in the SRI model which would be internationally consistent. Possible sources of such data are published: IRS data, savings information from FDIC, FRS, and savings and loan association data.

It is recommended that research be conducted which will lead to the adoption of a Keynesian multiplier approach using regionally specific value of  $\tau$  and  $\sigma$ . Additionally,  $omc$  should be investigated to determine its variability and the determinants of its variability.

The results of such research would be the following:

- (a) The SRI model would then be a self-sufficient model, not dependent upon other models for significant inputs.
- (b) The SRI model would be internally consistent with regard to the multiplier and values of  $omc$ ,  $\tau$  and  $\sigma$ .

2. Non-Wage Income (Lines 67-78). The SRI model estimates lost income to the ROI by adding to wage and salary income an increment to reflect additional sources of income. As currently modeled, the addition of non-wage income significantly overstates the income levels of base employees and thus significantly overstates the lost income to the ROI. The difficulty lies in the definition of non-wage income used. Many of the items included in the definition used by SRI are mutually exclusive of wage and salary income. For example, proprietor's income is not likely to accrue to wage earners, yet it is used in the current model. Other items represent fringe benefits to the employee and do not represent income lost to the ROI in a realignment. For example, employer contribution to social security, health plans, and retirement systems is technically "other labor income," but is not income lost to the ROI in the event of a realignment.

Other problems with this sector include line 72 which assumed that if K2 is not available, then K2 is equal to one-half K1. There does not appear to be any reason for such an approach and it should be proven or replaced.

The model also assumes that civilian and military permanent parties have different "non-wage incomes." Do they? It should be supportable if they do, changed if they do not. Now wage income is also calculated for workers in retail, wholesale, service and construction sectors.

It is recommended that research be conducted to find a reasonable estimate of non-wage income accruing to base employees and that based upon these studies the estimates of personal income lost to a community be rewritten in the model.

The results of the research will be:

- (a) A more realistic, creditable and accurate forecast of the income which will be lost to an ROI in a realignment.
- (b) A more realistic estimate of the number of jobs lost to the ROI.

3. Productivity Index (Lines 57-58, 37, 34). The model estimates lost jobs by dividing lost income by appropriate productivity measures (PGAM, PKS, PRS and PWS). Each of these measures is assumed to be constant in real terms. Since the basic data used in estimating these values is 1972 special studies (i.e., Census of Retail Sales, Census of Wholesale Trade, etc.), it follows that the model uses a 1972 real productivity index.

The question is whether or not real productivity is a constant or has there been a general trend toward greater or lower productivity. A subsidiary question is whether or not the average productivity is an appropriate measure of the need to add or delete employees. Finally, there is an important question of the variability of these measures over the business cycle. If, for example, PRS is developed based upon a year when the economy is in the bottom of a recession, it may be that PRS is relatively high as firms attempt to minimize costs. If we then forecast lost jobs at a period when the economy is in a peak of prosperity, we would tend to understate the impact of unemployment.

It is recommended that research into the question of trends in the productivity index be conducted to establish confidence in the manner in which they are currently modeled. If the facts warrant, the model should be changed to more accurately reflect the facts.

4. Estimates of Lost Income at  $t_2$ . The model is thought to project or forecast income lost to the local community at  $t_2$ , the date of completion of the action. However, the methodology used in the model only allows the estimation of lost income at  $t_4$  based upon the population at  $t_2$ . If a true estimate of lost income at  $t_2$  is to be made, the methodology cannot rely totally upon a ratio of consumer price indices.

This problem also appears in several other sections of the model and would need to be corrected if forecasts at  $t_2$  are desired.

It is recommended that this problem be examined further and that an appropriate measure of future lost income be adopted.

5. Labor Force Participation Rate (Line 111). If there are no available forecasts of the labor force at  $t_2$  or if interpolation from other forecasts is not possible, the model uses population forecasts and a projected labor force participation rate. In obtaining the participation rate, the model increments a historic rate at .007 per year.

Two questions arise here. The first is the obvious one of whether there is sufficient support for the rate. Preliminary evidence at the national level suggests that .007 is not representative of any "trend." A good look at both long-run trend and recent short-run changes is warranted, since this variable may tend to result in errors in the size of the labor force at  $t_2$ .

A second question is whether there should be a trend factor which is the same for all ROI's. An examination of regional variations seems appropriate if confidence in a national constant is to be established. If significant variations are found to exist, this item could become an input to the model, rather than a constant term.

Additional research is recommended.

6. Allocation Methodology used in Housing Sector. When estimating the impact of a proposed realignment on the housing market in each city, the SRI methodology currently allocates the number of civilians who rent in each city in the same proportion as the distribution of all civilians. However it appears that some cities around an installation are more

appropriately "renter" communities others more appropriately "owner" communities. The same methodology is used for civilians who own homes in each city, military permanent parties, and military trainees. This methodology probably leads to significant errors in both owner-occupied and renter-occupied vacancy rate in most of the cities (unless in fact the distribution of owner and renters is exactly the same as the distribution of each class of off-base employees).

Another problem area is the allocation of housing stock at  $t_2$  in the same proportion as that which existed at the date of the basic housing data. Since interest rates have moved higher and higher, there may be a shift toward proportionately more renter units in a community housing stock.

It is recommended a thorough study of the housing sector be made in order to provide realistic projections of housing vacancy rates.

7. Critical Review of "Gainer" Model and all Hand Calculations.  
It is recommended that the "gainer" portion of the SRI model be subjected to a critical review similar to that given the loser model. In addition, all hand calculations should be similarly evaluated.
8. It is recommended that additional research be conducted to establish a methodology to disaggregate personal income losses to various sectors in the local economy. The greater detail would provide planners with the ability to pinpoint specific areas for possible assistance.
9. It is recommended that research be conducted to establish a methodology which would provide significant detail on public sector impacts of base realignments.
10. Integration of Additional Attributes into the Computer Model.  
As currently used, the SRI Methodology Handbook contains many variables which are calculated by hand. Where possible,

these attributes should be programmed into the model. Additional work now being done by hand (tabular presentations) can also be added to the computer program.

11. Addition of Permanent Data into the Model. Regardless of the area or ROI, certain data in the model is used throughout. For example, there is little reason to have to input YT4, YT6, ET4, ET6 each time. These values can be loaded into the program and thus ease the burden of data collection each time. This researcher estimates that 26% of the data now being collected for each study can be stored within the program.
12. The specific treatment of NAF (non-appropriated fund) civilian employees should be carefully evaluated so that they are properly treated in income, unemployment, and housing calculations.
13. The structure of the equation which estimates working dependents jobs implicitly assumes that no family could have more than one working dependent. Moreover, the manner in which RHOWDC and RHOWDM have been estimated assumes that only wives/husbands of personnel occupy jobs. Research is needed to restructure this equation to be more descriptive of reality.
14. Complete restructuring of both inputs and outputs to a more legible and useable format. Additional error checks should be added as well as interactive statements to prompt the user.
15. The demographic sector needs critical reworking if the model is to be used in a predictive manner. Currently, there is no allowance for migration in the model, nor is there any allowance for age or sex adjustments occurring over time. Both changes would be important in forecasts of population growth rates. Additional research is needed in this area.

16. Sensitivity analysis should be conducted to develop a better understanding of the model's stability and the data areas where greatest care should be exercised. This should be done on the final revised model at the end of any future restructuring.

#### REFERENCES

1. SRI International, Socioeconomic Impact Assessment Methodology Handbook (Menlo Park, California: SRI International, September, 1978).
2. SRI International, Quick Reaction Socioeconomic Analysis System (QRSAS), Phase II (Menlo Park, California: SRI International, February, 1978).

APPENDIX A

SAMPLE DATA INPUT SHEET

EMPLOYMENT DATA

VALUE	COMPUTER SYMBOL	DEFINITION
_____	YT4	National output in year $t_4$
_____	YT6	National output in year $t_6$
_____	ET4	National employment in year $t_4$
_____	ET6	National employment in year $t_6$
_____	MU	Fraction of output from new construction that goes to the purchase of materials in each of the following sectors: <ol style="list-style-type: none"> <li>1. Manufacturing</li> <li>2. Transportation, communications, utilities</li> <li>3. Trade</li> <li>4. Finance, insurance, real estate</li> <li>5. Services</li> </ol>
_____	GAMM	Fraction of output from new construction that goes to employee compensation (wages)
_____	GAMN	Fraction of output from new construction that goes into property income
_____	SJT6	National output for $t_6$ in each of the following sectors: <ol style="list-style-type: none"> <li>1. Manufacturing</li> <li>2. Transportation, communications, utilities</li> <li>3. Trade</li> <li>4. Finance, insurance, real estate</li> <li>5. Services</li> </ol>
_____	EJT6	National employment for $t_6$ for each of the following sectors: <ol style="list-style-type: none"> <li>1. Manufacturing</li> <li>2. Transportation, communications, utilities</li> <li>3. Trade</li> <li>4. Finance, insurance, real estate</li> <li>5. Services</li> </ol>
_____	PDCT5	Price deflator for the construction sector, $t_5$
_____	PDCT4	Price deflator for the construction sector, $t_4$
_____	SKST5	State construction sector receipts for the most recently recorded year ( $t_5$ )
_____	EKST5	State employment in the construction sector in $t_5$

VALUE	COMPUTER SYMBOL	DEFINITION
_____	SWST3	Regional wholesale sector sales for the most recently recorded year (t <sub>3</sub> )
_____	PDWT4	Price deflator, wholesale trade sector, t <sub>4</sub>
_____	PDWT3	Price deflator, wholesale trade sector, t <sub>3</sub>
_____	SRST3	Regional retail sector sales for year t <sub>3</sub>
_____	PDRT3	Price deflator, retail trade sector, t <sub>3</sub>
_____	PDRT4	Price deflator, retail trade sector, t <sub>4</sub>
_____	SSST3	Regional service sector sales for year t <sub>3</sub>
_____	PDST4	Price deflator, service sector, t <sub>4</sub>
_____	PDST3	Price deflator, service sector, t <sub>3</sub>
_____	EWST3	Regional employment in the wholesale sector in t <sub>3</sub>
_____	ESST3	Regional employment in the service sector in t <sub>3</sub>
_____	ERST3	Regional employment in the retail sector in t <sub>3</sub>
_____	YPI	Amount of procurement expenditures in ROI
_____	YQ	Amount of procurement expenditures in ROI for commissary and BX goods purchased by retirees
_____	LI	Number of persons employed by and assigned to the base before the action (if data for YPG exists, set LI=0)
_____	YKG	Change in construction expenditures because of the action
_____	TAU	Fraction of total personal income remaining after taxes
_____	SIGMA	Fraction of after-tax total personal income remaining after savings
_____	WMT	The average wages of military trainees affected by the action
_____	WMMP	Average wages of military permanent parties affected by the action
_____	WWC	The average wages of civilian personnel affected by the action
_____	OMMP	Fraction of military permanent party disposable total personal incomes spent in the ROI, exclusive of on-base expenditures
_____	OMMT	The fraction of military trainee disposable total personal income spent in the ROI, exclusive of on-base expenditures
_____	OMC	Fraction of civilian disposable total personal income spent in the ROI

VALUE	COMPUTER SYMBOL	DEFINITION
_____	RHOWDC	The fraction of new USAF civilian personnel in the region who will have a dependent who will seek employment
_____	RHOWDM	The fraction of military personnel transferring to region who have a dependent who will seek employment
_____	ZETWD	Working dependent full-time employment equivalency factor
_____	LBZ	The size of the ROI labor force at $t_{2+x}$ (or $t_{1-y}$ if projections are not available)
_____	TLBZ	The date of $L_{bz}$
_____	LAZ	The size of the labor force at $t_{1-y}$ (or $t_{70}$ if projections are not available)
_____	TLAZ	The date of $L_{az}$
_____	E2	The unemployment rate at $t_2$ if available. If not available, enter 0
_____	T2	The date of completion of the action
_____	T1	The date of the initiation of the action
_____	RPBZ	The projected population of the region at $t_{2+x}$ or $t_{1-y}$
_____	TRPBZ	Date of RPBZ data
_____	RPAZ	The projected population of the region at $t_{1-y}$ or $t_{70}$
_____	TRPAZ	Date of RPAZ data
_____	YPG	The change in USAF procurement expenditures as a result of the action (if no data exists, input YPI, YQ and LI)
_____	M	Net regional export base income multiplier
_____		Run 1
_____		Run 2
_____		Run 3
_____		Run 4
_____		Run 5
_____		Run 6

PERSONAL INCOME DATA

VALUE	COMPUTER SYMBOL	DEFINITION
_____	K2	Ratio of non-wage income to wage income for region of influence
_____	KY	Number of years of personal and labor income data (up to ten years)
_____	Y	Total personal income for ROI number of years specified in KY
_____		Year 1 _____
_____		Year 2 _____
_____		Year 3 _____
_____		Year 4 _____
_____		Year 5 _____
_____		Year 6 _____
_____		Year 7 _____
_____		Year 8 _____
_____		Year 9 _____
_____		Year 10 _____
_____	YL	Labor income (wages and salary) for ROI for years specified in KY
_____		Year 1 _____
_____		Year 2 _____
_____		Year 3 _____
_____		Year 4 _____
_____		Year 5 _____
_____		Year 6 _____
_____		Year 7 _____
_____		Year 8 _____
_____		Year 9 _____
_____		Year 10 _____
_____	CPI	Consumer price index for number of years specified in KY
_____		Year 1 _____
_____		Year 2 _____
_____		Year 3 _____
_____		Year 4 _____
_____		Year 5 _____
_____		Year 6 _____
_____		Year 7 _____
_____		Year 8 _____
_____		Year 9 _____
_____		Year 10 _____
_____	PDRT4	Price deflator, retail trade sector, $t_4$
_____	PDRT3	Price deflator, retail trade sector, $t_3$
_____	PDRTH	Price deflator, retail trade sector, $t_h$
_____	PDRTF	Price deflator, retail trade sector, $t_f$

VALUE	COMPUTER SYMBOL	DEFINITION
_____	ENU	Total national employment for $t_f$
_____	YH	Regional per capita income for the most recently recorded year, $t_h$
_____	YK	National personal income from other labor income in $t_f$
_____	YM	National personal income from wages and salaries in $t_f$
_____	YN	National personal income of proprietors in $t_f$
_____	WWST3	The total regional wages in the wholesale sector in $t_3$
_____	WSST3	The total regional wages in the selected services sector in $t_3$
_____	WRST3	The total regional wages in the retail sector in $t_3$

POPULATION AND HOUSING DATA FOR THE REGION

<u>VALUE</u>	<u>COMPUTER SYMBOL</u>	<u>DEFINITION</u>
_____	LMP	The number of military permanent parties currently assigned to the installation
_____	LMT	The number of military trainees currently assigned to the installation
_____	FT	Median number of persons per household of USAF civilian employees at the installation
_____	FMP	Median number of persons per household of USAF military permanent parties at the installation
_____	FMT	Median number of persons per household of USAF military trainees at the installation

POPULATION AND HOUSING DATA FOR EACH CITY

(complete one set of forms of pages through for each city)

VALUE	COMPUTER SYMBOL	DEFINITION
_____	PBZ	The projected population of the city (or community under study) at $t_{2+x}$ or $t_{1-y}$
_____	TPBZ	The date of $P_{bz}$ data
_____	PAZ	The population of the city (or community under study) at $t_{1-y}$ or $t_{70}$
_____	TPAZ	The date of $P_{az}$ data
_____	NYEAR	Number of years of population data for city (up to 10 years)
_____	PP	Population of city for number of years specified in NYEAR
_____		Year 1 _____
_____		Year 2 _____
_____		Year 3 _____
_____		Year 4 _____
_____		Year 5 _____
_____		Year 6 _____
_____		Year 7 _____
_____		Year 8 _____
_____		Year 9 _____
_____		Year 10 _____
_____	TP	Date of PP data
_____		Year 1 _____
_____		Year 2 _____
_____		Year 3 _____
_____		Year 4 _____
_____		Year 5 _____
_____		Year 6 _____
_____		Year 7 _____
_____		Year 8 _____
_____		Year 9 _____
_____		Year 10 _____
_____	HBZ	The size of the housing stock at $t_{2+x}$ (or $t_{1-y}$ if projections are not available)
_____	THBZ	The date of $H_{bz}$ data
_____	HAZ	The size of the housing stock at $t_{1-y}$ or $t_{70}$
_____	THAZ	The date of $H_{az}$ data
_____	H700	The number of 1970 housing units that were either owner-occupied or for sale
_____	H70R	The number of 1970 housing units that were either renter-occupied or for rent

VALUE	COMPUTER SYMBOL	DEFINITION
_____	VE	The most recently recorded total housing stock vacancy rate. If data exists for VEO and VER, set VE=0.
_____	HEO	The most recently recorded number of housing units that are owner-occupied or for sale
_____	HER	The most recently recorded number of housing units that are renter-occupied or for rent
_____	VEO	The most recently recorded owner-occupied housing vacancy rate (use only if VE=0)
_____	VER	The most recently recorded renter-occupied housing vacancy rate (use only if VE=0)

UNIQUE DECLINER INPUT

VALUE	COMPUTER SYMBOL	DEFINITION
_____	RL	The total number of positions to be terminated at the base
_____	ALT	Fraction of positions terminated or relocated held by civilians who will transfer with the realignment
_____	ALMT	Fraction of positions terminated or relocated held by military trainees who transfer
_____	ALSP	The fraction of positions terminated or relocated held by civilians who will separate from the USAF
_____	ALP	The fraction of positions terminated or relocated held by civilians who will be placed elsewhere
_____	ALRC	The fraction of positions terminated or relocated held by civilians who will retire
_____	ALMP	The fraction of positions terminated or relocated held by military permanent parties who transfer
_____	ALRM	The fraction of positions terminated or relocated held by military permanent parties who retire
_____	PIP	The fraction of civilians placed by DOD in positions outside the ROI
_____	PIRC	The fraction of civilian retirees who leave the ROI labor force (i.e., retire from work or leave region)
_____	PIRM	The fraction of military retirees who do not enter the ROI labor force
_____	PISP	The fraction of USAF personnel that separate who do not become employed elsewhere before $t_2$
_____	RHOSJC	The fraction of USAF civilian personnel in the region who have a second job
_____	RHOSJM	The fraction of military personnel transferring from the region who have a second job
_____	ZETSJ	Second job full-time employment equivalency factor
_____	EEE	The most recently recorded unemployment rate
_____	EE1	The unemployment rate in the ROI for the most recently completed calendar year
_____	EE2	The unemployment rate in the ROI two years before the most recently recorded data
_____	ESS	The most recently recorded seasonally adjusted unemployment rate for the state

VALUE	COMPUTER SYMBOL	DEFINITION
_____	NYEAR	Number of years of unemployment data for the ROI (up to ten years)
_____	EE	Unemployment rate for the ROI for number of years specified in NYEAR
_____		Year 1 _____
_____		Year 2 _____
_____		Year 3 _____
_____		Year 4 _____
_____		Year 5 _____
_____		Year 6 _____
_____		Year 7 _____
_____		Year 8 _____
_____		Year 9 _____
_____		Year 10 _____
_____	EN	Years of unemployment rates stated in EE
_____		Year 1
_____		Year 2
_____		Year 3
_____		Year 4
_____		Year 5
_____		Year 6
_____		Year 7
_____		Year 8
_____		Year 9
_____		Year 10
_____	THETA	The fraction of USAF personnel who currently reside in the ROI
_____	BETCO	The fraction of civilian personnel who own their homes
_____	BETMPO	The fraction of incoming military permanent parties who own a dwelling unit
_____	BETMTO	The fraction of incoming military trainees who own a dwelling unit
_____	DKMF	The number of on-base family housing units occupied at $t_1$
_____	FOMP	The fraction of military permanent parties who live on-base
_____	FOMT	The fraction of military trainees who live on-base
_____	LRC	The fraction of civilian retirees who leave the region
_____	LP	The fraction of civilians placed by DOD outside the region
_____	LRM	The fraction of military retirees who leave the region

VALUE	COMPUTER SYMBOL	DEFINITION
_____	NCITY	Number of cities to be analyzed (up to 20 cities)
_____	NC	Number of civilian personnel residing in
_____		City 1 _____
_____		City 2 _____
_____		City 3 _____
_____		City 4 _____
_____		City 5 _____
_____		City 6 _____
_____		City 7 _____
_____		City 8 _____
_____		City 9 _____
_____		City 10 _____
_____		City 11 _____
_____		City 12 _____
_____		City 13 _____
_____		City 14 _____
_____		City 15 _____
_____		City 16 _____
_____		City 17 _____
_____		City 18 _____
_____		City 19 _____
_____		City 20 _____
_____	MC	Number of military personnel currently residing in
_____		City 1 _____ (City 1 must be the city in which the base is located)
_____		City 2 _____
_____		City 3 _____
_____		City 4 _____
_____		City 5 _____
_____		City 6 _____
_____		City 7 _____
_____		City 8 _____
_____		City 9 _____
_____		City 10 _____
_____		City 11 _____
_____		City 12 _____
_____		City 13 _____
_____		City 14 _____
_____		City 15 _____
_____		City 16 _____
_____		City 17 _____
_____		City 18 _____
_____		City 19 _____
_____		City 20 _____

APPENDIX B  
VARIABLE DEFINITIONS, "LOSER" MODEL

Variable	Definition
ALC	= Fraction of positions terminated or relocated held by civilians.
ALMP	= Fraction of positions terminated or relocated held by military permanent parties who transfer.
ALMS	= Fraction of positions terminated or relocated held by military permanent parties.
ALMT	= Fraction of positions terminated or relocated held by military trainees who transfer.
ALP	= Fraction of positions terminated or relocated held by civilians who will be placed elsewhere.
ALRC	= Fraction of positions terminated or relocated held by civilians who retire.
ALRM	= Fraction of positions terminated or relocated held by military permanent parties who retire.
ALSP	= Fraction of positions terminated or relocated held by civilians who will separate from USAF.
ALT	= Fraction of positions terminated or relocated held by civilians who will transfer with the realignment.
BETCO	= Fraction of civilian personnel who own their own home.
BETCR	= Fraction of civilian personnel who rent.
BETMPO	= Fraction of military permanent parties who own their own homes.
BETMPR	= The fraction of military permanent parties who rent housing off-base.
BETMTO	= The fraction of military trainees who own their own home.
BETMTR	= The fraction of military trainees who rent housing units off-base.
COL	= The number of civilians who own their own home who will leave the region.
COLC	= The number of civilians who own their own home who will leave the city.
CPI	= Consumer price index.
CPIt3	= Consumer price index at t3.
CPIt4	= Consumer price index at t4.
CPITF	= Consumer price index at tf.

CPITH = Consumer price index at th.  
 GNP Price Deflator for th.

CRL = The number of civilian personnel who rent who leave the region.

CRLC = The number of civilian personnel who rent in city who leave the city.

DDY = Deviation from the mean change in personal income (in constant dollars).

DEL = Percentage deviation from the mean change in total personal income.

DELMIN = Lower bound threshold for annual change in personal income.

DHAT2 = Change in total housing vacancies caused by realignment.

DHAT2R = Change in renter housing vacancies caused by the realignment.

DKMD = The number of on-base dormitory units occupied at tl.

DKMF = The number of on-base family housing units occupied at tl.

DLMP = The number of military permanent parties living on-base.

DLMT = The number of military trainees living on-base.

DHAT20 = Change in owner occupied vacancies caused by the realignment.

DMP = Number of military permanent parties living off-base at tl.

DMT = Number of military trainees living off-base at tl.

DY = Change in real income in constant dollars.

E = Unemployment rate at t2, including the effects of the AF action.

E2 = The employment rate at t2 excluding the effects of the action.

EAF = The change in the size of the labor force due to the USAF action.

ECAP = The threshold level of the ratio of regional unemployment to national unemployment.

EE = The most recently recorded unemployment rate in ROI.

EE1 = The unemployment rate in the ROI for the most recently completed calendar year.

EE2 = The unemployment rate in the ROI two years before the most recently recorded date.

EEE = The most recently recorded unemployment rate.

EJT6 = National Employment for t6 in each of 5 sectors (Mfg., Trade, Finance, Services).

EK = The change in the number of persons employed due to the change in base construction expenditures caused by USAF action.

EKSt5 = Total state employment in the construction sector at t5.

EMAX = The threshold unemployment level.

EMP = Number of military permanent parties who transfer.

EMT = Number of military trainees who transfer.

EN = The most recently recorded national unemployment rate.

ENU = Total national employment for tf.

EP = Number of civilian personnel who are placed by DOD in other positions.

EPSIF = Wage adjustment factor for tf.

EPSIH = Per capita income adjustment factor for th.

EPSIT3 = Wage adjustment factor for t3.

ERC = Number of civilian personnel who retire.

ERM = Number of military permanent parties who retire.

ERST3 = Total regional employment in the retail sector in t3.

ES = The number of secondary jobs (indirect and induced) estimated to be lost as a direct result of the action.

ESJ = The number of personnel who leave the ROI who hold second jobs.

ESP = Number of civilian personnel who separate from the USAF.

ESS = The most recently recorded seasonally adjusted unemployment rate for the state.

ESST3 = Total regional employment in the service sector in t3.

ET = The number of civilian personnel who transfer with the realignment.

ET4 = National employment in year t4.

ET6 = National employment in year t6.

ETN = Reads i-th value of EE.

EWd = Number of dependents of USAF personnel who are employed.

EWST3 = Total regional employment in the wholesale sector at t3.

FL = The average family size of the personnel affected by the action.

FMP = Median number of persons per household of military permanent parties.

FMT = Median number of persons per household of military trainees.

FOMP = The fraction of military permanent parties who live on-base.

FOMT = The fraction of military trainees who live on-base.

FT = Median number of persons per household of USAF civilian transferees.

G2 = The average annual population growth rate of the area of analysis at t2 excluding the effects of the realignment.

G2ROI = The average annual population growth rate of the ROI before the action.

GAF = Annualized percentage change in population associated with USAF action.

GAM = The fraction of output from new construction that goes to wages, salaries and property.

GAMM = Fraction of output from new construction that goes to employees compensation (wages and salaries).

GAMN = Fraction of output from new construction that goes to property income.

GDIF = Projected growth rate including realignment minus minimum permissible growth rate.

GHAT = The average annual population growth rate over the period of analysis.

GI = The average annual population growth rate of the ROI for the period between  $t_{i+1}$  and  $t_i$ .

GMIN = The minimum permissible average annual population growth rate, i.e., threshold.

H2 = The total number of year-round housing units at t2.

H2O = The total number of year-round owner occupied or for sale housing units at t2.

H2R = The total number of year-round renter occupied or for rent housing units at t2.

H70 = Total housing stock in 1970.

H70O = Total owner occupied or for sale housing stock in 1970.

H70R = Total renter occupied or for rent housing stock in 1970.

HAZ = The total housing stock at t1-y or t70.

HBZ = The size of the housing stock at t2 + x (or t1-y if projections are not available).

HEO = The most recently recorded number of housing units that are owner-occupied or for sale.

HER = The most recently recorded number of housing units that are renter-occupied or for rent.

I = Counter

J = Counter

JEND = Counter

K = Counter

K1 = Average of the time series for the ratio of personal income to labor income.

K2 = Ratio of non-wage to wage income of primary workers.

KEND = Counter

KY = Number of years of personal and labor income data ( $K_y \leq 10$ ).

L2 = The size of the labor force in the ROI at t2.

LAMBCC = Not Used

LAMBMC = Not Used

LAZ = The size of the labor force at t1-y or t70.

LBZ = The size of the labor force at t2+x or t1-y.

LI = The total number of persons employed by and assigned to the base.

LMP = The number of military permanent parties currently assigned to the base.

LMT = The number of military trainees currently assigned to the base.

LOG10 = Not used except in Ulman-Dacy Factor.

LP = The fraction of civilians placed by DOD outside the region.

LPRT2 = Labor force participation rate at t2.

LRC = The fraction of civilian retirees who leave the region.

LRM = The fraction of military retirees who leave the region.

M = The net regional export base multiplier.

MC(K) = The number of military personnel residing in city i. (Note: City 1 must include military on base.)

MOLC = Total number of military personnel who own their own home in city i who leave the city.

MPOL = Military permanent parties who own their own home who leave the region.

MPRL = Total number of military permanent parties who rent who leave the region (including on-base).

MPRLC = Total number of military permanent parties who rent in city i who will leave the city.

MT = The total number of military personnel assigned to the base.

MTOL = Number of military trainees who own their own homes.

MTRL = Number of military trainees who rent who live in the region (including on-base).

MTRLC = Number of military trainees who rent in city being analyzed.

MU(K) = Fraction of output from new construction that goes to the purchase of materials in each of the 5 sectors (Mfg., Trans, Trade, Finance, Services).

NC(K) = Number of civilian personnel residing in city i.

NCITY = Number of cities being analyzed ( $NC \leq 20$ ).

NT = Total number of civilians assigned to the base.

NU = Fraction of output from new construction that goes to the purchase of materials in other sector.

OMC = Fraction of disposable total personal income of civilian spent in the ROI.

OMMP = Fraction of disposable total personal income of military permanent parties wages spend in the ROI, exclusion of on-base expenditures.

OMMT = Fraction of disposable total personal income of military trainees spent in the ROI.

P2 = Population of region at t2.

P2AFC = Population of city after the effect of the realignment.

P2CI = Population of city at t2 (before action).

PAF = The total population associated with base employees.

PAFC = The total population associated with base employees who live in city i.

PAZ = Population of city being analyzed at  $t1 - y$  or  $t70$ .

PBZ = Population of city being analyzed at  $t2 + x$ .

PDCT4 = Price Deflator, Construction Sector, t4.

PDCT5 = Price Deflator, Construction Sector, t5.

PDIVT3 = Price Deflator, Wholesale Sector, t3.

PDIVT4 = Price Deflator, Wholesale Sector, t4.

PDRT3 = Price Deflator, Retail Sector, t3.

PDRT4 = Price Deflator, Retail Sector, t4.

PDST3 = Price Deflator, Service Sector, t3.

PDST4 = Price Deflator, Service Sector, t4.

PGAM = Regional labor productivity in the sectors that supply the construction sector.

PIP = The fraction of civilians placed by DOD in positions outside the ROI.

PIRC = The fraction of civilian retirees who leave the ROI labor force (i.e., retire from work or leave the ROI).

PIRM = The fraction of military retirees who do not enter the ROI labor force.

PISP = The fraction of USAF personnel that separate who do not become employed elsewhere before t2.

PKS = Regional labor productivity in the construction sector.

PP = Population of city for number of years specified in NYEAR.

PRS = The productivity (sales per employee) in the retail trade and personal service sectors in the ROI.

PRTLZ = Calculated participation rate of civilian labor force.

PSIO = The fraction of the t2 housing stock that is owner-occupied or for sale.

PSIR = The fraction of the t2 housing stock that is renter-occupied or for rent.

PT4 = Productivity of the national labor force in t4.

PT6 = Productivity of the national labor force in t6.

PWS = Productivity in the wholesale trade and service sectors in the ROI.

R = Ratio of unemployment rate to year of that unemployment.

RHOSJC = The fraction of USAF civilian personnel in ROI who will hold a second job.

RHOSJM = The fraction of military permanent parties who transfer who held a second job.

RHOWDC = The fraction of USAF civilian personnel in the ROI who have dependents who are employed.

RHOWDM = The fraction of military permanent parties transferring who have dependents who are employed.

RL = Total size of realignment.

RLC = Total number of civilian personnel who will leave the region.

RLMP = The number of military permanent parties who will leave the region as a result of the realignment.

RLMT = The number of military trainees who will leave the region as a result of the realignment.

RLOC = Total number of base personnel who own their own homes who leave the city.  
 RLRC = Total number of off-base personnel who were renting who will leave city i.  
 RLTC = Total number of military and civilians who will leave city being analyzed.  
 RMEAN = The mean of the time series of the ratio of regional unemployment to national unemployment.  
 RPAZ = The population of the region at t1-y or t70.  
 RPBZ = The population of the region at t2+x or t1-y.  
 RPLBZ = The projected total population at same date as labor force (LBZ).  
 RSIGM = The standard deviation of the unemployment rate in the ROI.  
 SIGMA = Fraction of after-tax total personal income remaining after savings.  
 SJT6(K) = National output for t6 in each of 5 sectors (Mfg., Trans., Trade, Finance, Services).  
 SKST5 = State Construction sector receipts for the most recently recorded year (t5).  
 SQRT = Square root function.  
 SRST3 = Regional retail sector sales for year t3.  
 SSST3 = Regional service sector sales for year t3.  
 SWST3 = Regional wholesale sector sales for the most recently recorded year (t3).  
 T1 = The date of initiation of the action.  
 T2 = The date of completion of the action.  
 TAU = Fraction of total personal income remaining after taxes.  
 TEMPM = Temporary multiplier inputed.  
 THAZ = Date of Haz data.  
 THBZ = Date of Hbz data.  
 THETA = The fraction of USAF personnel who currently reside in the ROI.  
 THETAC = The fraction of USAF personnel who currently reside in the city being analyzed.  
 TLAZ = Date of Laz.  
 TLBZ = Date of Lbz.  
 TP = Date of PP data.  
 TPAZ = Date of Paz data.

TPBZ = Date of Pbz data.  
 TRPAZ = Date of RPAZ data.  
 TRPBZ = Date of RPBZ data.  
 U2 = The number of unemployed in the ROI at t2 excluding the effects of the USAF action.  
 UAF = The change in the number of unemployed as a result of the USAF action.  
 UD = The Ullman-Dacey factor.  
 V = New (post-closure) housing vacancy rate.  
 VDIF = New vacancy rate minus old vacancy rate.  
 VDIFO = New owner occupied vacancy rate minus old rate.  
 VDIFR = New renter occupied vacancy rate minus old rate.  
 VE = The most recently recorded total housing stock vacancy rate.  
 VEO = The most recently recorded owner-occupied housing vacancy rate.  
 VER = The most recently recorded renter-occupied housing vacancy rate.  
 VHAT2 = Percentage change in the number of total housing units which will become vacant.  
 VHAT20 = Percentage change in the number of owner-occupied housing units which will become vacant.  
 VHAT2R = Percentage change in renter-occupied housing units which will become vacant.  
 VMAX = The allowable housing vacancy rate threshold.  
 VMAXO = The allowable owner occupied housing vacancy rate threshold.  
 VMAXR = The allowable renter occupied housing vacancy rate threshold.  
 VO = The new (post-closure) owner-occupied vacancy rate.  
 VR = The new (post-closure) renter-occupied vacancy rate.  
 WC = Total personal income of civilian personnel affected by the action.  
 WMP = Total personal income of military permanent parties affected by the action.  
 WMT = Total personal income of military trainees affected by the action.  
 WNU = Total personal income per employed worker at tf.  
 WRS = The average wage in the region's retail trade and personal services sector.

WRST3 = The total regional wages in the retail sector in t3.  
 WSST3 = The total regional wages in the selected services sector in t3.  
 WWC = The average wage in civilian personnel affected by the action.  
 WWMP = The average wage of military permanent parties affected by the action.  
 WWMT = The average wage of military trainees affected by the action.  
 WWS = Average gross wage per worker in wholesale and services sector at t4.  
 WWST3 = The total regional wages in the wholesale sector in t3.  
 XIMP = The fraction of military who live off-base who are permanent parties.  
 XIMT = The fraction of military who live off-base who are trainees.  
 Y = Total personal income for ROI for number of years specified in Ky.  
 Y2 = The total regional personal income at t2.  
 YAF = The total change in personal income resulting from the action.  
 YC = Disposable total personal income in ROI associated with civilian personnel affected by action.  
 YDELTA = Percentage change in total personal income in the ROI resulting from the realignment.  
 YH = Regional per capita income for the most recorded year, th.  
 YIG = The change in total amount spent by military civilian personnel in the ROI due to the realignment.  
 YK = National personal income from other labor income in tf.  
 YKG = Change in construction expenditures because of the action.  
 YKST4 = Total state output for the construction sector in t4.  
 YL = Wages and salaries for ROI for years specified in KY.  
 YM = National personal income from wages and salaries.  
 YMEAN = Average annual change in total regional income.  
 YMP = Disposable total personal income in ROI associated with military permanent parties affected by the action.  
 YMT = Disposable total personal income in ROI associated with trainees affected by action.  
 YN = National personal income of proprietors.

YPG = The change in USAF procurement expenditures in the ROI due to the realignment.  
 YPI = Total amount of procurement expenditures in ROI.  
 YQ = Total amount of procurement expenditures in ROI for commissary and BX goods purchased by retirees.  
 YRST4 = Total regional output or sales for the retail sector in t4.  
 YS = The total income of people holding secondary jobs (included and indirect jobs affected by unemployment) adjusted for multiplier effects.  
 YSNW = Non-wage income associated with secondary job estimate.  
 YSST4 = Total regional output or sales for the service sector in t4.  
 YT = Not Used. Delete  
 YT4 = National output in year t4.  
 YT6 = National output in year t6.  
 YW = The total personal income of USAF personnel involved in realignment.  
 YWST4 = Total regional output or sales for the wholesale sector in t4.  
 YY2 = The per capita personal income at t2.  
 Z = The number of workers entering the area.  
 ZETSJ = Second job full-time employment equivalency factor.  
 ZETWD = Working dependent full-time employment equivalency factor.

APPENDIX C

```

RELTL CF*ORSAS.ORSAST#0
ELT077 RL1870 08/17-18:11:51-(2,)
000001 002 C PROGRAM GR11(INPUT,OUTPUT,TAPE1,TAPE3,TAPE6
000002 001 C *,TAPE5=OUTPUT)
000003 000 C* 6 EBCDIC LOSER
000004 000 C* FILE 1(KIND=DISK,ITITLE='FRANKC1',FILETYPE=7)
000005 000 C* FILE 3(KIND=DISK,ITITLE='FRANKC3',FILETYPE=7)
000006 000 C* FILE 5(RMT,UNIT=REMOTE,IO,RECORD=13)
000007 000 REAL MU(5),SJT6(5),EJT6(5),M,NU,LI,LRZ,LA7,L2,FF(10),EN(10)
000008 000 REAL PI(20),TP(20),ALMT,LMP,MC(20),NC(20),K1,K2,YT(10),YL(10)
000009 000 REAL CPI(4),CPI(3),CPI(2),CPI(1),CPI(10),DY(10),DDY(10),DFL(10)
000010 000 REAL LAMBCC,LAMRMC,G2ROI,RPLBZ,PRTLRZ,LPRZ
000011 000 REAL LRC,LRM,YY2,EEE,EE1,EE2,THFTAC
000012 000 REAL MPRL,MTRL,CHL,CRLC,MPRI C,MPOL,MTOL,COL,COI C,MOLC
000013 000 C* UNEMPLOYMENT CALCULATIONS
000014 001 READ(4,*)YT4,YT6,ET4,ET6,MU,GAMM,GAMN,SJT6,FJT6,PDCT5,
000015 000 PDCT4,SKST5,FKST5,SWST3,PDIVT4,PDIVT3,SRST3,
000016 000 PDRT3,PDRT4,SSST3,PDST4,PNST3,EWST3,FSST3,FRST3,
000017 001 YPI,YQ,LI,YKG,TAU,SIGMA,
000018 000 WMT,WMP,WWC,OMMP,OMMT,OMC,
000019 000 RHOWDC,RHOWNM,ZETWD,LRZ,TLRZ,LA7,TLA7,E2,
000020 000 T2,T1
000021 001 READ(4,*) RPBZ,TRPBZ,FFAZ,TRPAZ
000022 002 READ(3,*) RL,ALM,ALSP,ALP,ALRC,ALMP,ALRM
000023 000 READ(3,*) PIP,PIRC,PIRM,PISP,RHOSJC,RHOSJM,ZETSJ
000024 001 READ(4,*) K2,KY,(Y(I),I=1,KY),(YL(I),I=1,KY),(CPI(I),I=1,KY)
000025 002 CALL CONNEX(6)
000026 000 PT4=YT4/ET4
000027 000 PT6=YT6/ET6
000028 000 DO 10 K=1,5
000029 000 NU=NU+MU(K)
000030 000 CONTINUE
000031 000 GAM=GAM+GAMM+GAMN
000032 000 PGAM=U.
000033 000 DO 20 K=1,5
000034 000 PGAM=PGAM+PT4+SJT6(K)+1000.0*MU(K)/(PT6*FJT6(K)*NU)
000035 000 CONTINUE
000036 000 YKST4=SKST5*PDCT4/PDCT5
000037 000 PKS=YKST4/EKST5
000038 000 P2=((RPBZ-RPAZ)*(T2-TRPAZ))/(TRPBZ-TRPA7))+RPAZ
000039 000 UD=.1*ALOG10(P2)-.1
000040 000 ME1./(1.-UD)-1.
000041 002 WRITE(6,1) M
000042 002 PRINT(5,1) M
000043 000 1 FORMAT(' CALCULATED M VALUE=',F5.4)
000044 002 WRITE(6,2)
000045 000 2 FORMAT(' IF YOU WISH TO CHANGE M ENTER NON ZERO VALUE M=')
000046 001 READ(5,3) TEMPM
000047 000 READ(5,3) TEMPM ***** CHANGED TO ABOVE CARD *****
000048 002 CALL DISCON(6)
000049 000 3 FORMAT(F10.5)
000050 000 IF(TEMPM .GT. 0.0) M=TEMPM
000051 002 WRITE(6,2)
000052 002 WRITE(6,400) TEMPM
000053 000 400 FORMAT(1H,T50,F6.4//)
000054 000 Y#ST4=SWST3*PDIVT4/PORT3
000055 000 YRST4=SRST3*PDRT4/PORT3

```

```

000056 YSST4=SSST3*PDST4/PDST3
000057 P#S=(YVST4+YSSST4)/(EWST3+ESSST3)
000058 PRS=(YRST4+YSSST4)/(ERST3+ESSST3)
000059 IF(LI.EQ.0.0) GO TO 21
000060 YPG=(YPI-YQ)*RL/LI
000061 GO TO 25
000062 21 READ(4,*) YPG
000063 25 CONTINUE
000064 ALC=ALT+ALRC+ALSP+ALP
000065 ALMS=ALMP+ALRM
000066 EK=YKG/PKS+M*TAU*SIGMA*GAM*YKG/PRS+NU*YKG/PGAM
000067 K1=0.0
000068 DO 110 K=1,KY
000069 K1=YIK)/YL(K)+K1
000070 110 CONTINUE
000071 K1=X1/KY
000072 IF (K2.LE.0.0) K2=(K1-1.0)/2.0
000073
000074 WMP=RL*ALMS+WMP*(K2+1)
000075 WMP=RL*ALMP+WMP*(K2+1)
000076
000077 WMT=RL*ALMT+WMT
000078 WC=RL*ALC*WC*KI
000079 YMP=WMP*OMMP*TAU*SIGMA
000080 YMT=WMT*OMMT*TAU*SIGMA
000081 YC=WC*OMC*TAU*SIGMA
000082 YIG=YC+YMT+YMP
000083 ES=M*YIG/PKS+M*YPG/PWS+EK
000084 ET=ALT*RL
000085 EMP=ALMP*RL
000086 EMT=ALMT*RL
000087 ERM=ALRM*RL
000088 EP=ALP*RL
000089 ESP=ALSP*RL
000090 ERC=ALRC*RL
000091 ESJ=(ET+PIP*EP)*RHOSJC+EMP*RHOSJM
000092 EWD=(ET+PIP*EP)*RHOWDC+EMP*RHOWDM
000093 UAF=(1-PIRC)*ERC+(1-PIRM)*ERM+PISP*ESP-7FTSJ*ESJ-ZETWD*EWD+ES
000094 EAF=-ET-PIRC*ERC-PIP*EP-ZETWD*EWD+(1-PIRM)*FRM
000095 L2=(LBZ-LAZ)*(T2-TLAZ)/(TLB7-TLAZ)+LAZ
000096 G2R01=(RPBZ-RPAZ)/(RPAZ*(TRPBZ-TRPAZ))
000097 C* THE FOLLOWING STATEMENT WAS ADDED PER SRI 10 NOV 7A
000098 IF (TLBZ.LT.T2) GO TO 27
000099
000100 L2=(LBZ-LAZ)*(T2-TLAZ)/(TLB7-TLAZ)+LAZ
000101
000102 C* THE FOLLOWING STATEMENTS WERE ADDED PER SRI 10 NOV 7A
000103 GO TO 28
000104
000105 27 CONTINUE
000106 C* ALTERNATIVE LABOR FORCE CALCULATIONS
000107 C#
000108 C# G2R01=(RPBZ-RPAZ)/(RPAZ*(TRPBZ-TRPAZ))
000109 RPLBZ=(RPAZ*G2R01*(TLBZ-TRPAZ))+RPAZ
000110 PRTLBZ=LRZ/RPLBZ
000111 LPRT2=PRTLBZ+(PRTLBZ*0.007*(T2-TLAZ))
000112 L2=LPLRT2*P2

```

```

000113 WRITE(6,*) 'G2ROI=',G2ROI
000114 WRITE(6,*) 'RPLRZ=',RPLRZ
000115 WRITE(6,*) 'PRTLKZ=',PRTLKZ
000116 WRITE(6,*) 'LPRT2=',LPRT2
000117 WRITE(6,*) 'L2=',L2
000118 UZ=L2*E2
000119
000120 E=(U2+UAF)/(L2+EAF)
000121 WRITE(6,*) 'PT4=',PT4
000122 WRITE(6,*) 'PT6=',PT6
000123 WRITE(6,*) 'NU=',NU
000124 WRITE(6,*) 'GAM=',GAM
000125 WRITE(6,*) 'PGAM=',PGAM
000126 WRITE(6,*) 'YKST4=',YKST4
000127 WRITE(6,*) 'PKS=',PKS
000128 WRITE(6,*) 'P2=',P2
000129 WRITE(6,*) 'UD=',UD
000130 WRITE(6,*) 'M=',M
000131 WRITE(6,*) 'YWST4=',YWST4
000132 WRITE(6,*) 'YRST4=',YRST4
000133 WRITE(6,*) 'YSST4=',YSST4
000134 WRITE(6,*) 'PWS=',PWS
000135 WRITE(6,*) 'PRS=',PRS
000136 WRITE(6,*) 'YPG=',YPG
000137 WRITE(6,*) 'ALC=',ALC
000138 WRITE(6,*) 'ALRC=',ALRC
000139 WRITE(6,*) 'ALNSE=',ALNSE
000140 WRITE(6,*) 'ALM=',ALM
000141 WRITE(6,*) 'ALMP=',ALMP
000142 WRITE(6,*) 'EK=',EK
000143 WRITE(6,*) 'K1=',K1
000144 WRITE(6,*) 'K2=',K2
000145 WRITE(6,*) 'WMP=',WMP
000146 WRITE(6,*) 'WMT=',WMT
000147 WRITE(6,*) 'WC=',WC
000148 WRITE(6,*) 'YMP=',YMP
000149 WRITE(6,*) 'YMT=',YMT
000150 WRITE(6,*) 'YC=',YC
000151 WRITE(6,*) 'YIG=',YIG
000152 WRITE(6,*) 'ES=',ES
000153 WRITE(6,*) 'ET=',ET
000154 WRITE(6,*) 'EMP=',EMP
000155 WRITE(6,*) 'EMT=',EMT
000156 WRITE(6,*) 'ERM=',ERM
000157 WRITE(6,*) 'EP=',EP
000158 WRITE(6,*) 'ESP=',ESP
000159 WRITE(6,*) 'ERC=',ERC
000160 WRITE(6,*) 'ESJ=',ESJ
000161 WRITE(6,*) 'EWD=',EWD
000162 WRITE(6,*) 'UAF=',UAF
000163 WRITE(6,*) 'EAF=',EAF
000164 WRITE(6,*) 'U2=',U2
000165 WRITE(6,*) 'L2=',L2
000166 WRITE(6,*) 'E=',E
000167 READ(3,*) EEE,EE1,EE2,ES
000168 EMAX=AMAX1(1.2*EEE,EE1,EE2,ES)
000169

```

C\* UNEMPLOYMENT THRESHOLDS

```

000170      WRITE(6,*) 'EMAX=', EMAX
000171      READ(3,*) I,(EE(J),J=1,I),(FN(J),J=1,I)
000172      ETN=EE(I)
000173      RMEAN=0.0
000174      RSIGN=0.0
000175      DO 30 K=1,I
000176      IF(EN(K) .EQ. 0.0) GO TO 30
000177      RMEAN=RMEAN+R
000178      RSIGN=RSIGN+R*R
000179      CONTINUE
000180      RSIGN=(I*RSIGN-RMEAN+RMEAN)/(I*(I-1))
000181      RMEAN=RMEAN/I
000182      RSIGN=RSIGN
000183      ECAP=RMEAN*RSIGN
000184      IF(1/E/ETN) .LT. ECAP) GO TO 40
000185      Z=0.0
000186      GO TO 50
000187      40 EMAX=ECAP*ETN
000188      -----
000189      C*
000190      Z=(L2*EMIN+EAF*EMIN-U2-UAF)/(1-EMIN)
000191      C* THIS EQUATION WAS CHANGED TO THE FOLLOWING
000192      Z=(U2+UAF-L2*EMAX-EAF*EMAX)/(1-EMAX)
000193      -----
000194      C*
000195      50 CONTINUE
000196      WRITE(6,*) 'RMEAN=', RMEAN
000197      WRITE(6,*) 'RSIGN=', RSIGN
000198      WRITE(6,*) 'ECAP=', ECAP
000199      -----
000200      C* THE FOLLOWING PRINT WAS CHANGED FROM
000201      WRITE(6,*) EMIN
000202      C* TO THE FOLLOWING STATEMENT ....
000203      WRITE(6,*) 'EMAX=', EMAX
000204      -----
000205      C*
000206      WRITE(6,*) 'Z=', Z
000207      Z=0.0
000208      C* PERSONAL INCOME
000209      READ(4,*) CPIT4,CPIT3,CPITH,CPIIF,ENU,YH,YK,YM,YN,WWST3,WSST3,
000210      * WRST3
000211      EPSIH=CPIT4/CPITH
000212      Y2=YH*EPSIH*P2
000213      YY2=YH*EPSIH
000214      EPSIF=CPIT4/CPIIF
000215      WNU=(YK+YM+YN)*EPSIF/ENU
000216      EPSIT3=CPIT4/CPIT3
000217      WWS=(WST3+WSST3)*EPSIT3/(EUST3+FSST3)
000218      WRS=(WST3+WSST3)*EPSIT3/(FAST3+FSST3)
000219      YS=WRS*MYIG/PRS+WWS*YPG/PWS+GAM*YKG+
000220      * WRS*SIGMA*TAU*GAM*YKG/PRS+WNU*NU*YKG/PGAM
000221      YW=WC*WMP+WAT
000222      YSHW=(K1-1.)*YS
000223      YAF=YH+YS+YSNW
000224      YDELTA=YAF/Y2
000225      WRITE(6,*) 'EPSIH=', EPSIH
000226      WRITE(6,*) 'Y2=', Y2
000227      WRITE(6,*) 'EPSIF=', EPSIF
000228      WRITE(6,*) 'WNU=', WNU

```

```

000227 WRITE(6,*) 'EPSIT3=', EPSIT
000228 WRITE(6,*) 'WSE=', WWS
000229 WRITE(6,*) 'WRS=', WRS
000230 WRITE(6,*) 'YS=', YS
000231 WRITE(6,*) 'YW=', YW
000232 WRITE(6,*) 'YSMW=', YSNW
000233 WRITE(6,*) 'YAF=', YAF
000234 WRITE(6,*) 'DELTA=', YDELTA
000235 WRITE(6,*) 'EPSIH=', EPSIH
000236 WRITE(6,*) 'YY2=', YY2
000237 C* PERSONAL INCOME THRESHOLD
000238 KEND=KY-1
000239 YMEAN=0.0
000240 DO 120 K=1,KEND
000241 DY(K)=Y(K+1)*CPI4/CPI(K+1)-Y(K)*CPI4/CPI(K)
000242 YMEAN=YMEAN+DY(K)
000243 CONTINUE
000244 120
000245 YMEAN=YMEAN/(KEND*E2)
000246 DELMIN=999999999.
000247 DO 130 K=1,KEND
000248 DDY(K)=DY(K)-YMEAN
000249 DEL(K)=DDY(K)/(Y(K)*CPI(K))
000250 IF(DEL(K) .LT. DELMIN) DELMIN=DEL(K)
000251 CONTINUE
000252 130
000253 DELMIN=DELMIN*.67
000254 WRITE(6,*) 'YMEAN=', YMEAN
000255 WRITE(6,*) 'DELMIN=', DELMIN
000256 C* POPULATION
000257 C* READ ALL DATA FOR REGION FOR HOUSING AND POPULATION
000258 C* READ POPULATION DATA FOR REGION
000259 READ(3,*) THETA
000260 READ(4,*) LMP
000261 READ(4,*) LMT
000262 WRITE(6,*) 'LMT=', LMT
000263 READ(3,*) RETCO,RETMO,BETMO,BETCR,BETMPR,RETMR
000264 READ(3,*) DKMF,FOMP,FOMT,LRC,LP,LRM,
000265 NCITY,((NC(K),MC(K)),K=1,NCITY)
000266 C* DO HOUSING AND POPULATION CALCULATIONS FOR REGION
000267 DLMT=LMT*FOMT
000268 DKMD=DLMP+DLMT-DKMF
000269 IF (DKMD .LT. 0.0) DKMD=0
000270 WRITE(6,*) 'DKMF=', DKMF
000271 WRITE(6,*) 'FOMP=', FOMP
000272 WRITE(6,*) 'FOMT=', FOMT
000273 WRITE(6,*) 'LMP=', LMP
000274 WRITE(6,*) 'DLMT=', DLMT
000275 WRITE(6,*) 'DLMP=', DLMP
000276 WRITE(6,*) 'DKMD=', DKMD
000277 DMP=LMP-DLMP
000278 DMT=LMT-DLMT
000279 IF (DMT .LT. 0.0) DMT=0
000280 XIMT=DMT/(DMT+OMP)
000281 XIMP=1.-XIMT
000282 WRITE(6,*) 'DMP=', DMP
000283 WRITE(6,*) 'DMT=', DMT

```

```

000284 WRITE(6,*) 'DKMF=', DKMF
000285 WRITE(6,*) 'DKMD=', DKMD
000286 WRITE(6,*) 'XIMP=', XIMP
000287 WRITE(6,*) 'XIMT=', XIMT
000288 RLC=ET+LRC+ERC+LP*EP
000289 RLMT=EMT
000290 RIMP=EMP+LRM+ERM
000291 WRITE(6,*) 'RLC=', RLC
000292 WRITE(6,*) 'RLMT=', RLMT
000293 WRITE(6,*) 'RLMP=', RLMP
000294 NT=0.0
000295 MT=0.0
000296 DO 70 K=1,NCITY
000297 NT=NT+NC(K)
000298 MT=MT+MC(K)
000299 70 CONTINUE
000300 WRITE(6,*) 'NT=', NT
000301 WRITE(6,*) 'MT=', MT
000302 READ(4,*) FT,FMP,FMT
000303 FL=(FT*ALT+FMP*ALMP+FMT*ALMT+FT*ALRC+FMP*ALRM)/(ALT+ALMP
* +ALMT+ALRC+ALRM)
000304 WRITE(6,*) 'FL=', FL
000305 WRITE(6,*) 'FT=', FT
000306 WRITE(6,*) 'FMP=', FMP
000307 WRITE(6,*) 'FMT=', FMT
000308
000309
000310
000311
000312
000313
000314
000315
000316
000317
000318
000319
000320
000321
000322
000323
000324
000325
000326
000327
000328
000329
000330
000331
000332
000333
000334
000335
000336
000337
000338
000339
000340

```

C\* THE FOLLOWING STATEMENTS WERE ADDED PER SRI 10 NOV 78  
PAF=(RLC+RLMT+RLMP)\*FL  
BETCR=1-BETCO  
BETMPR=1-BETMPO  
BETMTR=1-BETMTO  
C\* -----  
WRITE(6,\*) 'PAF=', PAF  
C\* -----  
MPRL=BETMPR\*RLMP  
MTRL=BETMTR\*RLMT  
CRL=BETCR\*RLC  
WRITE(6,\*) 'MPRL=', MPRL  
WRITE(6,\*) 'MTRL=', MTRL  
WRITE(6,\*) 'CRL=', CRL  
WRITE(6,6)  
6 FORMAT(' POPULATION GROWTH RATE IN ROI')  
GAF=PAF\*THETA/((T2-T1)\*P2)  
GHAT=62ROI-GAF  
WRITE(6,\*) 'GAF=', GAF  
WRITE(6,\*) '62ROI=', 62ROI  
WRITE(6,\*) 'GHAT=', GHAT  
C\* -----  
C\* DO HOUSING AND POPULATION CALCULATIONS FOR CITY  
DO 200 K=1,NCITY  
WRITE(6,4)  
4 FORMAT(' NEW CITY')  
READ(4,\*) PBZ,TPRZ,PAZ,TPAZ  
P2CI=((PBZ-PAZ)\*(T2-TPAZ))/(TPRZ-TPAZ)+PAZ  
THETAC=(NC(K)+MC(K))/(MT+NT)  
PAFC=THETAC\*PAF

```

000341 GAF=PAFC/((T2-T1)*P2CI)
000342 G2=(PBZ-PAZ)/(PA7*(TPBZ-TPA7))
000343 GHAT=G2-GAF
000344
000345 C* P2AFC=P2CI+PAF*THETAC
000346 C* P2AFC=P2CI-PAFC
000347
000348 WRITE(6,*) 'PAFC=', PAFC
000349 WRITE(6,*) 'GAF=', GAF
000350 WRITE(6,*) 'G2=', G2
000351 WRITE(6,*) 'GHAT=', GHAT
000352 *WRITE(6,*) 'P2CI=', P2CI
000353 *WRITE(6,*) 'P2AFC=', P2AFC
000354 *WRITE(6,*) 'THETAC=', THETAC
000355
000356 C* POPULATION THRESHOLDS
000357 READ(4,*) I,(PP(J),J=1,I),(TP(J),J=1,I)
000358 JENDE=I-1
000359 GMIN=999999999.
000360 DO 60 J=1,JEND
000361 GI=(PP(J+1)-PP(J))/(TP(J+1)-TP(J))*PP(J)
000362 IF (GI .LT. GMIN) GMIN=GI
000363
000364 60 CONTINUE
000365 IF (GMIN .GT. 0.0) GMIN/=GMIN*.8
000366 IF (GMIN .EQ. 0.0) GMIN=-.02
000367 IF (GMIN .LT. 0.0) GMIN=GMIN*1.2
000368 GU1F=GHAT-GMIN
000369 WRITE(6,*) 'GMIN=', GMIN
000370 WRITE(6,*) 'GDIFF=', GDIF
000371
000372 C* HOUSING
000373 IF (G2 .GE. .010) GO TO 75
000374 VMAXO=-.010
000375 VMAXR=.040
000376 GO TO 85
000377 IF (G2 .GT. .050) GO TO 80
000378 VMAXO=0.015
000379 VMAXR=.060
000380 GO TO 85
000381 VMAXO=-.020
000382 VMAXR=.080
000383 CONTINUE
000384 READ(4,*) HBZ,THBZ,HAZ,THAZ,H700,H70R
000385 READ(4,*) VE
000386 IF (VE .NE. 0.0) GO TO 90
000387 READ(4,*) HEO,HER,VEO,VER
000388
000389 C* THE FOLLOWING STATEMENTS WERE ADDED PER SRI 10 NOV 78
000390 90 CONTINUE
000391 CRLC=CRL*NC(K)/NT
000392 IF (K.GT.1.0) GO TO 95
000393 MPRLC=MPRL*MC(K)/MT-OLMP*RL*(ALMP+ALRM)/LMP
000394 IF (LMT.EQ.0.0) GO TO 96
000395 MTRLC=MTRL*MC(K)/MT-OLMT*RL=ALMT/LMT
000396 GO TO 96
000397 95 MPRLC=MPRL*MC(K)/MT
000398 MTRLC=MTRL*MC(K)/MT
000399 96 RLC=CRLC+MPRLC+MTRLC
000400 MPOL=BETMPO*RLMP

```

```

000198 MTOL=BEIMTO*RLMT
000199 COL=BETCO*RLC
000200 COLC=COL*NC(K)/NT
000201 MOLC=(MPOL+MTOL)*MC(K)/MT
000202 RLOC=MOLC*COLC
000203 WRITE(6,*) 'NC=', NC
000204 WRITE(6,*) 'MC=', MC
000205 WRITE(6,*) 'RLOC=', RLOC
000206 WRITE(6,*) 'RLRC=', RLRC
000207 RLTC=(RLMP+RLMT)*MC(K)/MT+RI C*NC(K)/NT
000208 IF(K.GT.1.0) GO TO 97
000209 IF(LMT.EQ.0.0) GO TO 97
000210 RLTC=RLTC-DLMP*RL*(ALMP+ALRM)/LMP-DL*MT*RL*ALMT/LMT
000211 97 CONTINUE
000212 DHAT2=RLTC
000213 WRITE(6,*) 'CRLC=', CRLC
000214 WRITE(6,*) 'MPRLC=', MPRLC
000215 WRITE(6,*) 'MTRLC=', MTRLC
000216 WRITE(6,*) 'MPOL=', MPOL
000217 WRITE(6,*) 'MTOL=', MTOL
000218 WRITE(6,*) 'COL=', COL
000219 WRITE(6,*) 'COLC=', COLC
000220 WRITE(6,*) 'MOLC=', MOLC
000221
000222 C* THE FOLLOWING STATEMENT WAS CHANGED FROM
000223 C* IF (K.EG.1.0) RLRC=RLRC-DI MF-DLMD
000224 C* TO THE NEW STATEMENT AS FOLLOWS ...
000225 C* IF (K.EG.1.0) RLRC=RLRC-DKMF-DKMD
000226 C* --THE ABOVE STATEMENT DELETED PER SRI 10 NOV 78
000227 C*
000228 C* END OF ADDITIONS PER SRI 10 NOV 78
000229 C*
000230 -----
000231 DHAT2=RLRC
000232 DHAT20=RLC
000233 H2=(HBZ-HAZ)*(T2-THAZ)/(THB7-THAZ)+HAZ
000234 IF (VE.GT.0.0) GO TO 93
000235 PSIR=HER/(HEO+HER)
000236 H20=PSIO*H2
000237 H2R=PSIR*H2
000238 VHAT20=DHAT20/H20
000239 VHAT2R=DHAT2R/H2R
000240 VO=VHAT20+VEO
000241 VR=VHAT2R+VER
000242 VDIFR=VO-VMAXO
000243 WRITE(6,*) 'DHAT2R=', DHAT2R
000244 WRITE(6,*) 'DHAT20=', DHAT20
000245 WRITE(6,*) 'H2=', H2
000246 WRITE(6,*) 'PSIO=', PSIO
000247 WRITE(6,*) 'PSIR=', PSIR
000248 WRITE(6,*) 'H2R=', H2R
000249 WRITE(6,*) 'H20=', H20
000250 WRITE(6,*) 'VHAT2R=', VHAT2R
000251 WRITE(6,*) 'VHAT20=', VHAT20
000252 WRITE(6,*) 'VO=', VO
000253
000254

```

```

000455      WRITE(6,*) 'VR=', VR
000456      WRITE(6,*) 'VMAXO=', VMAXO
000457      WRITE(6,*) 'VMAXR=', VMAXR
000458      WRITE(6,*) 'VDIFO=', VDIFO
000459      WRITE(6,*) 'VDIFR=', VDIFR
000460      GO TO 200
000461      VHAT2=DHAT2/H2
000462      V=VE+VHAT2
000463      VMAX=H700*VMAXO+H70R*VMAXR
000464      H70=H700+H70R
000465      VMAX=VMAX/H70
000466      VDIF=V-VMAX
000467      000
000468      000
000469      001
000470      000
000471      001
000472      000
000473      001
000474      000
000475      000
000476      001
000477      000
000478      001
000479      000
000480      001
000481      001
000482      001
000483      000
000484      000
000485      000

          93
          C* THE FOLLOWING STATEMENT WAS CHANGED FROM ....
          C* WRITE(6,*) DHAT
          C* TO THE FOLLOWING STATEMENT ....
          WRITE(6,*) 'DHAT2=', DHAT2
          C*
          C* WRITE(6,*) 'H2=', H2
          C*
          C* THE FOLLOWING STATEMENT WAS CHANGED FROM ....
          C* WRITE(6,*) VHAT
          C* TO THE FOLLOWING STATEMENT ....
          WRITE(6,*) 'VHAT2=', VHAT2
          C*
          C* WRITE(6,*) 'V=', V
          C* WRITE(6,*) 'VMAX=', VMAX
          C* WRITE(6,*) 'VDIF=', VDIF
          C* CONTINUE
          STOP
          END
          200

```

END ELT.

98K

```

QELT,L CF*QRSAS,QRSAST*0
ELT077 RLI070 08/17-14:11:51-(2,)
000001 002 C PROGRAM QRII(INPUT,OUTPUT,TAPE1,TAPE3,TAPE6
000002 001 C *TAPES=OUTPUT)
000003 000 C* 6 EBCDIC LOSER
000004 000 C* FILE 1(KIND=DISK,ITITLE=FRANKC1,FILETYPE=7)
000005 000 C* FILE 3(KIND=DISK,ITITLE=FRANKC3,FILETYPE=7)
000006 000 C* FILE 5(RMT,UNIT=REMOT,IO=RECORD=13)
000007 000 REAL MU(5),SJT6(5),EJT6(5),W,NU,LI,LRZ,LA7,LA2,FF(10),EN(10)
000008 000 REAL PP(20),TP(20),LMT,LMP,MC(20),NC(20),K1,K2,YT(10),YL(10)
000009 000 REAL CPIT4,CPIT3,CPITH,CPITF,Y(10),CPI(10),DY(10),DDY(10),DNL(10)
000010 000 REAL LAMBC, LAMFMC, G2ROI, RPLRZ, PRTLZ, LPRT2
000011 000 REAL LRC, LPL, LRM, Y2, FEE, EE1, EE2, THEFAC
000012 000 REAL MPRL, MTRL, CHL, CRLC, MPRI, C, MPOL, MTOL, COL, COL, C, MOLC
000013 000 C* UNEMPLOYMENT CALCULATIONS
000014 001 READ(4,*)YT4,YT6,ET4,ET6,MU,GAMM,GAMN,SJT6,EJT6,PDCT5,
000015 000 PDCT4,SKST5,EKST5,SWST3,POIVT4,POIVT3,SRST3,
000016 000 PORT3,PDRT4,SSST3,PNST4,PNST3,EWST3,FSST3,FRST3,
000017 001 YPI,Y0,LI,YKG,TAU,SIGMA,
000018 000 WMT,WMP,WWC,OMMP,OMMT,OMC,
000019 000 RHOWDC,RHOWDM,ZETWD,LRZ,TLRZ,LA7,TLA7,E2,
000020 000 T2,T1
000021 001 READ(4,*)RPBZ,TRPBZ,RPZ,TRPAZ
000022 002 READ(3,*)RL,AL,ALMT,ALSP,ALP,ALRC,ALMP,ALRM
000023 002 READ(3,*)PIP,PIRC,PIRM,PISP,RHOSJC,RHOSJM,ZETSJ
000024 001 READ(4,*)K2,KY:(Y(I),I=1,KY),(YL(I),I=1,KY),(CPI(I),I=1,KY)
000025 002 CALL CONNEX(6)
000026 000 PT4=YT4/ET4
000027 000 PT6=YT6/ET6
000028 000 DO 10 K=1,5
000029 000 NU=NU*MU(K)
000030 000 CONTINUE
000031 000 GAM=GAM+GAMM+GAMN
000032 000 PGAM=PGAM+PT4*SJT6(K)*1000.0*MU(K)/(PT6*EJT6(K)*NU)
000033 000 DO 20 K=1,5
000034 000 CONTINUE
000035 000 YKST4=SKST5*PDCT4/PDCT5
000036 000 PK5=YKST4/EKST5
000037 000 P2=((RPBZ-TRPAZ)*(T2-TRPAZ))/((TRPBZ-TRPAZ))*RPZ
000038 000 UD=.1*ALOG10(P2)-.1
000039 000 M=1/(1.-UD)-1.
000040 000 WRITE(6,1) M
000041 002 PRINT(5,1) M
000042 000 CONTINUE
000043 000 C 1 FORMAT(' CALCULATED M VALUE=',F5.4)
000044 002 WRITE(6,2)
000045 000 C 2 FORMAT(' IF YOU WISH TO CHANGE M ENTER NON ZFRO VALUF M=')
000046 001 READ(5,3) TEMP
000047 000 READ(5,3) TEMP
000048 002 CALL DISCON(6)
000049 000 C 3 FORMAT(F10.5)
000050 000 IF(TEMPM.GT.0.0)M=TEMPM
000051 002 WRITE(6,2)
000052 002 WRITE(6,400)TEMPM
000053 000 FORMAT(1H+,T50,F6.4//)
000054 000 YKST4=SWST3*POIVT4/POIVT3
000055 000 YKST4=SRST3*PORT4/PORT3

```

**1979 USAF - SCEE SUMMER FACULTY RESEARCH PROGRAM**

**Sponsored by the**

**AIR FORCE OFFICE OF SCIENTIFIC RESEARCH**

**Conducted by the**

**SOUTHEASTERN CENTER FOR ELECTRICAL ENGINEERING EDUCATION**

**FINAL REPORT**

**ANALYSIS OF THE ADVANCED SIMULATOR FOR PILOT TRAINING (ASPT):**

**COMPUTER SYSTEM ARCHITECTURE**

<b>Prepared by:</b>	Dr. John Hadjilogiou
<b>Academic Rank:</b>	<b>Associate Professor</b>
<b>Department and University:</b>	Electrical Engineering Department Florida Institute of Technology
<b>Research Location:</b>	Air Force Human Resources Laboratory Flying Training Division Williams Air Force Base, Arizona
<b>USAF Research Colleague:</b>	Mr. Alex Shaw
<b>Date:</b>	August 1979
<b>Contract No:</b>	<b>F49620-79-C-0038</b>

ANALYSIS OF THE ADVANCED SIMULATOR FOR PILOT TRAINING (ASPT):  
COMPUTER SYSTEM ARCHITECTURE

by

Dr. John Hadjilogiou

The goal of this research was to investigate the matter of reliability in a class of distributed information processing systems composed of highly autonomous nodes, e.g. CPU's, connected through common-shared memory modules. Distributed systems are often claimed to be inherently more reliable than systems based on a large central processor. That is, given that a distributed system is properly designed, it offers better reliability. This claim is based on several factors. First, distributed systems by their very nature provide opportunities for redundancy. Second, error propagation is restricted by physical separation of processes and resources. And finally, individual nodes in the distributed system may be less complex than a large central processor and, as a result, ought to have lower probability of failures. Basically, distributed systems have a potential for being more reliable than systems based on a large central processor; however, this potential needs to be exploited through proper design.

Reliability of an information processing system is not merely a question of the hardware components. Software errors, synchronization failures, and errors of the human users must be anticipated and handled gracefully. The only way to design a reliable system is to make it "fault-tolerant", or robust in the face of a large variety of internal failures and misuse.

This report documents the engineering design and development of the ASPT general purpose computer system in its present configuration and contains recommendations for future modification and expansion.

### ACKNOWLEDGEMENT

The author would like to thank the Air Force Systems Command, the Air Force Office of Scientific Research and the Southeastern Center for Electrical Engineering Education for providing him with the opportunity to spend a very worthwhile and interesting summer at the Flying Training Division, Air Force Human Resources Laboratory, Williams Air Force Base, Arizona.

Appreciation is extended to Mr. Glen P. York, AFHRL/FTE Contract Monitor; Major John Kiselyk, AFHRL/FTE; Mr. Terry Templeton, AFHRL/FTE; Mr. Bruce McCreary, University Contractor; Mr. Lynn Thompson, Mr. A. C. Snow, Mr. Dave Palmer, Mr. Art Rossi, and Mr. Jim Waldrop, Systems Engineering Laboratories; and Mr. George Turnage, General Electric Company for the time and support they devoted to this report.

Gratitude is also extended to Ms. Joy Murray for her efforts in typing and proofreading this report.

## TABLE OF CONTENTS

### Acknowledgement

#### I. Introduction

#### II. ASPT System Computation

##### II.1 General Purpose Computation

##### II.2 Special Purpose Computation

#### III. ASPT System Computer Configuration

##### III.1 Basic System Configuration

###### III.1.1 Hardware Architecture

###### III.1.2 Software Function Allocation

##### III.2 Visual System Configuration

###### III.2.1 Hardware Architecture

###### III.2.2 Software Function Allocation

#### IV. Recommendations for Future Development

##### IV.1 Basic Distributive Processor System

###### IV.1.1 A Host Computer

###### IV.1.2 A Multiport Switch System

###### IV.1.3 A Development Support Subsystem

###### IV.1.4 A Portable Diagnostic Console

##### IV.2 Writable Control Storage

##### IV.3 Operating System

##### IV.4 System Expansion for Third Simulator

#### V. Summary

## LIST OF ILLUSTRATIONS

Figure		Page
1	ASPT Basic Five-CPU Distributive Processor System	14
2	ASPT Visual Four-CPU Distributive Processor System	17
3	ASPT Visual Six-CPU Distributive Processor System	18
4	ASPT Basic Six-CPU Distributive Processor System	22

## I. INTRODUCTION

The goal of this research was to investigate the matter of reliability in a class of distributed information processing systems composed of highly autonomous nodes, e.g. CPU's, connected through common-shared memory modules. Distributed systems are often claimed to be inherently more reliable than systems based on a large central processor. That is, given that a distributed system is properly designed, it offers better reliability. This claim is based on several factors. First, distributed systems by their very nature provide opportunities for redundancy. Second, error propagation is restricted by physical separation of processes and resources. And finally, individual nodes in the distributed system may be less complex than a large central processor and, as a result, ought to have lower probability of failures. Basically, distributed systems have a potential for being more reliable than systems based on a large central processor; however, this potential needs to be exploited through proper design.

Reliability of an information processing system is not merely a question of the hardware components. Software errors, synchronization failures, and errors of the human users must be anticipated and handled gracefully. The only way to design a reliable system is to make it "fault-tolerant", or robust in the face of a large variety of internal failures and misuse.

This report documents the engineering design and development of the ASPT general purpose computer system in its present configuration and contains recommendations for future modification and expansion.

## II. ASPT SYSTEM COMPUTATION

The overall simulator system is composed of several SEL's general purpose computers and one GE's large size special purpose computer.

### II.1 General Purpose Computation

The ASPT computation system configuration consists of several high performance SEL 32 general purpose computer systems. The 32-bit computing system is built around a multiple high-speed, synchronous, shared, multiplexed SEL bus and one or more Memory Buses.

The communication between all functional elements of the system is provided by the SEL BUS. The modules that connect to the SEL BUS include: Central Processing Unit (CPU), High-Speed Floating-Point Option (HSF), Writable Control Storage Option (WCS), Real Time Option Modules (RTOM), Input/Output Microprogrammable Processors (IOM), Regional Processing Units (RPU) and High-Speed Data (HSD) Interfaces. Multiprocessor Shared Memory Options and Memory Ports are connected to the SEL bus to support shared and private memory. The SEL Bus distributes information at a rate of 26.67 million bytes per second and is capable of transferring information every 150 nanoseconds. The SEL BUS sends and receives data between the CPU, the Memory Subsystem, the Interrupt Subsystem, and the Input/Output subsystem.

Functionally the computer consists of three major divisions: the CPU, Main Memory, and I/O (External Device interfaces). The three divisions of the computer are interconnected by a network of signal paths. Data processing programs and data are stored in the main memory. Parameters, status, commands, and processor results are exchanged with external devices. All arithmetic and logical functions are processed by the CPU, using its internal Arithmetic Logic Unit (ALU) function.

The CPU which employs instruction look ahead for fast instruction execution consists of four major sections: The Control Section (CROM), containing the controlling microprogram; the Control, Sequencing, and Test logic; the internal storage registers; and the ALU. The instruction repertoire includes 163 standard instructions and a set of eight high-speed general purpose registers for use by the programmer for arithmetic, logical, and shift operations. The High-Speed Floating-Point Option Unit (FPU) provides a 64-bit wide data structure which optimizes floating-point performance.

The Memory Bus Controller (MBC) which can support up to 16 memory modules provides an interface between the SEL BUS and the Memory Bus. If a system is configured with more than four MBC's, every fourth MBC shares an MBC Inhibit line and ID Tag code. In shared memory systems, two MBC's are plugged into dedicated slots at the top and bottom of the shared memory chassis. Inter MBC communication is provided by a group of lines connected across the foreplane section of the MBC boards. All timing in dual processor systems is derived from a single Master 150 - nanosecond clock. The Memory Interface Adapter (MIA) provides a method for connecting remote memory systems.

The IOM consists of three functional parts: a SEL Bus interface, a microprogrammable Processor and a device interface. A number of devices are available to provide custom interfacing. The High Speed Data (HSD) interface is capable of transferring 32 bit data at 3.2 megabytes per second. The Regional Processing Unit (RPU) consists of 2,048 32 bit words of PROM and 4096 32 bit words of RAM for firmware and data. For

the Serial Data Interface (SDI) data, commands, and status are transmitted over the serial link in 20-bit frames at a rate of 10 MHz. Each frame contains a start bit, two tag bits, 16 bits of information and a stop bit. A Manchester bi-phase technique, which is self-clocking and has a narrow bandwidth, is used for transmission on the serial link. The teletypewriter line printer and card reader (TLC) controller is also available and plugs directly into the SEL Bus. The Moving-Head Disc (MHD) subsystem consists of a controller and a master MHD drive and transfers data at the rate of 1.2 million bytes per second. The Asynchronous Data Set Interface (ADS) provides for half or full duplex asynchronous RS232C channels. The basic ADS operates at rates of 50 to 9600 baud and is fully programmable on an individual channel basis. The Magnetic Tape Control Unit (MTC) is also implemented on a single plug-in module.

The computer can accommodate up to 112 hardware priority interrupt levels. These levels are used for IOM's and external signals. Interrupts associated with I/O are provided within the IOM's. External interrupts are provided by Real-Time Option Modules (RTOM). Each RTOM provides 16 external interrupt levels, a real time clock, and a 32-bit programmable internal timer. A system control panel is included in all packages to provide a complete set of operator controls and indicators.

The Program Status Word (PSW) is the control mode which allows the CPU to emulate the environment to run the Real Time Monitor (RTM) Operating System. The CPU may run in the privileged or unprivileged mode. In the privileged mode, the CPU performs all of its control functions and can modify any part of the system. Privileged operation

relates to input/output and to changes in the basic control state of the computer. Unprivileged operation is the problem-solving mode of the CPU. In this mode, memory protection is in effect, and all privileged operations are prohibited.

## II.2 Special Purpose Computation

The special purpose computer performs real time high speed processing on the data received from the general purpose computers and generates the required video signals to simulate the visual environment. The video signals are fed to the CRT electronics subsystems and to the operator stations. Each of the 14 display channels contains 985 active television raster 1000 element lines which are updated at each television frame of 1/30 seconds. Each element requires 10 bits to generate one of the 1024 ( $2^{10}$ ) gray shades which ranges from black to maximum brightness. The CIG system is thus capable in outputting  $(14 \times 985 \times 1000 \times 30 \times 10)$  4137 megabits per second.

The Special Purpose Computer is housed in 17 cabinets. The active environment data is stored in the core memory of cabinet A1. Its function is to accept data and supply the edge data to the edge processor, priority data to the priority processor and channel assignment data to the data product calculator. Active block storage is completely updated as is viewpoint storage. The interface between the core memory and the general purpose computer memory is handled by the interface function contained in the Priority Processor cabinet A2. The priority processor determines the proper priority of objects when in conflict and sets up a listing of all active objects according to their priority. The

vector processor is also contained in cabinet A2 and provides a high speed vector arithmetic data processing. The edge processor cabinet A3 performs edge projections, curved surface shading calculations, three dimensional object fading and light brightness control. It utilizes channel-specific viewpoint data to transform the active environment numerical description held in dynamic and environment storage into a stream of object-and channel-specific visible edges. The output of the edge generator is a series of display edges which are sequentially loaded into the edge generators 1 through 4 located in cabinets A4 and A5. Each edge generator simultaneously generates television raster scan line edge crossing data for the same four successive television raster field scan lines.

The orderer functions to arrange the edge data words received from the edge generator in an ordered sequence. Each orderer cabinet (A6 to A9) processes raster line edge crossing data for one out of every four television raster field lines. With each ordered cabinet, the raster line edge crossing data is ordered in raster line element sequence, and the priority resolver resolves priority conflicts concurrent with digital edge smoothing calculations. The output of each orderer cabinet is put on a data bus which connects the output to the input of the linepaths in all 14 video processor channels, cabinets (A10 to A16). With each video processor, four television raster lines are simultaneously processed, one raster line per line path. The video processor outputs one television raster line at a time in sync with the display television raster. The 10 bit binary gray shade of each display raster element line is converted

into television video signal by means of a precision high speed digital-to-analog converter. The master timing generator generates all of the basic timing clocks for the special purpose computer and provides 30 per second interrupts to both the CIG general purpose computer and the basic simulator general purpose computer. Synchronization of the total ASPT simulator is provided by the master timing which is part of cabinet A5.

### III. ASPT SYSTEM COMPUTER CONFIGURATIONS

The ASPT System is an advanced simulation system that is used in the research program by Air Force Human Resources Laboratory (AFHRL) to investigate the simulator role in the USAF fighter pilot training programs.

The ASPT system is composed of two major configurations: (1) Basic System Configuration and (2) Visual System Configuration. The Basic System uses five Systems Engineering Laboratory's (SEL) 32/75 computers. These five computers form a distributed processor system which has sufficient computation capacity for simultaneous operation of both simulators, all simulator sub-systems, and limited background data processing.

The Visual System, also referred to as Computer Image Generation (CIG) System, is organized into three major equipment areas: (i) the general-purpose computation subsystem (GPC), which consists of four SEL 32/75 computers; two SEL 8600 computers, which are used as an interface between the General Purpose (GP) computer and the Special Purpose (SP) computer; and an Array Processor; (ii) the Special Purpose Computation

Subsystem (SPC), driven by General Electric Special Purpose Computer; and  
(iii) the CRT's electronics.

### III.1 Basic System Configuration.

The Basic System simulates the aircraft flight information which includes the avionics, motions, G-seat, etc.

#### III.1.1 Hardware Architecture.

A five CPU system is configured as shown in Figure 1 with a full complement of peripheral equipment. The Master (OMEGA) CPU has a total of 128K-word of core memory contained in 16 Memory Modules which are divided into two categories: the shared memory modules and the private memory modules. The private memory modules have 96K-word of core which will perform both the RTM and the Terminal Support Subsystem (TSS) operations. The shared memory modules consist of two 16-K-word of core shared between each aircraft simulator and the master CPU, respectively.

The slave (Alpha, Beta, Delta, and Gamma) CPU's each has 32 K-word of core for its private memory and also two 32 K-word of core shared between Alpha and Gamma and between Beta and Delta, respectively.

#### III.1.2 Software Function Allocation

The ASPT Basic simulator on-line software is functionally allocated among the five CPU's as follows:

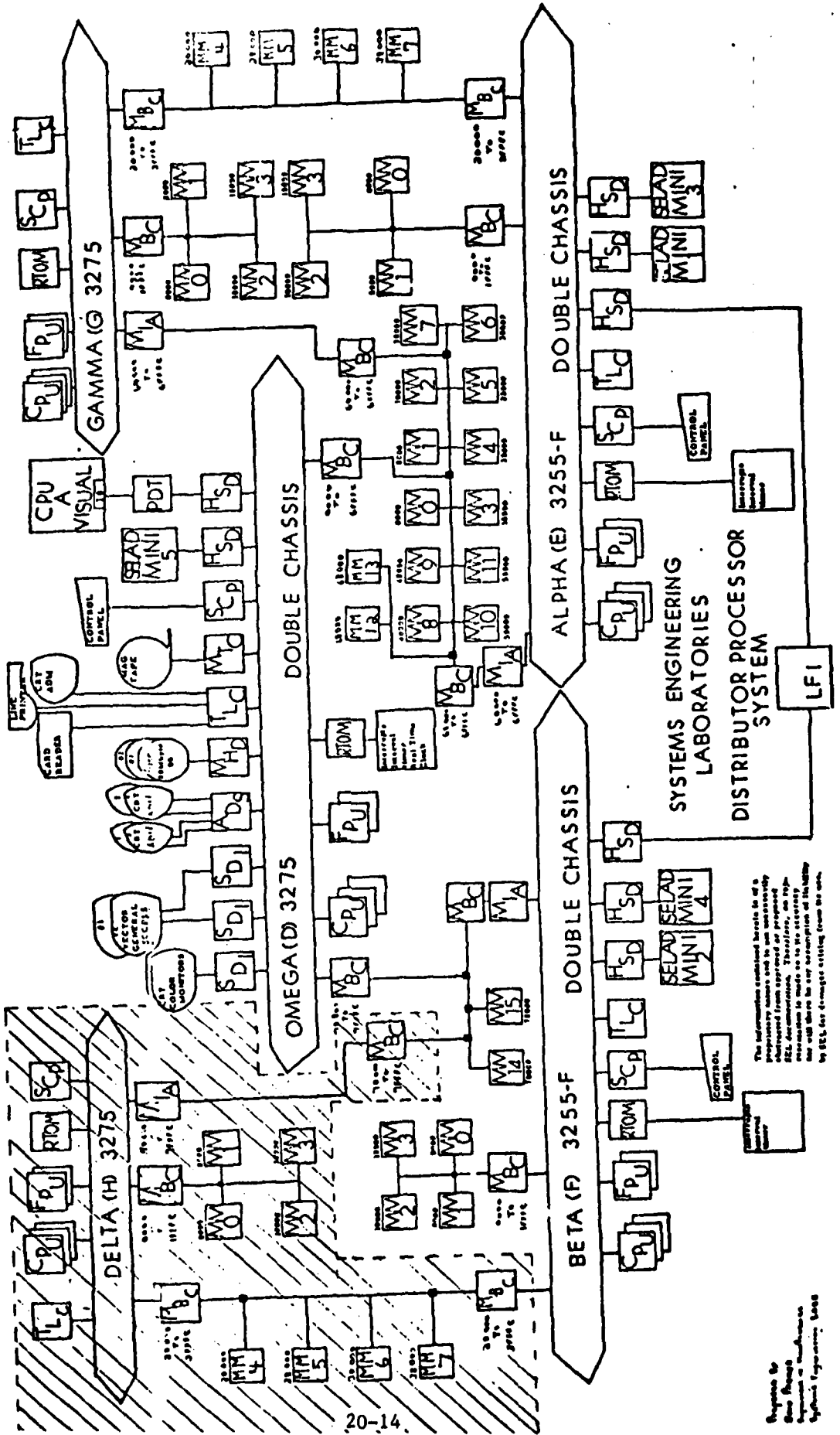
a. Omega (Master) CPU Functions:

RTM

Basic Systems Master Executive

Load slave (boot load)

Two Formation Flight Module



The information contained herein is of a proprietary nature and is not to be disseminated outside the ASPT organization. Therefore, no reproduction is made or to be accepted, in any form, without the prior written permission of the ASPT. All rights reserved.

Prepared by  
 IBM Research  
 Division  
 Systems Engineering, 1968

FIG 1 ASPT BASIC FIVE-CPU DISTRIBUTIVE PROCESSOR SYSTEM

Visual Interface

Navigation Communication

Background Batch Operation

b. Beta and Alpha CPU's Functions

Slave Executive

Flight Module

Accessory Modules (including instrument, sound, electrical,  
hydraulic, etc.)

Engine module

Navigation

Motion Module

G-seat module

Visual fast linkage

c. Delta CPU's Functions

The Delta CPU is dedicated to the Avionic Subsystem of the  
F-16 simulator due to the advanced on-board computer  
system on the F-16. This software includes:

Fire control computer

Bombing and Strafing

Radar Slant

HUD Display

Navigation

Store Management

Visual Initial Module

d. Gamma CPU Functions

For future expansion

III.2 Visual System Configuration. The visual system generates a video signal that, when used with a television display, presents a simulated visual scene to the pilot.

#### III.2.1 Hardware Architecture.

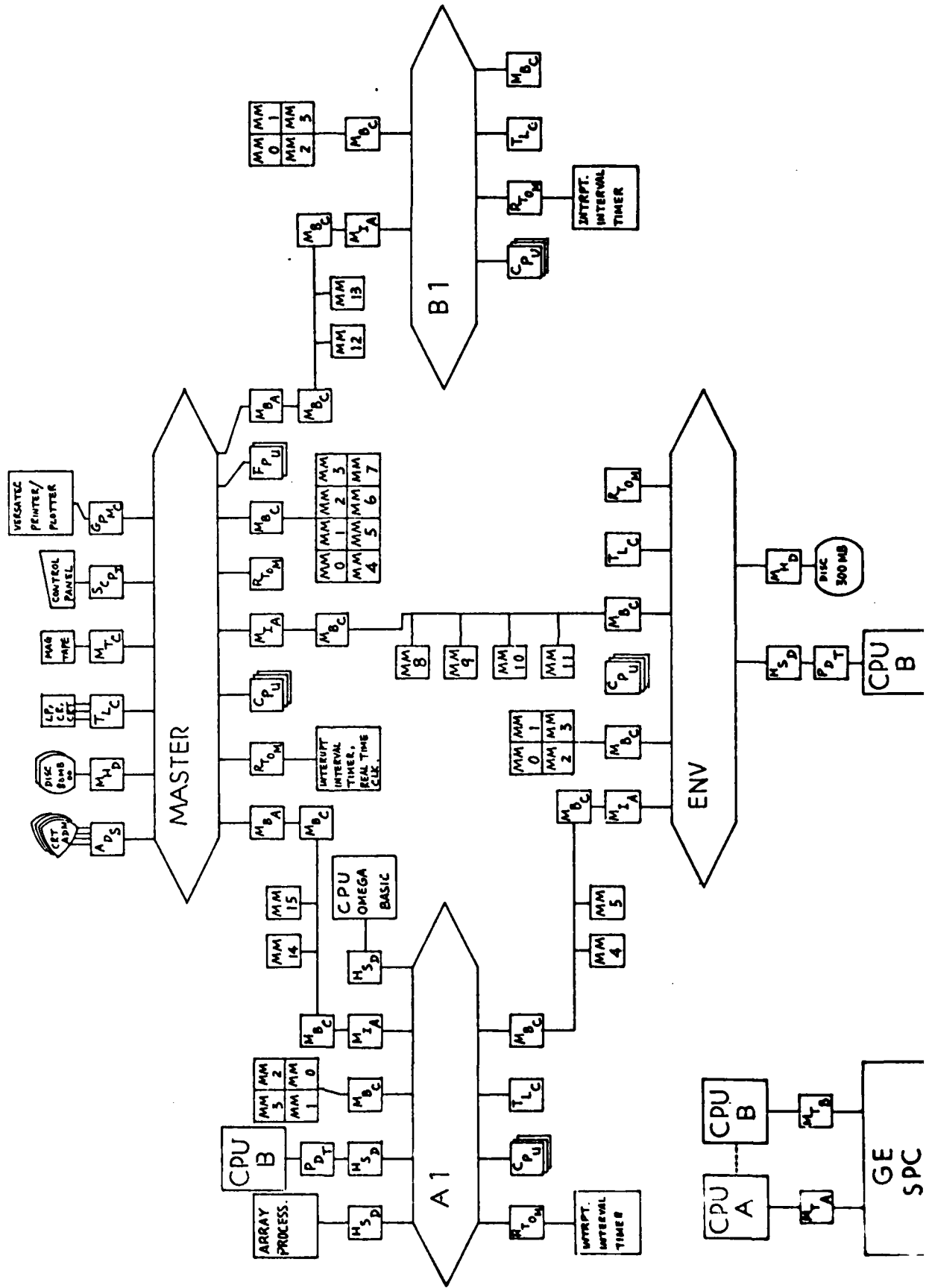
The ASPT Visual GP system requires four SEL 32/75 minicomputers and two SEL 8600 computers with a full complement of peripheral equipment shown in Figure 2. Two SEL 8600 computers are used strictly for interfacing between visual GP computer and visual SP computer, and they will be replaced by two new SEL 32/75 computers in the near future. For the new six CPU's ASPT visual system, (shown in Fig 3) there will be a slight modification on each CPU's function: The Master CPU with 32K-word and the Environment CPU with 32K-word of core will perform the data base updating for the Special Purpose Computer. Four SEL 32-75 minicomputers (A1, A2, B1, and B2) each with 32k words of core will perform the dynamic computation required for dual cockpit operations and will provide room for expansion and system refinements. After being replaced, the two SEL 8600 computers will be used for the Data Base Modeling System for performing the simulation of Frame 1, Frame 2, and user interactive data base development software processing.

#### III.2.2 Software Function Allocation.

ASPT Visual Simulator's on-line software will be functionally located among the four SEL 32/75 CPU's and the two SEL 8600 CPU's as follows:

a. Master CPU functions

RTM





Visual System Master Executive

Load Slaves (Boot Load)

Field-of-view program

Background batch operations

b. Environment CPU Functions

Slave Exec

FIND A10M, IMPACT, INIT

Adjust range for LOD/LOD Processing

Model Read from Disc

Model/object Allocation

Model Ship to B

Impact ship to B

PARAMOD

Stripe Bookkeeping

c. Dynamic A1 CPU Functions

Slave Exec

Receive viewpoint (VP), Moving Model (MM) and Impact data  
from Basic side and convert LAT/LONG to CIG Coordinates  
or Execute JOYSTICK

Ship PAOL/DIRLITE

Transform (RP-MM) to MM coordinates

Compute VP to MM DIR COS Matrix

Channel Assignment Start

Rotate U, V, W's Cockpit A

Blink Lights

- Build Active Object List
- Build Model Priority List
- Array Processor Handler
- d. Dynamic B1 CPU Functions
  - Slave Exec
  - Directional Light Range Adjustments
  - Terrain Elevation Computation
  - Fading
  - MM Size Adjustment
  - Rotate U, V, W's CKPT B
  - Transfer SW vector to MM
  - Pseudo Edge Vector Calc
  - MM Priority
  - Area of Interest (AOI) Bounding Planes
  - Hood Dynamics
  - FINTRAN (Prepare for Dynamic Ship)
- e. CPU A Functions
  - Slave Exec
  - A Serial Terminal
  - B Serial Terminal
  - Channel Assignment
  - Ship Dynamic Data to SPC
- f. CPU-B Functions
  - Slave Exec
  - Ship Environment to SPC

#### IV. RECOMMENDATIONS FOR FUTURE DEVELOPMENT

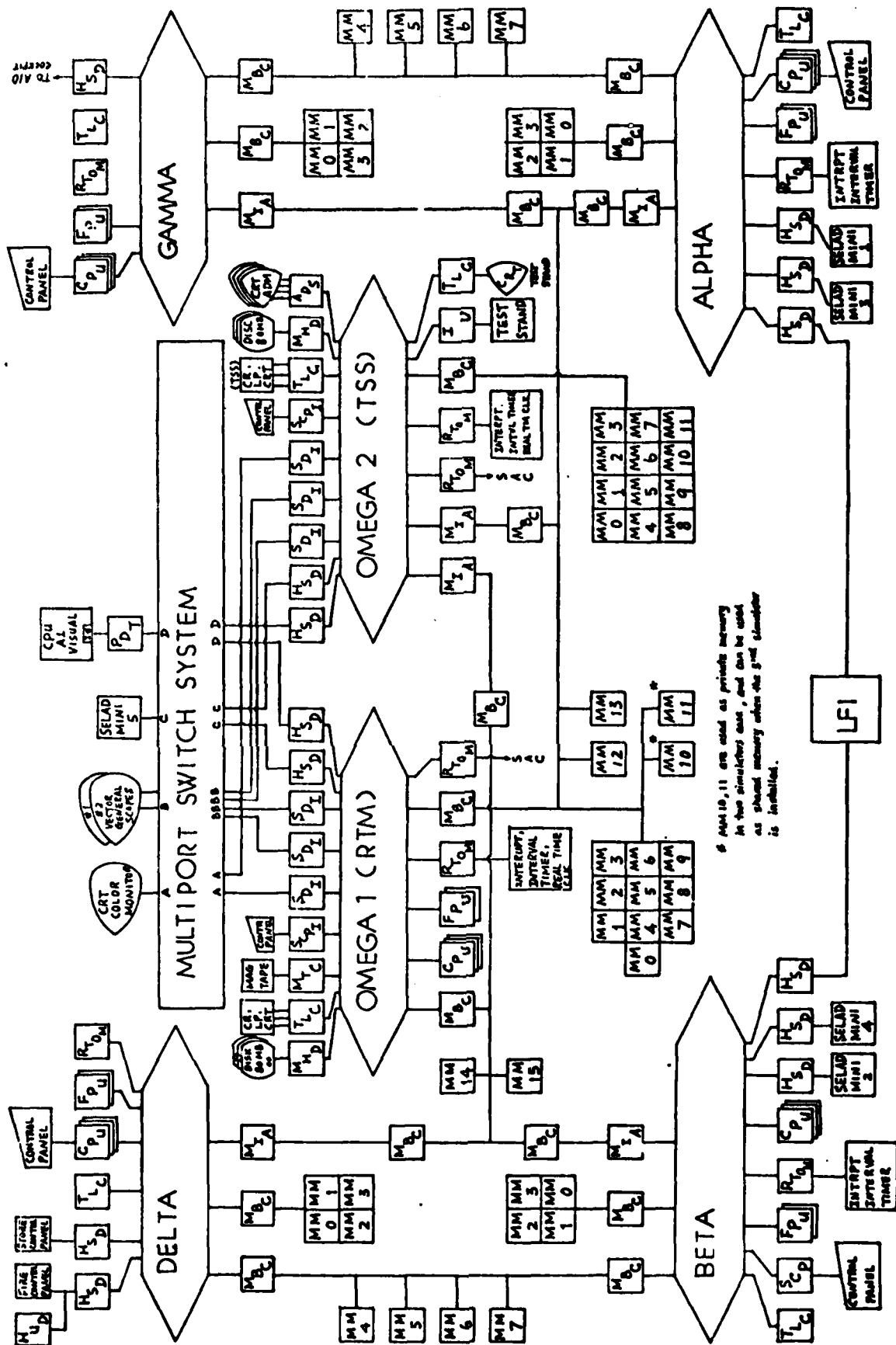
General Description. Distributed systems present a number of new problems that have to be solved to achieve reliable operations. The major problem is uncertainty - the fact that it is impossible to always know the entire global state of the system. Also, in distributed systems, the trade off between reliability and performance becomes much more prominent than in the centralized systems.

##### IV.1 The Basic Distributive Processor System.

The complexity of operations performed by the Distributive Processor's 5 CPU system is increasing. Efficient maintenance becomes more difficult because in order to trouble shoot problems, the entire Basic Simulator processor is needed, and all of the simulator operation will be interrupted. In order to make this system more fault-tolerant, we recommend that the following items be added to the present ASPT Basic System: (a) a new SEL 32/75 computer, (b) a multiport switch system, (c) a Development Support System with a Test Stand and (d) a portable diagnostic console. The advantages of adding each of these components to the present system are described below.

##### IV.1.1 The Host Computer

A new SEL 32/75 computer will serve as a duo-purpose processor, shown in Fig. 4 (a) It will act as a back-up CPU for the Basic Simulator's Master processor, Omega and (b) as a host computer for the Terminal Support Subsystem (TSS). The TSS in conjunction with the Test Stand, which is for Development Support System, will serve multiport terminal users, including text editing, interactive debugging, running



\* MM 10, 11 are used as private memory in the simulator case, and can be used as shared memory when the simulator is inhibited.

FIG 4 ASPT BASIC SIX-CPU DISTRIBUTIVE PROCESSOR SYSTEM

diagnostics, checking and updating IOM and RTOM boards, and batch job submission. This host CPU will be connected to the Omega through the shared memory modules and through a Multiport Switch System. While Omega is under normal operation, the new CPU will act as a host computer for TSS operation. If the Basic system goes down due to a malfunction of the Omega CPU, the new CPU will be released from its TSS mode and switched over to serve as the Master CPU. With this configuration, the Basic system will be up and running within 15 minutes without removing any boards or cables. The malfunctioned Omega will then be available off-line to run the diagnostics.

#### IV.1.2 Multiport Switch System

A Multiport Switch System (MSS) provides a manual/microprogrammable switch between two CPU's i.e., OMEGA and its back up to their common-shared peripheral devices without removing any cables and boards from either chassis. The system consists of (a) 1 x N Universal Switch Controller to interface with up to 8 CPU controlling channels (asynchronous) and its software support compatibility for the 1 x 2 switch system and 1 x 4 switch system, (b) Multiport Switch Panel with (1) 16 single pole-single throw switch for manual control, (2) hexadecimal display for each channel, (c) Multiport ADI/SDI switch for Quad 2 x 1 serial data switch or 8 x 1 serial data switch, if selected, (d) Multiport HSD Switch for a dual 1 x 2 port and 1 x 4 port operation, if jumpered internally.

An alternative to use of the Multiport Switch System is the Fast Multiplexer System (FMS) which is just being introduced by SEL, at their

new product presentation at WAFB, AZ on 12 August 1979. The FMS is a high speed multipurpose interface which consists of an FMS chassis, a Command/status interface (CSI), Memory Port Interface (MPI) and a Fast Multiplexer Controller (FMC). The FMC connects external devices to the FMS. A further study should be conducted to investigate the feasibility of using an FMS in place of an MSS.

#### IV.1.3 Development Support System

The Development Support System (DSS) is a computer-based tool for developing a total hardware/firmware/software system. Major elements of the DSS are the universal RAM modules and their affiliated Test Interface (TI) modules that enable a multiplicity of capabilities such as snapshot, ROMSIM, Writable Control Store (WCS), and ROM decode. The TI modules have been specifically designed for the DSS and can be used in various combinations to instrument a target system. The TI Snapshot module is the heart of the complex control hardware for the target system in the DSS and controls all of the snapshot memory control functions. The TI ROMSIM module is an interface to control the RAM/ROM Simulator, RAM/Writable Control Store, and RAM/decode modules. The DSS is structured to operate in both the instrumentation of microprogram/hardware development mode and in the system development mode.

The DSS with the aid of the host computer, provides an external monitor system. The monitor is logically invisible and totally noninterfering with both the software and the ongoing process. It monitors the behavior of the system programs both for debugging a system and for measuring parameters needed to design higher performance

programs. The host computer executes the Development Support Control System (DSCS) software specifically designed for the instrumentation of the system being developed. The host system contains modes of control and display of snapshot information, as well as control over target machines. The snapshot instrumentation includes a high-speed random access memory that captures certain conditions under the control of the instrumentation software system. The DSS provides control over the snapshot. Information can be captured either every cycle or on cycles when a logical condition is met. The snapshot provides the history of events that occurred just prior to a symptom and is under the control of the host machine which set up the conditions for capturing the data in the snapshot. The snapshot can store 64 bits of events every cycle. If more than 64 events must be observed simultaneously, several snapshot storage elements may be required. All DSS memory modules, whether used for snapshot or for control memory, use a single type of high-speed memory module which is identical to the Writable Control Storage (WCS) used for RPU or CPU.

The development of a hardware/firmware product utilizing the DDS involves several distinct phases. Each phase requires the support of a segment of the total DSS capability. Microprogram Development, Microprogram/Hardware Checkout and Burn-in of Programmable Read-Only Memory (PROM) are the three major steps involved in the development process. Currently, the DSS supports the Register Transfer Language (RTL) source code for two major target machines. One supports microcode development for a 32-bit microword structure (RPU) and the other a 64-bit

microword structure (CPU). The primary difference between the two, from a programming standpoint, is the amount of parallelism that can be achieved in a single microinstruction. The RTL compiler generates all addresses, makes all appropriate translations between symbolic representation of addresses (labels), equate values, register numbers, test addresses, order addresses, flip-flop addresses, etc. One major capability of the DSS is the interactive microprogram/hardware debug facility offered through the IU, ROM image memory and snapshot support of the Unit under test in concert with the DSCS software residing in the host computer. All communication between the DSCS software and user is via the control CRT. All microprogram object code is stored on user-defined disc storage under control of the host computer. The user can change the microprogram usage or modify the contents of any specified microprogram. The DSS commands allow the user to step through his object code sequentially and direct the hardware status information both to the CRT and to the printer to allow a detailed analysis away from the DSS work station. When all problems in the hardware and microprogram have been solved and the product is operational, the microprogram is transferred from the RAM/ROMSIM to the PROM. The DSS loads the debugged microprogram into the RAM/ROMSIN and then transfers its contents to the PROM Burner which in turn burns the microprogram into the appropriate PROM. The DSS can also be used as a stand alone unit.

#### IV.1.4 Portable Diagnostic Console

A portable diagnostic console consists of a card reader an alphanumeric CRT, and a parallel system control panel with hex display.

In order to perform efficient maintenance and easy trouble shooting, this mobile station is needed to free the master CPU from halting so it can serve as a debugging tool from its system control panel.

#### IV. 2. Writable Control Storage

One of the desirable optional features of the SEL computer, which is not presently incorporated in the ASPT, is the Writable Control Storage (WCS). With this feature, users can expand the instructions repertoire with macro level functions defined in microcode. The microprogrammer writing a WCS routine has his program in direct control of the Data Structure of the computer CPU, and this results in greater program efficiency and faster execution time. Once control of the CPU has been passed to a user program in WCS, the WCS routine is in total control of the computer.

The 32 Series SEL computer uses a microprogrammed Control Section (CROM) to decode and execute machine instructions. The WCS consists of one or two 64 x 2K bit high-speed Random Access Memory (RAM) boards that provide a physical extension of the Control Storage (CROM). The WCS may be used as a CROM extension in the host computer, or it may be used with the Development Support System (DSS), residing in the DSS Test stand. Each instruction in the Main Memory is performed by a sequence of Micro-instructions in CROM that defines the logical functions to be performed. Software can execute much faster with the application of microprogramming. This speed is achieved by several factors: The ratio of Control Store speed over Main Memory; the ability of micro-instructions to allow parallel operations within the execution

timing of a single instruction; the direct interface of micro-instruction to the hardware, thereby eliminating the requirement to do memory fetches and decoding for all the instructions. Programming the WCS requires a user with experience in assembly language programming. To successfully implement microprograms, the user must learn about the computer hardware. To write an efficient microprogram, an understanding of the CROM is required. The CROM consists of a series of manufacturer supplied READ-Only Memories (ROMs) which contain the decode and vector tables within CROM to the microprogrammed routines that operate the computer. There are a total of 297 internal registers accessible within the CPU by the Micro-instructions. The control, sequencing, and test logic consists of hardwired logic circuitry, interfacing directly with the output of the Control Store (CROM). All control, sequencing, and testing is accomplished directly by this logic, based on the signals received from CROM. The ALU is controlled directly by the microprogram and provides addition, subtraction, and logical functions utilizing the entire array of registers available in the CPU. Most routines, when microprogrammed in WCS, will show very significant increases in processing speeds. For a benchmark program, the time improvement was 19 to 1 over FORTRAN and 6 to 1 over the Micro Assembled program. There are 64 entry points to WCS from software. Entry into WCS is accomplished by the Micro-Instruction Jump WCS, which addresses one of the first 64 locations in WCS, where a micro-instruction jump to a routine WCS is accomplished using the WRITE WCS Micro-Instruction. The reading of the information contained in WCS is accomplished using the READ WCS Micro-Instruction which is intended

for use in verification of data that was previously written into WCS. The reading or writing of WCS is accomplished in 64-bit words. Overflow conditions in loading or reading WCS are reported to the software through the use of the Condition Codes. All executable code contained in WCS is written in micro-code. In the CPU, the controlling hardware which executes the microprogram is referred to as the Micro-engine. Timing within the microengine generally requires two machine cycles, the first being the CROM cycle, and the second being the CREG cycle. During the CROM cycle, the basic tests and the sequencing are accomplished. The second cycle (CREG cycle) executes all orders that the micro-instruction directs. The CROM of the present micro-instruction and the CREG of the previous micro-instruction are executed at the same time, thus effectively a micro-instruction is executed in a 150 nanosecond cycle. The control structure includes Read-Only Memory, containing 4096 micro-instructions. With the WCS installed, an additional 2048 or 4096 user programmed micro-instruction locations are available. These microinstructions control the CPU operations by testing, controlling, and directing the various functions to be performed. The sequence control section selects the source of addressing used for the control store for conditional and unconditional changes in processing sequence. The CROM consists of a main 48 - X 4K-bit Read-Only Memory (ROM), which contains micro-coded routines that control the operation of the CPU.

There are several additional smaller ROMS that are used for functions such as instruction decoding, floating-point, and ALU decoding. The data structure contains a 32 X 32-bit general file

register, hardware registers and two multiplexers organized around an arithmetic logic unit and a 256 x 32-bit local store. The full CPU micro-word contains 64 bits. Only 48 of these 64 bits are directly associated with CPU operations. The remaining 16-bits are used for the optional high-speed floating point unit. Decode of the micro-word is accomplished by division of the micro-word into specific test or control fields. Decoding occurs during one or more CROM/CREG timing cycles. The micro-word is divided into 13 main fields. Traps and interrupts do not exist in the firmware environment. This decision is generally based on the length of time occupied in the WCS routine. If the WCS routines are kept short, there would be no need to service interrupts or traps, whereas if long WCS routines are used, it may be necessary to identify and service interrupts and traps. Trap or interrupt occurrence information is available to the WCS programmers through the process of testing the condition of various flip-flops in the CPU hardware. As previously mentioned, the DSS system will support the development of microcode routines.

#### IV.3 Operating System

System Engineering Laboratories recently announced a new operating system. This new Optional Mapped Programming (MPX-32) Operating System will be continuously updated and will support all of the SEL's new standard devices such as Extended I/O, Mag Tape Controller, Disk Tape Controller, etc. The MPX-32 has interactive and batch processing capabilities and claims to meet extremely demanding scientific processing requirements. Other features include: multilevel batch

processing; improved intertask communication; faster response to indirect interrupts; less overhead; supports up to 64 interactive terminals; interactive debugging; better editing capabilities; no memory fragmentation; and it possesses dynamic memory expansion and contraction. It also supports the newly announced FOTRAN 77+ three-pass optimizing compiler which exceeds ANSI X3.9-1978, ISA S61.1, S61.2, S61.3 and MIL 1753 standards. At the 14 August 1979 new product meeting, SEL's representatives announced that some companies engaging in real time applications are starting conversion from RTM to the MPX-32 Operating Systems.

Conversion to the MPX-32 Operating System requires, however, additional hardware and extensive software modification. It is thus recommended that further studies are needed before changing to the new MPX-32 system. At the present time, the RTM is quite adequate for ASPT simulator operation.

#### IV.4 System Expansion for the Third Simulator

There are two ways for introducing the third simulator to the ASPT system: (a) as a stand alone unit, (b) as an addition to the existing system.

##### IV.4.1 Stand Alone Unit

It will be beneficial for the stand alone unit from both software and hardware point of view to duplicate, with some modifications, the structure of the existing system. This new system will be composed of the Basic configuration and the Visual configuration. With some minor updates, the new Basic configuration

should be similar to the existing one. It will include one Master and two Slave computers. With the exception of the special purpose computer, the new Visual configuration should also preserve the structure of the existing one. The new Visual configuration should include a newer version of the special purpose computer. By updating and performing as much duplication as possible from the present structure, the design, development, and testing phase of the third simulator will be kept to a minimum. With the addition of two Slave computers, the capability will also exist for supporting a fourth simulator.

#### IV.4.2 Addition to the Existing System

The Basic configuration, with an addition of the two Slave CPU's, will support the third simulator as shown in Fig. 4, provided, that the recommended host computer is incorporated into the existing system to support the TSS functions. If no simultaneous operation is required with the existing simulators, the Visual configuration will support this structure. To successfully utilize this configuration, the special purpose computer down-time must be kept to a minimum. One possible way of achieving this is by performing, on a weekly or monthly basis, failure analysis and system reliability performance tests. Data from this task could be used to predict failures and some down time could be avoided if certain failure prone parts were replaced whenever their operational life was equal to or had exceeded their expected life. Accurate failure history and strict control of the thermal and electrical environments of the components are essential for reliable expected life predictions.

## V. SUMMARY

During the period of this investigation, several recommendations were suggested to improve the operation and reliability of the ASPT system.

Some of the highlights of the suggestions are summarized below:

1. Dedicate a host computer into the system for sharing some of the tasks and acting as a back-up Master computer.
2. Incorporate a switching mechanism for speed and reliability.
3. Acquire a Development Support System for troubleshooting and hardware/software/firmware development.
4. Make available a portable diagnostic system to ease testing and improve reliability.
5. Firmware implementation of software routines for increasing the speed of instruction execution.
6. System expansion possibilities for a third simulator.
7. MPX-32 Operating System as possible alternative of the present operating system.

## REFERENCES

### Systems Engineering Laboratories, Ft Lauderdale, Florida

1. "32/70 Series Writable Control Storage (WCS) User Manual", Publication Number 301-322344-000 (1979).
2. "Reference Manual 32/70 Series Computer", Publication Number 301-320070-000 (1979).
3. "Multiport Switch System Technical Specification", Document Series No. 232 (1979).
4. "Technique Manual SEL 32 Series Computer", Publication Number 303-322000-000 (1977).
5. "Reference Manual SEL Development Support System", Publication Number 324-329900-000 (1978).

### Air Force Human Resources Laboratory (AFHRL)

6. "Advanced Simulation in Undergraduate Pilot Training Computer Image Generation" AFHRL-TR-75-59(V) (1971).
7. Turnage, G., "Detailed Design Document for the ASPT General Purpose Computer Subsystem". General Electric Company Ground Systems Department Space Division, Daytona Beach, Florida (1979).

1979 USAF - SCEE SUMMER FACULTY RESEARCH PROGRAM

Sponsored by the

AIR FORCE OFFICE OF SCIENTIFIC RESEARCH

Conducted by the

SOUTHEASTERN CENTER FOR ELECTRICAL ENGINEERING EDUCATION

FINAL REPORT

OPTIMIZED HOLOGRAPHY OF MICROSCOPIC PARTICLES

Prepared by:	Keith M. Hagenbuch, Ph. D.
Academic Rank:	Assistant Professor of Physics
Department and University:	Division of Natural Sciences & Engineering, Behrend College of Penn State University
Research Location:	W.P.A.F.B. AFFDL/FX
USAF Research Colleague:	Eugene Maddox
Date:	11 September 1979
Contract No:	F49620-79-C-0038

OPTIMIZED HOLOGRAPHY OF MICROSCOPIC PARTICLES

BY

K. M. Hagenbuch

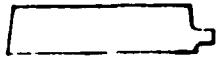
ABSTRACT

A systematic application of holographic geometries leads to optimized optical systems for producing high resolution holograms of particles in the size range 10-50 microns. It is found that where as in-line geometry with premagnification of the dust is the simplest experimentally to employ, off-axis image plane holograms give the highest resolution with lowest noise. Loss of contrast in double exposure holograms is counteracted by image subtraction both in the recording and in the reconstruction process. Recommendations for additional research are made.

#### ACKNOWLEDGMENTS

The author would like to express his gratitude to the Air Force Systems Command, the Air Force Office of Scientific Research, and Air Force Flight Dynamics Laboratory for making this effort possible. Also special thanks are given to Capt. George Havener, Dr. Eugene Maddox, and Dr. Daniel Parobeck for making their equipment available for this work, and to Dr. Eugene Maddox for his encouragement, helpful suggestions, and darkroom work which made the plates in this report possible.

LEGEND HEADINGS



laser



shutter



microscope objective



pin hole



lens or microscope objective



object field



film plate



beam splitter



mirror



image of object field

## I. INTRODUCTION

The study done during this research effort concerns holography of microscopic particles. The eventual goal of the continuation of this work is to observe the impact of rapidly moving dust on a target so as to understand the erosion process. This study relates directly to two areas of interest to the Air Force: (1) the erosion of air craft skins by impacting atmospheric aerosols; (2) the erosion of combustion chamber walls by impacting particles carried by air or fuel.

The projected reentry of the space shuttle, for example, and the flight of other supersonic aircraft produce considerable ablation of leading edges because of impacting particles through the shock waves associated with these surfaces. Even fog or ice particles encountered in high attitude clouds cause considerable damage, in addition to that caused by solid dust. Such erosion, of course, can be produced in wind tunnel facilities on aircraft models. Indeed, it is difficult to avoid such erosion because of the naturally occurring aerosols contained in air used in flow studies. Others have observed the propagation of aerosol particles through shock waves,<sup>(1)</sup> although observation of impacts were not reported. In those situations the impacting particles are cold and the targets may be either cold or hot.

Virtually any contained combustion process produces erosion of the combustion chamber walls through impacts with combusting particles, hot gases, and abrasive, non-combustible particles contained in fuel or air. In jet engines there is the additional erosion of turbine components. In these situations the impacting particles, the gases which carry them, and the target surfaces are hot. Although the observation of the combustion of individual microscopic particles has recently been reported,<sup>(2)</sup> surface impacts in combustion environments has not.

Research presently being carried on at the Behrend College of Penn State is directed at the single and double pulsed holography of the impacting of microscopic abrasive particles with a variety of targets in both hot and cold environments. To carry out this work a study was required of various possible optical arrangements to produce high resolution holograms of microscopic particles. The laser facilities at Wright-Patterson AFB are very adequate to do this study. The results of the holography study, then of the impact study will illucidate the erosion process.

## II. OBJECTIVES

The objectives of this effort are: (1) to survey the possible optical arrangements for making holograms of microscopic particles; (2) to produce the highest resolution holograms possible; (3) to improve contrast in double exposure holograms. The last goal became an important one to achieve as the work progressed on the first two. These goals were accomplished with a helium-neon gas laser. A final goal related to holography of rapidly moving particles is to align and fire a pulsed laser system and to produce double pulses using a Pockel's cell Q-switch.

### III. HOLOGRAPHY WITH A HELIUM-NEON GAS LASER

The reasons for doing holography rather than ordinary photography are three-fold. First for rapidly moving particles a pulsed laser is required to give sufficiently short exposures. Second, for microscopic particles to obtain sufficiently high intensity to give good exposure at short exposure times, a pulsed laser is required. Third, sufficient depth of field is obtained in holograms so as to see all particles in a three dimensional sample in a single exposure.

Before attempting double pulsed holography of moving dust particles, it was decided to find the best optical arrangement to obtain high resolution. This can be done with a continuous laser at low power with fixed sample objects.

#### A. Production of sample objects

Two sample objects were produced. The first was a dust field of abrasive grit of maximum size 25 microns. The field was simply produced by placing a standard microscope slide in a small plastic box fitted with two small holes. A small sample of dust was placed on the bottom of the box and a jet of air directed at the sample. Dust settled and naturally adhered to both sides of the slide, and a remarkably stable field of particles was produced.

The second object was a 50 micron diameter hair set in a projection lamp film mount.

## B. In-Line Holograms

Physically, the easiest type of hologram to make is the simple in-line type (Figure 1). Here one uses a single suitably filtered, expanded, and collimated beam (a collimated beam is used here and elsewhere mainly because of the ease of reproducing it in reconstruction). The field to be "holographed" is placed in the beam and the holographic film is located a suitable distance behind the field.

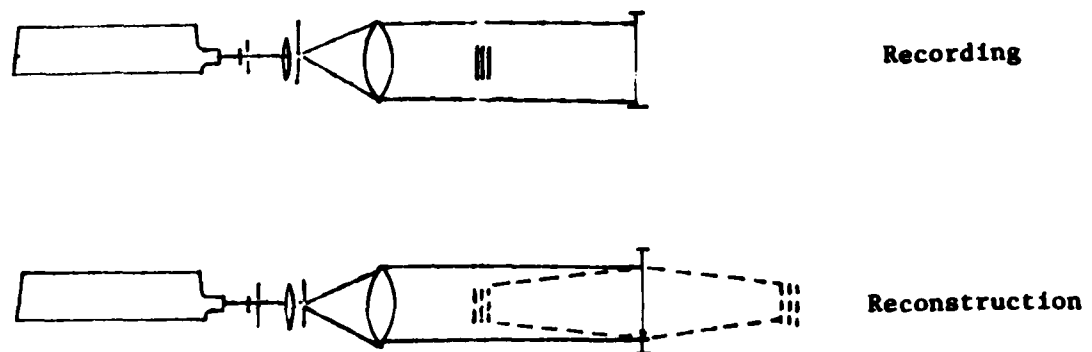


Figure 1. Geometry for In-Line Holography

In reconstruction, the same beam is used except that the field is removed. A virtual image is reconstructed in the original position of the field, and a real image in the "conjugate" position as shown. To view the reconstructed image, a telescope is used on the virtual or a microscope objective on the real image. If the images are both sufficiently close to the film plane then a microscope objective may be used to view both the real and virtual images.

Plate I is a photographic reproduction of the reconstructed real image. One immediately sees that the particles are not well resolved, that there is a lot of noise in the background, and that contrast is low. In addition, the particles, which are quite dark when viewed through a microscope, appear bright on a relatively dark background. The noise and lack of good resolution are caused by a number of factors: (1) the reference beam, which interferes with the beam scattered by the particles, is

distorted through being scattered by other particles in the field. During reconstruction, when the field is absent, no such distortion occurs. Thus the reference beam is not the same in reconstruction as in construction. (2) In viewing either image the scattered wave which would produce the other image is also present. (3) Resolution is limited by the film grain size which is on the order of a micron.

The low contrast occurs because one views the hologram by looking directly into the reconstructing reference beam, and the particles are bright on an already bright background. The reason that the particles appear bright is shown in Appendix A.

A double exposure in-line hologram is shown in Plate II. The particle field has been displaced 25 microns between exposures. Particle "pairs" may be easily seen to a size of about 10 microns, but resolution is sufficiently low that it would be difficult to match up pairs, were the displacements considerably larger. Contrast is actually reduced even further in the double exposure, though this may not be apparent from the photographs.

To improve these holograms, some magnification was done prior to recording (Figure 2). This has an advantage from a practical point of view. In wind tunnel or furnace experiments the field and holographic film may be physically distant from one another, thus making film images extremely small--causing resolution problems. With a microscope objective, or other lens, one can put a real magnified image conveniently near a film plane. The true image is viewed with a second microscope objective or lens. Plate III is a photographic reproduction of such a view. Although considerable background noise is still present, the resolution is considerably improved, with particles of 2 or 3 microns clearly visible. Contrast is still low and is further decreased in a double exposure.

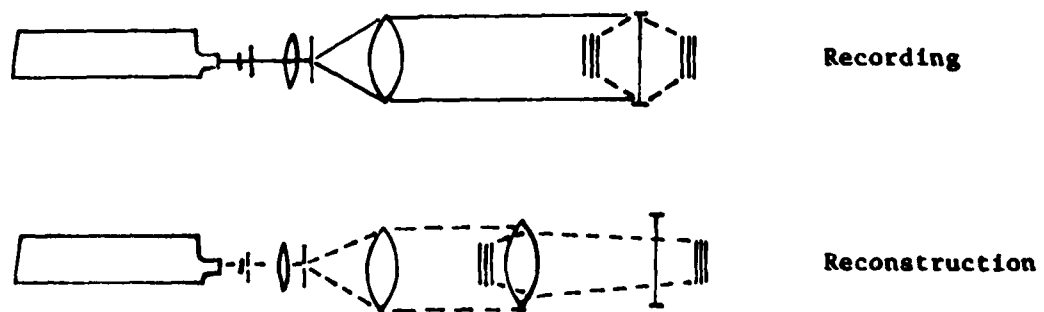


Figure 2. Geometry for In-Line Holography with Pre-magnification

### C. OFF-AXIS HOLOGRAMS

To eliminate the problem of looking directly into the reference beam in reconstruction, an off-axis geometry was produced (Figure 3). This has the added advantages of separating spatially the real and virtual images, during reconstruction, thus reducing noise, and of producing dark particles on a bright background with better contrast. The main disadvantage is the same as with all off-axis systems--that of requiring two separate beams. Plate IV is a reproduction of the view of the real image produced by such a hologram. Contrast is better and the particles are dark, but resolution is still poor--no better than with in-line geometry.

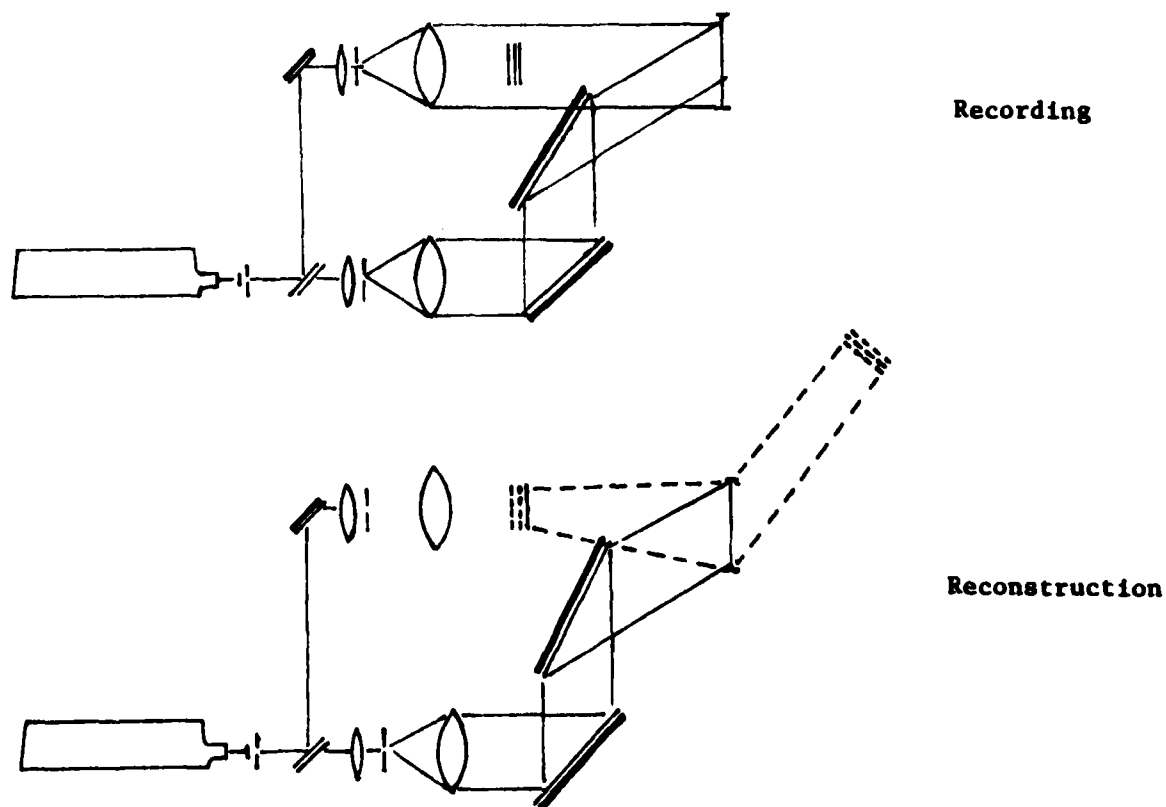


Figure 3. Geometry for Off-Axis Holography

With premagnification (Figure IV) by a 10 X microscope objective, advantages are again gained as with the in-line geometry. The true image may be put at any convenient location and resolution is considerably

improved. Plate V shows a view of such a reconstructed image. The concentric rings are produced by a flaw in one of the microscope objectives. The double exposure, reproduced in Plate VI again shows good resolution, considerable noise, and reduced contrast.

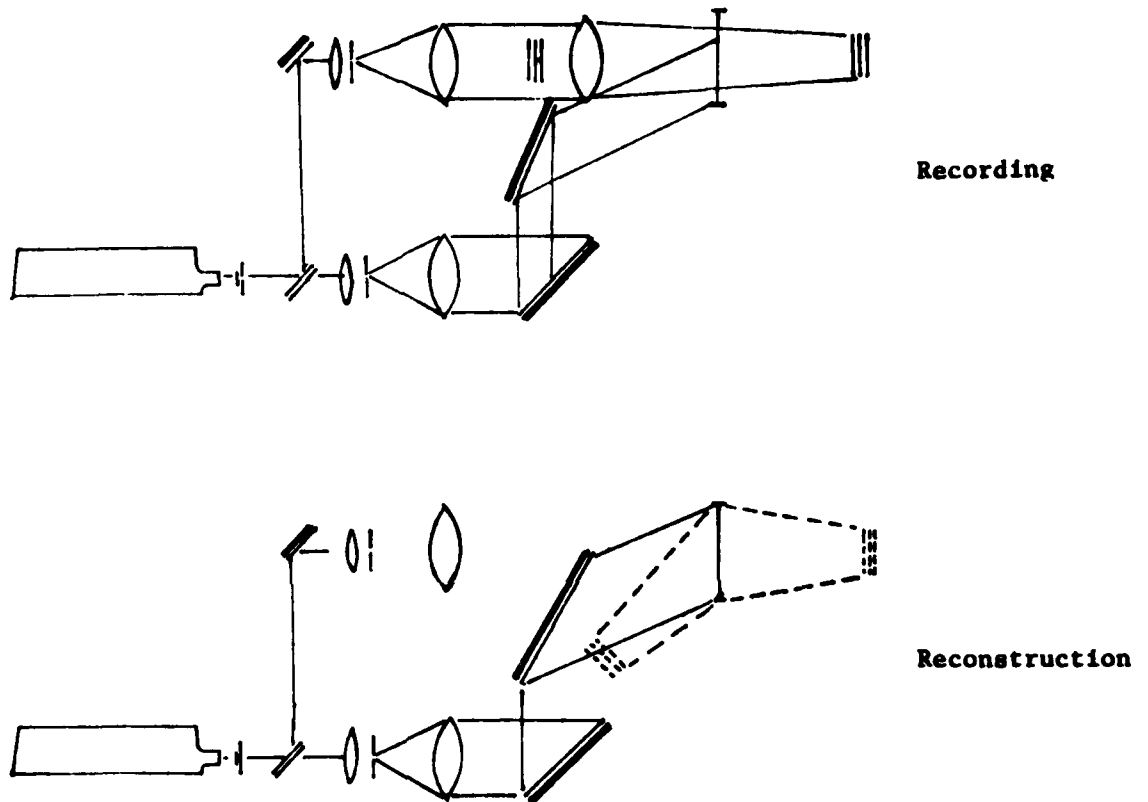


Figure 4. Geometry for Off-Axis Holography with Pre-magnification

A final arrangement was tried to get rid of noise. This is the off-axis image plane. This is a simple modification of Figure 4 in which the image of the field is made to fall in the plane of the hologram. The holograms thus formed may be viewed in white light.<sup>(3)</sup> In white light, speckle noise is absent. Plate VII is a photograph of such a "white light" hologram taken in white light. Background noise is virtually eliminated, and resolution is essentially as good as the objectives used in the production of the photograph. Plates VIII, IX, X

are photographs in white light of double exposure image-plane holograms where the particle field has been displaced 25 microns between exposures. Again contrast loss occurs. Efforts to improve contrast were made by adjusting the beam ratios. High reference/object ratios produce the highest contrast.

Based on the initial parts of this study a number of conclusions seem clear. First some premagnification is necessary. Not only can the particle field be "brought out of" the wind tunnel or furnace optically for close viewing, but also resolution in holograms is considerably increased by so doing. Good resolution is crucial to correlating particles in double exposures. Second, off-axis holograms are much more noise free than the in-line counterparts. Image plane holograms with premagnification give the most faithful reproduction of a particle field. Unfortunately only those particles in the plane of the hologram may be viewed in white light. And if the particle field has considerable depth, then confusion will occur in reconstruction and viewing between the real and virtual images, since they will overlap. That is since part of that image is in front of and part behind the film plane and since each side has its real and conjugate virtual images, the virtual image of particles on one side will be confused with the real image of particles on the other. Third, contrast is better in off-axis holograms than in in-line. However, all holograms suffer the problem of contrast reduction when multiple exposures are made.

#### D. Efforts at Contrast Enhancement

The first efforts at contrast enhancement in double exposures have been referred to above, namely, increasing the reference/object beam ratio. A certain improvement was gained thereby.

The cause of the loss of contrast can be seen from Appendix A and the simple illustration, A3. Each additional exposure further reduces contrast.

The effect is seen in Plates XI, XII, XIII. Plate XI is an image plane hologram of an 80 micron hair. Plate XII is a double exposure of the same hair with 80 micron displacement between exposures. Loss of contrast is evident. Plate XIII is a double exposure with the hair present in the first exposure, and absent in the second.

An obvious method for restoring contrast is image subtraction, i.e., instead of summing amplitudes, subtract them.<sup>(4,5)</sup> This can be done either during construction, or during reconstruction. To accomplish subtraction during construction, one must reverse the sign of the amplitude function during one of the exposures. This is done using a half wave plate in the reference beam (the same could be accomplished in the object beam). One exposure is made, the field is displaced and the half wave plate rotated so as to produce the required reversal, then the second exposure is made.

This process is not as simple to do as to imagine. The reason is that thermal gradients in the optical path of reference or object beams are sufficient to produce half-wave path differences alone. One can thus accomplish subtraction by chance and a number of trials. Likewise, if thermal gradients are not minimized, subtraction will occur only by chance with use of the half-wave plate.

The best efforts at subtraction of two images are shown in Plates XIV, XV. Here the background is essentially dark and the hair bright, as to be expected.

The best effort at producing a dark hair on a bright background can be seen in Plate XVI. Here two ordinary exposures were made, then a third with no field, but with the half-wave plate suitably rotated. This process is easily understood by considering the algebraic addition of the three object wave amplitudes.

The conclusion here is that contrast can be restored, or maintained by image subtraction during the construction process. However, this is not easy to do, even with a continuous laser. With a pulsed laser, the half wave path difference could be produced with a suitably switched Pockel's cell in the reference beam path. This has not yet been tried.

Such subtraction can be done during reconstruction by using two reference beams. One hologram is recorded using one reference beam. A second is recorded on a separate plate using the other reference beam and displaced particle field. Suitable spacing plates must be used in this process, since the two plates will be "sandwiched" for viewing. Both reference beams are used in reconstruction and the two plates are adjusted to do subtraction. The result of such subtraction is shown in Plate XVII. Again the particles appear bright on a dark background.

This method has the advantage that one can adjust the holograms at leisure while viewing to accomplish subtraction, whereas subtraction during construction is not so easy to control. It does have a disadvantage that the plates must be viewed in coherent light--thus produce a noisy image. In addition with double pulsed holography some means for rapidly changing plates between exposures must be employed. (6)

Conclusions based on this study are: (1) Particles in the range 10-50 microns may readily be holographed with high resolution, with either in-line or off-axis geometries, provided about 10 X magnification takes place before recording. In-line geometry is by far simplest and foolproof. However, noisy, low contrast holograms are produced. Off-axis geometry produces higher contrast, lower noise holograms--especially if the in-plane arrangement is used. In double exposure holograms--especially of rapidly moving particles--some form of image subtraction to maintain contrast may be necessary. Several possibilities exist for doing this, any one of which may be made to work.

#### IV. PULSED LASER ALIGNMENT

In the original project proposal, most of the work was to have been done on pulsed laser systems. However, it was determined that sufficient problems existed in holographing stationary particles, that this should be approached first, then work with pulsed systems would be done in the remaining time available. It turned out to be a wise thing to do because one of the originally available pulsed lasers developed a fault just before this study began and the other available system turned out to be faulty in the Q-switch function.

After repair of a pulsed laser with dye cell Q-switch, several pulsed holograms were made without fault after careful alignment of the laser cavity. Practice was gained in the use of a dye cell.

In the final week of this study another pulsed laser with Pockel's cell Q-switch was cleaned up and brought into operation. A digital storage oscilloscope, photomultiplier tube, and power supply were obtained to study the pulse shapes produced by the Q-switching. It was discovered that the laser power supply was not applying sufficient voltage to the Pockel's cell to enable the laser to fire with the Q-switch in place. Insufficient time

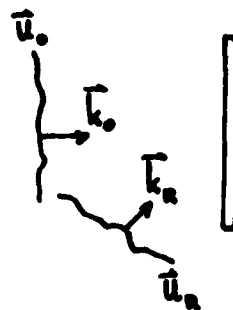
remained to have the power supply repaired. This part of the study was very valuable to this participant in providing opportunities to diagnose problems with operation of pulsed laser systems.

#### V. RECOMMENDATIONS

High resolution holograms of stationary microscopic particles can be routinely made provided magnification of about 10 X of the particles is done prior to recording. Off-axis in plane holograms viewin in white light give for the most faithful reproduction of the particles. Image subtraction to maintain contrast in double exposures can also be done if necessary. Pulsed holograms now should be made of rapidly moving dust to determine the range of conditions for which the optimized optics will produce fair resolution images.

APPENDIX A. BASIC EQUATIONS FOR HOLOGRAPHY

Let  $\vec{u}_o$  be the wave front to be recorded and reconstructed, and  $\vec{u}_R$  the reference wave used in the recording and reconstruction process. These functions may be taken in the form



A1 
$$\vec{u}_o = \vec{A}_o e^{i\vec{k}_o \cdot \vec{r}} \quad \vec{u}_R = \vec{A}_R e^{i\vec{k}_R \cdot \vec{r}}$$

Figure A1. Wavefront Geometry

where  $\vec{k}_o$  and  $\vec{k}_R$  have the same magnitude. At the film

A2 
$$\vec{u} = \vec{u}_o + \vec{u}_R$$

The exposure E is proportional to

A3 
$$|u|^2 = \vec{u}_o \cdot \vec{u}_o^* + \vec{u}_R \cdot \vec{u}_R^* + \vec{u}_o \cdot \vec{u}_R^* + \vec{u}_o^* \cdot \vec{u}_R$$

The transmissivity T is proportional to  $E^{-\Gamma}$  where for a negative hologram  $\Gamma \approx 2$ . Then the reconstructed wavefront using the reference wave is essentially

A4 
$$\vec{u}'_o = \vec{u}_R E^{-\Gamma}$$

which may be expanded for  $|\vec{u}_R| \gg |\vec{u}_o|$

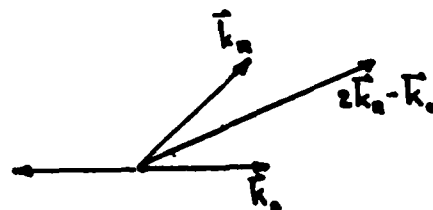


Figure A2.

A5 
$$\vec{u}'_o = |\vec{u}_R|^{-2\Gamma} \left[ \vec{u}_R - \Gamma \hat{R} \left( u_o \cos \Theta + \frac{u_o^* u_R^2}{|\vec{u}_R|^2} \cos \Theta \right) \right]$$
 Wave Number Addition for Conjugate Image

where  $\hat{R}$  is the polarization vector for  $\vec{u}_R$ , and  $\Theta$  is the angle between the polarization vectors of  $\vec{u}_R$  and  $\vec{u}_o$ . By considering the forms A1 and Figure A2, the three terms in A5 are seen to represent.

1. The reference wave.
2. The object wave with reference wave polarization.

3. A complex wave conjugate to the object wave about the reference wave direction, having reference wave polarization.

In both in-line and off-axis holograms  $\hat{U}_0$  is light "forward scattered" by particles. This light is phase shifted by nearly  $180^\circ$  for small particles. When in-line holograms are viewed one "sees" all three terms in A5. The last contributes noise if one is focusing on the true image. The first two terms add because of the scattering process, and the particles look bright. When off-axis holograms are viewed one normally only sees the second term. This is what one would see if the particles were viewed through an ordinary microscope. Thus the particles appear dark on a bright background.

In a double exposure, one uses the same reference wave, but different object waves. Following the development from A2 to A5 with two exposures

$$E_1 = |\hat{U}_{O1} + \hat{U}_R|^2 \quad E_2 = |\hat{U}_{O2} + \hat{U}_R|^2$$

one finds that the two object wave amplitudes (not intensities) add in A5, making possible image addition or subtraction during hologram construction.

The source of the loss in contrast is thus seen in this addition of object wave amplitudes in double or multiple exposures. Figure A3 illustrates this addition for a single-particle-field in which the particle the amplitudes are added and the enhancement of contrast is also evident when the amplitudes are subtracted.

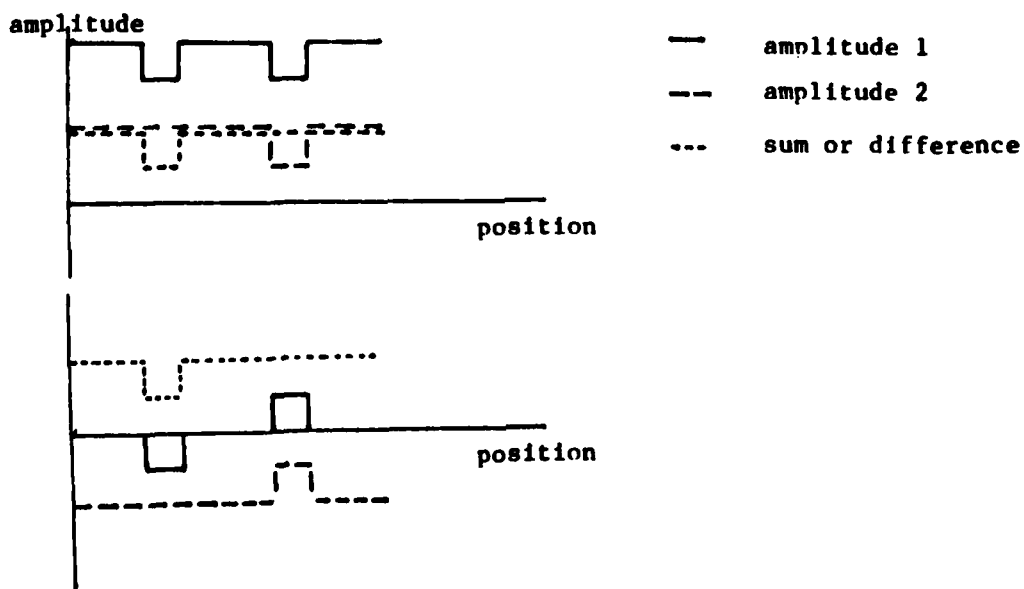


Figure A3. Amplitude Addition and Subtraction

## REFERENCES

1. J. D. Trolinger, "Particle Field Holography." Opt. Engr. 14, 5 p. 383-392 (1975).  
J. D. Trolinger, "Flow Visualization Holography," Opt. Engr. 14, 5 p. 470-481 (1975).
2. J. D. Trolinger and M. P. Heap, "Coal Particle Combustion Studied by Holography," Appl. Opt. 18, 11 p.1757-1762 (1979).
3. G. W. Stroke, "White Light Reconstruction of Holographic Images Using Transmission Holograms Recorded with Conventionally Focused Images and In-line Background," Phys. Lett. 23, p. 325 (1966).
4. J. D. Trolinger, "Application of Generalized Phase Control During Reconstruction to Flow Visualization Holography," Appl. Opt. 18, 6 p. 766-774 (1979).
5. H. Bjellehagen, "Pulsed Sandwich Holography," Appl. Opt. 16, 6 p. 1727-1731 (1977).



Plate I



Plate II



Plate III



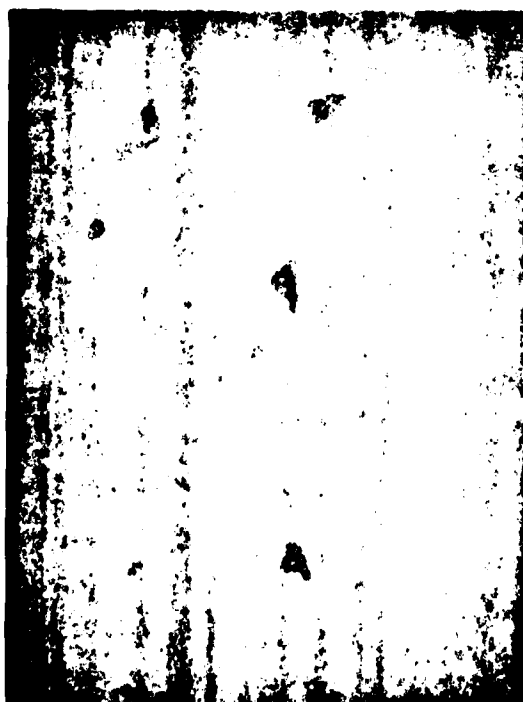
Plate IV



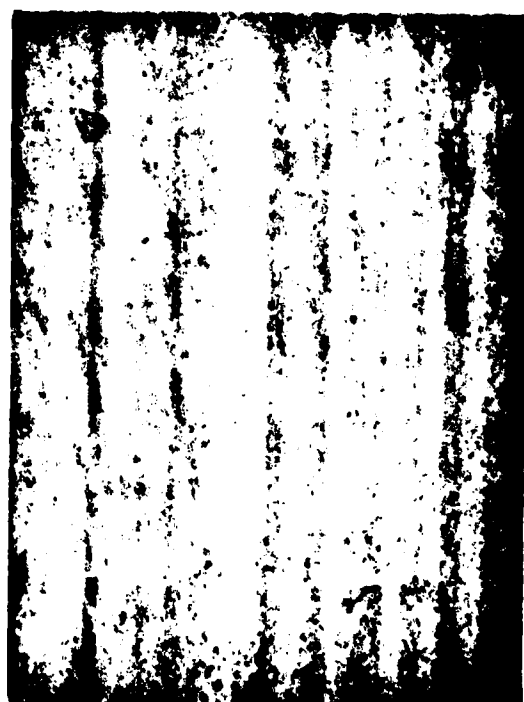
[REDACTED]



Page 11



[REDACTED]



[REDACTED]



Plate IX



Plate X



Plate XI

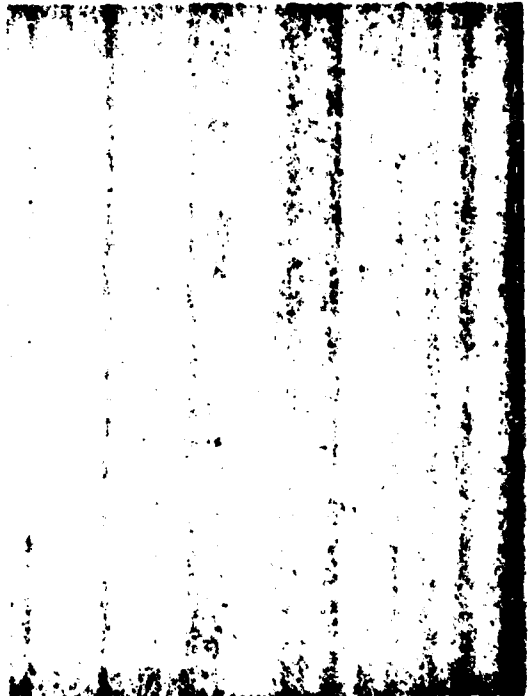


Plate XII



Plate XIII



Plate XIV

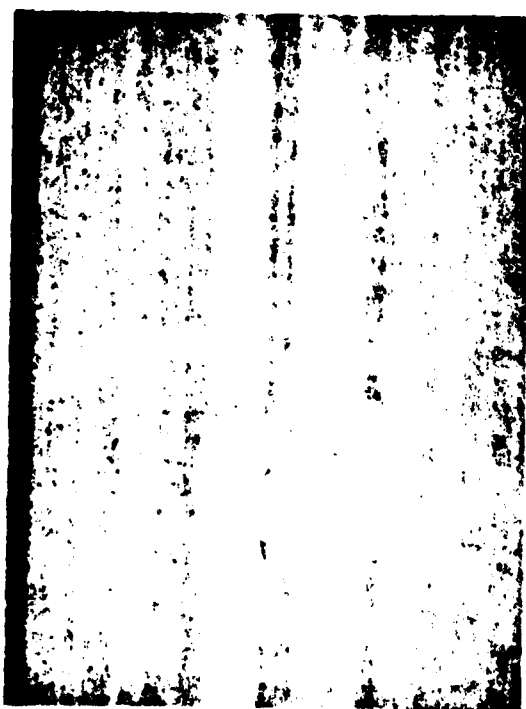


Plate XV

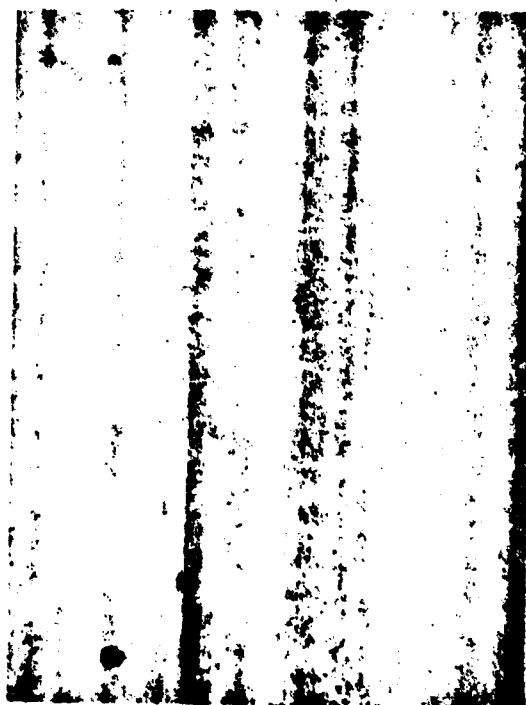


Plate XVI

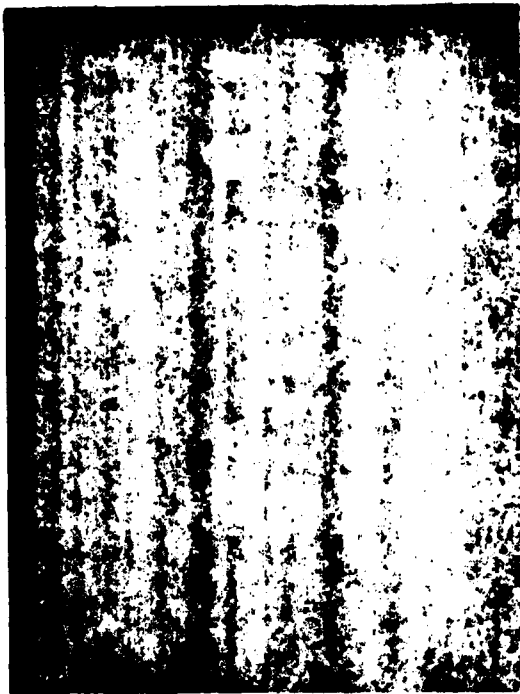


Plate XVII